FINAL REPORT

Risk Evaluation of Potential Environmental Hazards From Low Frequency Electromagnetic Field Exposure Using Sensitive *in vitro* Methods

A project funded by the European Union
under the programme
Quality of Life and Management of Living Resources
Key Action 4 "Environment and Health"
Contract: **QLK4-CT-1999-01574**
Start date: **01 February 2000**
End date: **31 May 2004**
Acronym: **REFLEX**

Table of contents

FOREWORD

Prof. William Ross Adey, who made fundamental contributions to the emerging science of the biological effects of electromagnetic fields (EMFs), died on May 20, 2004, in Redlands, California, USA. He was scheduled to deliver his personal views of EMF research at a REFLEX workshop held in Bologna in October 2002. But by then he was already too frail to travel. Dr. Adey who was an informal advisor of the REFLEX consortium sent us his talk in written form. In memory of his achievements as a scientist and in recognition of his support of the REFLEX work, the consortium decided that his message would be an inspiration to all those scientists who are willing to accept the challenges posed by EMF research, and in addition, make a fitting introduction to the final report.

THE FUTURE OF FUNDAMENTAL RESEARCH IN A SOCIETY SEEKING CATEGORIC ANSWERS TO HEALTH RISKS OF NEW TECHNOLOGIES

The Challenge to Conventional Wisdom

The history of bioelectromagnetics epitomizes a range of problems that arise whenever a community of sciences is confronted with a frontier that delves deeply into the established orthodoxies of biology, the physical sciences and engineering. These conflicts have become even more sharply defined when emerging new knowledge in bioelectromagnetics research has challenged the conventional wisdom in each part of this trinity.

Thirty-five years ago, we, who first voiced our observations of physiological responses to a spectrum of environmental EMFs at levels below thresholds for significant tissue heating, were promptly challenged by acolytes of orthodoxies in the biological and physical sciences. At best, we were euphemistically described as “controversial,” a designation that persists to this day. A Yale physicist recently added the charming term “crackpot” to describe a highly qualified biophysicist investigator.

What is the basis of this deep thorn of discontent? Historically, excitation in biological systems has been modeled and tested in terms of equilibrium thermodynamics. In this classic tradition, it was assumed that the potential effectiveness of an exciting agent could be assessed by its ability to transfer energy to the receptor in excess of its random thermal atomic and molecular collisions. Thus, the physical expression kT, the union of the Boltzmann constant and temperature, has been regarded as an expression of an immutable threshold below which an exciting agent would not be physiologically effective. In like fashion from the quantum realm of the physicist, photon energies of low-frequency magnetic fields, now known to act as effective physiological stimuli, would also fall below this thermal barrier.

Here is one example: The human auditory threshold involves a hair cell vibration of 10-11 meters, or about the diameter of a single hydrogen atom. But, by an as-yet-unknown mechanism, the ear suppresses the vastly larger noise of its thermal atomic and molecular collisions, functioning as an almost “perfect” amplifier close to 0°K.

Clearly, we face a profound paradox, with answers to be sought in cooperative states and nonequilibrium thermodynamics, as first suggested in a biological context almost 60 years ago by Herbert Fröhlich.

The lesson is clear. The awesome complexity of biological organization demands our most careful consideration.

The Recent History of Technology Applications

We also find the heat of controversy in the recent history of technological applications in western societies. At no point in the last 20 years has public school education ensured that a majority of citizens has even a basic understanding of sophisticated communication devices and systems, such as telephones, radio and television. Similarly, automotive engineering remains a sea of vast ignorance for most users. Nor is such knowledge considered appropriate or necessary.

In summary, we have become superstitious users of an ever-growing range of technologies, but we are now unable to escape the web that they have woven around us.

Media reporters in general are no better informed. Lacking either responsibility or accountability, they have created feeding frenzies from the tiniest snippets of information gleaned from scientific meetings or from their own inaccurate interpretation of published research. In consequence, the public has turned with pleading voices to government legislatures and bureaucracies for guidance.

Public Concerns and the Evolving Pattern of Research Funding

We face the problem brought on by the blind leading the blind. Because of public pressure for rapid answers to very complex biological and physical issues, short-term research programs have been funded to answer specific questions about certain health risks.

Participating scientists have all too often accepted unrealistic expectations that, in a matter of a few years, they will provide answers to pivotal questions in cell and molecular biology that can only be achieved slowly, painstakingly and collaboratively over a decade or more.

Using EMFs as tools, we have launched our ship on a vast, uncharted ocean, seeking a new understanding of the very essence of living matter in physical processes at the atomic level. This is an awesome and humbling prospect, surely not to be ignored or forgotten in the pragmatic philosophies of most risk research.

In many countries, and particularly in the USA, the effects of such harassing and troublesome tactics on independent, careful fundamental research have been near tragic. Beguiled by health hazard research as the only source of funding, accomplished basic scientists have diverted from a completely new frontier in physical regulation of biological mechanisms at the atomic level. Not only have governments permitted corporate interests in the communications industry to fund this research, they have even permitted them to determine the research questions to be addressed and to select the institutions performing the research.

These policies overlook the immutable needs of the march of science. In their hasty rush to judgment, they have sought a scientific consensus where none can yet exist. Such a consensus will occur only after experimental convergence emerges from a spectrum of related but certainly not identical experiments.

Defining the Role of Epidemiology in Current Controversies

Much in the fashion of ancient Romans, standing four-square and reading the auguries of future events by noting flight patterns of passing birds, the modern-day epidemiologist has become the high priest in the search for correlates of disease processes with a constellation of environmental observables. It is rare for them to be competent in delving into questions of causality, particularly where no exposure metric has been established for a suspected environmental factor. Nevertheless, in courts of law, in legislatures, and among a concerned public, epidemiological opinions have become a gold standard, typically outranking evidence based on a balanced and often cautionary review of current medical science.

We should remind ourselves that their professional tool is biostatistics —they build endless Byzantine edifices of levels of statistical risk, with little or no commitment to the underlying science or medicine. Their mutual discussions have produced the technique of meta-analysis, the pooling of statistical analyses from a series of epidemiological studies. The method ignores the nuances of both experimental design and epidemiological findings in the separate studies, and blinds us to options for further research based on the possible uniqueness of these separate observations.

It appears reasonable that there should be no more large epidemiological studies on human EMF exposures until essential exposure metrics are established, based on mechanisms of field interactions in tissues.

Repairing the Body Politic of Science: Some Personal Reflections

The passage of time across the years has not diminished in any way the importance, even the urgency, that one feels towards the growing edifice of science. We must not fail to engender in younger minds a passionate curiosity and an imagination sufficient to kindle their commitment to all that is great and good in the scientific method.

As I reflect on major changes wrought in the U.S. national research scene over the past 40 years, I sense a deep and growing concern that research training and the culture of research accomplishment have stifled

the burning thorn of personal discontent that should be the creative option of all young minds entering on a research career.

Graduate students are assigned a project that is typically a segment of their advisor's grand vista. They may not deviate to ask creative “what if?” questions. They emerge from the chrysalis of their training, bearing a parchment for the professional market place, affirming proficiency in certain techniques, but in no way proclaiming the arrival of that precious citadel of a creative mind.

Please allow me to conclude with an urgent proposal that comes from my own research experience. Formal instruction in physics, theoretical and applied, has become the weakest link for those entering on a career in medical research. Bioelectromagnetics research has opened the door to a new understanding of the very essence of living matter in physical regulation at the atomic level, beyond the realm of chemical reactions in the exquisite fabric of biomolecules. Without versatility in biophysics that matches their typical knowledge in molecular biology and biochemistry, none of these students may cross this threshold to the cutting edge of in future medical research. Let us not see this opportunity lost prematurely through prostitution of mechanistic research in the market place of possible health risks.

Thank you for the great privilege of offering these personal reflections.

LIST OF PARTICIPANTS

1. VERUM - Stiftung für Verhalten und Umwelt, München, Germany
   (Scientific person in charge of the project: Prof. Franz Adlkofer)
2. Institut für Klinische Chemie, Universitätsklinikum Benjamin Franklin, Berlin, Germany
   (Scientific person in charge of the project: Prof. Rudolf Tauber)
3. Abteilung für Arbeitsmedizin, Universitätsklinik für Innere Medizin, Wien, Austria
   (Scientific person in charge of the project: Prof. Hugo W. Rüdiger)
4. Institut für Pflanzengenetik und Kulturpflanzenforschung, Gatersleben, Germany
   (Scientific person in charge of the project: Prof. Anna M. Wobus)
5. Insalud, Ramon y Cajal Hospital, Madrid, Spain
   (Scientific person in charge of the project: Dr. Angeles Trillo)
6. STUK - Radiation and Nuclear Safety Authority, Helsinki, Finland
   (Scientific person in charge of the project: Prof. Dariusz Leszczynski)
7. Institut für Biophysik, Universität Hannover, Germany
   (Scientific person in charge of the project: Prof. H. Albert Kolb)
8. Laboratoire PIOM, ENSCPB, Bordeaux, France
   (Scientific person in charge of the project: Dr. Isabelle Lagroye)
9. Universita degli Studi di Bologna, Italy
   (Scientific person in charge of the project: Prof. Fernando Bersani)
10. Institut für Integrierte Systeme, ETH Zentrum, Zürich, Switzerland
    (Scientific person in charge of the project: Prof. Niels Kuster)
11. Cattedra di Farmacologia, Universita degli Studi di Milano, Italy
    (Scientific person in charge of the project: Prof. Francesco Clementi)
12. Ressourcenzentrum für Genomforschung GmbH (RZPD), Heidelberg, Germany
    (Scientific person in charge of the project: Dr. Christian Maercker)

1.0 INTRODUCTION

Based on the state of knowledge acquired during the last 50 years of research on possible biological effects of electromagnetic fields (EMF), the majority of the scientific community is convinced that exposure to EMF below the existing security limits does not cause a risk to the health of the general public. However, this position is questioned by others, who are of the opinion, that the available research data are contradictory or inconsistent and therefore, unreliable. As a consequence, it is necessary that the methodology applied in EMF research to be considerably improved and complemented by the most recent molecular biological techniques. In the REFLEX project, biological effects of extremely low frequency electromagnetic fields (ELF-EMF) and radio frequency electromagnetic fields (RF-EMF) are studied using sophisticated and diverse research methodologies separately since it is assumed that the generation of effects, if verifiable at all, may be based on different mechanisms.

Many laboratory investigations have been performed to test the hypothesis that ELF-EMF exposure may constitute a risk to the health of people. This hypothesis is almost entirely based on epidemiological studies, some of which indicate that ELF-EMF may contribute to the development of leukaemia in children, and other cancers in adults chronically exposed in residential environments or occupational settings (NRPB 2001; California EMF Program 2002; IARC Monographs 2002). The existing uncertainty is a source of increasing concern for the public, the health authorities and also the industry. *In vitro* studies have shown that ELF-EMF induces significant biological alterations in a variety of cells and tissues. These changes concern the up-regulation of several early response genes, including c-myc (Jin et al. 2000), c-fos (Rao and Henderson 1996) and hsp70 mRNA (Goodman and Blank 1998), thus increasing the production of stress inducible heat shock proteins (Goodman and Henderson 1988; Tokalov and Gutzeit 2003). In spite of this, it is still an unsolved issue whether or not exposure to ELF-EMF may promote pathological processes such as carcinogenesis and if so, whether or not the field effects are exerted through mechanisms influencing the genome of cells, cell proliferation, differentiation or programmed cell death (apoptosis). Results from several studies have indicated that ELF-EMF does not exert any direct genotoxic effect, but may promote carcinogenesis indirectly by interfering with the signal transduction pathways of cells (Blackman et al. 1985; Liburdy et al.1993). Of course, the present uncertainty could considerably be diminished by increasing our knowledge on the parameters of the electromagnetic field which are critical for the generation of biological effects and of the biological systems which are crucial for the occurrence of pathological cellular events.

As with ELF-EMF, several epidemiological and animal studies also cast suspicion on RF signals to promote cancer and other diseases in chronically exposed individuals (Stewart Report 2000; Hardell et al. 2003). Because of its overwhelming presence in our society, the potential influence of RF-EMF exposure on the development of adverse health effects has become a major topic of interest for all concerned, including the government, the general public, and the industry. Putatively non-thermal, immediate and reversible responses have been described in the literature for several years (Roschke and Mann 1997; Wagner et al.1998; Borbely et al.1999; Preece et al. 1999; Koivisto et al. 2000; Huber et al. 2000; Krause et al. 2000). However, these effects, because of their unspecific nature have been regarded as indications of potential biological responses to electrical excitation, rather than harmful effects able to produce permanent damage to health. To date, several *in vitro* studies have been carried out to investigate the disease causing potential of RF radiation. While most of these studies using different cell systems, exposure set-ups and molecular-biological and toxicological methodologies did not show any biological effect, increasing numbers of studies have come up with contradicting results (Moulder et al. 1999; Vescovic et al. 2002).

As stated above, although investigations of possible biological effects of EMF have been conducted for decades, reliable answers are still missing. Extensive epidemiological and animal studies commonly expected to provide the answer as to whether or not EMF might be hazardous are in progress. However, this approach alone might not be able to provide certain evidence whether EMF can or cannot contribute to the pathogenesis of diseases such as cancer or neurodegenerative disorders. The low sensitivity of the epidemiological methodology in detecting low risk associations is probably insufficient to reliably identify any risk to health caused by EMF. Therefore, although epidemiological studies will be needed to ultimately validate the extent of any potential health hazard of EMF, such research must be supplemented and supported by data from animal and *in vitro* studies. Therefore, *in vitro* studies using the most modern molecular biological techniques such as. genomics and proteomics are urgently needed in order to create at least a hypothetical basis for the understanding of disease development through EMF-exposure. If it can be determined that such a basis exists, it becomes even more important, to search for marker

substances which are specific for EMF exposure. Such marker substances could considerably increase the accuracy of epidemiological studies, so that even a low health risk due to EMF exposure would not escape epidemiological detection.

The main goal of the REFLEX project is to investigate the effects of EMF on single cells *in vitro* at the molecular level below the energy density reflected by the present safety levels. Most, if not all chronic diseases, including cancer and neurodegenerative disorders, are of diverse and heterogeneous origins. This variability is to a great extent generated by a relatively small number of critical events, such as gene mutations, deregulated cell proliferation and suppressed or exaggerated programmed cell death (apoptosis). Gene mutations, cell proliferation and apoptosis are caused by or result in an altered gene and protein expression profiles. The convergence of these critical events is required for the development of all chronic diseases. The REFLEX project is, therefore, designed to answer the question whether or not any of these disease-causing critical events could occur in living cells after EMF exposure. Failure to observe the key critical events in living cells *in vitro* after EMF exposure would suggest that further research efforts in this field could be suspended and financial resources should be reallocated for the investigation of more important issues.

2.0 MATERIAL AND METHODS

2.1 Exposure setups (Participant 10)

In order to compare the results of investigations carried out in the different laboratories and to ensure the conclusiveness of the data obtained in the studies, it is of the utmost importance that the conditions of exposure to EMF be strictly controlled. It was the task of Participant 10 to evaluate and modify already existing setups, to develop new optimised exposure systems and to provide technical quality control during the entire period of exposure. The latter was realised by (1) the conduct of a thorough dosimetry including an analysis of possible artefacts, (2) the continuous monitoring of exposure and environmental parameters and (3) blinded exposure protocols. Details about this work can be found in the appendix.

2.1.1 ELF-EMF exposure setup

A novel ELF setup was developed, and four copies were installed in the laboratories of Participants 3, 4, 7 and 11. The setup consists of two four-coil systems, each of which is placed inside a µ-metal shielding box. The coils produce a linearly polarised B-field over the area of the Petri dishes with a B-field vector perpendicular to the dish plane. The shielded design of the chamber guarantees non-interference between the two units, such that they can be kept close to each other inside the same incubator in order to guarantee identical ambient conditions for the cell dishes. Two fans per coil system ensure fast atmospheric exchange between the chambers and incubator. The airflow temperature is monitored with accurate Pt100 probes fixed inside the exposure chamber.

The signal is generated by a computer-controlled arbitrary function generator. A custom-designed current source allows arbitrary field variations in the range from MHz to 1.5 kHz. The maximum achievable magnetic flux density for a sinusoidal with a frequency of less than 80 Hz is 3.6 mT RMS. Sinusoidal signals with a frequency range from 3 Hz up to 1000 Hz can be applied, controlled and monitored. A powerline signal was defined which represents a worst-case scenario with respect to spectral content and corresponds to the maximum accepted distortions for power systems by the International Electrotechnical Commission (IEC 1995) (Figure 1). In addition to these waveforms, arbitrary field on/off intermittently in the range from seconds to hours can be applied.

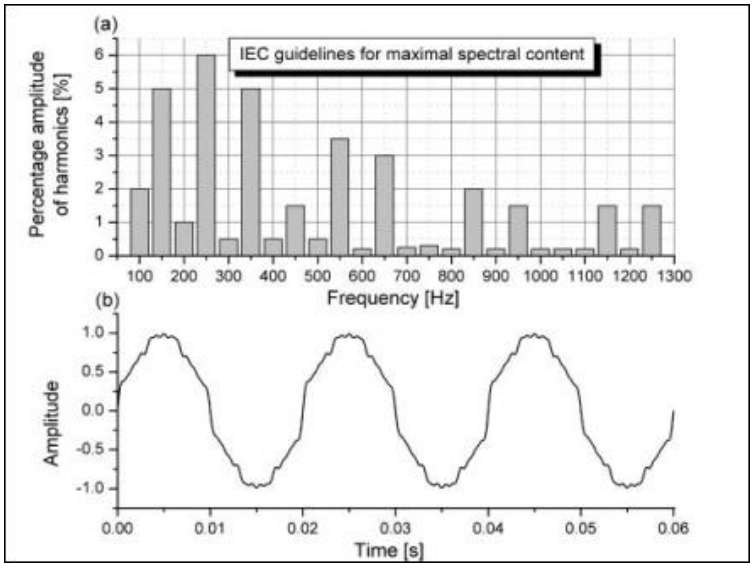

Figure 1. (a) Frequency composition of the powerline signal, corresponding to the maximum allowed spectral content according the IEC guidelines for low and medium voltage power networks (IEC 1995). Shown are the spectral amplitudes of the harmonics in relation to the main 50 Hz component. (b) The resulting powerline signal in the time domain.

The coil current and consequently the magnetic field is quasi-continuously (10s intervals) recorded and regulated using resistors providing low-temperature sensitivity. The currents in the bifilar coils can be randomly switched parallel for field exposure or nonparallel for sham control by the computer. This procedure is used to apply blind protocols and additionally to avoid temperature artefacts between exposed and control coils, since they are heated by the same current.

The evaluation and optimisation of the coil configuration was performed using numerical techniques (Mathematica V4.1) and experimental methods (3-axis Hall meter, FH49 Magnet Physik, Germany). A non-uniformity of less than 1% for the magnetic field over the exposure area of 16 cm x 16 cm x 23 cm is achieved. An uncertainty of 4.3% for the B-field assessment and a B-field variability of 1.6% were found. The average deviation of 2.9% between simulation and measurement is integrated in the uncertainty assessment. Parasitic electric fields generated by the coil system are reduced to less than 1 V/m by a grounded, metallic shielding box between the coil and Petri dishes. The temperatures inside the cell media have been analysed and no temperature differences due to field or sham exposures could be detected (i.e., temperature differences were below 0.1°C). The induced electric fields resulting from a sinusoidal exposure can be expressed as E = 3.2*f*B*r [V/m] and for the powerline exposure as E = 664*B*r [V/m], whereby f is the frequency of the sinusoidal [Hz], B is the average B-field [T] and r is the radial distance from the dish centre [m]. The estimated vibration of the exposed cells is less than 1 m/s^2 (= 0.1 g), which is a factor of 20 above the minimal background level for sham. If an elastically damped dish holder is used (as provided for Participant 4) the vibration load can be further reduced by a factor 12 to 0.1 m/s^2.

In addition to the newly developed exposure systems, it was decided to use two existing setups (Participants 5, 8).

The ELF setup of Participant 5 is based on a pair of Helmholtz coils placed inside a µ-metal shield; exposure and sham are kept in different incubators (no blinded protocols); and sinusoidal B-fields (50 Hz) up to 0.1 mT can be applied.

The ELF setup of Participant 8 is based on two unshielded 4-coil systems arranged in the same incubator; B-fields up to 1 mT (50 Hz) can be applied under non-blinded exposure conditions.

2.1.2 RF-EMF exposure setup

A novel RF setup (GSM) was developed, and four copies were installed in the laboratories of Participants 2, 5, 6, and 8. The system enables EMF exposure of cells under defined conditions with respect to field strengths, polarisation, modulation and temperature and is operated within the GSM DCS mobile frequency band. The setup consists of two single-mode resonator cavities for 1.8 GHz that are placed within an CO_2 incubator. Up to six 35 mm diameter Petri dishes can be exposed in one waveguide resonator. A dish holder guarantees that the dishes are placed exactly in the H-field maximum of the standing wave inside the waveguide.

Each waveguide is equipped with a fan for rapid environmental atmospheric exchange. In order to ensure stable exposure independent of the loading and drifts, monopole antennas are integrated to monitor and control the incident field. The system enables the exposure of monolayers of cells with a non-uniformity of SAR of less than 30% and an efficiency of better than 20 W/kg per W input power.

Much care has been taken to avoid artefacts due to temperature differences between exposed and sham exposed cells. The temperature response of the medium has been assessed by measurements in terms of the incident field strength, cell medium volume and air flow. A temperature load of less than 0.03°C per W/kg SAR was found. The air flow temperature is monitored with accurate Pt100 probes, resulting in differences of less than 0.1°C between the air flow temperature of the exposed and sham waveguides. A numerical heat flow analysis has shown that the possibility of temperature hot spots inside the medium can be excluded.

Field strengths, temperatures and fan currents as well as all commands are continuously logged to encrypted files which are evaluated after the experiments in order to ensure studies under 'blind' conditions (exposure and sham conditions are blindly assigned to the two waveguides by the computer-controlled signal unit).

Field, SAR and temperature characterisations were performed with numerical methods (FDTD simulation platform SEMCAD, SPEAG, Switzerland) and were experimentally verified using the near field scanner DASY3 (SPEAG, Switzerland) equipped with dosimetric field and temperature probes. An uncertainty and variability analysis resulted in an absolute uncertainty for the SAR assessment of 20% and a variability of 5%. The average deviation of 15% between SAR measurement and simulation is within the range of the uncertainty and therefore verifies the reliability of the numerical dosimetry.

The signal unit allows the application of the following five different exposure signals (Figure 2):

- Continuous Wave (CW): An unmodulated CW signal can be applied as a reference (same thermal load, but no ELF modulation components).
- GSM-217Hz: GSM signals are amplitude modulated by rectangular pulses with a repetition frequency of 217 Hz and a duty cycle of 1:8 (pulse width 0.576 ms), corresponding to the dominant modulation component of GSM. The ratio between slot average SAR and time average SAR is 8.
- GSM-Basic: In addition to this basic GSM-217Hz TDMA frame, every 26th frame is idle, which adds an 8 Hz modulation component to the signal. The ratio between slot average SAR and time average SAR is 8.3.
- GSM-DTX: The discontinuous transmission mode (DTX) is active during periods without speaking into the phone. To save battery power, the transmission is reduced to 12 frames per intermediate multiframe of 104 frames (compared to 100 frames for GSM Basic). The frame structure of the DTX signal results in 2, 8 and 217 Hz components. The ratio between slot average SAR and time average SAR is 69.3.
- GSM-Talk: GSM-Talk generates temporal changes between GSM-Basic and GSM-DTX and simulates a conversation with an average duration of 97s and 50s for Basic and DTX, respectively. The ratio between slot average SAR and time average SAR is 11.9. Furthermore, arbitrary field on/off intermittence in the range from seconds to hours can be applied.

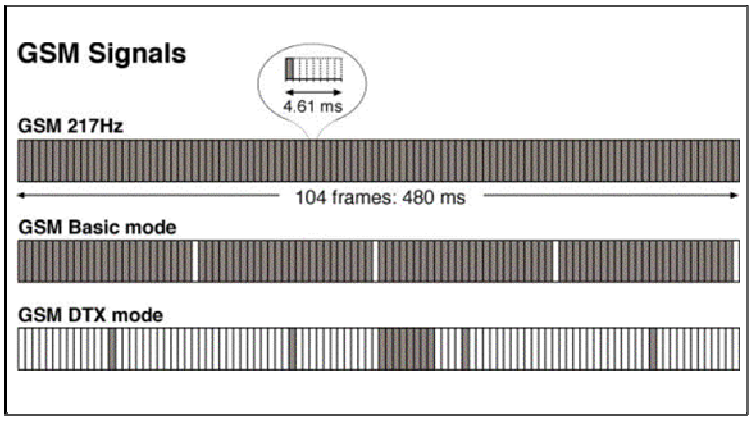

Figure 2. Pulse structure of the applied GSM signals. The basic frame has a period of 4.61 ms and contains a 576 µs burst including 15 µs rising and falling edges. 26 frames make up a GSM multiframe (MF) and 104 frames a GSM intermediate multiframe (IMF). GSM-217Hz is composed of a repetition of basic frames (104 bursts per IMF), whereby every 26th frame is blanked for the GSM-Basic signal (100 burst per IMF). The GSM DTX mode is active during periods of silence and transmission is reduced to 12 bursts per IMF.

In addition to the newly developed exposure systems, it was decided to use three existing setups (Participants 4, 6, 9) and to modify and improve the two setups of Participants 4 and 9.

The RF setup of Participant 4 is based on two R14 waveguides operated at 1710 MHz (Schönborn et al. 2000). Eight 60 mm diameter Petri dishes are exposed with the same concept as for the RF setup (GSM). An identical signal unit is applied, and similar performance is achieved. However, different settings for GSM-Talk were used: Average duration of Basic and DTX was 50s and 97s (instead of 97s and 50s). Therefore the ratio between slot average SAR and time average SAR is 19.8 (instead of 11.9).

The existing RF setup of Participant 6 is based on a R9 resonator cavity operated at 900 MHz. Active water cooling of the Petri dishes is integrated; for details see Toivo et al. (2001). The signal unit can apply GSM-217Hz. Blinded exposure protocols are not possible. In the course of the project, Participant 6 was additionally equipped with the standard RF-setup (GSM).

The RF setup of Participant 9 is based on the Wire-Patch cell and is operated at 900 MHz (Laval et al. 2000). The system was equipped with a new signal unit, allowing the full spectrum of GSM signals. However, also this setup does not allow for computer-controlled blinded exposure conditions. On the other hand, Participant 9 assures that exposure using this system was done blinded (see 2.6.2 below)

2.2 Experiments with human fibroblasts, lymphocytes, monocytes, melanocytes and muscle cells and with granulosa cells of rats (Participant 3)

2.2.1 ELF and RF-EMF exposure setups

See 2.1

2.2.2 Cell culture and exposure conditions

Human diploid fibroblasts (obtained from healthy donors) and SV40 transformed GFSH-R17 rat granulosa cells (Keren-Tal 1993) (provided by Participant 7) were cultivated in Dulbecco´s modified Eagle's medium (DME) supplemented with 10% fetal calf serum (FCS), 20 mM Hepes buffer, 40 µg/ml neomycin, 2 mM L-glutamine, 100 IU/ml penicillin and 100 µg/ml streptomycin. Human melanocytes (male, 3 years old) and skeletal muscle cells (male, 63 years old) were received from Promocell (Heidelberg, Germany) and cultured according to the supplied protocol. Cells were incubated at 37°C in an atmosphere of 5% CO_2 and at 90-100% relative humidity and supplied with fresh culture medium every 48h.

Leukocytes from a healthy donor (female, 31 years old) were isolated from venous blood using Ficoll Paque gradient centrifugation. Cells were washed twice with PBS, resuspended in DME medium with additives and seeded into 35 mm Petri dishes. After 2 hours monocytes had become completely attached on the bottom surface and were separated from lymphocytes by decantation. Monocytes were washed twice with PBS and taken up in 3 ml DME medium.

Lymphocytes from a healthy donor (female, 27 years old) were isolated from venous blood with Ficoll Paque gradient centrifugation. Cells were resuspended in fresh culture medium (DME, 25% FCS, 20 mM Hepes buffer, 40 µg/ml neomycin, 2 mM L-glutamine, 100 IU/ml penicillin and 100 µg/ml streptomycin) with or without stimulation with phytohemagglutinine (1%). The cells were seeded into 35 mm Petri dishes at a density of 2×10^5 cells/3 ml, 24 hours prior to ELF-EMF exposure.

The cells mentioned above were exposed or sham-exposed in suitable waveguides connected with an ELF-EMF generation system provided by Participant 10 within a Heraeus incubator (model Kendro BBD 6220). After exposure cells were detached with trypsin and suspended in fresh culture medium for Comet assay analysis or maintained in culture for cytogenetic testing. Each exposure level was tested in duplicate. In another series of experiments human fibroblasts (cell strain ES-1) and SV40 transformed GFSH-R17 rat granulosa cells (Keren-Tal 1993) (provided by Participant 7) were exposed or sham-exposed in suitable waveguides connected with a RF-EMF generation system (RF 1800 MHz) provided by Participant 10 within a Heraeus incubator (model Hera cell 150l). These experiments were first performed by E. Diem in the laboratories of Participant 2 and later on continued in our own laboratories with a comparable RF-EMF exposure setup, but a RF of 1950 MHz. After exposure cells were detached with trypsin and suspended in fresh culture medium for Comet assay analysis or maintained in culture for cytogenetic testing. Each exposure level was tested in duplicate.

Combined exposures to UVC and ELF-EMF were performed on ice using a germicidal lamp (60 W, Desaga, Heidelberg, Germany), the output of which predominantly contains UVC (253.7 nm). Exposure to UVC prior to ELF-EMF was carried out at an intensity of 2 W/m^2 (measured with a radiometer, Blak-

ray®, Ultra-violet products. Inc., model J225, San Gabriel, USA) for 10 minutes, which equals 1.2 kJ/m^2. Exposure to UVC post to ELF-EMF exposure was performed at an intensity of 2.5 W/m^2 for 30 minutes, which equals 4.5 kJ/m^2.

For thermal exposure cells were incubated at 38.5°C for 4 hours in a commercial incubator (BBD 6220, Kendro, Vienna, Austria). To study repair kinetics, cells were further incubated at 37°C for up to 24 hours.

2.2.3 Comet assay

We followed the technique described by Östling and Johanson (1984) with minor modifications by Singh et al. (1988, 1991). EMF-exposed and sham-exposed cells (10,000 – 30,000) were mixed with 100 µl low melting agarose (0.5%, 37°C) to form a cell suspension, pipetted onto 1.5% normal melting agarose pre-coated slides, spread using a cover slip, and maintained on a cold flat tray for about 10 minutes to solidify. After removal of the cover slip the third layer of 0.5% low melting agarose was added and solidified. The slides were immersed in freshly prepared cold lysis solution (2.5 M NaCl, 100 mM Na_2EDTA, 10 mM Tris, pH 10, 1% sodium sarcosinate, 1% Triton X-100, 10% DMSO, pH 10) and lysed for 90 minutes at 4°C. Subsequently, the slides were drained and placed in a horizontal gel electrophoresis tank side by side, nearest the anode. The tank was filled with fresh electrophoresis buffer (1mM Na_2EDTA, 300 mM NaOH, pH>13 or pH=12.1 in case of alkaline Comet Assay and 100 mM Tris, 300 mM sodium acetate, 500 mM sodium chloride, pH 8.5 in case of neutral Comet Assay) to a level approximately 0.4 cm above the slides. For both, alkaline and neutral Comet assay, slides were left in the solution for 40 minutes for equilibration and unwinding of the DNA before electrophoresis. Electrophoresis conditions (25 V, 300 mA, 4°C, 20 min, field strength: 0.8 V/cm) were the same for neutral and alkaline Comet assay. All steps were performed under dimmed light to prevent the occurrence of additional DNA damage. After electrophoresis the slides were washed 3 times with Tris buffer (0.4 M Tris, pH 7.5) to neutralise, then air-dried and stored until analysis. Comets were visualised by ethidium bromide staining (20 µg/ml, 30 seconds) and examined at 400 X magnification using a fluorescence microscope (Axiophot, Zeiss, Germany). One thousand DNA spots from each sample were classified into 5 categories corresponding to the amount of DNA in the tail according to Anderson et al. (1994) with modifications. The proposed classification system provides a fast and inexpensive method for genotoxic monitoring. Due to the classification to different groups by eye, no special imaging software is required. The different classification groups are not weighted equally, due to the fact that they do not represent equal grades of damage. Moreover, the technique becomes more sensitive, because many cells can be scored in a short time (1000 cells instead of 50-100 cells with image analysing). The subsequent calculation of a "Comet tailfactor" allows quantifying DNA damage as a single figure, which makes it easier to compare results. Due to the scoring of 1000 cells in one experiment, which are tenfold the cells processed with image analysing, standard deviations are very low. Reproducibility has been thoroughly checked. Results expressed as "Comet tailfactors" were calculated according to Diem et al. (2002). All experiments were performed in duplicate by the same investigator.

2.2.4 Micronucleus assay

Micronucleus (MN) assay was performed according to Fenech and Morley (1985) and Fenech (1993). Fifty thousand cells were seeded into slide flasks (Nunc, Roskilde, Denmark) and exposed to ELF-EMF. In order to block cytokinesis, cytochalasin B (3 µg/ml, Sigma, St. Louis, USA) was added four hours before the first round of replication. After termination of the culture, fibroblasts were treated with hypotonic KCl solution (0.075 M, 30 min.) and fixed with a mixture of methanol : aqua bidest. (7:3) for 10 min. Slides were air-dried and stained with 4,6-diamidino-2-phenylindole (DAPI, Sigma, St. Louis, USA) for 3 minutes. MNs were visualised under a fluorescence microscope and 2000 binucleated cells were scored according to criteria published by Lasne et al. (1984). The results are expressed as MN events/500 binucleated cells.

2.2.5 Chromosomal aberrations

For evaluation of chromosomal aberrations 2 x 10^5 cells were seeded into 35 mm petri dishes (Nunc, Roskilde, Denmark) and exposed to EMF at conditions producing maximum effects in the Comet assay.

After EMF exposure, fibroblasts were trapped at metaphase by incubation with colcemid (0.2 µg/ml, Invitrogen Corporation, Paisely, Scotland) for the last 4h prior to harvesting. Subsequently, the cells were detached with trypsin (Invitrogen Corporation, Paisely, Scotland) and subjected to a hypotonic treatment (0.075 M KCl, 37°C, 30 min.). Thereafter, cold fixative (methanol : acetic acid 3 : 1) was slowly added and cells were collected by centrifugation. Fixation procedure was repeated twice. Finally, the cells were resuspended in 0.5 ml of fixative, dropped on clean slides, air dried, stained for 12 minutes with 4% GIEMSA, prepared in Sorensen's buffer (38 mM KH_2PO_4, 60 mM Na_2HPO_4 x 12 H_2O, pH=7) and rinsed with aqua bidest. Chromosomal aberrations were evaluated in 10,000 well-spread and complete (46 chromosomes) metaphases (5,000 ELF-exposed, 5,000 sham-exposed). The identification of chromosome aberrations was carried out following the criteria recommended by the WHO (1985). Different types of aberrations (chromosome gaps, chromosome breaks, ring chromosomes, dicentric chromosomes and acentric fragments) were scored separately. Five independent experiments were performed. Results are expressed as percent chromosomal aberrations per cell.

2.2.6 Fluorescence *in situ* hybridisation (FISH)

For evaluation of stable translocations, cells were seeded into 35 mm petri dishes at cell density of 2 x 10^5/3ml. After ELF-EMF exposure and an additional repair time of one replication round, fibroblasts were trapped at metaphase by incubation with colcemid (0.2 µg/ml, Invitrogen Corporation, Paisely, Scotland) for the last 4h prior to harvesting. Subsequently, the cells were detached with trypsin (Invitrogen Corporation, Paisely, Scotland) and subjected to a hypotonic treatment (0.075 M KCl, 37°C, 30 min.). Thereafter, cold fixative (methanol : acetic acid 3 : 1) was slowly added and cells were collected by centrifugation. Fixation procedure was repeated twice. Finally, the cells were resuspended in 0.5 ml of fixative, dropped on clean slides and air-dried. Subsequently, slides were denatured (70% formamide/2×SSC pH 7, 72°C, 2 min) and immediately dehydrated through a cold (-20°C) ethanol series (70%, 80%, 90%). The rhodamine-labelled whole chromosome probes (chromosome 1-22, X, Y) were prepared according to the recommendation of the manufacturer (Appligene Oncor Q-biogene, Illkirch, France). Aliquots of 30 µl were applied to the metaphase preparations, the slides were covered with a cover slip and incubated overnight in a moist chamber at 37°C. The following day, slides were immersed in 0.5×SSC at 72°C for 5 min, transferred to 1×PBD at room temperature for 2 min and counterstained with DAPI (4,6-diamidino-2-phenylindole, 0.02 µg/ml, Sigma, St. Louis, USA). Fluorescence signals were evaluated using a fluorescence microscope equipped with filters capable of simultaneously passing DAPI/Rhodamine. 1,000 well spread and complete (46 chromosomes) metaphases were scored for translocations for each labelled chromosome.

2.2.7 Changes in mitochondrial membrane potential (JC-1 staining)

Changes in the mitochondrial membrane potential ($\Delta\Psi_m$) upon ELF-EMF exposure were assessed by staining mitochondria with 5,5',6,6'-tetrachloro-1,1',3,3'-tetraethyl-benzimidazolcarbo-cyanine iodide (JC-1, Molecular Probes, Leiden, The Netherlands), a fluorescent dye with high sensitivity to $\Delta\Psi_m$ in intact cells (Cossarizza et al. 1993b; Salvioli et al. 1997). This lipophilic cation forms J-aggregates in the matrix of intact mitochondria (emitting at 590 nm) or is released in a monomeric form (527 nm) from depolarised mitochondria. A good correlation between the J-aggregate fluorescence of JC-1 and $\Delta\Psi_m$ has been reported previously (Smiley et al. 1991). Immediately after exposure to ELF-EMF (50 Hz, 1 mT, 15h, intermittent 5 min on/10 min off) or RF-EMF (GSM basic 1950 MHz, SAR=1 W/kg, 15h, intermittent 5 min on/10 min off), cells were trypsinated, centrifuged (700 g, 5 min) and resuspended in medium (RPMI 1640 with 10% fetal calf serum). Subsequently, the cells were incubated in triplicates at a density of 0.45 x 10^6 cells/ml in complete medium for 15 min at 37°C in the dark with 10 µg/ml JC-1. After incubation with JC-1 the fibroblasts were washed twice with phosphate buffered saline (Gibco, Vienna, Austria) and adjusted to 2.15 x 10^5 cells/ml. From each of the three stained samples per ELF-EMF exposure and sham exposure, respectively, 8 x 250 µl cell suspension have been transferred to a 96 well sample plate. Measurement of red fluorescence (excitation 540 nm, emission 590 nm) and green fluorescence (excitation 485 nm, emission 535 nm) was done on a Wallac Victor 2 fluorescence plate reader (EG&G Wallac, Turku, Finland). Results were expressed as ratios of red/green fluorescence. For positive controls cell cultures were treated for 18h with 20 µM camptothecin (Sigma-Aldrich, Vienna, Austria), a well known inducer of apoptosis.

2.2.8 Statistical analysis

Statistical analysis was performed with STATISTICA V. 5.0 package (Statsoft, Inc., Tulsa, USA) and SPSS 10.0 package (SPSS Inc., Illinois, USA). All data are presented as mean ± standard deviation (SD). The differences between exposed and sham-exposed, as well as between different exposure conditions were tested for significance using independent Student's t-test or one-factorial ANOVA with post hoc Student´s t-test Bonferroni-correction. A difference at $p<0.05$ was considered statistically significant. Correlation was assessed by multiple regression analysis using linear regression.

2.3 Experiments with human HL-60 cells (Participant 2)

2.3.1 RF-EMF exposure setup

See 2.1.2

2.3.2 Cell culture and exposure conditions

Human HL-60 cells (ATCC, Rockville, MD, USA) were cultured in RPMI 1640 medium supplemented with 10% fetal calf serum (Promocell, Heidelberg, Germany), 1% L-glutamine, 1% HEPES buffer and 2% penicillin/ streptomycin (Gibco BRL Life Technologies, Rockville, MD, USA) under temperature- and pH-control conditions. The cell line was maintained in logarithmic growth phase at 37°C in a 5% CO_2 atmosphere. For radio-frequency (RF) exposure experiments the initial seeding density per 35 mm petri dish was 7.5×10^5 cells. In addition to sham-exposed cells, cells incubated under these normal cell culture conditions without the waveguides being connected to the generator system (see below) were examined as incubator controls. In positive control cells DNA breakage was induced either by incubation of cells for 60 min in cell culture medium containing hydrogen peroxide at a final concentration of 100 µmol/l or by 6 MeV γ-irradiation (0.5 Gy, exposure time: 5.2 s). In case of assessing indirectly the generation of reactive oxygen species and directly the modulation of detoxifying capacities of HL-60 cells, culture medium was supplemented with ascorbic acid (10 µmol/l) prior to RF-exposure.

The following exposure conditions were examined with respect to direct and indirect genotoxic effects in HL-60 cells using the alkaline Comet assay, the cytokinesis-block micronucleus assay, the flow cytometric measurement of micronuclei induction and DNA alterations, cytotoxicity testing, assessment of cell viability and cell growth:

- 1800 MHz, continuous wave (C.W.) exposure, 24 hours, SAR=0.2 W/kg, 1.0 W/kg, 1.3 W/kg, 1.6 W/kg, 2.0 W/kg and 3.0 W/kg, compared with the corresponding sham exposed cells, incubator control cells and positive controls.
- At 1800 MHz, SAR 1.3 W/kg, C.W., different periods of exposure, ranging from 2h up to 72h exposure.
- 1800 MHz, SAR of 1.3 W/kg different RF-signals: C.W., 5 min on/10 min off; GSM-217Hz; GSM-Talk were examined.
- 1800 MHz, GSM-DTX, 24 hours, 5 min on/5 min off, SAR 1.0 W/kg, compared with the corresponding sham exposed cells, for gene expression profiling studies.
- 1800 MHz, C.W., 24 hours, SAR1.3 W/kg, compared with the corresponding sham exposed cells and incubator controls for gene expression profiling studies.

Cells were exposed or were sham-exposed in waveguides connected with a RF-generator system in a Heraeus incubator (Model Hera Cell). After each run the cells were immediately taken out of the incubator for subsequent analyses unless otherwise stated. Experiments were performed under blinded conditions in the following way: after the cells were placed in the two waveguides, and the incubator chamber was closed, the selection which of the two waveguides was connected to the RF generator and which remained disconnected, i.e. served as a sham control, was controlled by the computer system provided by Participant 10 and remained concealed to the experimentalists until analyses by the Comet assay and the micronucleus assay were completed and results documented. For decoding which of the two waveguides was connected to the RF-generator or remained disconnected, respectively, and for control of

the experimental conditions of each run, technical data were mailed independently to Participant 10 and returned electronically with electronic documentation of the time points of dispatching and return. Temperature within the waveguides was monitored during each run for as well sham-exposed and RF-field exposed cells and documented electronically. Additionally, at the end of the experiment pH values were controlled within the cell culture medium of sham-exposed, RF-field exposed and control cells.

An independent experiment consisted of 6 exposed and 6 sham-exposed petri dishes (35 mm diameter) with an initial seeding density of 7.5 x 10^5 cells per petri dish. In order to rule out potential differences of the six positions within the waveguide, the cells from the six exposed petri dishes and of the six sham-exposed dishes, respectively, were pooled prior to further analysis. Differences between exposed cells and corresponding controls were tested for significance, employing the Student´s t-test at a level of $p \leq 0.05$.

2.3.3 *in vitro* genotoxicity tests

The cytokinesis-block in vitro micronucleus (MN) assay

The MN assay was carried out as described by Natarajan and Darroudi (1991) according to the guidelines developed by Fenech (1993, 2000), Fenech and Morley (1985, 1986), Fenech and Rinaldi (1995), Fenech et al. (1994) and Garriott et al. (2002). In order to evaluate the frequency of MN in binucleated (BN) human HL-60 cells, cytochalasin B (final concentration 3.0 µg/ml) was added to the growth medium after exposure and washing. Cytochalasin B prevents the cells from completing cytokinesis resulting in the formation of multinucleated cells (Fenech and Morley 1985). The cells were fixed after 24 hours. For fixation the cells were washed and treated with cold hypertonic KCl solution (5.6 g/l). Then the cells were fixed 3 times with a solution of acetic acid/methanol (1:3) and subsequently air dried preparations were made. For the detection of MN in binucleated cells (BNC) the slides were stained with 2.0% Giemsa solution. To determine the frequency of MN of RF-exposed, sham-exposed or control cultures the number of MN in 1000 BNC cells were scored microscopically at 400 fold magnification by one person in 2 slides for each experimental point. All particles about the size smaller than one-third that of the main nuclei, round-shaped with similar staining characteristics as the main nuclei were counted as micronuclei. In particular after high doses of γ-irradiation (2 and 3 Gy, respectively), it was sometimes difficult to distinguish between "true" micronuclei and apoptotic bodies that occurred also in BN cells. Experiments were repeated at least three times independently.

To study the effects of RF-EMF on cell division, the number of BNC relative to the number of mono-, bi-, tri- and tetranucleated cells (% BNC) was determined according to Fenech (2000). Furthermore, apoptotic cells can be recognised by a characteristic pattern of morphological changes, which may be broadly defined as cell shrinkage, cell shape change, condensation of cytoplasm, nuclear envelope changes, nuclear fragmentation and loss of cell surface structures.

Alkaline single cell gel electrophoresis assay (SCGE, Comet assay)

The alkaline SCGE assay was carried out as described by Singh et al. (1988) according to the guidelines developed by Tice et al. (1990, 2000), Fairbairn et al. (1995) and Klaude et al. (1996). After exposure and washing, a single cell suspension of 1 x 10^4 cells was mixed with 100 µl of 0.7% LMP agarose in PBS and transferred to the fully frosted slides precoated first with 1% and then with 0.5% NMP agarose in PBS. Finally, a covering layer (0.7% LMP agarose) was transferred to the slide. All procedures were performed under dimmed light. Subsequently, the slides were covered with a coverslip and allowed to solidify in the refrigerator. Then the coverslips were removed and the slides were immersed for 1 hour at 4°C in lysing solution (2.5 M NaCl, 100 mM Na_2EDTA, 10 mM Tris, pH 10) containing 1% Triton-X 100 and 10% DMSO added just before use. Thereafter, the slides were exposed to 0.3 M NaOH for 20 min to allow the DNA to unwind. After this, the slides were placed in a horizontal gel electrophoresis tank containing freshly prepared cold electrophoresis buffer (1 mM Na_2EDTA and 300 mM NaOH, pH 13.5) following electrophoresis at 0.8 V/cm (25 V, 300 mA) for 20 min. After electrophoresis, the slides were rinsed 2x with 400 mM Tris, pH 7.5 and were stained with 80 µl ethidium bromide (0.02% in water), covered with a coverslip. To prevent additional DNA damage all steps described above were conducted under dimmed light or in the dark. 50 randomly chosen cells per slide (two slides per culture) were analysed using a 400-fold magnification with a Zeiss fluorescence microscope (Zeiss Axioplan). A computerized image analysis system (Kinetic Imaging 4.0, Optilas, München, Germany) was employed to measure different Comet parameters. As a measure of DNA damage tail length (in µm), Tail Extent Moment, Olive Tail Moment (OTM) and % of DNA in tail were automatically calculated. To determine

DNA migration of exposed, sham-exposed or control cultures, 100 cells were scored microscopically for Comet formation on 2 slides for each experimental point. As a positive control hydrogen peroxide at a final concentration of 100 µmol/l for 1h was used. Experiments were repeated at least three times independently. The results reported are the mean values ± standard deviation (SD).

Positive control through Gamma-Irradiation

Irradiation was administered with 6 MeV X-rays on an linear accelerator to the HL-60 cells (0.75×10^6) in dishes at doses of 0.5, 1.0, 2.0 and 3.0 Gy (dose rate: 5.8 Gy/min). A control dish received no irradiation. Then, both irradiated and non-irradiated samples were returned to the incubator and cultured until analyses at each relevant point were performed.

Viability test

Viability of the cell samples was assessed using the trypan blue exclusion test. The percentages of viable cells were then determined by placing aliquots of the treated cells in a Neubauer chamber and scoring cells for either the absence (viable cells) or the presence (dead cells) of blue staining. Only cultures with a viability more than 90% were analysed.

2.3.4 *in vitro* cytotoxicity testing

In order to exclude in vitro cytotoxic effects different approaches were used to verify cell viability, including trypan blue staining, flow cytometry tests, by which cells with reduced viability are marked by nuclear propidium iodide and the MTT assay, a colorimetric assay, that is based on the ability of viable, i.e. metabolically active cells to cleave tetrazolium salts to form formazan dye.

Cell viability and cell cytotoxicity were assessed by using the MTT assay. MTT is a sensitive first indicator of mitochondrial damage induced by oxidative stressors (Wasserman and Twentyman 1988). To analyse HL-60 cell proliferation, the MTT assay (Cell Proliferation Kit I, Roche, Mannheim, Germany) was used according to the manufacturer's protocol, and the data reported as OD units. This assay is very sensitive for the measurement of cell proliferation based upon the reduction of the tetrazolium salt 3,[4,5-dimethylthiazol-2-yl]-2,5-diphenyltetrazolium bromide (MTT).

Briefly, around 2×10^3 cells per well were plated in 96-well microtiter plates with 100 µl of medium. 10 µl of a MTT (5 mg/ml) solution (Roche, Mannheim) was added. Incubation occurred for 4h at 37°C. 100 µl of solubilisation solution was added to each well. The plate was allowed to stand overnight in the incubator (37°C, humidified atmosphere). Absorbance was measured at 570 nm. Performing analysis on micronuclei induction, the ratio of BNC against mono-, bi-, tri- and tetranucleated cells is determined, giving a measure of cell division and cell cycle progression. Performing the flow cytometric analysis of micronuclei induction, an assessment of cell viability and also of DNA distribution and therefore of cell cycle alterations become feasible.

2.3.5 Preparation of nuclei suspensions from cells for flow cytometry analysis

The method was performed according to Nüsse and Kramer (1984), Nüsse and Marx (1997) and Wessel and Nüsse (1995). After exposure of cells and subsequent incubation for 24h (recovery time) the medium was removed and cells were washed twice with PBS and counted. Cells were then spun at 100 x g for 5 min at room temperature. Supernatants were removed carefully, the remaining cell pellet was re-suspended by gently shaking. FACS solution I (10 mM NaCl, 3 mM sodium citrate, 10 mg/l RNase A, 3 ml/l of 10% Igepal solution in water, 25 µg/l ethidium bromide freshly prepared before use) was added to the cell pellet and cells were suspended to a density of approximately 1×10^6 cells per ml. The suspension was stirred for 2 sec and was kept for 30-60 min at room temperature in the dark. After adding FACS solution II (70 mM citric acid, 250 mM sucrose, 40 mg/l of ethidium bromide) the suspension was stirred for 2 sec and subjected to FACS analysis.

2.3.6 Flow cytometric exclusion of apoptosis via Annexin V assay and TUNEL assay

Annexin V assay

After exposure to RF-EMF 10^7 cells were centrifuged, washed several times with PBS and the pellet was resuspended with Annexin V binding buffer (Becton Dickinson Biosciences, Heidelberg, Germany), 1 ml of this suspension was incubated for 20 min in the dark in the presence of 100 µl Annexin V binding buffer and 3 µl Annexin V FITC (Becton Dickinson Biosciences, Heidelberg, Germany). After washing with Annexin V binding buffer, cells were resuspended in 300 µl Annexin V binding buffer + 5 µl Propidium Iodide (PI) solution (50 µg/ml) and were analysed by flow cytometry using a FACSCalibur Analytic Flow Cytometer (Becton Dickinson Biosciences, Heidelberg, Germany).

TUNEL assay

After exposure to RF-EMF 10^7 cells were centrifuged, washed several times with PBS and then fixed for 1h by PBS/formaldehyde (4%). Then the cells were washed again, resuspended with PBS and permeabilised with 100 µl Triton X solution (0.01% Triton in 0.1% sodium citrate solution) for 2 minutes, followed by labelling with 50 µl TUNEL reaction mixture (Roche, Mannheim) for 1 h at 37°C. After this incubation the cells were washed and resuspended with 500 µl PBS. The cells then underwent flow cytometric analysis in order to determine the number of green stains (representing apoptotic DNA fragmentation). DNA content analysis was performed on a Becton Dickinson FACScan according to the manufacturer's protocol.

2.3.7 Reactive oxygen species (ROS) and antioxidant enzyme activity

Reactive oxygen species (ROS), including superoxide anion (O_2^-), hydrogen peroxide (H_2O_2), hydroxyl free radical (OH^-) and singlet oxygen ($^1O_2$) have powerful oxidative potential. ROS are capable of attacking lipids, nuclear acids and proteins, resulting in certain degree of oxidative damage. The cell possesses an efficient antioxidant defence system, mainly composed of antioxidative enzymes such as superoxide dismutase, and glutathione peroxidase. These enzymes are able to scavenge excessive ROS to cellular metabolism, and thereby lead to a relative stabilisation of the ROS level under physiological conditions. To evaluate the ROS level differences in RF-exposed and sham-exposed HL-60 cells the Nitric Oxide Assay, the oxyDNA assay, the direct detection by flow cytometry using the fluorescent dye Dihydrorhodamine 123 and the Lipid Peroxidation Assay were used. For measuring the antioxidative enzyme capacity the activities of superoxide dismutase and glutathione peroxidase were evaluated. The tests mentioned above were chosen within a first screening approach in order to assess qualitatively gross changes in ROS levels and antioxidative enzyme activities. All analyses were performed at room temperature unless otherwise stated.

Nitric oxide (NOx)

Nitric oxide (NOx) was measured using the colorimetric Nitric Oxide Assay Kit from Calbiochem (Cat. No. 482650, Calbiochem-Novabiochem GmbH, Bad Soden, Germany). Briefly, nitrate in aqueous solutions (supernatant after centrifugation of 7 x 10^5 cells/ml) was reduced to nitrite by enzymatic conversion by nitrate reductase and was estimated spectrophotometrically at 540 nm using the Griess reaction. The absorbance obtained is compared against a standard curve of known concentrations of NOx (1-25 µmol/l) and the results were expressed as µmol/l NOx. Detection limit is <1 µmol/l for NOx (Miles et al. 1996).

oxy DNA

Oxidative DNA damage, with 8-oxoguanine as the major oxidative DNA product, was measured using the fluorogenic OxyDNA Assay Kit from Calbiochem (Cat. No. 500095, Calbiochem-Novabiochem GmbH, Bad Soden, Germany). The assay utilizes a direct fluorescent probe directly binding to the DNA adduct of 8-oxoguanine (de Zwart et al. 1999, Kasai 1997, Cooke 1996). Briefly, cells (1 x 10^6) were washed first in 1× PBS, then in wash solution, and then by the addition of 100 µl blocking solution with a 1-hour incubation at 37°C. After 2 washes in working solution, cells were incubated with 100 µl FITC conjugate for 1 hour in the dark at room temperature before they were washed twice in washing solution and once in PBS. The FITC labelled protein conjugate binds to the 8-oxoguanine moiety present in the 8-oxoguanosine of oxidized DNA. Finally, cells were resuspended in FACS buffer and were analysed by flow cytometry (FACScan, Becton Dickinson). The presence of oxidized DNA is indicated by a

green/yellow fluorescence. A partial augmentation (shoulder at the right side of the signal) of FL-1 fluorescence intensity indicates an increase in level of oxidative DNA damage, i.e. 8-oxoguanine. In the present study, assays for the screening of oxidative DNA damage were performed after exposure to RF-field (1800 MHz, continuous wave, SAR 1.3 W/kg, 24h) or sham-exposed cells. Oxidatively damaged DNA was quantified by determination of the area under the curve (AUC) of the shoulder at the right side of the signal fluorescence intensity in RF-field exposed cells.

Detection of ROS level with Dihydrorhodamine 123

7.5 x 10^5 cells were incubated with 5 µmol/l dihydrorhodamine123 (DHR123, Sigma, Germany), as a ROS capture (Lopez-Ongil et al. 1998), during sham- or RF-exposure for 24h. Additionally, positive controls were run, in which 100 µmol/l of hydrogen peroxide (H_2O_2) was added for 1h prior to the end of the experiment. Intracellularly, DHR123 is oxidized by ROS to form the fluorescent compound rhodamine123 (Rh123), which is pumped into mitochondria and remains there. After the experiment, cells were harvested, washed with PBS and immediately analysed for Rh123 fluorescence intensity by flow cytometry (FACScan, Becton Dickinson). The percentage of oxidative damage was defined as the percentage of gated HL-60 cells with Rh123 fluorescence. The results presented represent the means of three independent experiments.

Lipid Peroxidation Assay

Lipid Peroxidation was measured using the colorimetric Lipid Peroxidation Assay Kit from Calbiochem (Cat. No. 437634, Calbiochem-Novabiochem GmbH, Bad Soden, Germany). Malondialdehyde (MDA) and 4-hydroxy-2(E)-nonenal (4-HNE), products of lipid peroxidation, can be estimated spectro-photometrically at 586 nm after reaction with a chromogenic reagent at 45°C to obtain an index for lipid peroxidation (Melchiorri et al. 1995, Öllinger and Brunmark 1994, Sewerynek et al. 1995).

Briefly, 3 x 10^6 cells were used per assay. The cells were lysed by repetitive freezing/thawing in 1000 µl distilled water. The cellular membranes were not removed until after the incubation with reagent R1 and R2. The samples were centrifuged at 15.000 x g for 10 minutes to clarify the homogenate supernatant. Immediately prior to reading the absorbance at 586 nm, 200 µl of sample solution, 650 µl of diluted reagent R1 and 150 µl of diluted reagent R2 were mixed to a volume of 1000 µl. A least-square linear regression demonstrates that the standard curve (concentration range 0-20 µmol/l) is a linear function of the concentration of either MDA or 4-HNE. The absorbance values obtained were compared against a standard curve of known concentrations of MDA/4-HNE (1-20 µM). The results were reported as µmol (MDA + 4-HNE)/l. Detection limit is 0.1 µmol/l for (MDA + 4-HNE).

To screen the possible effect of RF-EMF on endogenous antioxidant enzyme activity, the activities of superoxide dismutase (SOD) and glutathione peroxidase (GPX) were determined in HL-60 cells that exposed to RF-EMF (1800 MHz, continuous wave at SAR 1.3 W/kg for 24h) or sham-exposed

Superoxide dismutase (SOD) activity

Superoxide dismutase (SOD) activity of cell homogenates was determined using the Superoxide Dismutase Assay Kit from Calbiochem (Cat. No. 574600, Calbiochem-Novabiochem GmbH, Bad Soden, Germany). Briefly, 4 x 10^6 cells were washed with PBS buffer, diluted in 250 µl of PBS buffer and extracted with 400 µl of a chloroform/ethanol mixture (62.5/35.5 v/v). 40 µl of the aqueous layer of this sample extract was mixed with 30 µl of diluted chromogenic reagent (R1) and 30 µl reagent R2 in 900 µl of an aqueous alkaline solution buffer. The SOD-mediated increase in the rate of auto-oxidation of this reaction mixture was utilised to yield a chromophore with maximum absorbance at 525 nm (Wang et al. 1991, Vilim and Wilhelm 1989). Results were expressed as SOD units. Detection limit for SOD activity is 0.2 U/ml.

Glutathione peroxidase (GPx) activity

Glutathione peroxidase (GPx) activity of cell homogenates was determined using a cellular glutathione peroxidase assay Kit from Calbiochem (Cat. No. 354104, Calbiochem-Novabiochem GmbH, Bad Soden, Germany). Briefly, to assay cellular glutathione peroxidase, 70 µl of cell homogenisate of 1 x 10^6 cells is added to a 1050 µl of a solution containing glutathione (GSH, 1 mmol/l), as a source of reducing equivalents, GSH reductase (0.4 U/ml) and NADPH. The reaction is initiated by the addition of 350 µl of the diluted organic peroxide t-butyl hydroperoxide and the absorbance at 340 nm was recorded over a period of 5 minutes. The rate of decrease in the absorbance (NADPH is converted to NADP) is directly proportional to the GPx activity in the cell homogenisate. Therefore, the difference in absorbance per min

was used to calculate the enzyme activity and results were expressed as GPx units/ mg protein. As a positive control cellular glutathione peroxidase at an activity of 288 mU/ml was assayed at 23°C.

2.3.8 Analysis of cellular growth behaviour

Cellular doubling time

Cellular growth behaviour of HL-60 cells following RF-exposure for 24h (1800 MHz, continuous wave, SAR 1.3 W/kg) with respect to growth velocity as compared to sham and incubator controls was assessed by determination of the cellular doubling time td:

$$\mathrm{td} = \frac{\log 2 \cdot dt}{\log N - \log No}$$

with *dt* = time of exposure with RF field or sham-exposure, *No* = number of cells at the beginning of the experiment and *N* = number of cells at the end of experiment.

Thymidine kinase (TK) assay

Thymidine kinase activities were determined by radioenzyme assay Prolifigen® TK-REA (AB Sangtec Medical, Bromma, Sweden) with ^{125}I-deoxyuridinemonophosphate as substrate. Briefly, assay buffer containing ^{125}I-labelled substrate was added to the HL-60 cell lysate (lysate diluted 1:100) and incubated for 4h. Lysis was performed with 5 x 10^4 cells and a NP40/Tween 20 containing lysis buffer. The reaction was stopped by addition of a separator tablet which binds the phosphorylated product. After washing, radioactivity was measured. The level of radioactivity is directly proportional to the enzyme activity in the original sample. The TK value was calculated from the standard curve and expressed as U/l.

2.3.9 Statistics

To compare the results of the different groups listed above, the Student´s t-test (two-sided test) was used.

2.3.10 Proteomics

Different optimisation strategies for enhancement of 2-dimensional resolution of highly complex cellular protein mixtures were performed during the project. First of all we started with the IPG-strip approach/Pharmacia. Alternatively we also tested the tube gel approach and found, that for our system this proofed to be the most suitable one with the best resolution. This is essential for the following identification steps. Therefore we here focus on the description of the tube gel technology. In general, the methodology for two-dimensional electrophoresis of protein mixtures described by Klose and Kobalz (1995), was performed. Alternatively, a protocol with slight modifications was applied, described below.

IEF-sample preparation

For separation of cellular proteins by 2-dimensional gel electrophoresis cells were lysed after thorough washing with PBS by repeated freezing and thawing. Proteins were solubilised in: 56 mg urea lyophilised with 16.8 µl 0.6 M DTE, 41 µl protein (corresponds to 250 µg of protein)/water, 5 µl Ampholyte 9-11, 8 µl 25% CHAPS, mixed for 30 minutes at room temperature, centrifuged 6 minutes at 14000 g, then the supernatant was taken off as sample.

IEF/2-D PAGE

High resolution 2-dimensional SDS-polyacrylamide gel electrophoresis (2-D PAGE, 23 x 30 cm gels, pI 2-9.5; 14 x 16 cm gels alternatively, pI 2-11) was performed as follows. For the isoelectric focussing of the small gels a pH-gradient extending from pH 2 to pH 11 was generated by means of carrier ampholytes. For the 14x16 cm 2D-gels six 13 cm long and 2.2 mm thick isoelectric focusing gels were prepared with 3.3 g urea, 780 µl acrylamide / N,N'-methylene-bis-acrylamide (30% T, 5.4% C), 480 µl 25% CHAPS, 1.92 ml water and 300 µl ampholyte mix. The ampholyte mix, which can be stored at -20°C, consisted of 340 µl servalytes 5-7, 340 µl ampholines, 113 µl servalytes 3-10, 113 µl servalytes 2-11 and 113 µl servalytes 3.5-10. The IEF-samples were loaded on the tube gel, overlaid with 10 µl sample overlay (12 M urea, 8% w/v CHAPS, 4% ampholyte 9-11, 0.16 M DTE) and with the upper chamber

buffer consisting of a sodium hydroxide solution (20 ml 1N NaOH in 980 ml water). The lower chamber buffer contained 0.6 ml 85% phosphoric acid in 900 ml water. Gels were run in a tube gel apparatus at room temperature. The samples are focused for 9000 Vh. After extrusion gels were equilibrated for 5 minutes in SDS equilibration buffer (10% v/v 0.5 M Tris HCl pH 6.8, 5% v/v 20 mM EDTA 2Na, 20% of a 10% SDS solution, before usage 1.54% w/v DTE was added) and then loaded onto the 14 x 16 cm second dimension vertical slab gel. This gel consisted of a 12.5% SDS separation gel (7.5 ml 2M Tris HCl pH 8.8, 0.4 ml 10% SDS, 1.9 ml 20 mM EDTA 2Na, 12.7 ml water, 15.1 ml of an acrylamide/bisacrylamide solution (30% T, 2.67% C), 12.7 ml water; polymerisation with 20 µl TEMED and 200 µl of a 10% ammonium persulfate solution) and a stacking gel (2 ml Tris HCl pH 6.8, 80 µl 10% SDS, 400 µl 20 mM EDTA 2 Na, 1.1 ml of an acrylamide/bisacrylamide solution (30% T, 2.67% C), polymerised with 8 µl TEMED and 80 µl of a 10% ammonium persulfate solution). The lower chamber buffer for the second dimension consisted of 400 ml Tris/glycine 10x stock solution, 40 ml 10% SDS, diluted to 4000 ml with water, the upper chamber buffer consists of 50 ml Tris/glycine 10x stock solution, 5 ml 10% SDS, diluted to 500 ml with water, 230 mg DTE and 50 µl 0.5% BPB. The isoelectric focussing gel was layered on top of the SDS stacking gel and overlaid with top chamber buffer. Each gel was run for approximately 4 h beginning with 20 mA, 30 mA within the stacking gel and finally 50 mA in the separation gel. After finishing electrophoresis the gels were fixed in 40% ethanol/10% glacial acetic acid overnight, then silver stained according to the method applied by Klose and Kobalz (1995) and then dried.

Two-dimensional polyacrylamide gels were first qualitatively analysed on a light box visually. Clear changes in the protein secretion pattern like newly expressed or disappearing proteins can be detected by this means. The human eye is capable of registering even very small variations like an increasing or decreasing secretion of a characteristic protein, whereas a quantitative analysis of changes protein secretion is not possible. Protein spots of the 2-D gels were displayed by standard staining procedures with silver for image analysis. The corresponding gels were digitised. The spots were detected and the master gel image was calibrated. Image analysis was performed with Proteom Weaver (Definiens, München, Germany). Known proteins serve as "landmark proteins". With the help of their isoelectric points and molecular weights an internal two-dimensional co-ordinate system can be generated. In this system an evaluation of the isoelectric point and molecular weight of any protein of interest together with the determination of its amount expressed in the sample is possible. Qualitative and quantitative analysis of single gels and a direct gel-to-gel comparison was performed by this method.

2.3.11 Gene expression profiling

In an approach to examine effects of RF-EMF on gene expression on the transcriptional level (transcriptome), changes of cellular RNA profiles were analysed by use of the array technology in collaboration with the Resource Center of the German Human Genome Project (Participant 12). Methodological details and detailed presentations of the results obtained together with Participant 12 are provided under 2.10.3 and 2.10.4.

2.4. Experiments with the human neuroblastoma cell line NB69 (Participant 5)

2.4.1 ELF-EMF exposure setup

50 Hz, sine wave magnetic fields (MF) at 10 µT, 100 µT or 2000 μT_{rms} were generated by a pair of coils in a Helmholtz configuration energised by a wave generator Newtronic Model 200MSTPC, (Madrid, Spain). The exposure setup used in these experiments was reproduced from that described by Blackman et al., (1993). Each exposure system consisted of two 1000-turn, 20-cm-diameter coils of enamelled wire, aligned coaxially 10 cm apart and oriented to produce vertically polarised magnetic fields. Cell culture dishes were placed in the uniform MF space within the coils for exposure or sham-exposure. Currents in the coils were adjusted and monitored using a multimeter (Hewlett Packard, model 974A, Loveland, CO) after the flux density was established with fluxgate magnetometers (Bartington, model MAG-3, GMW Assoc and Wandel and Goltermann S.A, EFA-3, Model BN 2245/90.20. Two pairs of coils were mounted

in the centre of magnetically shielded (co-netic alloy) boxes (Amuneal Corp., Philadelphia, PA) housed in incubators (Forma, Models 3121 and 3194) with a 5% CO, 37ºC. The magnetic shielding allowed for reduced environmental fields at the samples' locations. With DC MF = 0.02-0.08 μT and AC MF = 0.07 - 0.1 μT. Each incubator contained a coil system and shielding box, but only one set was energised for each experiment.

Two sets of coils, shielding rooms and incubators were used. In each experimental run, one set of coils was energised at random. The samples in the unenergised set were considered sham-exposed control. See also 2.1.1

2.4.2 RF-EMF exposure setup

See 2.1.2

2.4.3 Cell culture and EMF-Exposure

The human neuroblastoma cell line NB69 was obtained from Dr. M.A. Mena, (Hospital Ramón y Cajal, Madrid) and cultured in Dulbecco's Minimum Essential Medium (D-MEM) supplemented with 15% (ELF-EMF) or 10% (RF-EMF) heat inactivated foetal calf serum (FCS, Gibco), 2 mM L-Glutamine and 100 U/ml penicillin / 100 U/ml streptomycin. The cells were grown at 37ºC in a CO_2 incubator. In each experiment, cells were seeded at a density of 4.5 x 10^4 cells/ml in ∅ 60 mm plastic dishes. NB69 cells cultured in D-MEM were exposed and/or incubated in the presence or absence of retinoic acid (RA). In the experiments with RA, 40 dishes were supplemented with 0.0 μM (20 dishes) or 2.0 μM all trans RA (20 dishes) in absolute ethanol dissolved (1:1000) in culture medium. This vehicle was proven not to affect significantly cell growth when compared to cultures treated with the same volume of medium alone. In the RF-EMF experiment, cells were seeded at a density of 4.5 x 10^4 cells / ml in ∅ 35 mm dish (NUNC) in 12 dishes, supplemented with 0.0 ng/ml (6 dishes) or 20 ng/ml of bFGF (human recombinant, Boehringer Mannheim GmbH, 6 dishes). Immunocytochemical and *in situ* hybridisation studies were carried out 4 days post-plating.

Isolated embryonic neural stem cells

Striata from E15 Sprague-Dawley rat embryos were dissected and mechanically dissociated. Cell suspensions were grown in a defined medium (DF12), composed of Dulbecco's modified Eagle's medium and Ham's F-12 (1:1), 2 mM L-glutamine, 1 mM sodium piruvate (all from Gibco BRL, Life Technologies Inc, Grand Island, New York), 0.6% glucose,25 mg/ml insulin, 20 nM progesterone, 60 μM putrescine, and 30 nM sodium selenite (all from Sigma Chemical Co, St Louis, MO), 100 mg/ml human transferrin and 50 ng/ml human recombinant EGF (both from Boehringer Mannheim GmbH, Germany). After a minimum of five passages, cells were plated at a density of 500.000 cells/dish (Ø 35 mm) on 12 mm glass coverslips coated with 15 μg/ml poly-l-ornithine (immunocytochemistry) or 50 μg/ml poly-l-lysine (in situ hybridisation). The cultures were maintained in DF12 and EGF for 3 days and then switched to DF12 without EGF for longer culture periods. Immunocytochemical and in situ hybridisation studies were carried out at day 3 post-plating. For additional information see Reimers et al., (2001). Neural stem cells (NSCs) are self-renewable, multipotential cells capable of differentiating into the three major neural cell types. The mechanisms, involved in the regulation of NSC's differentiation are not fully understood.

Test for cellular response to retinol (ROL) or retinoic acid (RA)

Different concentrations of ROL and RA were selected within the physiological range in mammals: 0.1 μM to 5 μM. Cells were seeded and supplemented with ROL concentrations of 0.0, 0.1, 0.5, 1.0, 2.0, or 5.0 μM or with RA concentrations of 0.0, 0.5, 1.0, 2.0, or 5.0 μM. Seventy-two hours after plating, the medium was removed and replaced with fresh medium supplemented with the corresponding ROL or RA concentrations. Each of the retinoid concentrations was triple tested (a total of 15 petri dishes per experimental replicate), and a total of 3 experimental replicates were carried out. At the end of five days of incubation in the absence or presence of ROL or RA the cells were scrape-collected in 1 ml of culture medium. Aliquots of the cell suspensions received 1 ml of 0.4% Trypan Blue, and the number of total cells and of viable cells were calculated using a Neubauer chamber. Each sample was double counted.

ELF-EMF exposure conditions

In each experimental replicate 20 dishes with cells (10 with 0.0 µg/ml RA and 10 with 2.0 µg/ml RA) were incubated for three days inside pairs of unenergised Helmholtz coils placed in a shielded chamber, inside a 5% CO_2 incubator, at a 37ºC and 100% RH atmosphere. At the end of day 3 the media were renewed and 10 dishes (5 with 0.0 µg/ml RA and 5 with 2 µg/ml RA) were placed in one incubator; the remaining ten dishes (5 with 0.0 µg/ml RA and 5 with 2 µg/ml RA) were placed in an identical incubator. Both incubators were used, in a random sequence, alternatively for MF exposure and sham-exposure. The exposed group was treated intermittently, 3h on/3h off, to 50 Hz ELF-EMF at 10 or 100 µT magnetic flux densities (MFD) for 42h or 63 hours. At the end of this period the cells were checked for appropriate viability and proper inmunocytochemical characteristics before being processed for analysis of their responses to the physical and chemical treatments. Spectrophotometric analysis of total protein and DNA contents were done following the methods described in Mena et al., (1995). As we described below, cell counting by Trypan Blue exclusion, BrdU incorporation in DNA, PCNA labelling and flow cytometry were assayed in cells exposed to 10 or 100 µT as an estimation of the proliferative activity of NB69 cell line. The percent of apoptotic cells was estimated with TUNEL-labelling (TdT-mediated dUTP nick labelling) and the expression of the phosphorilated cyclic adenosine monophosphate response-element binding protein (p-CREB) was analysed using phosphorylation site-specific antibodies. Assays and analysis were performed blinded to treatment condition. The statistical test used was ANOVA followed by Student's T-test for unpaired data.

RF-EMF exposure condition

Neural stem cells (NSC) and NB69 cells grown on coverslips were exposed for 21 or 24 hours, respectively to 1800 GSM signals (Talk, Basic, CW and DTX signals), at 1-2 W/kg SAR), in 5 min On/10 min Off cycles. In the experiments with neural stem cells a total of 10 replicates were carried out. In each replicate a total of 12 dishes (with three coverslips per dish) were RF-EMF-exposed or sham-exposed, in groups of 6 samples. In the experiments with human neuroblastoma cells a total of 27 replicates were carried out. In each replicate a total of 12 dishes were exposed, in groups of 3 samples, to one of the following treatment combinations: untreated controls, bFGF alone, EMF alone, bFGF + EMF. The sham-exposure and the RF-EMF exposure were carried out inside shielded chambers (IT'IS Setup, Schuderer et al., 2001), in a 5% CO_2, 37ºC and 100% humidity atmosphere. At the end of the 21-h (NSC) or 24-h (NB69) period of RE-EMF exposure or sham-exposure the cell responses were checked for appropriate viability and proper inmunocytochemical characteristics before being processed for analysis of their responses to the physical and chemical treatments through Trypan Blue exclusion, immunocytochemical and in situ hybridisation studies.

Cell counting and cell viability

After treatment the cells were detached from culture dishes and resuspended in 1 ml of media. The cell number was determined in aliquots of 50 µl using a haemocytometer and each sample was double-counted by Trypan Blue exclusion. Doubling time (DT) of proliferating cells was calculated according to Falasca et al., (1999) using the formula DT = T2 - T1 / 3.32 log (X2 / X1), where T1 and T2 are the culture times in hours, and X1 and X2 are number of cells at the corresponding time. The ANOVA test followed by Student's T-test for unpaired data was used for statistical significance ($p < 0.05$).

2.4.4 Immunocytochemical characterisation of NB69 Cells

Cells were grown in Ø 60 mm dishes onto 12 mm-diameter round coverslips for immunocytochemical detection. After fixation with 4% (wt/vol) paraformaldehyde in 0.1 M phosphate buffer, the cells were incubated for 30 min in a blocking solution containing 2.5% (wt/vol) BSA in phosphate-buffered saline (PBS) to prevent non-specific antibody binding. The same solution was used to dilute the different antibodies. Cells were successively incubated with a mouse monoclonal antibody raised against the neuron-specific intermediate filament BIII-tubulin, and for the astrocyte-specific glial fibrillary acidic protein, GFAP), (1:1000, Promega; 1:300, Sigma, respectively). Nestin immunostaining was carried out by 1:5000 dilution of a rabbit antiserum, followed by an anti-rabbit IGL labelled with FITC (1:200; Jackson ImmunoResearch, West Grove, PA, USA).

2.4.5 Immunocytochemical characterisation of neural stem cells (NSC)

EGF-expanded neurospheres were seeded onto adherent substrate and treated with EGF during their first 3 days in culture, in order to enhance expansion of precursor cells. After this period the mitogen was withdrawn, and cells grew in a defined medium, which promoted cell differentiation to neurons, astrocytes and oligodendrocytes. Between 2h and 3 days, the cultures, mainly contained nestin-positive, undifferentiated precursors. At later stages, the total number of cells dropped, as a gradual loss of nestin content occurred, together with and an enhancement in the differentiation processes of neurons, oligodendrocytes and astrocytes.

2.4.6 Immunocytochemical staining for the Cell Nuclear Antigen (PCNA).

PCNA, the auxiliary component of DNA polimerase delta, is a proliferation-induced, 36 kD nuclear protein. The expression of PCNA in tissues has been found to be correlated with proliferative activity. In fact, it has been suggested (Kawasaki et al. 1995) that PCNA levels may reflect differences in the proliferative activity of neuroblastomas, as they evolve through different stages of the disease. However, PCNA is also necessary for nucleotide-excision repair of DNA. In the present work, we estimate PCNA positive cells in eight experiments with cells exposed to the MF at 10 μT on day 3 after plating. At the end of the 42-h exposure period, PCNA positive cells were determined by immunostaining, using PCNA-labelling and Hoechst for quantification of total number of cells. Cells were stained with 2 μg/ml Hoechst dye 33342 for 10 min at room temperature, studied and photographed with fluorescence microscope. In a total of 13 experiments the cells were exposed to the MF at 100 μT on day 3 after plating, and processed for PCNA labelling at the end of the 42 and 63-h exposure (day 5 and 6 postplating). The proportion of PCNA+ cells was quantified by counting 15 microscope fields per coverslip, in a total of 4 coverslips (two control and two exposed) per experimental replicate. All determinations were carried out following blind protocols.

2.4.7 5-bromo-2'-deoxyuridine (BrdU) labelling for identification of cells synthesising DNA.

Samples exposed to 100μT were labelled with BrdU at different times during the exposure period: Time 0 of exposure, (day 3 after plating); time 21h (day 4) or time 42h (day 5). The cells were always analysed 21 hours after the BrdU application, i.e. at 21, 42 or 63 hours of exposure. The results were compared to those in the respective controls (BrdU-treated, MF-unexposed). The analysis was performed through total cell number counting (Trypan Blue exclusion protocol) and by quantification of anti-BrdU antibody positive cells. The proportion of BrdU+ cells was quantified by counting 15 microscope fields per coverslip, in a total of 4 coverslips per experimental replicate. All determinations were carried out following blind protocols.

2.4.8 Flow cytometry assay

DNA content and cell cycle phase distribution were analysed by flow cytometry with propidium iodide DNA staining, in cells exposed to 100 μT for 42 or 63 hours (day 5 or 6 post-plating, N= 3 or 6 experiments, respectively, with two replicates per experimental condition). Cells were harvested, fixed with 70% ethanol and incubated with RNAse A (100 μg/ml) and the DNA intercalating dye propidium iodide (20 μg/l) in citrate buffer (3.4 mM). The cell cycle phase analysis was performed by flow cytometry using a Becton Dickinson FAC flow cytometer and Becton Dickinson CellQuest software. All determinations were carried out following blind protocols.

2.4.9 Apoptosis assay

In order to investigate the potential influence of 50 Hz MF on apoptosis the percent of apoptotic cells was estimated with TUNEL-labelling (TdT-mediated dUTP nick labelling) after 63 hours of exposure. Additional assays for apoptosis were carried out through flow cytometry in propidium iodide-stained neuroblastoma cells, exposed to the MF for 42 or 63 h (N= 7 experimental replicates).The distribution pattern of apoptotic nuclear DNA was determined using a Becton Dickinson FAC flow cytometer and Becton Dickinson CellQuest software. Three additional experiments were conducted and the cellular

response was analysed through TUNEL procedure. After fixation in 4% paraformaldehide, cells were washed with PBS, permeabilised with 0.1% Triton X-100 in 0.1% sodium citrate, washed again with PBS, and incubated for 60 min at 37ºC with biotin-conjugated dUTP in a TdT (terminal deonucleotidyl transferase, 25 U/ml) catalysed reaction (Roche Molecular Biochemicals) in a humidified atmosphere in the dark. The labelled nuclei (dUTP) were revealed with 3,3'-diaminobenzidine. The cells were counterstained with methyl green. *In situ* labelled nuclei were quantified by image analysis and photographed under light microscope. All determinations were carried out following blind protocols.

2.4.10 Immunocytochemical staining for the expression p-CREB

CREB is a nuclear transcription factor that regulates expression of genes controlling cell proliferation, differentiation, and survival. In fact, this protein is known to play an important role in neuronal survival and plasticity. Besides, different alterations of the CREB family of transcription factors have been observed in tumours. The cells were grown on coverslips. The MF-exposed samples (50 Hz; 100 μT, 30 or 60 minutes exposure) and their respective controls were labelled at the end of the exposure period for 30 min, 60 min, or 2 hours using phosphorylation site-specific antibodies. As positive controls, samples were treated with bFGF at a concentration known to activate p-CREB immunoreactivity in neuronal cells. The proportion of p-CREB cells was quantified by counting 15 microscope fields per coverslip, in a total of 4 coverslips per experimental replicate. All determinations were carried out following blind protocols. For analysis of Ser^{133}- phosphorilated CREB and total CREB, Western blotting was performed on 2 $x10^6$ cells per experimental point. Cell pellets were added at 4ºC with a lysis buffer containing 1% deoxycholate, 1 μg/ml aprotinin, 2 μg/ml leupectin, 1 mM phenylmethylsulfonyl fluoride, and 1mM sodium orthovanadate for 10 min. Cell lysates were sonicated and either immediately processed by Western or kept frozen until assayed. Protein concentration in the samples was estimated by the method of Lowry et al., (1951). Equivalent (50 μg) amounts of proteins per sample were subjected to electrophoresis on a 10% sodium dodecyl sulphate-acrilamide gel. The gel was then blotted onto a nitrocellulose membrane. Blotted membranes were blocked for 1h in a 4% suspension of dried skimmed milk in PBS and incubated overnight at 4ºC with a rabbit polyclonal anti-P-CREB serum; against the phosphorilated Ser133 form of CREB (1:1000 dilution). The membranes were washed and incubated for 1h at room temperature with peroxidase-conjugated anti-rabbit immunoglobulin G (dilution 1:1000). Specific reactions were revealed by the ECL Western blotting detection reagent (Amersan Biosciences).

2.4.11 Indirect immunocytochemistry

Rabbit polyclonal antibodies and mouse monoclonal antibodies against neural antigens and receptors for FGF were used as primary antibodies for indirect immunocytochemistry. Polyclonal anti-FGFR1, anti-FGFR2 and anti-FGFR3 were purchased to Santa Cruz Biotechnology Inc. Burlingame, CA. Anti-GFAP was obtained from Dakopatts a/s, Glostrup, Denmark. Monoclonal antiβ-tubulin isotype III and anti-GFAP were obtained from Developmental Studies Hybridoma Bank (University of Iowa), Sigma Chemical Co, and Boehringer Mannheim GmbH, respectively. Secondary antibodies raised in goat against rabbit, and in sheep against mouse immmunoglobulins, conjugated to alexafluor were purchased to Jackson Boehringer Mannheim GmbH. After appropriate culture time, cells grown on poly-l-ornithine coated coverslips were fixed with 4% paraformaldehyde for 10 min, rinsed 3 times in phosphate-buffered saline, then blocked with 10% foetal calf serum, and subsequently incubated in primary antibodies for 1 hour at room temperature (for growth factor receptors). Permeabilisation for intracellular antigens was achieved by incubation with ethanol acetic solution at –20ºC for 20 min. To assess non-specific binding for each antibody, adjacent cultures were incubated in buffer, without primary antibody. For dual labelling, primary antibodies generated by different species were added together. Secondary antibodies were administered for 45 min in the dark at room temperature. The coverslips with cells were mounted in a medium containing p-phenylenediamine and bisBenzimide (Hoechst 33342, Sigma Chemical Co). In selected experiments, FGFR1 was immunoperoxidase detected, using a biotin-linked (Vector Laboratories Inc, Burlingame, CA), instead of a fluorescence-linked secondary antibody, followed by incubation with an avidin-biotinylated horseradish peroxidase complex (Vectastain Elite ABC Kit, Vector Laboratories Inc). Finally, peroxidase was developed with 0.05% DAB, 0.005% hydrogen peroxide. The samples were counterstained with haematoxylin.

2.4.12 Hybridisation histochemistry

The hybridisation protocol has been adapted for all cell cultures from that reported by Simmons et al. (1989). The cells were fixed with 4% paraformaldehyde for 30 min at room temperature, dehydrated, air dried for 2 hours, and stored at –80ºC. Before hybridisation, the cultures were treated with proteinase K at a doses ranging from 0.1 to 1 µg/ml for 10 min at 37ºC, acetylated with acetic anhydride, dehydrated and air dried. Each coverslip was overlaid with 50 µl of hybridisation solution (50% formamide, 0.3M ClNa, 10mM Tris pH 8.0, 1mM EDTA, 0.5 mg/ml transfer RNA, 0.5 mg/ml total yeast RNA, 1x Denhardt's solution, 10% dextran sulphate, 10 mM DTT) containing $1x10^7$cpm/ml [^{35}S]-radio-labelled probe (FGFR1, FGFR2, FGFR3, FGFR4 cRNAs). In each experiment parallel cultures were hybridised with the complete probes and with the hydrolysis product of each type of probe. Alkaline hydrolysis was performed by incubating probes at 60ºC with bicarbonate buffer, pH 10.2, during appropriate periods of time, in order to obtain fragments of 250 bp. Hybridisation was carried out at 55ºC overnight, and thereafter coverslips were treated with 20 µg/ml ribonuclease A for 30 min at 37ºC. Coverslips were washed at increasing stringency with the final wash in 0.1x SSPE (10mM NaH_2PO_4, pH 7.4, 0.15M NaCl, 1mM EDTA), containing 1mM DTT, for 1 hour at 45ºC. After dehydration, cultures were air dried for 2 hours. In order to facilitate subsequent manipulation of coverslips, they were fixed to slides with DPX, so that 2 similar cultures, hybridised with the antisense and sense probes respectively, were attached to the same slide. Cultures were exposed to X-ray film for 5 days, and then dipped in Kodak NTB-2 liquid autoradiographic emulsion, and exposed for 4 weeks at 4ºC prior to development in Kodak D-19. Finally, the cultures were counterstained with haematoxylin and eosin and analysed.

2.4.13 Nucleic acid probes

[^{35}S]-UTP (ICN Pharmaceuticals Inc, Irvine, CA) labelled probes were synthesised in a run-off transcription reaction, using T3 or T7 and SP6 or T7 polymerases to generate antisense or sense RNAs, respectively.

2.4.14 Analysis of inmunocytochemical data

The results were expressed as mean ± SEM from 4 to 6 independent experiments (per treatment) done in duplicates (two coverslips). Where indicated, data are normalised in relation to their own controls, and represent the mean ± SEM of two coverslips from 4 independent experiments. In each coverslip, 30 predetermined visual fields (400X amplification) were counted under fluorescence microscopy through a program of Image Analysis. Statistical analyses were performed using Student's T test, and differences were considered significant when $p \leq 0.05$.

2.5 Experiments with human lymphocytes and thymocytes and embryonic stem cells of mice during cardiac differentiation (Participant 8)

2.5.1 ELF-EMF exposure setup

The ELF-EMF exposure setup used by Participant 8 is based on two unshielded 4-coil systems arranged in the same incubator; B-fields up to 1 mT (50 Hz) can be applied (see 2.1.1). It was composed by two systems, one used for the active exposure and one used as sham. Each system was composed by four circular coils; each coil being double-wrapped, in order to obtain a wound (active) or counter-wound (sham) configuration. The characteristics of the coils were the following: internal radius of the top and bottom coils 9.2 cm, numbers of turns 40 (20+20); internal radius of the two central coils 6.6 cm, numbers of turns 40 (20+20); distances between the coil centres 7.9 cm. The coil configuration was calculated in order to have a large zone of high uniformity (1%). The two systems were powered in series by an home-made DC amplifier connected to a function generator (Beckman FG3A). The ELF set up was kept inside a commercial CO_2 incubator (HeraCell) and the temperature was monitored by means of an high precise thermoresistor. At variance with the ELF set up used by Participant 4 the automated blind protocol was not implemented in the system by means of a suitable switcher and the experiments were

done in blind by the experimental protocol.

2.5.2 RF-EMF exposure setup

See 2.1.2

2.5.3 Cell proliferation by ^{3}H-TdR incorporation test

Peripheral blood mononuclear cells (PBMCs) from 20 young donors, were separated by centrifugation on Histopaque-1077 (Ficoll Histopaque, Sigma Chemical, St. Louis, MO, USA) discontinuous density gradient (Böyum 1968). One hundred µl of cell suspension containing 10^5 PBMC in complete medium (RPMI 1640 with 2 mM glutamine, 100 U/ml penicillin, 100 µg/ml streptomycin and 10% heat-inactivated AB serum from a pool of 10 human donors) was distributed in microplate wells (Costar, Cambridge, Ma, USA) and added with 0.1 ml of medium with or without mitogen. The following mitogens were used to promote lymphocyte proliferation: phytohemoagglutinin (PHA-P, Difco, Detroit, MI, USA) at the final concentrations of 0.1, 1, 5 and 10 µl/ml; anti-CD3 monoclonal antibody (mAb) (OKT3, an IgG2a mAb, from ATCC, Rockville, MD, USA) at the final concentration of 10 ng/ml. Each point was performed in quadruplicate. Cultures were incubated and sham-exposed or exposed to 50 Hz magnetic field (50 µT) for 2 up to 6 days (5% CO_2 in a humidified atmosphere). ^{3}H-methyl-thymidine (^{3}H-TdR, Amersham Int., UK, specific activity 5 Ci/mM) was added for the last 6 hours of culture (0.5 µCi/well). At the end of the incubation period, PBMC were harvested and washed on fibre filters by a multiple cell culture harvester (Skatron, Norway); ^{3}H-TdR incorporation was measured by liquid scintillation counting (*b*-counter, Beckman).

2.5.4 Cell proliferation by flow cytometry

PBMCs from young donors were marked by using the fluorescent cell tracer Carboxyfluorescein diacetate, succinimidyl ester (CFDAse, Serotec, UK). It couples irreversibly intracellular proteins by reaction with lysine side-chains and other available amine groups. Cells become fluorescent and after mitogenic stimulation (with 1 or 0.1 µl/mL PHA, phytohaemoagglutinin; in some experiments anti-CD3 10 ng/mL was also used), the dye is divided between the daughter cells. Each division results in generation of a population of cells that is marked by half of the cellular fluorescence intensity. PBMCs were cultured in petri dishes (35mm) at the concentration of $1x10^6$/mL of medium and exposed to RF. Two intermittent types of exposure were applied using Talk modulated RF signal (SAR 2 W/kg): (1) 10 min on/20 min off for 44 h; (2) 2h on/22h off for 72 hours. We performed experiments with cells from 6 donors using the former, from 11 donors using the latter. All cells were acquired and analysed after 72 h and 120 h of culture. At the end of time culture, cells were harvested and labelled by anti-CD4, anti-CD8 and anti-CD28 monoclonal antibodies (Serotec, UK), in order to discriminate helper and cytotoxic T cells with or without the co-stimulating molecule CD28, fundamental for the activation of lymphocytes.

2.5.5 Cell cycle analysis by flow cytometry

Cell cycle was analysed in PBMCs exposed either to ELF and RF-EMF. In ELF experiments, PBMCs from 9 young donors were stimulated by PHA (optimal dose, i.e. 1 µl/ml) or anti-CD3 (10 ng/mL) and exposed or sham-exposed for 24, 48, 72 and 96 hours. In RF experiments, PBMCs from 8 young donors were exposed to GSM basic signal (SAR=2W/Kg), PBMCs from 10 young and 8 elderly donors to TALK signal (SAR=2W/Kg) and PBMCs from 8 young subjects were exposed to DTX signal (SAR= 1.3 W/Kg).The exposure time was 10 minute on and 20 minute off for 44 hours.

Cell cycle analysis was performed by the method of 5-bromo-2'-deoxyuridine (BrdU) incorporation and propidium iodide (PI) staining. Briefly, at the end of the incubation period, cells were labelled with 20 µM BrdU for 30 min., centrifuged for 1 min., washed twice with 1 ml of PBS solution containing 0.5% Tween 20, and resuspended in 1 ml HCl 1N. After a 30 min. incubation at room temperature, cells were centrifuged at 300g for 1 min. washed once in 0.1 M $Na_2B_4O_7$, and added with 5 µl of anti-BrdU mAb (Becton Dickinson, San Josè, CA, USA). Cells were incubated for 60 min. at 4°C, washed twice and

resuspended in 200 µl of diluted secondary antibody (goat-anti-mouse IgG conjugated with fluorescein isothiocyanate, FITC). After a 30 min. incubation at 4°C, cells were washed twice and resuspended in 200 µl of PBS solution with 0.5% Tween 20 and 200 µl of PI working solution (50 mg/ml in 3.4 mM trisodium citrate, 9.65 mM NaCl plus 0.03% Nonidet P40). After 15 min. at 4°C in the dark, cells were acquired and analysed by flow cytometer.

2.5.6 Expression of membrane receptors on T lymphocytes by flow cytometry

Phenotypical analysis of T lymphocytes was performed in PBMCs exposed either to ELF and RF. In ELF experiments, HLA-DR and CD25 membrane expression were analysed on CD3+ T and CD4+ T helper lymphocytes respectively. The analysis was performed on cells from 9 young donors, before and after stimulation with PHA (1 µl/ml) or anti-CD3 mAb (10 ng/ml). Briefly, cells were stimulated and exposed from 24h to 72 h, collected, washed twice with cold PBS and stained with different mAbs directly conjugated with FITC or phycoerythrin (PE). The following mAbs from Becton Dickinson and from Serotec (Oxford, UK), were used: anti-CD3, recognising all T cells; anti-HLA-DR, recognising B cells and activated T cells; anti-CD4, reactive with helper/inducer T cell subset; anti-CD25, reactive with the p55 chain of IL-2 receptor. The expression of HLA-DR and CD25 molecules was studied on CD3+ and CD4+ lymphocytes at 24, 48, 72h after mitogen stimulation. In RF experiments, PBMCs from 8 young donors were exposed to GSM basic signal (SAR=2W/Kg), PBMCs from 10 young and 8 elderly donors were exposed to TALK signal (SAR=2 W/Kg) and PBMCs from 8 young subjects were exposed to DTX signal (SAR=1.3 W/Kg). CD25, CD95 and CD28 in CD4+ helper and CD8+ cytotoxic T lymphocytes, respectively, were analysed by flow cytometry technique. (In specific: CD95 is the receptor activating the pathway of programmed cell death). Lymphocytes before and after exposure to RF were phenotypically analysed. Cells, unstimulated or stimulated with anti-CD3 mAb (10 ng/ml), immediately after exposure or sham-exposure, were collected, washed twice with cold PBS and stained with three different mAbs (CD25, CD95, CD28, CD4 and CD8, Serotec, Oxford, UK) directly conjugated with FITC or phycoerythrin (PE), or tricolor fluorocromes. The analysis was performed on 10,000 lymphocytes for each sample and the three fluorescences were analysed using “paint-a-gate” software (Becton Dickinson).

We performed also from 5 up to 8 replications, using PBMCs from the same young donor. Cells were un-stimulated or anti-CD3-stimulated (10 ng/mL) and exposed or sham-exposed to TALK modulated RF (SAR 2 W/kg) for 44h (10 min on/20 min off). After exposure, cells were stained using the same protocol describe before. The following membrane molecules were analysed: CD25, CD95, CD28, CD45RO, HLA-DR on CD4+ and CD8+ T lymphocytes, respectively. Moreover, a more sophisticated analysis was performed on fluorescence distribution of CD4+ helper T lymphocytes from 10 young and 8 elderly donors

2.5.7 Spontaneous and induced apoptosis by flow cytometry

PBMCs from 8 young donors were exposed to GSM basic signal (SAR=2W/Kg), PBMCs from 10 young and 8 elderly donors to TALK signal (SAR=2W/Kg) and PBMCs from 8 young subjects were exposed to DTX signal (SAR=1.3 W/Kg). PBMCs were induced to undergo apoptosis by 2-deoxy-D-ribose (dRib) (Barbieri et al, 1994), which acts through an oxidative pathway (Monti et al. 2000) and the early stage of apoptosis was assessed by Annexin-V and propidium iodide kit (ANX-V , Bender, Vienna, Austria) using flow cytometry technique. Briefly, cells were collected, washed in PBS and resuspended in 200 µL of ANX-V binding buffer (10 mM Hepes/NaOH pH 7.4, 140 mM NaCl, 2.5 mM $CaCl_2$), stained with 5 µL of ANX-V and incubated for 10 minutes at room temperature. Then, cells were washed with binding buffer to remove the excess of ANX-V, resuspended in PBS, counterstained with 5 µg/ml PI and analysed by flow cytometry. ANX-V, the probe used for the detection of early stage apoptotic cells, is able to recognise phosphatidylserine (PS) when present on the outer leaflet of the plasma membrane. It is well known that PS is normally found only on the inner leaflet of the cell membrane double layer, but it is actively transported to the outer layer as an early event in apoptosis and becomes available for annexin binding (Green and Steinmetz 2002).

2.5.8 MMP modifications in induced and spontaneous apoptosis

PBMCs from 8 young donors were exposed to GSM basic signal (SAR=2W/Kg), PBMCs from 10 young

and 8 elderly donors to TALK signal (SAR=2W/Kg) and PBMCs from 8 young subjects were exposed to DTX signal (SAR=1.3 W/Kg). Changes in MMP have been evaluated by using the lipophilic cationic probe JC-1, which changes reversibly its colour from green to orange as MMP increases (over values of about 80-100 mV). This property is due to the reversible formation of JC-1 aggregates upon membrane polarisation that causes a shift in the emitted light from 530 nm (*i.e.*, emission of JC-1 monomeric form) to 590 nm (*i.e.*, emission of J-aggregates) when excited at 490 nm; the colour of the dye changes reversibly from green to orange/red as the mitochondrial membrane becomes more polarised. Both colours can be detected using the filters commonly mounted on flow cytometers, so that green emission can be analysed in one fluorescence channel, and orange/red emission in the other. Briefly, cells were stained with 2.5 μg/mL JC-1 and kept at room temperature for 10 minutes, washed twice with PBS, resuspended in a total volume of 400 μL PBS and analysed (Cossarizza et al. 1993b; Salvioli et al. 1997).

2.5.9 Cytokine production by ELISA

The production of interleukin-1 β (IL-1 β) and interleukin-6 (IL-6) in unstimulated and stimulated PBMCs from young donors was determined in the surnatant of cultures. Two types of stimuli were used: a) 10 ng/mL anti-CD3, b) 10 ng/mL TPA (12-O-tetradecanoylphorbol-13-acetate) plus 1 μ/mL PHA (phytohaemoagglutinin). PBMCs from 26 donors were stimulated with the former and 24 were stimulated with the latter. The second stimulus is stronger than the first, since it is directed on monocytes. PBMCs were exposed both to GSM talk (2 W/kg SAR) and DTX only (SAR 1.4 W/kg) RF for 44 hours (10 min on/20 min off). At the end of time culture, surnatants were harvested and frozen. After the collection of all the samples we analysed the presence of cytokines by ELISA (Enzyme linked Immuno-adsorbant assay), a well known immuno-enzimatic method, by which cytokine is revealed by a coloured end-product. By using an ELISA plate reader final data are produced as pg/mL units.

2.5.10 Hsp70 levels in induced and spontaneous apoptosis by flow cytometry

PBMCs, obtained from 7 healthy young donors, were treated by 2-deoxi-d-Ribosio (dRib, 10 mM) for 44 h and in the meantime cells were exposed to RF (GSM Talk signal, SAR 2W/kg; 10 min ON and 20 min OFF). Detection of intracellular Hsp70 was performed by flow cytometry techniques (Bachelet et al., 1998). At the end of culture, cells were collected, fixed and permeabilised by ethanol 95% and acetic acid 5% for 15-30 minutes, at -20°C. Then, cells were washed with PBS with 1% of BSA and labelled with Hsp70 primary antibody (Mouse IgG, 70 KDa for human target, Pharmingen, BD, San Josè, CA, USA) for 1h at 4°C in the dark. Then, cells were incubated with a secondary fluorescent antibody (GOT anti-mouse, Becton Dickinson), FITC conjugated (isothiocyanate of fluorescein) for 30 min at 4°C in the dark. At the end of the incubation cells were washed and analysed by flow cytometer (FCScalibur, BD). Fluorescence intensity was evaluated by CellQuest® programme.

2.5.11 Thymocyte development and apoptosis by HTOC and flow cytometry

Pieces of human thymus were obtained by cardio-surgery from S.Orsola-Malpighi Hospital (Bologna, Italy) from 6 human newborn. (5 days-8 months). Small fragments of tissue (2-3 mm^3) were cut and cultured above a sterilised filter on a small piece of gelfoam which was embedded of medium (20% of FCS, 1% of penicillin-streptomycin, 79% of DMEM). Each gelfoam was placed inside the Petri dishes containing the DMEM medium. This is a standard technique used to analyse in vitro thymocyte differentiation (Anderson and Jenkinson 2000). Human thymus organ cultures (HTOC) were incubated for 48 h, but the exposure (or sham-exposure) was performed only during the first 24h (DTX only at SAR 1.4 W/kg; 10 min on / 20 min off). At the end of culture (48 h), thymocytes were separated by gentle pressing through a fine stainless steel screen submerged in PBS. Single cell suspensions were obtained by passing the cells through a steel filter, and washing twice in PBS. Thymocytes were directly labelled with FITC or PE conjugated mAbs; such as, CD4, CD8, αβTCR (T cell receptor), γδTCR, CD71 (transferrin receptor on proliferating cells) and CD16 (receptor for IgG) in order to discriminate different phenotypical phases of differentiation. Moreover, apoptosis and viability were assessed by annex-V (see the methods described above) and PI staining, respectively. 10,000 cells from each sample were acquired by flow cytometer and analysed by paint-a gate-software.

2.5.12 T lymphocyte gene expression by microarray technology

Quiescent T lymphocytes were separated by MACS® (Magnetic Cell Sorting, Miltenyi Biotec, Germany). Three samples were obtained from control cultures, sham-exposure and exposure to DTX only RF for 44h (10 min on/20 min off). These samples were sent to Participant 12 for gene expression analysis by microarray technology. Data analysis were performed in Bologna by Participant 8.

2.5.13 Cell culture of embryonic stem cells and EMF-Exposure

GTR1 ES cells, a derivative of R1 ES mouse cells (Nagy 1993) bearing the puromycin-resistance gene driven by the cardiomyocyte-specific MHC promoter (GTR1 cells were kindly provided by Dr. William L Stanford (University of Toronto and Centre for Modelling Human Disease, Canada). ES cells were maintained in the undifferentiated state by culturing in DMEM containing 15% FBS, supplemented with a final concentration of 1000 U/ml ESGRO-LIF (LIF). To induce cardiac differentiation, cells were plated onto bacterial Petri dishes, containing DMEM lacking supplemental LIF. After 2 days of culture, the resulting embryoid bodies (EBs) were plated onto tissue culture dishes. When spontaneous contractile activity was noticed, puromycin (2 µg/ml) was added to eliminate non-cardiomyocytes. After 2 days, puromycin-selected myocytes were transferred to new tissue culture dishes. As indicated in the legend of each figure, EBs, collected at several stages after plating, as well as puromycin-selected cells, were processed for gene expression analyses. Following LIF removal and throughout puromycin selection, GTR1 cells were exposed to ELF-EMF (50 Hz, 0.8 mT_{rms}).

2.5.14 Analysis of mRNA expression

Expression of GATA-4, Nkx-2.5, prodynorphin, alpha-myosin heavy chain and myosin light chain-2V mRNA was assessed by RT-PCR as previously described (Ventura 2000), using GAPDH mRNA as a measure of equal loading and mRNA stability. GATA-4 mRNA levels were also quantitated by RNase protection assay, as described elsewhere (Ventura 1997, Ventura 2003a, Ventura 2003b). Briefly, fragments of the main exon of the mouse GATA-4 (292 bp) gene was inserted into pCRII-TOPO (Invitrogen, CA). Transcription of the plasmid linearised with *BamHI* generated a sense strand of GATA-4 mRNA, which was used to construct a standard mRNA curve. Transcription in the presence of [^{32}P]CTP (800 Ci/mmol) (Amersham International) of plasmids linearised with *Xba*I produced an antisense strand of GATA-4 mRNA (radio-labelled cRNA probe). Samples were then incubated with a combination of RNase A and T1 and exposed to proteinase K. The protected fragments were recovered after phenol chloroform extraction and electrophoretically separated in a polyacrylamide non-denaturing gel. Autoradiographic exposure was performed for 48h. The individual bands were counted for radioactivity by liquid scintillation spectrometry, and cpm values were translated to pg values on a correlated standard curve. Data were expressed as pg of mRNA/µg of total RNA.

2.5.15 Transcriptional analysis in isolated nuclei

Nuclear run-off was performed. 90 µl of nuclear suspension were added with 100 µl of 2 x reaction buffer (10 mmol/L Tris/HCl, pH 7.5, 5 mmol/L $MgCl_2$, 0.3 mol/L KCl, 5 mmol/L dithiothreitol, 1 mmol/L each of ATP, GTP, and CTP), and 5 µl of [α-^{32}P]UTP (3000 Ci/mmol), followed by incubation at room temperature for 15 min. DNA was digested by incubating the transcription mixture for 5 min at room temperature in the presence of 1 µl of 20,000 units/ml RNase-free DNase. Equal counts of ^{32}P-labeled nuclear RNA (about 5 x 10^6 cpm) were then subjected to a solution hybridisation RNase protection assay and were hybridised for 12h at 55°C in the presence of unlabelled antisense GATA-4 mRNA Samples were then incubated with a combination of RNase A and T1 and exposed to proteinase K. The protected fragments were recovered after phenol chloroform extraction and electrophoretically separated in a polyacrylamide non-denaturing gel. Autoradiographic exposure was for 48h. ^{32}P-labeled nuclear RNA was also hybridised with unlabeled antisense cyclophilin mRNA synthesised from a *Nco*I-linearised pBS vector containing a 270-base pair fragment of plB15, a cDNA clone encoding for rat cyclophilin (6). Cyclophilin mRNA was utilised as a constant mRNA for control.

2.6 Experiments with brain cells of different origin and human monocytes and endothelial cells (Participant 9)

2.6.1 Exposure setup and exposure conditions

The wire-patch cell (WPC) is the setup that was used for exposure to frame-scheme (FS) GSM-900 signals. This exposure system accommodates 8 Petri dishes to be built as a double Petri dish, i.e. a 3.5-cm diameter Petri dish (where cells are cultured) is positioned inside a 5-cm diameter dish (outer dish with distilled water inside). Two double Petri dishes are pilled-up and placed in the wire-patch antenna (Figure 3) so that a total of 8 dishes can be exposed at a time. Two successive WPC models were used. The second one shown in Figure 1, built by Participant 10, was fitted with electric field probes that allowed monitoring of the SAR in real time.

Cells were cultured in 3.2 ml of culture medium and the outer Petri dishes are filled with 5 ml of distilled water. Cultured cells in Petri dishes were placed in a standard CO_2 air-flow incubator inside a WPC for a minimum of 3 hours to allow for temperature stabilisation. Sham exposed samples were treated in the same way in a non-activated WPC placed in a second, identical incubator. Each WPC was fitted with a square annular ring made of absorbing foam (Figure 3) to block emission sideways towards the metallic walls of the incubators and allow for a good adaptation at 900 MHz. The foam is sealed with waterproof lining.

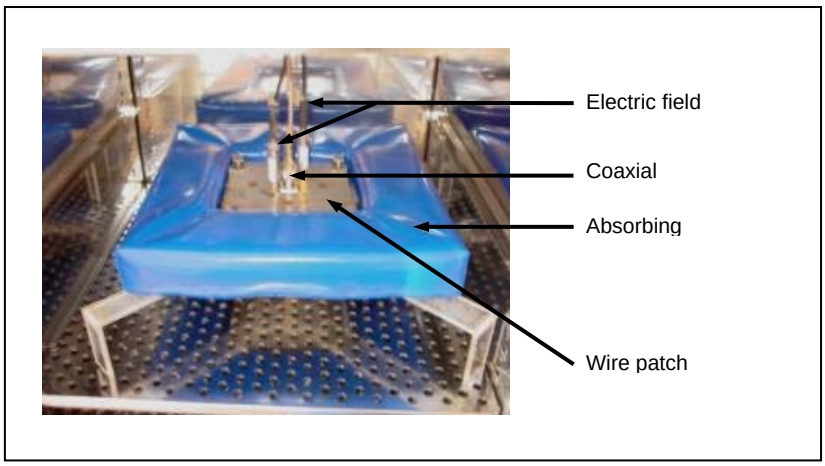

Figure 3. Image of a wire-patch antenna surrounded by the absorbing foam in a dedicated incubator

Dosimetry

The WPC's dosimetry (temperature measurement and modelling) was performed in collaboration with French experts (P. Lévêque, IRCOM, France and J. Wiart, France Télécom R&D). A good efficiency was found (around 0.6 W/kg per incident watt) and the uniformity for cell exposure was found to be very good (ca. 15%) (Figure 4). Experimental Specific Absorption Rate (SAR) evaluation was undertaken in order to validate the data obtained by numerical dosimetry (see Participant 10). Based on the measurement of temperature increase after the RFR generator was turned on, this technique gives also information on the thermal consequences at the level of the whole setup. Temperature was recorded in the inner part of a double Petri dish using optical fibres (Luxtron probes, that are immune to the microwaves), as well as in the incubator throughout the first hours of exposure (until temperature stabilisation was reached). Temperature measurements also showed that it took at least 2 hours for temperature to equilibrate, after the cell cultures were introduced, in the absence of microwaves. This needed to be taken in account in the exposure protocol. Experimental dosimetry showed that the mean SAR was 0.77 W/kg at the level of the cell monolayer, which is in good agreement (within 15%) with numerical data. The corresponding temperature rise was 0.2°C (i.e. temperature difference between the Petri dish inner part and the incubator).

Since heating is produced by absorption of the microwaves by the samples, care was taken to keep the temperature of the exposed and sham-exposed samples identical during the experimental trial. For that purpose, the "exposed " incubator temperature was first set at a lower value than that of the "sham" side, depending on the SAR level chosen for a given experiment. For a SAR of 2 W/kg for instance, the temperature difference was 0.5°C for an input power of 3.4 W, in very good agreement with numerical FDTD modelling (Figure 4) Those data have been confirmed for quality control purposes by Participant 10.

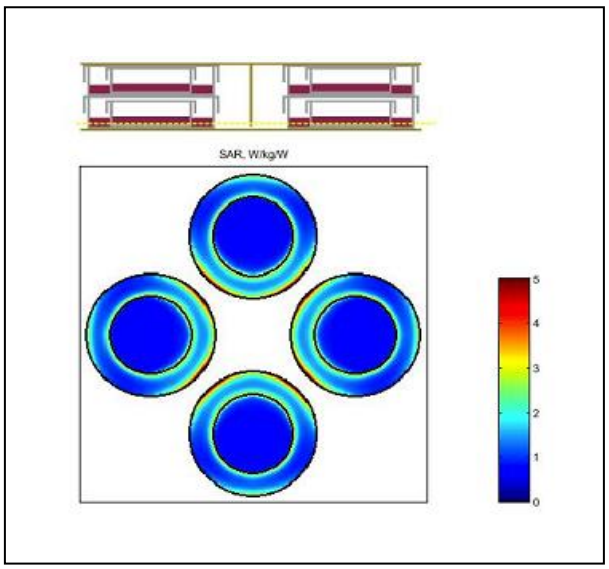

Figure 4. FDTD simulation of SAR in the Petri dishes (outer and inner parts) using an input power of 1 W. Upper panel shows the Petri dishes disposition in the wire-patch antenna.

2.6.2 Cell culture and RF-EMF exposure

For each exposure condition, at least three independent experiments were performed in a blind manner. For that purpose, all samples are coded prior to exposure, one researcher is in charge of exposure and codes are broken after completion of the analysis of all parameters investigated in the experiment by researchers unaware of the exposure conditions.

Culture of nerve cells

Rat primary neurons (granule cells) - a very critical cell type in the central nervous system-, rat primary astrocytes and rat C6 astrocytic cell line were used. Both primary cell types were prepared from newborn rat cerebella. Human nerve cell lines were also used to look at possible species specificity as well as at differences between transformed and normal cells. Human U87 astrocytic- and SH-SY5Y neuronal- cell lines were chosen as models.

i) Rat brain primary cultures: Primary cultures were prepared from postnatal day 4-9 (P4-P9) rat cerebella. Two types of cultures were prepared: neuronal-astroglial and glial (astrocytes) cultures.

Neuronal-astroglial cultures, with approximately 80% neurons and 20% glia in the cell population, were obtained from P4 rat cerebella. The cells were plated on polylysine-coated dishes at 10^6 cells/dish in Hanks Minimum Essential Medium supplemented with 10% horse serum. They were maintained in 3% CO_2 in air at 37°C for 4-6 days. Astrocyte cultures, where very few neurons survived, were obtained from P8 rat cerebella and plated at 10^6 cells/dish in Dulbelco Miminum Essential Medium (DMEM) supplemented with 10% fetal calf serum (FCS) and antibiotics (AB, 100 U/ml penicillin and 100 µg/ml streptomycin) and maintained in 9% CO_2 in air at 37°C for 13-15 days. For the experiments, all primary cells were plated in 35 mm diameter Petri dishes and used as it, without any further handling. The endpoint investigated in these cells was apoptosis. Rat primary neurons were sham-exposed or exposed to GSM-900 for one or 24 hours and apoptosis was evaluated following a time-kinetics (4, 8 and 24 hours

after exposure began) or immediately after exposure, respectively. Rat primary astrocytes were sham-exposed or exposed to GSM-900 for 1 hour and apoptosis was evaluated as described previously. Three to six independent experiments were performed for each exposure condition. Results are expressed as the percentage of apoptotic cells in GSM-900- exposed versus sham-exposed samples. The Student t test was used for statistical analyses.

ii) Human neuroblastoma cells: Human SH-SY5Y neuroblastoma cells (ECACC N° 94030304) were cultured in Ham's F12 medium supplemented with 15% FCS, 1% non-essential amino-acids and AB The endpoint investigated in these cells was apoptosis. Human SH-SY5Y neuronal cells – as rat primary neurons – were sham-exposed or exposed to GSM-900 for one or 24 hours and apoptosis was evaluated following a time-kinetics (4, 8 and 24h after exposure began) or immediately after exposure, respectively. Three to six independent experiments were performed for each exposure condition. Results are expressed as the percentage of apoptotic cells in GSM-900- exposed versus sham-exposed samples. The Student t test was used for statistical analyses.

iii) Human glioblastoma cells: Human U87 glioblastoma cells (ECACC N° 89081402) were grown in Eagle Minimum Essential Medium supplemented with 10% FCS, 1% non-essential amino-acids and AB. The endpoint investigated in these cells was apoptosis. Human U87 astrocytic cells -as rat primary astrocytes - were sham-exposed or exposed to GSM-900 for 1 hour and apoptosis was evaluated following a time-kinetics (4, 8 and 24h after exposure began). Three to six independent experiments were performed for each exposure condition. Results are expressed as the percentage of apoptotic cells in GSM-900- exposed versus sham-exposed samples. The Student t test was used for statistical analyses.

iv) Rat glioma cells : Rat C6 glioma cells were obtained from the European Collection of Cell Cultures (ECACC N° 85040101, UK) and maintained in DMEM-F12 medium (Biomedia, France) containing 10% fetal bovine serum (Gibco), 2 mM sodium pyruvate (Biomedia, France) and 1% antibiotics (100 U/ml penicillin and 100 µg/ml streptomycin, Biomedia, France) at 37°C in a standard culture incubator. The endpoint investigated in these cells was expression and activity of the inducible isoform of the Nitric Oxide Synthase (iNOS or NOS_2). C6 cells were sham-exposed or exposed to GSM-900 alone (0.2 W/kg or 2.0 W/kg, 48h) or in the presence of a cocktail of lipopolysacharide and cytokines CK (see below). Following RFR or sham-exposure the cells were harvested for western blot analysis and culture medium collected for the determination of nitrite accumulation, to test iNOS expression and activity, respectively. Randomised sham/sham exposures were included in the schedule of exposure, so that the engineer responsible for the analysis never was aware of any exposure condition. A total of four sham/sham exposures, six sham/exposed experiments at 0.2 W/kg and three sham/exposed experiments at 2 W/kg were conducted. The Student t test was used for statistical analyses.

Culture of immune cells

i) Human monocytes: Human U937 monocytic cells (ECACC N° 85011440) are grown as a cell suspension in RPMI 1640 medium complemented with 10% FCS plus AB. Two endpoints were investigated in these cells:

- Apoptosis in cells submitted either to a 48 hour-exposure to GSM-900 at a SAR of 0.7 W/kg or to a 1 hour-exposure at 0.7 W/kg and 2.0 W/kg followed by a treatment with camptothecin (CPT). Three to six independent experiments were performed for each exposure condition. Results were expressed as the ratio of apoptotic cells in GSM-900-exposed versus sham-exposed samples with or without CPT treatment. The Student t test was used for statistical analyses.
- Gene expression in cells submitted to a 1 hour-exposure to GSM-900 at a SAR of 2.0 W/kg.

ii) Human microglial cells: The human cloned microglial cells (CHME 5) were plated at a density of 10^6 cells/35mm diameter dishes in 2 ml of complete Dulbecco's MEM medium. Cultures were carried out for 3 days in water-saturated 5% CO_2 in air at 37°C before GSM exposure. The endpoint investigated in these cells was gene expression in cells after a 1 hour-exposure to GSM-900 at a SAR of 2.0 W/kg.

Culture of endothelial cells

Two EA.hy926 cell lines were tested: one was a generous gift from Participant 6, the other one from Dr. Cora-Jean S. Edgell who first developed the cell line and gave permission to use these cells in Bordeaux. The purpose for using both cell lines was to look at potential different behaviour of cells cultured in slightly different conditions that may have led to possible genotypic drift. Human EA.hy926 endothelial cells were cultured according to the provider's instructions.

i) EA.hy926 (a gift from Participant 6): Cells were grown in DMEM supplemented with 1% penicillin-streptomycin, 2% L-glutamine (200 mM), HAT-supplement and 10% FCS.

ii) EA.hy926 (a gift from Dr. Cora-Jean S. Edgell, North Carolina University at Chapel Hill, NC, USA): Cells were grown in DMEM supplemented with 1% penicillin- streptomycin, 2% L-glutamine (200 mM) and 10% FCS. For the RF-EMF experiments, cells were removed from culture flasks with trypsin, washed and seeded at a density of 0.26 x 10^6 cells/12 mm-diameter glass coverslips corresponding to 1.2 x 10^6 cells/55 mm-diameter dishes (as mentioned in Leszczynski et al. 2002). After an overnight culture, coverslips were transferred to 35-mm diameter Petri dishes and EA.hy926 cells were sham-exposed or exposed to RF-EMF for one hour at 2.0 W/kg. The endpoint to be studied in these cells is the expression of the heat-shock protein 27 (hsp27). EA.hy926 cells were sham-exposed or exposed to RFR for one hour at 2.0 W/kg.

2.6.3 Chemicals and other treatments

Positive controls used chemicals or other treatments. In order to look at possible interactions between RFR and chemicals, different protocols used RFR exposure combined to or prior chemical treatment.

Lipopolysaccharide plus cytokine treatment

Lipopolysaccharide plus cytokine treatment was used as a positive control for iNOS expression in C6 glial cells (Hewett et al., 1993; Nomura 1998). Two days before RFR exposure, C6 cells are plated in custom-made Petri dishes at a density of $5x10^4$ cells/dish. At the day of experiment, Petri dishes are filled with culture medium containing 4% FCS for cell deprivation. Half of the samples are treated with a cocktail of *e.coli* lipopolysacharide (LPS 10 µg/ml) and cytokines IFNγ (50 U/ml) plus TNFα (50 ng/ml) before Petri dishes are placed in the wire-patch antenna. Cells were then put in the exposure-dedicated incubators during 3 hours for temperature stabilisation before exposure to RFR started.

Camptothecin treatment

The apoptosis-inducer camptothecin (4 µg/ml, 4 hours) as a positive control in U937 monocytic cells. Camptothecin is a topoisomerase I inhibitor. As such, it inhibits the topoisomerase molecule from religating DNA strands after cleavage. This leaves a cell with DNA breaks, which if not repaired, become lethal (Holden 2001). When cells of the immune system are exposed the topoisomerase I inhibitor campthothecin, they rapidly undergo cell death via apoptosis, irrespective of what phase of the cell cycle a cell is in (Cotter 1992).

Heat shock

Positive controls for heat shock proteins (Hsp27 and Hsp70) induction were performed by exposing the different cell lines (U87, C6 and SH-SY5Y cell lines) to a heat shock at 43°C for 20 min.

2.6.4 Detection of apoptosis

The occurrence of apoptosis was assessed using two markers and flow cytometry.

Double staining with Annexin-V/FITC and propidium iodide

During apoptosis, phosphatidyl-serine is exposed on the outer leaflet of the plasma membrane that causes a loss of membrane asymmetry. Annexin V preferentially binds to phosphatidylserine (Van Engeland et al. 1998) and can be detected by flow cytometry using the APOPTEST^{TM}-FITC kit (Dako, France) according to manufacturer' instructions. Immediately after the complete treatment, cells were harvested so that all cells, including floating cells, were taken in account for the apoptotic test. Where needed, cells were scrapped (nerve cells) before being washed with PBS, and centrifuged at 200 g for 5 minutes. Cell pellet was resuspended and 10^6 cells were incubated for 15 minutes in 100 µl of cold labelling solution (1 µl of Annexin-V/FITC and 2.5µl of propidium iodide (PI) 250 µg/ml) in 96 µl of the kit's labelling buffer. Then 250 µl of labelling buffer were added and samples are analysed on a flow cytometer.

Double staining with $DiOC_6(3)$ and propidium iodide

Mitochondrial physiology is disrupted in cells undergoing apoptosis via intrinsic pathways. Mitochondrial membrane potential ($\Delta\Psi_m$) decrease has been largely described which can be measured using the

carbocyanine dye ($DiOC_6(3)$, Zamzami et al., 1995). Briefly, immediately after exposure, cells were washed and centrifuged as indicated above. Then 10^6 cells were incubated for 10-15 minutes in 500 µl of PBS containing 40 nM of $DiOC_6(3)$. Propidium iodide (2.5 µl of PI; 50 µg/ml) was added before analysis on a flow cytometer.

Data acquisition was performed using a FacScan® flow cytometer (Becton Dickinson) with the following parameters: 488 nm excitation, 515 nm bandpass filter for the Annexin V and $DiOC_6(3)$ dyes and filter > 560 nm for PI detection. Analysis was performed on 10000 events using the Cell-Quest® software. Analysis was performed blindly.

2.6.5 Western Blot analysis

Western Blotting was used for the detection of iNOS expression in C6 cells. C6 cells were lysed using RIPA buffer [0.5 mM Tris (pH 8.0), 0.5% Sodium Deoxycholate, 10% SDS,150 mM NaCl, 1% Triton X100 and protease inhibitors (16 mg/ml Benzamidin, 10 mg/ml Aprotinin, 10 mg/ml Pepstatin, 10 mg/ml Leupeptin, 10 mg/ml Phenanthroline and 1 mM Phenylmethylsulfonyl Fluoride)] using methods adapted from Schreiber et al. (1989).

Proteins were extracted from cell lysates and the concentration was determined by Bradford reaction (Biorad Protein Assay®). Protein samples (10-20µg) were electrophoretically separated through a 7.5% polyacrylamide SDS-page gel, electroblotted to polyvinylidene difluoride membranes and probed with mouse anti-iNOS (Transduction Laboratories N-39120, 1/5000°). In addition, we used ß-actin as an internal control for protein loading (all blots were de-hybridised and reprobed for ß-actin detection). Immunoreactive bands were visualised using ECL Western Blotting System® (Amersham-Pharmacia Biotech, RPN 2108) followed by exposure to autoradiography film (Biomax, Kodak). The NIH Image 1.54 software was used for blot quantitative analysis (based on OD measurements).

2.6.6 Griess reaction

iNOS activity in C6 cells was quantified as nitrites accumulation in culture media by the colorimetric assay based on the Griess reaction. 50µl of culture medium collected in triplicate from the samples were added to 60µl of Griess A solution (sulfanilamide 1% in 1.2N HCl) and 60µl of Griess B solution (Naphtylene Diamine Dichlorhydrate 0.3% in distilled water). The mixture was incubated 10 min at room temperature and red at 540 nm with a spectrophotometer. Fresh corresponding culture medium served as blank for NO_2^- content determination. Results were expressed as µg of nitrite per million cells.

2.6.7 Hsp immunolabelling and image analysis

Hsp70 expression was evaluated in human neuronal (SH-SY5Y) and rat (C6) or human (U87) astrocytic cell lines. Three days before the experiment, cells were plated on glass coverslips in 24-well plates at a density of 0.5×10^5 cells/well. The day before the experiment, coverslips were transferred to 35-mm diameter Petri dishes before being placed in the sham- and RFR-dedicated incubators.

U87, C6 and SH-SY5Y cell lines were sham-exposed or exposed to GSM-900 for 24 hours and the expression of Hsp70 was evaluated at the end of exposure. Hsp27 expression was evaluated in human EA.hy926 cells at the end of a-one hour sham- or RFR exposure at 2.0 W/kg. Following RFR or sham exposure, the cells were fixed in PBS-paraformaldehyde (4%) for immunocytochemistry. Anti-hsp70 and anti-hsp27 antibodies were obtained from Stressgen®. The first antibody was revealed using a FITC-labelled antibody. Coverslips were mounted on slides with Mowiol® before microscopy observation. For each exposure condition, three (hsp70) to five (hsp27) independent experiments have been performed in a blind manner. After immunocytochemistry labelling, fluorescence analysis was performed using the Aphelion® image software. Results are expressed as arbitrary units of fluorescence intensity.

2.6.8 RNA extraction and cDNA array hybridisation

Based on the data available within the REFLEX consortium on the effect of RF-EMF exposure on gene expression (see Participant 12), we chose two human cell lines involved in inflammatory processes (brain

human microglial and monocytes cells). Indeed, one of the gene families that were shown to be sensitive to exposure to electromagnetic fields is the gene family involved in inflammation. The human cloned microglial CHME-5 cells and the monocytic U937 cells were sham-exposed or exposed for one hour at 2 W/kg. Immediately after exposure, they were harvested for RNA extraction using Nucleospin® RNA purification kit (BD Biosciences Clontech, Palo Alto, USA). Total RNA purification was performed following user manual instructions. The amount of total RNA was measured by spectrophotometry. RNA samples were then frozen at –80°C before being sent to Participant 12 who performed cDNA array hybridisation.

2.7 Experiments with embryonic stem cells of mice (Participant 4)

2.7.1 Exposure setups

See 2.1.1 and 2.1.2.

2.7.2 Cell culture and EMF exposure

Pluripotent R1 ES cells (Nagy et al. 1993), wild type (wt) D3 (Doetschman et al. 1985) and p53-deficient ES cells (p53-/-; a gift of Dr. T. Jacks, Howard Hughes Medical Institute, Cambridge, MA, see Jacks 1994) derived from D3 cells were cultured as described (Wobus et al. 2002) except that p53-/- ES cells were maintained on neomycin-resistant SNL feeder cells (a gift of Dr. A. Bradley, Baylor College of Medicine, Houston, TX) in presence of 300 µg/ml G418. EC cells of line P19 (Edwards and McBurney 1983) were cultured without feeder cells (Wobus et al. 1994). For differentiation, P19, R1, and wt or p53-/- D3 cells were cultivated as EB in hanging drops in Dulbecco's modified minimal essential medium (DMEM, Gibco) supplemented with 20% FCS, L-glutamine, non-essential amino acids (NEAA) and β-mercapthoethanol (β-ME) as described (Wobus et al. 2002). Briefly, cells (n=400) in 20 µl of differentiation medium were incubated in hanging drops as embryo-like aggregates ("embryoid bodies", EBs) for 2 days and in suspension for 3 days. EBs were plated separately onto gelatin-coated 24-well microwell or tissue culture plates (∅ 6cm) at day 5 for morphological and reverse transcriptase polymerase chain reaction (RT-PCR) analyses, respectively. For the induction of P19 cell differentiation, EBs were cultivated in the presence of 1% DMSO (Sigma) during the first 2 days of EB development (Wobus 1994).

EBs derived from p53-/- and wt D3 ES cells were RF- or ELF-EMF- exposed in hanging drops for 6 or 48 hours (Figure 5). For 6h experiments, samples were collected immediately after exposure and used for RT-PCR analysis (Figure 5). After 48h exposure, EBs were further cultivated and samples were sequentially collected during differentiation for RT-PCR analyses. EBs derived from R1 cells were EMF (GSM-217)- or sham-exposed in hanging drops (SAR: 1.5 W/kg) for 2 days and in suspension (SAR: 2.0 W/kg) for 3 days. P19 cells (n=200,000) were seeded into 0.1% gelatin-coated tissue culture dishes, cultured in DMEM (see above) and after 2h pre-incubation at 37°C placed into the exposure setup for EMF and sham-exposition. As control, non-exposed cells were cultured in a separate humidified 5% CO2 incubator at 37°C. P19 cells were exposed to EMF at SAR value of 2.0 W/kg for 22 or 40h. After exposure, cells were immediately processed for flow cytometric analysis (P19), and in parallel, R1 and P19-derived EBs were prepared for differentiation and RT-PCR analysis

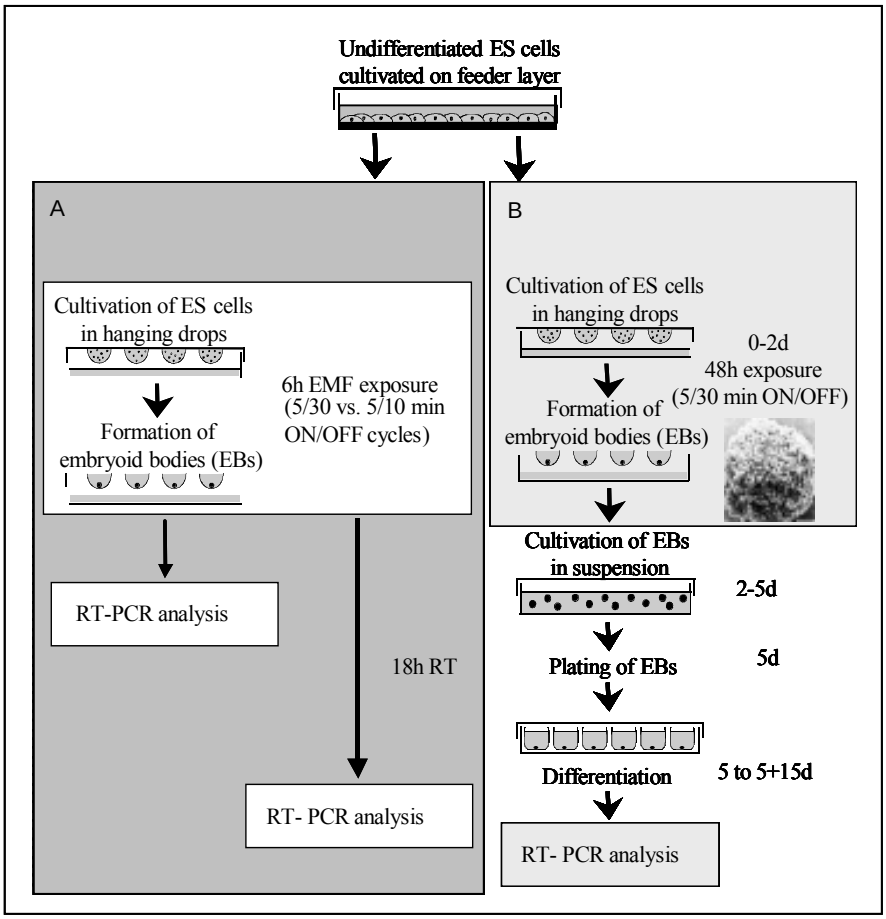

Figure 5. Experimental protocol for the exposure of undifferentiated and differentiating ES cells to EMF. Wild type (wt) and p53-deficient (p53-/-) D3 ES cells were grown on feeder layer. (A) ES cells were RF-EMF or PL-MF exposed for 6 h at the initial stage of hanging drop formation, when the differentiation processes are initiated. mRNA levels of genes encoding egr-1, p21, c-jun, c-myc, hsp70 and bcl-2 were analysed immediately after exposure (or after 18 h recovery time for PL-MF). (B) ES cells were exposed to EMF in hanging drops for 48 h and were monitored at different stages of the differentiation process.

For differentiation of neural phenotypes, R1 ESs were cultivated in 'hanging drops' (n = 200 cells/drop) for 2 days. EBs were transferred to bacteriological petri dishes (Greiner, Germany) and cultivated for two days in Iscove's modification of DMEM (IMDM, GIBCO) containing 20% FCS and supplements as described (Wobus et al., 2002), with the exception that ß-mercaptoethanol was replaced by 450 µM α-monothioglycerol (Sigma, Steinheim, Germany). EBs (n=20-30) were plated onto tissue culture dishes (∅ 6cm) at day 4 and cultivated in IMDM +20% FCS. The selection of neural precursor cells was carried out according to (Rolletschek 2001). After attachment of EBs, one day later, the medium was exchanged by DMEM/F12 medium supplemented with 5 µg/ml insulin, 30 nM sodium selenite (all from Sigma), 50 µg/ml transferrin and 5 µg/ml fibronectin (all from GIBCO) referred as "nestin-selection media". The culture medium was replenished every 2 days. RF-EMF or ELF-EMF exposure was performed for 48h between 4+4d and 4+6d. Nestin-positive neural precursor cells were selected after cultivation for 7 days (= 4+7d). At day 4+8, EBs were dissociated by 0.1% trypsin (GIBCO)/0.08% EDTA (Sigma) in PBS (1:1) for 1 min, collected by centrifugation, and replated onto poly-L-ornithine/laminin-coated tissue culture dishes into DMEM/F12 containing 20 nM progesteron, 100 µM putrescin, 1µg/ml laminin (all from Sigma), 25 µg/ml insulin, 50 µg/ml transferrin and 30 nM sodium selenite, referred to as "nestin-expansion media", for six days until day 4+13. The medium was changed every 2 days. 10 ng/ml basic fibroblast growth factor (bFGF) and 20 ng/ml epidermal growth factor (EGF; Strathmann Biotech, Hannover, Germany) were added daily. At day 4+14, the differentiation of neurons was induced by 'Neurobasal' medium plus 2% B27 (GIBCO), 10% FCS and maintained by the addition of survival

promoting factors such as interleukin-1ß (IL-1ß, 200 pg/ml daily; PeproTech, London, UK) and db-cAMP (700 µmol every four days; Sigma). Glial cell line-derived neurotrophic factor (GDNF, 2 ng/ml; R&D Systems) and transforming growth factor-ß3 (TGF-ß3, 2 ng/ml) were applied at day 4+18 and at day 4+21, respectively. Neurturin (NTN, 10 ng/ml; all from PeproTech) was applied at day 4+21. The application of survival promoting factors during terminal stages was combined with medium changes at three-day intervals. The total time of cultivation was 4+23d (Figure 6).

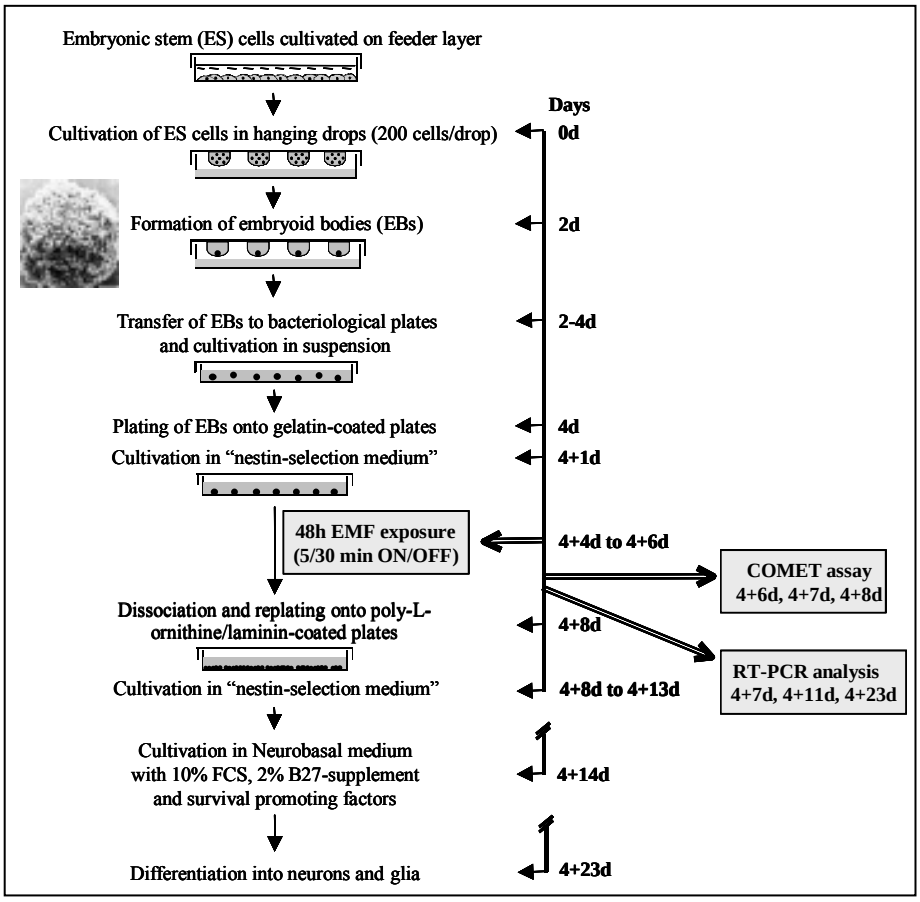

Figure 6. Experimental protocol for EMF exposure of R1 ES cells differentiating into the neural lineage. For differentiation of neural phenotypes, ES were cultivated in 'hanging drops' as EBs (embryoid bodies) for two days, then transferred to bacteriological petri dishes and cultivated two more days. EBs (n = 20-30) were plated onto tissue culture dishes (∅ 6cm) at day 4. After attachment of EBs, one day later, the medium was exchanged with medium supporting the development of neural precursor cells (replenished every 2 days). Nestin-positive neural precursor cells were selected after cultivation for 7 days (= 4+7d). Cell samples were analysed for primary DNA damage (24 and 48h after exposure) measured by the Comet assay, and mRNA levels of various regulatory, tissue-specific and neuronal genes at different stages of differentiation.

2.7.3 Detection of mRNA levels by semi-quantitative RT-PCR analysis

The expression of early response and growth regulatory genes as well as genes involved in neural and cardiac differentiation was analyzed in ES and EC cells after differentiation by semi-quantitative RT-PCR as described (Wobus et al. 2002). EBs or cells differentiating after the dissociation of EBs collected at days 4+4, 4+7, 4+11 and 4+23 were suspended in lysis buffer (4 M guanidinium thiocyanate, 25 mM sodium citrate, pH 7; 0.5% sarcosyl, 1% ß-mercaptoethanol). Total RNA was isolated by the single step extraction method according to (Chomczynski, 1987). RNA was reverse transcribed using Oligo $d(T)_{16}$ primers (Perkin-Elmer, Überlingen, Germany) for the genes encoding c-fos, c-jun, c-myc, early growth response-1 (egr-1), hsp70, p21, p53, bcl-2, bax, growth arrest and DNA-damage inducible –45

(GADD45), engrailed-1 (en-1), nurr-1, nestin, tyrosine hydroxylase (TH), GFAP (glial fibrillary acidic protein), α-myosin heavy chain (α-MHC) (primer sequences and the number of PCR cycles are available on request).

Reverse transcription was performed with MuLV reverse transcriptase (Perkin-Elmer) for 1h at 42°C, followed by denaturation for 5 min at 99°C and cooling to 4°C according to the protocol supplied by the manufacturer. For semi-quantitative determination of mRNA levels, PCR analyses were carried out with Ampli Taq DNA polymerase (Perkin-Elmer). For determination of relative mRNA levels, two separate PCR reactions, either using primers of the analyzed gene or primers specific for ß-tubulin were performed with 3 µl from each RT reaction.

One third of each PCR reaction was electrophoretically separated on 2% agarose gels containing 0.35 µg/ml ethidium bromide. Gels were illuminated with UV light and the ethidium bromide fluorescence signals were stored by the E.A.S.Y. system (Herolab, Wiesloch, Germany) and analysed by the TINA2.08e software (Raytest Isotopenmeßgeräte, Straubenhardt, Germany). Data of the target genes were plotted as percentage changes in relation to the expression of the housekeeping gene ß-tubulin. Gels of four independent experiments were analysed.

2.7.4 Detection of mRNA levels by quantitative RT-PCR (Q-RT-PCR)

Quantitative RT-PCR was performed with specific primers and TaqMan probes designed with Primer Express 2.0 (Applied Biosystems). All oligonucleotides were obtained by Metabion (Germany). The TaqMan probes for Q-RT-PCR were 5´-labelled with FAM (6-carboxyfluorescein) and with 3' prime quencher, TAMRA. The primer and TaqMan probe sequences are available on request. The mouse GAPDH gene was used as endogeneous reference. Reactions were carried out in 96-well plates using iCycler, Version 3.0.6070 (BioRad). The threshold cycle (Ct) , which is the cycle number, at which the amount of the amplified product of the analysed genes reached a fixed threshold, was determined subsequently. The relative quantitaion of bcl-2 and GADD45 mRNA levels was calculated using the comparative Ct method. In order to avoid amplification of contaminating DNA, all primers were designed with an intron sequence inside the amplicon, template-free controls were used as negative controls, the melting temperature of the TaqMan probe was adjusted to be at least 10° higher than the melting temperatures of the sense and anti-sense primers. After Real-time RT-PCR, gel electrophoresis was performed to confirm the correct size of the amplified product.

2.7.5 Single cell gel electrophoresis (Comet assay)

The lkaline version of the Comet assay was applied for detection of single-strand break and alkali-labile site induction, and neutral Comet assay for detection of double-strand breaks.In order to obtain single-cell suspensions, control, sham-exposed or exposed EB outgrowths were trypsinised by addition of 2 ml prewarmed at 37°C mixture of 0.1% Trypsin : 0.01% EDTA (1:1, v/v) per 6 cm tissue culture dish, incubated for 60 sec at room temperature, then the mixture was carefully aspirated as previously described (Wobus et al. 2002). The procedure was repeated. Thereafter, the cells were resuspended into cold Dulbecco's modified Eagle's medium (Gibco BRl, cat. No. 52100-039) with 15% FCS, the cell density was adjusted at ~$5x10^5$ cells/ml and the test-tubes were placed on ice.

For the Comet assay procedure, the protocol of the original technique described by Östling and Johanson (1984) was followed with minor modifications by (Singh et al. 1991, Morris et al. 1999, Speit et al. 2000, Ivancsits et al. 2002b). Briefly, 20 µl of cell suspension (~10 000 cells) was mixed with 200 µl prewarmed (37°C) 0.5% low melting point agarose in PBS. The cell suspension was rapidly pipetted onto slides with frosted ends precoated with 1.5% normal melting point agarose in PBS and evenly spread using a coverslip. The slides were incubated at 4°C for 15 min. to allow the microgel to solidify. Then the coverslips were removed by pulling them carefully aside. The slides were immersed in precooled (4°C) lysis solution (2.5 M NaCl, 100 mM Na_2EDTA, 10 mM Tris, 1% sodium sarcosinate, 10% DMSO, pH 10 for the alkaline Comet assay and pH 7.5 for the neutral COMET assay) and lysed for 60 min at 4°C in the dark. After lysis, the slides were removed from the lysis buffer, drained, placed into a horizontal electrophoresis tank and covered with the precooled (4°C) electrophoresis buffer (1 mM Na_2EDTA, 300 mN NaOH , pH 13 for the alkaline Comet assay and 100 mM Tris, 300 mM sodium acetate, 500 mM sodium chloride, pH 8.5 for the neutral Comet assay, respectively). After 20 min incubation for DNA

alkaline denaturation and expression of the various types of alkaline labile sites (alkaline Comet assay) and for washing away the lysis buffer and equilibration (neutral Comet assay), the electrophoresis was performed in the dark at 4°C for 10 min. The electrophoretic conditions (25 V, 300 mA, field strength 0.7 V/cm) were identical for both versions (alkaline and neutral) of the single cell gel electrophoresis assay. After removal from the electrophoresis tank, the slide surface was carefully covered 3x with a neutralization buffer (400 mM Tris, pH 7.5, 5 min. incubation), then the slides were rinsed briefly in distilled water and fixed in 100% ethanol for 5 min. The slides were air-dried at a slanted angle for at least 2 hours and stained with 50 µl ethidium bromide solution (20 µg/ml in bidistilled water). The analysis was done using the fluorescence microscope ECLIPSE E600 (Nikon, Germany), appropriate excitation and barrier filters (excitation 540-580 nM, barrier 600-660 nm) at 200 fold magnification and the imaging software Lucia (Version 4.71 for Windows). A total of 1000 nuclei were scored (500 per slide) for exposed, sham exposed and control cells and classified into 5 groups according to tail length and intensity using the classification proposed by Anderson et al. (1994): Group A corresponding to <5% DNA damage; B (5-20%); C (20-40%); D (40-95%) and E (>95%). All analyses were performed by the same investigator blind. Results were expressed as 'tail factors', calculated according to Ivancsits et al. (Ivancsits et al. 2002a; Ivancsits et al. 2002b) by the following formula: Tailfactor (%) $=AF_A+BF_B+CF_C+DF_D+EF_E/n$, where A is the number of nuclei classified to group A, F_A is the average DNA damage of group A, which is 2.5% in Anderson's classification; B is the number of nuclei classified to group B, F_B is the average DNA damage of group B (12.5%); C is the number of nuclei classified to group C, F_C is the average DNA damage of group C (30%); D is the number of nuclei classified to group D, F_D is the average DNA damage of group D (67.5%); E is the number of nuclei classified to group E, F_E is the average DNA damage of group E (97.5%); n – the number of scored nuclei (n= 1000).

The results on DNA damage in the alkaline and neutral Comet assay were obtained from 6 separate experiments. The statistical analysis was performed with the SigmaPlot for Windows Version 3.06 package (Jandel Corp.). All data are presented as mean values ± standard error of the mean (SEM). The differences between exposed, sham exposed and control cells were checked for statistical significance using the independent Student's *t* test.

2.7.6 Analysis of cardiac differentiation

Cardiac differentiation of EC or ES cells was used as a parameter of differentiation according to the embryonic stem cell test, EST (Spielmann et al. 1997), established for in vitro analysis of embryotoxic agents. Spontaneously beating cardiomyocytes were estimated at various stages after EB plating. The percentage of EB containing beating cardiomyocytes and mRNA levels of α-MHC were used for the estimation of the degree of cardiac differentiation.

2.7.7 Flow cytometric analysis of cell cycle phases

RF-EMF- and sham-exposed P19 cells were processed according to the two-step procedure of DNA staining (Sehlmeyer et al. 1996). Cells were analysed with a FACStar^{PLUS} flow cytometer (Becton Dickinson, Heidelberg, Germany). Data from 3 (22h) and 4 (40h) independent experiments with 3 to 6 parallels were subjected to statistical analysis performed with the 'ModFitLT' software (Verity Software House, Inc.).

2.8 Experiments with the human neuroblastoma cell line SY5Y (Participant 11)

2.8.1 ELF-EMF exposure setup

See 2.1.1

2.8.2 Cell culture and exposure conditions

The human neuroblastoma cell line was grown in RPMI, 10% foetal calf serum, 100 units/ml penicillin, 100 µg /ml streptomycin, and 2 mM L-glutamine at 37°C and 5% CO_2. Cells were plated one day prior to exposure at densities varying with the exposure protocol: $2.6x10^6$ cells per 100 mm dish for 16 hours exposure protocol; 2 x 10^6 cells per 100 mm dish for 48 hours exposure protocol followed by recovery of the cells immediately after the end of the exposure; and 10^6 cells per 100 mm dish when cells were exposed to the electromagnetic field for 48 hours and harvested 48 hours after the end of the exposure. This was to ensure the collection of the same amount of cells at the end of the different exposure protocols.

Human neuroblastoma cells (SY5Y) were exposed to ELF-EMF (50 Hz, powerline) in a "blind trial" system that allows direct comparison to control unexposed cells. Different exposure protocols, varying in the density of ELF-EMF and in the time of exposure, were applied: a) 2 mT magnetic flux density, intermittent exposure of 5 min on/5 min off, duration 16h; b) 1 mT magnetic flux density, intermittent exposure 5 min on/5 min off, duration 16h; c) 2 mT magnetic flux density, continuous exposure, duration 16h; d) 1 mT flux density, continuous exposure, duration 16hs; e) 1 mT magnetic flux density, continuous exposure, duration 48h. Harvesting of the cells was performed immediately after the end of exposure, unless indicated otherwise.

2.8.3 RNA preparation and Northern blot analysis

Total RNA from exposed and sham exposed SY5Y cells was extracted using RNA Fast II (Molecular Systems, San Diego, CA, USA) according to manufacturer's instructions and size fractionated on 1% agarose gel containing 2.2 M formaldehyde as described in Sambrook et al. (1989). RNA was subsequently transferred and cross-linked to a nylon membrane (Biodyne A, Pall Europe Ltd., UK). After two hours of pre-hybridisation at 65°C in 0.125 M Na_2HPO_4, 1 mM EDTA, 0.25 M NaCl, 7% SDS, 10% polyethylene glycole and 1% BSA, RNA was hybridised with 10^6 cpm/ml of ^{32}P labelled cDNA probe corresponding to the cytoplasmic domain of the human α3 (nucleotides +975/+1404; Fornasari et al. 1997) and α5 (nucleotides +1005/+1263, Chini et al. 1992) nAChR subunits and to the full length coding region of the human α7 nAChR subunit (Groot Kormelink and Luyten 1997). Following hybridisation, membrane was washed at a final stringency depending on the probe used: α3, 0.1x SSC/0.1% SDS at 50 °C; α5, 0.2x SSC/0.1% SDS at 55 °C; α7, 0.1x SSC/0.1 % SDS at 65°C.

The human Phox2a probe corresponds to the 5'UTR region (nucleotides +26/+219) obtained by digestion of the construct SacI-NcoI (Flora, 2001) with Eag I and NcoI. The human Phox2b probe corresponds to the 5'UTR specifying region (nucleotides -299/-90 with respect to the ATG; GenBank accession number NM_003924) and was obtained by RT-PCR. The primers used were: upper primer 5'-GTG CCA GCC CAA TAG ACG GAT G-3'; lower primer 5'-CTC AAC GCC TGC CTC CAA ACT G-3'. The human DβH probe (nucleotides +728/+1337; GenBank accession number NM_000787) was obtained by RT-PCR using the following primers: upper primer 5'-GCT TCT CTC GGC ACC ACA TTA TC-3'; lower primer 5'-TGA GGG CTG TAG TGA TTG TCC TG-3'. The final stringency washings were Phox2a, 0.2x SSC/0.1% SDS at 55°C; Phox2b, 0.2x SSC/0.1% SDS at 50°C; DβH, 0.1x SSC/0.1% SDS at 55°C, respectively.

After stripping the probe, blots were re-hybridised to a human 18S cDNA probe (nucleotides 715-794; Ambion, Austin, TX, U.S.A.) to check the quality of the RNAs and normalise the amount of RNA loaded.

2.8.4 Radioligand assay with ^{125}I-α Bungarotoxin and ^{3}H-Epibatidine

After the end of the exposure, the cells were detached with buffer A (50 mM Tris-HCl pH 7, 150 mM NaCl, 5 mM KCl, 1 mM $MgCl_2$, 2.5 mM $CaCl_2$, 2mM PMSF (buffer A) and centrifuged at 10000g for 60 min. The pellets were washed and then homogenised using an Ultra Turrax homogeniser in an excess of buffer A containing 10 µg/ml of a mixture of the protease inhibitors leupeptin, bestatin, pepstatin A and aprotinin in order to block possible proteolysis during the incubation time of the assays.

^{125}I-αBungarotoxin (αBgtx) was from Amershan, England, and had a specific activity of 200 Ci/mmol; ^{3}H-Epibatidine (Epi; NEN, Boston, USA) had a specific activity of 56 Ci/mmol.

In preliminary experiments we determined the affinity of ^{125}I-αBgtx by performing saturation binding experiments on the cell homogenate. The ^{125}I-αBgtx concentrations ranged from 0.1 to 20 nM, and aspecific binding was determined, after overnight incubation at room temperature, using 1 µM unlabeled αBgtx. The affinity of ^{3}H-Epi was determined by performing saturation binding experiments on the cell homogenate using ^{3}H-Epi concentrations between 0.005 and 10 nM, diluted in buffer A, and incubated overnight at 4°C.

After having determined the affinity of nicotinic ligands, the determination of the number of nicotinic receptors was performed using ^{3}H-Epi binding and ^{125}I-αBgtx-binding to membrane homogenates using saturating concentrations of nicotinic ligands (2 nM ^{3}H-Epi or 10 nM ^{125}I-αBgtx) and subtracted for the aspecific binding performed in parallel using 2 nM ^{3}H-Epi or 10 nM ^{125}I-αBgtx and 100 nM cold Epi or 1 µM cold αBgtx. For total and aspecific ^{3}H-Epi binding membranes were always preincubated with 2 mM cold αBgtx.^{125}I-αBgtx binding was performed overnight at room temperature and the ^{3}H-Epi binding overnight at 4°C. At the end of the incubation, the samples were filtered on GF/C filters and radioactivity counted in a α- or β- counter, respectively. The number of receptor present was expressed as fmol of ^{3}H-Epi or ^{125}I-αBgtx bound/mg of protein. Protein measurement was done using the BCA protein assay (Pierce) with bovine serum albumin as the standard.

2.8.5 Protein preparation and Western blot analysis

Total protein extract was prepared from sham and exposed cells by the freezing and thaw method. Briefly, cells were detached by scraping in PBS 1x and collected by centrifugation at 1000 rpm for 15 min at 4°C. The pellet was resuspended in PBS 1x containing protease and phosphatase inhibitors (purchased by SIGMA) and 20 mM Phenyl-Methyl-Sulphonyl-Fluoride (PMSF). Cells were lysed by four repeated passages between liquid nitrogen to freeze and 37°C to thaw. NaCl at a final concentration of 400 mM was subsequently added, to allow extraction of nuclear protein. Samples were incubated 10 min on ice and extract clarified by centrifugation at 14000 rpm for 30 min at 4°C in a table-top centrifuge (Eppendorf). Twenty micrograms of total extract were then separated by SDS-PAGE and transferred to nitrocellulose membrane (Schleicher & Schuell). The membranes were pre-incubated with blocking buffer (5% non-fat dry milk, 20 mM Tris-HCl pH 7.5, 150 mM NaCl, 0.1% Tween 20) for one hour, after which the primary antibodies were added at appropriate dilutions and incubated for two hours; the secondary antibodies conjugated with horseradish peroxidase were then added and incubated for one hour. The bands were revealed using Super Signal West Dura (Pierce). Standard molecular weights (New England Biolabs) were loaded in parallel.

2.9 Experiments with *Xenopus laevis* oocytes, granulosa cells of rats, HeLa cells, Chinese Hamster Ovary (CHO) cells and human fibroblasts (Participant 7)

2.9.1 ELF-EMF-exposure setup

See 2.1.1

2.9.2 ELF-EMF exposure, expression in Xenopus oocytes and RNA preparation of rCx46

The cDNA for rCx46 were subcloned in the SP64T vector for RNA transcription. SP64T contains 250 bp of the non-coding sequence from *Xenopus laevis* b-globin including a poly-A tract that increases translational efficiency. RNA was prepared by using a synthesis kit containing SP6 RNA polymerase and CAP analogue purchased from Ambion (Austin, USA). The Xenopus expressions construct was linearised with XbaI for RNA transcription. The transcript concentration was estimated spectrophotometrically and analysed on agarose gels. The oocytes were isolated from *Xenopus laevis* ovaries and stage V-VI oocytes were collected and defolliculated by collagenase treatment (5 mg/ml, 355 U/mg, 1.5 h; Worthington, Type 2) in Ca^{2+}-free ND96 solution (96 mM NaCl, 2 mM KCl, 1 mM $MgCl_2$, Na-HEPES at pH 7.4 and adjusted with sorbitol to 240 mosmol/l). An injection apparatus

(Nanoliter Injector, World Precision Instruments) was used to inject 23 nl of 25 ng/µl of Cx46 cRNA and 23 nl of DNA antisense to the endogenous XenCx38 oligo 5¢-gCT gTG AAA CAT ggC Agg Atg (500 ng/µl) (Tib Molbiol) to eliminate endogenous hemi-channel currents. Oocytes were incubated in ND96 supplemented with antibiotics (100 U/ml penicillin/streptomycin) at 17°C. During the expression period of 14h, 17h and 20h the oocytes were exposed to ELF-EMF of 50 Hz powerline or sham exposed. Field strength of 2.3 mT was either continuously or intermittently (5 min on/10 min off) applied. In a further series of experiments 1.0 mT was applied with the intermittent application protocol. For the cell-to-cell coupling assay of paired oocytes, each cell of a pair of oocytes were injected with 23 nl of DNA antisense to the endogenous XenCx38 in order to suppress endogenous coupling in addition 23 nl of rCx46 cRNA (25 ng/µl)were injected. The expressing oocytes were incubated for 16h in ND96 medium, followed by manual removal of the vitelline layers. Two oocytes were paired at their vegetal poles and incubated with ND96 at 17°C for further 8h in the ELF-EMF setup (Participant 10). During this incubation the oocytes pairs were exposed to ELF-EMF (50 Hz, powerline, 1.0 mT, intermittently (5 min on/10 min off)).

2.9.3 Electrophysiological recordings of single and paired oocytes

The two electrode voltage clamp technique was applied to measure the expressed and conducting rCx46 gap-junctional hemi-channels in single *Xenopus laevis* oocytes using a voltage-clamp amplifier Turbo TEC-10 CD (npi electronic, Tamm, Germany). Voltage protocols were applied by a Pentium 100 MHz Computer linked to an ITC-16 interface (Instrutech. Corp., NY). The following pulse protocol was used throughout the experiments: From a constant holding potential of -90 mV or -80 mV variable test potentials were applied for 15 s in the range from -110 mV to +70 mV in steps of 10 mV after repolarisation of the oocyte at a holding potential of -90 mV or -80 mV. The latter was constantly applied for at least 70s. The current signals were filtered at 1 kHz and were sampled at 0.5 or 0.25 kHz. Data acquisition and analysis were performed by using Pulse/PulseFit (HEKA, Germany), Igor Pro (Wave Metrics, USA), Origin (Microsoft), PatchMaschine (V. Avdonin, University of Iowa, USA). n denotes the numbers of individual oocytes. The data are given as mean ± s.e.m. For electrophysiological recordings on paired oocytes the setup was extended by a second amplifier and a further pair of micromanipulators /electrodes. For the pulse protocol of paired oocytes a holding potential of -40 mV, close to the resting potential, was used for both oocytes. The depolarising test pulses were applied for 5s (10s) in the range from -120 mV to +120 mV and the corresponding holding potential was held for 15s (30s). For the electrophysiological recordings the micropipettes were filled with 3 M KCl resulting in input resistances of 1-1.5 M. During the current recordings the oocytes were continuously superfused with the corresponding solution at a rate of 0.5 ml/min and all recordings were performed at room temperature (20-22°C). The standard bath was a nominal Ca^{2+}- free ND96 solution at pH 7.4. The different Ca^{2+} concentrations of ND96 were obtained by addition of suitable concentrations of $CaCl_2$ to the standard solution. For experiments on single oocytes Ca^{2+}-concentrations of 0.0, 0.25 and 0.5 mM and on paired oocytes 1.8 mM and 5 mM were used.

2.9.4 Voltage-jump current-relaxation and membrane conductance of hemi-channels

The steady-state current amplitudes were leak-subtracted and denoted as Iss. The Iss values are presented as function of driving voltage (V-Vrev). The leak current at the applied test potential V was determined by extrapolation of the corresponding current values in the range of -100 mV to -70 mV, at this voltage the voltage dependent hemi-channels are closed.. The reversal potential (Vrev) of the rCx46-mediated current was calculated by a 4-point interpolation polynom of third order. The corresponding membrane conductance G(V) was calculated from the steady-state current amplitude divided by the driving voltage (V-Vrev) and plotted as function of test potential V. In the absence of a significant time- and voltage-dependent current inactivation the corresponding G(V) values in the range of -110 mV < V < +40 mV could be fitted by a simple Boltzmann distribution according to: $G(V)=(A/(1+\exp(-(V-V1/2)zF/RT))+B)$. R, T, F have their usual meanings. V1/2 denotes the half-activation voltage at which 50% of the maximal membrane conductance is observed. z gives the number of membrane bound equivalent gating charges. The parameter A denotes the maximal membrane conductance Gmax of expressed and conducting rCx46-connexons hemi-channels and B the corresponding leak conductance of the oocyte. B is assumed to be voltage independent. For different experiments G(V) was normalised to the corresponding values

obtained at A=1 and B=0, respectively. A similar subtraction of the leak-current was considered in the experiments on paired oocytes.

2.9.5 Cell cultures

Granulosa cell line GFSHR-17 (rat) (Keren-Tal et al. 1993), HeLa cells (human), Chinese Hamster Ovary (CHO) cells and fibroblasts (human, Participant 3) were cultivated in Dulbecco´s modified Eagle´s medium F-12 Ham (DMEM-F12, Sigma Corp., USA) added with 10% fetal calfserum (FCS, Sigma Corp., USA) and 50 U/ml Penicillin, 50 µg/ml Streptomycin (Gibco BRL, G) (300 mosmol, pH 7.4). Both cell lines were incubated under an atmosphere containing 5% CO_2 at 37°C. The culture dishes (35 mm in diameter) for the measurement of the intercellular free calcium ($[Ca^{2+}]i$) contained six coverslips of 10 mm diameter. Under these conditions the cultured cells were ELF-EMF exposed (50 Hz sinusoidal, 4h - 24h, 1.0 mT, 5 min on/10 min off) or sham exposed. The culture dishes (50 mm in diameter) for the measurement of volume regulation and the Comet assay analysis for contained a coverslip of 25 x 50 mm diameter. Under these conditions the cultured cells were ELF-EMF exposed or sham exposed.

2.9.6 Measurement of [Ca2+]I

Measurement of $[Ca^{2+}]i$ was performed according to Grynkiewicz et al. (1985). For measurement of $[Ca^{2+}]i$ the cells were loaded with fura 2-AM (5 µM and 1% DMSO) for 60 min under ELF-EMF exposure. Fura 2-AM was added to the bath during an off phase of ELF-EMF exposure, respectively. After the indicated time of exposure Fura 2-Amloaded loaded cells grown on a coverslip were transferred to an exposure-free superfusion chamber mounted on an inverted Axiovert (Zeiss, Germany) microscope. The cells were superfused with a bath solution containing (in mM): 145 NaCl, 5 KCl, 2 $CaCl_2$, 1.5 $MgCl_2$, 5 glucose, 10 Hepes, (pH 7.4, adjusted with NaOH; 300 mosm) at 2 ml/min for 3 min to wash-off extracellular fura 2-AM and DMSO at room temperature. The cells were excited at 340 nm and 380 nm using a monochromator polychrome II (T.I.L.L. Photonics GmbH, Planegg; Germany) by a 75 W XBO xenon lamp and the corresponding fluorescence was registered with a digital CCD camera (C4742-95, Hamamatsu Photonics K.K.; Japan). The ratio of excitation at 340 nm to 380 nm was calculated and calibrated to determine $[Ca^{2+}]i$ using the program Aquacosmos (Hamamatsu Photonics K.K.; Japan). Measurement of $[Ca^{2+}]i$ was started about 10 min after completion of ELF-EMF exposure and recorded for 4-8 cells simultaneously. In a further series of experiments two additional stressors were applied after the period of ELF-EMF exposure, respectively. Either 200 µM H_2O_2 was added to the bath or 30 mM NaCl was replaced by KCl. The cells were superfused with the corresponding solution (2 ml/min) for 10 min. Thereafter the solution was replaced by the bath and the recording of $[Ca^{2+}]i$ started.

2.9.7 Comet assay

The granulosa cell line of rat (GFSHR-17), HeLa cells (human) and Chinese Hamster Ovary (CHO) were cultivated as described above. The cells were ELF- and sham- exposed at various frequencies using the exposure parameters 5 min on/10 min off, 1.0 mT applied during 12 to 20 hours. After exposure the Comet assay was performed as described by Ivancsits et al. (2003a, b). The viability of the cells was determined by trypan blue and only slides containing cells with a viability of more than 90% were analysed. For each experiment 3000 nuclei are scored (1000 per slide) for exposed and sham exposed cells and classified into 5 categories according to material and methods of Ivancsits et al. (2002b). The results for DNA damage in the Comet assay are obtained from at least 2 independent exposure experiments. Analysis of exposed and sham-exposed cells was performed in a double-blind approach.

2.9.8 Measurement of cell volume regulation

For measurement of the cell volume the cells were trypsinised (0.25% Trypsin, pH 7.4), collected and centrifuged for 5 min at 500 xg after ELF exposure (18h expression time, 1.0 mT, 50 Hz, 5 min on/10 min off). The pellet was resuspended in 10 ml PBS (in mM: 140 NaCl, 2.7 KCl, 8 Na_2HPO_4, 1.5 KH_2PO_4, 300 mosmol, pH 7.4). For the volume measurements, 1-2 µl of the cell suspension were placed on a cover slip in an exposure-free superfusion chamber mounted on an inverted Axiovert (Zeiss, Germany) microscope. After 5 min, the cells adhered and 2-3 ml of PBS-solution (300 mosmol) were added to the

dish. The cells were superfused with the PBS-solution (300 mosmol) and the cell volume was recorded at time intervals of 30s about 40 minutes. The cell sizes were registered with a digital CCD camera (C4742-95, Hamamatsu Photonics K.K.; Japan). After 30 sec the 300 mosmol PBS-solution was replaced by a 250 mosmol PBS-solution (or 350 mosm solution). This hypotonic (or hypertonic) solution was exchanged after 20 min by PBS-control (300 mosmol), again. The diameter of the cells of spherical shape (breath, height) were measured and the corresponding rotationellipsoid volume determined. The time dependent volume V(t) was subtracted by the basis volume V0, normalised to the maximal volume and the mean calculated.

2.10 Experiments with the human endothelial cell lines EA.hy926 and EA.hy926v1 (Participant 6)

2.10.1 RF-EMF 900 MHz GSM signal exposure system dosimetry

Cells were irradiated with a simulated mobile phone microwave radiation in specially constructed exposure system, which is based on the use of high Q waveguide resonator operating in TE_{10} mode. The irradiation chamber has been placed vertically inside a cell culture incubator with two 55 mm-diameter glass Petri dishes placed so that the E-field vector was parallel to the plane of the culture medium. Temperature controlled water was circulated through a thin (9 mm) rectangular glass-fiber-molded waterbed underneath the Petri dishes. In all experiments reported here, cells were exposed for 1 hour to 900 MHz GSM signal at an average SAR of 2.4 W/kg. SAR values ranged from 1.8 W/kg to 2.5 W/kg depending on the area of the dish, what was caused by the non-uniform distribution of the RF-EMF radiation field. The average SAR level of 2.4 W/kg was selected because it is slightly above of the safety limit for the mobile phone microwave radiation emission as defined by ICNIRP (International Commission on Non-Ionizing Radiation Protection). RF-EMF signal was generated with EDSG-1240 signal generator and modulated with pulse duration 0.577 ms and repetition rate of 4.615 ms to match the GSM signal modulation scheme. Signal was amplified with RF Power Labs R720F amplifier and fed to the exposure waveguide via monopole type feed post. The SAR distribution in the cell culture and the E-field above the cell culture were determined using computer simulations (FDTD method). The simulations were done with commercial XFDTD code (Remcom, USA) with simulation grid size of 3x3x3 mm^3 in the main grid and 1x1x1 mm^3 in sub grid, consisting of the culture dishes and part of the waterbed. The maximum SAR was obtained in the centre of Petri dish, decreasing to about 6 dB at the edges of dish. Simulation results were verified with measurements. Electric field in the air above cell cultures was measured with a calibrated miniature Narda 8021B E-field probe. The measured E-field values differed less than 15% from the corresponding simulated E-fields. The SAR distribution was measured with small, calibrated temperature probes (Luxtron and Vitek) directly from the culture medium. The measurements were done at room temperature outside the incubator with increased culture medium height, in order to reduce the measurement uncertainty at air-medium boundary. The temperature was measured (Vitek probe, BSD Medical, USA) for 10 sec. in order to limit the effect of heat convection and conduction (Moros and Pickard, 1999). The Luxtron probe has lower temperature resolution (0.1°C) compared to Vitek probe (0.001°C) and thus the temperature had to be measured for 1 min. to achieve sufficient temperature rise (1°C). Due to these short measurement times the power fed to the chamber was increased up to 25 W and the resulting SAR value was afterwards scaled down to 1 W of input power. The measured SAR values at the centre of the culture medium (3-mm depth) were 2.5 W/kg (Luxtron, USA) and 5.0 W/kg (Vitek, USA). These values can be compared to the simulated value of 2 W/kg and 3.6 W/kg, respectively, with simulation parameters changed to correspond with the measurement situation. The measured values can be considered as the upper and lower limits of SAR due to measurement uncertainties described above and thus they validate the simulations. Waveguide resonator's water-cooling system was tested with long-term temperature measurements by using Luxtron probe. The temperature was recorded twice a minute over normal 1-hour exposure period at 2 W/kg. The temperature remained at 37 ± 0.3°C during the whole measurement time. Therefore, the reported biological effects are of non-thermal nature. Additionally, human endothelial cells were also exposed to GSM 1800 MHz radiation in talk and cw mode. See also 2.1.

2.10.2 Cell cultures and exposure

EA.hy926 and EA.hy926v1 cells (gift from Dr. Cora-Jean S. Edgell, North Carolina University at Chapel Hill, NC, USA) (Edgell et al. 1983) were grown Dulbecco's MEM, supplemented with antibiotics, 10% fetal bovine serum, L-glutamine and HAT-supplement. For experiments, cells were removed from culture flasks with trypsin, washed and seeded at density of 1.2 x 10^6 cells per 55 mm-diameter glass Petri dish (900 MHz GSM exposure) or seeded at density of 0.4 x 10^6 cells per 35 mm-diameter plastic Petri dish (1800 MHz GSM signal exposure). After overnight culture semi-confluent monolayers of EA.hy926 cells were exposed to sham or RF-EMF radiation. Cell cultures for sham and irradiation were prepared in the same kind of glass dishes, derived from the same batch of cells, were seeded at the same cell density and were grown for the same period of time before experiment. The only difference between irradiated and sham samples was that the irradiated dishes resided for 1-hour in incubation chamber with RF-EMF radiation turned-on whereas sham dishes resided in the irradiation chamber for the same period of time but with irradiation turned off.

2.10.3 ^{32}P-othophosphate metabolic labelling

To determine changes in protein phosphorylation ^{32}P-orthophosphate was present in cell culture during the 1-hour sham or RF-EMF exposure. In experiments where the time-course of hsp27 phosphorylation was determined, ^{32}P-orthophosphate was present in cell cultures during the whole post-exposure incubation period. During the phosphorylation cells were incubated in culture medium consisting of phosphate-free DMEM that was supplemented with dialysed FBS and with ^{32}P- orthophosphate (NEN, Cat no. NEX-053s). Briefly, confluent monolayers of endothelial cells were washed twice with the pre-warmed (37°C) labelling medium that did not contain ^{32}P-orthophosphate, in order to wash away residual phosphates from the cell cultures. Thereafter, pre-warmed ^{32}P-orthophosphate-containing medium (5 mCi) was added to the cells and dishes were irradiated immediately for one hour. Following irradiation petri dishes were placed on ice, labelling medium was aspirated, cells were rinsed with cold PBS supplemented with protease/phosphatase inhibitors (1 mM PMSF; 0,4 mM orthovanadate) and cells were scraped and collected with ice cold PBS. From this point onwards orthovanadate was present in all solutions used to extract phosphoproteins. In experiments where the time-course of hsp27 phosphorylation was determined, ^{32}P-orthophosphate was present in cell cultures during the whole post-exposure incubation period (up to 5 hours).

2.10.4 2D-electrophoresis - for protein phosporylation studies

Cells were harvested, washed once with ice cold PBS containing 1mM PMSF and lysed on ice for 10 minutes in buffer consisting of 9.5 M Urea, 2% CHAPS, 0.8% Pharmalyte pH 3-10 and 1% DTT. Lysates were cleared of debris by centrifugation 42000 xg at +15°C for 1 hour. The pellet containing insoluble debris was discarded and supernatant was collected and its protein concentration was measured with the Bradford method. Proteins in the lysates were separated using standard 2D-electrophoresis method - isoelectrofocusing (IEF) in the first dimension and SDS-PAGE in the second dimension.

1st-dimension isoelectric focusing

The 125 ug protein was applied to the groove of the re-swelling tray that contained 11 cm-long IPG strip with pH range of 3-10 (APBiotech, Sweden). The IPG strips were incubated overnight with the protein lysate solution. The proteins in IPG strips were separated by isoelectrofocusing (IEF) using the programmable power supply with the following protocol:

- 300 V, 1 W, 1 mA for 6 minutes at 20°C
- 3500 V, 1 W, 1 mA for 6 minutes at 20°C
- 3500 V, 1 W, 1 mA for 24 hours at 20°C

After completion of the IEF-separation the strips were equilibrated for 10 minutes on a rocking platform in solution-I consisting of urea (6 M), glycerol (30% w/v), SDS (2% w/v), DTT (100 mg/10 ml) in 50 mM Tris-HCl buffer pH 8.8 with a trace of bromphenol blue (migration marker). Thereafter, the strips were placed in a solution-II that contained iodocetamide (480 mg /10 ml) instead of DTT and equilibrated on a rocking platform for another 10 minutes at room temperature.

2nd-dimension SDS-PAGE

Equilibrated IPG strips were attached on the top of 8% SDS-PAGE gel with melted agarose to ensure firm contact. Gels were run with 40 mA/gel for ca. 2.5 hours at 4°C.

After completion of the electrophoretic separation gels were silver stained using Morrissey's modification of the Merril's method and images for computerised analysis were acquired into PC using the Bio-Rad GS-710 densitometer.

2.10.5 ^{32}P-autoradiography

2D-gels, containing metabolically ^{32}P-labelled phosphoproteins, were dried in gel dryer and used for autoradiography. Images generated on X-ray films were acquired into PC for computerised analysis using the Bio-Rad GS-710 densitometer.

2.10.6 2D-electrophoresis - protein expression screening

Immediately after the end of the exposure to 900 MHz GSM mobile phone radiation-like signal at the average specific absorption rate (SAR) of 2.4 W/kg cells were placed on ice, washed with ice-cold PBS and lysed with buffer consisting of: 7 M urea, 2 M thiourea, 4% chaps, 2% IPG buffer pH 3-10 NL, and 1% dithioreitol (DTT), 1 mM sodium orthovanadate and 1 mM PMSF. Protein concentration in lysates was measured using Bradford-method and 175 µg of total protein was used for 2-DE.

IEF was performed using IPGphor apparatus and non-linear pH 3-10 18 cm long IEF strips (Amersham Biosciences, Sweden). The samples were loaded using in-gel rehydration in a buffer containing 9 M urea, 2% chaps, 0.2% DTT, 0.5% IPG buffer pH 3-10 NL for 12 hours. IEF was run at 20°C using step-and-hold and gradient methods as follows: 30 V - 2 hrs, 100 V - 0.5 hrs, 300 V - 0.5 hrs, 600 V - 0.5 hrs, 1500 V - 0.5 hrs, 8000 V gradient 4 hrs, 8000 V - until the 65000 volt-hours were achieved.

For SDS-PAGE the IEF strips were equilibrated for 15 min with 6 M urea, 30% glycerol, 50 mM Tris-HCl pH 8.8, 2% SDS, and 10 mg/ml DTT for 15 min and then for another 15 min in the same buffer 25 mg/ml iodoacetamide replacing DTT. SDS-PAGE was run in 8% gel using Protean IIxi Multicell apparatus (Bio-Rad, UK) and a constant current of 40 mA/gel at 10°C.

After electrophoresis gels were fixed with 30% ethanol and 0.5% acetic acid overnight, washed with 20% ethanol and ddH_2O, sensitised with sodium thiosulfate (0.2 g/l), incubated in silver nitrate solution (2 g/l) and developed in a solution of potassium anhydride (30 g/l), 37% formaldehyde (0.7 ml/l) and sodium thiosulfate (0.01 g/l). The development was stopped with Tris (50 g/l) and acetic acid (0.05%) solution. Silver stained gels were stored in ddH_2O at 4°C. The gels were scanned using GS-710 densitometer (Bio-Rad, UK).

The MALDI-MS analysis service was purchased from the Protein Chemistry Laboratory of the Institute of Biotechnology at the Helsinki University, Finland. The spots were reduced with DTT and alkylated with iodoacetamide before overnight digestion with trypsin (Sequencing Grade modified Trypsin, promega, USA). The peptide mixture was concentrated and desalted using Millipore ZipTip^{TM} µ-C18 pipette tips. The peptide mass fingerprints were measured with Bruker Biflex^{TM} MALDI-ToF mass spectrometer in a positive ion reflector mode using α-cyano-4-hydroxycinnamic acid as a matrix. The MALDI spectra were internally calibrated with the standard peptides, angiotensin II and adrenocorticotropin-18-39. The database searches were performed using ProFound (http://prowl.rockefeller.edu/cgi-bin/ProFound) and Mascot (http://www.matrixscience.com) searches.

2.10.7 Western blotting

Immediately after the completion of 2D-electrophoretic separation of protein lysates, gels were placed into the transfer buffer (25 mM Tris, 192 mM glycine, 20% methanol and 0.1% SDS) and blotted onto PVDF membrane (Bio-Rad) using Novablot semi-dry blotting apparatus (APBiotech, Sweden). The transfer of proteins on the membrane was performed with current of 0.8 mA/cm^2 for 45 minutes at room temperature. Following transfer, the membranes were blocked overnight at 4^{o}C in Tris-buffered-saline (TBS, pH7.4) containing 5% of non-fat milk proteins. The expression of Hsp27, MAP p38 kinase and protein phosphatase-1α was detected in western blot membranes by ECL method using specific polyclonal antibodies, peroxidase-conjugated second antibody and West Pico ECL kit (Pierce, USA).

2.10.8 Immunoprecipitation

Immunoprecipitation experiments were performed using cells that were metabolically labelled with ^{35}S-methionine (APBiotech, Sweden) as follows. Briefly, confluent EA.hy926 monolayers were washed twice with the pre-warmed (37°C) labelling medium (phosphate-free) to remove phosphates. After completion of washing, the pre-warmed ^{35}S-methionine-containing (2 mCi) labelling medium was added to culture dishes and cells were allowed to incorporate ^{35}S-methionine overnight. Then, ^{35}S-methionine-containing cultures were irradiated for 1 hour. After the end of irradiation dishes were placed on ice, cells scraped in 1 mM PMSF containing PBS and used in immunoprecipitation. In experiments where the time-course of protein expression changes was determined the ^{35}S-methionine was present in the cell cultures during the whole post-exposure incubation period (up to 8 hours). Harvested cells were lysed in ice-cold RIPA buffer. Lysates were centrifuged 10000 xg at 4°C for 10 minutes to remove debris and lysates' protein concentration was measured with the Lowry-Ciocalteau method. Samples containing 230 µg of proteins were placed in eppendorf tubes and pre-cleared with 2.3 µg of non-immune goat IgG (Santa-Cruz, USA; sc-2028) and 20 µl of recombinant-Protein-G-conjugated Sepharose-4B (Zymed, USA, Cat. no. 10-1242) at 4°C on a shaker for 30 minutes. After pre-clearing the Sepharose-beads were removed by centrifugation (1000 xg; 4°C; 10 min) and selected proteins (hsp27, MAP p38 kinase, protein phosphatase-1α) were immunoprecipitated with 2 µg of specific antibody and 20 µl of recombinant-Protein-G-Sepharose-4B-conjugate (overnight at 4°C on a shaker). Thereafter, beads were collected by centrifugation, washed 4 times with RIPA buffer, dispersed in the electrophoresis sample buffer, boiled on water-bath for 3 minutes and proteins released from the beads were resolved using 8% SDS-PAGE gel (40 mA/gel). Gels were stained with coomassie blue, dried between cellophane sheets and exposed with X-ray film for different periods of time to detect the ^{35}S-methionine labelled immunoprecipitated proteins.

2.10.9 cDNA Expression Arrays

Total RNA isolation

For the isolation of total RNA from RF- or sham-exposed cells we used NucleoSpin RNA II kit (Clontech, USA). Briefly, confluent cell cultures we directly lysed on glass culture dishes. RNA, from the cleared cell lysates, was directly immobilised in Spin columns provided by the manufacturer. After DNAse treatment the total RNA was eluted from the columns and analysed for the possible remaining DNA contamination by PCR using b-actin primers against genomic DNA. RNA from several independent experiments were pooled and stored at -80^{o}C for further use.

Probe synthesis and analysis of gene expression

For the synthesis of cDNA probes and differential analysis of gene expression we used Atlas Pure Total RNA Labelling System (Clontech) and Atlas cDNA Expression Arrays (Clontech), respectively. In this system mRNA was enriched from the total RNA by binding it to Streptavidin-biotin-oligo- (dT) coated magnetic beads. After enrichment of the mRNA they were reverse transcribed to radioactive cDNA probes directly when still bound to magnetic particles. Purified probes were hybridised with Atlas filters containing complementary cDNA spots and analysed by autoradiography. AtlasImage 2.0 software was used for the differential gene expression analysis of autoradiograms.

2.10.10 Cell cycle analysis

Cell cycle distribution among the EA.hy926 cells was detected by staining the DNA with propidium iodide followed by flow cytometry analysis. Briefly, cells were collected by centrifugation, washed once with phosphate-buffered saline (PBS) and fixed in 90% methanol on ice for 10 min. After fixation, the cells were washed twice with PBS and suspended in RNAse solution in PBS (100 units/ml) and incubated at 37^{o}C for 30 minutes. At this point the propidium iodide solution (10 mg/ml in PBS) was added to the cells in RNAse solution, and the incubation was continued on ice overnight. Upon termination of incubation, cells were washed once with PBS and analysed by FACScan (Becton Dickinson, USA).

2.10.11 Caspase-3 activity

Caspase-3 activity was detected in non-fixed cells using CaspaTaq Caspase-3 Activity Kit (Intergen, USA). The active caspase-3 molecules are labelled in cells with a green fluorescent probe (FAM-DEVD-FMK) which only binds to the active caspase-3. Dead cells were excluded from the analysis by staining with propidium iodide that, when used with non-fixed cells, labels only cells with permeable membrane (necrotic or late apoptotic cells). The cell cultures were either sham- or RF-EMF-exposed with or without staurosporin (positive control of caspase-3 activation). Activity of caspase-3 was analysed either immediately after the exposure or 4h to 24h after exposure. Fluorescent content of the cells was analysed by flow cytometry with Lysys II software (Becton-Dickinson, USA).

2.10.12 Immunhistochemistry

A standard indirect immunofluorescence method was used for immunohistochemistry. Cells were washed twice with PBS and fixed in cold 3.7% paraformaldehyde in fixing buffer (0.1 M Pipes, 1 mM EGTA, 4% polyethyl glycol 8000, 0.1 M NaOH pH 6.9) overnight at 4°C. After fixing cells were rinsed twice with PBS, permeabilised with 0.5% Triton X-100 in fixing buffer 10 min, rinsed with PBS and permeabilised with 0.1% sodiumborohydride in PBS. After permeabilisation cells were rinsed with PBS and blocked with 5% BSA in PBS for 30 min. The primary antibody (Hsp27 StressGen, Canada) was incubated for an hour as well as the TRITC-labelled secondary antibody (DAKO, Denmark). After antibody incubations cells were rinsed with PBS and stained with Alexa Fluor 488 phalloidin for 30 min. Specimens were observed using a Leitz fluorescense microscope and computerized image acquisition system (Metafer, Germany)

2.10.13 Image analysis

Images of 2D-gels and X-ray films were analysed with the PDQuest 6.1.0/6.2.0 software (Bio-Rad, UK) or Phoretix 1D Advanced 5.0 (Nonlinear Dynamics, USA).

2.10.14 cICAT method

Protein Labelling and Purification

1 mg each of sample (talk and cw exposed) was labelled separately using the acid cleavable isotope-coded affinity tag (cICAT) reagent (Applied Biosystems, USA) following the vendors protocols as has been described (Burlingame). Briefly, the protein samples were separately reduced at cysteine residues using Tris (2-carboxyethyl) phosphine (TCEP, Pierce, USA), and the free sulfhydryl groups labelled using either the normal ($C^{13}(0)$) cICAT reagent, or the isotopically heavy ($C^{13}(9)$) cICAT reagent containing nine C^{13} atoms. The samples were then combined, enzymatically digested using trypsin (Promega, USA) and the resulting peptides were fractionated using strong-cation exchange (SCX) HPLC. The SCX HPLC was carried out on an Integral HPLC system (Applied Biosystems, USA) using a 2.1 mm x 250 mm polysulfoethyl A SCX HPLC column (PolyLC). The A buffer was 5 mM KH_2PO_4/25% acetonitrile pH 3.0 and the B buffer was 5 mM KH_2PO_4/25% acetonitrile pH 3.0 containing 300 mM KCl. The peptides were eluted and collected in one minute fractions using a gradient profile of 0-25% B over 30 minutes, followed by 25-100% B over 20 minutes, followed by washing of the column for 10 minutes at 100% B. Collected peptide fractions were affinity purified using avidin chromatography columns. The purified, labelled cysteine-containing peptides were then subjected to an acid incubation to cleave the biotin affinity tag from the peptides (Burlingame). The cleaved samples were then separated using offline microcapillary reverse-phase liquid chromatography (μLC) with collection in one minute fractions onto a MALDI sample target using a 180 μm x 15 cm reverse phased column home-packed with 5 μm, 300 Å C18 material (Magic, Michrom Inc., USA) and an Ultimate capillary LC system coupled to a Probot sample spotter (Dionex, USA). The MALDI matrix α-cyanohydroxycinnamic acid (CHCA, Agilent, USA) was automatically added to the eluent at each spot on the sample plate.

Automated mass spectrometric analysis

After μLC fractionation to the MALDI sample plate, the samples were analysed using an abundance-ratio dependent methodology on a oMALDI qQTOF mass spectrometer (oMALDI Qstar, MDS-Sciex/Applied

Biosystems). First, a single-stage mass spectrum of each sample spot on the plate is acquired for 30 seconds at each spot. The relative intensity ratios, as well as singlet peaks for all of the detected, cICAT labelled peptides are then automatically calculated using an automated software algorithm. Those peptides showing $C^{13}(0):C^{13}(9)$ relative intensity ratios of >1.7 or <0.6 were outputted to an inclusion list for identification by tandem mass spectrometry (MS/MS). All those peaks identified as singlets (i.e. no matching $C^{13}(0)$ or $C^{13}(9)$ peak) were also selected for MS/MS analysis. The peptide masses contained in the inclusion list at each sample spot were then analysed by MS/MS analysis, using one minute data acquisition time for each peptide.

Sequence database searching and quantitative analysis

The acquired MS/MS data were searched against the human protein sequence database maintained at the National (USA) Cancer Institute using the search program Sequest. For all MS/MS data, the search was run with no enzyme constraint, or amino-acid composition constraint (i.e. only those sequences containing cysteine), and a mass tolerance of 0.1 Da was used for the precursor peptide mass. A differential mass addition to cysteine of 227.13 was indicated in the search parameters for the $C^{13}(0)$ reagent, and 236.16 for the $C^{13}(9)$ reagent. Only matches to peptide sequences containing cysteine were kept after the database search. The results were further statistically scored using a recently described statistical algorithm for validation of sequence database search results. Only those peptides having a confidence score of 0.85 or greater using this tool were considered to be accurate matches. The quantitative $C^{13}(0)/C^{13}(9)$ values determined by the automated software described above were matched to each identified peptide, and these ratios were each checked for accuracy by manual inspection of the raw mass spectral data.

2.11 Effects of ELF-EMF and RF-EMF on gene expression in human cells analysed with the cDNA array (Participant 12)

2.11.1 ELF-EMF and RF-EMF exposure setups

See 2.1

2.11.2 Cell cultures and RNA isolation

See reports of the REFLEX Participants who provided samples for this investigation.

2.11.3 RZPD cDNA arrays

The whole-genome Human Unigene RZPD-2 cDNA array contains about 75,000 cDNA clones (I.M.A.G.E. clone collection), the Mouse Unigene RZPD-1 array about 25,000 clones, each selected from UniGene clusters (group of Bernhard Korn (RZPD), see also: http://www.ncbi.nlm.nih.gov/entrez/query.fcgi?db=unigene). The cDNA products were PCR amplified by M13 forward and reverse standard primers and spotted in duplicates on 22 x 22 cm nylon membranes (mouse: 1 part, human: 3 parts) in a 5 x 5 pattern (group of Uwe Radelof (RZPD), see also Boer et al. (2001) Genome Res. 11, 1861-1870). Each 5 x 5 field contained 11 genes spotted in duplicates as well as the E.coli kanamycin gene (1 spot) and an Arabidopsis gene (2 spots) as "empty" spots for background subtraction during data analysis. For quality control, M13 forward and reverse primers were end labelled with ^{33}P gamma ATP and hybridised to each membrane to control of all filters of the same robot run were spotted even and complete. After quality control, the membranes were stripped and used for complex hybridisation after about 6 weeks. Only filters from the same robot run containing comparable concentrations of PCR products representing single genes or ESTs were used for hybridisation with the different samples to be compared. One individual hybridisation experiment was done on the same filter batch with all 4 samples. Repetitions, however, were performed with different filter batches to exclude biases caused by using filters from only one robot run.

2.11.4 Hybridisation of global cDNA arrays and image analysis

RNA was isolated from exposed and as a control sham-exposed cells from different cell lines (Table 1). RNAs coming from individual experiments were checked separately for degradation (28S/18S rRNA ratio 1.5-2.0) and concentration (at least 1 µg/µl in H2O) with the Bioanalyzer (Agilent). Afterwards, RNAs from 2 individual exposures were pooled for each hybridisation sample in same concentrations. Hybridisation was performed according to Boer et al. (2001) with minor modifications: 10 µg of total RNA per sample was reversely transcribed using (dT)18 primer and 33P alpha-dCTP without amplification (Superscript II reverse transcriptase, Invitrogen) and purified. The labelled cDNA was hybridised with the arrays. The hybridisation solution contained 6 x SSC/5 x Denhardt's, as well as Cot-1 DNA (Invitrogen Co., Germany) and (dA)40 oligonucleotide for blocking. After exposition of the hybridised membranes, the PhosphorImager screens were scanned (Fuji FLA-3000, 100 µm resolution, Fuji BAS-reader software). The primary image analysis (estimation of nVol grey level values for each individual spot) was done by the help of the ArrayVision software package (Interfocus), which had been adjusted to the 5x5 array before. The background was corrected locally in each 5x5 field by subtracting the empty spot signal (average signal of 3 spots, see above). Normalisation was done via the average signal intensity (without empty spots) on the whole membrane. Two independent hybridisations were performed for each experiment (4 data points per gene because of spotting of each gene in duplicates).

2.11.5 Pre-processing (data cleaning) and Modified SAM method (and Selective SAM method)

Original expression profiling data ("control" data *ctrl*, related to gene expression without the applied EMF, and "exposed" *exp*, related to gene expression after EMF exposure) were normalised and the background was removed as mentioned above. For each experiment (Table 1) at least two hybridisations were performed. In a first pre-processing, signals were removed giving a zero or an infinite ratio (*ratio = exp/ctrl*), that could lead to a reduction of the available measurements for some genes.

Table 1. Gene expression profilings on human and mouse global cDNA arrays

Cell line	Exposition	Exposure experiments/ profiling	Array	Participant
ES-1	ELF/EMF: 50 Hz, 1 mT	4	Human	3
human primary fibroblasts	5 min ON, 10 min OFF, 24 h		Unigene RZPD-2	
ES-1	ELF/EMF: 50 Hz, 1 mT	4	Human	3
human primary fibroblasts	5 min ON, 10 min OFF,15 h		Unigene RZPD-2	
SY5Y	ELF/EMF: 2 mT	4	Human	11
human neuroblastoma	5 min ON, 5 min OFF, 16 h		Unigene RZPD-2	
ES	ELF/EMF: 50 Hz powerline	3	Mouse	4
mouse embryonic stem cells	2.3 mT		Unigene RZPD-1	
NB69	RF/EMF: 1800 MHz (GSM Basic)	2	Human	5
human neuroblastoma	SAR 2 W/kg		Unigene RZPD-2	
	5 min ON, 10 min Off, 24h			
EA.hy926	RF/EMF: 900 MHz, GSM	2	Human	6
human endothelial	SAR 1.8-2.5 W/kg, 1h		Unigene RZPD-2	
EA.hy926	RF/EMF: 1800 MHz, GSM	2	Human	6
human endothelial	SAR 1.8-2.5 W/kg, 1h		Unigene RZPD-2	
EA.hy926	RF/EMF: 1800 MHz, GSM	2	Human	6
human endothelial	SAR 1.8-2.5 W/kg, 1h		Unigene RZPD-2	
T-lymphocytes	RF/EMF: 1800 MHz	2	Human	8
human, quiescent	DTX only		Unigene RZPD-2	
from peripheral blood	SAR 1.4 W/kg			
	10 min ON, 20 min OFF, 44 h			
	(RNA prepared in Heidelberg)			
U937	RF/EMF	5	Human	9
human lymphoblastoma	GSM-900 MHz		Unigene RZPD-2	
	2 W/kg, 1 h			
CHME5 (µglie)	RF/EMF	5	Human	9
human microglial	GSM-900 MHz		Unigene RZPD-2	
	2 W/kg, 1 h			
HL-60	RF/EMF: 1800 MHz	3	Human	2
human hematopoietic	DTX		Unigene RZPD-2	
	SAR 1.0 W/kg			
	5 min ON, 5 min OFF, 24 h			
HL-60	RF/EMF: 1800 MHz	3	Human	2
human hematopoietic	DTX		Unigene RZPD-2	
	SAR 1.3 W/kg			
	continuous waves, 24 h			
HL-60	RF/EMF: 1800 MHz	3	Human	2
human hematopoietic	DTX		Unigene RZPD-2	
	SAR 1.3 W/kg			
	continuous waves, 24 h			

2.11.6 Biostatistics (Dr. Daniel Remondini, Participant 8)

The statistical analysis to find those genes that significantly changed their expression level between the ctrl and the exp state was done as follows: In order to increase the statistical significance of the test, we considered only those genes with *NG* = 4 "good" measurements (both for ctrl's and exp's). The genes of each experiment were kept separated in 3 different groups, related to each part (nylon membrane) they belonged to ("Part 1", "Part 2", "Part 3"). Normalisations and analysis were performed on each part separately, in order to avoid possible biases due to different behaviour of the arrays during hybridisation or scanning. Data were processed in order to evaluate and reduce possible artefacts due to the array reading procedure:

- as a first step, data were rescaled by means of a cubic root function in order to gather the data in a smaller interval: $ctrl' = \sqrt[3]{ctrl}$, $\exp' = \sqrt[3]{\exp}$;

- the averages of all 8 measurements for each gene were taken as a "reference" set. A scatter plot was made of each measurement (ctrl or exp) versus the reference set, and the resulting plot was fitted linearly. On the basis of the fit parameters a rescaling was performed on data if they were not on a Y=X curve.

The "interesting" genes were found by calculating a normalised difference *diff(i)* between exp and ctrl values for each gene *i*:

$$diff(i) = \frac{E[\exp(i)] - E[ctrl(i)]}{\sqrt{\frac{\sigma_{ctrl}^{2}}{NG-1} + \frac{\sigma_{\exp}^{2}}{NG-1}} + s_0},$$

where "E[]" denotes "expected value of ", and s_0 is a correction term that removes possible divergences in the denominator, calculated as the median of the σ_i distribution for each gene (ctrl and exp distributions were merged). For a first selection, genes were considered outliers if they exceeded the threshold of 3σ calculated from the resulting distribution of *diff(i)*.

To increase the robustness of our selection, following the bootstrapping procedure as shown in [PNAS 2001, Vol. 98 no. 9, pg. 5116-5121], new datasets were generated as permutations of the original ones, and the same analysis was performed over these datasets, ranking the differences $diff_p(i)$ (p referring to the p-th permutation) from larger to smaller. A plot of *diff(i)* vs. $E[diff_p(i)]$ was generated for each group of genes, and the interesting genes were chosen as those that significantly deviated from the y=x line: the distance of *diff(i)* from the y=x line, defined as *dist(i)*, was to be larger than a threshold value Δ=1.2.

Finally, the outlier genes selected for each part in each experiment were chosen from the intersection between the initial outliers ($|\text{diff(i)}| \geq 3\sigma$) and those from the bootstrapping procedure ($|dist(i)| \geq \Delta$). In this way the outlier selection results more selective than just applying the technique as shown in [PNAS 2001, Vol. 98 no. 9, pg. 5116-5121].

2.11.7 Data mining

The ratio of the spot-to-spot comparison was taken for further analysis, without values smaller than 0.001 or bigger than 1,000, respectively, which were eliminated before. Since each PCR fragment was spotted twice on each membrane, and each hybridisation experiment was performed twice, four ratios went into an own database tool (Martin Holst, access database program, Microsoft) to make an analysis in a non-statistical manner: All eight values coming from two hybridisations had to show the same tendency to be taken over in the final list showing clones appearing up- or down-regulated in both experiments. The clones of this list were connected to the gene ontology data via a Stanford database (http://genome-www5.stanford.edu/cgi-bin/SMD/source//sourceBatchSearch) according to IMAGE IDs. With the help of these data and a text query tool (Microsoft Excel, Matthias Schick) regulated genes belonging to certain gene families of interest could be extracted manually. The same procedure was applied on genes extracted by bio-statistical analysis.

3.0 RESULTS

The studies in REFLEX cover a wide range of frequencies within the spectrum of electromagnetic fields (EMF). Based on the assumption that possible biological effects may be generated by EMF in a different way dependent on their frequencies the results of the REFLEX project are reported separately for extremely low frequency electromagnetic fields (ELF-EMF) and radio frequency electromagnetic fields (RF-EMF).

3.1 Results in ELF-EMF research

3.1.1 Genotoxic effects

3.1.1.1 Human fibroblasts, lymphocytes, monocytes, melanocytes and muscle cells and granulosa cells of rats (Participant 3)

Intermittent ELF-EMF exposure, but not continuous ELF-EMF exposure induced DNA strand breaks in human fibroblasts.

In the first set of experiments fibroblasts were continuously exposed to ELF-EMF at 1000 µT for 24h. In these experiments significant differences in DNA-breaks between exposed and sham-exposed cells were observed neither with the alkaline nor with the neutral Comet assay. As Nordenson et al. (1994) reported positive genotoxic effects applying intermittent field exposure, our next experiments concentrated on exposures at different intermittence conditions. Intermittence of 5 min on/5 min off and 15 min on/15 min off revealed an increase of DNA-breaks in both, the alkaline and the neutral Comet assay, compared to sham-exposed cells, whereas at 5 min on field/25 min off field did not enhance the frequency of DNA-breaks (Tables 2, 3).

Table 2. Mean values of alkaline Comet tailfactors at different exposure conditions (n = 2), cell strain IH-9

Alkaline Comet Assay - different exposure conditions				
	exposed		sham	
	Comet tailfactor %	±SD[#]	Comet tailfactor %	±SD[#]
Continuous exposure (24h)	4.29	0.02	4.27	0,03
15'/15' on/off	6.47*	0.14	4.23	0.05
5'/5' on/off	6.98*	0,04	4.41	0.16
5'/10' on/off	7.47*	0.13	4.48	0.05
5'/15' on/off	6.68*	0.17	4.42	0.03
5'/20' on/off	5.90*	0.12	4.38	0.12
5'/25' on/off	4.27	0.04	4.23	0.03
1'/10' on/off	5.89*	0.19	4.21	0.14
3'/10' on/off	6.60*	0.06	4.19	0.22
10'/10' on/off	6.91*	0.07	4.24	0.07
15'/10' on/off	6.56*	0.15	4.11	0.08
25'/10' on/off	5.37*	0.05	4.21	0.04

[#] SD indicates standard deviation

* indicates significant differences ($p < 0.05$) exposed vs. sham

Table 3. Mean values of neutral Comet tailfactors at different exposure conditions (n = 2), cell strain IH-9

Neutral Comet Assay - different exposure conditions				
	exposed		sham	
	Comet tailfactor %	±SD[#]	Comet tailfactor %	±SD[#]
Continuous exposure (24h)	4.20	0.03	4.17	0.05
15'/15' on/off	5.72*	0.01	4.25	0.04
5'/5' on/off	6.09*	0.02	4.31	0.08
5'/10' on/off	6.21*	0.01	4.35	0.07
5'/15' on/off	5.66*	0.06	4.23	0-13
5'/20' on/off	4.52	0.16	4.50	0.21
5'/25' on/off	4.25	0.05	4.34	0.07
1'/10' on/off	4.16	0.15	4.16	0.13
3'/10' on/off	5.94*	0.05	4.20	0.06
10'/10' on/off	6.19*	0.11	4.11	0.11
15'/10' on/off	6.02*	0.03	4.21	0.10
25'/10' on/off	5.44	0.01	4.15	0.01

[#]SD indicates standard deviation
* indicates significant differences ($p < 0.05$) exposed vs. sham

Based on these findings, we tried to find out the optimal exposure conditions for maximal effects on DNA strand break levels. We started with a fixed field-on time of 5 min and varied field-off times from 5 to 25 min. These experiments indicated that DNA strand break levels (SSB and DSB) culminated at an off-time of 10 min and reached control levels at extended off-times (Figure 7). Significant differences ($p< 0.01$) between exposed and sham-exposed cells were found at 5 min on/5 min off, 5 min on/10 min off, 5 min on/15 min off and 5 min on/20 min off intermittence for alkaline Comet assay and at 5 min on/5 min off, 5 min on/10 min off and 5 min on /15 min off intermittence for neutral Comet assay, but not at 5 min on/ 25 min off for both assays.

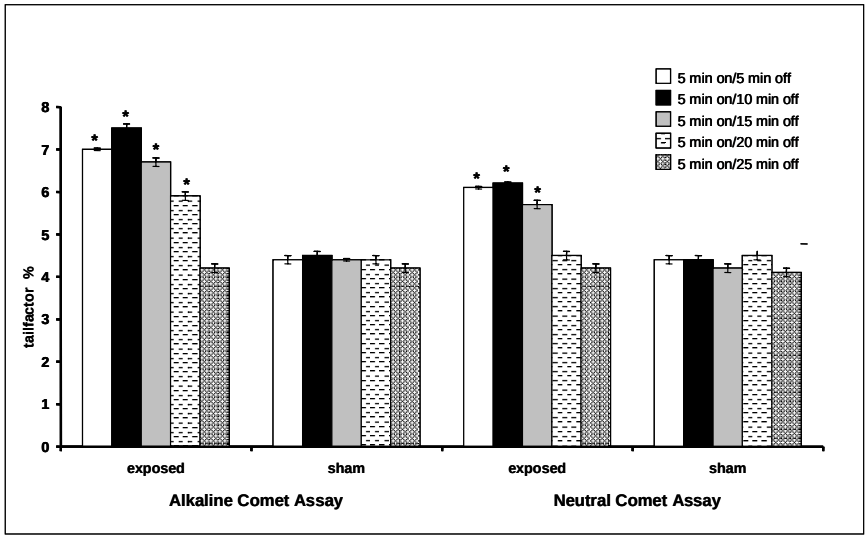

Figure 7. Alkaline and neutral Comet Assay tailfactors of ELF exposed fibroblasts (cell line IH-9, 50 Hz sinus, 24h,1000 µT, intermittent) - variation of off-time. * $p<0.01$ exposed versus sham-exposed

Subsequently, a fixed off-time of 10 min was chosen and on-times have been varied from 1 to 25 min. Again, the highest level of DNA strand breaks was obtained at an intermittence of 5 min on/10 min off (Figure 8). Comet tailfactors of exposed and sham-exposed cells differed significantly at each on-time in

alkaline Comet assay and at 3 to 15 min on in the neutral Comet assay. Solely the alkaline Comet tailfactors of 5 min on/10 min off, 5 min on/25 min off and 25 min on/10 min off-EMF exposed cells differed significantly to the other applied intermittence conditions. Since an intermittence of 5 min on/10 min off was able to induce the highest levels of DNA strand breaks in both alkaline and neutral Comet assay, further experiments were performed at 5 min on/10 min off.

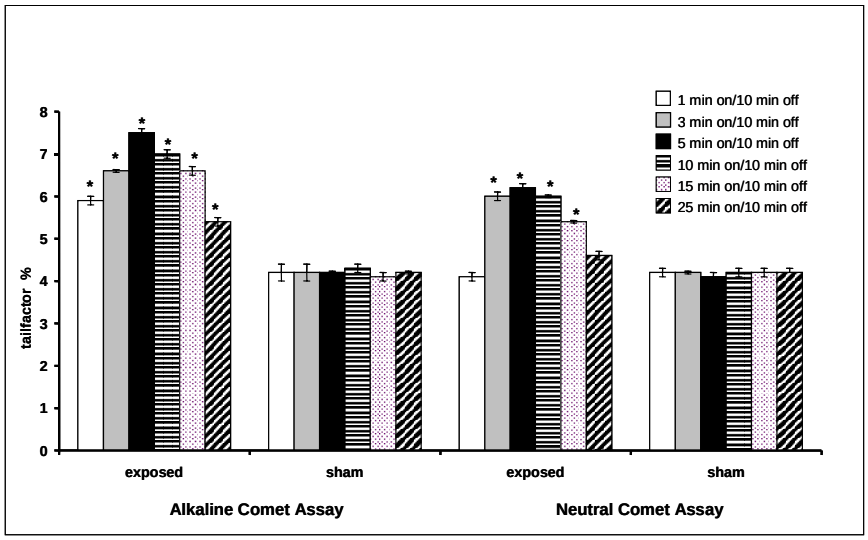

Figure 8. Alkaline and neutral Comet assay tailfactors of ELF exposed fibroblasts (cell line IH-9, 50 Hz sinus, 24 h, 1000 µT, intermittent) - variation of on-time. * $p < 0.01$ exposed versus sham-exposed

ELF-EMF 50 Hz sinus generated a higher rate of DNA strand breaks in human fibroblasts than ELF-EMF powerline.

By comparing 50 Hz sinus to the 50 Hz powerline signal it was found out that at 50 Hz powerline Comet assay tailfactors were significantly lower than at 50 Hz sinusoidal (Figure 9). All further experiments in the ELF-EMF range were, therefore, carried out with 50 Hz sinus.

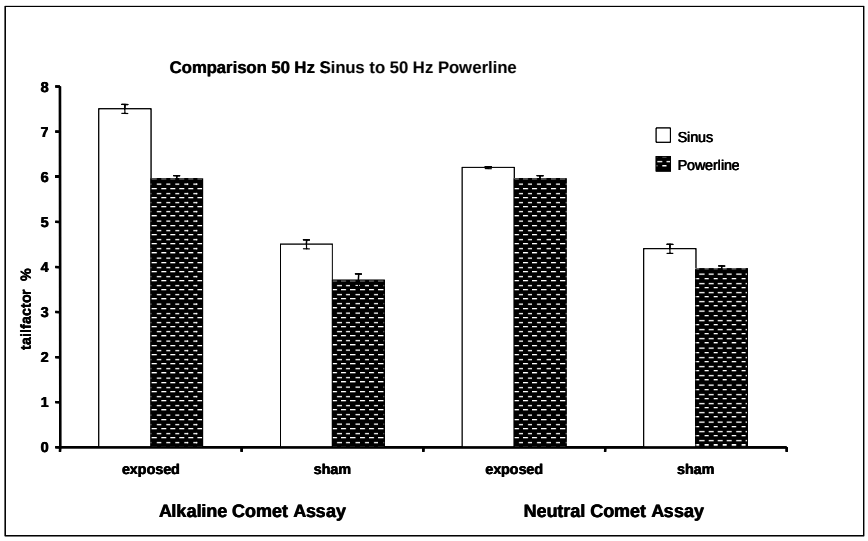

Figure 9. Alkaline and neutral Comet Assay tailfactors of ELF exposed fibroblasts (cell line IH-9, 24 h, 1000 µT, intermittent)

Genotoxic effects were frequency dependent.

In order to investigate the frequency dependence of genotoxic effects of ELF-EMF (1 mT, 5 min on/ 10 min off) cultured human fibroblasts were exposed to different frequencies (3-550 Hz). Exposure time was set to 15 hours. Genotoxic effects were evaluated using the alkaline Comet assay. Figure 10 presents the tailfactors in exposed and sham exposed cells. Significant increases in DNA damage could be found at 3 Hz, 16 2/3 Hz, 30 Hz, 50 Hz, 300 Hz, and 550 Hz. Effects on strand break levels varied with the applied frequencies and could be ranked as follows: 50 Hz > 162/3 Hz > 3 Hz > 300 Hz > 550 Hz > 30 Hz. Quite obviously, the extent of induced DNA damage did not correlate with the applied frequency.

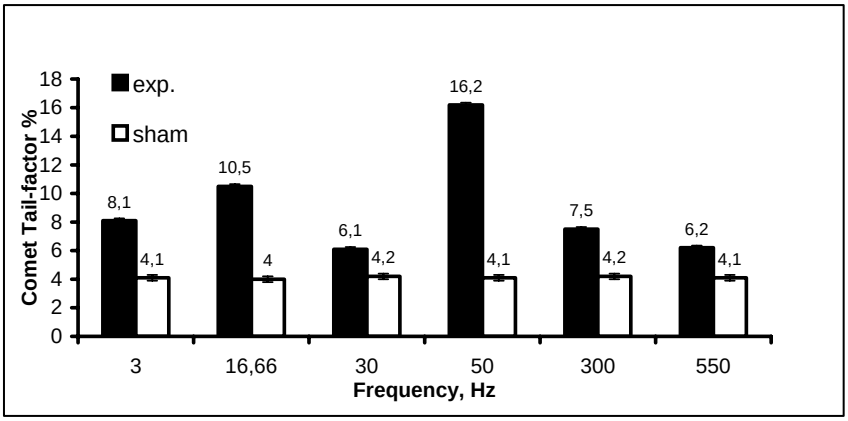

Figure 10. Alkaline Comet Assay tailfactors of ELF-EMF exposed and sham exposed fibroblasts (cell line ES-1, 15 hrs, 1000 µT, intermittent) after variation of exposure frequency (3-550 Hz).

Increase in DNA strand breaks in human fibroblasts after ELF-EMF exposure was dependent on exposure time.

Alkaline and neutral Comet tailfactors increased with exposure time (1-24 hours, 1000 µT, intermittent (5 min on/10 min off)), being largest at 15 hours (Figure 11). Comet assay levels declined thereafter, but did not return to basal levels.

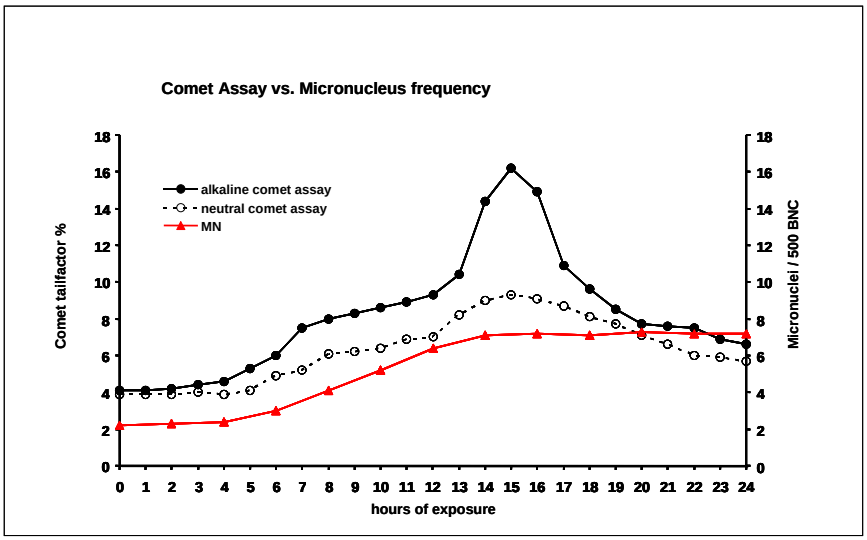

Figure 11. Influence of exposure time on formation of DNA single and double strand breaks and micronuclei in human fibroblasts (cell strain ES-1, 1 mT, 5 min on/10 min off cycles).

Increase in DNA strand breaks in human fibroblasts after ELF-EMF exposure was dependent on the age of the donors.

Fibroblasts from six healthy donors (ES1, male, 6 years old; AN2, female, 14 years old; IH9, female, 28 years old; KE1, male, 43 years old; HN3, female, 56 years old; WW3, male, 81 years old) revealed differences in response to ELF-EMF exposure (Table 4). Cells from older individuals exhibited a higher rate of single and double strand breaks and their break levels started to decline later than in cells from younger donors (Figures 12, 13).

Table 4. Alkaline and neutral Comet assay tailfactors of donors with different age (ES-1: 6, AN2: 14, IH9: 28, KE1: 43, HN3: 56, WW3: 81 years of age) - variation of exposure duration (basal-, maximum-, and end-levels)

			Alkaline Comet Assay		Neutral Comet Assay	
	cell strain	hours exposure duration	Comet tailfactor %	±SD#	Comet tailfactor %	±SD#
basal levels	ES1	0	4.112	0.018	3.901	0.006
	AN2	0	4.077	0.064	3.900	0.035
	IH9	0	4.223	0.047	4.161	0.148
	KE1	0	6.227	0.044	5.224	0.013
	HN3	0	6.802	0.018	6.313	0.064
	WW3	0	7.101	0.064	6.816	0.023
maximum levels	ES1	15	16.155	0.184	9.305	0.057
	AN2	15-16	16.501	0.004	9.394	0.134
	IH9	16	16.707	0.040	9.716	0.054
	KE1	18	17.300	0.064	10.462	0.277
	HN3	18-19	18.311	0.078	11.364	0.122
	WW3	19	18.517	0.069	12.822	0.076
and levels	ES1	24	6.611	0.017	5.742	0.023
	AN2	24	7.210	0.062	5.824	0.030
	IH9	24	7.511	0.017	6.127	0.054
	KE1	24	8.242	0.038	6.738	0.023
	HN3	24	8.718	0.008	6.761	0.006
	WW3	24	9.229	0.037	8.010	0.063

#SD ….standard deviation

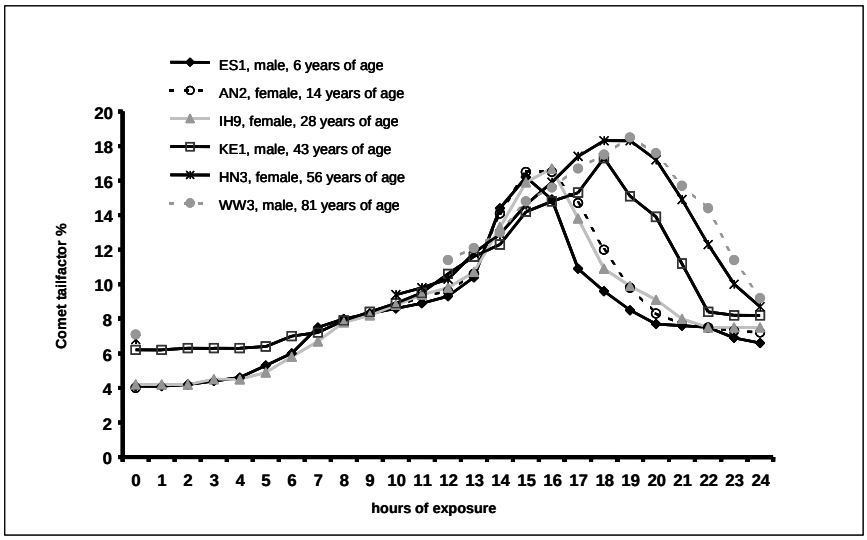

Figure 12. Alkaline Comet tailfactors of human diploid fibroblasts of donors with different years of age exposed to ELF-EMF (1 mT, intermittent 5 min on/10 min off) for 1-24 hours

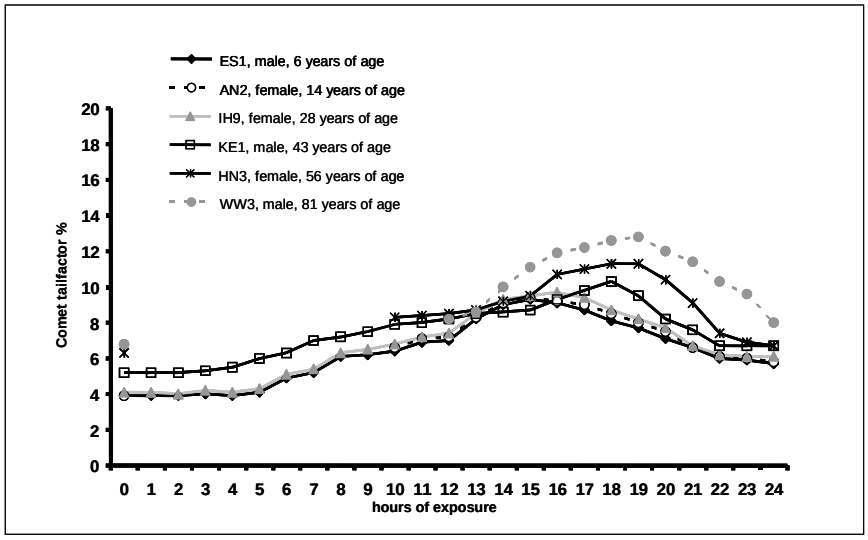

Figure 13. Neutral Comet tailfactors of human diploid fibroblasts of donors with different years of age exposed to ELF-EMF (1 mT, intermittent 5 min on/10 min off) for 1-24 hours

Increase in DNA strand breaks in human fibroblasts after ELF-EMF exposure was accompanied by a rise in micronuclei frequencies.

In addition, variation of exposure time from 2 to 24 hours revealed a time dependent increase in micronucleus frequencies. As shown in Figure 11, this increase became significant ($p<0.05$) at 10 hours of ELF-EMF exposure. Thereafter, micronucleus frequencies reached a constant level, which was about 3-fold as compared to the basal levels (Figure 14).

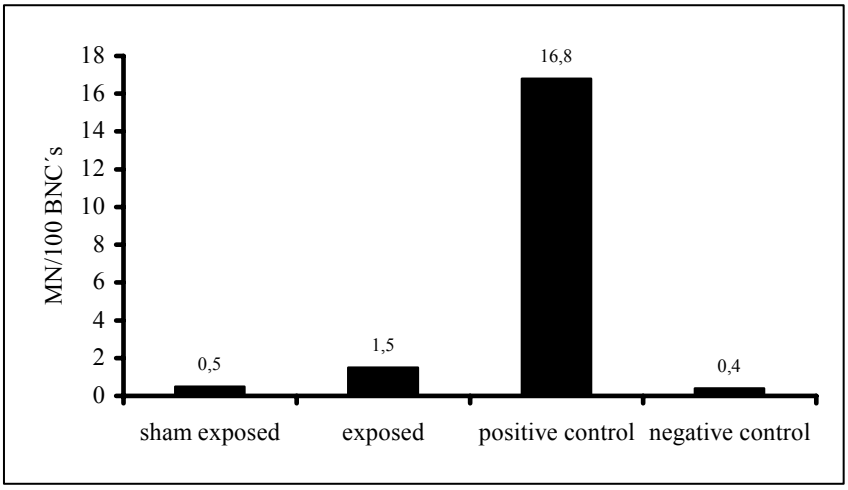

Figure 14. Micronucleus frequencies of ELF-EMF exposed (50 Hz, 1 mT, 15 h, 5 min on/10 min off) cultured human fibroblasts and controls (Vienna). Bleomycin 10µg/ml was used as a positive control.

ELF-EMF exposure did not diminish the number of fibroblasts in culture.

No differences in cell count between exposed and sham exposed cells at any exposure duration could be detected. Therefore, an elimination of cells by apoptosis and cell death during ELF-EMF exposure can probably be ruled out.

ELF-EMF exposure induced DNA strand breaks in human fibroblasts in a dose dependent way.

When magnetic flux density increased from 20 to 1,000 µT, a dose dependent rise in Comet assay tailfactors could be observed. At an exposure time of 24 hours a magnetic flux density as low as 70 µT produced significantly elevated ($p < 0.01$) alkaline and neutral Comet assay levels as compared to sham-exposed controls (Figure 13). At 15 hours of exposure genotoxic effects already occurred at 35 µT (Table 5, Figure 12). Using regression analysis, a significant correlation between Comet tailfactors and applied magnetic field (alkaline Comet assay: $r = 0.843$, $p = 0.004$; neutral Comet assay: $r = 0.908$, $p = 0.0007$), as well as between alkaline and neutral Comet assay could be found ($r = 0.974$, $p = 0.00001$).

Table 5. Mean values of alkaline and neutral Comet tailfactors at intermittent ELF exposure (5/10 on/off, 1000 µT, 24 h) (n = 2) dose response, cell line ES-1

	Alkaline Comet Assay				Neutral Comet Assay			
	exposed		sham		exposed		sham	
µT magnetic flux density	tailfactor %	±SD#	tailfactor %	±SD#	tailfactor %	±SD#	tailfactor %	±SD#
20	4.16	0.02	4.21	0.13	3.63	0.01	3.60	0.08
50	4.16	0.06	4.20	0.12	3.70	0.16	3.72	0.03
70	4.87*	0.03	4.28	0.02	3.99*	0.01	3.71	0.01
100	5.25*	0.06	4.28	0.05	4.32*	0.00	3.73	0.04
250	5.31*	0.02	4.25	0.07	4.24*	0.06	3.60	0.02
500	5.52*	0.01	4.22	0.01	4.48*	0.02	3.79	0.05
750	6.17*	0.08	4.26	0.11	5.08*	0.08	3.67	0.10
1000	6.50*	0.18	4.27	0.10	5.71*	0.01	3.79	0.16
2000	6.62	0.01	4.13	0.04	5.79*	0.05	3.70	0.01

SD indicates standard deviation
• indicates significant differences ($p < 0.05$) exposed vs. sham

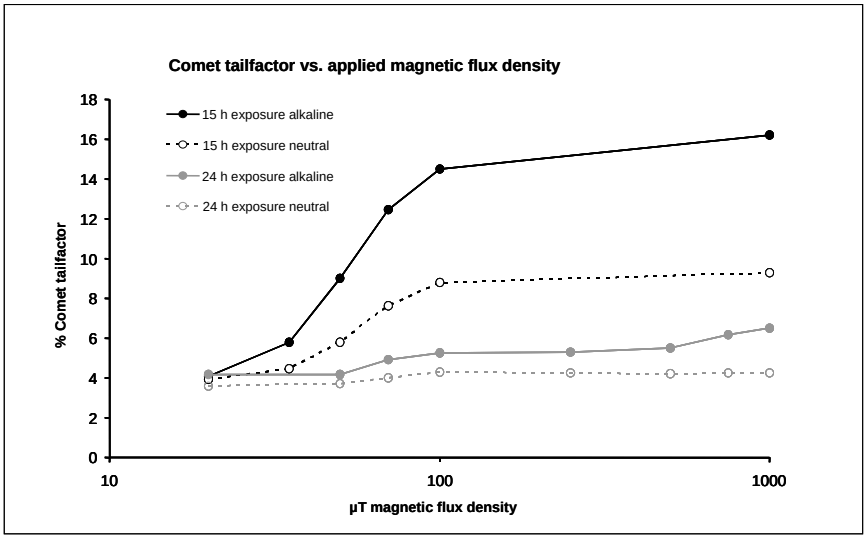

Figure 15. Dose dependent formation of DNA single and double strand breaks determined with Comet assay under alkaline and neutral conditions with cell strain ES-1 (exposure time 15 and 24 hours, 5 min on/10 min off cycles)

DNA strand breaks in human fibroblasts after ELF-EMF exposure were rapidly repaired.

After having demonstrated a time dependent relationship between alkaline and neutral Comet assay tailfactors and ELF-EMF exposure, the next aim was to find an explanation for the declining of the Comet assay levels after reaching the peak value. When exposure was terminated after 12 or 15 hours the Comet tailfactors returned to basal levels after a repair time of 7 to 9 hours (Figures 15, 16), comprising in a fast repair rate of DNA single strand breaks (< 1 hour) and a slow repair rate of DNA double strand breaks (> 7 hours). The marked Comet peak value between 12-17 hours disappeared when the Comet assay was performed at pH 12.1 instead of pH >13, thereby eliminating the cleavage of alkali labile sites in the DNA (Figure 18). The decline of Comet tailfactors after 15-20 hours of exposure could be prevented, when the cells were exposed in the presence of 10 µg/ml cycloheximide, an inhibitor of protein synthesis (Figure 18.

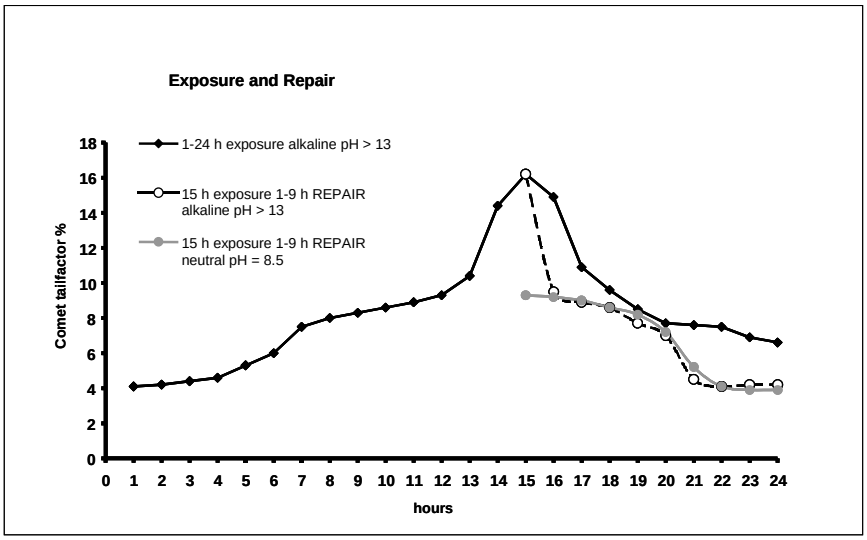

Figure 16. Repair kinetics of DNA single and double strand breaks in human fibroblasts (cell strain ES-1) after termination of ELF-EMF exposure (cell strain ES-1, 1 mT, 5 min on/10 min off cycles) using alkaline and neutral Comet assay - repair after 15 h ELF-EMF exposure

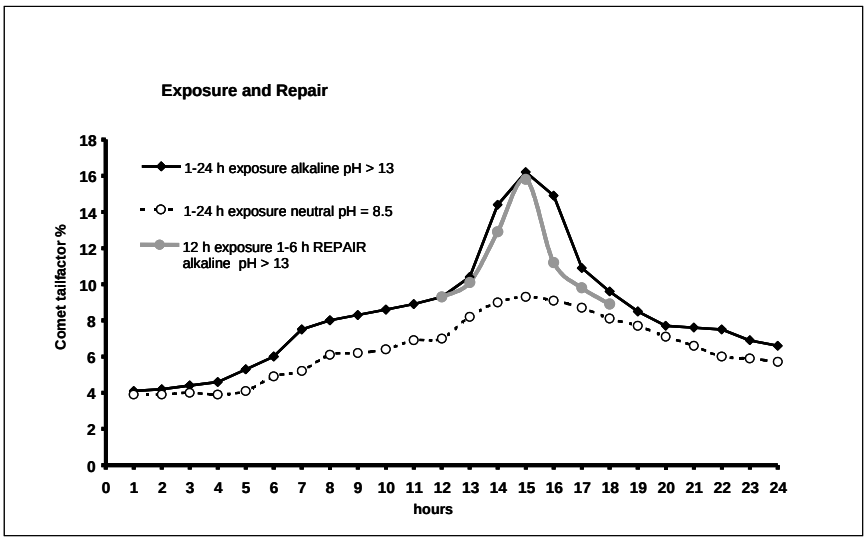

Figure 17. Repair kinetics of DNA single and double strand breaks in human fibroblasts (cell strain ES-1) after termination of ELF-EMF exposure (cell strain ES-1, 1 mT, 5 min on/10 min off cycles) using alkaline and neutral Comet assay - repair after 12 hours ELF-EMF exposure

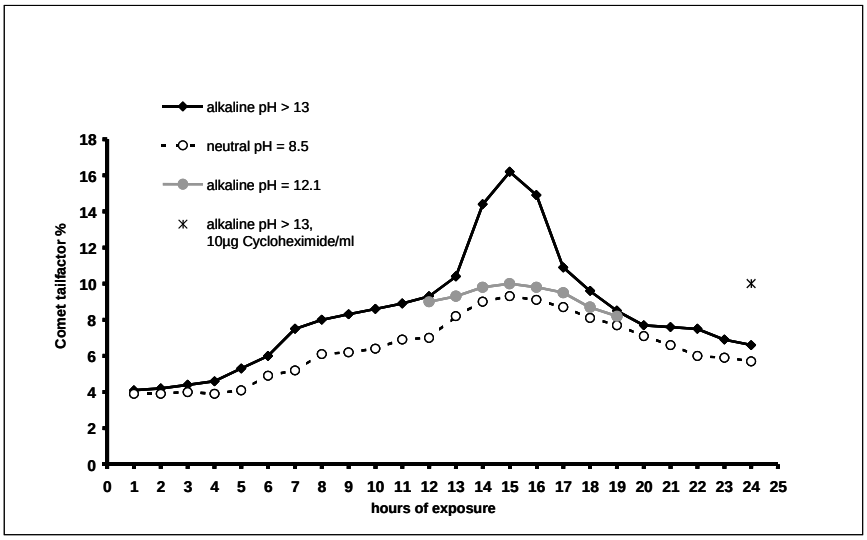

Figure 18. Comet assay of exposed human fibroblasts was performed at different pH (1 mT, intermittent 5 min on/10 min off)

DNA repair deficient cells react differently to ELF-EMF exposure.

Diploid human fibroblasts from patients with the genetically determined DNA repair defects Cockayne Syndrome, Ataxia Teleangiectatica, and Bloom Syndrome were obtained from Coriell Cell Repository (Camden, New Jersey, USA). The cells were cultured under standardized conditions and exposed (24 hours, 1 mT, 5 min on/10 min off) or sham exposed, and alkaline Comet assay was performed as described. As a result the Cockayne and Bloom Syndrome fibroblasts exhibited a similar pattern of genotoxicity as normal control fibroblasts, whereas the cells from a patient with Ataxia Teleangiectatica showed an almost threefold increased ELF-EMF induced Comet tailfactor as compare to normal cells (Figure 19).

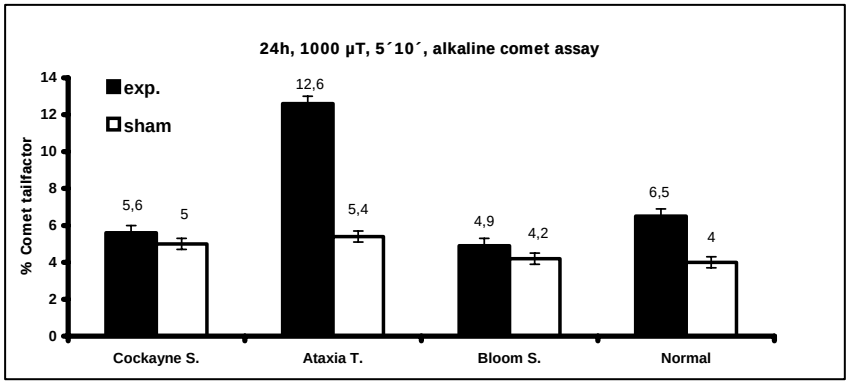

Figure 19. Alkaline Comet assay tailfactors of ELF-EMF exposed human fibroblasts from patients with various genetically determined DNA repair defects and normal controls.

Generation of DNA strand breaks through ELF/EMF was cell type specific.

ELF-EMF exposure (50 Hz sinusoidal, 1 mT, 5 min on/10 min off, 1-24 hours) of different human cell types (melanocytes, skeletal muscle cells, fibroblasts, monocytes, stimulated and quiescent lymphocytes) and of SV40 transformed rat granulosa cells revealed differences in induced DNA damage. Rat granulosa cells exhibited the highest DNA strand break levels and seemed to be most sensitive to intermittent ELF-

EMF exposure (Figures 20, 21). Human melanocytes also reacted, but not as strong as fibroblasts or rat granulosa cells. In contrast, stimulated or non-stimulated lymphocytes, monocytes and skeletal muscle cells did not respond at all.

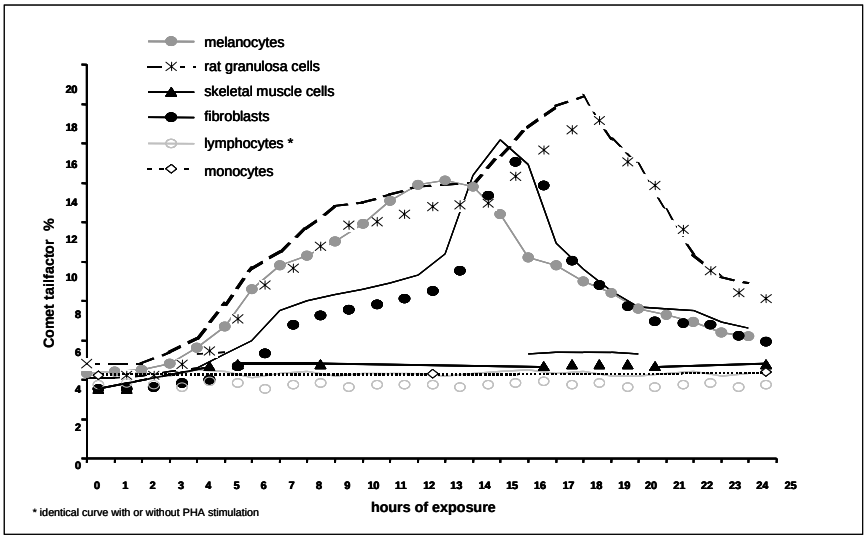

Figure 20. Alkaline Comet tailfactors of different human cell types (fibroblasts, melanocytes, monocytes, lymphocytes, skeletal muscle cells) and SV 40 transformed rat granulosa cells exposed to ELF-EMF (50 Hz sinusoidal, 1 mT, intermittent 5 min on/10 min off) for 1 to 24 hours.

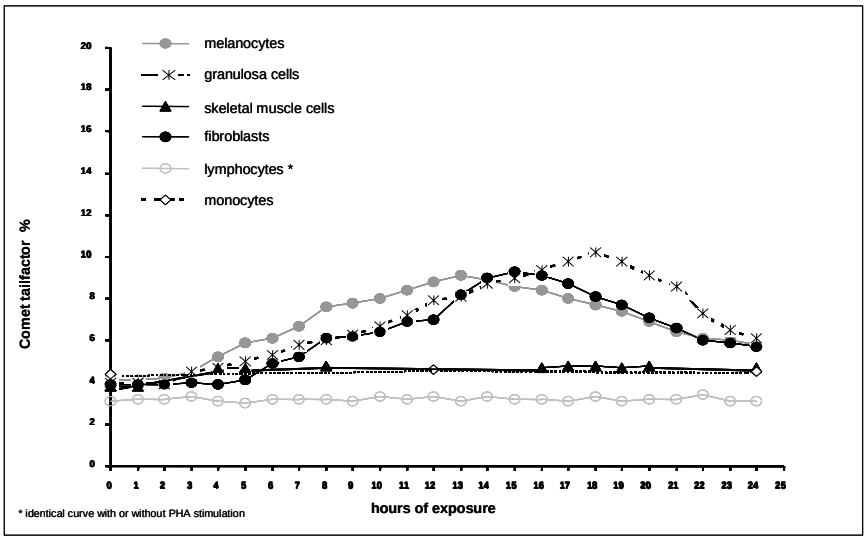

Figure 21. Neutral Comet tailfactors of different human cell types (fibroblasts, melanocytes, monocytes, lymphocytes, skeletal muscle cells) and SV 40 transformed rat granulosa cells exposed to ELF-EMF (50 Hz sinusoidal, 1 mT, intermittent 5 min on/10 min off) for 1 to 24 hours.

Generation of DNA strand breaks in human fibroblasts through ELF-EMF and their repair were modified by UVC or heat stress.

To test a possible impact of ELF-EMF exposure on DNA repair, cells were subjected to combined exposures to ELF + UVC or ELF-EMF + heat stress. In the first set of experiments fibroblasts were pre-exposed to UVC (10 min., 1.2 kJ/m^2). Subsequently, ELF-EMF exposure (50 Hz, sinus, 1000 µT) was varied from 1-24 hours. Results of the alkaline Comet assay showed that DNA damage caused by UVC could be removed within 7 hours of ELF-EMF exposure (Figure 22). UV/ELF-EMF exposed cells

resulted in 50 % higher Comet assay levels than UV/sham exposed cells after 1 hour of ELF-EMF exposure. In UV/ELF-exposed cells DNA-damage was repaired very slowly, but the maximum at 15 hours ELF-EMF-exposure could not be detected any more. The results were similar with the neutral Comet assay, but DNA damage (DNA double strand breaks) was repaired within a shorter time (Figure 23)

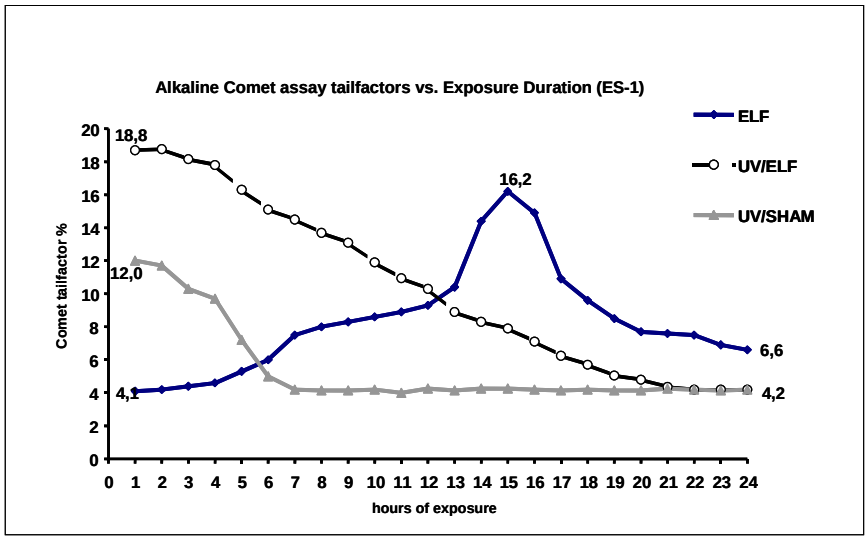

Figure 22. Repair kinetics of DNA single and double strand breaks in human fibroblasts (cell strain ES-1) after exposure with UV-C, ELF-EMF or UV C + ELF-EMF (cell strain ES-1, 1 mT, 5 min on/10 min off cycles) using alkaline Comet assay

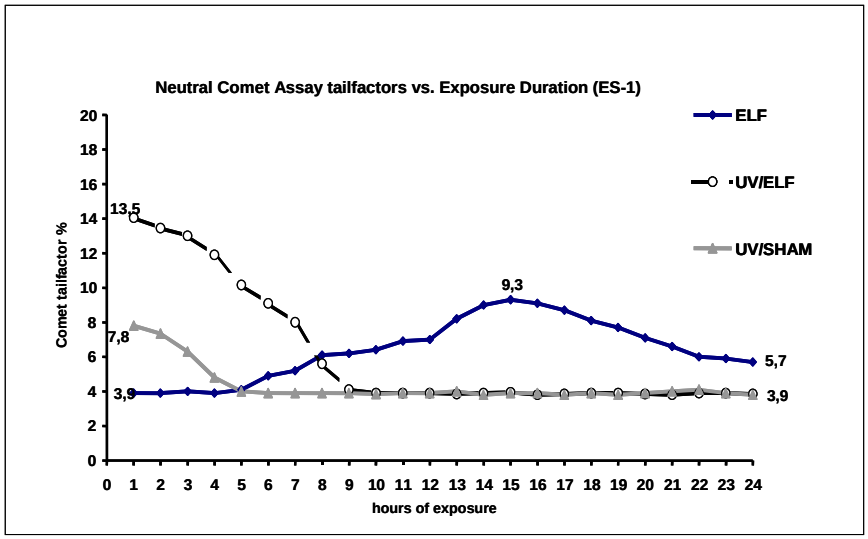

Figure 23. Repair kinetics of DNA single and double strand breaks in human fibroblasts (cell strain ES-1) after exposure with UV-C, ELF-EMF or UV C + ELF-EMF (cell strain ES-1, 1 mT, 5 min on/10 min off cycles) using neutral Comet assay

Based on the results with human fibroblasts, which suggest an induction of DNA repair upon intermittent ELF-EMF exposure, we concluded that pre-exposure to ELF-EMF would have a protective effect and diminish effects of additional exposures from other genotoxic factors. To check this assumption, fibroblasts were pre-exposed to ELF-EMF (50 Hz sinusoidal, 5 min on/10 min off, 1 mT) for 20 hours to ensure maximum induction of DNA repair. Subsequently, cells were either exposed to UVC (254 nm, 4.5

kJ/m², 30 min) or to mild heat stress (38.5°C, 4 h). Recovery of DNA damage was evaluated using alkaline and neutral Comet assay. UVC-exposure produced 50 % higher DNA strand break levels than ELF-EMFs alone and DNA damage was completely repaired after 3 hours (Figure 24). DNA damage induced by mild thermal stress was even higher and persisted longer than 6 hours after exposure termination. Pre-exposure to ELF-EMF intensified and elongated UVC or temperature induced DNA damage. After 24 hours of recovery time ELF-EMF pre-exposed cells still exhibited higher DNA strand break levels and just about 50% of the initially induced DNA damage had been repaired after this time. The results were similar with the neutral Comet assay, indicating induction and repair of DNA double strand breaks (Figure 25).

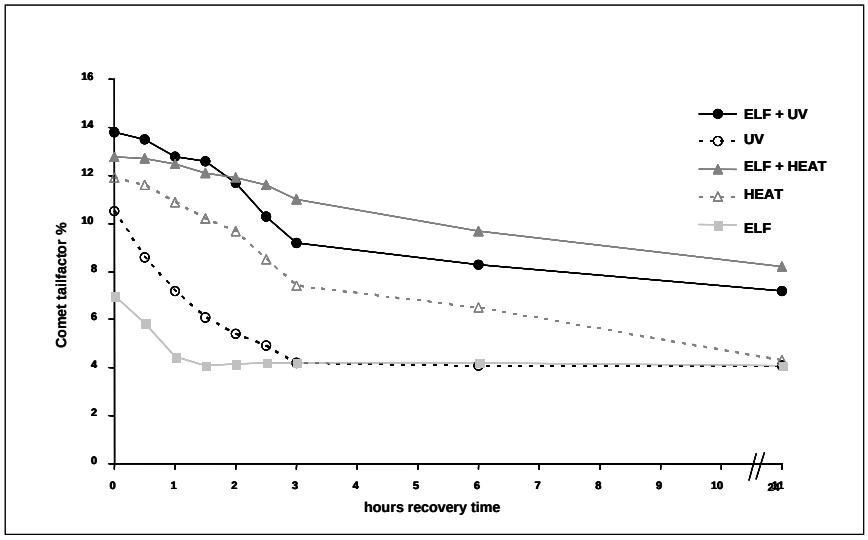

Figure 24. DNA damage and repair of cultured human fibroblasts pre-exposed to ELF-EMF (50 Hz sinusoidal, 5 min field-on/10 min field-off, 1 mT, 20 hours) and additionally exposed to UVC (254 nm, 30 min, 4.5 kJ/m²) or mild thermal stress (38.5°C, 4 hours) evaluated using alkaline Comet assay.

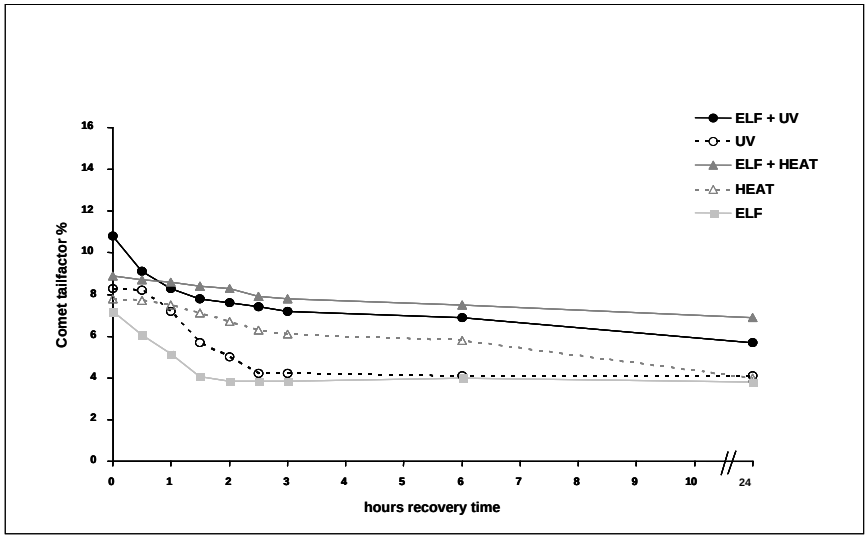

Figure 25. DNA damage and repair of cultured human fibroblasts pre-exposed to ELF-EMF (50 Hz sinusoidal, 5 min field-on/10 min field-off, 1 mT, 20 hours) and additionally exposed to UVC (254 nm, 30 min, 4.5 kJ/m²) or mild thermal stress (38.5°C, 4 hours) evaluated using neutral Comet assay.

ELF-EMF generated chromosomal aberrations in human fibroblasts.

Chromosomal aberrations were evaluated at exposure conditions producing maximum effects in the Comet assay and in the micronucleus test (15 h, 1 mT, 5min on/10 min off). Five different types of aberrations were separately scored (gaps, breaks, rings, dicentric chromosomes, acentric fragments). Significant increases ($p < 0.05$) between exposed and sham exposed cells could be demonstrated for all types of aberrations (Table 6). Gaps were 4-fold increased, breaks 2-fold, and dicentric chromosomes and acentric fragments 10-fold. Translocations were evaluated using the fluorescence in situ hybridisation (FISH) technique. 1,000 metaphases were scored for each specifically labeled chromosome (1-22, X and Y) after ELF-EMF exposure (50 Hz, 24h, 5 min on/10 min off, 1 mT). No stable translocation in any of the 24,000 metaphases of ELF-EMF exposed cells could be detected (data not shown).

Table 6. Percentage of chromosomal aberrations induced by ELF-EMF exposure (50 Hz, 5´field-on/10´field-off, 1 mT, 15 h) in cultured human fibroblasts.

Types of aberrations	ELF-exposed (% ± SD)	sham-exposed (% ± SD)	p-value*
chromosome gaps	24.3 ± 1 %	5.5 ± 0.7 %	< 0.001
chromosome breaks	2.2 ± 0.3 %	1.3 ± 0.3 %	0.0015
ring chromosomes	0.1 ± 0.07 %	---	0.0133
dicentric chromosomes	0.4 ± 0.1 %	0.06 ± 0.05 %	< 0.001
acentric chromosomes	0.3 ± 0.07 %	0.02 ± 0.04 %	< 0.001

[a] A number of 1,000 metaphases were scored in each of five independent experiments. Results are expressed as percentage chromosomal aberrations per cell.
[b] Significant differences ($p < 0.05$) as compared to sham-exposed controls using Student's t-test for independent samples

ELF-EMF did not alter the mitochondrial membrane potential in human fibroblasts.

The experimental settings in the present tests were based on conditions, which resulted in the highest inducible frequencies of these DNA strand breaks in human fibroblasts. Evaluating changes in the mitochondrial membrane potential after ELF exposure (50 Hz, 15 hours, 1 mT, 5 min on/10 min off) using JC-1, revealed no significant differences between exposed and sham-exposed fibroblasts.

3.1.1.2 Granulosa cells of rats, Chinese hamster ovary cells (CHO) and HeLa cells (Participant 7)

ELF-EMF exposure caused a significant increase of DNA strand breaks in cultured rat granulosa cells, CHO cells and HeLa cells.

The effect of ELF-EMF was analysed on the genomic level by use of the Comet assay. Especially the dependence on exposure time and frequency was analysed. Figure 26 shows that exposure to ELF-EMF at 16 2/3 Hz (5 min on/10 min off, 1.0 mT) caused a significant increase in single and double DNA strand breaks in cultured granulosa cells. The same result was obtained with CHO and HeLa cells (not shown). The data presented in Figure 26 indicate that the genotoxic effect at 16 2/3 Hz is time dependent with a maximum after about 18 hours of exposure, which resembles the results obtained at 50 Hz by Participant 3 (Ivancsits et al., 2003).

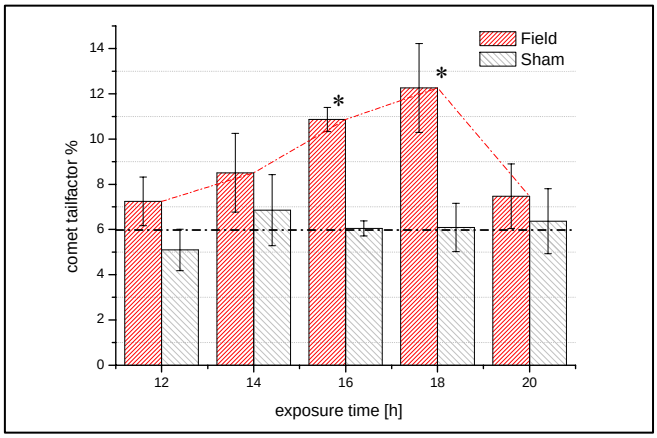

Figure 26. DNA damage of rat granulosa cells after exposure for 12 to 20 hours to ELF-EMF (16 2/3 Hz, 5 min on/10 min off, 1 mT) evaluated using alkaline Comet assay. For values of n see Material and Methods. (* p< 0.05)

To investigate the frequency dependence of the genotoxic effect of ELF-EMF (5 min on/10 min off) exposure of rat granulosa cells a constant exposure time of 18h was selected. Figures 27 and 28 present the tailfactors of exposed and sham exposed granulosa cells using the alkaline and neutral Comet assay. At the applied frequencies within the range of 8 Hz to 1000 Hz a significant frequency dependence was not observed for the rate of double DNA strand breaks as derived from the neutral Comet assay (Figure 28). The corresponding results of the alkaline Comet assay are presented in Figure 27. At 8 Hz, 16 2/3 Hz and 50 Hz an intensity of 1 mT could be applied (Figure 27a). A significant increase of DNA strand breaks was found at 16 2/3 Hz. Surprisingly, especially at 50 Hz the s.e.m. data of sham and ELF-EMF exposed cells differ significantly. The large error could be caused by a variable time dependent location of the maximum and/or the influence of the specific cell passage. Further experiments are under analysis to confirm the data presented in Figure 27a. At 1000 Hz the recorded DNA damage is significantly lower than observed at 16 2/3 Hz (Figure 27b). But it has to be noted that the maximal applied flux density was limited to 0.6 mT due to the used exposure system (Participant 10). Furthermore, DNA damage was measured at 20 µT, which approximately corresponds to the maximal acceptable magnetic flux density as recommended by the 26. BlmSchV[1]. Again a significant increase of DNA strand breaks was observed (Figure 27b).

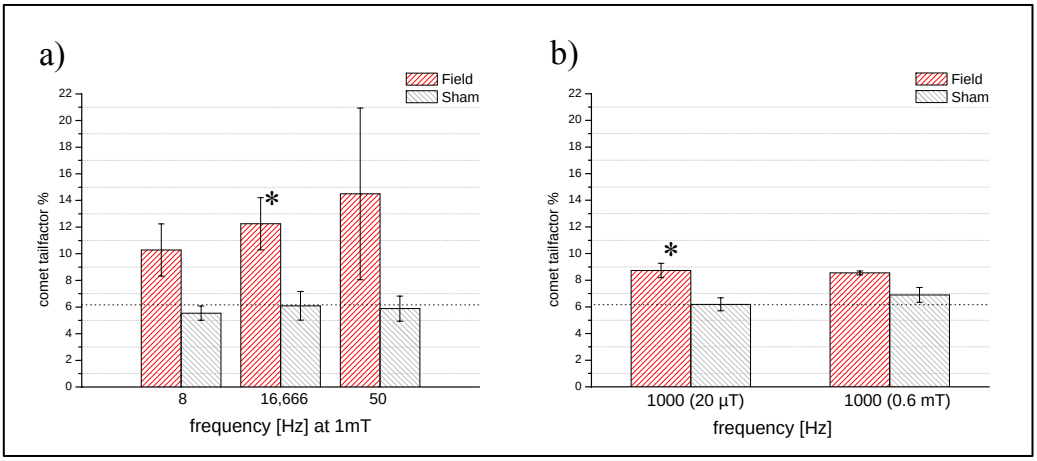

Figure 27. DNA damage of rat granulosa cells as function of frequency of ELF-EMF (5 min on/10 min off) after an exposure for 18 hours as derived by the alkaline Comet assay. **a)** In the frequency range of 8 to 50 Hz the flux density was set to 1 mT. **b)** At 1000 Hz the flux density was adjusted to 20 µT and 0.6 mT (for further explanation, see text). For values of n see Material and Methods. (* p< 0.05)

[1] 26. Verordnung zur Durchführung des Bundes-Immissionschutzgesetzes (Verordnung über elektromagnetische Felder – 26. BlmSchV)

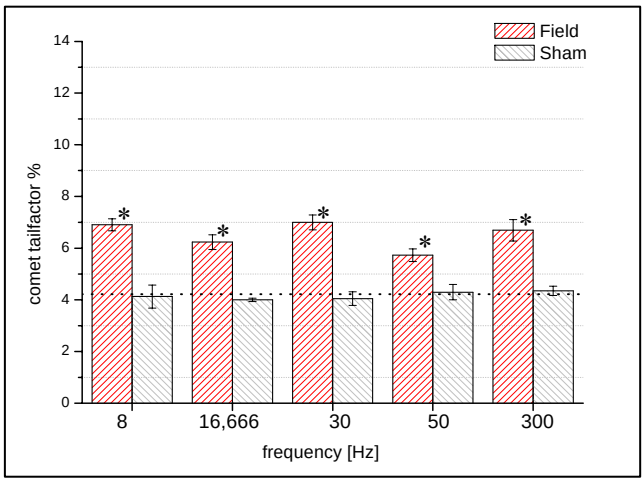

Figure 28. Double DNA strand breaks of rat granulosa cells as function of frequency of ELF-EMF (5 min on/10 min, 1 mT) after an exposure time of 18 hours as derived by the neutral Comet assay. For values of n see Material and Methods. (* $p < 0.05$)

3.1.1.3 Embryonic stem cells (ES) of mice (Participant 4)

Lack of effects on single and double strand break induction 0, 18, 24 and 48 hours after completion of a 6 or 48 hours ELF-EMF exposure.

The effects of ELF-EMF on the integrity of DNA strands in differentiating ES cell from EB outgrowths were studied. Two schemes were applied: (1) For ELF-EMF exposure (50 Hz Powerline, 2.0 mT, 5 min on/30 min off, 6 hours) the percentage of primary DNA damage was measured immediately after ELF-EMF exposure at the stage of neural differentiation (4+4d - 4+6d) and 18 hours after exposure using the alkaline and neutral Comet assay. (2). In the second set of experiments, the same ELF-EMF exposure conditions were applied for 48 hours instead of 6 hours, and the alkaline Comet assay was done immediately after exposure, while the neutral Comet assay was done 24 or 48 hours post exposure. No significant differences were observed in the induction of single or double DNA strand breaks between sham-exposed or ELF-EMF exposed neural progenitors.

3.1.1.4 Summary (Participant 1)

Our data indicate a genotoxic action of ELF-EMF in various cell systems. This conclusion is based on the following findings:

- Intermittent exposure to 50 Hz ELF-EMFs generated DNA single and double strand breaks in various cell systems such as human fibroblasts, melanocytes, granulosa cells of rats, Chinese hamster ovary cells (CHO) and HeLa cells, but not in human lymphocytes, monocytes, myelocytes and neural progenitors from mouse embryonic stem cells (see 3.1.1.1, 3.1.1.2 and 3.1.1.3).
- DNA damage generated by ELF-EMF in human fibroblasts was dependent on time and dose of exposure, on the age of the donors the cells derived from, and on the genetic background of the cells. A flux density of 35 µT was high enough to significantly increase the number of DNA strand breaks (see 3.1.1.1)
- The increase in DNA strand breaks in human fibroblasts due to ELF-EMF exposure was accompanied by an enhanced formation of micronuclei which was also dependent on the exposure time (see 3.1.1.1).
- The DNA repair system in human fibroblasts which was strongly activated by ELF-EMF during exposure did not work error-free as shown by a significant increase of different types of chromosomal aberrations (see 3.1.1.1).
- Genotoxic effects were frequency dependent. Significant increases in DNA strand breaks were found, when an ELF-EMF of 3 Hz, 16 2/3 Hz, 30 Hz, 50 Hz, 300 Hz, 550 Hz and 1000 Hz was applied. The

effect was strongest with 50 Hz ELF-EMF and second strongest with 16 2/3 Hz (see 3.1.1.1 and 3.1.1.2).

3.1.2 Cell proliferation and differentiation

3.1.2.1 Human neuroblastoma cell line NB69 (Participant 5)

ELF-EMF promoted the growth rate of NB69 neuroblastoma cells.

Immunocytochemical staining using antibodies against phenotype-specific antigens revealed that NB69 cells contain the neuroblast-specific protein ßIII-tubulin. However, these cells do not contain the neuroepithelial marker nestin, which is present in immature progenitors and in some neuroblastoma cells, nor the astrocyte-specific antigen GFAP. The cells remained in an undifferentiated state throughout the experimental period. Only the treatment with retinoic acid induced neurite extension accompanied by cell growth reduction.

Two series of experiments were carried out to analyse the cell growth response of NB69 cells to ELF-EMF. In the first series, the ELF-EMF administrated alone (42 hours) provoked a modest, though significant increase in the number of cells at day 5 postplating (5 dpp), both at 10-µT (12% over controls, **p<0.01) and 100-µT MFD (17 % increase over controls, ***p<0.001) as shown in Figure 29A). Retinol (ROL) alone or in combination with ELF-EMF did not change significantly the cell growth (data not shown). The ELF-EMF exposure also provoked modest increases in the total DNA levels, the effect being statistically significant at 10 µT (8 % over controls, p<0.05, Figure 29B). However no significant changes were observed in the protein or protein/DNA contents in the ELF-EMF exposed samples. Taken as a whole, these results indicate that exposure to 50 Hz ELF-EMF at 10 or 100 µT promote cell growth in the NB69 human neuroblastoma cell line.

In the second series of experiments, the 42-hours exposure to ELF-EMF at a flux density of 100 µT significantly increased cell growth (11 % over controls, ***p<0.001, Figure 30A). This result confirms the growth-promoting response obtained in the first experimental series. However, such an effect was not observed, when the ELF-EMF exposure was maintained for a longer period of time, i.e. 90 hours (Figure 30B). The treatment with retinoic acid (RA) alone significantly reduced the cell number, both at 42 and 90 hours, when compared to untreated controls. Also, RA-treated cells did show the growth-promoting effects of a 100 µT ELF-EMF, these samples demonstrating reduced growth rates when compared to unexposed controls: 35% reduction at the end of 42 hours-treatment (p<0.0001) and 57% reduction at the end of 90 hours-treatment (p<0.0001).

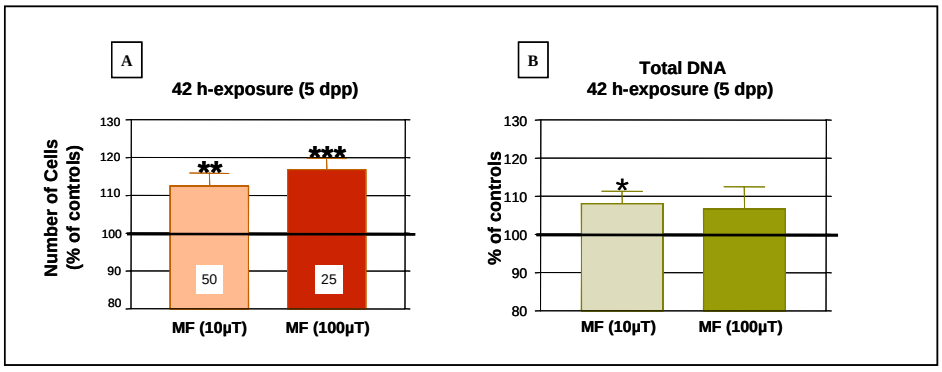

Figure 29. First series of experiments. A-Cell growth estimated by cell counting (Trypan blue exclusion) and B-Total DNA estimated by spectrophotometry.

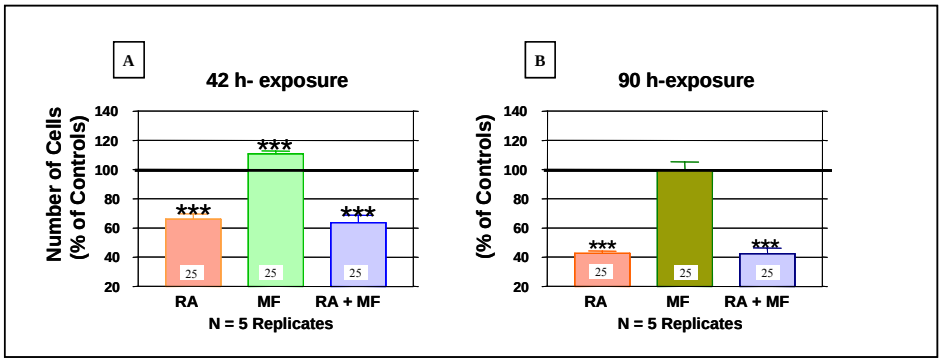

Figure 30. Second series of experiments: A-Number of cells at day 5 postplating (after 42 hours-exposure) and B-Number of cells at day 7 postplating (after 90 hours-exposure).

No experiment could be performed at a flux density of 2.0 mT following the 3 hours on/3 hours off exposure protocol, since the ohmic heat in the coils due to the electric current could not be compensated by the incubator resulting in an unstable ambient temperature. When the samples were exposed to 2 mT ELF-EMF in a 5min on/30 min off cycle, no effect was observed on the cell growth. Similarly, the cells did not respond to a 5 min on/30 min off cyclic exposure to a 100 µT ELF-EMF. It is possible that the NB69 cell line requires a longer exposure cycle to show significant changes in the cell growth.

A growth-promoting effect of ELF-EMF in NB69 neuroblastoma cells was not observed after an extended exposure period.

As described above, the growth promoting effect of a 100-µT EMF was not observed when the exposure was maintained for a longer period of time, i.e. 90 hours (Figure 30B). In NB69 cultures kept in control conditions, the number of cells peaks at day 6 and then decays (Figure 31). In the present experiments, long-term cultures (7 days postplating) reached a confluence stage close to saturation. This physiological condition could be the cause of the lack of response to ELF-EMF after long-term exposures between 3 and 7 days postplating.

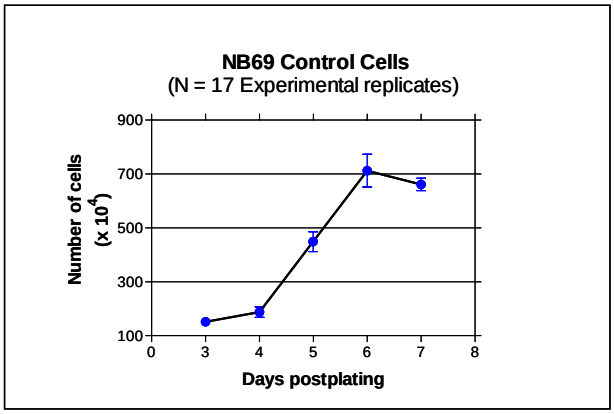

Figure 31. Growth pattern of NB69 cells: On day 7 the number of cells is reduced when compared to that at day 6. Long-term cultures (7 days postplating), reached a confluence stage close to saturation.

ELF-EMF did not counteract the retinoic acid-induced inhibition of cell proliferation in NB69 neuroblastoma cells.

To better characterise the potential ELF-EMF effects on the proliferation/differentiation rate, NB69 cells were treated with a chemical agent that inhibits proliferation and induces differentiation. All trans retinoic

acid (RA) promotes differentiation in NB69 cells, inducing outgrowth of long neurite-like processes and driving of the cell morphology along a neural pathway. As shown in Figure 30AB, the cell growth decreases after treatment with RA (2 µM) for 5 or 7 days. This response to RA remained unchanged after exposure to the ELF-EMF during 42 or 90 hours.

ELF-MF enhanced the cellular proliferation rate NB69 neuroblastoma cells as revealed through analysis of cell proliferation markers (PCNA).

Studies of expression of cell proliferation markers (PCNA) reinforce the described effects of ELF-EMF on cell growth: To determine whether the above growth-promoting effect detected by Trypan Blue exclusion involves changes in cell proliferation, we searched for changes in the proliferating cell nuclear antigen (PCNA). PCNA immunolabelling shows that exposure to 10 µT ELF-EMF significantly increases the proportion of PCNA-positive cells (24% increase; Figure 32). This effect was associated with an increase in the number of cells (15% increase), showing a significant linear correlation between both of the parameters, PCNA positive cells and total number of cells, at the end of 42 hours exposure ($p<0.01$). These results confirm and reinforce the previous observations that a 42 hours exposure to ELF-EMF at a flux density of 10 µT can modulate cell growth in NB69 cells. The mean value of PCNA positive cells in controls is 32 % ± 1,3).

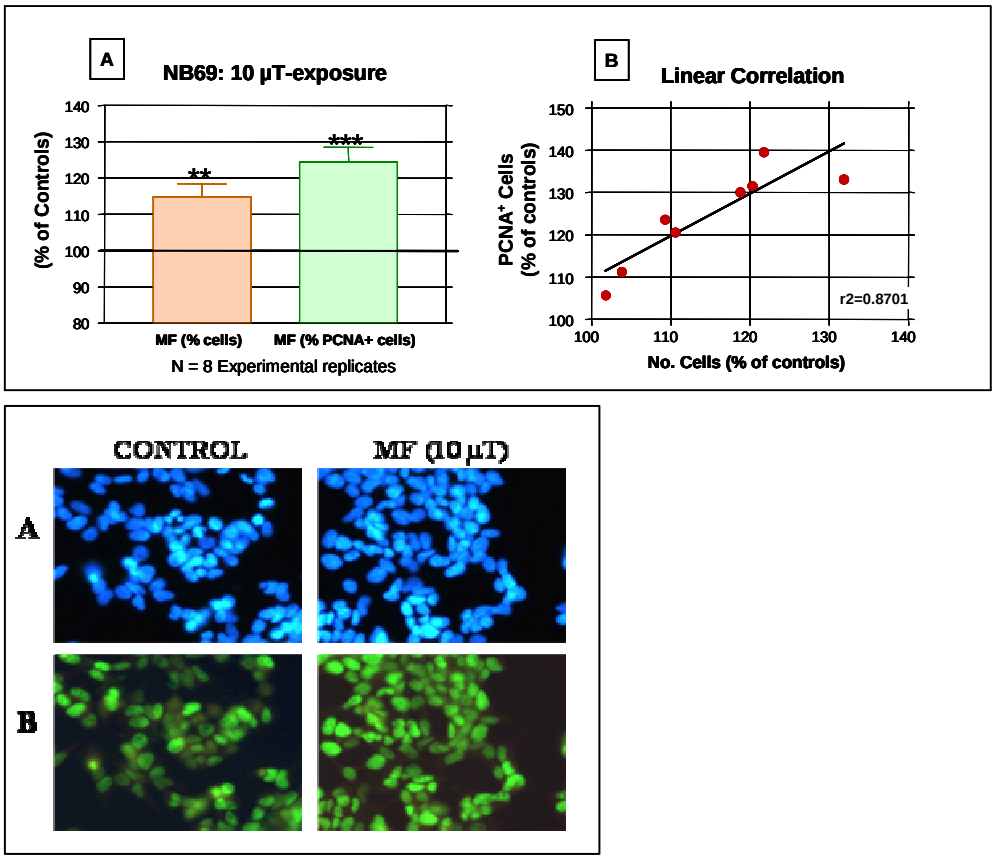

Figure 32. A) Growth response of NB69 to 10 µT after a 42 hours exposure as revealed by Trypan (brown) and PCNA content (green). Student T' test: **p<0.01; ***p<0.001. B) Linear correlation between these two parameters. Photomicrographs of NB69 cells. A: Hoechst-marked nuclei. B: PCNA labelling. The ELF-EMF exposure induced an increase in the number of cells expressing PCNA.

Neuroblastoma cell cultures contain two different phenotypes. One type is characterised by flattened, "sail-like" morphology and shows a strong adherence to the culture flask. These cells are called S-cells. The second phenotype corresponds to much smaller, triangular cells that adhere to the culture flask loosely. These cells, called N cells have a neuroblastic phenotype, are clonigenic and tumorigenic and

grow rapidly in the culture flask. We have observed that the relative proportion of both phenotypes evolves along the successive subcultures, which seems to significantly influence the response of the culture, as a whole, to the field exposure. In fact, young passages, having a high proportion of N cells, are particularly sensitive to ELF-EMF, whereas older passages, very rich in S-cells and with virtually no N cells, are not responsive to ELF-EMF exposure. Consequently, we conducted experiments with young passages, where the cells were exposed to a 100-µT ELF-EMF during 63 hours (day 6 post-plating). A significant increase in the number of cells was observed in the exposed samples (9.7% over controls $p<0.0001$, Figure 33A). The mean cell number in controls was 621.689 ± 62.314 ($x10^4$). The increase in the number of cells was found to be associated with significant increases in the proportion of PCNA-positive cells. Figure 33B shows the percent of PCNA positive cells at days 5 and 6 post-plating (dpp). Only at 6 dpp significant changes in the number of PCNA positive cells were observed (31.7% over controls, $p<0.01$, N = 3 experimental replicates). Those changes do not represent an ELF-EMF-induced increase in PCNA labelling, since the percent of PCNA positive cells in the control cultures spontaneously decreased between days 5 and 6 post-plating (Student T'test *, $p<0.05$). Such a decrease did not occur in the exposed cultures. The present results indicate that the regulation of the kinetics of the cell cycle could be altered by ELF-EMF at 100 µT. Provided that in the proliferating cell the PCNA levels are maximal at late G1 and S phases, it is possible that such phases of the cell cycle are implicated in the above described responses.

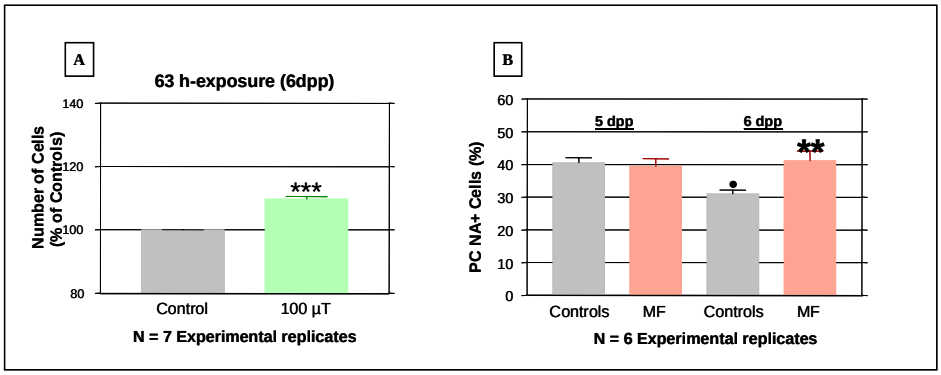

Figure 33. A) Percent of cells at the end of 63-hours exposure and/or incubation (6 day post-plating). B) Percent of PCNA positive cells at 5-6 days post-plating (dpp). In controls the percent of PCNA positive cells significantly decreases between the days 5 and 6 post-plating (Student T'test ●, $p<0.05$), whereas in exposed cells at 100 µT this decrease did not occur).

ELF-EMF increased the DNA synthesis in NB69 neuroblastoma cells.

We also tested the BrdU incorporation into DNA. As shown in Figure 31, at the end of a 42-hours exposure (5 pp) to the 100 µT ELF-EMF a significant increase of BrdU- positive cells was observed in the treated cultures (41 % over controls, Student's T test $p<0.01$). Such an effect was followed (63-hours exposure, 6 pp) by a subsequent increase in the number of cells (9.7% over controls, $p<0.001$, Figure 34). This response was accompanied by a significant reduction in the percent of spontaneously apoptotic cells (58.5 % of that in controls, $p<0.05$).

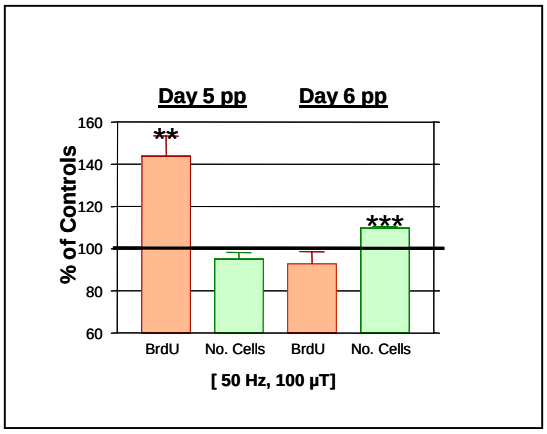

Figure 34. Cell growth in a total of 18 experiments: ELF-EMF effects at 5 days post-plating (42 hours exposure) or at 6 days post-plating (63 hours exposure): Red, percent of BrdU-positive cells; Green, Number of Cells analysed by Trypan blue exclusion. Student T'test: **p< 0.01; ***p< 0.001.

ELF-EMF affected the cell cycle in NB69 neuroblastoma cells.

The experiments performed to test the DNA content and the cell cycle distribution by flow cytometry showed that at the end of day 5 post-plating (Figure 35A), the 42-hours exposure to 100 µT ELF-EMF induces increases in the number of cells in G2-M phase of the cell cycle (28% over controls; N= 3 experimental replicates). The exposure also provoked a modest reduction of cells in G0-G1. However, no significant changes were observed in the number of cells in S-phase and in the number of total cells (Trypan Blue exclusion, Figure 352A). The flow-cytometry assay at the end of day 6 post-plating did not reveal EMF-induced changes in the cell cycle (G0-G1; S and G2-M), even thought a significant increase in the number of alive cells was observed (16.7% over controls, p<0.05; N= 5 experimental replicates, Figure 35B). These results confirm and reinforce our previous observations using other techniques, that 100 µT 50-Hz ELF-EMF can promote cell growth in the NB69 cell line from a human neuroblastoma.

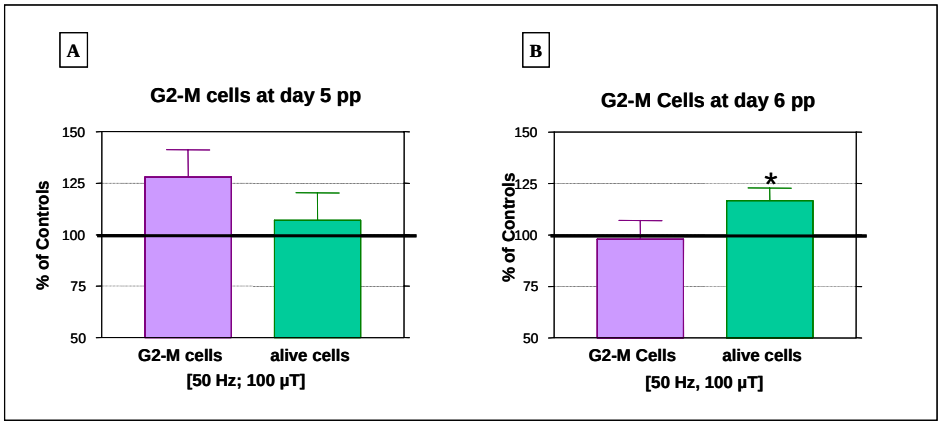

Figure 35. A) A 42 hours-exposure to a 100-µT field provokes an increase in the percent of G2-M cells at day five postplating (5 pp). B) This increase was not observed one day later, after 63 hours- exposure, however, a significant increase in the number of alive cells occurred.

ELF-EMF diminished the spontaneous apoptosis in NB69 neuroblastoma cells.

In order to investigate the potential influence of 50 Hz ELF-EMF on apoptosis the percent of apoptotic cells was estimated with TUNEL-labelling after 63 hours of exposure. Also, the number of cells was

quantified by Trypan Blue exclusion. The results (Figure 36A) indicate that ELF-EMF of 50 Hz at a flux density of 100 μT (3 hours on/3 hours off) induces a significant reduction in the spontaneous apoptosis of the NB69 cell line. This response was associated with an increase in the number of cells (9.7% over controls, $p<0.001$, Figure 36B as we previously observed in experiments described above. Apoptosis was also determined through flow cytometry analysis; the results confirming a reduction at the end of 63 hours-exposure (data not shown).

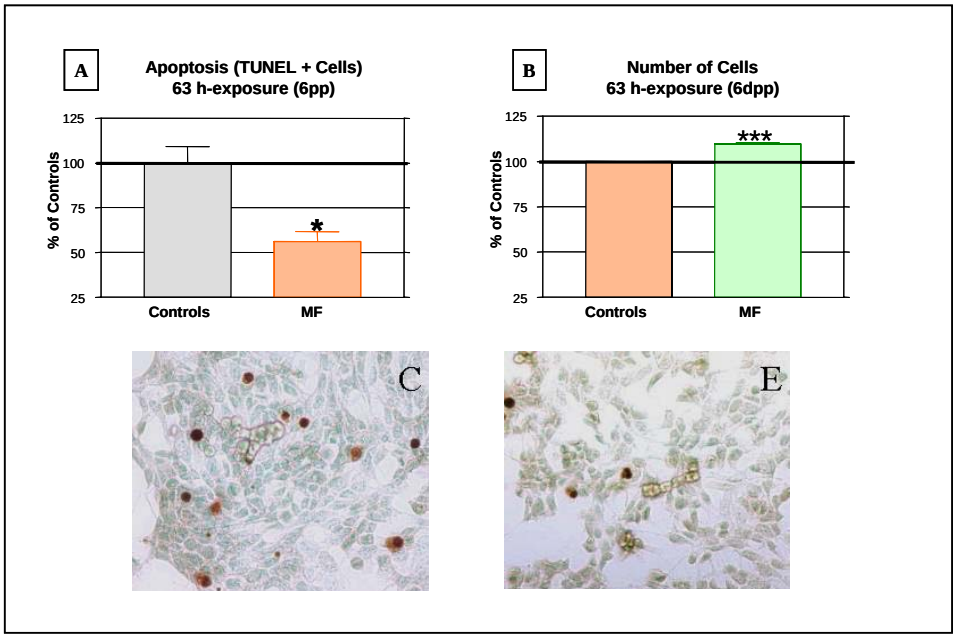

Figure 36. A) ELF-EMF (50 Hz, 100 μT) induce a significant reduction in the spontaneous apoptosis of the NB69 cell line. B) This described response is associated with an increase in the number of cells. (* $p< 0.05$, ***$p<0.001$, Student T´ test, three independent experimental replicates).Photomicrographs showing TUNEL-positive cells in controls (C) and exposed (E) samples.

ELF-EMF altered the activation of the phosphorylated cyclic adenosine monophosphate response-element binding protein (p-CREB).

The results of a total of 8 experiments show that both, the labelling/cell in NB69 cells and the proportion of phospho-CREB positive cells increase after 60 min of exposure (35.4% over controls, $p<0.01$, Figure 37 and photomicrograph). The percent of p-CREB positive cells in controls after 60 min of exposure was 32%. However, no differences were observed between ELF-EMF-exposed and controls samples after 30 or 120 min of exposure. These preliminary results suggest that the activation of p-CREB is involved in the previously described effects of 50 Hz 100 μT ELF-EMF on cell growth/apoptosis. In additional experiments the analysis of Western confirms that the ELF-MF induced a short-time dependent activation of the transcriptional factor CREB, with a peak at 60 min followed by a recovering of the basal levels at 120 minutes of exposure (data not shown).

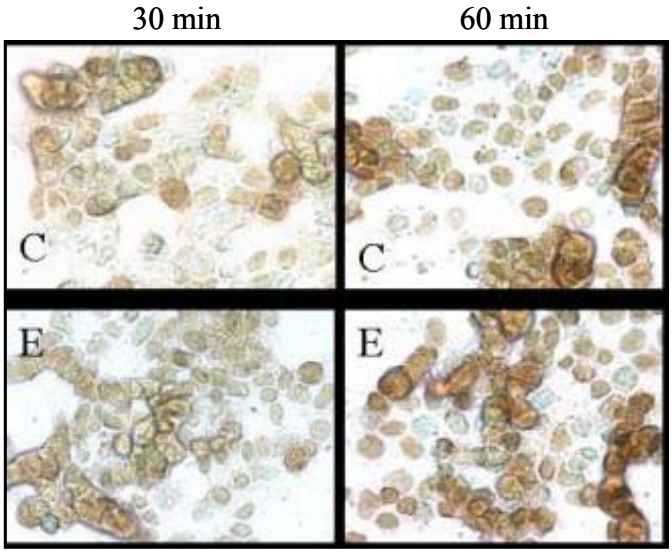

Figure 37. Immunocytochemistry for phospho-CREB. Changes in p-CREB positive cells showed a time-dependent response in the presence of the 100μT ELF-EMF. Photomicrograph showing the p-CREB labelling in brown and the counterstaining in green(methylgreen).

3.1.2.2 Embryonic stem cells of mice during cardiac differentiation (Participant 8)

ELF-EMF accelerated the cardiac differentiation of embryonic stem cells through enhanced expression of cardiac genes.

See 3.1.4.3

3.1.2.3 Human lymphocytes (Participant 8)

ELF-EMF exposure did not have any influence on proliferation, cell cycle and functionality of human lymphocytes.

The experiments with ELF-EMF (50 Hz) were performed at 50 μT magnetic field intensity on cells from 20 donors. Cell proliferation, cell cycle together with membrane activation markers were studied on lymphocytes from young donors. Data obtained by all the experiments performed indicated that no significant differences exist on cell proliferation or DNA synthesis at any time during the continuous exposure up to 6 days, as well as on cell cycle during the continuous exposure up to 96 hours. Cell activation phase was studied on CD3+HLA-DR+ T lymphocytes and CD4+CD25+ T helper lymphocyte subpopulation, but also in this case no differences were found between cells exposed and not exposed.

3.1.2.4 Embryonic stem cells of mice (Participant 4)

ELF-EMF did not have any influence on the growth and neuronal differentiation of embryonic stem cells of mice.

See 3.1.4.1

3.1.2.5 Summary (Participant 1)

Our data show some influence of ELF-EMF on proliferation and differentiation of some, but not all cell systems investigated. This conclusion is based on the following findings:

- ELF-EMF at a flux density of 0.1 mT significantly increased the proliferation of neuroblastoma cells (NB69 cell line) after exposure for 42- and 63-hrs (see 3.1.2.1).
- ELF-EMF at a flux density of 0.8 mT accelerated the cardiac differentiation of embryonic stem cells through enhanced expression of cardiac genes (see 3.1.2.2 and 3.1.4.3)

- ELF-EMF at a flux density of 2 mT did not have any influence on the growth and neuronal differentiation of embryonic stem cells of mice (see 3.1.2.4 and 3.1.4.1)
- ELF-EMF at a flux density of 0.8 mT did not have any influence on proliferation, cell cycle and activation of lymphocytes, either (see 3.1.2.3).

3.1.3 Apoptosis

3.1.3.1 Embryonic stem cells of mice (Participant 4)

ELF-EMF at a flux density of 2 mT up-regulated the transcript levels of the anti-apoptotic gene bcl2 and the growth arrest and DNA damage inducible gene GADD45 and down-regulated bax in ES cell-derived neural progenitor cells. This may indirectly influence the apoptotic process in neural progenitor cells.

See 3.1.4.1

3.1.3.2 Neuroblastoma cell line NB69 (Participant 5)

ELF-EMF at a flux density of 100 µT inhibited the spontaneous apoptosis in NB69 neuroblastoma cells.

See 3.1.2.1

3.1.3.3 Human fibroblasts (Participant 3)

No differences in cell count between ELF-EMF exposed and sham exposed human fibroblasts at any exposure duration could be detected. Therefore a possible elimination of cells by apoptosis and cell death can probably be ruled out.

See 3.1.1.1

3.1.3.4 Summary (Participant 1)

Our data indicate that ELF-EMF may have some indirect effect on apoptosis in certain, but not all cell systems investigated. This conclusion is based on the following findings:

- ELF-EMF at a flux density of 2 mT up-regulated in neural progenitor cells the transcript levels of the GADD45 gene and down-regulated the transcript levels of the bax gene by which the apoptotic process may be modulated (see 3.1.3.1 and 3.1.4.1).
- ELF-EMF at a flux density of 0.1 mT inhibited the spontaneous apoptosis in neuroblastoma cells in a way which is at present not well understood (see 3.1.3.2 and 3.1.2.1).
- ELF-EMF at a flux density of 1 mT did neither measurably affect the apoptotic process nor could a cytotoxic effect be detected in human fibroblasts in the course of a 24h exposure (see 3.1.1.1 and 3.1.3.3).

3.1.4 Gene and protein expression

3.1.4.1 Embryonic stem cells of mice (Participant 4)

ELF-MF exposure resulted in up-regulation of egr-1, c-jun and p21 transcript levels in p53-deficient, but not in wild type ES cells.

To analyse the effects of ELF-EMF, undifferentiated wild type (wt) and p53-deficient ES cells were exposed at different intermittence schemes and flux densities of 0.1, 1,0 and 2.3 mT for 6 and 48 hours, respectively (Table. 7). The exposition of ES cells to 5 min on followed by 30 min off cycles applied at

the high flux density of 2.3 mT resulted in a statistically significant up-regulation of egr-1, p21 and c-jun mRNA levels in p53-deficient ES cells (Figure 38A and C), whereas wild type cells showed no variations in transcript levels compared to sham exposure and control cells (Figure 38A). In contrast, low flux densities of 0.1 and 1 mT ELF-EMF applied at 5 min on/30 min off intermittence cycles induced no significant effects on transcript levels indicating that a high flux density of ELF-EMF signals is necessary to affect mRNA levels of regulatory genes (Table 7).

Table 7. Conditions of the exposure of p53-proficient and deficient pluripotent embryonic stem cells embryonic stem cells to ELF-EMF and summary of the effects on transcript levels of regulatory genes.

Intermittent exposure (5min on/30 min off)			
6 hours ELF-EMF exposure ; wt, $p53^{-/-}$		48 hours ELF-EMF exposure; wt, $p53^{-/-}$	
0.1 mT	no ELF-EMF effect (n=3)	0.1 mT	no ELF-EMF effect (n=3)
1.0 mT	no ELF-EMF effect (n=3)	1.0 mT	no ELF-EMF effect (n=3)
2.3 mT	up-regulation of egr-1, p21 and c-jun in $p53^{-/-}$ cells (without recovery time, RT); no ELF-EMF effect after 18 h RT (n=6)	2.3 mT	no ELF-EMF effect (n=3)

Intermittent exposure (5min on/10 min off)			
6 hours ELF-EMF exposure; wt, $p53^{-/-}$; without RT		6 hours ELF-EMF exposure; wt, $p53^{-/-}$; 18h RT	
2.3 mT	no ELF-EMF effect (n=6)	2.3 mT	no ELF-EMF effect (n=6)

Continuous exposure			
6 hours ELF-EMF exposure; wt, $p53^{-/-}$		48 hours ELF-EMF exposure; wt, $p53^{-/-}$	
0.1 mT	no ELF-EMF effect (n=3)	0.1 mT	no ELF-EMF effect (n=3)
1.0 mT	no ELF-EMF effect (n=3)	1.0 mT	no ELF-EMF effect (n=3)

ELF-MF exposure of p53-deficient cells induced only short-term and transient effects on gene expression levels.

To elucidate, whether ELF-EMF induce short- or long-term responses, p53-deficient and wt ES cells were exposed to intermittent 5 min on/30 min off ELF-EMF signals for 6 hours. In parallel, the cells were analysed after a recovery time of 18 hours. No statistically significant effects could be seen after 18 hours recovery in control, sham- and field-exposed variants suggesting that ELF-EMF induced only an immediate transient response in p53-deficient cells (Figure 38B).These observations correlated with the results of the 48 hours ELF-EMF exposure to p53-deficient ES cells at early differentiation stage, where no ELF-EMF effects on transcript levels were found (data not shown, see Table 7).

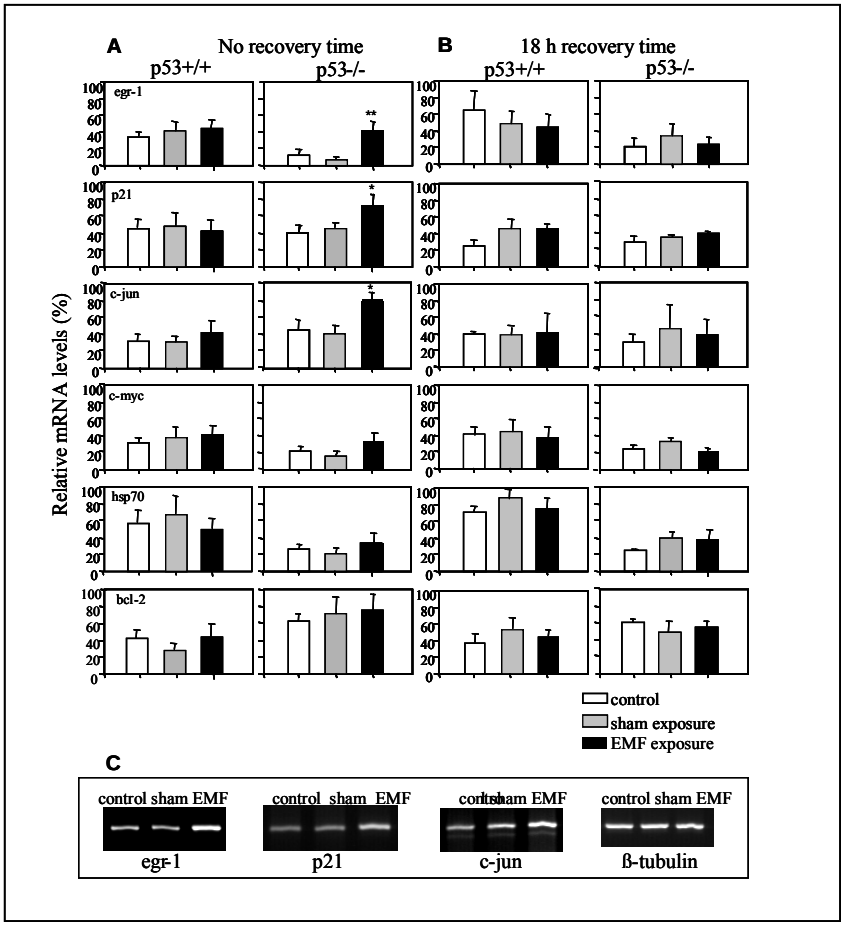

Figure 38. Relative mRNA levels of genes encoding egr-1, p21, c-jun, c-myc, hsp70 and bcl-2 in p53-deficient ($p53^{-/-}$) EC cell-derived embyoid bodies (EB) compared to wild-type (wt, $p53^{+/+}$) D3 cells immediately after 6h ELF-EMF (2.3 mT, intermittency 5 min on / 30 min off cycles) exposure (A) and after 18h recovery time (B) analysed by semi-quantitative RT-PCR. ELF-EMF exposure resulted in a significant, but transient up-regulation of egr-1, c-jun and p21mRNA levels in undifferentiated p53-deficient (C), but not wt ES cells. Statistical significance was tested by Studentt's t-test for significance levels of 1% and 5% (**p<0.01; *p<0.05)

ELF-MF effects on transcript levels of regulatory genes in p53-deficient cells were dependent on intermittence cycles (on/ off cycle duration).

In addition, we analysed in wt and p53-deficient ES cells the influence of ELF-EMF signals applied at another intermittence scheme of 5 min on/10 min off for 6 hours with a flux density of 2.3 mT. We found that 5 min on/10 min off ELF-EMF signals with or without recovery time had no effects on the transcript levels of the investigated regulatory genes in both, wt and p53-deficient cells. Further, continuous ELF-EMF signals at flux densities of 0.1 and 1 mT were applied to wt and p53-deficient ES cells. We found no influence of continuous ELF-EMF on the mRNA levels of the regulatory genes included in the study (data not shown). Experiments with the highest flux density (2.3 mT) could not be performed with the continuous exposure protocol, because the generated ohmic heat of the coils could not be compensated by the incubator and would have resulted in an unstable ambient temperature.

ELF-EMF exposure up-regulated the transcript levels of bcl-2, the growth arrest and DNA damage inducible gene (GADD45) and down-regulates bax in ES cell-derived neural progenitor cells.

Elf-EMF (50 Hz-Power line, 2 mT, 5 min.on/30min. off, Table 8) was applied for 6 or 48 hours on neural progenitors (Table 8). Semi-quantitative RT-PCR analysis revealed no effect of ELF-EMF on transcript levels of genes involved in neuronal differentiation (nurr1, en-1) and on markers of differentiating

(nestin) or differentiated neuronal (TH) or astrocytic (GFAP) cells. In addition, we studied the effect of ELF-EMF on transcript levels of genes involved in the regulation of cell homeostasis (hsp70), cell cycle (p21) and anti-apoptosis (bcl-2). RT-PCR analysis revealed that, whereas transcript levels of p21 and hsp70 remain similar in sham and ELF-EMF exposed variants, a significant up-regulation of the growth arrest inducible gene GADD45 was observed at stage 4d+11d. (Figure 39). The quantitative RT-PCR (Q-RT-PCR) with specific primers and TaqMan probes showed that bcl-2 was first down-regulated at stage 4+7d ($p<0.05$), then up-regulated in the intermediate stage 4+11d ($p<0.01$) and at the terminal stage 4+23d ($p<0.05$). GADD45 was significantly up-regulated at stage 4+11d, then down-regulated at the terminal stage 4+23d (Figure 40). These studies were further substantiated by immunofluorescence analyses of neuronal markers. However, by immunofluorescence analysis, no changes in intracellular distribution and number of cells expressing neuronal markers (ßIII-tubulin, TH, GFAP) were observed (data not shown).

Table 8. Conditions of the exposure of neuronal progenitor cells to ELF-EMF and summary of the effects on transcript abundance, neural differentiation induction and DNA break induction.

Intermittent exposure (5min on/30 min off)			
48 hours, ELF-EMF (Power line, 50Hz)		6 hours, ELF-EMF (Power line, 50Hz)	
2.0 mT	up-regulation followed by down-regulation of GADD45 up-regulation of bcl-2 down-regulation of bax no effect on neural differentiation no effect on DNA break induction (n=6)	2.0 mT	no effect on DNA break induction (n=3)

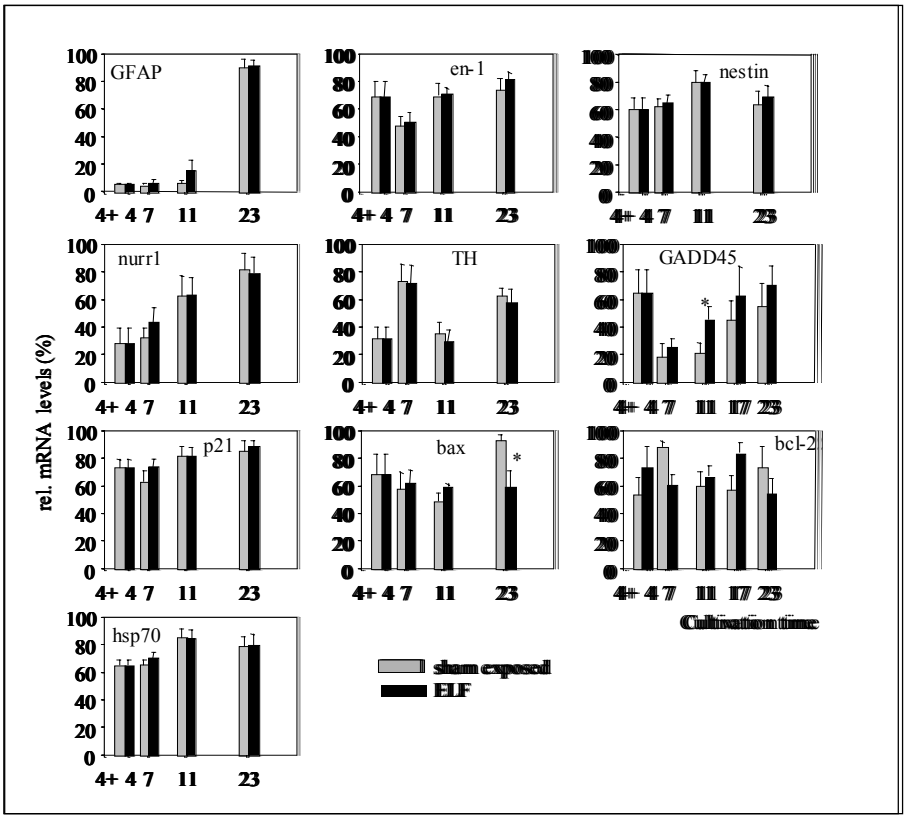

Figure 39. Relative mRNA levels of genes encoding the regulatory genes bcl-2, bax, p21, hsp70 and the genes involved in neuronal differentiation en-1, nurr1, TH, GFAP and nestin in ES-derived neural progenitors after 48 hours ELF (50Hz Powerline) EMF exposure (2.0 mT, intermittence 5 min ON/30 min OFF), at stage 4+4d - 4+6d. EMF exposure resulted in a significant transcript up-regulation of GADD45 and down-regulation of bax. Error bars represent standard deviations. Statistical significance was tested by the Student's t-test for a significance level of 5% (*, p£ 0.05).

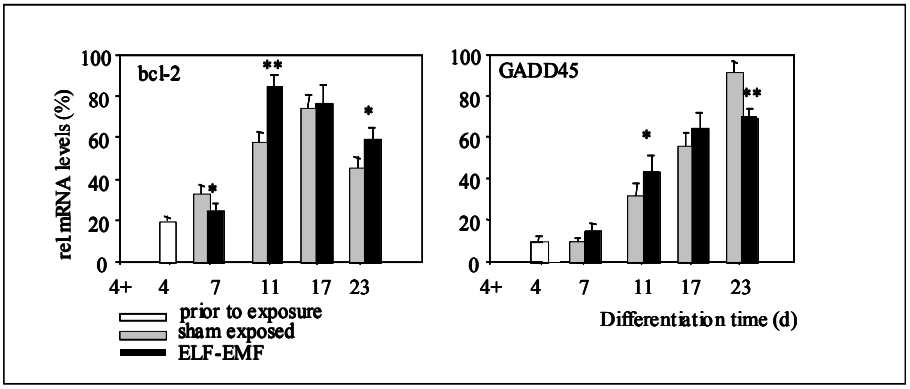

Figure 40.: Quantitative RT-PCR for estimation of relative mRNA levels of genes encoding the regulatory genes bcl-2 and GADD45 in ES-derived neural progenitors after 48 hours ELF (50Hz Powerline) EMF exposure (2.0 mT, intermittence 5 min on/30 min off), at stage 4+4d - 4+6d. EMF exposure resulted in a significant transcript down-regulation followed by up-regulation of bcl-2, which correlated with up-regulation followed by down-regulation of GADD45. Error bars represent standard deviations. Statistical significance was tested by the Student's t-test for a significance level of 5% and 1% (*, p< 0.05 ;**, p< 0.01).

3.1.4.2 Human neuroblastoma cell line SY5Y (Participant 11)

In order to obtain cellular models to study ELF-EMF, we have characterised some neuroblastoma cell lines for their ability to express nAchRs and evaluate whether ELF-EMF can interfere with the expression of alpha3, alpha5 and alpha7 nAchR subunits, as well as with that of Phox2a, Phox2b and dopamine-beta-hydroxylase (DβH).

Three human neuroblastoma cell lines (SH-SY5Y, SK-N-BE and IMR32) have been analysed, by means of northern blot analysis, for the expression of neuronal acetylcholine receptor subunits. Due to the high degree of homology between different subunits, the experiments have been carried out with probes derived from the cytoplasmic portion, the least conserved region of nAchR subunits, in order to avoid cross-contamination. The results showed that these cells express the ganglionic type of nAchRs (alpha3, alpha5 and alpha7), but not alpha 4, mainly expressed in the CNS (data not shown and Fornasari 1997; Flora 2000). Furthermore only human neuroblastoma cell lines SY5Y and IMR-32 appeared to express either Phox2a, Phox2b or DβH (Flora, 2001 and data not shown), although with differences in the level of expression. As the SY5Y lineage shows higher expression of the three genes, we decided to use this as a model in all the experiments.

ELF-EMF did not affect the expression of nicotinic acetylcholine receptors (nAchRs) which represent the neuronal nicotinic system in human neuroblastoma cells.

At the beginning of our experiment we decided to use field strengths which are larger than the maximum real-world exposure and eventually scale-down, in the case of measurable effect, establishing the minimum threshold level to which ELF-EMF do not represent a risk to human health. Neuroblastoma cell line SY5Y was then exposed to ELF-EMF (50 Hz, powerline signal) continuously for 16 hours at flux densities of 2 mT and 1 mT and the expression level of humaṇ alpha 3,alpha 5 and alpha 7 nAchRs subunits analysed by means of Northern blotting. Figure 41 (panel A) shows the results obtained by three independent exposures at 2 mT (lanes 1, 4 and 5) together with that of sham-exposed cells (lanes 2, 3 and 6). The densitometric quantification of the mRNA level, however, has shown no effect on the expression level of nAchR subunits as compared to that of the sham-exposed cells set as 100%, when cells were exposed either at 2 mT or 1 mT (Figure 41), panel B and C respectively). We then decided to explore whether an intermittent exposure might be influent on the expression of the nAchR subunits tested. Exposing the cells to intermittent magnetic field (5 min on/5 min off), 2 mT and 1 mT flux density, for 16 hours did not affect the expression of the alpha3, alpha5 and alpha7 nAchR subunit genes (Figure 42, panel A and B respectively).

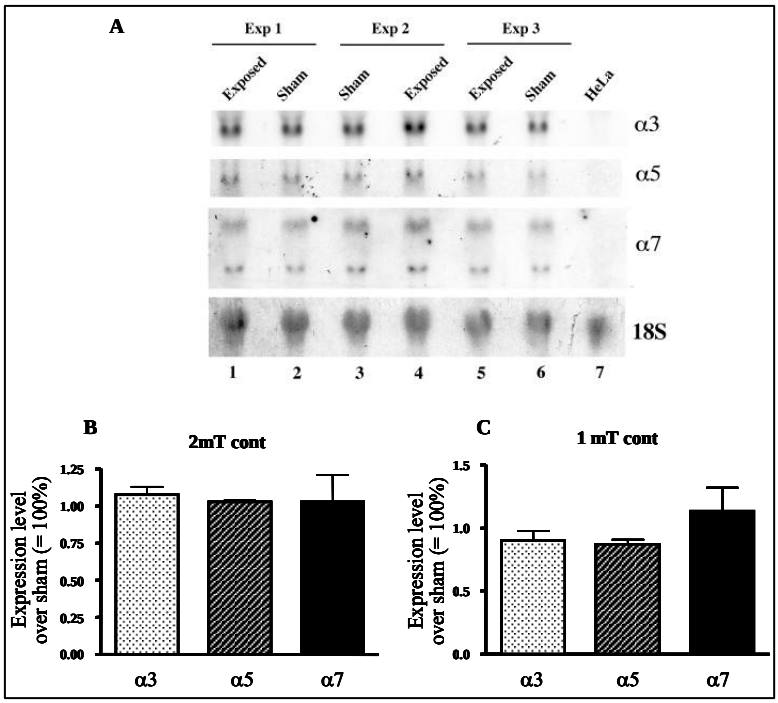

Figure 41. nAchR subunits expression upon exposure to 16 hours continuous ELF-EMF. 20 µg of total RNA extracted from SY5Y cells exposed to 2mT and 1 mT continuous 50 Hz magnetic field, for 16 hours, was hybridised to cDNA probes corresponding to the human alpha3, alpha5 and alpha7 nAchR subunits. The expression level was normalised to that of 18S RNA. A, Northern blot analysis of total RNA extracted upon exposure to 2mT ELF-EMF. Here reported are the results of three independent experiments (Exp1, lanes 1-2; Exp 2, lanes 3-4; Exp 3, lanes 5-6). Lane 7, HeLa total RNA has been used as a negative control. B and C, Densitometric quantification of the expression level of nAchR subunits upon exposure to 2 mT and 1 mT continuous ELF-EMF, respectively. The data are the mean of three independent experiments ± S.E., expressed as a percentage of the sham-exposed sample set equal to 100%.

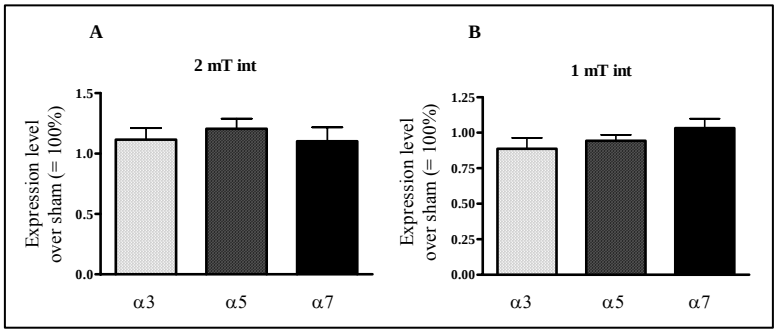

Figure. 42. nAchR subunits expression upon exposure to 16 hours intermittent ELF-EMF. 20 µg of total RNA extracted from SY5Y cells exposed to 2mT and 1 mT continuous 50 Hz magnetic field, for 16 hours, was hybridised to cDNA probes corresponding to the human alpha3, alpha5 and alpha7 nAchR subunits. The expression level was normalised to that of 18S RNA. The data are the mean of three independent experiments ± S.E., expressed as a percentage of the sham-exposed sample set equal to 100%. A, Densitometric quantification of the expression level of nAchR subunits upon exposure to 2 mT intermittent ELF-EMF. B, Densitometric quantification of the expression level of nAchR subunits upon exposure to 1 mT intermittent ELF-EMF.

As we were not able to measure any effect at the mRNA level, we wondered whether the exposure to ELF-EMF might have an effect at the level of receptor proteins. To this purpose we carried out radioligand assays on cells exposed to either continuous or intermittent 50 Hz ELF-EMF, flux densities of 1 mT and 2 mT for 16 hours, to assess the amount of protein functionally assembled in the receptors. The

binding was performed in the presence of radiolabelled ligands, ^{3}H-Epibatidine to quantitate alpha3-containing receptor and ^{125}I-alpha-bungarotoxin to quantitate alpha7-containing receptor. However, as shown in Figure 43, no change in the amount of either alpha3- or alpha7-containing receptor was detected under the same conditions used in Northern blot analysis of Figures 41 and 42, as compared to that of the sham-exposed cells set as 100%.

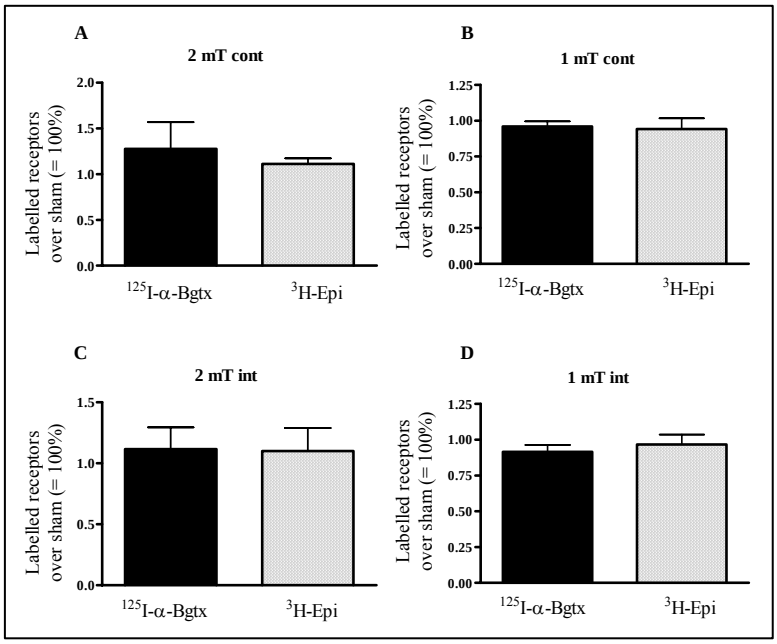

Figure 43. Quantitative analysis of the alpha3- and alpha7-containing receptors upon continuous and intermittent ELF-EMF exposure for 16 hours

The amount of labelled receptors were obtained from the binding of saturating concentration of ^{3}H-Epibatidine (grey bars) and ^{125}I-alpha-bungarotoxin (black bars) to the cell homogenates, performed in quadruplicate. The values are the mean of three independent experiments ± and S.E. are expressed as percentage of labelled receptors in the exposed samples with respect to the sham-exposed cells set as 100%. A and B, continuous exposure to 1 mT and 2 mT ELF-EMF, respectively. C and D, intermittent (5 min on/5 min off) exposure to 1 mT and 2 mT ELF-EMF.

The experiments carried out until now have showed that the ELF-EMF does not influence the expression of nAchRs upon exposure of the cells to magnetic field with flux densities of either 1 mT or 2 mT for a relatively short period of time (16 hours). We then investigated whether the duration time of the exposure of SY5Y cells to ELF-EMF might affect the expression of the genes encoding the nAchR subunits, and especially, whether longer exposure to ELF-EMF might affect the expression of some of the genes. To answer this question two different exposure protocols have been used: a) 50 Hz powerline signal, flux density 1 mT, continuous exposure, duration 48 hours. The RNA or proteins were extracted immediately after the end of exposure (immediate recovery); b) 50 Hz powerline signal, flux density 1 mT, continuous exposure, duration 48 hours. The RNA or proteins were extracted 48 hours after the end of exposure (delayed recovery).

As shown in Figure 44, panel A, the expression of nAchR subunits, as measured at mRNA level, was again not affected by a prolonged exposure to the ELF-EMF followed by an immediate recovery of the cells (protocol a). Furthermore, no effect was detected at the level of receptor proteins (Figure 44, panel B). We then wondered whether the effect could be a delayed one, that is mediated by the activation of a cascade of second messengers that results in a change of gene expression. To test this hypothesis, cells were collected for RNA and protein analysis 48 hours after the end of the exposure (protocol b). The

results shown in Figure 44 seemed to rule out an indirect effect as neither the level of mRNA (Figure 45, panel A) nor of the receptor proteins (Figure 45, panel B) changed under these experimental conditions.

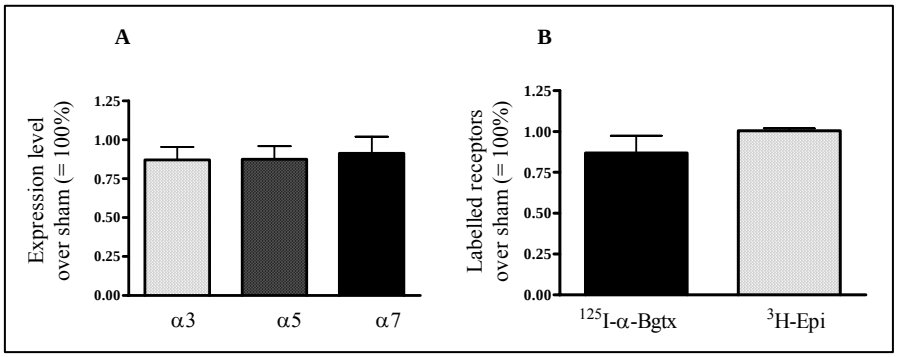

Figure 44. nAchR subunits expression and quantitative analysis of the alpha3- and alpha7 containing receptors upon continuous exposure to 1 mT ELF-EMF for 48 hours: Immediate recovery

Cells were exposed to 1 mT ELF-EMF for 48 hours and recovered immediately after the end of the exposure. A, Densitometric quantification of the expression level of nAchR subunits after Northern blot analysis. The data are the mean of five independent experiments ± S.E., expressed as a percentage of the sham-exposed sample set as 100%. B, quantification of the alpha3- (grey bars) and alpha7-containing (black bars) receptors. The values are the mean of three independent experiments ± and S.E. are expressed as percentage of labelled receptors in the exposed samples with respect to the sham-exposed cells set as 100%.

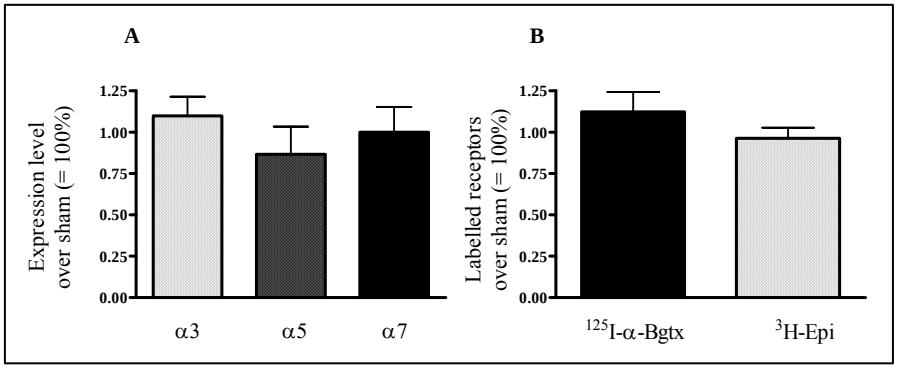

Figure 45. nAchR subunits expression and quantitative analysis of the alpha3- and alpha7 containing receptors upon continuous exposure to 1 mT ELF-EMF for 48 hours: Delayed recovery

Cells were exposed to 1 mT ELF-EMF for 48 hours and recovered 48 hours after the end of the exposure. A, Densitometric quantification of the expression level of nAchR subunits after Northern blot analysis. The data are the mean of five independent experiments ± S.E., expressed as a percentage of the sham-exposed sample set as 100%. B, quantification of the alpha3- (grey bars) and alpha7-containing (black bars) receptors. The values are the mean of three independent experiments ± and S.E. are expressed as percentage of labelled receptors in the exposed samples with respect to the sham-exposed cells set as 100%.

ELF-EMF did not affect the expression of markers of the cathecolaminergic system in neuroblastoma cells.

In collaboration with Participant 1 we decided to investigate the influence of ELF-EMF on neurotransmitter release. In particular, the activity of the dopamine-beta-hydroxylase (DβH) which is a key enzyme in the synthesis of noradrenaline has been studied. Furthermore, we investigated possible modifications on the expression of two related homeo-domain transcription factors, Phox2a and Phox2b, that are relevant for the specification of the autonomic nervous system. Moreover, in noradrenergic cells, they are directly involved in the determination of the neurotransmitter phenotype by regulating the expression of DβH. As protocols, we applied the same exposure conditions used for the analysis of the human nAchR subunits. As shown in Figure 46, panels A and B, continuous exposure of SY5Y neuroblastoma cells to 1 mT and 2 mT 50 Hz ELF-EMF did not affect the expression level of either Phox2a, Phox2b and DβH genes, as compared to that of the sham-exposed cells set to 100%. Again we asked whether an intermittent exposure might have an effect on gene expression of these proteins. We then measured the mRNA level upon intermittent exposure (5 min on/5 min off) to 1 mT ELF-EMF, but no change was observed (Figure 47). Previous experiments have shown that an exposure of SY5Y cells for 48 hours at 1 mT flux density reduced the amount of mRNA of Phox2a, but not of Phox2b and DβH. We then exposed the cells under these conditions up to nine times independently.

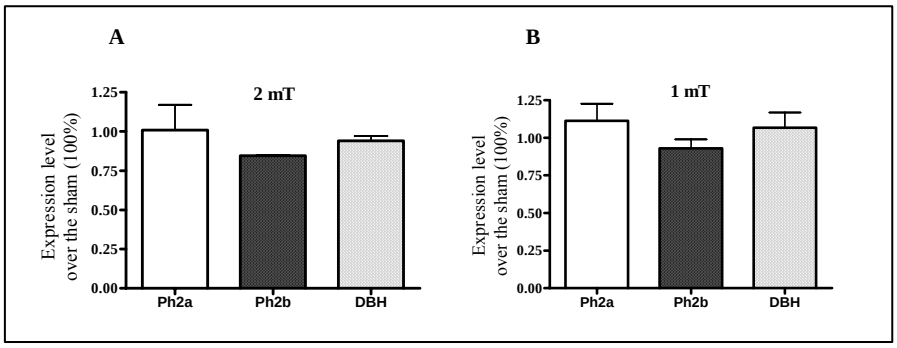

Figure 46. Noradrenergic phenotype specifying genes expression upon continuous exposure to ELF-EMF for 16 hours

20 µg of total RNA extracted from SY5Y cells continuously exposed to 1mT and 2 mT 50 Hz ELF-EMF for 16 hours was hybridised to cDNA probes corresponding to the human Phox2a, Phox2b and DβH genes. The expression level was normalised to that of 18S RNA. A Densitometric quantification of the expression level of the three genes upon continuous exposure to 2 mT ELF-EMF. B, Densitometric quantification of the expression level of the three genes upon continuous exposure to 1 mT ELF-EMF. The data are the mean of five independent experiments ± S.E., expressed as a percentage of the sham-exposed sample set as 100%.

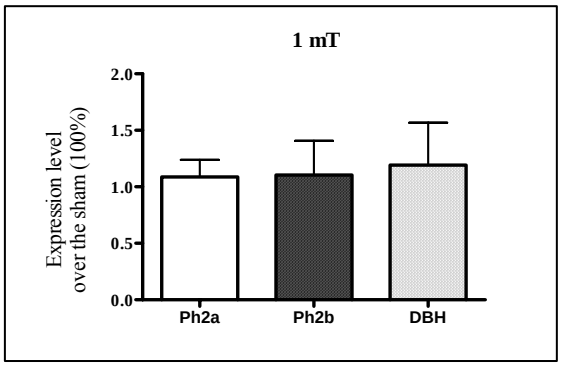

Figure 47. Noradrenergic phenotype specifying genes expression upon intermittent exposure (5 min on/5 min off) to ELF-EMF for 16 hours.

Densitometric quantification of the expression level of the three genes upon intermittent exposure to 1 mT ELF-EMF, after Northern blot analysis. The data are the mean of five independent experiments ± S.E., expressed as a percentage of the sham-exposed sample set as 100%.

Statistical analysis has ruled out that, upon this exposure protocol, the expression of the noradrenergic specifying genes was affected, as shown in Figure 48, either harvesting the cells immediately after the end of the exposure (Figure 48, panel A) or 48 hours later (Figure 48, panel B). As no change was seen at the level of mRNA we asked whether the exposure to ELF-EMF might affect the expression of Phox2a and Phox2b at protein level. To this purpose we decided to measure, by western blot analysis, the protein level upon continuous exposure to 50 Hz ELF-EMF, flux density 1 mT, for 16 and 48 hours (Figure 49). Cells were harvested immediately after the end of the exposure (Figure 49, lanes 10-13 and lanes 6-9, respectively). Also protein extract from cells harvested 48 hours after the end of the continuous 48 hours exposure was tested (Figure 49, lanes 2-5). Densitometric analysis of the signal obtained for Phox2a (Figure 49, panel A) and Phox2b (Figure 49, panel B), normalised to that of the beta-tubulin, revealed that exposure of SY5Y cells to relatively short or longer period of time did not affect the expression of Phox2a and 2b, at protein level, as compared to that of the sham-exposed cells (Figure 49, panel C).

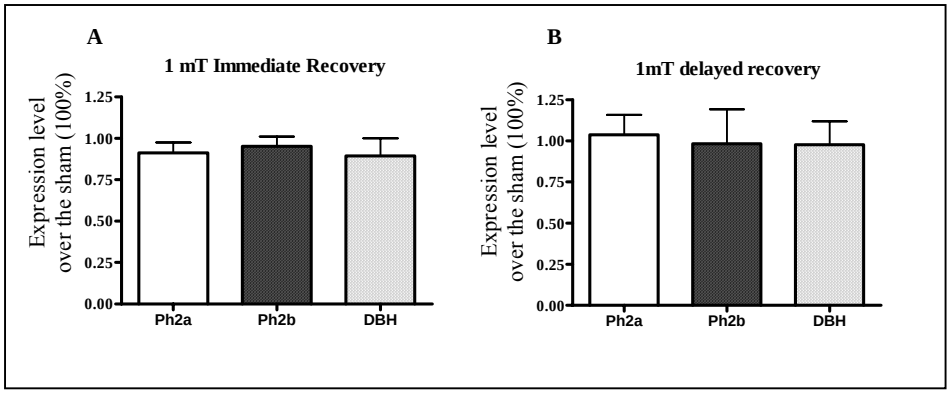

Figure 48. Noradrenergic phenotype specifying genes expression upon continuous exposure to ELF-EMF for 48 hours

SY5Y cells were continuously exposed to 1 mT 50 Hz ELF-EMF for 48 hours and collected either immediately (panel A) or 48 hours (panel B) after the end of the exposure. After northern blot analysis, the expression level of Phox2a, Phox2b and DβH genes was quantified by densitometric scanning of the autoradiogram. The data are the mean of six independent experiments ± S.E. (Phox2b and DβH) and nine independent experiments (Phox2a), expressed as a percentage of the sham-exposed sample set equal to 100%.

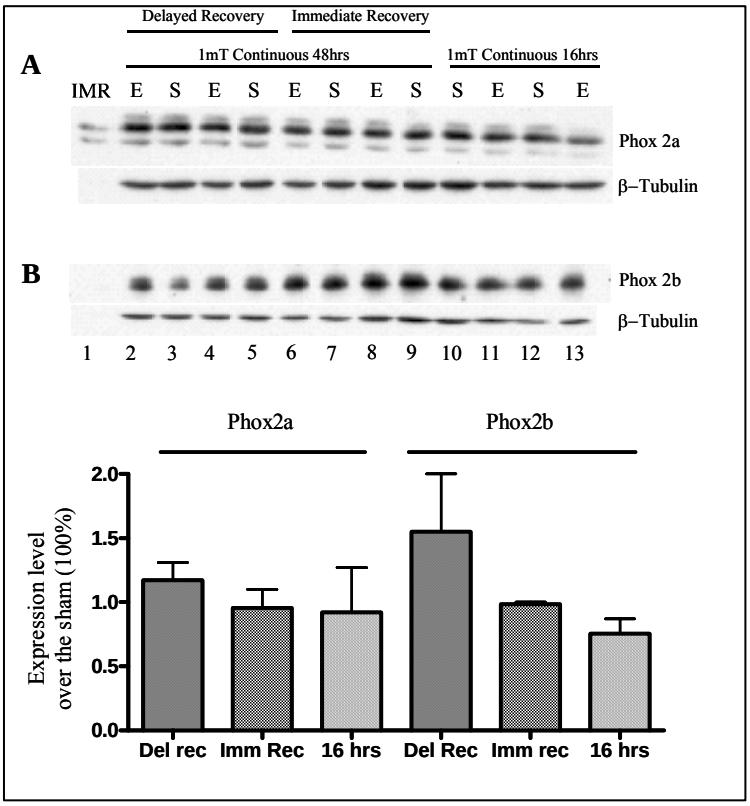

Figure 49. Western blot analysis of Phox2a and Phox2b expression upon continuous exposure to 1 mT ELF-EMF.20 µg of total protein extract were size-fractionated by SDS-PAGE and transferred to nitrocellulose membrane. The expression of Phox2a and Phox2b was detected by incubation with anti-Phox2a (panel A) and anti-Phox2b antibodies (panel B). Lanes 2-9, samples from continuous exposure to 1 mT ELF-EMF for 48 hours recovered 48 hours (lanes 2-5) or immediately (lanes 6-9) after the end of the exposure. Lanes 10-13, samples from 1 mT continuous exposure for 16 hours. Lane 1, IMR 32 neuroblastoma cells nuclear extract used as a control. E= exposed, S= sham-exposed. The expression of Phox2a and Phox2b was normalised to that of β-tubulin. C, quantification of the expression level of Phox2a and Phox2b. The data are the mean of two independent exposures ± S.E. and are expressed as percentage of the sham-exposed samples set as 100%. Del Rec = recovery 48 hours after the end of the exposure; Imm rec = recovery immediately after the end of the exposure; 16 hours = samples were exposed for 16 hours to 1 mT continuous ELF-EMF.

3.1.4.3 Embryonic stem cells of mice during cardiac differentiation (Participant 8)

In higher vertebrates, heart formation is a complex phenomenon that starts at early stages of embryogenesis, prior to the end of gastrulation, with commitment of anterior lateral plat mesoderm cells to cardiogenic lineage. Studies in different organ systems have shown that tissue-specific transcription factors which control the expression of differentiation markers are also regulators of cellular differentiation. Basic helix-loop-helix proteins such as the myogenic factor are key regulators of skeletal muscle differentiation, while the erythroid cell-specific zinc finger protein GATA-1 is crucial for erythroid cell differentiation. It is now becoming evident that inactivation of the mouse homologue of the Drosophila melanogaster homeobox gene tinman, the homeobox gene Nkx2.5 or Csx affects heart morphogenesis (Biben 1997, Lints 1993). Moreover, the GATA-4 protein, a member of the GATA family of transcription factors, has been found to be restricted to the hearts and to characterise very early stages of heart formation during embryonic development (Grepin 1995).

ELF-EMF affected the expression of cardiogenic genes in murine embryonic stem cells (GTR1).

In the first step of our study we looked at the effects of ELF-EMF (0.8 mT, 50 Hz sinusoidal) on the expression of cardiogenic genes in mouse embryonic carcinoma (EC) cells (P19 cells). Despite the encouraging results obtained in our pilot experiments, in a subsequent set of ten separate experiments P19

cells exposed to ELF-EMF desultorily underwent a gene program of cardiogenesis and revealed structural and functional cardiomyocyte features. Only in 2 experiments, exposure to ELF-EMF primed the expression of both GATA-4 and Nkx-2.5 genes, and led to the appearance of alpha-myosin heavy chain (MHC) and myosin light chain-2V (MLC), two cardiospecific transcripts. A representative RT-PCR analysis of cardiogenic and cardiac specific gene expression from ELF-EMF responsive cells is shown in Figure 50).

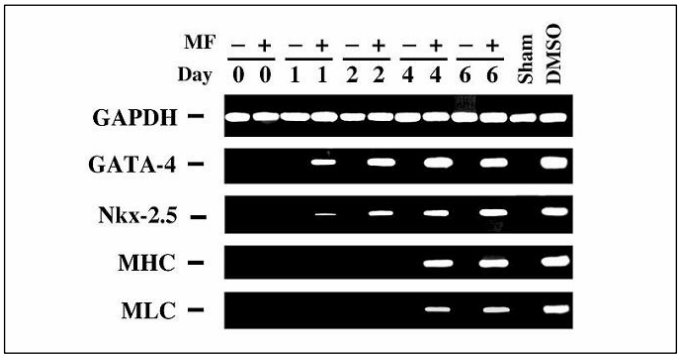

Figure 50. RT-PCR analysis of cardiogenic and cardiospecific transcripts in P19 cells exposed to ELF-EMF (continuous exposure, 4 days). MHC, alpha-myosin heavy chain. ML*C,* myosin light chain-2V.

We reasoned that the lack of data reproducibility of these results could be due to the consistent dilution of the myocardial phenotype within multiple non-myocardial cells encompassed by the P19 model of cell differentiation. To circumvent this problem, we decided to change the biological model, by using a line of pluripotent embryonic stem (ES) cells engineered for a gene trapping selection of a virtually pure population of ES-derived cardiomyocytes. RT-PCR analysis of targeted transcripts in unexposed cells indicated that, differently from undifferentiated LIF-supplemented cells, EBs expressed both GATA-4 and Nkx-2.5 mRNA (Figure 51). The expression of these cardiogenic genes resulted to be further enhanced in puromycin selected, ES-derived cardiomyocytes (Figure 52). Figures 51 and 52 show that ELF-EMF exposure remarkably increased GATA-4 and Nkx-2.5 gene expression in both EBs and cardiomyocytes, as compared to unexposed GTR1 cells. Interestingly, in both groups of cells ELF-EMF also increased the expression of the prodynorphin gene, an endorphin gene that has been recently shown to play a major role in orchestrating ES cell cardiogenesis (Ventura 2003(a), 2003(b), 2000). These responses were further inferred by the quantitative analysis of mRNA levels as shown in RNase protection experiments (Figure 53). Interestingly, nuclear run-off analyses of GATA-4 gene transcription indicated that the ELF-EMF action occurred at the transcriptional level (Figure 54). The activation of a program of cardiogenic gene transcription was also associated with the appearance of the cardiac specific transcripts alpha-myosin heavy chain and myosin light chain-2V (Figure 55).

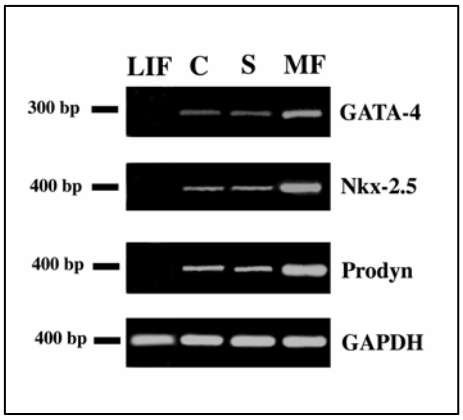

Figure 51. ELF-EMF was applied from the time of LIF removal and EBs were collected after 3 additional days. C: control EBs; S: sham. (Ethidium bromide-stained agarose gels, representative of 4 separate experiments).

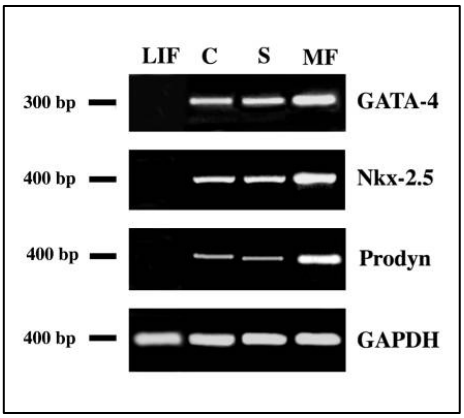

Figure 52. Effect of ELF-EMF (MF) on Cardiogenic gene expression in puromycin-selected cells. ELF-EMF was applied from the time of LIF removal throughout puromycin selection. Four days after puromycin addition (10 days from LIF withdrawal), ES-derived cardiomyocytes were processed gene expression analyses. C: control puromycin-selected cardiomyocytes; S: sham. (Ethidium bromide-stained agarose gels, representative of 4 separate experiments).

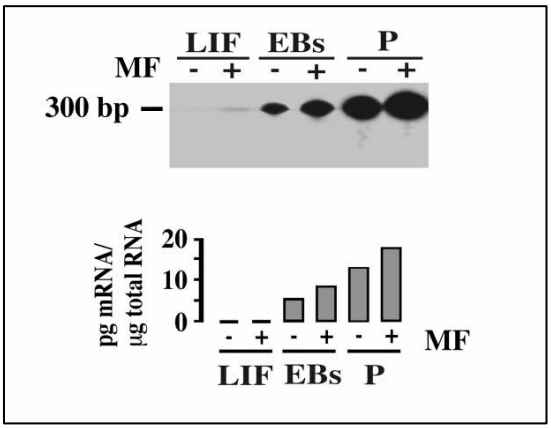

Figure 53. RNase protection analysis of GATA-4 mRNA expression in GTR1 ES cells cultured in the absence or presence of ELF-EMF.LIF, undifferentiated GTR1 cells. EBs, embryoid bodies collected 5 days after LIF removal. *P*, puromycin-selected cardiomyocytes: puromycin was added at day 8 following LIF removal. Each group of cells was cultured in the absence (-) or presence (+) of ELF-EMF. Autoradiograms are representative of 3 separate experiments.

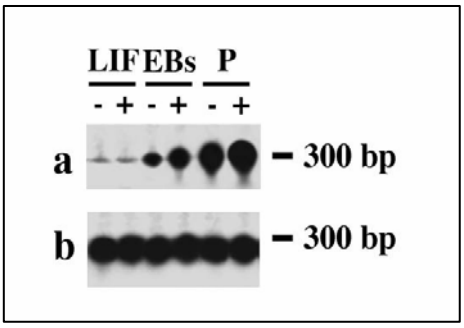

Figure 54. Nuclear run-off analysis of GATA-4 gene transcription in isolated ES cell nuclei. Nuclei were isolated from undifferentiated GTR1 cells (LIF), from EBs collected 5 days after LIF removal (EBs) or from puromycin-selected cardiomyocytes (P): puromycin was added at day 8 following LIF removal. Each group of cells was exposed in the absence (-) or presence (+) of ELF-EMF (MF). Puromycin was added at day 8 following LIF removal. Row a, GATA-4 gene transcription. Row b, cyclophilin gene transcription (cyclophilin was assessed as a constant gene for control). Autoradiograms are representative of 3 separate experiments.

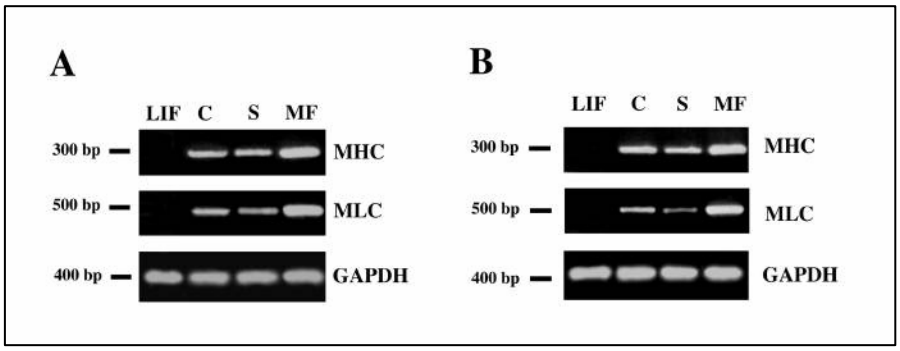

Figure 55: Effect of MF on the expression of cardiac specific genes.A: ELF-EMF (MF) was applied from the time of LIF removal and EBs were collected after additional 3 days. B: MF was applied from the time of LIF removal throughout puromycin selection. Four days after puromycin addition (10 days from LIF withdrawal), ES-derived cardiomyocytes were processed gene expression analyses. C: control cells; S: sham. (Ethidium bromide-stained agarose gels, representative of 4 separate experiments).

Exposure of GTR1 ES cells to ELF-EMF after LIF removal and throughout 4 days of puromycin selection for an overall period of 10 days from LIF withdrawal was able to increase the yield of ES-derived cardiomyocytes: the number of beating colonies reached 170.44 ± 28.0 % of the control value, estimated in cardiomyocytes selected from untreated cells (mean ± SEM of 4 separate experiments).

We finally investigated whether the transcriptional responses evoked by ELF-EMF may encompass genes that are essential for the specification of non-myocardial lineages. Noteworthy, the expression of MyoD, a gene involved in skeletal myogenesis was not affected in both EBs and puromycin selected cells (Figure 56), while the expression of neurogenin1, a neuronal specification gene, was slightly enhanced only in EBs (Figure 56).

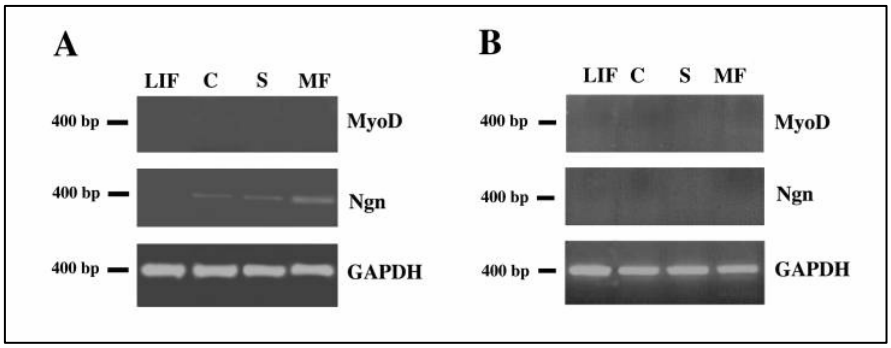

Figure 56. Effect of ELF-EMF (MF) on the expression of genes promoting non-myocardial lineages. A: MF was applied from the time of LIF removal and EBs were collected after additional 3 days. B: MF was applied from the time of LIF removal throughout puromycin selection. Four days after puromycin addition (10 days from LIF withdrawal), ES-derived cardiomyocytes were processed gene expression analyses. C: control cells; S: sham. MyoD and neurogenin1 (Ngn) are skeletal muscle and neuronal specification genes, respectively. (Ethidium bromide-stained agarose gels, representative of 4 separate experiments).

3.1.4.4 Membrane currents of oocytes of *Xenopus laevis* expressing rCx46 (Participant 7)

ELF-EMF did not significantly affect the leak-current of oocytes of Xenopus laevis expressing hemi-channels of rCx46.

During expression of hemi-channels, composed of the connexin rCx46, the oocytes were exposed to ELF-EMF (50 Hz). As suitable parameter for functional integrity of an oocyte the leak-current was selected which was electrophysiologically measured at voltage-clamp. A representative experiment of a sham exposed oocyte is shown in Figure 57. Figure 57a) shows membrane currents recorded at depolarising test potentials starting from a holding potential of –90 mV. The figure indicates that the rCx46-mediated current becomes activated by depolarising test potentials above about –10 mV. Figure 57b) shows the corresponding leak subtracted steady-state current values (I_{ss}) as function of driving voltage ($V-V_{rev}$) where V_{rev} denotes the corresponding reversal potential. The corresponding steady-state current values were derived at the end of the applied test pulse.

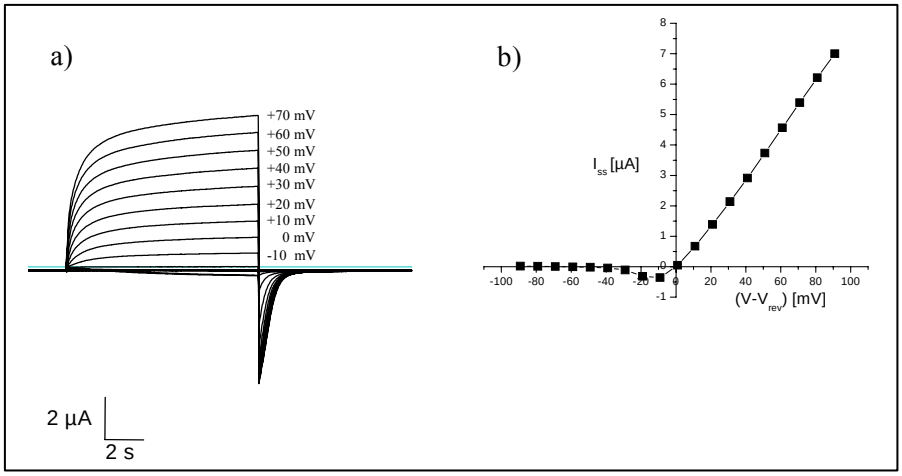

Figure 57. Voltage-dependent current activation of sham exposed *Xenopus* oocytes expressing rCx46 after an expression time of 16 hours.**a)** Representative voltage-jump current-relaxations at given test potentials. The common holding potential was set to -90 mV. The dotted line denotes the zero current level. **b)** Leak subtracted steady-state current amplitudes (I_{ss}, , ■) derived from the data in a) as function of driving voltage ($V-V_{rev}$)

The leak-current was derived at test potentials in the range of -70 mV to -100 mV using a constant holding potential of -90 mV. A comparison of leak-currents for exposed and sham exposed oocytes is given in Figure 58. Figure 58a shows the leak-current for oocytes which were continuously exposed for 16 hours at 2.3 mT and Figure 55b) the corresponding leak-current after an intermittent exposure (5 min on/10 min off) at 1.0 mT for 16h. A significant influence of ELF-EMF exposure on the leak current could not be observed for the different exposure conditions.

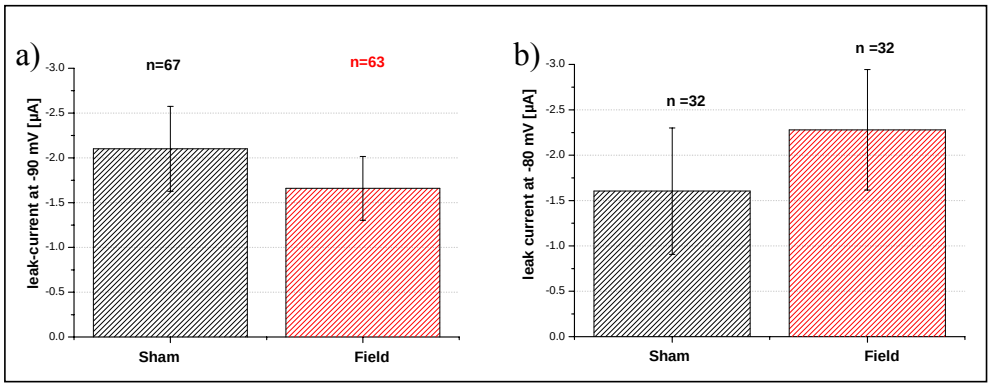

Figure 58. Leak-currents of single oocytes after expression of rCx46- hemi-channels at different holding potential.**a**) Leak current amplitudes at holding potential –90 mV of sham and ELF-EMF (2.3 mT, 16 hours) continuously exposed oocytes. **b**) Leak-currents at holding potential –80 mV of sham and ELF-EMF (1.0 mT, 16 hours, 5 min on/10 min off) exposed oocytes. Data are given as mean ± s.e.m. n denotes the number of different oocytes.

No significant influence of ELF-EMF on the number of expressed and conducting hemi-channels composed of rCx46 in oocytes.

The expression level of hemi-channels composed of rCx46 was estimated from the number of conducting hemi-channels which corresponds to the mean steady-state current amplitude (I_{ss}) and/or the maximal membrane conductance G_{max} at depolarising test potentials. Expression of endogenous hemi-channels was suppressed by injection of the corresponding anti-sense. Figures 59a, 60a and 61a show the relationship I_{ss} vs ($V-V_{rev}$) for different oocytes for the selected exposure condition. For clearer presentation G(V) was normalised to a maximal value of G(V) which is obtained at V = +50 mV (Figures 59b, 60 and 61b). A significant influence of ELF-EMF exposure on the number of expressed and conducting hemi-channels of rCx46 could not be read from the analysed data. This finding is also reflected in the frequency distribution of G_{max} for sham and exposed oocytes (Figure 59c).

No significant influence of ELF-EMF on the voltage-dependent gating properties of rCx46 expressing oocytes

A possible effect of ELF-EMF exposure on the voltage dependent gating properties of conducting hemi-channels of rCx46 was analysed. I_{ss} vs ($V-V_{rev}$) was measured and the corresponding relation G(V) vs ($V-V_{rev}$) derived. The latter relationship could be fitted by a simple Boltzmann equation. The fit yields as essential parameter the number of apparent equivalent voltage gating charges z. z was determined for the different exposure conditions. As can be read from Figure 59a) a significant effect of ELF-EMF exposure on the voltage-dependent gating which is reflected in the apparent number of equivalent charges z (Figure 59b) was not observed.

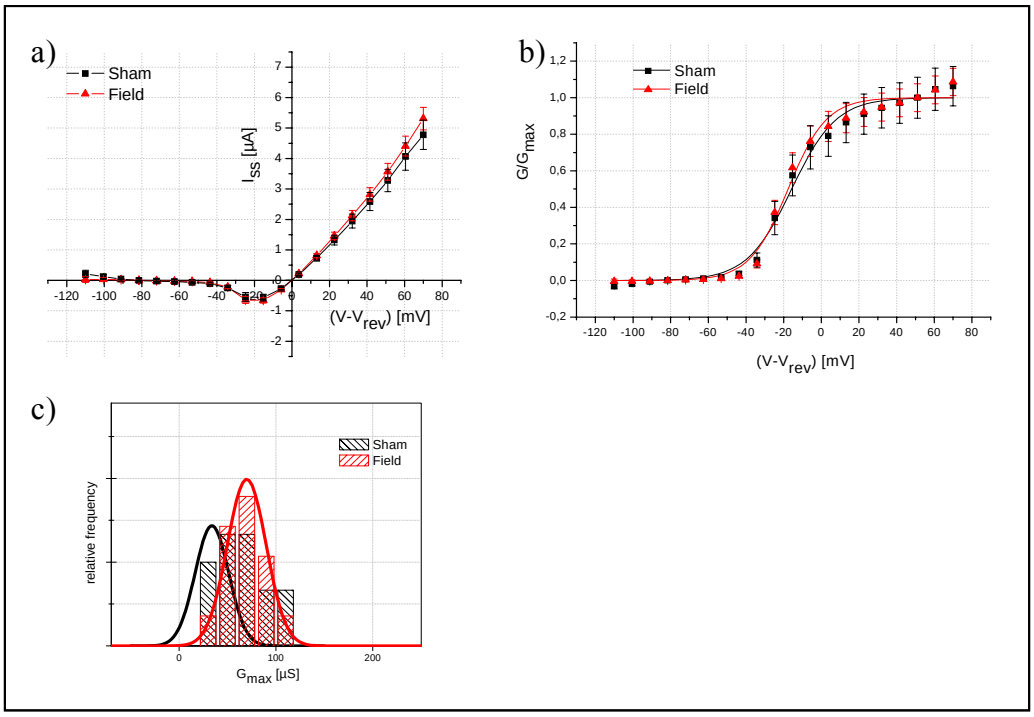

Figure 59. Voltage dependence of macroscopic rCx46-mediated membrane current and corresponding conductance after continuous ELF-EMF exposure for 16 hours at 2.3 mT. **a)** Mean ± s.e.m. of leak subtracted steady-state current amplitudes (I_{ss}) as function of (V-V_{rev}) in the absence and presence of ELF-EMF exposure (sham ■, n = 14; field ▲, n=15). **b**) Mean ± s.e.m. of corresponding normalised membrane conductance G/G_{max} = G(V)/G(V=+50 mV) as function of (V-V_{rev}) in the absence (■, n = 14) and presence of ELF (▲, n = 15). The solid lines show fits of the data by a simple Boltzmann function (for details see Materials and Methods). The derived parameters are z(sham) = 2.11 ± 0.17; z(field) = 2.45 ± 0.23; $V_{1/2}$(sham) = (-15.76 ± 1.06) mV; $V_{1/2}$(field) = (-17.66 ± 1.07) mV. **c**) Distribution of relative frequency of G_{max} = G(V=+50 mV) in the absence (n = 14) and presence (n = 15) of ELF-EMF. Solid lines present the Gauss distribution with the parameters: $G_{max, mean}$(sham)=64.2µS, corresponding standard deviation (sd) sd(sham) = 7.8 µS and $G_{max, mean}$(field) = 69.8 µS, sd(field) = 20.0 µS

To investigate an influence of field intensity on the results presented above, the experiments were repeated at 1.0 mT and the EMF-ELF was intermittently applied (5 min on/10 min off) for 16 hours. The corresponding results are given in Figure 60. Again, a significant effect of ELF-EMF on the number of expressed hemi-channels of rCx46 (Figure 59a) as well as their voltage dependent gating properties was not observed (Figure 60b).

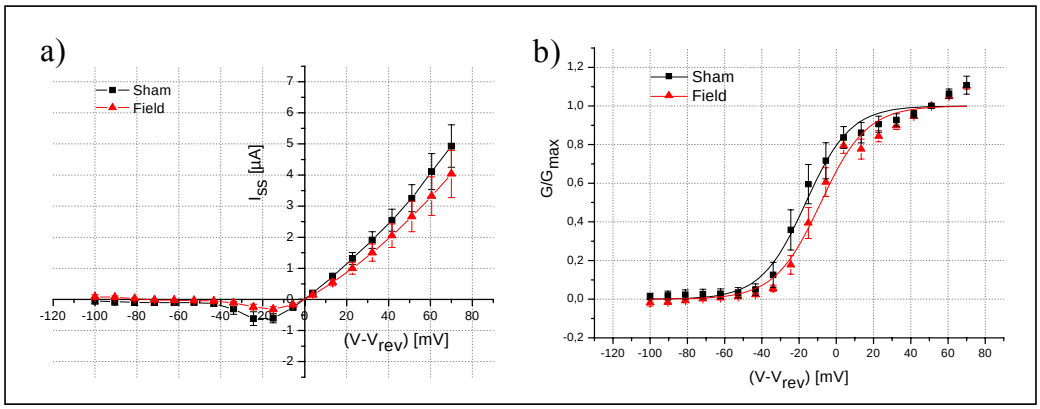

Figure 60. Voltage dependence of rCx46-mediated membrane currents and corresponding membrane conductance after intermittent ELF-EMF exposure (5 min on/10 min off) for 16 hours at 1.0 mT. **a)** Mean ± s.e.m. of leak subtracted steady-state current amplitudes (I_{ss}) as function of (V-V_{rev}) in the absence and presence of ELF-EMF exposure (sham ■, n = 5; field ▲, n = 5). **b)** Mean ± s.e.m. of normalised membrane conductance G/G_{max} = G(V)/G(V = +50 mV) as function of driving voltage (V-V_{rev}) in the absence (■, n = 5) and presence of ELF-EMF (▲, n = 5). The solid lines present fits of the data by a simple Boltzmann function, respectively (for details see Materials and Methods). The derived parameters are z(sham) = 2.08 ± 0.19; z(field) = 2.02 ± 0.20; $V_{1/2}$(sham) = (-16.39 ± 1.29) mV; $V_{1/2}$(field) = (-8.32 ± 1.38) mV

In a further series of experiments ELF-EMF at an intensity of 2.3 mT was intermittently (5 min on/10 min off) applied for 16 hours. The corresponding results are given in Figure 61. A significant effect of ELF-EMF exposure on the number of expressed hemi-channels of rCx46 (Figure 61a) was not observed. The data indicate a decrease of z after ELF-EMF exposure which appears not be significant (see legend of Figure 61b).

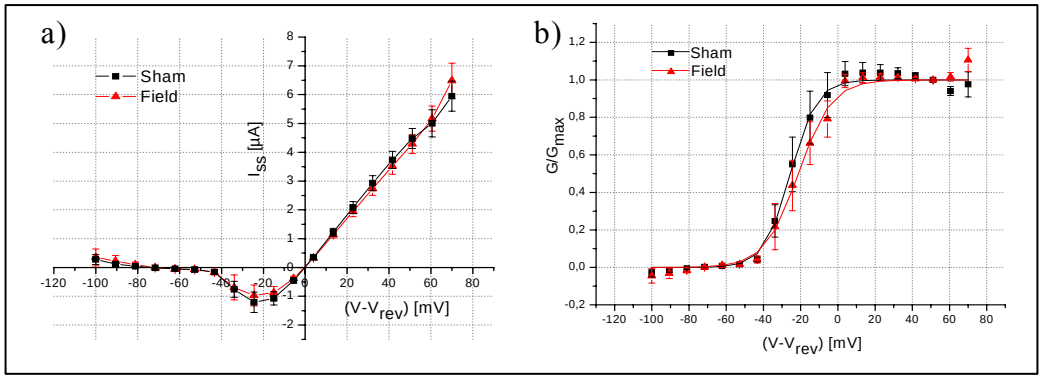

Figure 61. Voltage dependence of macroscopic rCx46-currents (I_{ss}) and corresponding membrane conductance (G) after intermittent exposure (5 min on/10 min off) for 16 hours at 2.3 mT. **a)** Mean ± s.e.m. of leak subtracted steady-state current amplitudes (I_{SS}) as function of (V-V_{rev}) in the absence and presence of ELF-exposure (sham ■, n = 4; field ▲, n = 5). **b)** Mean ± s.e.m. of normalised membrane conductance G/G_{max} = G(V)/G(V = +50 mV) as function of (V-V_{rev}) in the absence (■, n = 4) and presence of ELF-EMF(▲, n = 5). The solid lines show fits of the data by a simple Boltzmann function (see Material and Methods). The derived parameters are z(sham) = 3.54 ± 0.26; z(field) = 2.77 ± 0.24; $V_{1/2}$(sham) = (-25.51 ± 0.59) mV; $V_{1/2}$(field) = (-21.31 ± 0.88) mV

For a more detailed analysis of the voltage dependent gating properties the kinetics of rCx46- mediated current activation was considered. The time dependent current activation could be described by a sum of two exponential functions: $I(t) = a_0 + a_1*\exp(1-\exp(-t/\tau_1)) + a_2*\exp(1-\exp(-t/\tau_2))$. The corresponding time constants of activation τ_1 and τ_2 were obtained from corresponding fits to the experimental data and the

results are presented in Figures 62a-c. The figure indicates that ELF-EMF exposure does not influence the voltage dependent time constants of channel activation significantly.

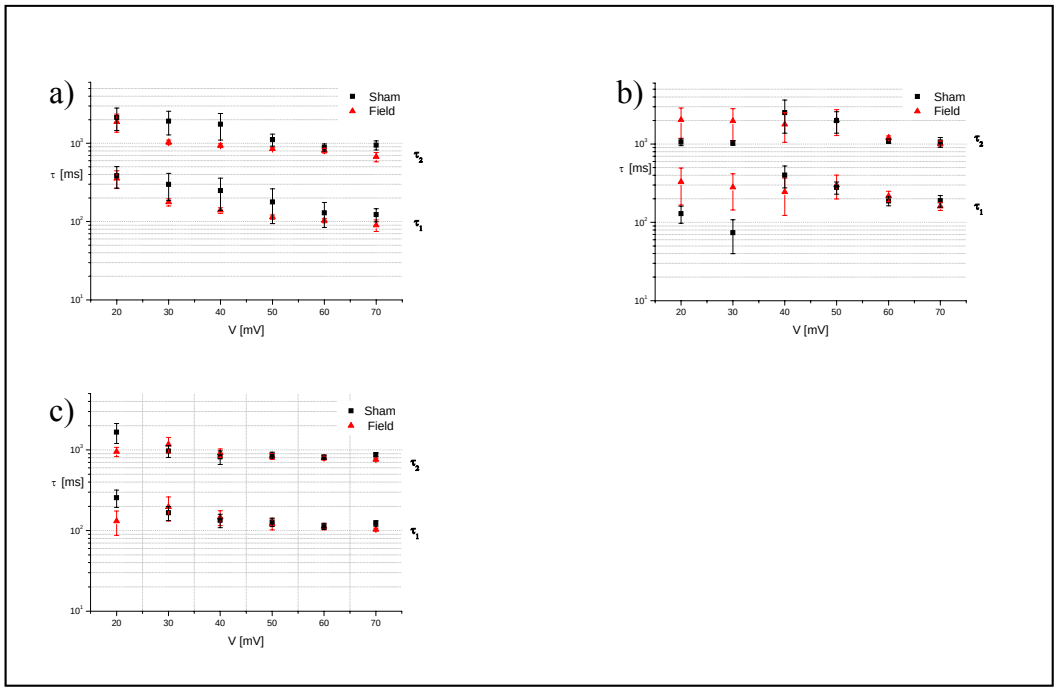

Figure 62. Time constants of voltage-dependent current activation. Time constants of current activation were plotted as function of voltage. Each point represents mean ± s.e.m of five different oocytes. The time constants of activation were obtained by fitting the time course of current activation by a sum of two exponential functions (see text). **a**), **b)** and **c)** present the time constants τ_1 and τ_2 at different exposure conditions: **a)** 2.3 mT, 16 hours continuous, **b)** 2.3 mT, 16 hours intermittent (5 min on/10 min off) and **c)** 1.0 mT, 16 hours intermittent (5 min on/10 min off).

No significant influence of ELF-EMF on the reversal potential of rCx46-mediated membrane current in oocytes.

Finally, the reversal potential V_{rev} of the rCx46-mediated membrane current was considered at different exposure conditions (Figure 63). The reversal potential is mainly determined by the expressed and conducting hemi-channels composed of rCx46, but also includes the contribution of all electrogenic transport systems. A field induced shift of the reversal potential would indicate a change of the intrinsic voltage sensor of the channel of by variation of the intracellular ion composition. No significant effect on the reversal potential of rCx46-mediated membrane current could be observed.

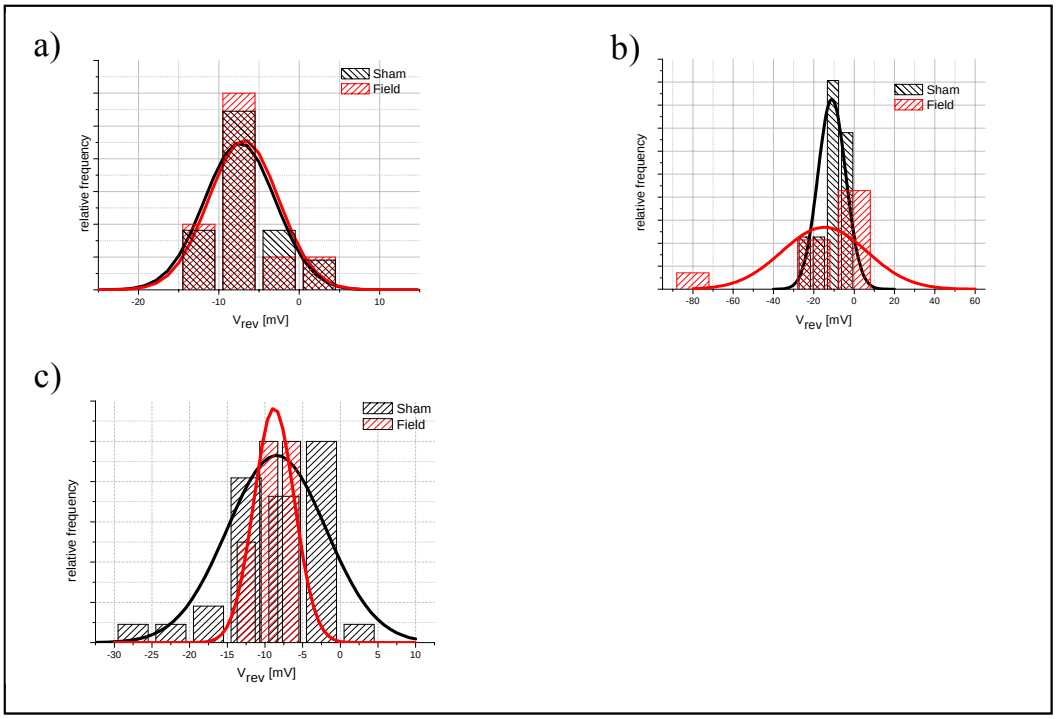

Figure 63. Relative frequency of reversal potential (V_{rev}) of conducting hemi-channels composed of rCx46 for different exposure conditions during an expression period of 16 h. The data were derived from the corresponding experiments given in Fig. 59. **a)** 1.0 mT, intermittent exposure: n = 11 for sham exposed and n = 10 for ELF-EMF exposed oocytes; **b)** 2.3 mT, permanent exposure: n = 18 for sham exposed and n = 20 for ELF-EMF exposed oocytes; **c)** 2.3 mT intermittent exposure: n =5 for sham exposed and n = 4 for ELF-EMF exposed oocytes. Solid lines present the corresponding Gauss distributions using the parameters mean of relative frequency ($V_{rev,\,mean}$) and standard deviation (sd): **a)** $V_{rev,\,mean}$(sham) = -6.9 mV, sd(sham) = 4.4 mV, $V_{rev,\,mean}$ (field) = -7.4 mV, sd(field) = 4.4 mV; **b)** $V_{rev,\,mean}$(sham) = -11.1 mV, sd(sham) = 6.9 mV, $V_{rev,\,mean}$(field) = -14.8 mV, sd(field) = 2.1 mV; **c)** $V_{rev,\,mean}$(sham) = -8.8 mV, sd(sham) = 2.1 mV, $V_{rev,\,mean}$(field) = -8.5 mV, sd(field) = 0.7 mV

A slight but not significant influence of ELF-EMF on the gating properties of hemi-channels expressed in Xenopus oocytes dependent on the external calcium concentration was observed.

The expression level of rCx46 in single were characterised by detailed biophysical analysis of corresponding voltage-jump current relaxation experiments. In parallel the gating by external Ca^{2+} concentration was characterised. A significant influence on the rCx46 mediated membrane conductance, the corresponding half-activation voltage ($V_{1/2}$) and the number of apparent equivalent gating charges (z) of the rCx46-hemi-channels in exposed and sham-exposed *Xenopus laevis* oocytes could not be observed for intermittently applied ELF-EMF at 50 Hz powerline signal (1.0 mT, 5 min on/10 min off) after an exposure time of 14 hours, 17 hours and 20 hours, respectively. Since it is known that external calcium significantly modulates the voltage dependent gating behaviour of expressed hemi-channels composed of rCx46, the experiments were repeated at various external calcium concentrations. The results indicate an influence by ELF-EMF exposure, but the differences are not significant (Figure 64). The membrane conductance and the gating parameters of exposed oocytes expressing rCx46 are smaller than those of sham exposed cells after an exposure time of 14 hours and 20 hours, respectively.

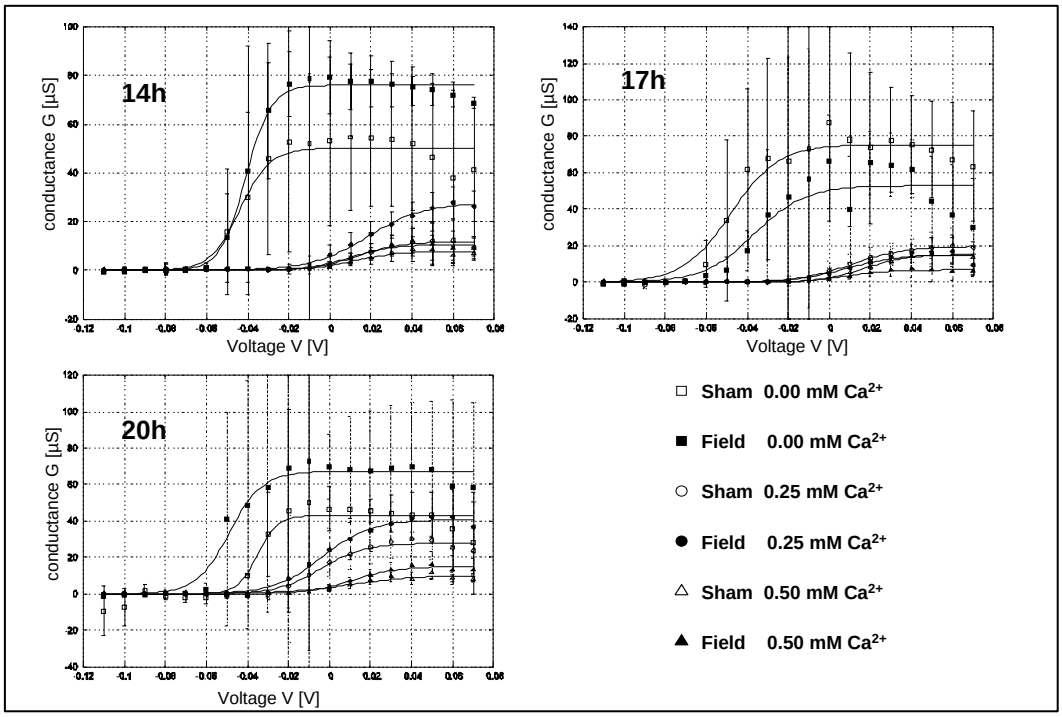

Figure 64. Conductance of hemi-channels composed of rCx46 expressed in oocytes after intermittent exposure (5 min on/10 min off) for 14 hours, 17 hours and 20 hours at 1.0 mT in the presence of 0.0 mM (n = 2-6), 0.25 mM (n = 2-4) and 0.5 mM (n = 2-5) Ca^{2+} in the bath. Closed symbols denote results of exposed oocytes and open symbols those of sham exposed oocytes.

ELF-EMF did not significantly affect the results of electrophysiological recordings of paired Xenopus oocytes.

The voltage-clamp experiments were repeated using paired oocytes. Paired oocytes expressing rCx46 form cell-to-cell channels (gap junctions) by head-to-head association of two hemi-channels which results in an increase of transjunctional conductance (G) between paired oocytes. Paired oocytes were intermittently ELF-EMF exposed (5 min on/10 min off) for 8 hours at 50 Hz powerline signal of 1.0 mT. The half-activation voltage ($V_{1/2}$) and the number of apparent equivalent gating charges (z) derived from the voltage-gating of junctional conductance of paired oocytes expressing rCx46 showed no significant change by ELF-EMF exposure (Figure 65). But the conductance of exposed paired oocytes is smaller than the conductance of sham exposed cell pairs. This finding is not significant on the basis of the 3 paired oocytes analysed so far.

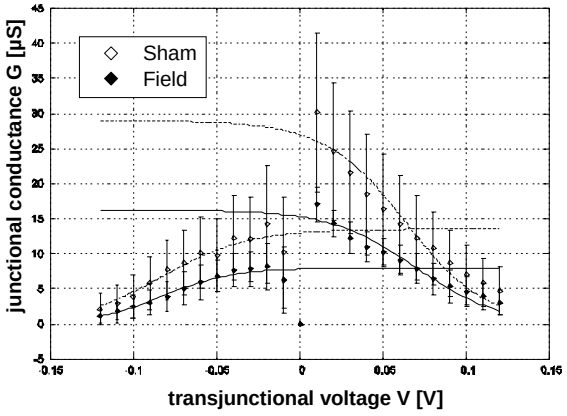

polarity of trans-junctional voltage	$G_{\pm 70}$ [µS]	$V_{1/2}$ [mV]	z
	Sham		
negative	13.53	-82.94	0.96
positive	28.97	69.32	-1.03
	Field		
negative	08.00	-82.54	1.19
positive	16.27	68.94	-0.99

Figure 65. Mean junctional conductance (G) of paired oocytes expressing cell-to-cell channels composed of rCx46 as function of transjunctional voltage. The table summarizes the maximal conductance $G_{\pm 70}$ = G(V=±70 mV) and the voltage-dependent gating parameters: the half-activation voltage ($V_{1/2}$) and number of apparent equivalent gating charges (z) of cell-to-cell channels after intermittent exposure (5 min on / 10 min off) for 8 hours at 1.0 mT, 50 Hz powerline (closed symbol: exposed cell pairs (n = 3); open symbol: sham exposed cell pairs (n = 3)). The parameter values were obtained by fitting the experimental data of G vs. V by a simple Boltzmann-distribution.

No significant influence of ELF-EMF on gap junctional coupling of rat granulosa cells was observed.

Gap junctional coupling by cell-to-cell channels of pairs of cultured granulosa cells was recorded after continuous exposure to ELF-EMF of 2.3 mT for 30 min. Figure 66a shows the maximal gap junctional conductance in the absence and presence of ELF-EMF exposure. The data were obtained as function of days in culture after passage, respectively. The corresponding mean gap junctional conductance of sham- and field-exposed cell all pairs is given in Figure 66b. No significant influence of ELF-EMF exposure on gap junctional coupling of rat granulosa cells was found.

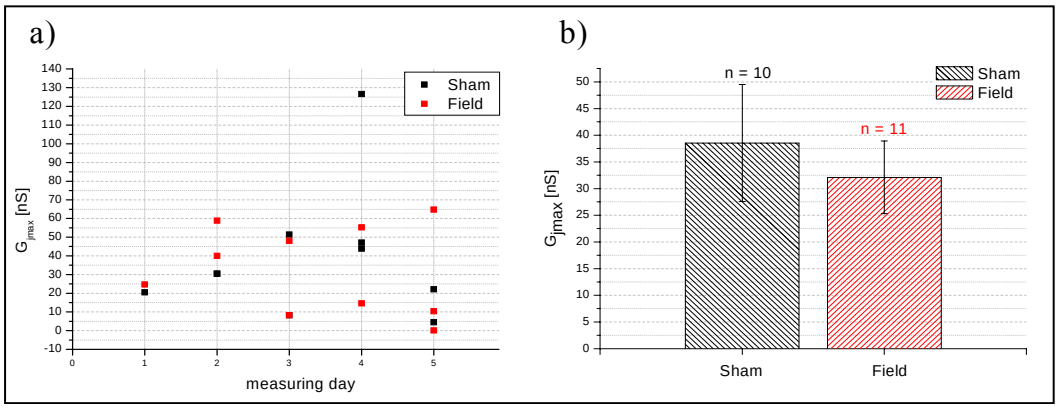

Figure 66. Gap junctional coupling of rat granulosa cell pairs as function of culture time in the presence and absence of ELF-EMF. **a.)** Maximal gap junctional conductance G_{jmax} of cultured pairs of granulosa cells in the absence (■, n = 10) and presence of ELF (■, n = 11) as function of time in culture. ELF-EMF was continuously applied with 2.3 mT for 30 min at room temperature, respectively. Measurements were performed by application of the double whole-cell patch clamp technique. **b**.) Mean ± s.e.m. of gap junctional conductance measured at 1 to 5 days (see a)), in the absence (n = 10) and presence of ELF-EMF (n = 11). n denotes the number of different cell-pairs.

An effect of ELF-EMF on cytoplasmic free calcium of cultured human fibroblasts and granulosa cells of rats was not observed.

After exposure of fibroblasts for 5, 6, 7, 9, 10 and 11 hours to ELF-EMF $[Ca^{2+}]_i$ was recorded. Measurement of $[Ca^{2+}]_i$ was started 10 min after end of exposure and recorded up to 40 min under exposure –free incubation conditions. In Figure 67 $[Ca^{2+}]_i$ was followed after exposure for 11 h (Figure 67a) and 15h (Figure 67b). During the presented recording time no significant change of $[Ca^{2+}]_i$ was observed. The described experiments were repeated for a cultured granulosa cell line (not shown). The observed variability in the time course of $[Ca^{2+}]_i$ of some sham- and field exposed cells seems not to be significant. As in the case of fibroblasts a long-lasting influence of ELF-EMF on the time course and amplitude of $[Ca^{2+}]_i$ was not observed for cultured rat granulosa cells. For clearer presentation the results of $[Ca^{2+}]_i$ recorded for fibroblasts and rat granulosa cells are summarised in Table 9.

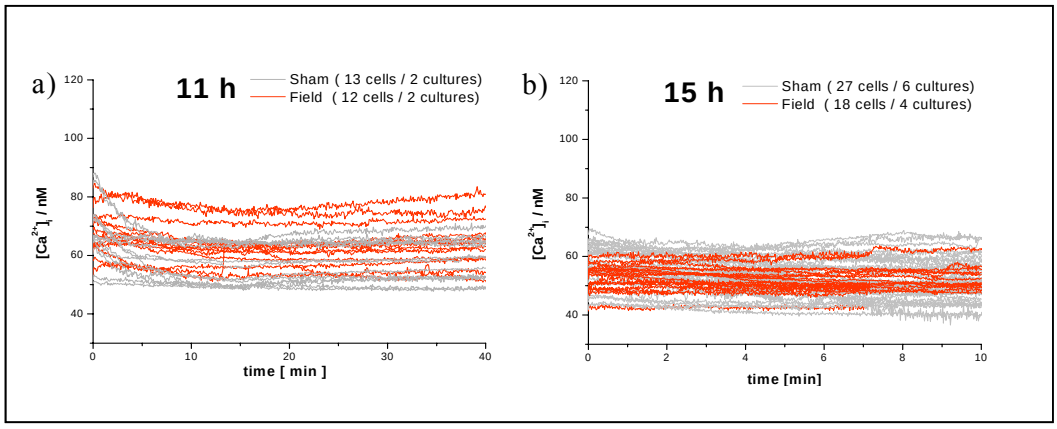

Figure 67. Time course of $[Ca^{2+}]_i$ in fibroblasts after ELF-EMF exposure at 50 Hz sinusoidal, 1.0 mT, intermittent (5 min on/10 min off) for **a)** 11 hours and **b)** 15 hours exposure time (grey curves denote sham- and red curves field-exposure)

Table 9. Summary of $[Ca^{2+}]_i$ data obtained on cultured fibroblasts and rat granulosa cells after ELF-EMF (5 min on/10 min off, sinusoidal 50 Hz, 1.0 mT) exposure

cell system	exposure time	7 h	9 h	11 h	15 h	17 h
Fibroblasts	sham	35 cells / 6 cultures	27 cells / 5 cultures	13 cells / 2 cultures	27 cells / 6 cultures	56 cells / 7 cultures
	field	37 cells / 6 cultures	15 cells / 3 cultures	12 cells / 2 cultures	18 cells / 4 cultures	14 cells / 3 cultures
		no ELF-EMF effect	**no ELF-EMF effect**	**no ELF-EMF effect**	**no ELF-EMF effect**	**no ELF-EMF effect**
Granulosa	**exposure time**	**4 h**	**5 h**	**6.5 h**	**7.75 h**	
	sham	11 cells / 1 culture	54 cells / 5 cultures	60 cells / 5 cultures	51 cells / 3 cultures	
	field	19 cells / 2 cultures	57 Cells / 5 cultures	47 cells / 3 cultures	7 cells / culture	
		no ELF-EMF effect	**no ELF-EMF effect**	**no ELF-EMF effect**	**no ELF-EMF effect**	
ELF-EMF stimulation: 50 Hz, sinusoidal, 1 mT (5 min on / 10 min off)						

In a further series of experiments the cells were exposed to an additional stressor added to the bath after the end of ELF-EMF exposure. Figure 65 shows the time course of $[Ca^{2+}]_i$ of fibroblasts during an additional exposure to 200 µM H_2O_2 in the bath. No significant effect on $[Ca^{2+}]_i$ could be found during a consecutive treatment by H_2O_2. Application of another stress condition like cell- depolarisation by high external KCl (30 mM) also did not affect the time course and amplitude of $[Ca^{2+}]_i$ for ELF-EMF exposed cells (data not shown).

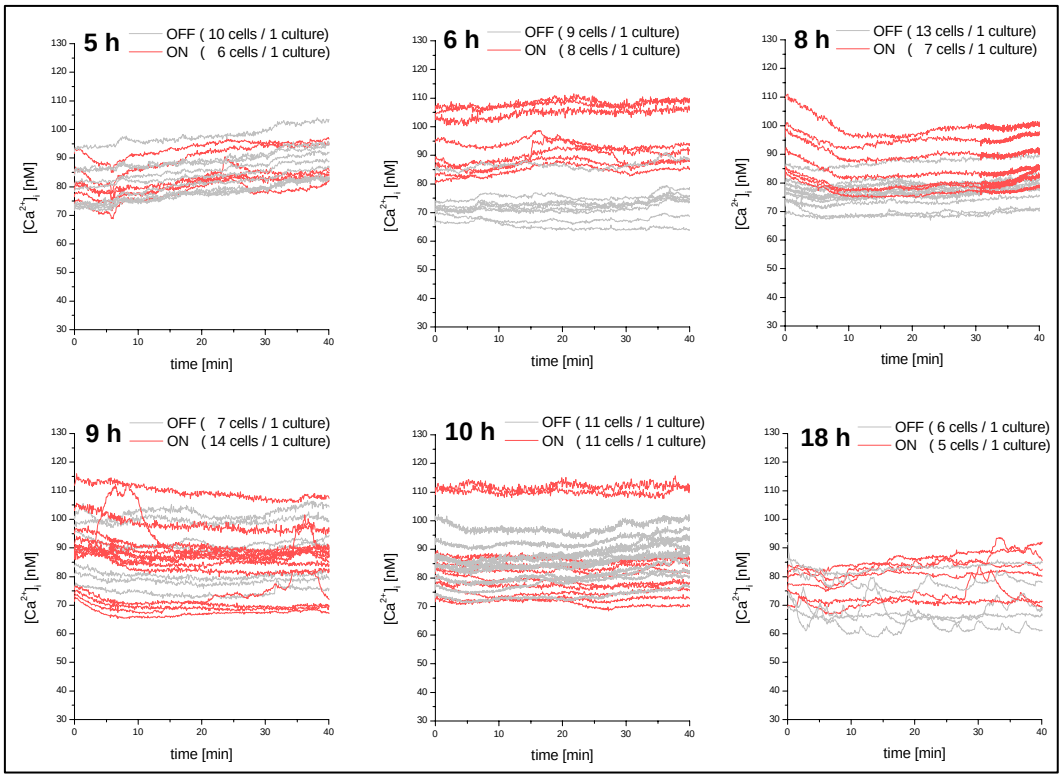

Figure 68. Time course of $[Ca^{2+}]_i$ in fibroblasts after end of ELF-EMF (5 min on/10 min off, 50 Hz sinusoidal, 1.0 mT) exposure for 5 , 6, 8, 9, 10 and 18 hours which was followed by an addition of 200 µM H_2O_2 to the bath for further 10 min (grey curves denote sham- and red curves field-exposure). For further details see text.

A summary of $[Ca^{2+}]_i$ measurements on fibroblasts and rat granulosa cells after application of ELF-EMF followed by addition of H_2O_2 to the bath is given in Table 10. $[Ca^{2+}]_i$ was recorded in the presence of 200 µM H_2O_2.

Table 10. Summary of $[Ca^{2+}]_i$ data obtained on cultured fibroblasts and rat granulosa cells after ELF-EMF (5 min on/10 min off, sinusoidal 50 Hz, 1.0 mT) exposure followed by addition of H_2O_2 to the bath.

cell system	stimulation	exposure time	5 h	6 h	8 h	9 h	10 h	18 h
Fibroblasts	ELF-EMF and 200 µM H_2O_2	sham	10 cells / 1 culture	9 cells / 1 culture	13 cells / 1 culture	7 cells / 1 culture	11 cells / 1 culture	6 cells / 1 culture
		field	6 cells / 1 culture	8 cells / 1 culture	7 cells / 1 culture	14 cells / 1 culture	11 cells / 1 culture	5 cells / 1 culture
			no ELF -EMF effect	no ELF -EMF effect	no ELF -EMF effect	no ELF -EMF effect	no ELF -EMF effect	no ELF -EMF effect
	ELF-EMF and 30 mM KCl	**exposure time**	**6.5 h**	**7.5 h**	**8.5 h**	**9.5 h**		
		sham	7 cells / 1 culture	7 cells / 1 culture	6 cells / 1 culture	7 cells / 1 culture		
		field	5 cells / 1 culture	5 cells / 1 culture	10 cells / 1 culture	8 cells / 1 culture		
			no ELF -EMF effect	no ELF -EMF effect	no ELF -EMF effect	no ELF -EMF effect		
Granulosa	ELF-EMF and 200 µM H_2O_2	**exposure time**	**5 h**	**6 h**	**7 h**	**8 h**	**18 h**	
		sham	14 cells / 1 culture	14 cells / 1 culture	20 cells/ 2 cultures	14 cells / 1 culture	14 cells / 1 culture	
		field	5 cells / 1 culture	5 cells / 1 culture	10 cells / 1 culture	8 cells / 1 culture	14 cells / 1 culture	
			no ELF -EMF effect	no ELF -EMF effect	no ELF -EMF effect	no ELF -EMF effect	no ELF -EMF effect	
ELF-EMF stimulation: 5o Hz, sinusoidal, 1 mT, 5 min on / 10 min off								

The volume regulatory response of granulosa cells appeared not to be influenced by ELF-EMF.

The volume regulatory response of cultured granulosa cells was studied after application of a hypotonic shock followed by a hypertonic shock. For clearer presentation for each experiment the volume change (v(t)–v(t=0)) of 10 cells was analysed as function of time and normalised to the maximal value v_{max}, respectively. As exposure period again 18 h were selected, since after this exposure period rat granulosa cells show the maximal response on the genomic level. The volume regulatory behaviour of rat granulosa cells appears not to be influenced by ELF-EMF. In addition, there was no significant difference between exposed and sham exposed cells for hypotonic (Figure 69) as well as hypertonic conditions (not shown). The volume analysis was started 15 min after end of ELF-EMF exposure.

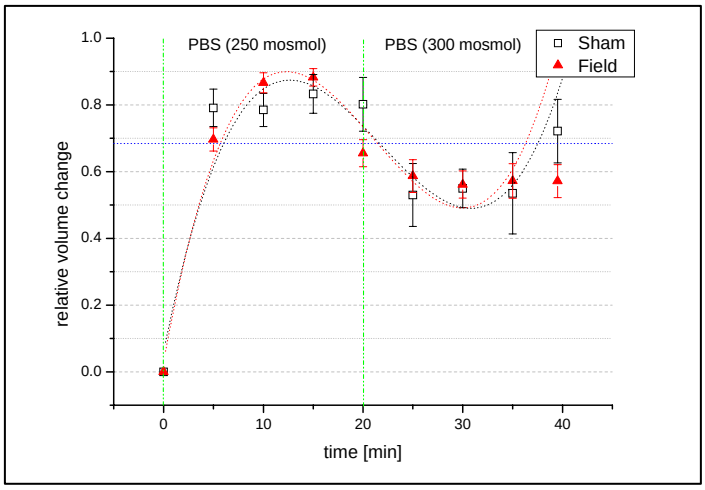

Figure 69. Relative volume change of granulosa cells (GFSHR-17) after addition of a hypotonic solution at t = 0. Prior to this treatment the cells were sham exposed (n = 7) or ELF-EMF exposed (n = 24) for 18 hours at 50 Hz, 1.0 mT, (5 min on/10 min off)). The mean ± s.e.m. is given, respectively.

3.1.4.5 Whole-genome analysis of various cell lines exposed to ELF-EMF (Participant 12)

Altogether, 58 whole-genome analyses of 10 different cell lines (sham-exposed cells and control cells) were performed (Table 1). After primary data analysis, we only worked on genes which were reproducibly regulated in several experiments (see materials and methods) and which belonged to certain gene families (Table 11). We defined gene families which are potentially relevant for the cellular answer on EMF exposure: signal transduction, ion/electron transport, metabolism of energy/proteins, cell proliferation/apoptosis, immune answer/inflammation and extracellular matrix/ cytoskeleton. Each gene family was sub-divided in subgroups again, e.g. GTP proteins in the signal transduction family (Tables 11, 12). In a first step, we did not go into single genes, but simply counted genes up- or down-regulated in the different gene families. The total number of regulated genes in a certain gene family is not very meaningful, because the sizes of the gene families are of course very different. Therefore, the total numbers of genes on the human array belonging to a gene family are shown in the first column of Tables 11 and 12. Although a single gene might appear in different categories (e.g. all small G proteins are GTP binding proteins), the Tables give a good overview on what might happen in the cells after EMF exposure on the molecular level.

In human fibroblasts (Participant 3), a number of G proteins and calcium associated proteins involved in signal transduction seem to be strongly regulated. Genes involved in adhesion of cells and cytoskeletal genes appear strongly regulated in several hybridizations, although the variances in numbers between the experiments are high (Table 11).

The fibroblast experiments (Participant 3) were also assessed by bio-statistics (Participant 8: Dr. Remondini, Table 12): Mitochondrial and ribosomal genes appeared strongly regulated, also Ca-related genes, cell cycle, apoptosis, extracellular matrix, and the cytoskeleton. The overall number of significantly regulated genes is higher in the ELF-EMF treated fibroblasts than e.g. in endothelial cells

exposed to RF-EMF (Participant 6). This was expected, since the number of regulated genes in fibroblasts after ELF-EMF exposure is pretty uniform in the non-statistically evaluated gene numbers (compare Table 12 with Table 11). From the experiments with SY5Y human neuroblastoma cells (Participant 11) and mouse embroyonic stem cells (Participant 4) it was not possible to extract bio-statistically significant data.

In detail, the following genes were extracted by bio-statistics so far:

Actin associated proteins (belong to cytoskeleton):
- Caldesmon (tropomysin binding, actin binding. Activation of ERK MAP kinases lead to phosphorylation of caldesmon. Regulatory protein of the contractile apparatus): down-regulated (fibroblasts, participant 3).
- Gamma-actin: down-regulated (fibroblasts, Participant 3).
- "coactosin-like": down-regulated (fibroblasts, Participant 3).
- "actin-binding": down-regulated (fibroblasts, Participant 3).
- "procollagen-proline 2": down-regulated (fibroblasts, Participant 3).
- "actin modulating activity": up-regulated (fibroblasts, Participant 3).
- "actin-binding, calcium ion binding": down-regulated (fibroblasts, Participant 3).
- CD2-associated protein, actin binding: down-regulated (fibroblasts, Participant 3).
- Tropomodulin 3: actin binding down-regulated (fibroblasts, Participant 3).

Calcium (Ca2+)-associated proteins:
- protein phosphatase 4: down-regulated (fibroblasts, Participant 3).
- Thrombospondin (cell adhesion): down-regulated (fibroblasts, Participant 3).
- "EGF-containing fibulin-like…" (cell adhesion): down-regulated (fibroblasts, Participant 3).
- matrix metalloproteinase 2 MMP 2 (extracellular matrix, collagen metabolism): down-regulated
- follistatin (extracellular matrix, heparin binding): down-regulated (fibroblasts, Participant 3).
- SPARC (extracellular matrix, collagen binding): down-regulated (fibroblasts, Participant 3).
- ("myosin light polypeptide": up-regulated (fibroblasts, Participant 3).
- ("hypothetical protein": up-regulated (fibroblasts, Participant 3).

Extracellular matrix (ECM):
- thrombospondin (see Ca): down-regulated (fibroblasts, Participant 3).
- "EGF-containing…." (see Ca): down-regulated (fibroblasts, Participant 3).
- MMP2 (see Ca): down-regulated (fibroblasts, Participant 3).
- Connective tissue growth factor CTGF (cell adhesion, obviously not influenced by Ca): up-regulated (fibroblasts, Participant 3).
- Collagen XV (obviously not influenced by Ca): up-regulated (fibroblasts, Participant 3).
- Lysyl oxidase (also processed by bone morphogenetic protein 1 BMP1, obviously not influenced by Ca): up-regulated (fibroblasts, Participant 3).

Cytoskeleton (see also actin and calcium-associated proteins):
- "hypothetical protein": down-regulated (fibroblasts, Participant 3).
- "protein phosphatase 4, caldesmon): down-regulated (fibroblasts, Participant 3).
- "SH3 protein interacting with Nck": down-regulated (fibroblasts, Participant 3).
- "in kinesin complex": down-regulated (fibroblasts, Participant 3).

Ion transport:
- "potassium channel activity": down-regulated (fibroblasts, Participant 3).
- SLC12A5 KCl (potassium chloride) transporter: down-regulated (fibroblasts, Participant 3).
- SLC26A3 sulfate porter: down-regulated (fibroblasts, Participant 3).
- "ferric ion binding": down-regulated (fibroblasts, Participant 3).
- (ATP synthase, H+ transport): down-regulated (fibroblasts, Participant 3).
- ("H+ transporter): down-regulated (fibroblasts, Participant 3).
- "iron ion transport": down-regulated (fibroblasts, Participant 3).

Ribosomal proteins:
- 7 ribosomal proteins down-regulated, 3 ribosomal proteins up-regulated, 1 ribosomal protein up-regulated in profile nr.1, down-regulated in profile nr.2 (fibroblasts, Participant 3).

Table 11. Numbers of genes regulated within different gene families

Gene Family	total number of clones in Human Unigene RZPD-2	partner 3 fibroblasts Exp1 ELF up-regulated genes	partner 3 fibroblasts Exp2 ELF up-regulated genes	partner 3 fibroblasts Exp1 ELF down-regulated genes	partner 3 fibroblasts Exp2 ELF down-regulated genes	Gene "Superfamily"
Signal	2528	251	232	296	190	signal transduction
GTP	560	66	73	66	52	signal transduction
Small G	235	31	32	28	27	signal transduction
Jak	23	0	0	5	3	signal transduction
Rab	80	0	9	11	13	signal transduction
Ras	66	10	7	10	5	signal transduction
wnt	5	0	0	0	0	signal transduction
phosphatase	334	39	36	35	26	signal transduction
protein kinase	304	28	29	35	24	signal transduction
phospholipase	72	9	8	10	7	signal transduction
calcium	715	67	72	80	50	signal transduction
calmodulin	131	6	13	17	11	signal transduction
channel	348	31	25	36	22	ion/electron transport
voltage-gated	164	16	13	16	6	ion/electron transport
electron transport	423	52	52	57	37	ion/electron transport
ion transport	501	49	48	45	29	ion/electron transport
metaboli	1241	122	128	135	96	metabolism of energy/proteins
ATP	1234	113	112	157	82	metabolism of energy/proteins
mitochon	574	84	82	70	65	metabolism of energy/proteins
ribosom	254	47	48	32	39	metabolism of energy/proteins
translation	168	30	28	20	13	metabolism of energy/proteins
transcript	1991	201	190	228	136	metabolism of energy/proteins
cell cycle	478	46	52	54	43	cell proliferation/apoptosis/differentiation
apoptos	373	31	37	37	23	cell proliferation/apoptosis/differentiation
differentiat	177	14	21	22	11	cell proliferation/apoptosis/differentiation
immun	390	31	37	38	32	immune answer/inflammation/stress answer
inflamma	184	10	20	24	11	immune answer/inflammation/stress answer
stress	118	12	11	14	13	immune answer/inflammation/stress answer
peroxidase	32	6	5	4	6	immune answer/inflammation/stress answer
heat shock	188	4	7	5	3	immune answer/inflammation/stress answer
DNA repair	154	14	19	19	10	immune answer/inflammation/stress answer
early	8	2	2	0	2	immune answer/inflammation/stress answer
adhesion	573	46	49	53	43	extracellular matrix/cytoskeleton/adhesion
extracellular matrix	226	19	34	31	16	extracellular matrix/cytoskeleton/adhesion
cytosk	529	45	50	47	42	extracellular matrix/cytoskeleton/adhesion
junction	129	11	10	13	10	extracellular matrix/cytoskeleton/adhesion
actin	494	32	32	38	32	extracellular matrix/cytoskeleton/adhesion

Table 12. Numbers regulated genes in different expression profiling experiments (bio-statistical analysis by Dr. Remondini/Participant 8)

Gene Family	total number of clones in Human Unigene RZPD-2	partner 3 fibroblasts ELF up-regulated genes	partner 3 fibroblasts ELF down-regulated genes	Gene "Superfamily"
Signal	2528	0	12	signal transduction
GTP	560	0	2	signal transduction
Small G	235	0	1	signal transduction
Rab	80	0	1	signal transduction
Ras	66	0	1	signal transduction
phosphatase	334	1	2	signal transduction
protein kinase	304	0	1	signal transduction
calcium	715	2	6	signal transduction
calmodulin	131	0	1	signal transduction
channel	348	0	2	ion/electron transport
voltage-gated	164	0	1	ion/electron transport
ion transport	501	0	7	ion/electron transport
electron transport	423	0	3	ion/electron transport
metaboli	1241	0	4	metabolism of energy/proteins
ATP	1234	2	7	metabolism of energy/proteins
mitochon	574	0	5	metabolism of energy/proteins
ribosom	254	3	7	metabolism of energy/proteins
translation	168	3	0	metabolism of energy/proteins
transcript	1991	2	9	metabolism of energy/proteins
cell cycle	478	1	4	cell proliferation/apoptosis/differentiation
apoptos	373	0	4	cell proliferation/apoptosis/differentiation
differentiat	177	0	2	cell proliferation/apoptosis/differentiation
immun	390	0	2	immune answer/inflammation/stress answer
DNA repair	154	0	0	immune answer/inflammation/stress answer
inflamma	184	0	1	immune answer/inflammation/stress answer
adhesion	573	2	3	extracellular matrix/cytoskeleton/adhesion
extracellular matrix	226	2	5	extracellular matrix/cytoskeleton/adhesion
cytosk	529	1	6	extracellular matrix/cytoskeleton/adhesion
actin	494	1	4	extracellular matrix/cytoskeleton/adhesion
junction	129	0	0	extracellular matrix/cytoskeleton/adhesion

3.1.4.6 Summary (Participant 1)

Our data indicate that ELF-EMF may affect the gene and protein expression in various cell systems. This conclusion is based on the following findings:

- ELF-EMF at a flux density of about 2 mT up-regulated the expression of early genes, such as p21, c-jun and erg-1, in p53-deficient mouse embryonic stem cells, but not in healthy wild-type cells suggesting that the genetic background affects the responsiveness of the cells (see 3.1.4.1).
- ELF-EMF at a flux density of 2 mT up-regulated in neural progenitor cells the transcript levels of the GADD45 gene and down-regulated the transcript levels of the bax gene by which the apoptotic process may be modulated (see 3.1.3.1 and 3.1.4.1).
- ELF-EMF at a flux density of 0.8 mT up-regulated the expression of cardiac specific genes in cardiomyocytes derived from embryonic stem cells thus promoting cardiogenesis (see 3.1.4.3).
- ELF-EMF did not affect the expression of neuronal genes in neuroblastoma cells (SY5Y) such as nAchRs, DβH, Phox2a and Phox2b, either at mRNA or protein level (see 3.1.4.2).
- ELF-EMF did not affect either the expression level of conducting hemi-channels composed of rCx46, nor their gating properties by voltage, pH, Ca^{2+} in *Xenopus laevis* oocytes (see 3.1.4.4).
- ELF-EMF appeared to regulate the expression of a series of genes and proteins in human fibroblasts such as mitochondral and ribosomal genes as well as Ca-, cell cycle-, apoptosis-, extracellular matrix-, and cytoskeleton-related genes, although it must be considered that the variances observed between the various experiments was high (see 3.1.4.5).

3.2 Results in RF-EMF research

3.2.1 Genotoxic effects

3.2.1.1 Human HL-60 cell line (Participant 2)

Genotoxic effects of EMF may occur directly either by damage to chromosomes and/or by damage to DNA repair mechanisms. Indirect genotoxic effects may arise by various processes such as generation of oxygen radicals or impairment of radical-scavenging mechanisms. Direct and indirect genotoxic effects of defined RF-EMF were investigated in the human cell line HL-60.

A. Direct genotoxicity

RF-EMF increased the micronucleus frequency and the number in DNA strand breaks in HL-60 cells dependent on the energy of radiation as determined by the cytokinesis-block in vitro micronucleus assay and the Comet assay.

The effect of RF-EMF on the formation of micronuclei (MN) and DNA strand breaks was examined by use of the cytokinesis-block in vitro micronucleus assay and the alkaline Comet assay. To validate the MN assay and to prove the susceptibility of HL-60 cells to physical noxes, cells were exposed to ionising-irradiation. As shown in Figure 70, a dose-dependent induction of micronuclei in HL-60 cells was found for doses of exposure increasing from 0.5 to 3.0 Gy. Cell division was effected by ionising-irradiation at doses ≥1.0 Gy as shown in Figure 71, inferred from the ratio of BNC against mono-, bi-, tri- and tetranuclear cells (in %).

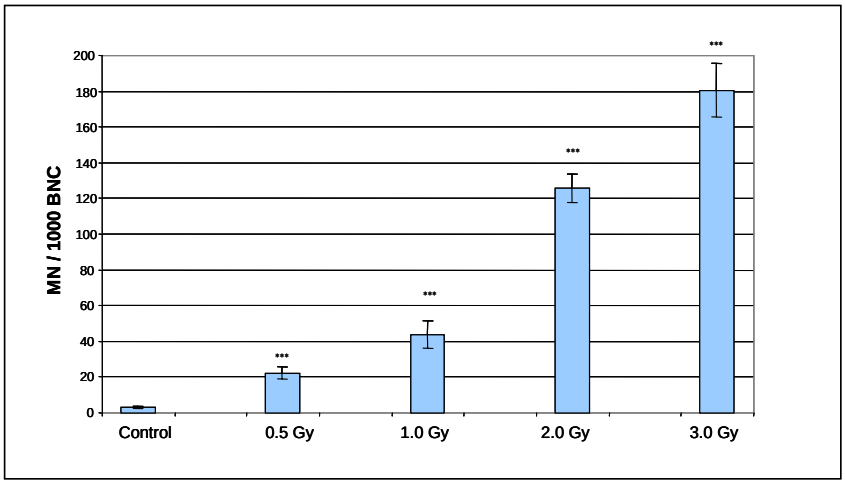

Figure 70. Effect of ionising-irradiation (6 MeV) on micronuclei formation in binucleated HL-60 cells. Each data point is based on at least three independent experiments. Each bar represents the mean ± SD of results obtained in three independent experiments. *** P<0.001 (Student's t-test, two-sided). All in all (mono-, bi-, tri-, and tetranucleated) 15000 cells were analysed.

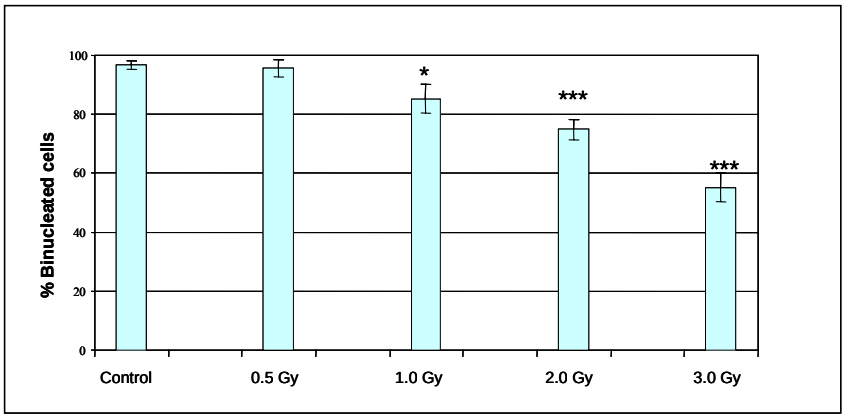

Figure 71. Effect of ionising-irradiation on HL-60 cell division. The number of binucleated cells relative to the number of mono-, bi-, tri-, and tetranuclear cells following ionising-irradiation (6 MeV) of HL-60 cells. Each bar represents the mean ± SD in % of results obtained in three independent experiments; *p<0.05, ***p<0.001 (Student's t-test, two-sided).

In a series of experiments SAR levels ranging from 0.2 W/kg to 3.0 W/kg were examined in order to clarify whether the effects of RF-EMF exposure (1800 MHz, continuous wave, 24 h) on MN frequencies in HL-60 cells are energy dependent (Figure 72). Whereas at SAR of 0.2 W/kg, 1.0 and 3.0 W/kg MN frequencies were not changed in RF-EMF-exposed cells as compared to sham controls and incubator controls, MN frequencies were significantly increased at SAR of 1.3 W/kg and above. The maximum increase was noted at a SAR of 1.3 and 1.6 W/kg. This effect was approximately 66 % of the effect observed after 0.5 Gy ionising-irradiation (6 MeV, exposure time: 5.2 s). At a SAR of 3.0 W/kg the MN frequency was similar to that found in sham-exposed cells. While MN frequencies of incubator controls were around 3.5, the MN frequency determined after RF-exposure at a SAR of 1.3 W/kg was 13.3 (approximately 3.8 fold higher). The MN frequency determined in cells after exposure to ionising-irradiation (0.5 Gy, exposure time: 5.2s), used as a positive control, was 22.3 ± 3.5 (n=3; 6.3 fold increase compared to control).

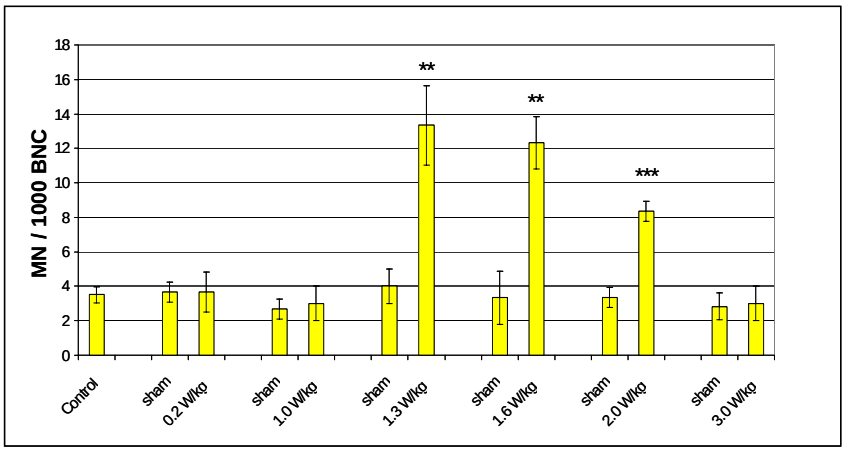

Figure 72. Micronucleus frequencies in binucleated HL-60 cells after exposure to RF-field (1800 MHz, continuous wave) for 24h ranging from SAR 0.2 to 3.0 W/kg, compared to control and sham-exposure. Each bar represents the mean ± SD of results obtained in three independent experiments (except of control: n = 11). Each data point is based on at least three independent experiments except of the control with 11 independent experiments and on a total number of 11000 (control), 18000 (sham-exposed) and 18000 (RF-exposed) bi-nucleated HL-60 cells. All in all (mono-, bi-, tri-, and tetra-nucleated) 47000 cells were analysed. The micronuclei frequency of BNC after exposure to ionising-irradiation (0.5 Gy, exposure time: 5.2s), which was used as a positive control, were on average 22.3 ± 3.5 (n=3). ** P<0.01; *** P<0.001 (Student's t-test, two-sided).

In order to compare micronuclei induction in cells exposed to RF-fields at different ranges of SAR, the average micronuclei frequencies (MN/1000 BNC) were calculated for the following groups: experiments performed at all SAR tested (range 0.2 W/kg to 3.0 W/kg, number of independent experiments n=18), experiments performed at SAR ranging from 1.0 W/kg to 2.0 W/kg (number of independent experiments n=12), and experiments at SAR of 0.2 W/kg and 1.0 W/kg (number of independent experiments n=6). While the calculated average of MN/1000 BNC in HL-60 cells at a SAR of 0.2 W/kg to 1.0 W/kg was not significantly different from that observed in sham-exposed controls, both groups ranging from 0.2 W/kg to 3.0 W/kg ($p<0.01$) or from 1.0 W/kg to 2.0 W/kg ($p<0.001$) exhibited a significant increase in micronuclei induction after RF-exposure as compared to sham-exposed controls (Figure 74A).

Previous experiments had clearly shown that RF-EMF exposure results in an increase of DNA strand breaks in HL-60 cells. In order to achieve a better understanding of whether these effects are energy dependent, additional experiments were performed applying RF-exposure (1800 MHz, continuous wave, 24h) at SAR of 0.2 W/kg to 3.0 W/kg. As shown in Figure 73 the effect of RF-EMF on DNA strand breaks at these exposure conditions exhibited a similar energy dependency as the effect of RF-EMF on micronucleus formation (Figure 72). RF-EMF exposure at a SAR of 1.0 W/kg and below had no effect on Comet formation in HL-60 cells (expressed as Olive Tail Moment OTM) as compared to control and sham-exposed cells. On the other hand RF-EMF at SAR of 1.3 W/kg and above caused a significant increase in DNA strand breaks. The maximum of this effect was observed at SAR 1.3 W/kg (OTM = 2.20 ± 0.16) and 1.6 W/kg (2.24 ± 0.10). At a SAR of 3.0 W/kg Comet formation in RF-EMF exposed cells (OTM 1.23 ± 0.12) was similar to that observed in sham-exposed cells (OTM 1.18 ± 0.03). While the Olive Tail Moment was around 1.0 in sham-exposed and incubator controls, the OTM determined after exposure at a SAR of 1.3 W/kg was approximately 2.2 fold higher (Figure 73). The OTM determined in cells after exposure to hydrogen peroxide (100 µmol/l, 1h), used as a positive control, was 8.3 ± 1.3 (n=3; 8 fold increase compared to control).

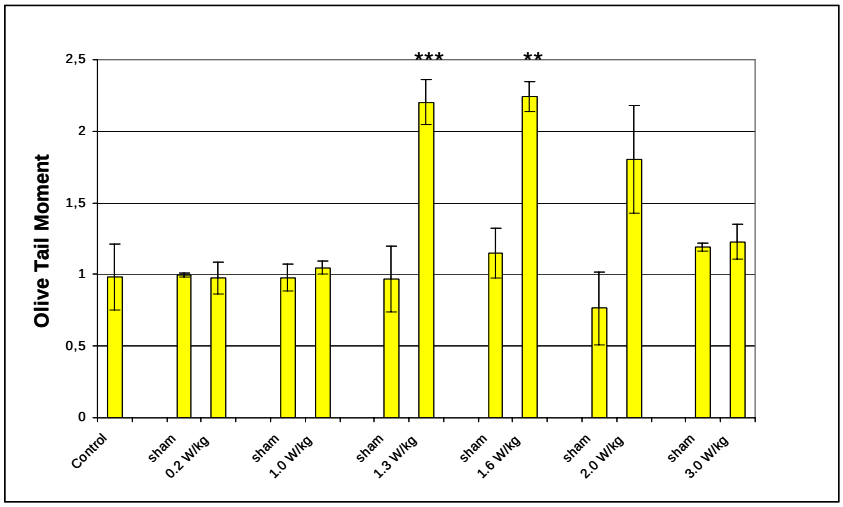

Figure 73. Comet formation in HL-60 cells after exposure to RF-field (1800 MHz, continuous wave) for 24h ranging from SAR 0.2 to 3.0 W/kg, expressed as Olive Tail Moment, compared to control and sham exposure. Each bar represents the mean ± SD of results obtained in at least three (except SAR 1.3 W/kg: n=4) independent experiments. The OTMs of the Comets after exposure to hydrogen peroxide (100 µmol/l, 1 h), which was used as a positive control, were on average 8.3 ± 1.3 (n=3). ** $P<0.01$; *** $P<0.001$ (Student's t-test, two-sided).

In order to compare Comet formation in cells exposed at different SAR ranges the average values of the Olive Tail Moments were calculated for the following groups: experiments performed at all SAR tested (range 0.2 W/kg to 3.0 W/kg, number of independent experiments n=18), experiments performed at SAR ranging from 1.0 W/kg to 2.0 W/kg (number of independent experiments n=12), and experiments at SAR of 0.2 W/kg and 1.0 W/kg (number of independent experiments n=6). While the calculated average of OTMs in HL-60 cells at SAR of 0.2 W/kg and 1.0 W/kg was not significantly different from that observed in sham-exposed controls, both groups ranging from 0.2 W/kg to 3.0 W/kg ($p<0.01$) or from 1.0

W/kg to 2.0 W/kg ($p<0.001$) exhibited a significant increase in Comet formation after RF-exposure as compared to sham-exposed controls (Figure 74B).

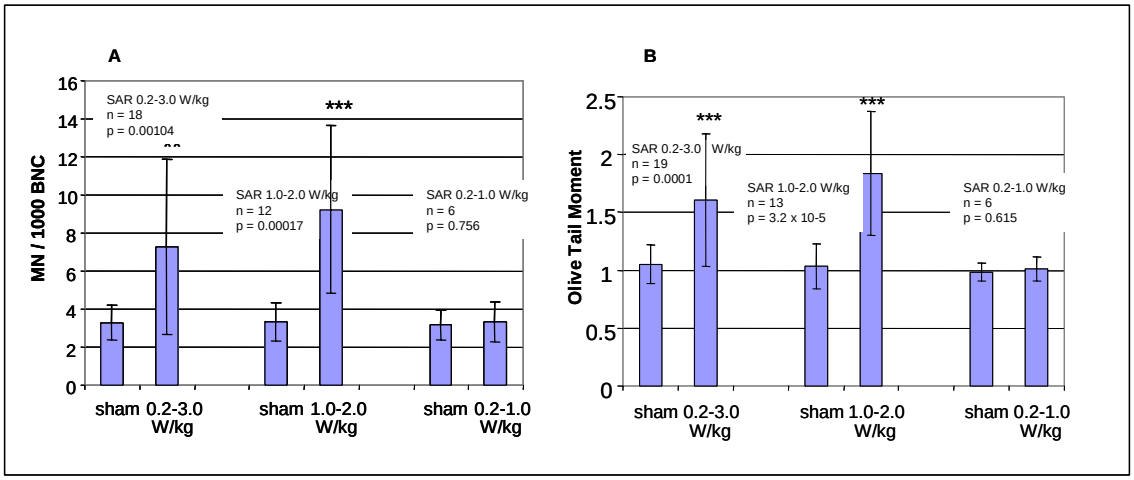

Figure 74. MN induction and Comet formation in HL-60 cells after RF-field exposure (1800 MHz, continuous wave, 24 h) over all SAR groups tested versus total sham, expressed as MN per 1000 BNC (A) and as Olive Tail Moment (B). Each bar represents the mean ± SD of results obtained in indicated number of experiments. ** $P<0.01$; *** $P<0.001$ (Student's t-test, two-sided).

RF-EMF increased the micronucleus frequency and the number of DNA strand breaks in HL-60 cells dependent on the exposure time as determined by the cytokinesis-block in vitro micronucleus assay and the Comet assay.

Using the cytokinesis-block MN assay it was also investigated, whether the duration of exposure of HL-60 cells to RF-fields has an influence on MN induction (Figure 75). Short exposure periods (6 h) caused no or less pronounced effects compared to longer exposure periods of 24 and 72h. The level of the effect on MN frequency noted after RF-EMF exposure for 72h (MN/1000 BNC: 20.22 ± 2.08) was comparable to that observed after 0.5 Gy ionising-irradiation (6 MeV, exposure time: 5.2 s) (MN/1000 BNC: 22.33 ± 2.48).

Furthermore, it was investigated, whether the duration of exposure of HL-60 cells to RF-EMF has an influence on Comet formation (Figure 76). Short exposure periods (2 and 6h) caused less pronounced effects compared to the longer exposure period of 24h. After 72h of exposure Comet formation was similar to that observed after short exposure times (2 and 6h).

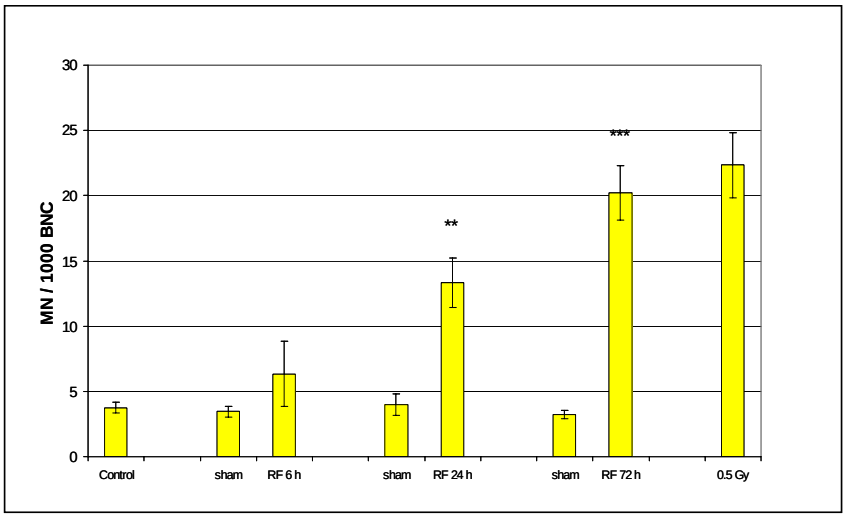

Figure 75. Micronucleus frequencies in binucleated HL-60 cells after exposure to RF-fields (1800 MHz, continuous wave, SAR = 1.3 W/kg) for 6, 24 and 72h, compared to control and sham-exposure. Positive control: 0.5 Gy ionising-irradiation (6 MeV). Each bar represents the mean ± SD of results obtained in three independent experiments (except control: n = 4). Data points are based on a total cell number of 4000 (control), 9000 (sham-exposed), 9000 (RF-exposed) and 3000 (0.5 Gy-exposed, exposure time: 5.2s) binucleated HL-60 cells. All in all (mono-, bi-, tri-, and tetranucleated) 25000 cells were analysed. ** P<0.01; *** P<0.001 (Student's t-test, two-sided).

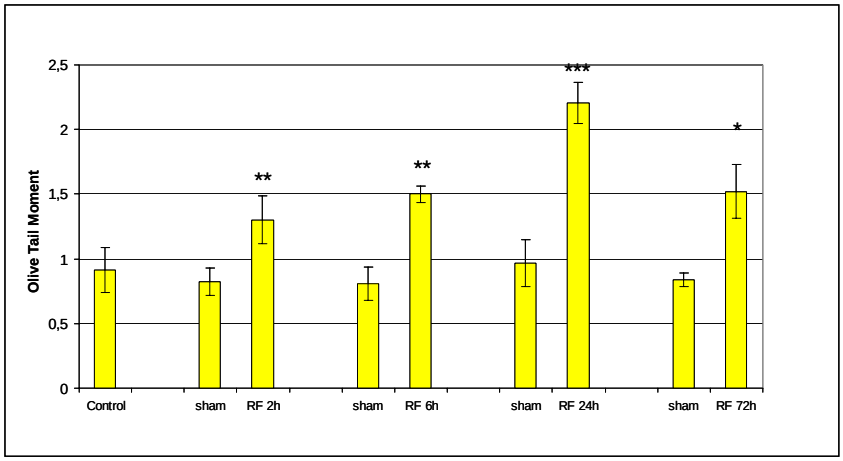

Figure 76. Comet formation in HL-60 cells after exposure to RF-fields (1800 MHz, continuous wave, SAR 1.3 W/kg) for 2, 6, 24 and 72h, expressed as Olive Tail Moment, compared to control and sham-exposure. Each bar represents the mean ± SD of results obtained in at least three (except RF-field exposure, 24h with n=4) independent experiments. * P<0.05; ** P<0.01; *** P<0.001 (Student's t-test, two-sided).

The effects of RF-EMF on genomic integrity of HL-60 cells were exposure-signal-dependent as determined by the cytokinesis-block in vitro micronucleus assay and the Comet assay.

In a further series of experiments it was studied, whether different RF-signals (1800 MHz, SAR 1.3 W/kg: continuous wave, C.W., 5 min on/10 min off; GSM-217Hz, GSM-Talk) for 24h are capable to cause MN induction in HL-60 cells (Figure 77) The number of independent experiments was extended to at least three independent experiments for each of the different types of RF-signals at that SAR with the most pronounced effect (SAR 1.3 W/kg). Using the cytokinesis-block MN assay the different RF-signals had similar effects on MN induction as observed following continuous wave exposure. While the MN frequency of continuous wave-exposed cells was 13.33 ± 1.89, the MN frequencies determined after different other RF-exposure signals were 16.11 ± 3.10 (C.W., 5 min on/10 min off), 13.22 ± 2.88 (GSM-

217Hz) and 17.66 ± 1.70 (GSM-Talk). The MN frequency determined in cells after exposure to ionizing-irradiation (0.5 Gy, 6 MeV, exposure time. 5.2 s), used as a positive control, was 22.3 ± 3.5 (n=3; 6.3 fold increase compared to control).

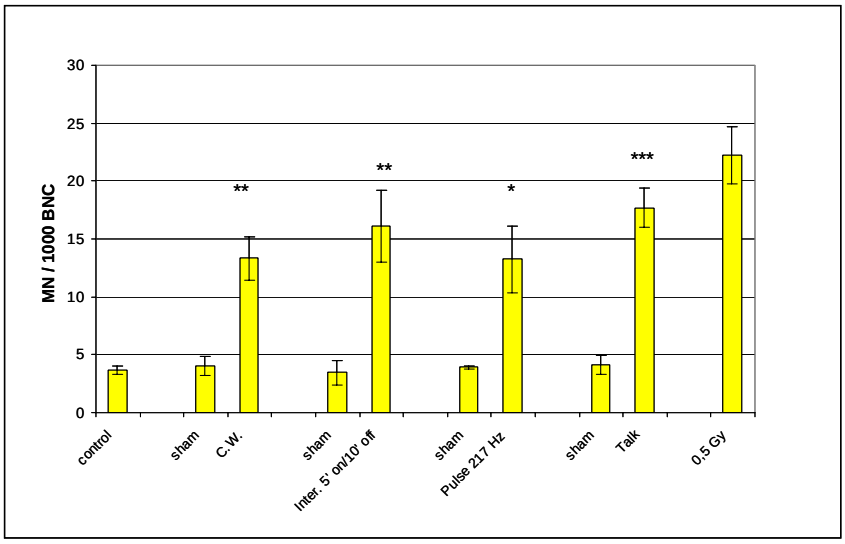

Figure 77. Micronucleus frequencies in binucleated HL-60 cells after exposure to RF-field (1800 MHz, SAR 1.3 W/kg, 24h) compared to control and sham-exposure for different signal modulations. Positive control: 0.5 Gy ionising-irradiation (6 MeV, exposure time: 5.2s). Bars represent means ± SD of three independent experiments (except control = 5). * P<0.01; ** P<0.01; *** P<0.001 (Student's t-test, two-sided). Each data point is based on at least three independent experiments except the control with five and the positive control with three independent experiments and on a total of 5000 (control), 12000 (sham-exposed), 12000 (RF-exposed) and 4000 (0.5 Gy-exposed) binucleated HL-60 cells. All in all (mono-, bi-, tri-, and tetranucleated) 32000 cells were analysed.

Calculation of the average numbers of micronuclei per 1000 BNC determined after exposure (SAR of 1.3 W/kg, 24h) to all RF-signals tested (continuous wave, C.W., 5 min on/10 min off; GSM-217Hz, GSM-Talk) showed an increase in micronuclei induction as compared to sham-exposure at a significant level (number of independent experiments n=12, P<0.001) (Figure 79A).

Using the Comet assay the different RF-signals had similar effects on Comet formation as observed after continuous wave exposure (Figure 78). While the OTM of continuous wave-exposed cells was 2.20 ± 0.16, the OTMs determined after different other RF-exposure signals were 2.11 ± 0.05 (C.W., 5 min on/10 min off), 1.77 ± 0.01 (GSM-217Hz) and 2.26 ± 0.24 (GSM-Talk).

Calculation of the average value of Olive Tail Moments determined after exposure to all RF-signals tested (continuous wave, C.W., 5 min on/10 min off; GSM-217Hz, GSM-Talk) showed a significant increase in Comet formation compared to sham-exposed controls (n=14, P<0.001 (Figure 79B).

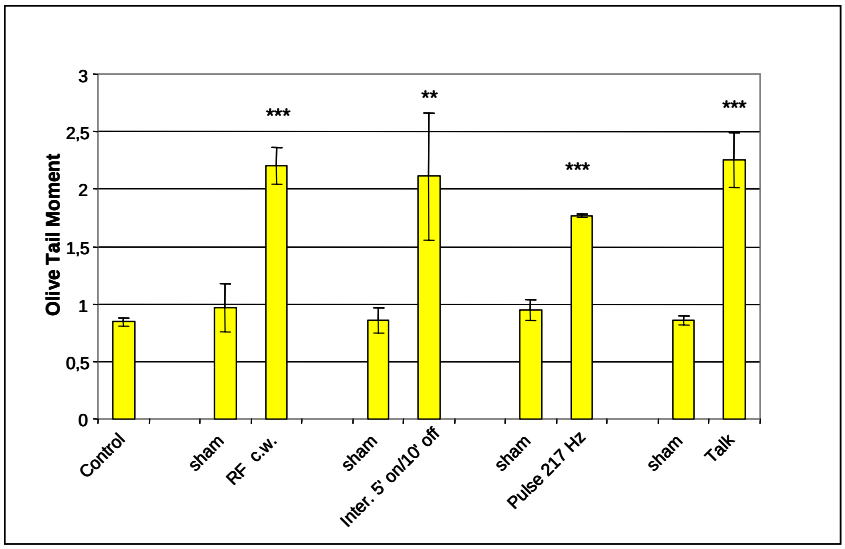

Figure 78. Comet formation in HL-60 cells after exposure to RF-fields (1800 MHz, SAR 1.3 W/kg) for different signal modulations, expressed as Olive Tail Moment, compared to control and sham exposure. Each bar represents the mean ± SD of results obtained in at least three (except continuous wave and C.W., 5 min on/10 min off: n=4) independent experiments. ** P<0.01; *** P<0.001 (Student's t-test, two-sided).

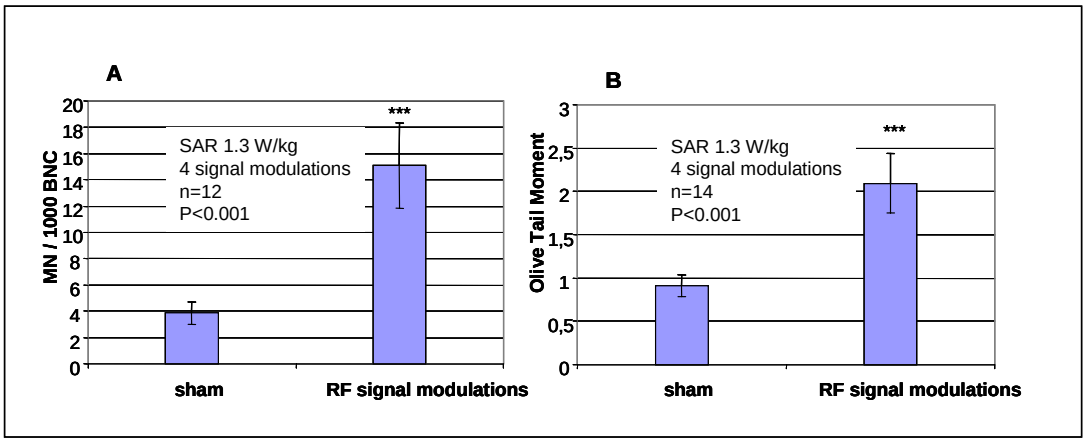

Figure 79. MN induction and Comet formation in HL-60 cells over all RF-field signal modulations at 1800 MHz, 24h, versus total sham, expressed as MN per 1000 BNC (A) and as Olive Tail Moment (B). Each bar represents the mean ± SD of results obtained in indicated number of experiments. *** P<0.001 (Student's t-test, two-sided).

As shown by flow cytometric analysis RF-EMF increased the micronuclei frequency, but did not affect cell cycle.

The results of the flow cytometric analysis of MN induction in HL-60 cells following RF-EMF exposure at the SAR level of 1.3 W/kg tested above using the continuous wave signal, according to the method of Nüsse et al. 1984, 1997, parallel the results obtained using the cytokinesis-block MN assay. Figure 80 shows a representative flow cytometric analysis of MN induction for sham-exposed (A) and RF-exposed (B) HL-60 cells after exposure to RF (1800 MHz, continuous wave, SAR 1.3 W/kg) for 24h. The DNA distribution of micronuclei (marker M1) and nuclei (marker M2) is obtained by projection of the particles defined by their side scatter intensities as micronuclei and nuclei. The percentage of MN is higher in the RF-exposed sample than in the sham-exposed sample (4.1% MN versus 2.7% MN).

The quantitative results of MN content analysis in four independent experiments are presented in Table 13. In all HL-60 cell experiments the MN content of the RF-exposed samples is higher than in sham-exposed samples. Normalisation of MN content in sham-exposed cells to 100% revealed a significant induction of MN after exposure to RF-field by 138.2 ± 18.4% ($P<0.01$; Student's t-test, two-sided). This result parallels those obtained using the microscopic analysis of MN frequencies.

Moreover, by means of flow cytometry the DNA-content of G1/G0, S and G2/M phase can be quantified by determining the fraction of each sub-population. The DNA-content distribution (ethidium bromide fluorescence) showed no differences between RF-field exposed and sham-exposed cells, indicating no influence of RF-EMF on cell cycle (Figure 80). Furthermore, cell cycle analysis demonstrated no accumulation of cells arrested in S and G2/M phase following exposure to RF fields. Additionally, for 24h RF-field exposure (1800 MHz, continuous wave, SAR 1.3 W/kg) no increase of the cell population in he sub G1 peak, which can be considered a marker of apoptotic cell death, was observed by flow cytometry.

Table 14 shows the data of DNA content distribution as percentage of gated cells for G1/G0, G2/M and S phase for RF-field exposed cells (continuous wave, SAR 1.3 W/kg, 24h), as compared to incubator control, sham-exposure and positive control hydrogen peroxide (100 µmol/l for 1 hour). The distribution of G1/G0, G2/M and S phase in the incubator control was 51.9 ± 4.2%, 18.3% ± 3.7 and 19.4 ± 1.7%; that of the positive control hydrogen peroxide: 28.4 ± 12.1%, 9.1 ± 5.2% and 9,0 ± 3.6%. Overall, the percentage of gated cells for the positive control was clearly lower than in all other conditions due to the fact, that here out of the gate analysed a high content of cellular debris was detected. This serves as a measure of cytotoxicity exerted by hydrogen peroxide. Sham-exposed and RF-exposed cells showed a similar DNA distribution as in the incubator control. No significant differences in DNA distribution of RF-exposed cells compared to sham-exposed cells were observed.

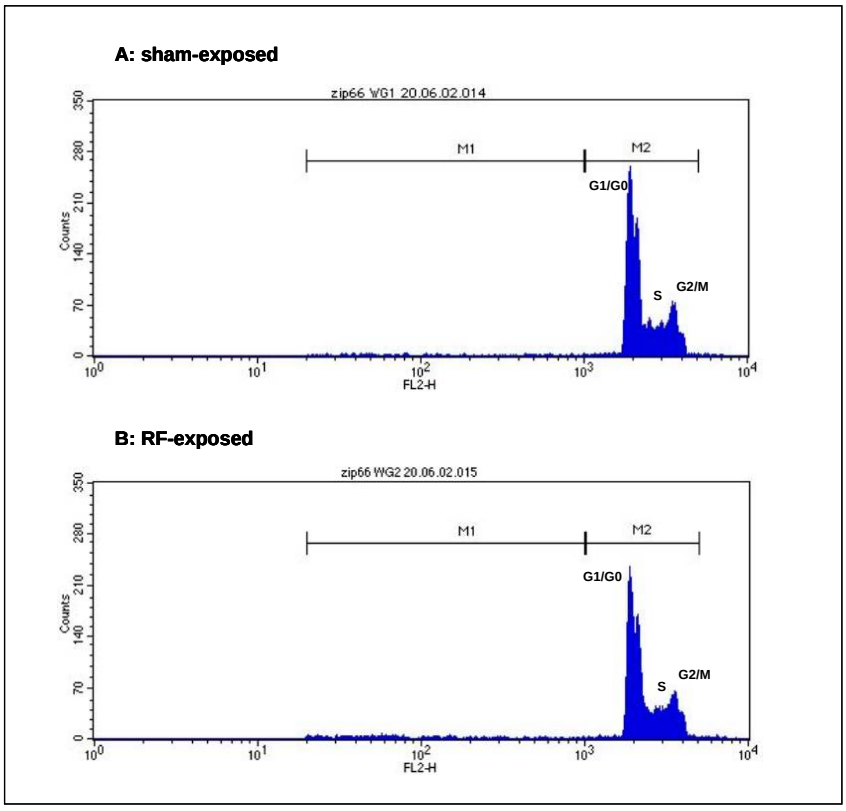

Figure 80. Flow cytometric analysis of micronuclei induction and determination of the proportions of cells in G1/G0, S and G2/M phases of the cell cycle after exposure of HL-60 cells to sham (A) or RF field (B, 1800 MHz, continuous wave, SAR 1.3 W/kg) for 24h.

The diagrams show representative ethidium bromide fluorescence histograms of micronucleated cells/nuclei suspension after treatment with FACS solution I and II. The method was performed according to Nüsse and Kramer (1984), Nüsse and Marx (1997) and Wessel and Nüsse (1995). G1/G0, S and G2/M peaks are indicated. For measurement of MN the G1/G0 peak was adjusted to approximately 2000 relative fluorescence units (FL2-H). The sort window for counting the MN comprised the relative DNA fluorescence units from 20 to 1000 (M1). For quantitative determination of MN the ratio of events in M1 (micronuclei) was compared to the events in M2 (nuclei) and expressed as % MN. For this representative experiment out of four the results for sham-exposure is 2.7% MN (A) and for RF-exposure is 4.1 % MN (B).

Table 13. Quantitative flow cytometric analysis of micronuclei frequencies after RF-field exposure (1800 MHz, continuous wave, SAR 1.3 W/kg, 24 h), compared to sham-exposure.

No. of experiment	Content of MN [%]		
	Sham-exposed	RF-field exposed	Content of MN in RF-exposed cells rel. to sham-exposed cells (100%)
1	2.69	4.08	151.67
2	5.49	6.37	116.03
3	4.24	6.57	154.95
4	1.85	2.41	130.70
mean	3.57 ± 1.62	4.86 ± 1.98	138.23 ± 18.41 **

Data of column 4 are values of RF-exposed cells in percentage relative to the corresponding sham-exposed value.
** Significant difference between the content of MN of RF-exposed cells to sham-exposed cells at P<0.01 (Student's t-test, two-sided).

Table 14. DNA distribution and cell cycle analysis of HL-60 cells after exposure to RF-field (1800 MHz, continuous wave, SAR 1.3 W/kg) for 24 h, compared to control, sham-exposure and positive control hydrogen peroxide (100 µmol/l for 1 h). Data represent DNA content distribution as percentage of gated cells in G1/G0, G2/M and S phase.

Group	n	G1/G0 [%]	S [%]	G2/M [%]
control	3	51.90 ± 4.17	18.25 ± 3.65	19.37± 1.71
sham	4	54.98 ± 6.69	19.45 ± 3.50	18.43 ± 4.07
RF-field	4	52.94 ± 6.19	19.01 ± 3.54	20.06 ± 2.73
positive control H_2O_2 (100 µmol/l for 1h)	3	28.37 ± 12.11	9.11 ± 5.17	8.96 ± 3.59

RF-EMF did not affect apoptosis as demonstrated by the Annexin V and TUNEL assay.

As the findings of structural alterations on the genomic level correlated with an external cellular stimulus do per se not prove a genotoxic effect, it has to be ruled out, that such changes are due to induction of apoptosis. Apoptotic cells typically undergo a series of structural changes: blebbing of the plasma membrane, condensation of the cytoplasm and intact organelles, and nuclear fragmentation. The most common biochemical property of apoptosis is the endonucleolytic cleavage of chromatin, initially to large fragments of 50-300 kilobase pairs and subsequently to monomers and multimers of 180-200 base pairs.

By establishing two flow cytometry methods for detection of apoptosis, Annexin V assay and TUNEL assay, a differentiation approach was included in the experimental strategy. By means of these two tests the detection of apoptotic changes at different stages in the apoptotic process became feasible. As a positive control for apoptosis induction by camptothecin, a topoisomerase I inhibitor, was used in the flow cytometry assays.

After initiation of apoptosis most cell types translocate phosphatidylserine (PS) from the inner plasma membrane leaflet to the cell surface. Once on the cell surface, PS can easily be detected by staining with a FITC conjugate of Annexin V, a protein that has strong natural affinity for phosphatidylserine. As

externalisation of phosphatidylserine occurs before nuclear changes, associated with apoptosis, take place, the Annexin V test detects apoptotic cells significantly earlier than do DNA-based assays.

Figure 81 shows a representative flow cytometric analysis of Annexin V staining following RF- (1800 MHz, 1.3 W/kg, continuous wave, 24h) and sham-exposure of HL-60 cells. As a positive control the apoptosis inducer camptothecin, a topoisomerase I inhibitor, was used to prove inducibility of apoptosis in the HL-60 cell system. The histograms show apoptosis associated Annexin V-FITC-signals (FL-1) versus DNA content propidium iodide (PI) signals. In order to prove that the gating of the corresponding cell populations for scoring the content of apoptotic cells did not select sub-populations, the histograms for "gated" and "not gated" cells are presented.

The TUNEL method (Terminal Deoxynucleotidyl Transferase Biotin-dUTP Nick End Labeling) identifies apoptotic cells *in situ* by using terminal deoxynucleotidyl transferase (TdT) to transfer FITC-dUTP to the free 3´-OH of cleaved DNA. These labelled cleavage sites can then be detected by flow cytometry.

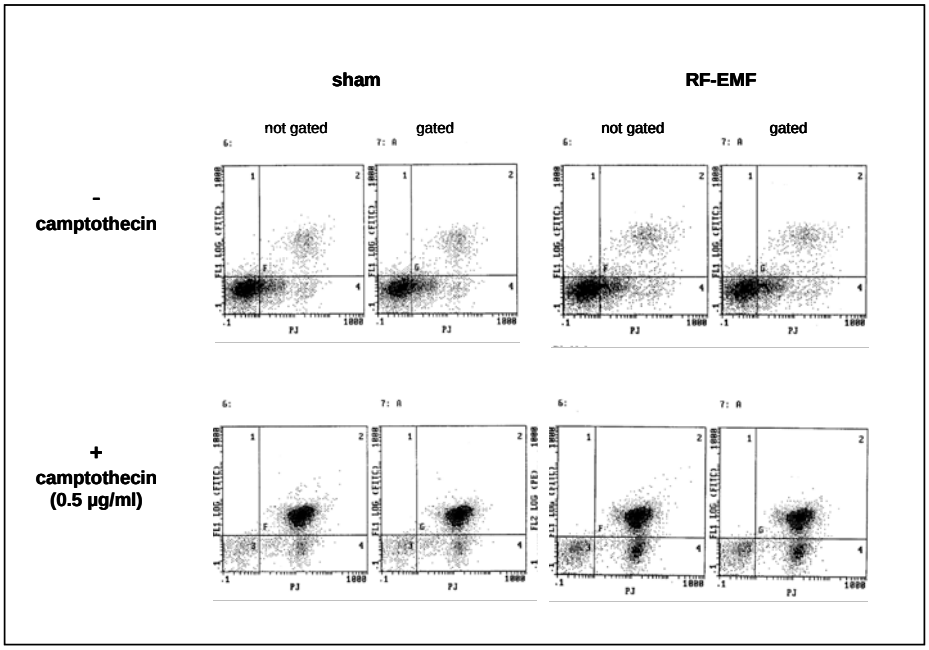

Figure 81. Flow cytometric analysis of RF- (1800 MHz, continuous wave, 1.3 W/kg, 24h) and sham-exposed HL-60 cells after staining with Annexin V-FITC (FL-1) and propidium iodide (PI, DNA content). The apoptosis inducer camptothecin is included as a positive control.

The histograms show apoptosis associated Annexin V-FITC (FL-1) versus DNA content propidium iodide (PI) signals. In order to prove that the gating of the corresponding cell populations for scoring the content of apoptotic cells did not select certain sub-populations, the histograms for "gated" and "not gated" cells are presented.

Figure 82 shows a representative flow cytometric analysis of TUNEL staining following RF-exposure (1800 MHz, , continuous wave, SAR 1.3 W/kg, 24h) and sham exposure of HL-60 cells. As a positive control the apoptosis inducer camptothecin, a topoisomerase I inhibitor, was used to prove inducibility of apoptosis in the HL-60 cell system. The histograms show apoptosis associated TUNEL-FITC-signals (FL-1) versus DNA content propidium iodide (PI) signals. In order to prove that within the quantification procedure no differences in cell population analysed occurs, histograms for "gated" and "not gated" cells are presented (Figure 82).

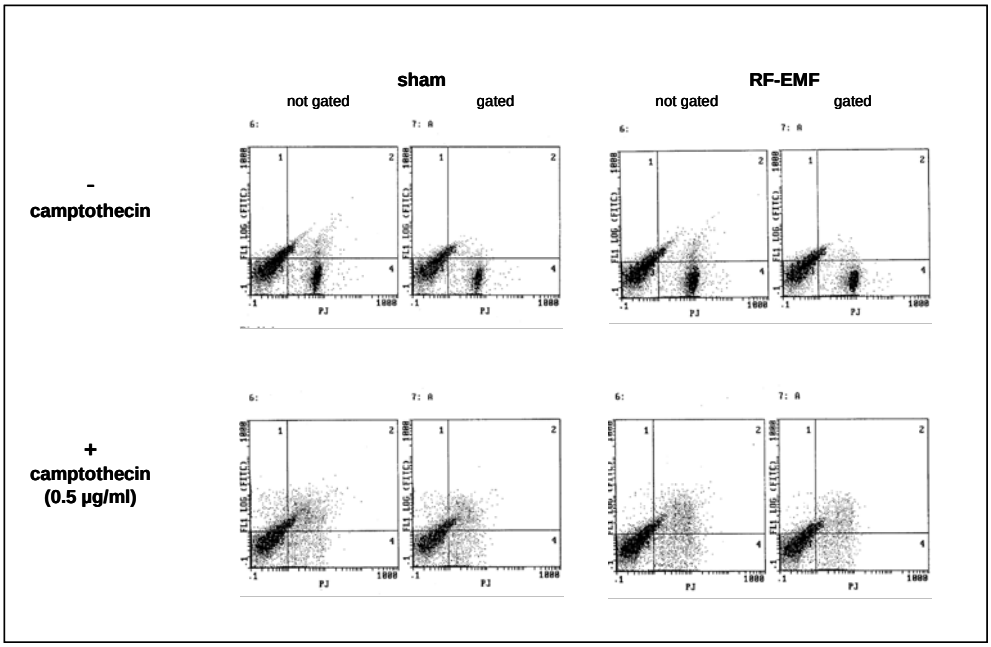

Figure 82. Flow cytometric analysis of RF- (1800 MHz, continuous wave, 1.3 W/kg, 24h) and sham-exposed HL-60 cells after labelling with TUNEL reaction mixture (Roche, Mannheim) for 1 hour at 37°C. The cells then underwent flow cytometric analysis in order to determine the number of green stains (representing apoptotic DNA fragmentation). DNA content analysis was performed on a Becton Dickinson FACScan by using the manufacturer's protocol. The apoptosis inducer camptothecin is included as a positive control.

The histograms show apoptosis associated TUNEL-FITC-signals (FL-1) versus DNA content propidium iodide (PI) signals. In order to prove that the gating of the corresponding cell populations for scoring the content of apoptotic cells did not select certain sub-populations, the histograms for "gated" and "not gated" cells are presented.

Neither by the Annexin V assay nor by the TUNEL assay, apoptosis induced by RF-electromagnetic fields (1800 MHz, continuous wave, SAR 1.3 W/kg, 24h) could be detected in HL-60 cells. Moreover, HL-60 cells exposed to RF-field at SAR 1.3 W/kg and continuous wave signal for 24h show no induction of the cell population in the sub G1 peak, which can be considered a marker of cell death by apoptosis (Figure 80).

RF-EMF did not exert a cytotoxic effect on HL-60 cells.

The trypan blue vitality test did not reveal any cytotoxic effects on the HL-60 cells from any RF-field applied. The vitality of the exposed cells was on the same order of magnitude (≈ 90%) as the cells of the sham-exposed and the incubator control. To exclude minor effects of RF-fields on viability of HL-60 cells, cell viability was examined spectrophotometrically by the MTT assay (Figure 83). Supplementary, also by this method no cytotoxic effect was detectable: absorbance A_{570nm} (RF-exposed HL-60 cells) = 0.91 ± 0.13 ; A_{570nm} (sham-exposed HL-60 cells) = 0.98 ± 0.15.

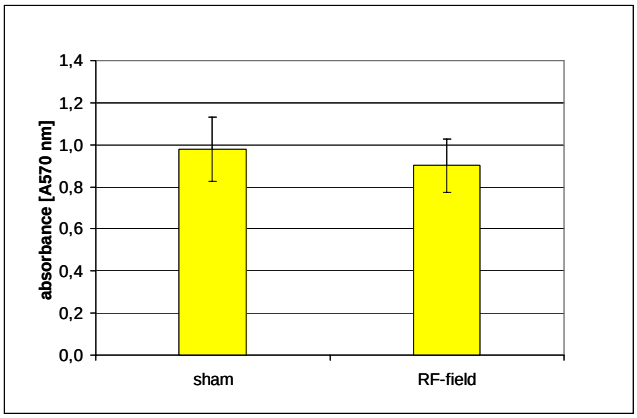

Figure 83. Viability of HL-60 cells after exposure to RF-field (1800 MHz, continuous wave, SAR 1.3 W/kg, 24h) compared to sham exposure. Cell viability was evaluated by the MTT assay and reported as absorbance at 570 nm. Bars represent means ± SD of 12 independent experiments.

In addition, the ratio of binucleated cells (BNC) against mono-, bi-, tri- and tetranucleated cells (% BNC) was determined as a measure of cell division and cell cycle progression. No effect of RF-EMF exposure on % BNC for different energies (Figure 84) or for different signal modulations (Figure 85) was found in comparison to sham-exposed or ionising-irradiated (0.5 Gy, 6 MeV, exposure time: 5.2s) HL-60 cells.

Additionally, no significant differences in DNA distribution of RF-exposed cells compared to sham-exposed cells were observed with respect to increased incidence of cellular debris as a measure of cytotoxicity (Table 14).

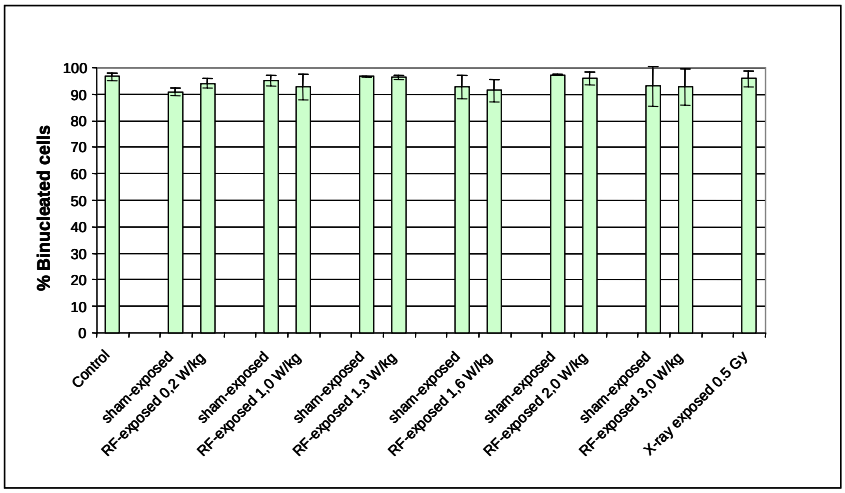

Figure 84. Effect of RF-field exposure on cell division. Shown is the number of binucleated HL-60 cells relative to the number of mono-, bi-, tri-, and tetra-nuclear cells (% BNC) following RF-field exposure (1800 MHz, continuous wave, different SAR levels, 24h). Positive control: 0.5 Gy ionising-irradiation (6 MeV, exposure time: 5.2s). Each bar represents the mean ± SD of results obtained in three independent experiments.

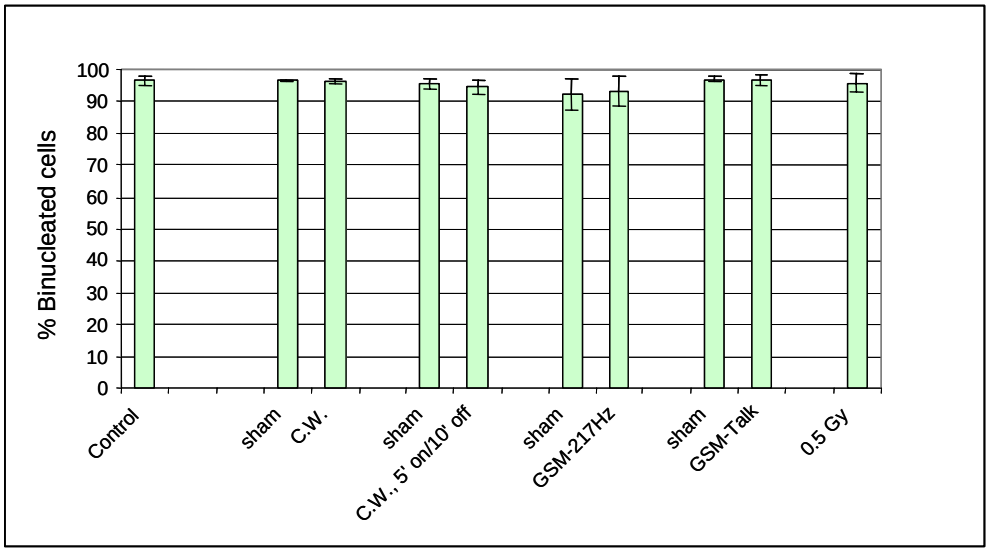

Figure 85. Effect of RF-field exposure on cell division. Shown is the number of binucleated HL-60 cells relative to the number of mono-, bi-, tri-, and tetranuclear cells (% BNC) following RF-field exposure (1800 MHz, SAR 1.3 W/kg, different signal modulations, 24h). Positive control: 0.5 Gy ionising-irradiation (6 MeV, exposure time: 5.2s). Each bar represents the mean ± SD of results obtained in three independent experiments.

Concludingly no in vitro cytotoxic effects of RF-EMF could be detected in RF-EMF-exposed and sham-exposed cells for the exposure conditions tested using either microscopic evaluation (trypan blue exclusion, % BNC), colorimetric MTT assay or flow cytometric analysis (nuclear ethidium bromide staining).

B. Indirect genotoxicity (by reactive oxygen species)

RF-EMF induced formation of reactive oxygen species as shown by flow cytometric detection of oxyDNA and rhodamine fluorescence.

It was the aim of these series of experiments to examine whether RF-EMF (1800 MHz at SAR 1.3 W/kg, 24h exposure) is capable to induce indirect genotoxic effects by affecting the generation and elimination of reactive oxygen species (ROS). For monitoring these ROS-formation and elimination steps, different assays, measuring nitric oxide, oxyDNA, oxidative DNA-damage via Dihydrorhodamine 123 (DHR123), lipid peroxidation, glutathione peroxidase activity, superoxide dismutase activity, have been established and were applied following RF-field exposure of HL-60 cells at that exposure condition with the most significant effect on DNA integrity (1800 MHz, continuous wave, 1.3 W/kg, 24h).

Nitric oxide (NOx)

Nitric oxide (NOx), was measured using the colorimetric Nitric Oxide Assay Kit, Calbiochem, Bad Soden, Germany. The data in Table 15 show the NOx production from HL-60 cells after exposure to RF-field (1800 MHz, continuous wave, SAR 1.3 W/kg, 24h), compared to control and sham-exposed cells. For an amount of 0.25 x 10^5 cells, in neither treatment group the detection limit of 1 µmol NOx/l was exceeded. The results presented are the means of three independent experiments. Concludingly, with this assay no in vitro effect of RF-field exposure on NOx formation was detected for the exposure conditions tested.

Table 15. NO_x formation in HL-60 cells after exposure to RF-field (1800 MHz, continuous wave, SAR 1.3 W/kg, 24h), compared to control and sham-exposure.

Group	NOx [µmol/l]
control	< 1
sham	< 1
RF-field	< 1

0.75×10^6 viable HL-60 cells/3 ml cell culture medium were cultivated for 24h at 37°C. After centrifugation, aliquots of culture media corresponding to 0.25×10^5 cells were collected and analysed for nitric oxide (NOx) by the colorimetric Nitric Oxide Assay Kit, Calbiochem, Bad Soden, Germany.
The results presented are representative for three independent experiments.

Flow cytometric detection of oxidative DNA damage (oxy-DNA)

The presence of oxidised DNA (by a fluorescent probe, directly binding to 8-oxoguanine as the major oxidative DNA product) was indicated by a green/yellow fluorescence that could be detected using a flow cytometry system. In Figure 86 a partial augmentation (occurring as a shoulder on the right side of the signal, see arrow Figure 86 of FL-1 fluorescence intensity), indicating the presence of oxidised DNA, was observed for the RF-exposed signal (green) in contrast to sham-exposed signal (blue). Additionally, RF-exposed cells showed a significant shift to the left as compared to sham-exposed cells. Table 16 shows the data for the quantification of ROS levels using oxyDNA-FITC conjugate to stain 8-oxoGuanosine residues on oxidatively damaged DNA of HL-60 cells. RF-field exposure of HL-60 cells induced a mean increase of oxidative DNA damage of 21.7 ± 2.0 %.

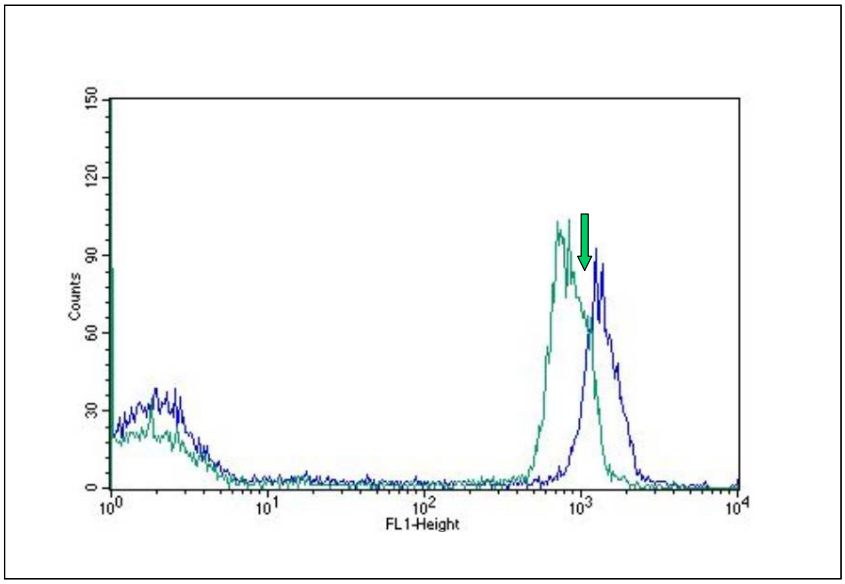

Figure 86. Flow cytometric detection of ROS levels using oxyDNA-FITC conjugate to stain 8-oxoGuo residues on oxidatively damaged DNA of HL-60 cells. The diagram shows the signal of oxidatively damaged DNA of RF-field exposed cells (green line) compared to sham-exposed cells (blue line). One representative histogram plot out of four independent experiments is shown. A partial augmentation (shoulder at the right side of the signal, indicated by arrow) of FL-1 fluorescence intensity was observed for the RF-exposed signal in contrast to sham-exposed signal.

Table 16. Quantification of ROS levels of HL-60 cells after exposure to RF-field (1800 MHz, continuous wave, SAR 1.3 W/kg) for 24h using oxyDNA-FITC conjugate to stain 8-oxoGuo residues on oxidatively damaged DNA.

No. of experiment	% augmentation of fluorescence signal of RF-field exposed cells (area under curve AUC of shoulder at the right side of the signal)
1	21.38
2	24.44
3	19.80
4	20.98
mean ± SD	21.65 ± 2.0

0.75 x 10^6 HL-60 cells/dish were sham- or RF-field exposed for 24 h. oxyDNA-FITC was used to stain 8-oxoGuo residues on oxidatively damaged DNA using the oxyDNA assay from Calbiochem-Novabiochem GmbH, Bad Soden, Germany. Oxidatively damaged DNA was quantified by determination of the area under the curve (AUC) of the shoulder at the right side of the signal fluorescence intensity (see arrow Figure 83) in RF-field exposed cells * Significant difference between the median of fluorescence intensity of RF-field exposed cells and sham-exposed cells at P<0.05 (n=4, Student's t-test, two-sided).

Oxidative DNA damage measured by DHR123 and flow cytometry

Cellular production of ROS was determined by measuring the rhodamine fluorescence of HL-60 cells, incubated in growth medium containing 5 µmol/l dihydrorhodamine 123 (DHR123) for 24h at 37°C. DHR123 is a non-fluorescent reduced Rhodamine 123 (Rh123) derivative that is freely permeable through cell membranes. Intracellular oxidation converts DHR123 to the fluorescent Rh123, which is retained intracellularly by the mitochondrial potential.

Figure 87 displays the overlay fluorescence histograms for RF-field exposed cells (1800 MHz, continuous wave, SAR 1.3 W/kg), compared to sham-exposed cells after simultaneous incubation with DHR123 for 24h. The figure shows that, in RF-field exposed cells, the fluorescence intensity signal shifts to the right in comparison to the signal of sham-exposed cells. In contrast, treating cells with 100 µmol/l H_2O_2 resulted in an even more pronounced shift of fluorescence signal. These shifts indicate enhanced fluorescence intensities and thereby increased production of intracellular ROS during RF-field exposure or H_2O_2 treatment of HL-60 cells.

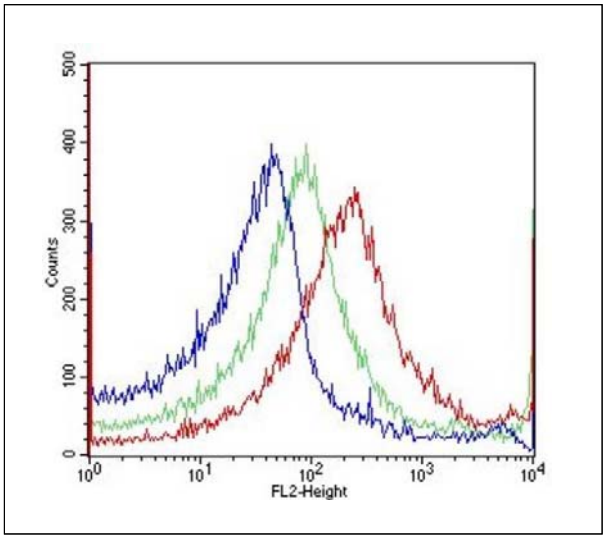

Figure 87. Fluorescence histograms for RF-field exposed (1800 MHz, continuous wave, SAR 1.3 W/kg, 24h) and sham-exposed HL-60 cells simultaneous treated with 5 µmol/l dihydrorhodamine 123 (DHR123). Blue line represents sham-exposed sample, green line represents RF-field exposed sample and red line represents H_2O_2-treated positive control (100 µmol/l for 1 hour). DHR123 reacts with intracellular ROS to form fluorescent Rh123, which is then retained by the mitochondria, enabling a flow cytometric assessment of cellular oxidant production.

By means of the DHR123 flow cytometry detection assay the shift of the signal can be quantified by determining the medians of the fluorescence intensities and the increase in rhodamine fluorescence for each population compared to sham, expressed in percent (Table 17). The data show that there is no difference in the level of oxidatively damaged DNA for control cells and sham-exposed HL-60 cells, expressed as the median of fluorescence intensity. The median values for control cells were 41.8 ± 5.8 and for sham-exposed cells 39.9 ± 8.5 (n=3). The values for the positive control (H_2O_2, 100 µmol/l, 1h) were 230.6 ± 100.3. In contrast, exposing cells to RF-fields resulted in a significant increase in median (75.5 ± 19.2; P<0.05, n=3). The percentage increase of rhodamine fluorescence for RF-field exposed cells compared to sham-exposed cells is 17.8 ± 9.7%, that of H_2O_2-treated cells 31.9 ± 12.4% (Table17).

Table 17. Detection and quantification of ROS levels with Dihydrorhodamine 123 after exposure to RF-field (1800 MHz, continuous wave, SAR 1.3 W/kg, 24 h), compared to control, sham-exposed and H_2O_2-treated HL-60 cells. For quantitative measurement the shift in median and the increase of fluorescence intensity was evaluated.

No. of exp.	Median of fluorescence intensity [units]				% increase of rhodamine 123 fluorescence relative to sham-exposure [a]	
	control	sham-exposed	RF-field exposed	H_2O_2-treated	RF-field exposed	H_2O_2-treated
1	39.95	30.51	95.60	149,89	28.98	43.12
2	37.18	42.17	57.26	199.02	12.35	18.53
3	48.26	46.98	73.65	342.89	11.97	33.91
mean	41.8 ± 5.8	39.9 ± 8.5	75.5 ± 19.2 *	230.6 ± 100.3	17.8 ± 9.7	31.9 ± 12.4

[a] differences of rhodamine 123 fluorescence (AUC, area under curve) of cells exposed to RF-field or those treated with H_2O_2 was determined and the values were plotted as percentage increase relative to sham-exposure.
* Significant difference between the median of RF-exposed cells to the median of sham-exposed cells and the median of RF-exposed cells to that of control cells at P<0.05 (Student's t-test, two-sided).

Lipid peroxidation

Lipid peroxidation was measured using the colorimetric Lipid Peroxidation Assay Kit, Calbiochem, Bad Soden, Germany. Malondialdehyde (MDA) and 4-hydroxy-2(E)-nonenal (4-HNE), products of lipid peroxidation, were estimated spectrophotometrically at 586 nm after reaction with a chromogenic reagent at 45°C. The absorbance values obtained for the samples were compared with a standard curve of known concentrations of MDA / 4-HNE (1 - 20 µmol/l). For MDA and 4-HNE the amounts of lipid peroxidation markers in all experiments and samples were below 1 µmol/l. Table 18 shows that there is no difference in the level of lipid peroxidaton for RF-field exposed HL-60 cells, compared to control and sham-exposed cells (n=3).

Table 18. Lipid peroxidation (LPO) in HL-60 cell homogenates after exposure to RF-field (1800 MHz, continuous wave, SAR 1.3 W/kg, 24h), compared to control and sham-exposed cells.

Group	amount of (MDA + HNE) [µmol/l]		
	exp. 1	exp. 2	exp. 3
control	< 1.0	< 1.0	< 1.0
sham	< 1.0	< 1.0	< 1.0
RF-field	< 1.0	< 1.0	< 1.0

Lipid peroxidation was measured using the colorimetric Lipid Peroxidation Assay Kit from Calbiochem, Bad Soden, Germany. Malondialdehyde (MDA) and 4-hydroxy-2(E)-nonenal (4-HNE), products of lipid peroxidation, were estimated spectrophotometrically at 586 nm in an aliquot corresponding to 6 x 10^5 cells after reaction with a chromogenic reagent at 45°C. The results presented are means of three independent experiments.

Antioxidant enzyme activities

RF-EMF did not affect antioxidant enzyme activities of HL-60 cells (SOD and GPx activity).

To screen the possible effect of RF-EMF on endogenous antioxidant enzyme activity, the activities of superoxide dismutase (SOD) and glutathione peroxidase (GPX) were determined in the HL-60 cells that were exposed to RF-fields (1800 MHz), continuous wave, SAR 1.3 W/kg for 24h. Positive controls as indicated in the assays by the manufacturer were included in the analysis.

Superoxide dismutase (SOD) activity

Superoxide dismutase (SOD) activity of cell homogenates was determined using the Superoxide Dismutase Assay Kit from Calbiochem, Bad Soden, Germany. The data in Table 19 show SOD activities in HL-60 cells after exposure to RF-field (1800 MHz, continuous wave, SAR 1.3 W/kg, 24h), compared to control and sham-exposed cells. For an amount of 4 x 10^5 cells, in neither treatment group the detection limit of 0.2 U/ml SOD activity was exceeded. The results presented are means of two independent experiments. Concludingly, no in vitro effect of RF-field exposure on SOD activity was detected for the exposure conditions tested.

Table 19. Superoxide dismutase (SOD) activity in HL-60 cell homogenates after exposure to RF-field (1800 MHz, continuous wave, SAR 1.3 W/kg, 24h), compared to control and sham-exposed cells.

Group	SOD_{525} activity [U/ml]	
	exp. 1	exp. 2
control	< 0.2	< 0.2
sham	< 0.2	< 0.2
RF-field	< 0.2	< 0.2

Superoxide dismutase (SOD) activity of cell homogenates was determined using the Superoxide Dismutase Assay Kit from Calbiochem, Bad Soden, Germany. The SOD-mediated increase in the rate of autooxidation of the reaction mixture was utilized to yield a chromophore with maximum absorbance at 525 nm. SOD activity was measured in an aliquot corresponding 4 x 10^5 cells (n=2). Detection limit for SOD activity is 0.2 U/ml.

Glutathione peroxidase (GPx) activity

Glutathione peroxidase (GPx) activity of cell homogenates was determined using a cellular Glutathione Peroxidase Assay Kit, Calbiochem, Bad Soden, Germany. The data in Table 20 show the GPx activity in HL-60 cells after exposure to RF-field (1800 MHz, continuous wave, SAR 1.3 W/kg, 24h), compared to control and sham-exposed cells. For an amount of 1 x 10^6 cells, in neither treatment group the detection limit of 5.6 mU/ml GPx activity was exceeded. The results presented represent two independent experiments. Concludingly, no in vitro effect of RF-field exposure on GPx activity was detected for the exposure conditions tested.

Table 20. Glutathione peroxidase (GPx) activity in HL-60 cell homogenates after exposure to RF-field (1800 MHz, continuous wave, SAR 1.3 W/kg, 24h), compared to control and sham-exposed cells.

Group	GPx activity [mU / ml]	
	exp. 1	exp. 2
control	< 5.6	< 5.6
sham	< 5.6	< 5.6
RF-field	< 5.6	< 5.6

Glutathione peroxidase (GPx) activity of cell homogenates was determined in two independent experiments using the cellular Glutathione Peroxidase Assay Kit from Calbiochem, Bad Soden, Germany.
Cell homogenisate of 1 x 10^6 cells is added to a 1050 µl of a solution containing glutathione (GSH, 1mmol/l), GSH reductase (0.4 U/ml) and NADPH. The reaction is initiated by the addition of 350 µl of the diluted organic peroxide t-butyl hydroperoxide and the absorbance at 340 nm was recorded over a period of 5 minutes. The rate of decrease in the absorbance is directly proportional to the GPx activity in the cell homogenisate. Detection limit for GPx activity is 5.6 mU/ml.

Summarising, the endogenous antioxidant enzyme activities of HL-60 cells (SOD and GPx activity) were not altered by RF-field exposure compared to sham-exposure using the conditions of the assays described above. This screening approach revealed, that the analysis of antioxidant enzyme activities does not show enough methodological sensitivity for the amounts of ROS to be generated by RF-field exposure of HL-60 cells.

Indirect genotoxicity by modulation of cellular toxifying and detoxifying capacities

The generation of genotoxic effects through RF-EMF was inhibited by ascorbic acid.

In a further series of experiments it was examined, whether ascorbic acid as a free radical scavenger and inhibitor of reactive oxygen species is capable to inhibit MN induction and DNA damage by co-administration to RF-field-exposure (continuous wave, SAR 1.3 W/kg, 24h). The inhibition of micronuclei induction and Comet formation was measured by use of the cytokinesis-block in vitro Micronucleus assay and the Comet assay. In both tests systems, ascorbic acid effectively reduced the RF-field induction of micronuclei and DNA damage (Figures 85 and 86).

Figure 88 displays the inhibition of MN induction induced by RF-fields (continuous wave, SAR 1.3 W/kg, 24h) and simultaneous treatment of cells with ascorbic acid (AA, 10 µmol/l) for 24h. MN frequencies for sham-exposed and RF-field exposed cells were 4.1 ± 0.2 and 11.6 ± 1.9 expressed as MN / 1000 BNC. After co-incubation of sham-exposed and RF-exposed HL-60 cells with ascorbic acid (AA, 10 µmol/l) for 24h the frequencies were 4.3 ± 0.4 and 4.8 ± 1.9. The MN frequency for the incubator control was 3.4 ± 0.4. Data show, that ascorbic acid inhibits RF-field associated MN induction significantly (n=3, P<0.05). The inhibition resulted in an induction by factor 1.08 compared to sham.

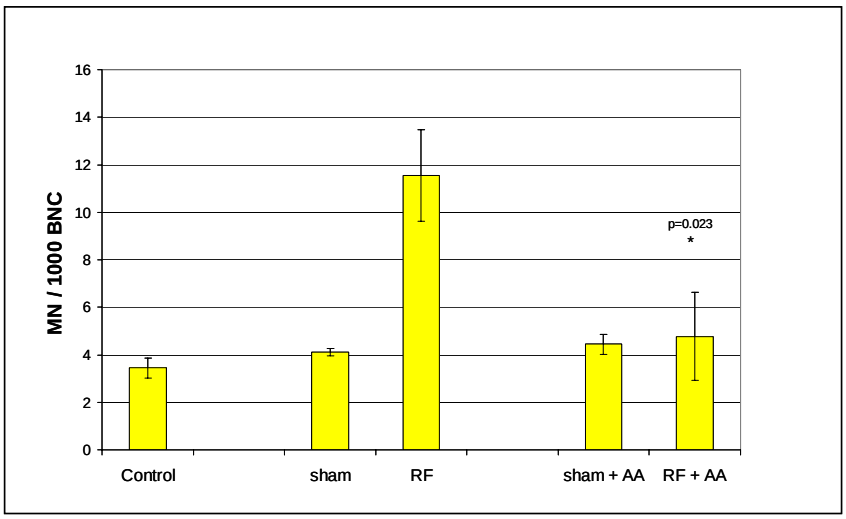

Figure 88. Effect of ascorbic acid (AA, 10 µmol/l) on RF-field (1800 MHz, continuous wave, SAR 1.3 W/kg, 24h) induced MN frequencies in HL-60 cells, compared to control and sham-exposed cells. Each bar represents the mean ± SD of results obtained in at least three independent experiments. Significant differences between RF-field exposure and sham-exposure with co-administration of AA is given by * P<0.05 (Student's t-test, two-sided).

Figure 89 displays the inhibition of DNA damage induced by RF-fields (continuous wave, SAR 1.3 W/kg, 24h) and simultaneous treatment of cells with ascorbic acid (AA, 10 µmol/l) for 24h. The values of Olive Tail Moment for sham-exposed and RF-field exposed cells were 0.9 ± 0.1 and 2.0 ± 0.2. After co-incubation of sham-exposed and RF-field exposed HL-60 cells with ascorbic acid (AA, 10 µmol/l) for 24h the values were 1.0 ± 0.1 and 1.2 ± 0.03. The OTM for the incubator control was 0.8 ± 0.05. Data show, that ascorbic acid inhibits the RF-field induced DNA damage significantly (n=3, P<0.01). The inhibition resulted in an induction by factor 1.2 compared to sham. Additionally, no induction of cytotoxicity (trypan blue test), no alteration of cell medium pH value and no influence on cell growth or cell cycle progression was observed for ascorbic acid alone and for co-administration of ascorbic acid together with RF-field exposure over 24h.

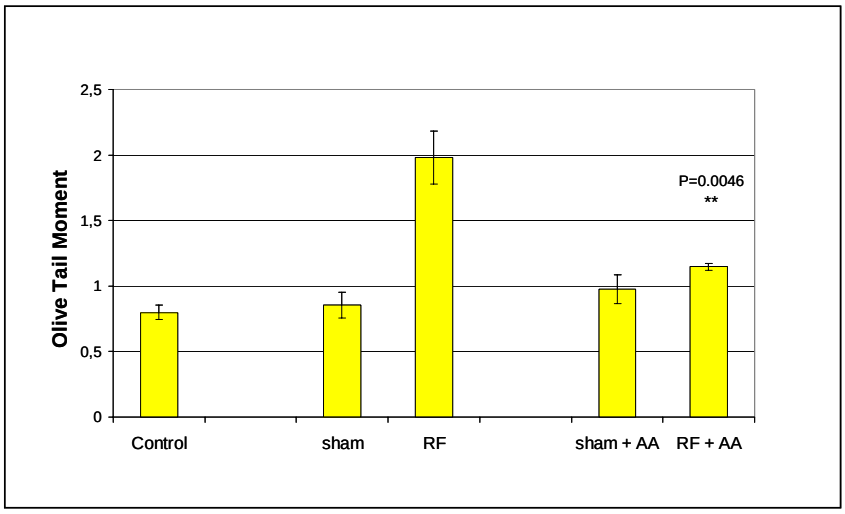

Figure 89. Effect of ascorbic acid (AA, 10 µmol/l) on RF-field induced Comet formation in HL-60 cells (1800 MHz, continuous wave, SAR 1.3 W/kg, 24 h), compared to control and sham-exposed cells. Each bar represents the mean ± SD of results obtained in at least three independent experiments. Significant differences between RF-field exposure and sham-exposure with co-administration of AA is given by ** P<0.01 (Student's t-test, two-sided).

Concludingly, this observed inhibition of genotoxicity by ascorbic acid supports the hypothesis that the effect of RF-field on genomic integrity may be explained by the generation of free oxygen radicals.

3.2.1.2 Human fibroblasts and granulosa cells of rats (Participant 3)

RF-EMF generated DNA strand breaks in human fibroblasts and in granulosa cells of rats.

The influence of RF-EMF exposure on the generation of DNA strand breaks in cells of two different tissues (human fibroblasts, rat granulosa cells) was evaluated using alkaline and neutral Comet assay. Four different sets of exposure conditions were tested: continuous (1800 MHz, 2 W/kg), intermittent (5 min on/10 min off, 1800 MHz, 2 W/kg), pulse modulation (1800 MHz, 2 W/kg, amplitude 217 Hz, 5 min on/10 min off) and talk modulation (1800 MHz, 1.2 W/kg, DTX 66%, GSM basic 34%, continuous). Different exposure duration was applied (4, 16 and 24 hours).

An elevation of Comet assay levels in exposed cells compared to sham-exposed controls could be detected in each of these experiments, even at continuous exposure (Figure 90). This elevation became significant at 16 hours of exposure, but no significant differences between 16 and 24 hours could be detected. At intermittent, pulse modulation and talk modulation Comet assay levels were significantly higher than at continuous exposure. Human fibroblasts and granulosa cells responded equally to RF-EMF, albeit the latter exhibited higher basal and higher end levels (Figure 91). The Comet factors with neutral Comet assay were similar, albeit lower (Figures 92, 93). Dose response investigations with human fibroblasts, which were exposed intermittently (5 min on/10 min off) for 24 hours, revealed a dose dependent increase of the Comet tailfactor beginning already at a SAR of 0.3 W/kg with a peak level at 1.0 W/kg (Figure 94).

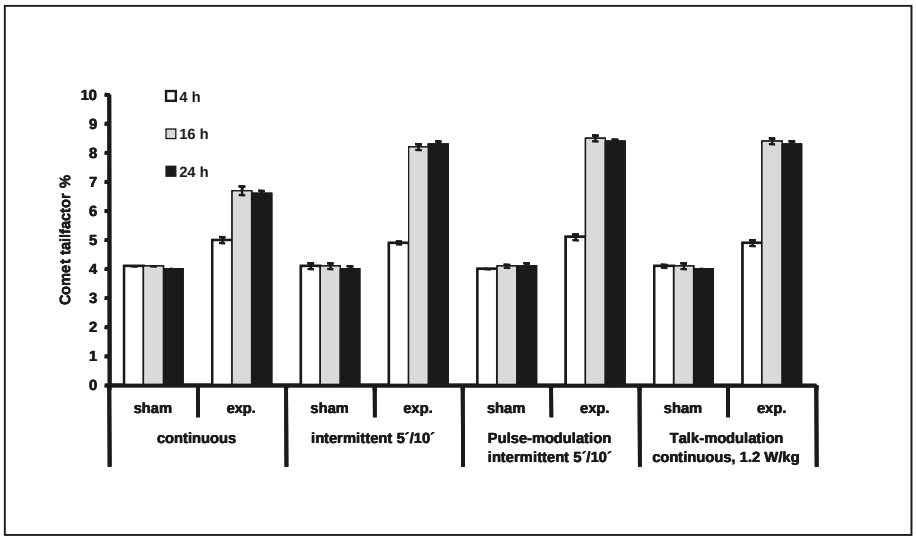

Figure 90. Influence of exposure time and of different exposure conditions on formation of DNA single and double strand breaks in human fibroblasts determined with Comet assay under alkaline conditions (cell strain ES 1, 1800 MHz, SAR 2 W/kg).

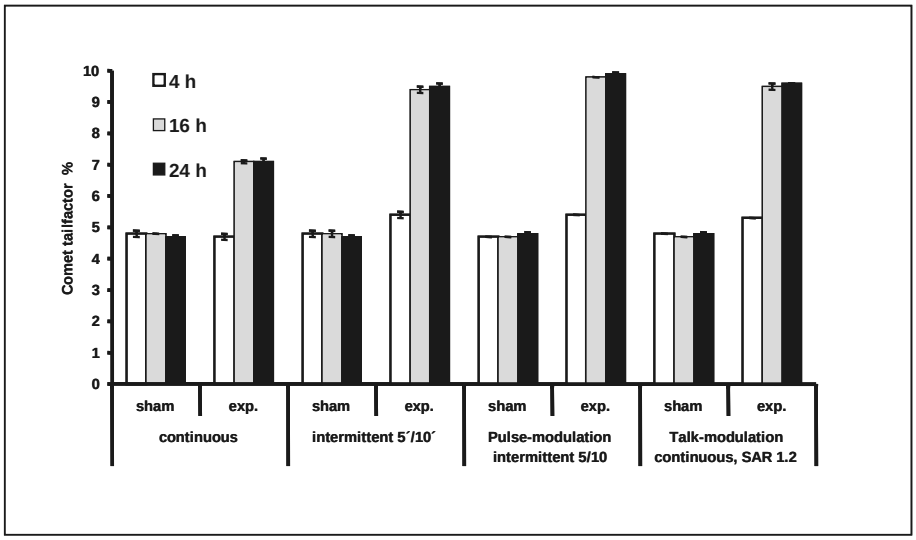

Figure 91. Influence of exposure time and of different exposure conditions on formation of DNA single and double strand breaks in granulosa cells determined with Comet assay under alkaline conditions.

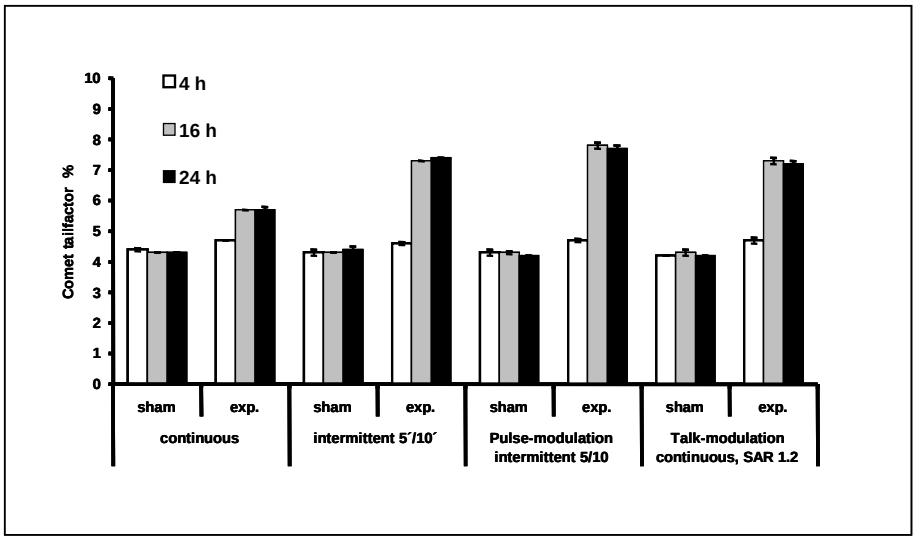

Figure 92. Influence of exposure time and of different exposure conditions on formation of DNA double strand breaks in human fibroblasts determined with Comet assay under neutral conditions (cell strain ES 1, 1800 MHz, SAR 2 W/kg).

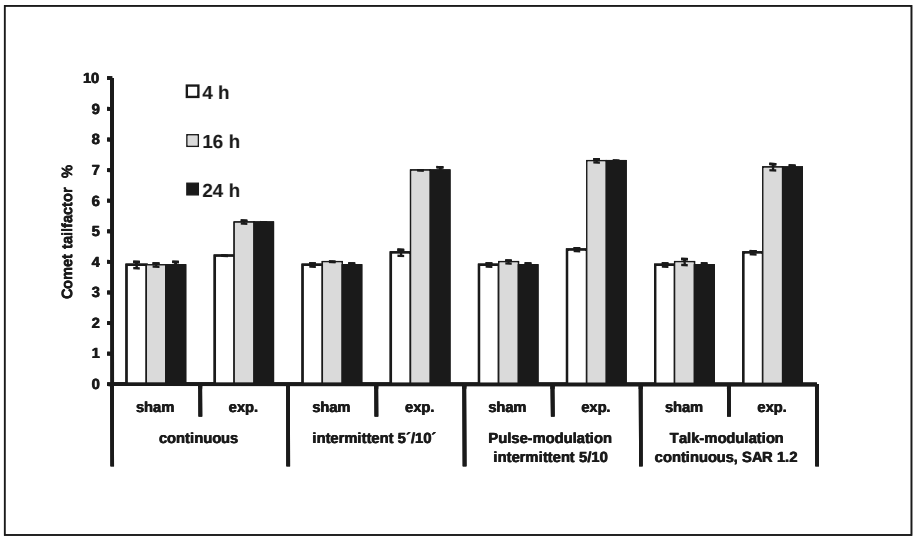

Figure 93. Influence of exposure time and of different exposure conditions on formation of DNA double strand breaks in granulosa cells determined with Comet assay under neutral conditions (1800 MHz, SAR 2 W/kg).

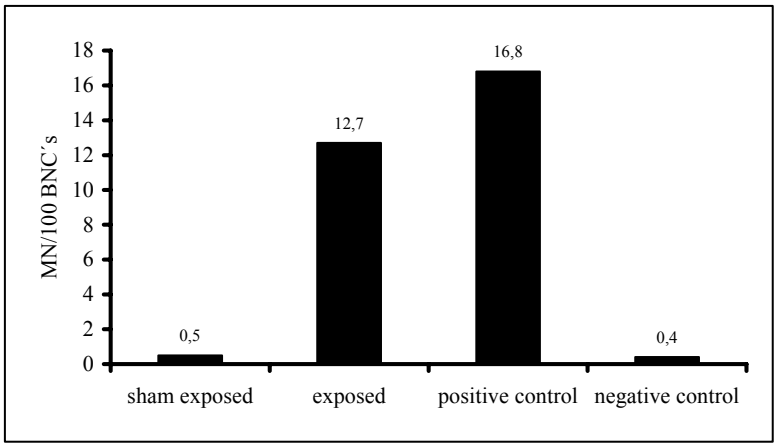

Figure 95. Micronucleus frequencies of RF-EMF exposed (GSM basic 1950 MHz, 15h, 2 W/kg) cultured human fibroblasts and control cells. Bleomycin-treated cell were used as a positive control.

Results on the influence of RF-EMF on the mitochondrial membrane potential were inconsistent.

Evaluating changes in the mitochondrial membrane potential after RF-EMF exposure (GSM basic 1950 MHz, 1 W/kg, 5 min on/10 min off, 15h) using JC-1, revealed a significant decrease in the mitochondrial membrane potential in one experiment, which could not be reproduced..

3.2.1.3 Mouse embryonic stem cells (Participant 4)

RF-EMF affected double-strand DNA break induction in ES cell derived neural progenitors immediately after exposure.

We studied the possible effects of RF-EMF on the integrity of DNA strands in differentiating ES cell from EB outgrowths. Two schemes were applied: (1) For RF-EMF exposure (GSM signal 217-Hz, 1.71 GHz, 1.5 W/kg, intermittency 5 min on/30 min off, 6h), the percentage of primary DNA damage was measured in the alkaline and neutral Comet assay immediately after the RF-EMF exposure at the stage of neural differentiation (4+4d - 4+6d) and 18 hours after the RF-EMF exposure. No differences in the induction of single-strand breaks as measured by the alkaline Comet assay were observed 0 and 18 hours after exposure. The tailfactor was slightly, but significantly increased in the neutral Comet assay immediately after exposure ($p<0.05$) (Table 26). In the second set of experiments, the same RF-EMF exposure conditions were applied for 48 hours instead of 6 hours, and the alkaline Comet assay was done immediately after exposure, while the neutral Comet assay was done 24 or 48 hours post exposure. However, no significant differences were observed in the induction of single- or-double DNA strand breaks between sham-exposed or EMF exposed neural progenitors after prolonged exposure (48h).

3.2.1.4 Summary (Participant 1)

Our data indicate a genotoxic action of RF-EMF in various cell systems. This conclusion is based on the following findings:

- RF-EMF exposure was able to induce DNA single and double strand breaks as well as an increase in micronuclei in HL-60 cells (3.2.1.1).
- The DNA damage generated by RF-EMF in HL-60 cells was dependent on the time of exposure, the field strength and the type of RF-EMF signals (3.2.1.1).
- The DNA damage in HL-60 cells probably resulted from an increase in free oxygen radicals induced during RF-EMF exposure (3.2.1.1).
- RF-EMF exposure at a SAR value between 0,3 and 2,0 W/kg produced DNA single and double strand breaks in human fibroblasts and in granulosa cells of rats dependent on the exposure time and the type of signals (3.2.1.2).

- RF-EMF exposure at a SAR value of 2 W/kg caused an increase in chromosomal aberrations in human fibroblasts demonstrating that the DNA repair was not error-free (3.2.1.2).
- RF-EMF exposure at a SAR value of 1,5 W/kg caused a slight, but significant increase in DNA double strand breaks in neural progenitor cells stemming from mouse embryonic stem cells (3.2.1.3).

3.2.2 Cell proliferation and cell differentiation

3.2.2.1 Human neuroblastoma cell line NB69 and neural stem cells (NSC) (Participant 5)

RF-EMF did not affect growth or viability of NB69 neuroblastoma cells and neural stem cells (NSC).

NB69 cells were exposed at day 3 postplating to GSM-Basic over a 24-hour period. After exposure, the cells were left to grow in the absence of field for an additional 24 hour lapse (5 days postplating). The field exposure was applied alone or in combination with bFGF. As it is shown in Figure 96, the GSM-Basic signal alone did not affect significantly cell growth or cell viability. The morphological analysis did not show significant differences between exposed and control groups, either (data not shown). The treatment with bFGF alone induces differentiation in NB69 cells, which exhibit significant increases in the number and the extension of processes per cell and in the cell size (see 3.2.4.2). An equivalent response was obtained after exposure to the combined treatment with bFGF plus GSM-Basic.

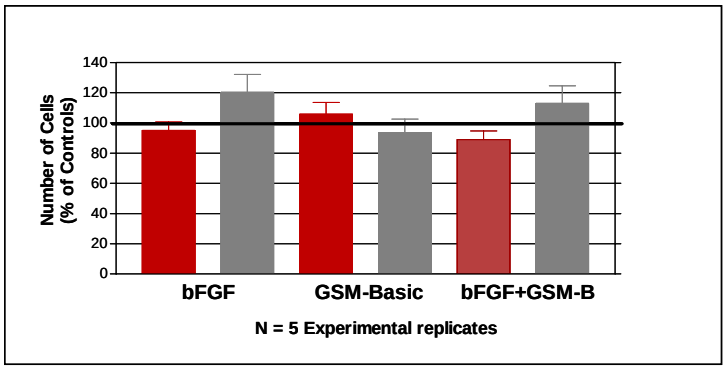

Figure 96. Number of living (red) and dead (grey) cells after a 24-h exposure to GSM-Basic signal followed by 24 additional hours of incubation in the absence of the RF-EMF. No significant changes were observed in the exposed samples when compared to the respective controls

NS cells were exposed at day 2 postplating to GSM-Basic over a 24-hour period. After exposure, the cells were left to grow in the absence of field for an additional 48-hour lapse (5 days postplating). At the end of this period, the samples were studied for cell growth and/or cell viability. The treatment did not affect cell growth (Figure 97A) and did not induce significant changes in the cells' morphology (data not shown). However, the cell size in the exposed samples was observed to be slightly, but not significantly augmented when compared to the respective controls (Figure 97B; image analysis of 60 microscope fields per condition of a total of 4 experimental replicates). The observed, slight reductions in the percent of dead cells, and in the increase of the cells' size after exposure to the GSM-Basic signal (Figure 97) could be due to an enhancement of the cell attachment to the substrate in the exposed samples. Such an attachment was microscope observed, though not image-analysis quantified (data not shown).

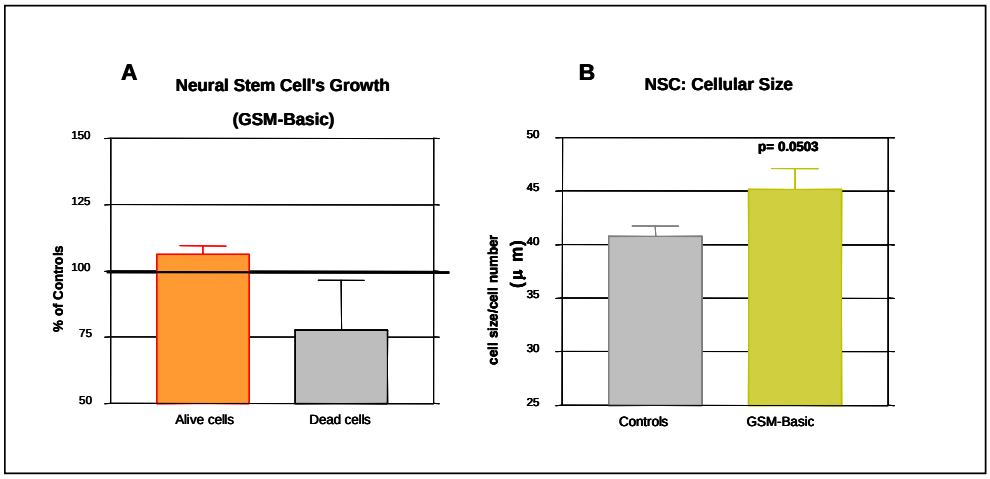

Figure 97. (A) Number of living and dead cells after a 21-h exposure to GSM-Basic signal followed by 48 additional hours of incubation in the absence of RF-EMF (5 days postplating). No significant changes were observed, even though a small reduction of dead cells occurs in the exposed samples. (B) The cell size in the exposed samples was observed to be slightly, but not significantly augmented when compared to the respective controls.

RF-EMF may affect the expression of FGF receptors in NB69 human neuroblastoma cells and in neural stem, potentially influencing cellular differentiation.

See 3.2.4.2

RF-EMF affected the differentiation of neural stem cells (NSC), but not of neuroblastoma cells (NB69).

The aim of the study was to determine whether the exposure of neural stem cells (NSC) to GSM-1800 signals (GSM-Basic signal, 21-hours, 5 min on/10 min off) can influence the evolution of the phenotypic differentiation at the middle term (6 additional days after exposure). As described in the methodology, the cells were exposed to RF-EMF at day 2 postplating. After the 21-hour exposure, the cells were grown for 6 additional days in the absence of the GSM stimulus. At the end of this period, the cells were immunostained with O1 for mature oligodendrocyte identification, GFAP for astrocytes and ß-tubulin III for neurons. All experiments and analysis were conducted following blind protocols. The data (N= 5 experimental replicates) indicate that the GSM-Basic signal promotes marked morphological changes in differentiating oligodendrocytes and astrocytes derived from NSC (Figure 98).

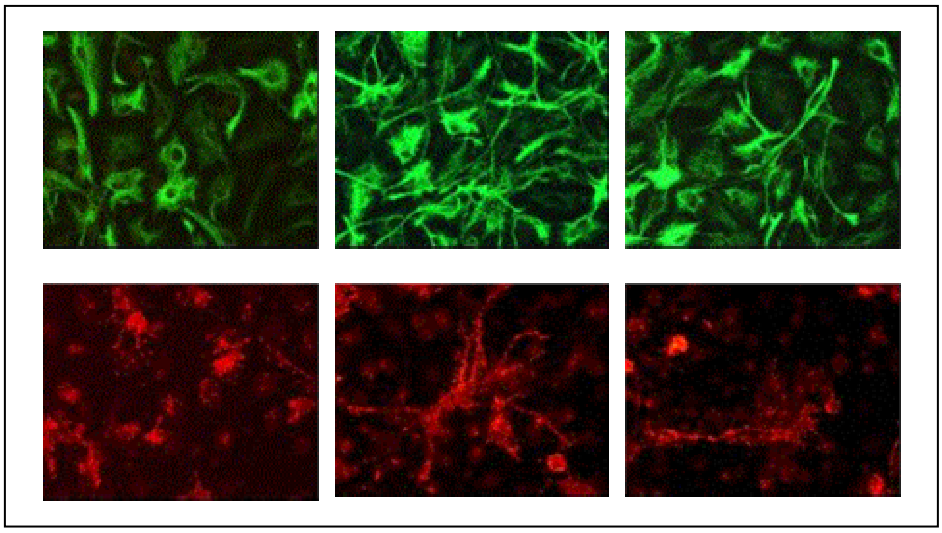

Figure 98. Photomicrographs of neural stem cells progeny. Astrocytes labelled with GFAP (green) and oligodendrocytes labelled with O1 (red) immunostaining: A, Control; B, and C, exposed to the GSM-Basic signal. The exposure increases cell extension in astrocytes and oligodendrocytes.

Similar experiments have been carried out to evaluate the phenotypic differentiation of NB69 cells treated with the above GSM-signal and exposure conditions, in the presence or absence of RA. As described in the methodology, the cells were exposed to the field at day 3 postplating, during a 24-hour period, and then grown for 2 additional days in the absence of GSM exposure. After that, the cells were analysed for expression of mature neuronal cell marker ß-tubulin III, and for tyrosine hydroxylase (TH) marker. Exogenous, basic fibroblast growth factor was used as a positive control. The data show that the neuronal outgrowth of NB69 cells (Figure 99) and the percent of TH+ cells seem not to be altered by the exposure to the GSM-Basic signal. Only the treatment with bFGF promoted the neuronal microtubules network in these cells.

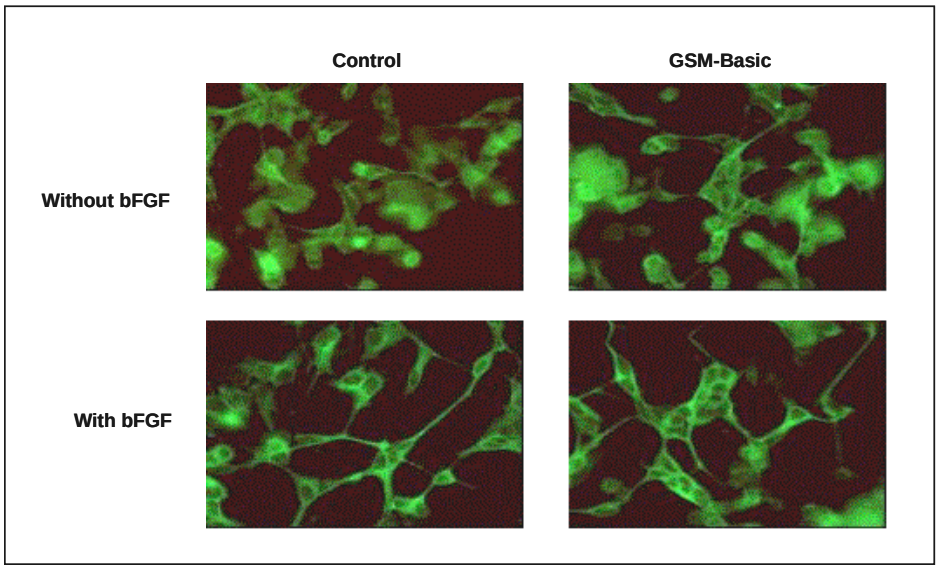

Figure 99. Photomicrographs of NB69 cells analysed 3 days after the exposure and/or incubation in the presence or absence of bFGF. Cells stained with anti-beta-tubulin antibody. The neuronal outgrowth of NB69 cells seems not to be altered by the exposure to the GSM-Basic signal. However, the treatment with bFGF promotes the neuronal microtubules network in these cells.

3.2.2.2 Human lymphocytes and thymocytes (Participant 8)

RF-EMF did not affect proliferation, cell cycle and activation of human lymphocytes.

The experiments with RF-EMF were performed at SAR 1,4-2,0 W/kg using different RF modulations or time exposure. Studies on cell proliferation were performed discriminating CD4+CD28+/- and CD8+CD28+/-lymphocytes subpopulation. Cells were exposed to Talk modulated RF-EMF (2 W/kg) and two intermittent types of exposure were applied: 1) 10 min on/20 min off for 44 hours; 2) 2 hours on/22 hours off for 72 hours. We performed experiments with cells from 6 donors using the former approach, from 11 donors using the latter approach. All cells were acquired and analysed after 72 hours and 120 hours of culture. A small increase (3%) of proliferating CD8+CD28+ T lymphocytes was observed in exposed cells both at 72 hours and 120 hours of culture. Since the differences observed are similar to the calculated standard error, we considered this effects not relevant. In Tables 22 and 23 data related to proliferating and not proliferating cells subsets after 72 hours and 120 hours of culture, respectively, are reported.

Table 22. T lymphocytes subsets exposed to talk modulated RF-EMF 2 hours on/22hours off for 72 hours. Data are reported as mean (% ± s.e.) of all experiments performed

Lymphocyte subsets	Sham % ± se	RF % ± se	p
P CD4+CD28+	30.7 ± 2	28.2 ± 2	ns
P CD4+CD28-	0.9 ± 0.4	0.7 ± 0.3	ns
NP CD4+CD28+	13.0 ± 2	12.4 ± 2	ns
NP CD4+CD28-	1.8 ± 0.9	0.8 ± 0.3	ns
P CD8+CD28+	19 ± 2	21 ± 2	0.042
P CD8+CD28-	7.9 ± 3	7.7 ± 3	ns
NP CD8+CD28+	8.0 ± 1	9.3 ±1	ns
NP CD8+CD28-	1.1 ± 0.2	1.0 ± 0.4	ns

P = proliferating; NP = non proliferating; ns = not significant

Table 23. T lymphocytes subsets exposed to Talk modulated RF-EMF 2 hours on/22 hours off for 72 hours and analysed at 120 hours of culture. Data are reported as mean (% ± s.e.) of all experiments performed

Lymphocyte subsets	Sham % ± se	RF % ± se	p
P CD4+CD28+	61.0 ± 2	62.1 ± 2	ns
P CD4+CD28-	0.60 ± 0.07	0.80 ± 0.11	ns
NP CD4+CD28+	9.3 ± 0.2	8.7 ± 0.2	ns
NP CD4+CD28-	1.4 ± 0.1	1.72 ± 0.11	ns
P CD8+CD28+	32 ± 4	35 ± 4	0.048
P CD8+CD28-	5.4 ± 3	4.3 ± 2	ns
NP CD8+CD28+	5.4 ± 0.7	4.7 ± 0.9	ns
NP CD8+CD28-	0.9 ± 0.3	0.8 ± 0.3	ns

P = proliferating; NP = non proliferating; ns = not significant

Cell cycle analysis was performed in PBMCs exposed at three RF-EMF modulations and in the case of Talk signal also PBMCs from old donors were analysed. In all the cases observed no differences were found between exposure and control cells. Some slight differences (1-2%, sometimes increase and sometimes decrease) were observed when analysis of activation markers on CD4+ and CD8+ T lymphocytes were performed on both young and old donors. Since the effects were really small, we

performed from 5 up to 8 replications of T lymphocyte phenotypical analysis, using cells from the same donor.

Results obtained from replications did not confirm the data previously obtained, thus suggesting that such small significant effects must be considered at the noise level of the statistical analysis. Moreover, we performed a more sophisticated analysis on fluorescence intensity in order to verify if the number of molecular markers could be changed in RF exposed cells in comparison with sham exposed cells. We found that in T helper lymphocytes from elderly, but not from young donors, and exposed to Talk modulated RF-EMF, CD95 molecules shifted significantly their fluorescence from bright to dim, as reported in Figure 96. This effect means that in the exposed cells the number of molecular markers on membrane surface was slightly decreased (around 9%).

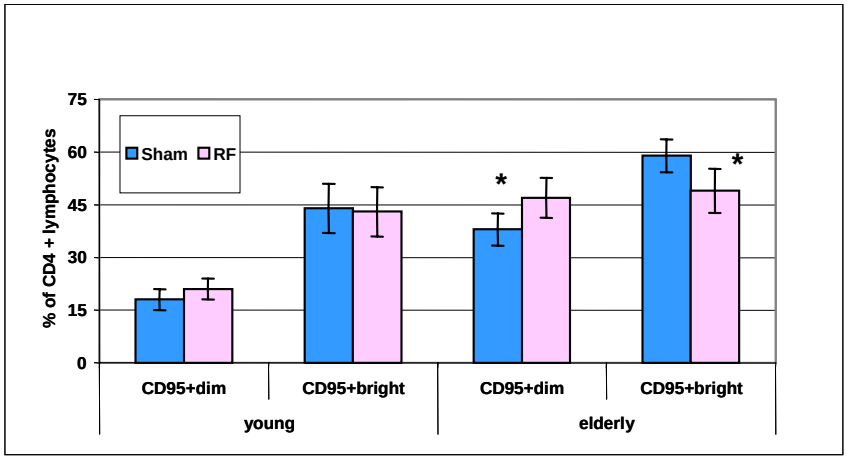

Figure 100. Analysis of fluorescence brightness of proliferating CD4+CD95+ from 10 young and 8 elderly donors, after sham and talk modulated RF-EMF exposure (2W/kg). * = $p < 0.05$. Data are represented as mean ± s.e.

RF-EMF (DTX) may inhibit the production of IL-1beta in human lymphocytes, but did not affect the production of IL 6.

The results obtained showed no significant differences between cells sham-exposed or differently modulated RF-EMF exposed, except in the case of IL-1beta. Indeed, we found a decrease of IL-1beta production (around 13%) in CD3-stimulated PBMCs exposed to DTX modulated RF-EMF in comparison with sham-exposed cells. As demonstrated in Figure 101, the decrease observed was statistically significant on 6 experiments performed. This result was not found when PBMCs were exposed to Talk modulated RF-EMF or using the other stimulus.

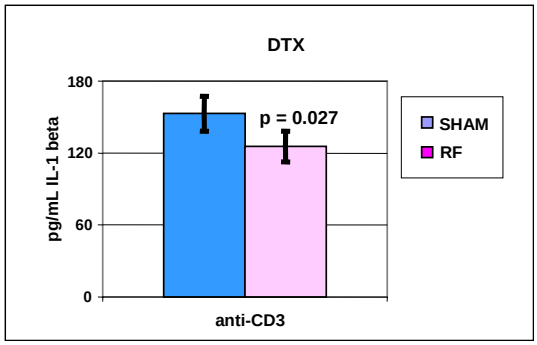

Figure 101. Effect of DTX modulated RF (SAR 1.4 W/kg) on IL-1 beta production in CD3-stimulated PBMCs.

RF-EMF did not affect thymocyte differentiation.

HTOC were performed in order to assess *in vitro* phenotypical differentiation and apoptotic phenomena due to negative selection, which usually occurs in vivo inside the thymus. Thus, different subsets of thymocytes were analysed such as CD71+CD4-CD8-, CD3-/+CD4+CD8+, abTCR-/+CD4+CD8+, gdTCR-/+CD4-CD8-, CD3+CD4+CD8-, CD3+CD4CD8+, abTCR+CD4+CD8-, abTCR+ CD4-CD8+ cells. Each population represents a different phase of development, which was monitored before the exposure and at the end of culture, in presence or absence of RF-EMF. Thymocyte apoptosis was assessed with two different methods, in the same conditions, but the data obtained from 6 human thymus on thymocyte differentiation and apoptosis did not suggest positive results on both the endpoints. Actually, a small increase (4%) of double positive thymocytes (CD4+CD8+) was found in RF-EMF-exposed cultures in comparison with sham-exposed tissue fragments. Also in this case the effect is of the order of the standard error thus we consider these results irrelevant.

3.2.2.3 Human promyelocytic cell line HL-60 (Participant 2)

RF-EMF did not affect the cell cycle of HL-60 cells as shown by flow cytometric analysis.

See 3.2.1.1

RF-EMF did not affect the growth behaviour of HL-60 cells with respect to growth velocity and DNA synthesis.

See 3.2.1.1

Indicators for HL-60 cell growth were the proliferation rate, reflected by the cellular doubling time, and the synthesis of the enzyme thymidine kinase (TK). The enzyme thymidine kinase plays an important role in DNA synthesis. It has been well established that the cellular activity of thymidine kinase is correlated with the growth rate of cells (Johnson et al. 1982). Its relation to the cell cycle has been shown in previous studies (Chang 1990; Kit 1976; Pelka-Fleischer et al. 1987; Piper et al. 1980).

Cellular doubling time

Cellular growth behaviour with respect to growth velocity was assessed by determination of the cellular doubling time. Cellular doubling time of HL-60 cells following RF-field exposure (1800 MHz, 24h) for different SARs (continuous wave, 0.2, 1.0, 1.3, 1.6, 2.0 and 3.0 W/kg) and different signal modulations (continuous wave, C.W., 5 min on/10 min off, GSM-217Hz, GSM-Talk) was compared to controls and sham-exposure. No alteration of the cellular doubling time was observed for any of the different SARs or signal modulations tested (Figures 101, 102). The value of the doubling time for the control was 20.8 ± 2.8 h. Calculation of the average HL-60 doubling time after exposure to all SAR levels tested revealed a value of 22.0 ± 3.8 h (n=21) versus that for all sham-exposed cells: 21.6 ± 4.5 hours (n=21). On the other hand the calculation of the average HL-60 doubling time after exposure to all signal modulations tested at SAR = 1.3 W/kg revealed a value of 21.3 ± 4.2 h (n=14) versus that for all sham-exposed cells: 21.7 ± 4.5 h (n=14).

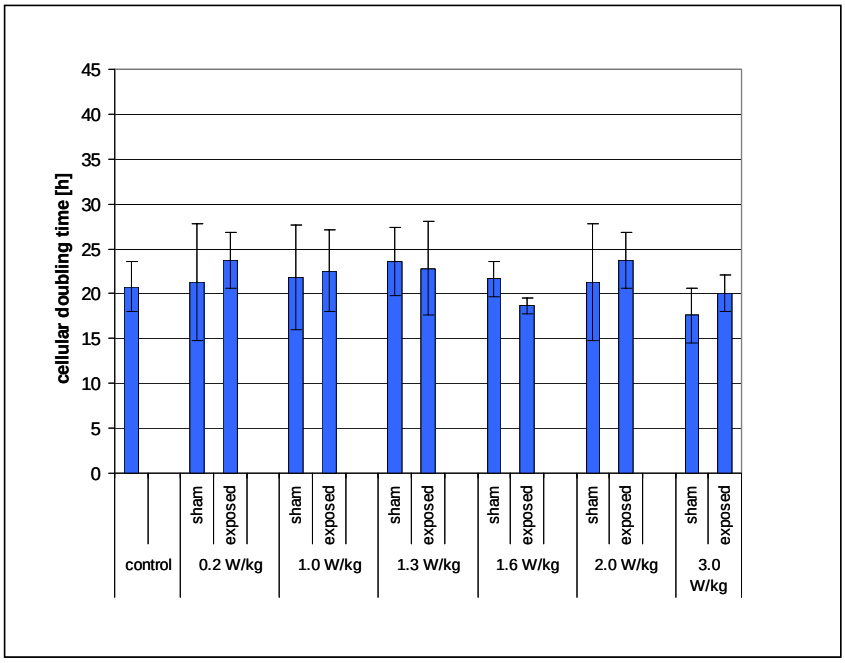

Figure 102. Effect of RF-field exposure (1800 MHz, continuous wave, SAR 0.2, 1.0, 1.3, 1.6, 2.0 and 3.0 W/kg, 24h) on HL-60 cell growth with respect to growth velocity compared to control and sham-exposure, determined by the cellular doubling time. Each bar represents the mean ± SD of results obtained in at least three independent experiments, except for control (n=6) and SAR 1.3 W/kg (n=6).

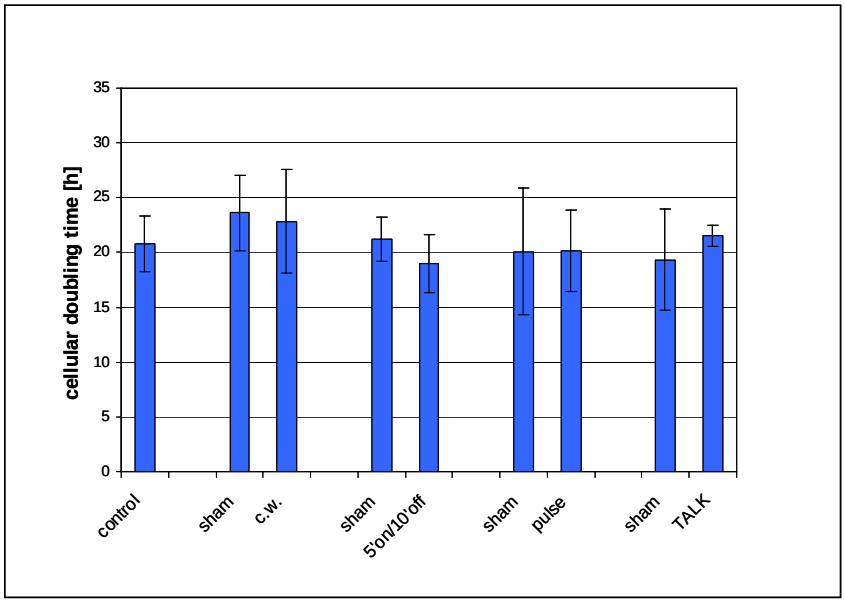

Figure 103. Effect of RF-field exposure (1800 MHz, different signal modulations, SAR 1.3 W/kg, 24h) on HL-60 cell growth with respect to growth velocity compared to control and sham-exposure, determined by the cellular doubling time. Each bar represents the mean ± SD of results obtained in at least three independent experiments, except for control (n=6), continuous wave (n=6) and GSM-Talk (n=2).

Thymidine kinase (TK) activity

Intracellular thymidine kinase (TK) activities were determined by radioenzyme assay with ^{125}I-deoxyuridine monophosphate as substrate (Prolifigen® TK-REA, AB Sangtec Medical, Bromma, Sweden). The level of radioactivity is directly proportional to the enzyme activity, the TK value is calculated from the standard curve and expressed as U/l.

TK activities of HL-60 cells following RF-field exposure (1800 MHz, continuous wave, 1.3 W/kg, 24 h) was compared to control and sham-exposure. Table 24 represent levels of thymidine kinase activities for two independent experiments. No changes in intracellular TK activities were found in HL-60 cells following RF-field exposure compared to control and sham-exposure. In summary, the growth behaviour of HL-60 cells with respect to growth velocity and DNA synthesis are not altered by RF-EMF exposure compared to control and sham-exposure using the assays described above.

Table 24. Thymidine kinase (TK) activity in HL-60 cells after exposure to RF-field (1800 MHz, continuous wave, 1.3 W/kg, 24h), compared to control and sham-exposed cells

Group	thymidine kinase activity [U/l]	
	exp. 1	exp. 2
control	121.4	126.8
sham	151.1	116.3
RF-field	121.9	118.4

3.2.2.4 Mouse embryonic stem cells (Participant 4)

RF-EMF did not induce cardiac differentiation of R1 ES cells and cardiac differentiation and proliferation of P19 EC cells, but may affect the bcl-2 mediated apoptotic pathway in ES-cell derived neural progenitors and neuronal differentiation by inhibiting nurr-1 and TH transcription.

See 3.2.4.1

3.2.2.5 Summary (Participant 1)

Our data did not reveal a significant effect of RF-EMF on proliferation and differentiation of various cell systems such as neuroblastoma cells (NB69) (see 3.2.2.1), R1-embryonic stem cells and embryonic cancer cells (P19) (3.2.2.4 and 3.2.4.1), human lymphocytes and human thymocytes (3.2.2.2) and HL-60 cells (3.2.2.3), though some effects on the differentiation process in neural stem cells were observed (see 3.2.2.1). These effects may be of indirect nature possibly through modulation of the expression of various genes and proteins. With respect to neural stem cells, RF-EMF may affect proliferation and differentiation via up-regulation of bcl-2 which mediates the apoptotic pathway and via inhibiting nurr-1 and TH transcription (see 3.2.2.4 and 3.2.4.1)

3.2.3 Apoptosis

3.2.3.1 Brain cells of different origin and human monocytes (Participant 9)

RF-EMF did not affect apoptosis in neuronal cells.

Spontaneous apoptosis was found higher in sensitive primary nerve cells than in the human neuroblastoma cell line SH-SY5Y) (around 20% versus 10% using the $DiOC_6$ dye). A high percentage of spontaneous apoptosis in granule cells was found using Annexin V staining compared to $DiOC_6$ staining. This observed difference seems to be cell type-dependent and it appeared difficult, in this case, to

correlate information given by these two dyes. Besides this technical consideration, exposure of primary granule cells to GSM-900 at 2.0 W/kg for one hour did not induce apoptosis as shown by the time-kinetics up to 24 hours after exposure (Figure 104). The same observation was made with the SH-SY5Y cell line. To test longer time exposure, we decided to expose granule cells and SH-SY5Y to GSM-900 during 24 hours and to quantify apoptosis at the end of exposure. In these exposure conditions, no significant difference was observed between sham and exposed cells in both cases (Figure 105).

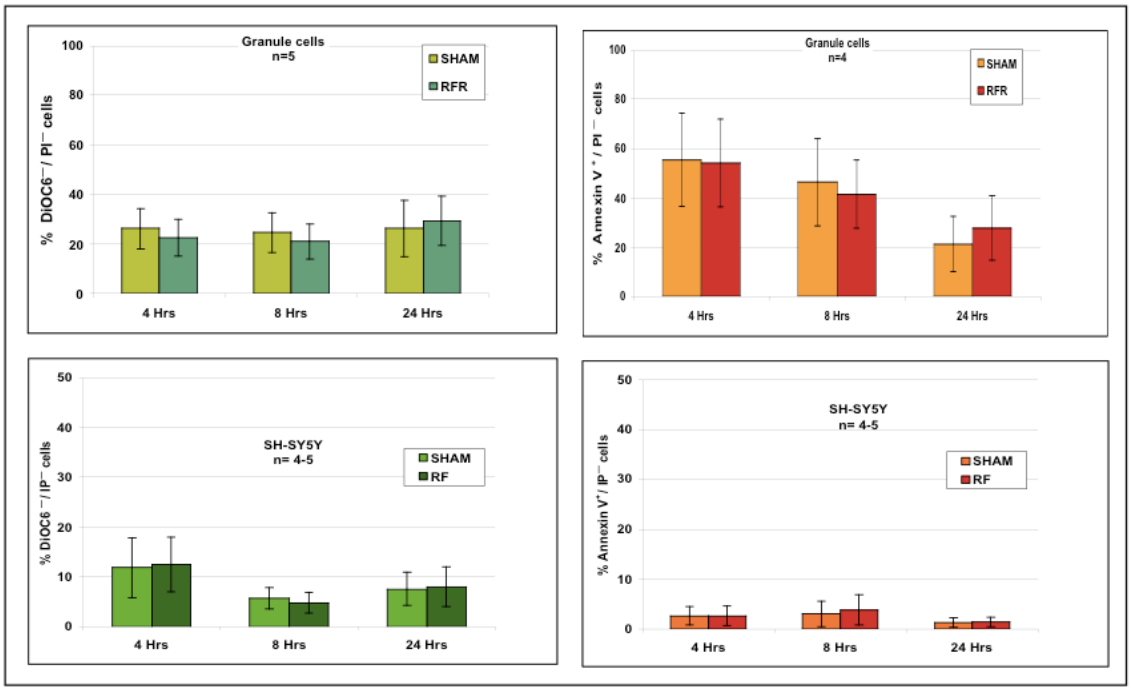

Figure 104. Effect of a one-hour exposure to GSM-900 on apoptosis in nerve cells. Results are expressed as the percentage of cells with depolarised mitochondrial transmembrane potential ($DIOC6^-/PI^-$, left panel) and apoptotic cells (ANX^+/PI^-, right panel) after exposure of primary granule cells (upper panels) and human neuronal cells (lower panels) to frame GSM-900 signal at 2.0 W/kg for 1 hour. Apoptosis was measured 4, 8 and 24 hours after the exposure began. Data are presented as the mean ± SEM of 4 to 5 independent and blind experiments.

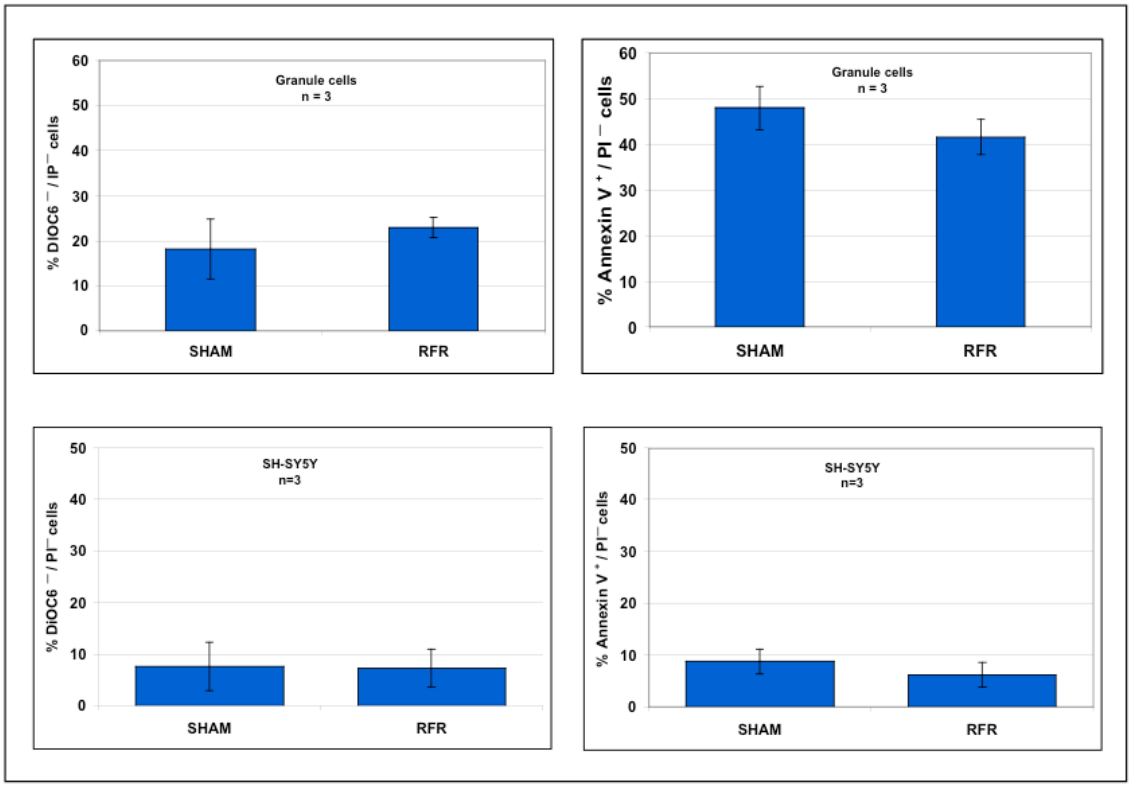

Figure 105. Effect of a 24-hour exposure to GSM-900 on apoptosis in nerve cells. Results are expressed as the percentage of cells with depolarised mitochondrial transmembrane potential ($DIOC6^-/PI^-$, left panel) and apoptotic cells (ANX^+/PI^{--}, right panel) after exposure of rat primary neurons (upper panels) and human SH-SY5Y neuroblastoma cells (lower panels) to frame GSM-900 signal at 2.0 W/kg for 24 hours. Apoptosis was measured immediately after exposure. Mean ± SEM of 3 independent, blinded experiments are presented.

We conclude from our results that granule cells and SH-SY5Y cells are not sensitive to GSM-900 exposure for up to 24 hours.

RF-EMF did not affect apoptosis in astrocytic cells.

Primary cultures of astrocytes and human U87 glioblastoma cells were sham-exposed or exposed to GSM-900 for one hour at 2.0 W/kg and apoptosis was followed up during 24 hours in the conditions described previously. Figure 105 shows the data obtained using the primary culture and the U87 cell line. In the two cell types, no difference in the number of cells with depolarised mitochondrial potential or in AnnexinV-positive cells could be evidenced after exposure to GSM-900. An increase in apoptotic astrocytic cell population measured with $DiOC_6$ was noticed, correlated to the time spent in culture. Nevertheless, no significant difference was observed between sham- and GSM-900 exposed cells. In the exposure conditions tested, no demonstration of a significant effect of GSM-900 signal on primary astrocytes or glioblastoma U87 cells could be made.

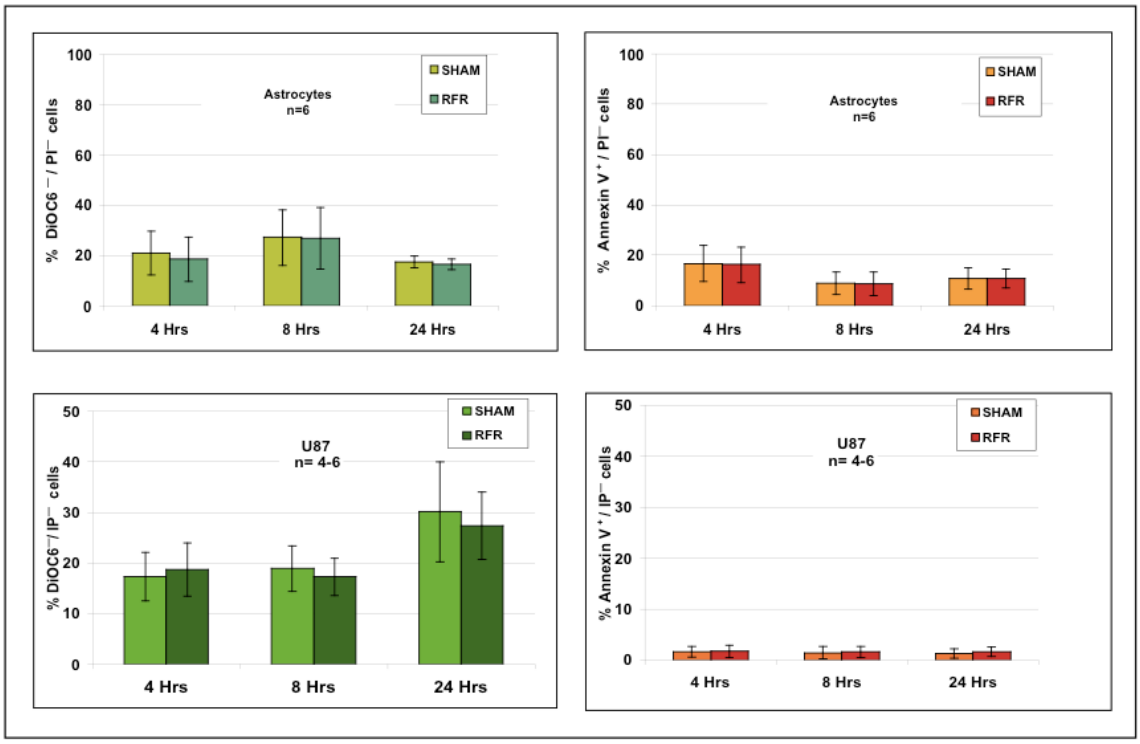

Figure 106. Effect of a 1-hour exposure to GSM-900 on apoptosis in astrocytic cells. Results are expressed as the percentage of cells with depolarised mitochondrial transmembrane potential ($DIOC6^-/PI^-$, left panel) and apoptotic cells (ANX^+/PI^-, right panel) after exposure of primary astrocytes (upper panels) and human astrocytic cells (lower panels) to GSM-900 signal at 2.0 W/kg for 1 hour. Apoptosis was measured 4, 8 and 24 hours after the exposure began. Data from 4 to 6 independent experiments are presented as the Mean ± SEM.

In summary, an immediate or delayed effect of RF-EMF on apoptosis in rat primary cells and human cell lines could not be demonstrated.

RF-EMF did not influence apoptosis in immune cells.

The ability of the human U937 promyeloma cells to undergo apoptosis was tested by using camptothecin as a positive control (Figure 107). We show a significant 4- to 8-fold increase ($p<0.01$), depending of the marker of apoptosis used, in U937 cells treated for 4 hours with CPT (4 µg/ml).

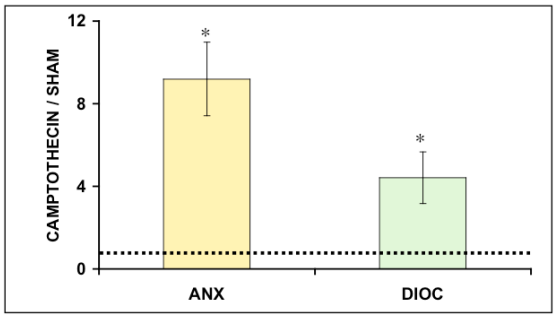

Figure 107. Effect of camptothecin treatment on apoptosis in human U937 cells. The results are expressed as the ratio of apoptotic cells (ANX^+/PI^-, left panel) and cells with depolarised mitochondrial transmembrane potential ($DIOC^-/PI^-$, right panel) in camptothecin-treated versus sham-exposed U937 promyeloma cells. U937 cells were sham-exposed for 1 hour and then treated for 4-hours with camptothecin (4 µg/ml). Data are presented as the mean ± SEM of 5 independent experiments. *=$p<0.01$

Sham-sham experiments (n=3-4) showed that inter-incubator (incubator used for RFR exposure versus incubator used for sham-exposure) variation of U937 apoptotic cells was around 1.1 ± 0.5 after one hour and 1.2 ± 0.6 when the cells were placed back in a control incubator for 4 hours after the one hour spent in the dedicated incubators (Figure 108). The effect of CPT treatment was very similar when the samples were put for one hour in either dedicated incubator. We therefore concluded that both dedicated incubators were equivalent within a range of 50% of ratio variation and that an at least two-fold increase in apoptosis in RFR-exposed cells could be considered as significant.

No statistically significant influence of GSM-900 could be evidenced on spontaneous apoptosis of U937 cells (Figure 109), when they were exposed for one hour at a SAR of 0.7 W/kg and even at the highest SAR tested (2.0 W/kg). No difference could be detected either immediately after exposure or after a 4-hour resting period in a control incubator. Hence, no delayed effect of GSM-900 on apoptosis could be evidenced. A longer exposure duration, i.e. 48 hours, to GSM-900 at the lowest SAR tested (0.7 W/kg) was also not able to alter spontaneous apoptosis in the human cell line.

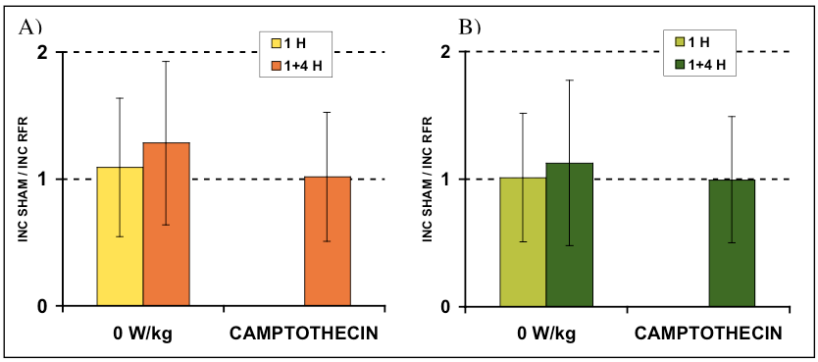

Figure 108. Comparison of occurrence of apoptosis in U937 cells in both dedicated incubators. Results are expressed as the ratio between apoptotic U937 cells in the incubator used for RFR exposure and apoptotic U937 cells in incubator used for sham-exposure. Sham-sham exposure lasted 1 hour and cells were harvested either immediately (1 H) or after an additional 4-hour resting period or campthotecin treatment (1+4 H). A) apoptotic U937 cells (ANX^+/PI^-) and B) U937 cells with depolarised mitochondrial transmembrane potential ($DIOC6^-/PI^-$). Data are presented as the mean ± SEM of 3 to 4 independent experiments.

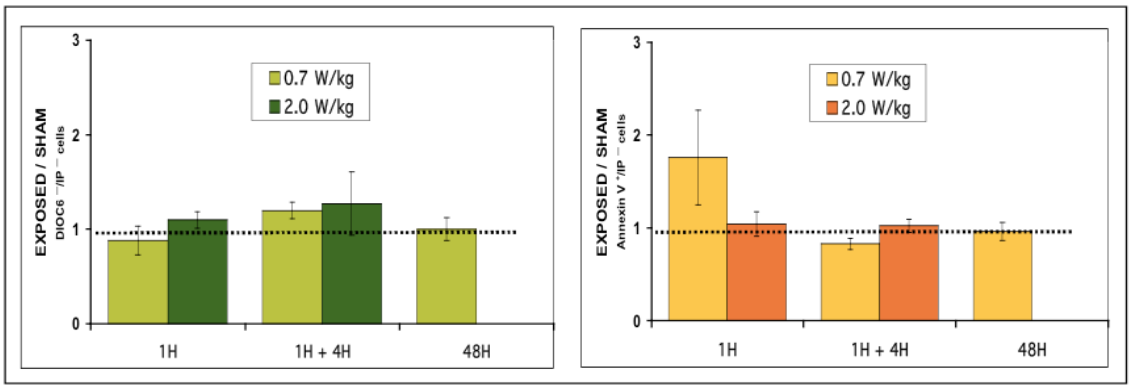

Figure 109. Effect of GSM-900 exposure on apoptosis in human U937 cells. Results are expressed as the ratio of cells with depolarised mitochondrial transmembrane potential ($DIOC6^-/PI^-$, left panel) and apoptotic cells (ANX^+/PI^-, right panel) in GSM-900- versus Sham-exposed U937 cells. U937 cells were exposed to GSM-900 at 0.7 W/kg (n=7) and 2.0 W/kg (n=6) for 1 hour, for 1 hour followed by a 4-hour resting period or for 48 hours. Data are presented as the mean ± SEM.

RF-EMF did not influence chemically-induced apoptosis in immune cells.

When possible interaction between RFR and camptothecin was tested, we show that a one-hour treatment with GSM-900 at either 0 .7 or 2.0 W/kg was not able to influence camptothecin-induced apoptosis (Figure 110).

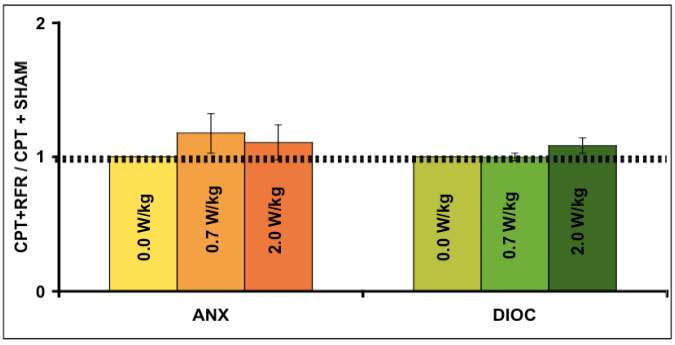

Figure 110. Effect of GSM-900 exposure on camptothecin (CPT)-induced apoptosis. The results are expressed as the ratio of apoptotic cells (ANX $^{+}$/PI $^{-}$, left panel) and cells with depolarised mitochondrial transmembrane potential (DIOC6 $^{-}$/PI $^{-}$, right panel) in GSM-900 plus camptothecin-treated versus GSM-exposed U937 promyeloma cells. U937 cells were sham-exposed or exposure to GSM-900 for 1 hour and then treated for 4-hour with camptothecin (4 µg/ml). The SAR level was 0.7 W/kg (n=7) or 2.0 W/kg (n=6). Data are presented as the mean ± SEM.

In summary, we showed no evidence for an immediate, cumulative or delayed effect of RF-EMF on apoptosis in a human monocytic cell line. We conclude from our results that U937 cells are not sensitive to GSM-900 exposure for up to 48 hours. Taken together, our results strongly suggest that the apoptotic process is not a major biological target for GSM mobile telephony-related signals.

3.2.3.2 Human lymphocytes (Participant 8)

RF-EMF did not affect apoptosis in human lymphocytes.

Negative results were obtained studying spontaneous or dRib-induced apoptosis, when PBMCs were exposed at all the three signal modulations. Moreover, PBMCs from old donors were exposed to Talk modulated RF, but also in this case no effects on spontaneous or oxidative stress-induced apoptosis were found. These results were also confirmed by mitochondrial membrane polarisation, since no differences were noticed in dependence of the exposure and age of donor.

RF-EMF did not increase the Hsp70 level in human lymphocytes after induction of apoptosis.

dRib induces an increase of hsp70 in treated cells in comparison with untreated cells already detectable after 3h of treatment (unpublished data) up to 44 hours of treatment. When we studied RF-EMF effects (1800 MHz, GSM talk signal, 2 W/kg), we did not found any alteration of hsp70 gene product, after 44 hours of intermittent exposure, in PBMCs from 7 young donors, as showed in Figure 111. In this figure it is possible to notice the significant difference between the level of hsp70 in untreated cells versus the dRib-treated cells. Additional analysis were performed in separated lymphocytes and monocytes, but no differences were found between RF-exposed and sham-exposed cell populations.

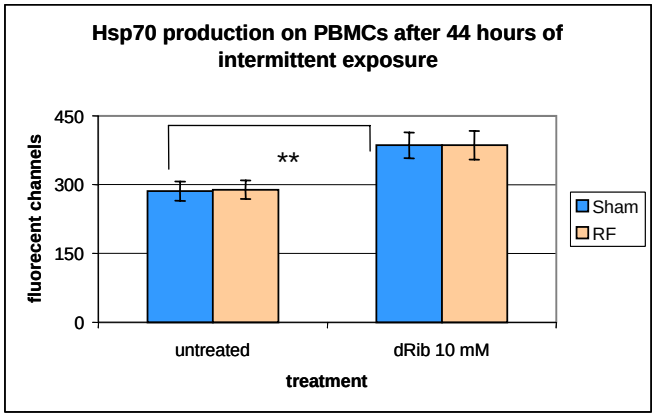

Figure 111. Hsp70 production in untreated and dRib treated PBMCs after 44hours of intermittent exposure. PBMCs were obtained from 7 donors and data are represented as mean of fluorescent channels ± s.e. ** = p< 0.01, untreated PBMCs versus dRib treated PBMCs.

RF-EMF did not affect apoptosis in thymocytes.

Thymocyte apoptosis was assessed with two different methods, in the same conditions, but the data obtained from 6 human thymus on thymocyte apoptosis did not suggest positive results on both the endpoints. Actually, a small increase (4%) of double positive thymocytes (CD4+CD8+) was found in RF-EMF-exposed cultures in comparison with sham-exposed tissue fragments. Also in this case the effect is of the order of the standard error thus we consider these results irrelevant.

3.2.3.3 Human promyelocytic cell line HL-60 (Participant 2)

RF-EMF did not affect apoptosis in HL-60 cells as shown by flow cytometric analysis and the Annexin V and TUNEL assay.

See 3.2.1.1

3.2.3.4 Embryonic stem cells of mice (Participant 4)

RF-EMF exposure may influence the bcl-2 mediated apoptotic pathway in ES-cell derived neural progenitors.

See 3.2.4.1

3.2.3.5 Human endothelian cell lines (Participant 6)

The RF-EMF-induced enhancement of hsp27 phosphorylation as well as the concomitantly RF-EMF-induced down-regulation of proteins of Fas/TNFα suggest that the anti-apoptotic pathway in RF-EMF exposed cell systems may be modified.

See 3.2.4.6

3.2.3.6 Summary (Participant 1)

Our data did not reveal a significant effect of RF-EMF on apoptosis in various cell systems such as brain cells and human monocytes (see 3.2.3.1), human lymphocytes and thymocytes (see 3.2.3.2), human endothelial cells (3.2.4.6) and HL-60 cells (see 3.2.3.3). On the other hand, an indirect effect on apoptosis through modulating the expression of various genes and proteins cannot be excluded at present. Up-

regulation of bcl-2 in differentiating embryonic stem cells (see 3.2.3.4 and 3.2.4.1) and of hsp27 in endothelial cells (see 3.2.4.6) both of which may affect the apoptotic process support such an assumption.

3.2.4 Gene and protein expression

3.2.4.1 Mouse embryonic stem cells (Participant 4)

Loss of p53 function rendered pluripotent ES cells sensitive to RF-EMF after prolonged exposure.

Exposure of undifferentiated cells to GSM-217 signals for 6 hours (Table 25) did not evoke any short-term modification of gene expression patterns neither in wt nor in p53-/- ES cells (Figure 112A). On the other hand, long-term (48 hours) GSM-217 exposure of p53-/- cells during EB development resulted in the up-regulation of transcript levels of 4 out of 6 analysed genes. Whereas c-jun, p21 and c-myc mRNA levels were only transiently up-regulated at early stages (days 2, 5 and 5+2 of EB differentiation, Figure 112B, a prominent induction of hsp70 levels in p53-/- cells was observed throughout the differentiation period. The same experimental protocol was applied to analyse the influence of GSM signals simulating talking and listening phases during a typical conversation (GSM-Talk). However, no changes of gene expression patterns in both wt and p53-/- cells were observed upon the exposure to GSM-Talk signals regardless of the protocol used. These observations indicate that the genetic constitution of cells determined by the p53 function affected cellular responsiveness to GSM-modulated EMF, whereas low frequency components characteristic for GSM-Talk modulation were not responsible for these effects.

Table 25. Conditions of the exposure of p53-proficient and deficient pluripotent embryonic stem cells to RF-EMF and summary of the effects on transcript levels of regulatory genes.

GSM-Basic	
1.5 W/kg (5min on/30 min OFF)	
$p53^{+/+}$ ES cells	**$p53^{-/-}$ ES cells**
6h, (5min ON/30 min OFF) (n=3) no EMF effect	6h, (5min on/30 min OFF) (n=3) no EMF effect
48h, (5min on/30 min OFF) (n=3) no EMF effect	48h, (5min on/30 min OFF) upregulation of hsp70, (n=3) c-jun,c-myc and p21

GSM-Talk (33% GSM-Basic, 66% DTX)	
0.4 W/kg (5min on/30 min OFF)	
$p53^{+/+}$	**$p53^{-/-}$**
6h, (5min on/30 min OFF) (n=3) no EMF effect	6h – (5min on/30 min OFF) (n=3) no EMF effect
48h,(5min on/30 min OFF) (n=3) no EMF effect	48h (5min on/30 min OFF) (n=3) no EMF effect

GSM – DTX (100% DTX)	
0.11W/kg	
$p53^{+/+}$	**$p53^{-/-}$**
6h, (5min on/30 min OFF) (n=3) no EMF effect	6h, (5min on/30 min OFF) (n=3) no EMF effect

n- number of experiments

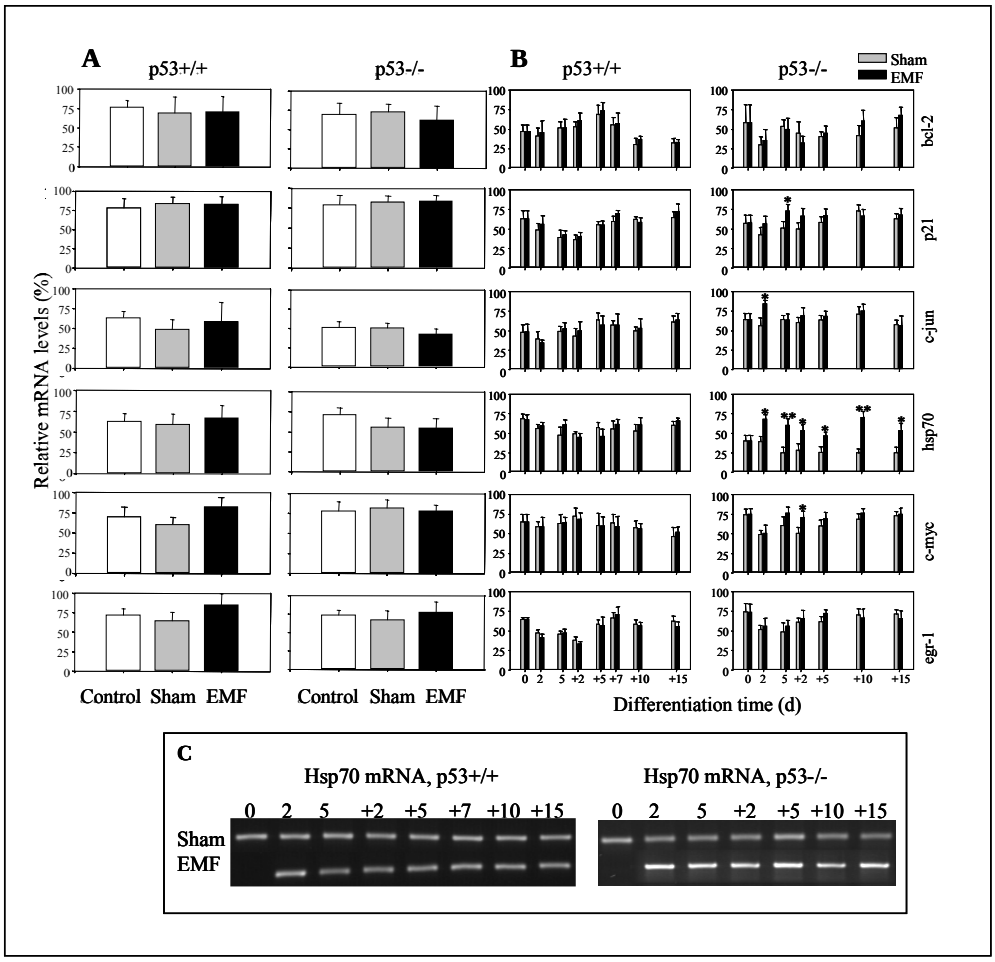

Figure 112. Relative mRNA levels of genes encoding bcl-2, p21, c-jun, hsp70, c-myc and egr-1 in p53-deficient ($p53^{-/-}$) and wild-type ($p53^{+/+}$) D3 ES cell-derived EBs after 6 (A) and 48 (B) hours GSM-217 Hz exposure. GSM-217 exposure resulted in a significant and long-lasting upregulation of hp70 transcripts (C) paralleled by a temporary upregulation of c-myc, c-jun and p21 levels in differentiating $p^{-/-}$ ES cells after 48h exposure (B), but not after 6h (A) exposure. Error bars represent standard deviations. Statistical significance was tested by the Student's t-test for significance levels of 1 and 5% (**, $p<0.01$, *,<0.05)

RF-EMF did not influence cardiac differentiation and gene expression levels in R1 ES cells.

For the evaluation of embryotoxic effects of chemical compounds in vitro, the mouse embryonic stem cell test, EST (Spielmann 1997), studying cardiac differentiation of ES cells as endpoint has been established. Therefore, we further analysed effects of EMF on cardiac differentiation in R1 ES and P19 EC cells. R1-derived EBs were exposed to EMF for 5 days and the cells were analysed after further differentiation. Similarly to D3 wt cells, no effect of GSM-217 signals on the expression of the regulatory genes including p53 was observed in R1 wt cells. Moreover, no significant differences in cardiac differentiation were found between sham- and EMF-exposed variants during EB differentiation. The results of morphological investigations were confirmed by RT-PCR analyses, where no differences in cardiac α-MHC mRNA levels between sham- and EMF-exposed variants were observed.

RF-EMF did not induce cardiac differentiation and gene expression and the proliferation of P19 EC cells.

Contrary to ES cells, which spontaneously differentiate into the cardiac lineage, differentiation of P19 cells has to be stimulated by external differentiation factors, i.e. DMSO or retinoic acid. To elucidate, whether EMF signals interfere with DMSO-induced cardiac differentiation, undifferentiated P19 EC cells were exposed to GSM-217 signals for 22 and 40h, respectively, and differentiated in the absence or

presence of 1% DMSO. The mRNA levels of regulatory genes were not affected by EMF exposition, and no significant differences were found between EMF-, sham-exposed and control variants of undifferentiated P19 cells, respectively.

Without DMSO induction, only low levels (5-10%) of spontaneous cardiac differentiation were found. By differentiation induction with DMSO during the first 48 hours of EB development, the differentiation of spontaneously beating cardiac cells was increased to a maximum level of 90% in both variants. Exposure of P19 cells to GSM-217 signals for 22 and 40 hours did not result in significant changes of cardiac differentiation suggesting that EMF had no effects on spontaneous or DMSO-induced cardiogenesis. Furthermore, undifferentiated EC cells were EMF- (GSM-217) and sham-exposed at a SAR value of 2.0 W/kg for 22 or 40 hours, and the lengths of cell cycle phases were analysed by flow cytometry. In both cases, no differences in the distribution of cells in G1, S or G2/M phases were observed between sham- and EMF-exposed variants.

RF-EMF exposure may affect the bcl-2 mediated apoptotic pathway in ES-cell derived neural progenitors and neuronal differentiation by inhibiting nurr-1 and TH transcription.

We used an experimental protocol that has been shown to be efficient for differentiation induction of ES cells into the neural lineage (Figure 6) for our experiments aimed at defining the influence of RF-EMF (1.71 GHz, 1.5 W/kg, 5 min on/30 min off) as shown in Table 26. Neural progenitors were analysed at stage 4+4d to 4+6d, where nestin-positive cells were detected in ca. 60-80% of the cells. The exposure conditions applied for 6 or 48 hours are shown in Table 23. The analysis of hsp70, bax and p21 mRNA levels after RF-EMF exposure of neural progenitor cells did not provide evidence of gene expression changes. Bcl-2 was significantly up-regulated after the RF-EMF exposure at the terminal stage 4+23d (Figure 109, $p<0.01$). In addition, we investigated the effect of RF-EMF exposure on GADD45 transcript levels and found that GADD45 mRNA levels were significantly up-regulated at the same stage of differentiation at 4+23d (Figure 113, $p<0.05$). The data on the influence of RF signals on gene expression pattern in differentiating neuronal cells revealed statistically significant down-regulation of nurr-1 at stage 4d+11 and TH at terminal stage 4d+23d, but no clear shifts in transcript levels of the tissue specific genes GFAP, Nestin and En-1 (Figure 113). Quantitative RT-PCR with specific primers and TaqMan probe confirmed the up-regulation of GADD45 at 4+23d stage, but not for bcl-2. According to the Q-RT-PCR data nurr-1 was down-regulated both at stage 4+7d and 4+11d, but the decrease in mRNA levels was statistically significant for stage 4+7d (Figure 114).

Table 26. Conditions of the exposure of neuronal progenitor cells to PL-MF or RF-EMF.

Intermittent exposure (5min on/30 min off)			
48h, GSM 217 Hz (1.71 GHz)		**6h, GSM 217 Hz (1.71 GHz**	
1.5 W/kg	Alterations of GADD45 transcript levels Down-regulation of nurr-1. No effect on DNA break induction (n=7)	1.5 W/kg	Low, but statistically significant induction of double-strand DNA breaks (n=7)

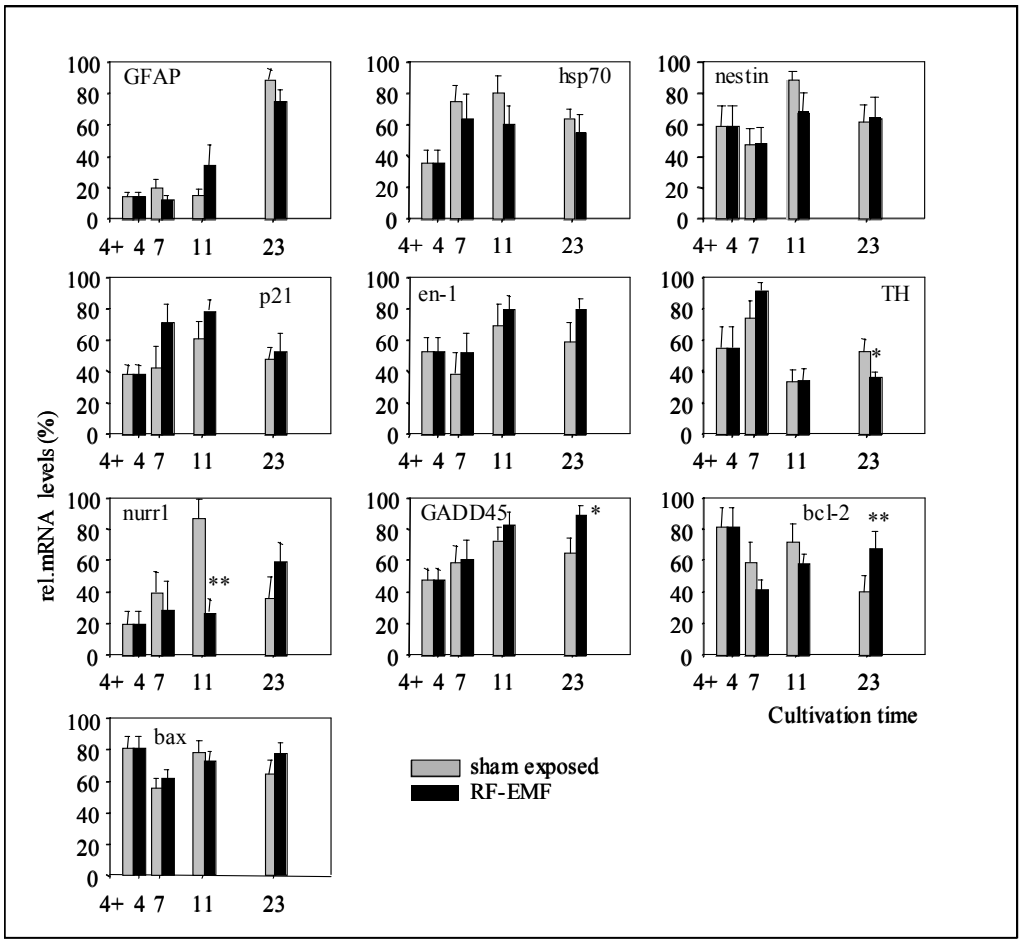

Figure 113. Relative mRNA levels analysed by semi-quantitative RT-PCR of genes encoding bcl-2, p21, c-jun, hsp70, c-myc and egr-1 in p53-deficient (p53-/-) and wild-type (p53+/+) D3 ES cell-derived EBs and EB outgrowths after 6 (A) and 48 hours (B) exposure to GSM-Talk. No effects of GSM-Talk on gene expression levels in ES cells were observed.

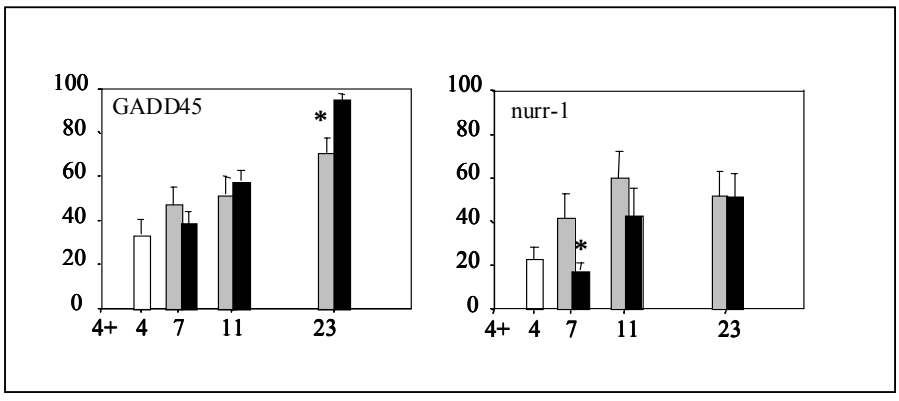

Figure 114. Quantitative RT-PCR with specific primers and Taqman probe for estimation of relative mRNA levels of the growth arrest and DNA damage inducible gene GADD45 and the nurr-1 gene involved in neuronal differentiation in ES-derived neural progenitors after 48 hours RF - EMF (GSM signal 217-Hz) exposure (1.5 W/kg, 1.71 GHz, intermittency 5 min ON/30 min OFF), at stage 4+4d - 4+6d. EMF exposure resulted in a significant transcript down-regulation, followed by up-regulation of GADD45 and down-regulation of nurr-1 at stage 4+7d. Error bars represent standard deviations. Statistical significance was tested by the Student's two-tailed paired t-test for a significance level of 5% (*, $p < 0.05$).

3.2.4.2 Human neuroblastoma cell line NB69 and neural stem cells (NSC) (Participant 5)

RF-EMF (GSM-CW and GSM-Basic) interfered with the expression of FGF receptors in NB69 human neuroblastoma cells.

In a first experiment the cellular response to a chemical promoter of differentiation was characterised. Immunocytochemical staining using antibodies against phenotype-specific antigens revealed that NB69 cells contain the neuroblast-specific protein ßIII-tubulin, but not the neuroepithelial marker nestin, which is present in immature progenitors and in some neuroblastoma cells (Kashima et al. 1995). Untreated NB69 cells remain in an undifferentiated state. Immunocytochemistry for FGFR1-3 revealed the three types of receptors in the human neuroblastoma cell line. On day 3 after plating approximately 70% of cells expressed R1, whereas FGFR3 and FGFR2 were present in a smaller proportion of cells, 30% and 20%, respectively (Figure 115, grey colour). Basic fibroblast growth factor (bFGF), which induces morphological changes including neurite extension at a 20-ng/ml concentration, was used as a positive control for the subsequent EM treatments. This growth factor reduced the number of NB69 cells expressing FGF receptors R1, R2 and R3. Such an effect was accompanied with changes in the cellular morphology associated to differentiate phenotypes. These changes included increased neural outgrowth, neural microtubule network and cell surface. As shown in this Figure 115, the 24-hour treatment with bFGF induced a consistent reduction in the percent of FGFR positive cells for the 3 receptors tested ($p<0.0001$; ANOVA).

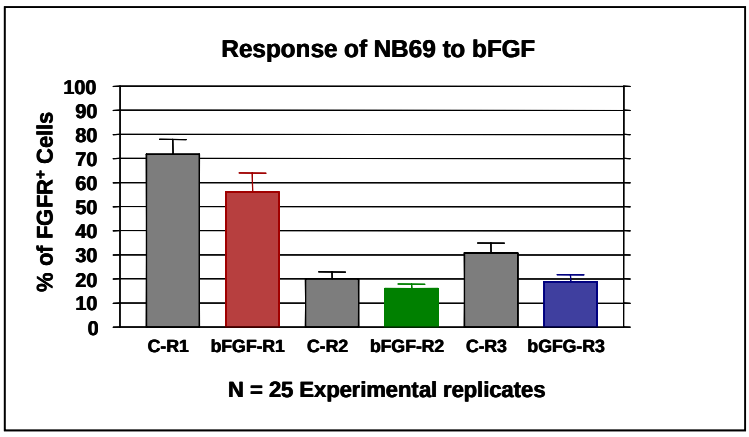

Figure 115. Expression of FGF Receptors 1, 2 and 3 in NB69 cells after a 24-hours treatment with 20-ng/ml bFGF. See text for details.

In the following experimental series, the cellular responsiveness to a differentiation-promoter was confirmed through treatment with bFGF, which induced a reduction of the percent of cells expressing FGF receptors R1, R2 and R3. Such an effect was associated with cell enlargement and neurite arborisation. In contrast, the treatment with GSM-Talk (SAR of 2 W/kg) signal alone (N= 4 experimental replicates), does not modify significantly the normal expression of the FGF protein receptors R1, R2 and R3 in NB69 cells (Figure 116). However, the results of the combined treatment bFGF + GSM-Talk signal show that the EMF seems to antagonize the significant reduction of FGFR-2 expression induced by bFGF. This indicates that the GSM-Talk signal might interfere with some of the cellular responses to bFGF.

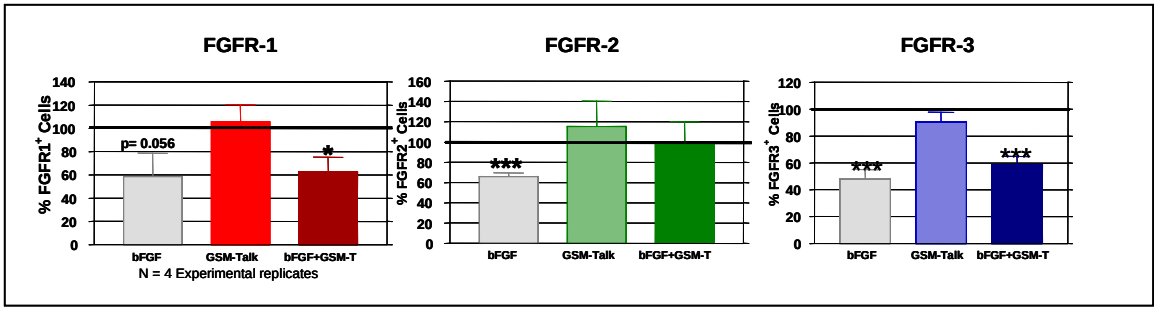

Figure 116. Response of NB69 cells to GSM-Talk signal. Percent of cells expressing FGF Receptors R1, R2 and R3. The treatment with bFGF induced significant reductions in the percent of cells expressing the receptors. Data normalised over the respective controls. (*, p<0.05; **, p<0.01; ANOVA followed by Student's T test).

When administered alone, the exposure to GSM 1800-Basic signal at a 2 W/kg SAR was found to induce a decrease in the number of cells expressing the FGFR-1 (15% reduction vs. controls, Figure 117) and photomicrographs of NB69 cell cultures) without affecting significantly the number of cells expressing receptors R2 and R3. The magnitude of the effect on R1 was equivalent to that induced by bFGF at a 20 ng/ml concentration. However, unlike bFGF, the exposure to GSM-Basic alone did not provoke changes in the cellular morphology. Provided that, as described previously, the GSM-Basic treatment does not induces significant changes in the total cell number or the cell viability, the present results indicate that the GSM-Basic-induced effect on FGFR-1 is not due to a reduction in the number of cells, but to a loss of expression of this receptor.

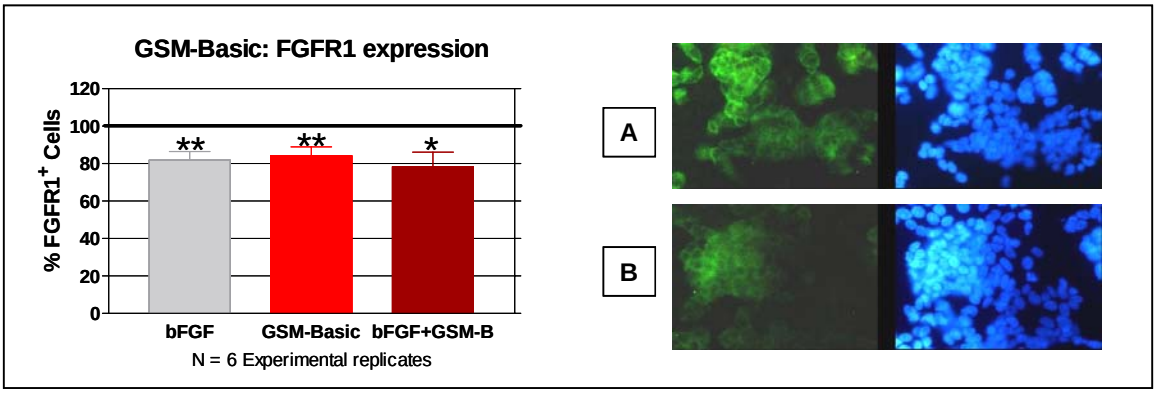

Figure 117. Photomicrographs of NB69 cell cultures: A, control; B, exposed to GSM-Basic signal. Immunocytochemistry for FGFR1. The image analysis showed a statistically significant reduction in the protein expression in the exposed cells (left). The matched fields (right) show the total cells stained with Hoechst.

The treatment with RF-CW signal (SAR 2 W/kg) induced effects on the expression of FGFR-1 equivalent to those induced by the GSM-Basic signal (Figure 118A), whereas the exposure to GSM-DTX signal at a lower SAR (1 W/kg) did not modify significantly the normal expression of the FGF protein receptors R1 in NB69 cells (Figure 118B).

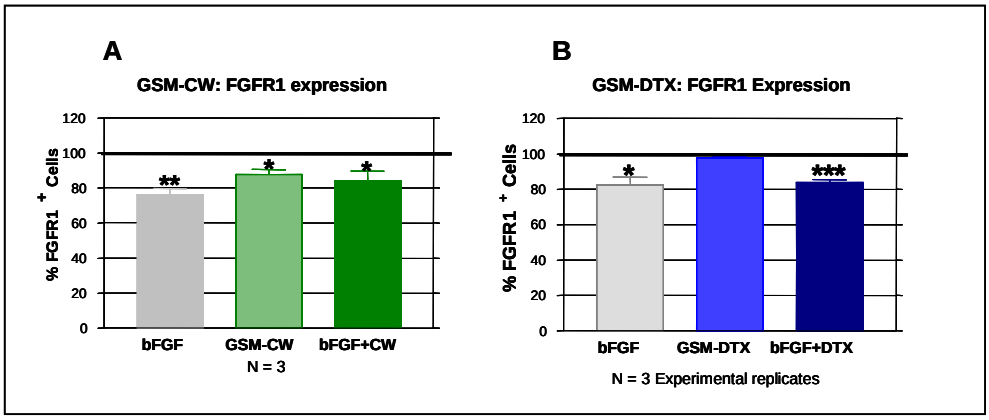

Figure 118. FGFR1 expression in NB69 cells after exposure to: (A) RF-CW signal, 2 W/kg and (B) GSM-DTX signal, 1 W/kg. Only RF-CW induced a significant response. *, $p<0.05$; **, $p<0.01$, ***, $p<0.001$ (ANOVA followed by Student's T test for unpaired data).

Taken together, the results on the expression of FGFRs in NB69 cells exposed to GSM-1800 MHz signals and RF-CW signals suggest that (1) these cells are sensitive to low-SAR signals, (2) the cellular response does not seem to be dependent on the tested low-frequency modulation and (3) the observed response on FGFR1 could be indicative of a EMF-induced promotion of cell differentiation. However, additional studies on the expression of differentiation markers have to be done to confirm this hypothesis. (4) The GSM signal does not seem to interfere significantly with the cellular response to bFGF.

RF-EMF affected the expression of FGF receptors in neural stem cells (NSC).

In order to enhance expansion of NS precursor cells, neurospheres were seeded onto adherent substrate and treated with the mitogen epidermal growth factor (EGF) during the first 3 days in culture. After this period the EGF was withdrawn, and cells grew in a defined medium, which promoted differentiation processes to neurons, astrocytes and oligodendrocytes. Between 2 h and 3 days cultures comprised mainly nestin-positive, undifferentiated precursors. At later stages, the total number of cells dropped, paralleling to a gradual loss of nestin content, and an enhancement in the differentiation processes of neurons, oligodendrocytes and astrocytes.

Immunocytochemistry for FGFR1-3 identified the three types of receptors in the progeny of EGF-expanded NSCs. During the first day after plating, approximately 70% and 50% of the precursors expressed FGFR1 and FGFR2, respectively, whereas FGFR3 was restricted to a less abundant population. At 3 days and thereafter the number of cells exhibiting FGFR1 and FGFR2 decreased gradually, so that at 3 days the percent of FGFR-1 was 35% and at 9 days postplating only approximately 15% of the cell population was immmunopositive for this receptor. FGFR1 immunostaining was preferentially localised in the cytoplasmic compartment, FGFR-3 was found in the cytoplasmic and/or nuclear compartments, and FGFR2 was frequently confined to the nucleus. In situ hybridisation studies on the third day postplating showed high levels of FGFR1 mRNAs in NSC.

On the basis of our previous data showing that the GSM-Basic signal induces a reduction in the percent of cells expressing FGF-R1 in human neuroblastoma cells, we tested firstly this signal (2 W/kg) on NSC. Like in NB69 cells, a significant decrease in FGFR1-positive NS cells was also observed after exposure to the GSM-Basic signal (50% reduction with respect to controls, Figure 119). Western blot analysis for FGFR1 confirmed this effect (data not shown). The study also indicates that the response of the neural stem cells seems to be dependent on the age of the culture (Figure 120).

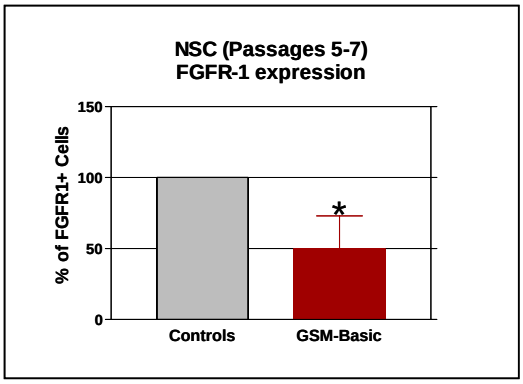

Figure 119. Percent of FGFR-1 positive labelling vs. total cell number normalised over their controls, quantification by the program for image analysis (IPWIN-3). Data represent the mean ± SEM of 3 independent experiments, done in duplicate (two coverslips), for the different treatment conditions. Student T-test *p< 0.05.

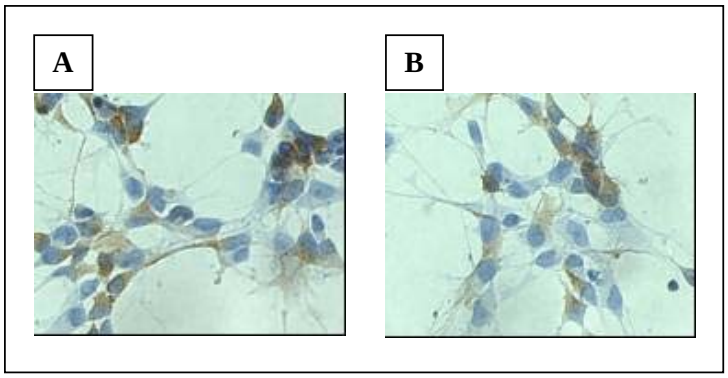

Photomicrographs of Neural Stem Cells, A, control and B exposed to GSM-Basic signal. Inmunocytochemistry for FGFR1-positive cells (brown).

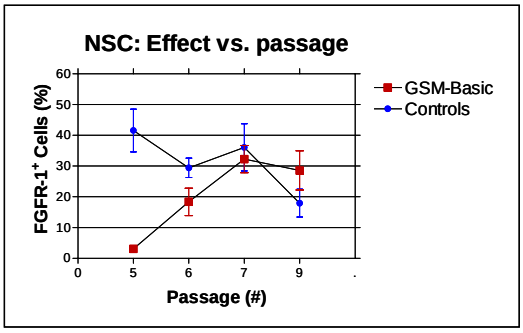

Figure 120. NSC exposed to GSM-Basic signal. The percent of FGFR-1 positive cells seems to be dependent on the passage number.

RF-EMF did not affect gene expression of FGF Receptor-1 in NB69 neuroblastoma cells and in neural stem cells (NSC)

In situ hybridisation studies were conducted on neural stem cells and in NB69 cells exposed for 21 hours (5 min on/10 min off) to the GSM-Basic signal. The objective is to evaluate potential EMF effects on gene expression of FGFR1. All experiments were conducted following blind protocols. The results on both cell types showed no differences in FGFR1 mRNA-expression between controls and exposed samples. An image-analysis study confirmed this result in NSC (Figure 121). Taken together, the

described effects on NB69 and NSC (FGFR1 protein-expression and FGFR1 mRNA-expression), suggest that the GSM-Basic signal can modulate FGFR1 protein translation without affecting protein transcription.

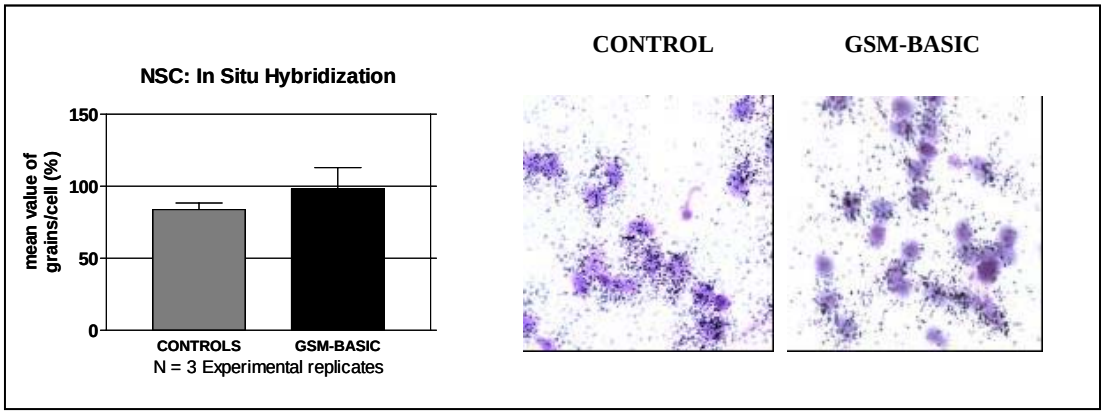

Figure 121. Quantification of in situ hybridisation staining by image-analysis technique (IPWIN 3.0) of the number of grains/cell. The photomicrographs show the developmental pattern of FGFR1 in NSC processed with Radiolabelled Probe Specific for Transcript of FGFR1.

3.2.4.3 Human promyelocytic cell line HL-60 (Participant 2)

RF-EMF exposure reproducibly up- and down-regulated protein expression in HL-60 cells (41 proteins showed to be up-, 1 protein to be down-regulated and 14 proteins appeared to be de-novo expressed).

The proteome screening approach included analysis of the entire HL-60 protein expression pattern by means of 2-D polyacrylamide gel electrophoresis (2D-PAGE). After having established the technique for HL-60 cells, cells were exposed to RF-fields at selected conditions in repeated independent experiments in order to obtain reproducible information on changes in the cellular protein pattern, correlated with RF-EMF-exposure.

HL-60 cells were exposed at 1800 MHz, continuous wave, SAR 1.3 W/kg, 24h, or were sham exposed in repeated independent experiments. Additionally, incubator controls were run and analysed for their protein expression pattern by 2D-PAGE. Cell samples were partly analysed as described above, partly stored at -80 °C for further analyses. Comparison of protein pattern after 2D-PAGE showed that optimal reproducibility is achieved when the 2-D separation step is performed in one series with identical reagent batches. In order to be able to perform statistics, appropriate numbers of comparable 2D-gels are required, also to have enough material for protein identification.

Figures 122, 123, and 124 show representative high-resolution 2-dimensional polyacrylamide gels (23 x 30 cm) for each of the conditions described above (incubator control, sham-exposure and RF-field exposure).

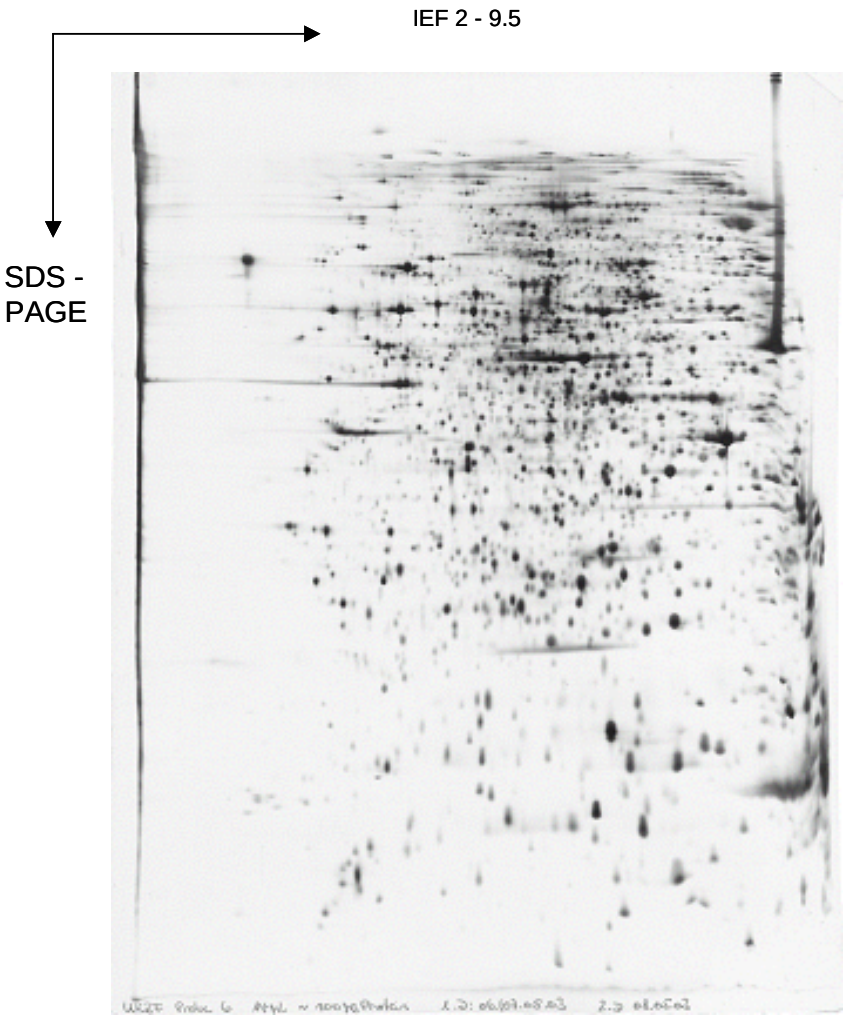

Figure 122. Two-dimensional polyacrylamide gel electrophoresis (2-D PAGE) profile of incubator control HL-60 cells (whole cell lysate). Incubation time: 24h. First dimension (isoelectric focussing): pH-gradient 2-9.5. Second dimension: 12.5% polyacrylamide gel, silver stain.

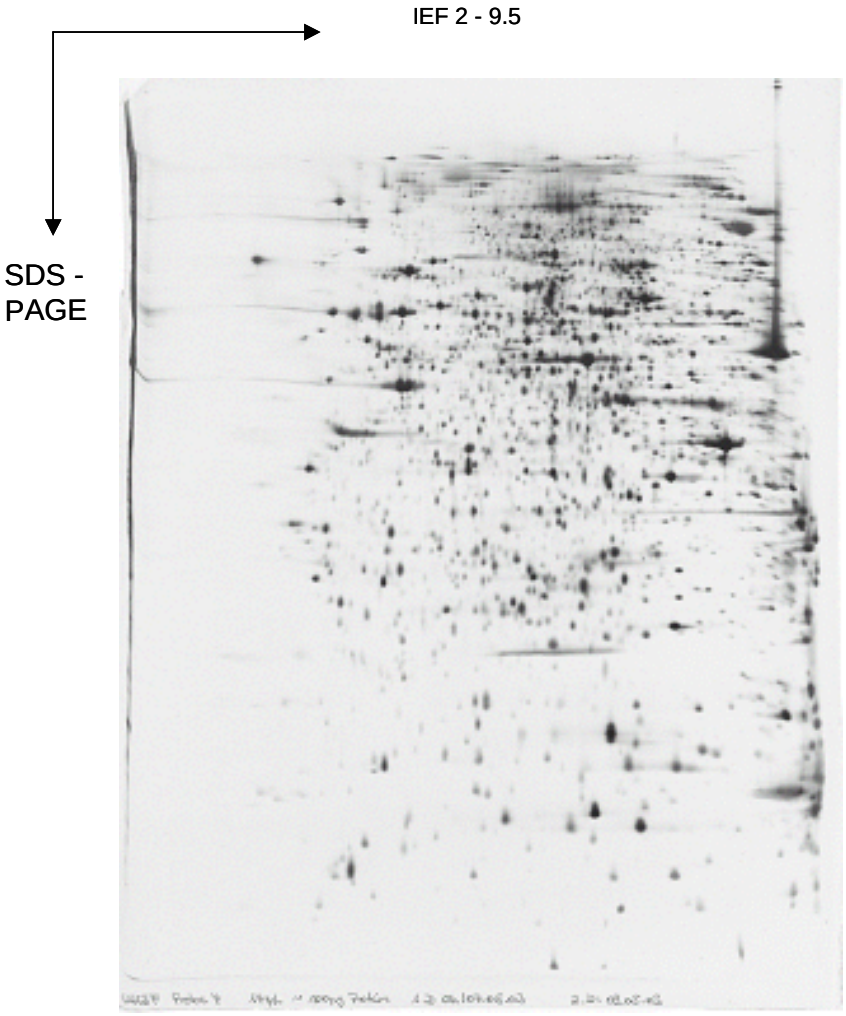

Figure 123. Two-dimensional polyacrylamide gel electrophoresis (2-D PAGE) profile of sham-exposed HL-60 cells (whole cell lysate). Exposure time: 24h. First dimension (isoelectric focussing): pH-gradient 2-9.5. Second dimension: 12.5% polyacrylamide gel, silver stain.

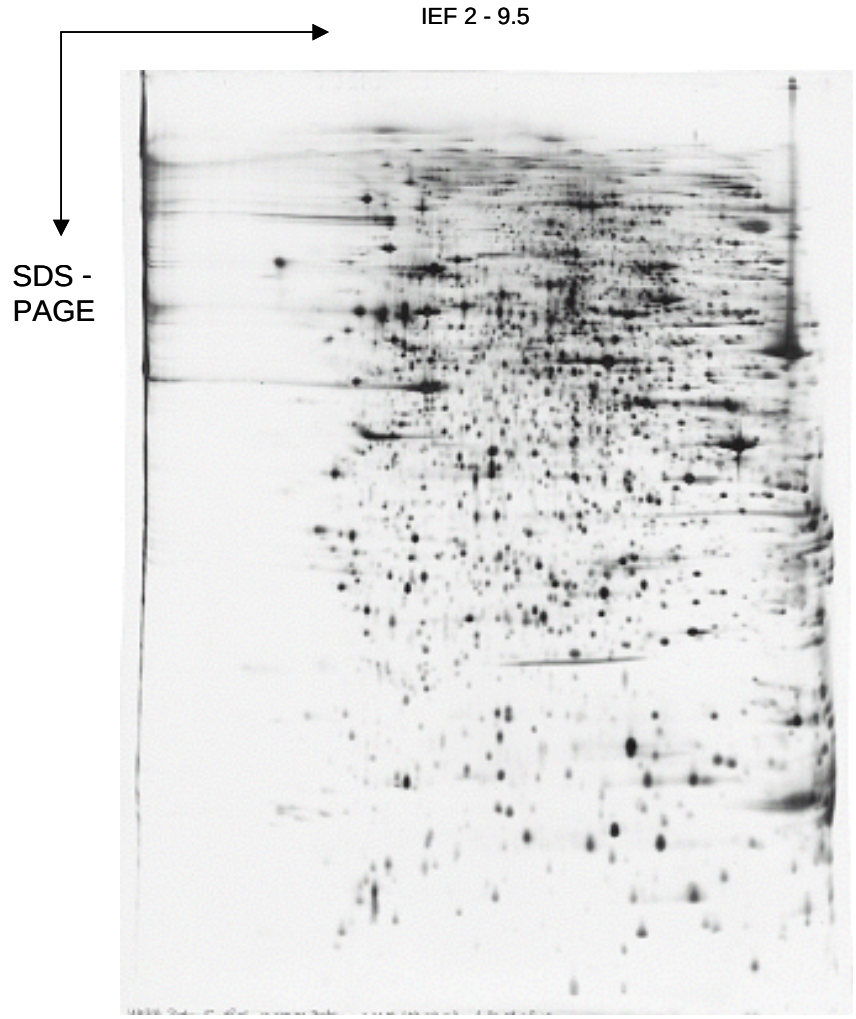

Figure 124. Two-dimensional polyacrylamide gel electrophoresis (2-D PAGE) profile of RF-exposed HL-60 cells (whole cell lysate). Exposure characteristics: 1800 MHz, continuous wave, 1.3 W/kg, 24h. First dimension (isoelectric focussing): pH-gradient 2-9.5. Second dimension: 12.5% polyacrylamide gel, silver stain.

Following digitalisation, in a second analysis step the qualitative and quantitative comparison of protein expression was performed by use of Proteom Weaver image analysis program. Figure 125 shows a representative comparative 2D-gel, in which expression differences between RF-field exposed and sham-exposed HL-60 cells are marked. Expression differences were quantified. In Table 27 (a-c) proteins up-or down-regulated and those that have disappeared after RF-field exposure are listed.

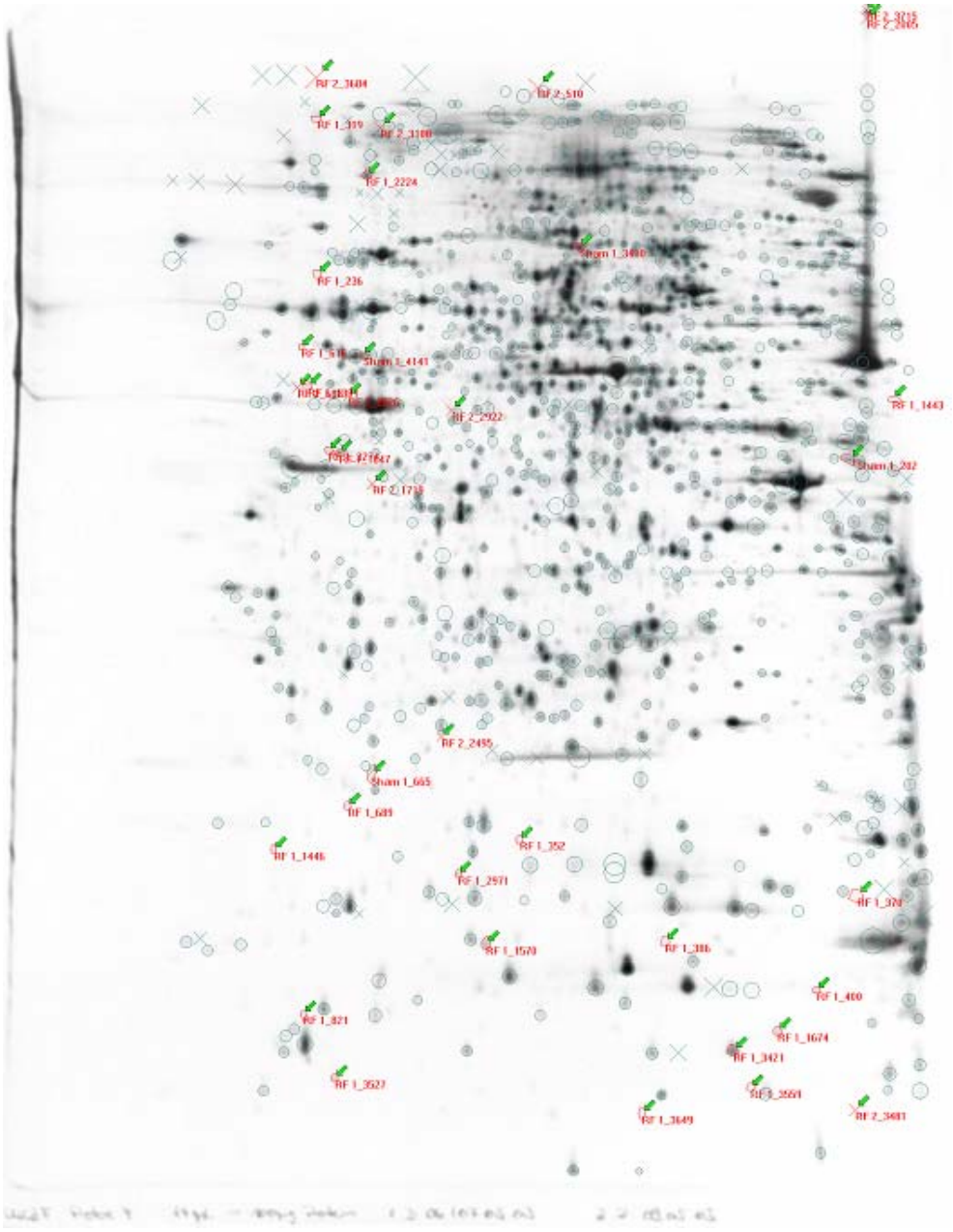

Figure 125. Representative qualitative and quantitative comparison of two-dimensional polyacrylamide gel electrophoresis (2-D PAGE) profiles of sham-exposed and RF-exposed HL-60 cells (whole cell lysate).

Exposure conditions: see above. Green arrows mark different proteins of sham-exposed cells compared to RF-field exposed cells (green arrows and red circles: up-regulated proteins; green arrows and red crosses: newly expressed or disappeared proteins).

Table 27. List of proteins in 2-DE patterns of HL-60 cells, differing between RF-field exposed and sham exposed cells. Exposure conditions: see above

a: List of proteins up-regulated in RF-field exposed HL-60 cells (average intensity see arrow) as compared to sham-exposed cells (average intensity see arrow).

				sham				⇩	RF-field				⇩
ID	ID	Name	Freq	X	Y	I	/	Avg	X	Y	I	/	Avg
1	1_3559	RF 1_3559	2	1163	1684	0,039	N.R.	0,039	1183	1726	0,278	7,1924	0,278
2	1_1443	RF 1_1443	2	1384	614	0,058	N.R.	0,058	1399	628	0,389	6,649	0,389
3	1_400	RF 1_400	2	1266	1533	0,055	N.R.	0,055	1278	1562	0,354	6,3801	0,354
4	1_689	RF 1_689	2	536	1247	0,048	N.R.	0,048	574	1271	0,267	5,5816	0,267
12	1_616	RF 1_616	2	464	533	0,031	N.R.	0,031	512	546	0,137	4,404	0,137
15	1_386	RF 1_386	2	1030	1458	0,057	N.R.	0,057	1056	1491	0,247	4,3329	0,247
16	1_1446	RF 1_1446	2	421	1315	0,046	N.R.	0,046	464	1345	0,193	4,2311	0,193
17	1_236	RF 1_236	2	489	421	0,047	N.R.	0,047	538	431	0,198	4,227	0,198
22	1_1391	RF 1_1391	2	474	594	0,094	N.R.	0,094	522	607	0,354	3,7725	0,354
24	1_821	RF 1_821	2	467	1570	0,042	N.R.	0,042	507	1611	0,157	3,7049	0,157
27	1_3274	RF 1_3274	2	506	694	0,067	N.R.	0,067	549	708	0,229	3,4382	0,229
28	1_1674	RF 1_1674	2	1205	1597	0,117	N.R.	0,117	1220	1631	0,394	3,3527	0,394
35	1_3649	RF 1_3649	2	994	1725	0,048	N.R.	0,048	1017	1778	0,15	3,102	0,15
36	1_370	RF 1_370	2	1329	1387	0,084	N.R.	0,084	1338	1406	0,261	3,0949	0,261
37	1_352	RF 1_352	2	804	1299	0,043	N.R.	0,043	834	1330	0,132	3,0908	0,132
41	1_1647	RF 1_1647	2	523	698	0,199	N.R.	0,199	565	712	0,59	2,9714	0,59
43	1_2971	RF 1_2971	2	708	1353	0,075	N.R.	0,075	743	1385	0,221	2,9515	0,221
45	1_2224	RF 1_2224	2	565	267	0,345	N.R.	0,345	607	275	1,016	2,9415	1,016
48	1_319	RF 1_319	2	489	178	0,058	N.R.	0,058	536	186	0,168	2,9054	0,168
49	1_3421	RF 1_3421	2	1136	1628	0,597	N.R.	0,597	1159	1669	1,728	2,8956	1,728
54	1_1570	RF 1_1570	2	751	1462	0,231	N.R.	0,231	784	1499	0,63	2,7259	0,63
61	1_3527	RF 1_3527	2	516	1670	0,075	N.R.	0,075	552	1717	0,187	2,5069	0,187

b: List of proteins down-regulated in RF-field exposed HL-60 cells (average intensity see arrow) as compared to sham-exposed cells (average intensity see arrow).

				sham				⇩	RF-field				⇩
ID	ID	Name	Freq	X	Y	I	/	Avg	X	Y	I	/	Avg
13	1_3400	Sham 1_3400	2	897	378	0,345	N.R.	0,345	927	389	0,12	0,3489	0,12

c: List of newly expressed or disappeared proteins in RF-field exposed HL-60 cells (average intensity see arrow) as compared to sham-exposed cells (average intensity see arrow) .

				sham				⇩	RF-field				⇩
ID	ID	Name	Freq	X	Y	I	/	Avg	X	Y	I	/	Avg
1	1_202	Sham 1_202	1	1317	708	0,417	N.R.	0,417	1326	716	X	N.A.	N.A.
2	2_2005	RF 2_2005	1	1343	21	X	N.R.	N.A.	1358	29	0,546	N.A.	0,546
3	2_1719	RF 2_1719	1	574	746	X	N.R.	N.A.	614	761	0,198	N.A.	0,198
4	2_3100	RF 2_3100	1	586	191	X	N.R.	N.A.	628	196	0,424	N.A.	0,424
5	2_688	RF 2_688	1	458	595	X	N.R.	N.A.	506	609	0,133	N.A.	0,133
6	2_2495	RF 2_2495	1	682	1138	X	N.R.	N.A.	718	1160	0,142	N.A.	0,142
7	1_4141	Sham 1_4141	2	560	546	0,158	N.R.	0,158	600	558	0,468	2,9721	0,468
8	2_2922	RF 2_2922	1	697	631	X	N.R.	N.A.	735	643	0,222	N.A.	0,222
9	2_3481	RF 2_3481	1	1325	1718	X	N.R.	N.A.	1337	1750	0,101	N.A.	0,101
10	2_510	RF 2_510	1	832	129	X	N.R.	N.A.	868	135	1,007	N.A.	1,007
11	2_3684	RF 2_3684	1	487	114	X	N.R.	N.A.	533	117	1,457	N.A.	1,457
12	2_2826	RF 2_2826	1	537	609	X	N.R.	N.A.	582	622	0,146	N.A.	0,146
13	2_3715	RF 2_3715	1	1343	8	X	N.R.	N.A.	1358	16	0,199	N.A.	0,199
14	1_665	Sham 1_665	2	572	1199	0,124	N.R.	0,124	609	1227	0,13	1,0504	0,13

Overall, 56 polypeptides of HL-60 cells are influenced in their expression under RF-EMF. Reproducibly, 41 proteins showed to be up- and 1 protein to be down-regulated following RF-field exposure. 14 proteins appeared to be de-novo expressed after RF-field exposure of HL-60 cells.

By use of these lists identification strategies are further performed. They will include in gel-cleavage, identification of selected proteins by mass spectrometry (MALDI-TOF) and mass spectrometric sequencing (ESI-MS/MS). Further identification of selected proteins will include immunoblotting and functional protein assays.

3.2.4.4 Human lymphocytes (Participant 8)

RF-EMF did not affect gene expression in human lymphocytes.

T lymphocyte gene expression analysis was performed in collaboration with Participant 12 and Dr. Daniel Remondini in Bologna. The results suggest that no differences in gene expression are found between

quiescent T lymphocytes exposed to RF-EMF (DTX only) in comparison with sham-exposed cells. This finding did not suggest any significant interaction of RF-EMF with gene profile expression.

3.2.4.5 Brain cells of different origin (Participant 9)

RF-EMF exposure did not affect expression and activity of the inducible nitric oxide synthase (iNOS or NOS2) in nerve cells.

A basal level of NOS_2, probably due to the SVF deprivation, was detected in C6 cells, although inter-experiment's variation could be seen. A 48-hour treatment with LPS plus CK increased the expression of the enzyme by a factor 5 (Figure 126)

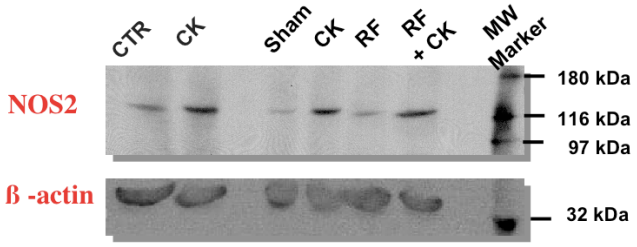

Figure 126. Representative blot for the detection of NOS_2 (upper blot) and ß-actin (lower blot) proteins.

Sham/sham experiments showed that a 15-20% inter-incubator variation had to be expected, so that a more than a 30% difference between sham- and RF-exposed data would be considered as a significant biological effect for both NOS_2 expression and nitrite accumulation (Figure 127).

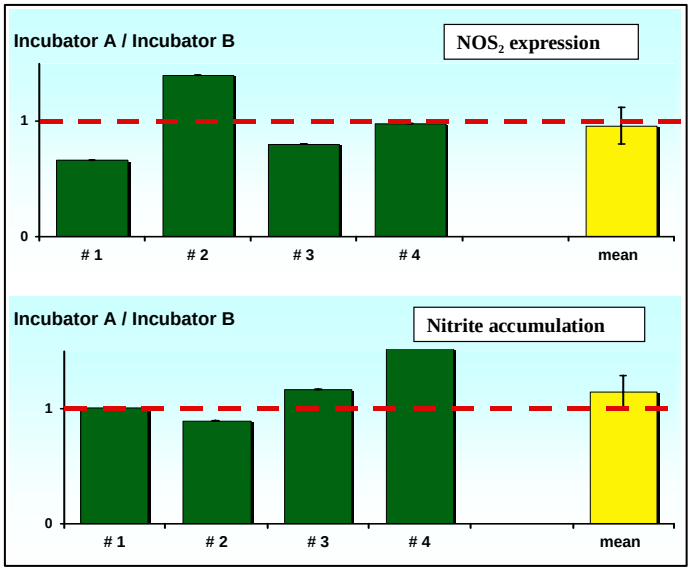

Figure 127. Expression of NOS_2 protein and nitrite accumulation (culture medium) in C6 cells in four sham/sham experiments (#1 to #4). Data are given as the ratio ± SEM between the levels found in the incubator A used for RF exposure and incubator B used for sham-exposure.

Exposure to GSM-900 at 0.2 W/kg and 2 W/kg for 48 hours was shown to not alter the expression of NOS_2 compared to sham exposure. Co-exposure to GSM and LPS plus cytokine was ineffective in modifying the effect of LPS plus cytokine treatment on NOS_2 expression (Figure 128).

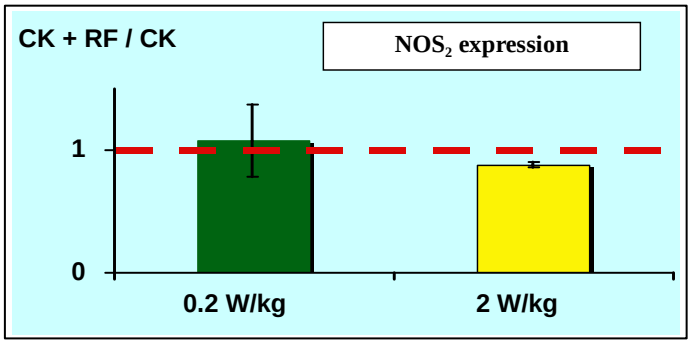

Figure 128. Expression of NOS_2 protein in C6 cells exposed to frame-GSM-900 at 0.2 and 2 W/kg for 48 hours. Data are given as the ratio ± SEM between the levels found in samples treated with CK+LPS (CK) and exposed to RF and those treated with CK alone.

Nitrite accumulation in culture medium was used as a marker of NOS_2 activation. No nitrite accumulation was shown in sham-exposed samples. Although inter-experiment variability, treatment with the cocktail of LPS plus CK led to a significant nitrite accumulation ($p<0.001$). As shown in Figure 129, a mean 20-fold increase in nitrite accumulation was measured after 48 hours of LPS plus CK treatment.

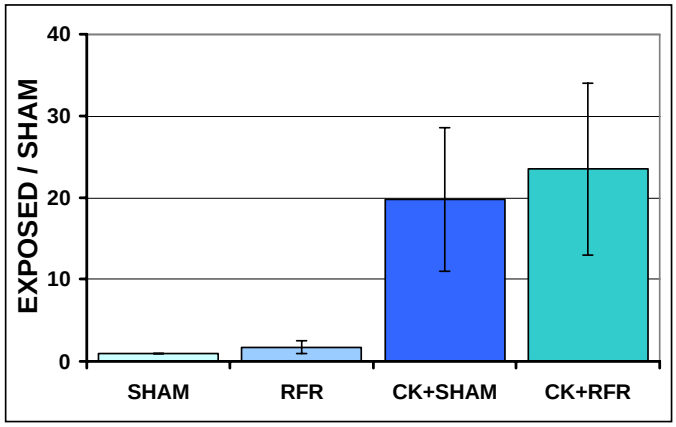

Figure 129. Nitrite accumulation in culture medium of C6 cells sham-exposed or exposed to GSM-900 at 0.2 W/kg and /or treated with CK+LPS (CK). In all cases, treatment duration was 48 hours. Data are given as the ratio ± SEM between the levels found in treated- versus sham-exposed samples.

No significant effect of GSM-900 exposure was detected on nitrite accumulation. When co-exposures to GSM-900 and LPS + CK treatment were performed, no modulation of chemically-induced NOS_2 expression. Overall, exposure to GSM-900 did not modulate CK+LPS-induced nitrite accumulation (Figure 130).

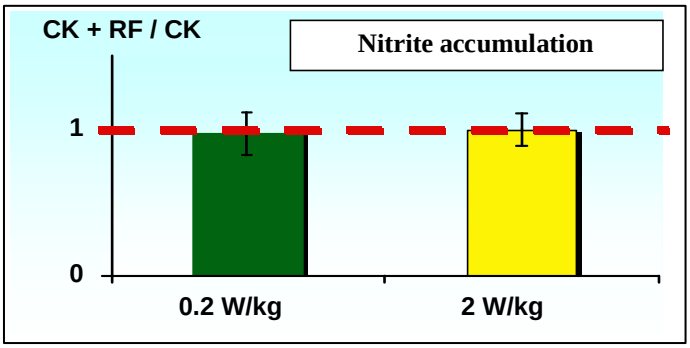

Figure 130. Nitrite accumulation (culture medium) in C6 cells exposed to frame-GSM-900 at 0.2 W/kg and 2 W/kg for 48 hours. Data are given as the ratio ± SEM between the levels found in samples treated with CK+LPS (CK) and exposed to RF and those treated with CK alone.

No evidence of an effect of RF-EMF (GSM-900) exposure on spontaneous expression and activity in C6 cells was obtained from our experiments. However, one can note that only strong treatments (serum deprivation plus long duration of chemical treatment) are shown to increase NOS_2 expression in C6 cells. It is noteworthy that most papers in the literature looked at the mRNA but not at the *protein* level as we did in the present work. Two SAR levels of GSM-900 were tested. Even at the highest SAR level of 2 W/kg corresponding to the public exposure limit recommended by the EU Commission, GSM-900 exposure was not shown able to influence NOS_2 expression or activity in activated C6 cells. Taken together, RF-EMF at a low SAR level were not identified as a stimulus for C6 cells activation.

RF-EMF (GSM-900 signals) did not affect heat shock protein expression in nerve cells.

When used as a positive control, heat shock (43°C for 20 min) increased expression of hsp70 in all nerve cell cultures, i.e. human U87 astrocytoma cells, rat C6 glioma cells and human SH-SY5Y neuroblastoma cell lines. However, when exposed to GSM-900 for 24 hours, none of the cell line showed a significant change in expression of hsp70 (Figures 131, 132). Altogether, our data show that exposure to ELF-EMF does not seem to be able to induce Hsp70 expression in rat and human nerve cells.

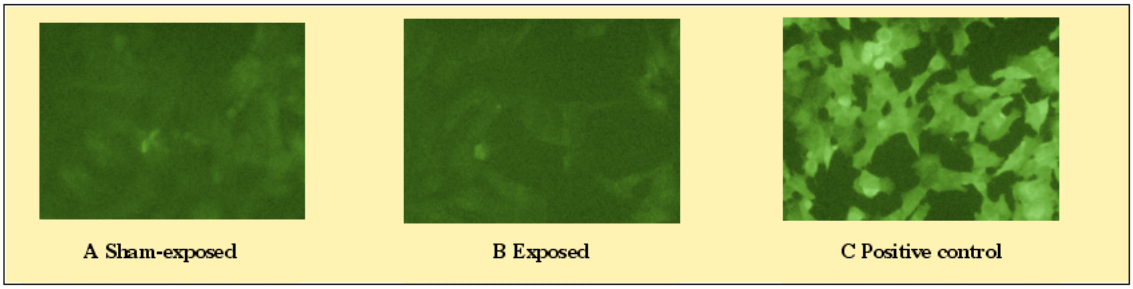

Figure 131. Fluorescent Hsp70 immunolabelling after sham-exposure or exposure of human SH-SY5Y neuroblastoma cells to frame GSM-900 signal at 2 W/kg for 24 hours (A and B) or to heat shock (43°C, 20 min) (C).

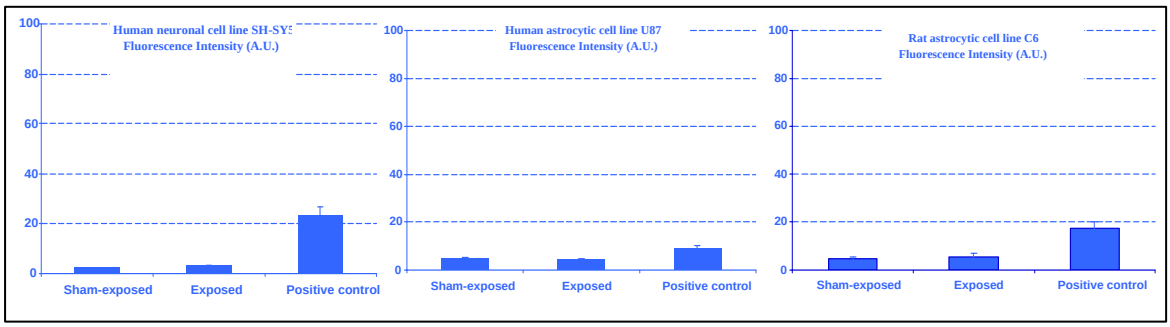

Figure 132. Effect of GSM-exposure (2 W/kg, 24h) or Heat Shock exposure (43°C, 20 min) (Positive control) on hsp70 expression in three different cell lines. Results are expressed in Fluorescence Intensity (A.U). Data from 3 independent experiments are presented as the Mean ± SEM

GSM-900 microwave exposure did not affect hsp27 expression in human endothelial cell line EA.hy926.

The hsp27 expression was measured using the immunofluorescence technique. Qualitative analysis did not allow for detecting any difference in fluorescence intensity in RFR exposed cells versus sham cells. Our quantitative results obtained after fluorescence image analysis of hsp27 expression in EA-hy926 revealed that no significant difference was observed between sham-or exposed cells in both cell lines (Figures 133, 134)

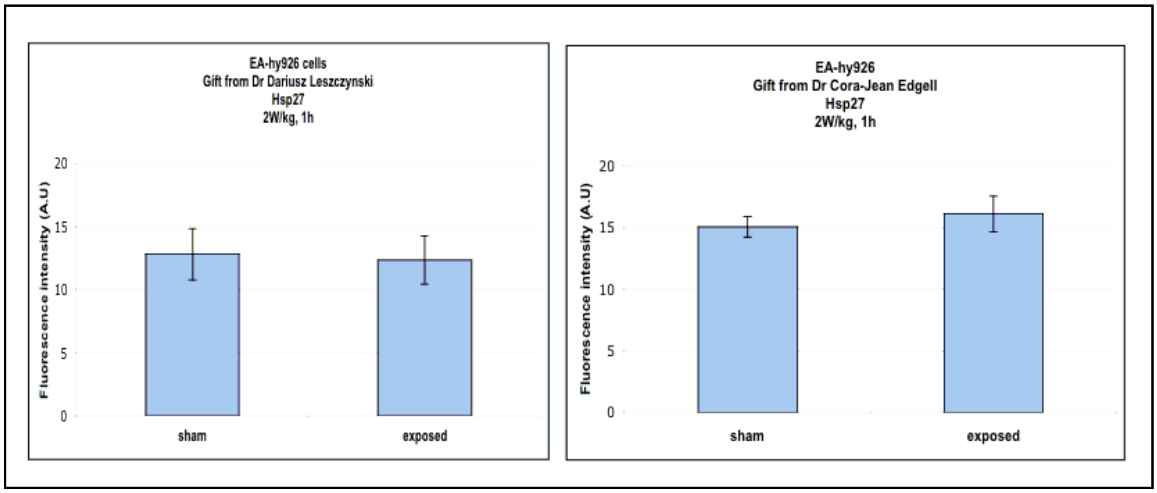

Figure 133. Effect of GSM-exposure (2 W/kg, 1 hour) on hsp27 in EA-hy926 cell lines given by Participant 6 and Dr Cora-Jean Edgell. Results are expressed as the fluorescence Intensity (A.U). Data from 5 independent experiments are presented as the Mean ± SEM.

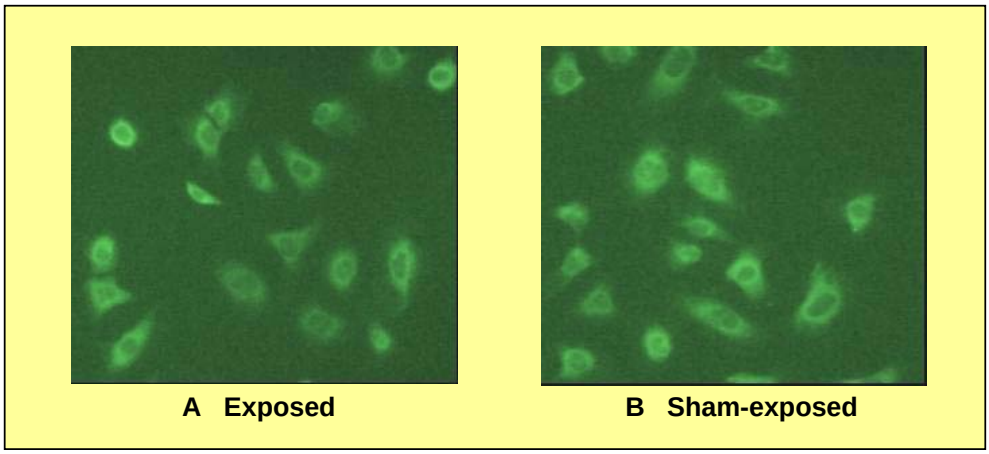

Figure 134. Fluorescent hsp27 immunolabelling after exposure(A) or sham-exposure(B) of EA-hy926 cell lines given by Participant 6 to GSM-900 signal at 2 W/kg for 1 hour.

A third method using Elisa test will allow us to quantify precisely if RFR are able to induce changes in hsp27 expression. However, with our method we were unable to confirm previous data on hsp27 expression in endothelial cell lines (Leszczynski et al., 2002). Therefore, we can not conclude that RFR induce stress response.

No conclusive data was obtained on the effect of RF-EMF exposure on Hsp27 expression in rat brain.

Table 28 shows results obtained on hsp27 expression in rat brains in the pilot experiment.

Results obtained on samples treated without perfusion show non-specific labelling disturbing the analysis. Results obtained on perfused brains show acceptable background noise. Image analysis obtained on perfused brains reveal conflicting and opposite results within groups preventing to draw conclusions.

Table 28. Hsp27 expression in rat brains

Experimental procedure	Background noise	Hsp27 labelling	Exposure conditions
Perfusion	-	+	Control
Perfusion	+	-	Control
Perfusion	-	-	Sham-exposed
Perfusion	-	+	Sham-exposed
Perfusion	-	-	Exposed
Perfusion	+	+/-	Exposed
Without perfusion	+	+	Control
Without perfusion	+	+	Control
Without perfusion	+	+/-	Sham-exposed
Without perfusion	+	++	Sham-exposed
Without perfusion	+	+	Exposed
Without perfusion	+	+/-	Exposed

– : negative labelling; + : positive labelling; +/- : negative or positive labelling depending of the area; +/+ : clear positive labelling

This pilot study did not allow us to draw conclusion on results obtained *in vitro* on hsp27 expression but it gave information on technical methodologies and on the number of animals to use.

RF-EMF (GSM-900) exposure weakly affected gene expression in immune cells.

This investigation was carried out in cooperation with Participant 12. Criteria for the selection of significantly altered gene expression was an exposed over sham ratio less than 0.5 for a significant decrease and more than 2.0 for a significant increase. Using these criteria, over 15588 human genes were detected, changes in expression of about 50 genes were significant corresponding to 0.3% of total number of detectable genes. Genes shown to be altered after RF-EMF exposure (increase or decrease) are known to be involved in signal transduction, ion electron transport, metabolism of energy and proteins, cell proliferation, apoptosis or differentiation, immune answer, inflammation, stress answer, extracellular matrix, cytoskeleton, adhesion and DNA repair. The largest modification in RNA expression corresponded to genes related to signal transduction (linked with GTP or calcium) and energy metabolism. Only a few genes involved in apoptosis or stress response were detected and show no significant sensitivity to RFR exposure. Concerning our purpose to investigate modification of genes involved in inflammatory response and processes, one gene corresponding to a component of major histocompatibilty complex class II and another acting as plasminogen activator were altered by RF-EMF. Finally, the largest increase of expression (30 fold increase), after mobile phone exposure, concerned genes described to participate in amine oxidase (copper containing) activity. This enzyme is involved in cell growth and proliferation but also in immune regulation.

3.2.4.6 Human endothelial cell lines EA.hy926 and EA.hy926v1 (Participant 6)

It has been suggested that high-throughput screening techniques (HTST) of transcriptomics and proteomics could be used to rapidly identify broad variety of potential molecular targets of RF-EMF and generate variety of biological end-points for further analyses (Leszczynski 2001). Combination of data generated by transcriptomics and proteomics in search for biological effects is called the “discovery science”. This term has been coined-in by Aebersold and co-workers (Aebersold et al. 2000) to define the new approach that will help in revealing biological mechanisms, some of which might be unpredictable using the presently available knowledge. This approach seems to be particularly suited for elucidation RF-EMF health hazard issue because it might reveal effects that are not possible to predict based on the present knowledge about the biological effects of RF-EMF. However, before committing large funds that are needed for HTST studies it is necessary to determine whether indeed this approach will be successful in unravelling physiologically significant biological events induced by RF-EMF. Due to their high sensitivity HTST are able to pick-up very small changes in protein or gene expression which changes might be of insufficient magnitude to alter cell physiology. Thus, although using HTST it might be possible to find biological effects induced by RF-EMF these effects might be of limited or no significance at all, from the physiological stand point. Therefore, to determine the usefulness of HTST approach to the issue of bio-effects induced by RF-EMF, we have performed a 5-step feasibility study and have shown that HTST might indeed help to identify experimental targets for physiological studies of RF-EMF-induced biological responses (Figure 135).

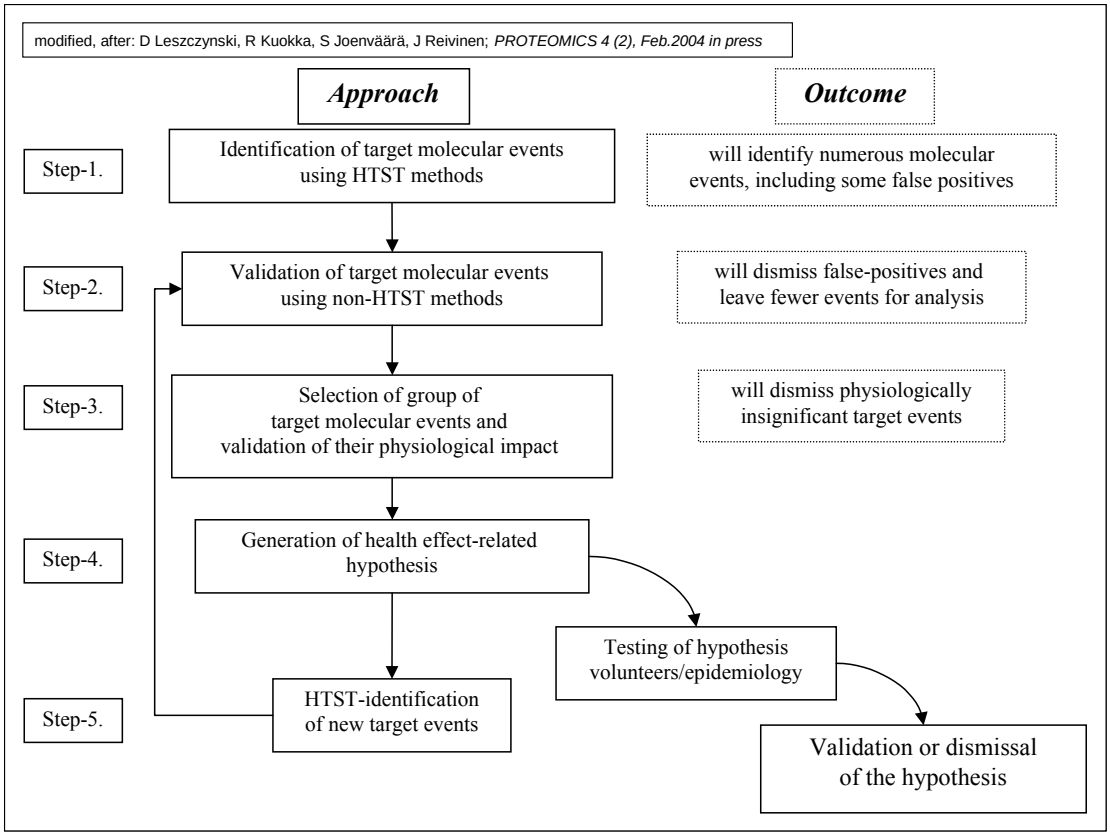

Figure 135. Scheme of experimental procedure which execution will elucidate new RF-EMF induced molecular events that might affect cell physiology. Events of magnitude sufficient to alter cell physiology could be then examined for their potential impact on the organ/whole body physiology in attempt to predict the extent of eventual health hazard.

A. The 5-step feasibility study

Step-1: HTST-identification of target molecular event

Firstly, we have determined the extent of cell response to RF-EMF (Leszczynski et al. 2002). This has been done by analysing global changes in the pattern of protein phosphorylation. As an experimental model we have used cultures of human endothelial cell line EA.hy926 (Edgell et al. 1983). Cells were exposed for 1 hour to 900MHz GSM mobile phone simulating signal at an average specific absorption rate (SAR) of 2.4 W/kg (Deli et al. 1995) that is slightly above the European safety limit (SAR=2.0 W/kg). In order to be able to determine changes in protein phosphorylation, the ^{32}P-labelled orthophosphate was present in the cell cultures during the 1 hour RF-EMF exposure period. Immediately after the end of exposure cells were harvested; proteins extracted and separated using standard two-dimensional electrophoresis (2-DE). Using PDQuest software (Bio-Rad, UK), some 1266 different protein spots were identified in silver-stained 2-DE gels (Figure 136A). Using autoradiography it was possible to determine that among the 1266 proteins spots, in non-irradiated control exposed cells, were detected some 110 phosphoproteins (Figure 136B), whereas in exposed cells were detected some 372 phosphoproteins (Figure 136C). The observed broad change in the pattern of global protein phosphorylation has suggested that cells respond to RF-EMF and that possibly any of the hundreds of phosphoproteins that have altered their phosphorylation status could, at least potentially, affect cell physiology. By using western blot or mass spectrometry, to identify the phosphoproteins present in the 2DE spots, it might be possible to find variety of protein targets that could be used in examining effects of mobile phone radiation on cell physiology. With this approach, the selection of molecular targets for further studies would not be based only on deduction of potentially affected events but on the knowledge of the identities of proteins that indeed respond to RF-EMF. Thus, in the continuation of Step-1, using

simple western blot screening with antibodies directed against various stress response proteins, we have identified hsp27 as one of the phosphoproteins responding to RF-EMF. Hsp27 is continuously expressed in endothelial cells (Edgell et al. 1983). In 2DE-western blots it appeared as two spots of 27kDa molecular weight but with different isoelectric points (pI=5.7 and pI=6.1) (Figure 136D). Only the $hsp27_{pI=5.7}$ isoform was phosphorylated and, following exposure to RF-EMF, the size of $hsp27_{pI=5.7}$-spot has increased (Leszczynski et al. 2002).

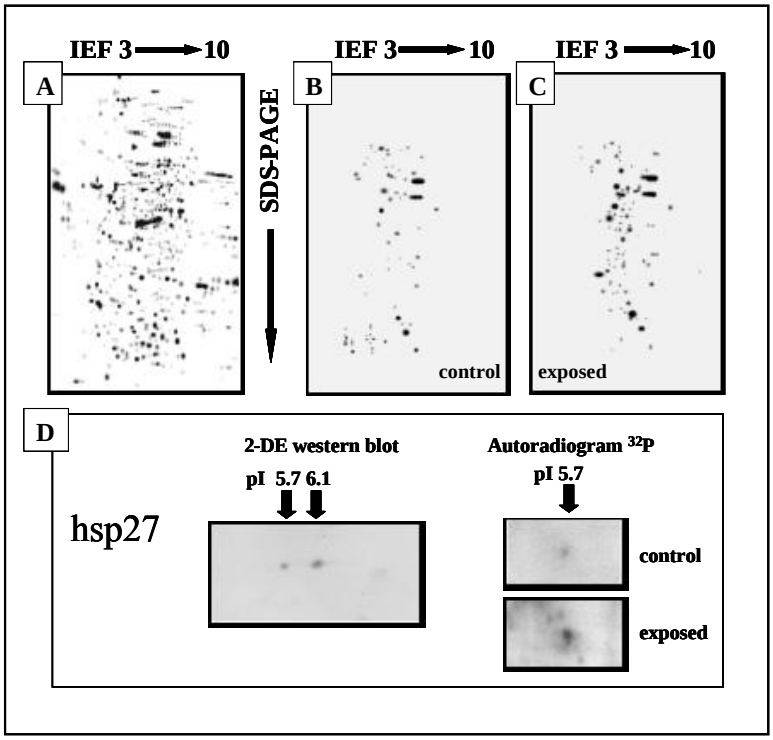

Figure 136. Identification of target molecular event for further studies – Step-1. Pattern of protein expression in EA.hy926 human endothelial cell line as determined by 2DE (panel A). Pattern of expression of ^{32}P-labeled phosphoproteins in control (panel B) and in exposed (panel C) cells. Hsp27 protein was identified, using 2DE western blot, as existing in EA.hy926 cells in two isoforms with different pI values (panel D-left). The pI 5.7 form was phosphorylated and its phosphorylation level has increased after RF-EMF exposure (panel D-right). For experimental details see Material and Methods section in Leszczynski et al. 2002.

Step-2: Validation of target molecular event

The change in phosphorylation status of hsp27 was confirmed in several ways to assure the validity of this observation (Leszczynski et al., 2002):

- immunoprecipitation of phosphorylated hsp27 (Figure 137A),
- immunoprecipitation of p38MAPK (Figure 137B), an up-stream kinase indirectly involved in phosphorylation of hsp27,
- inhibition of hsp27 phosphorylation by introduction to cell cultures of inhibitor of hsp27-up-stream kinase p38MAPK (SB203580) and determining hsp27 phosphorylation status by immunoprecipitation (Figure 137C).

Thus, in the Step-2 was confirmed that hsp27 is the valid molecular target event of the RF-EMF and that it is justified to further examine impact of this change on cell physiology.

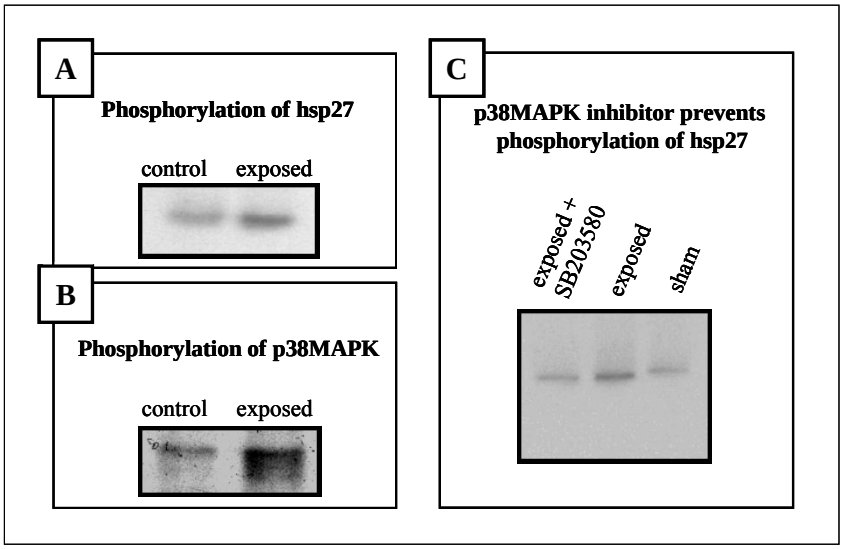

Figure 137. Validation of the target molecular event – Step-2. Increase in phosphorylation of hsp27 was confirmed by immunoprecipitation (panel A). Effect of p38MAP kinase on the RF-EMF-induced hsp27 phosphorylation was confirmed by determining, by immunoprecipitation, that p38MAPK is also activated by the RF-EMF exposure (panel B). As expected, presence of p38MAPK inhibitor, SB203580, in the culture medium during the exposure to RF-EMF, has prevented phosphorylation of hsp27 (panel C). For experimental details see Material and Methods section in Leszczynski et al. 2002.

Step-3: Cellular response – validation of the physiological event

Observed by us phosphorylation and increase in expression of hsp27 (Leszczynski et al. 2002) is a well-established mechanism of cell response to a broad variety of stress stimuli (Rogalla et al. 1999). Therefore, the observed by us doubling of Hsp27 expression and 2- to 7-fold increase in amount of phosphorylated hsp27 in cells (Leszczynski et al. 2002) have suggested that EA.hy926 cells have recognised RF-EMF as an external stress factor and that they have launched an hsp27-dependent counter response. Phosphorylation of hsp27 has been shown to regulate polymerisation of F-actin and stability of made of this protein - stress fibers (Landry and Huot 1995). Thus, we have examined status of the stress fibers in exposed cells by staining F-actin with AlexaFluor-labelled phalloidin. As shown in Figure 136A, RF-EMF exposure has caused increase in cellular staining with phalloidin what indicates increase in stability of F-actin stress fibers. The stability of stress fibers, as determined by the pattern of staining with phalloidin-AlexaFluor, increased after 1 hour irradiation and did not decline during the 1 hour of post-irradiation incubation. Induction of the stability of stress fibers caused cells to shrink and visible cell shrinking was observed among the cells brightly stained with AlexaFluor-phalloidin (Figure 138A; middle and right panels). The increase in the stability of stress fibers was prevented in the presence of p38MAPK inhibitor SB203580 (Figure 138B). Also it was possible to observe that in cells expressing high levels of hsp27 (Figure 138C), the cell edges were brightly stained with phalloidin-AlexaFluor, what indicates re-localisation of F-actin stress fibers to cell ruffles whereas in cells expressing low levels of hsp27, network of stress fibers was seen throughout the whole cytoplasm but not in the ruffles. Such behaviour of hsp27 and stress fibers in cells exposed to RF-EMF is in agreement with the general pattern of cellular response to stimuli that activate hsp27-dependent stress response (Landry and Huot 1995).

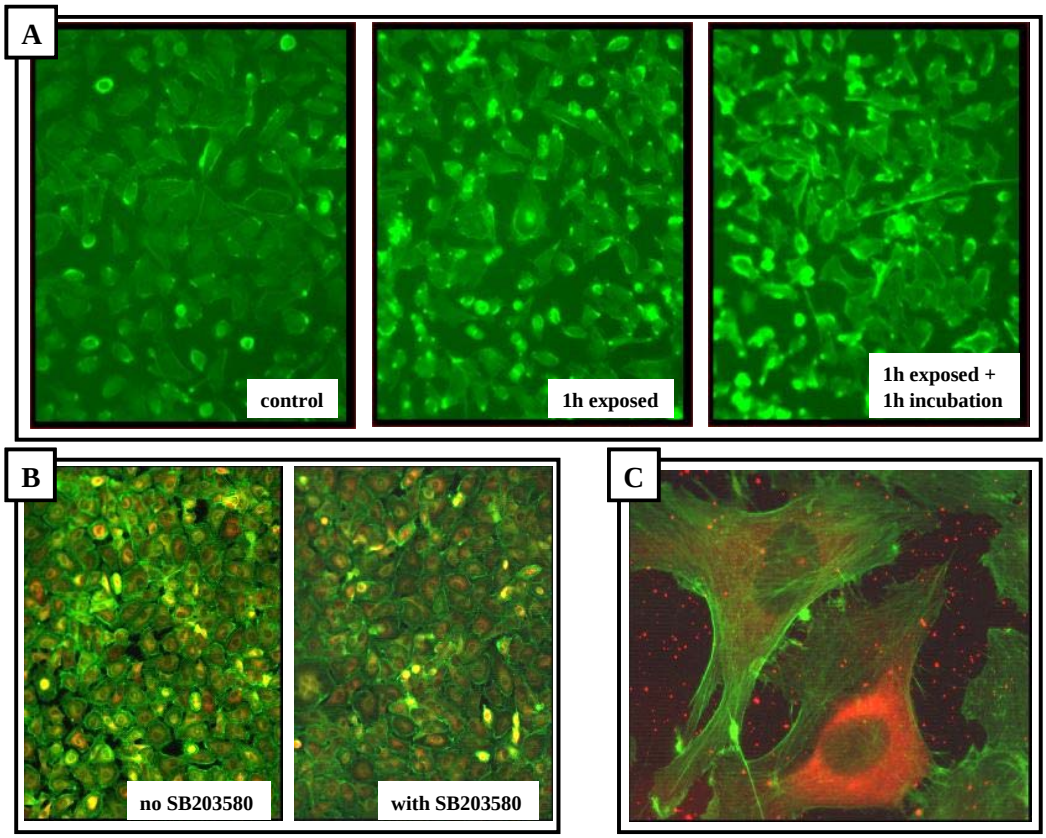

Figure 138. Cellular response to RF-EMF – validation of physiological event – Step-3.Exposure of cells to RF-EMF has caused increase in cell staining with AlexaFluor-labelled phalloidin (panel A). This suggests the increase in the expression/stability of F-actin, protein that forms cellular stress fibers. Rounding up is visible among the cells expressing highest F-actin content (the brightest staining with AlexaFluor-phalloidin). This effect persisted during the 1-hour post-exposure incubation of cells in control conditions. Presence of p38MAPK inhibitor, SB203580, in cell culture medium has prevented increase in AlexaFluor-phalloidin staining (panel B). Large magnification of cells shown in panel C demonstrates difference in distribution of AlexaFluor-phalloidin stained stress fibers (green colour) in cells with high (cell on the right) and low (cell on the left) content of hsp27 protein (indirect immunohistochemical staining; red fluorescence).

Step-4: Generation of hypothesis based on molecular and physiological events

The above results (Leszczynski et al. 2002) have formed basis and support for our working hypothesis (Figure 132, Step-4). Stabilisation of stress fibers and caused by it cell shrinking, when occurring in endothelial cells lining brain's capillary blood vessels, might be of importance for the functioning of blood-brain barrier. Stabilisation of stress fibers and cytoplasmic distribution of F-actin was previously shown to cause: (i) cell shrinkage (Landry and Huot 1995; Piotrowicz and Levin 1997a), that might lead to opening of spaces between cells, (ii) increase in the permeability and pinocytosis of endothelial monolayer (Deli et al. 1995; Lavoie et al. 1993), (iii) increase in formation of the so called "apoptosis-unrelated" blebs on the surface of endothelial cells (Becker and Ambrosio 1987), which eventually might obstruct blood flow through capillary blood vessels, (iv) stronger responsiveness of endothelial cells to estrogen and, when stimulated by this hormone, to secrete larger than normally amounts of basic fibroblast growth factor (bFGF) (Piotrowicz et al. 1997b) which might, in endocrine manner, stimulate de-differentiation and proliferation of endothelial cells and possibly led to the associated with cell's proliferative state - cell shrinkage and unveiling of basal membrane. Also, the activated (phosphorylated) hsp27 has been shown to inhibit apoptosis by forming complex with the apoptosome (complex of Apaf-1 protein, pro-caspase-9 and cytochrome *c*), or some of its components, and preventing proteolytic activation of pro-caspase-9 into active form of caspase-9 (Pandey et al. 2000; Concannon et al. 2001). This, in turn, prevents activation of pro-caspase-3 which is activated by caspase-9. Thus, induction of the

increased expression and phosphorylation of hsp27 by the RF-EMF exposure might lead to inhibition of the apoptotic pathway that involves apoptosome and caspase-3. This event, when occurring in RF-EMF exposed brain cells that underwent either spontaneous or external factor-induced transformation/damage, could support survival of the transformed/damaged cells. Therefore, based on the known cellular role of over-expressed/phosphorylated hsp27 we have proposed a hypothesis (Leszczynski et al. 2002) that: the activation (phosphorylation) of hsp27 by mobile phone radiation might be the molecular mechanism (i) regulating increase in blood-brain barrier permeability, which would explain, observed in some animal experiments, increase in blood-brain barrier permeability, and (ii) regulating apoptosis through interference with the cytochrome c/caspase-9/caspase-3 pathway (Figure 139). Thus, it is possible that the RF-EMF might have effect on cytoskeleton-related and on the apoptosis-related cell functions. This notion supports and justifies further examination of cytoskeleton and apoptosis related properties of RF-EMF exposed endothelial cells.

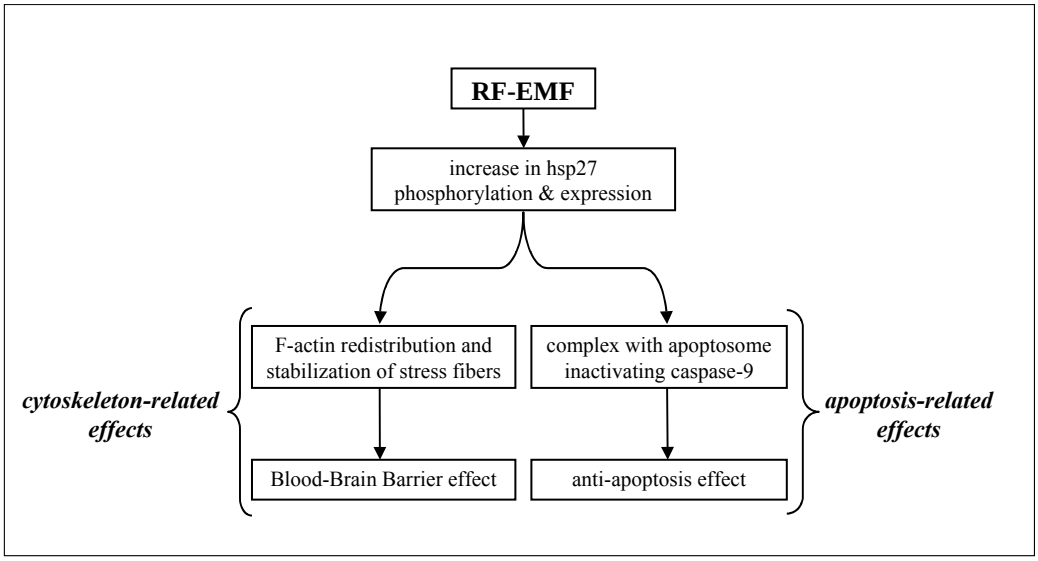

Figure 139. Hypothesis based on the molecular and physiological events – Step-4. Based on the known functions of hsp27 we have proposed that RF-EMF induced hsp27 phosphorylation might affect cell cytoskeleton and cell apoptosis. For full scheme and description of hypothesis see reference Leszczynski et al. 2002.

Step-5: HTST-identification of new target events, with support of hypothesis

Further experiments using HTST have revealed additional information pertinent to the cytoskeleton and apoptosis related properties of RF-EMF exposed endothelial cells.

The suggested changes in the cytoskeletal proteins were detected using 2-DE separated proteins. Approximately 1300 protein spots were detected 2-DE. Comparison of the control and exposed samples revealed some 49 protein spots which were statistically significantly (student T-test, $p<0.05$, $n=10$) affected by the exposure (increased or declined expression). Few of the spots were selected for the mass spectrometry identification using the following criteria: spots needed to be (i) enough separate from the adjacent spots, (ii) sufficiently large and (iii) well focused in all dimensions. Cytoskeletal proteins vimentins (Figure 140) and tubulin (not shown) were identified by mass spectrometry among the proteins that responded to RF-EMF. The suggested interference with apoptosis was further examined using cDNA Expression Arrays (Clontech) and screening expression of 3600 different genes. Among the genes that were down-regulated in cells exposed to RF-EMF were numerous genes encoding proteins of Fas/TNFα-apoptotic pathway (Figure 141). This pathway was suggested as target for the RF-EMF induced phosphorylated hsp27. Therefore, concomitantly observed increase in hsp27 phosphorylation, that is anti-apoptotic event, and down-regulation of proteins of Fas/TNFα apoptotic pathway suggest that further studies aiming at elucidation of RF-EMF effect on cell apoptosis are justified.

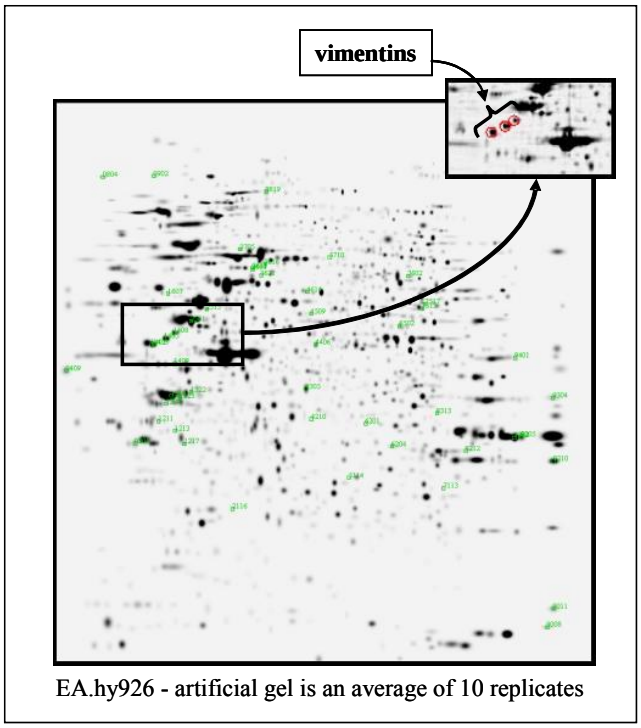

Figure 140. HTST-identification of new target events – cytoskeleton-related – Step-5. Using larger 2-DE gels (20x20 cm) and 10 replicates of each run we have identified some 49 proteins that, in statistically significant fashion, have altered their expression following RF-EMF exposure. Among the mass spectrometry identified spots were cytoskeletal proteins vimentins (inset) and tubulin (not shown).

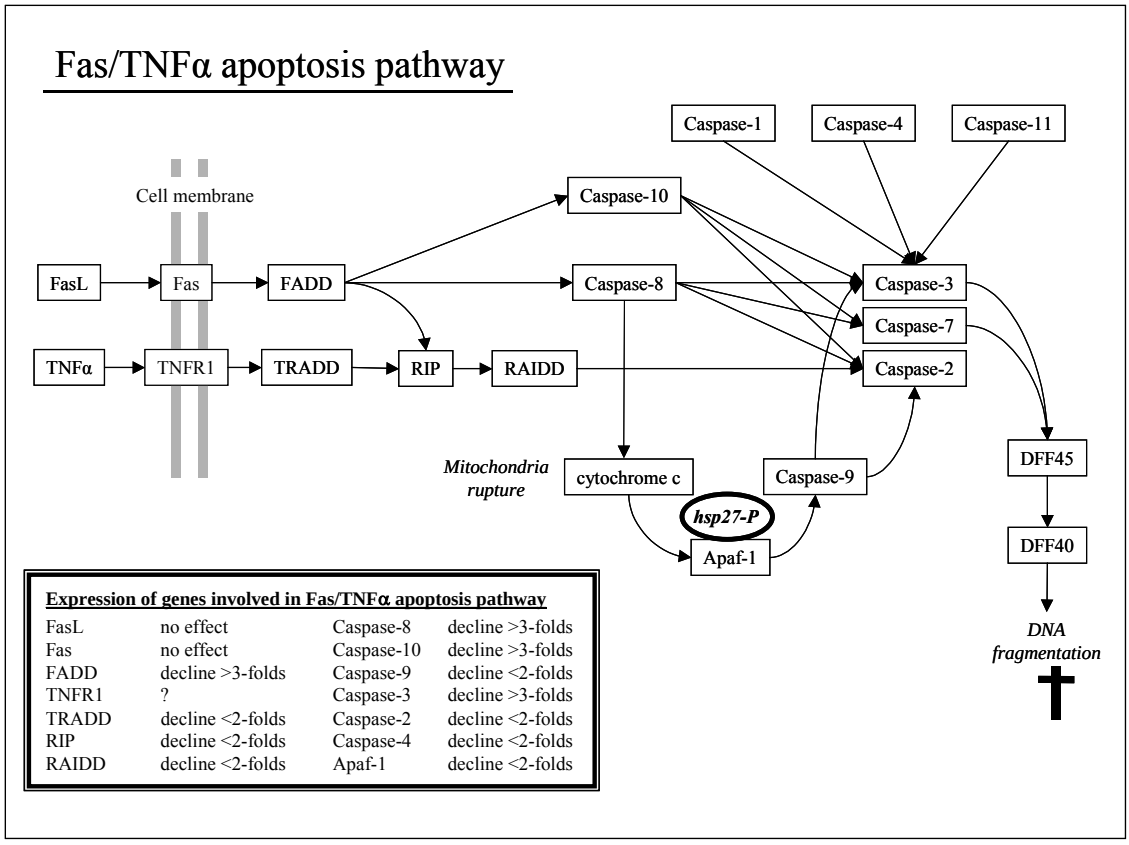

Figure 141. HTST-identification of new target events – apoptosis-related – Step-5. Analysis of RF-EMF-induced expression changes, using cDNA Expression Array for 3600 tumour-related genes, has revealed that the majority of genes that encode proteins forming Fas/TNFα apoptotic pathway are down-regulated (Table inset).

B. Genotype-dependent cell response to 900 MHz GSM radiation

We have compared response to mobile phone radiation of two human endothelial cell lines: fast proliferating EA.hy926 (Edgell et al., 1983) and its slow proliferating variant EA.hy926v1 (derived by sub-cloning from the EA.hy926 cell line).

Proteomics approach

Using 2-DE and MALDI-MS proteomics approach we have determined what proteins respond to the mobile phone radiation. Using PDQuest 6.2 software (Bio-Rad, UK) the 2-DE artificial gels (Figure 135) were generated from 10 independent protein samples from ten independent replicates of controls and irradiated cell cultures. The protein expression pattern in ten replicate control samples was then compared with the protein pattern in ten replicate irradiated samples. The normalised spot volumes of the proteins from control and exposed sample gels were statistically analysed using student t-test at the confidence level of 95%. The most striking observation was that the comparison in-between the two cell lines showed that their protein expression patterns are very different in spite of the closely related origin of both cell lines (Figures 142A, 142B). Only approximately half of all of the protein spots could be matched confidently between the cell lines. This difference in protein expression pattern might explain the observed differences in the growth rate between the cell lines. Because of the observed differences in the protein expression and proliferation between the cell lines, it was not a surprise that the response to the mobile phone radiation also varied between EA.hy926 and EA.hy926v1 cell lines. The comparison of the exposed and control samples has shown several tens of protein spots with radiation-induced statistically significant change in expression levels (t-test $p<0.05$). In EA.hy926 cell line there were 38 of protein spots which expression was altered by the radiation exposure (Figure 142A) whereas in EA.hy926v1 cell line there were 45 differentially expressed protein spots (Figure 142B). The identity of

the all radiation-responding protein spots is being determined by MALDI-MS and will be reported in due time.

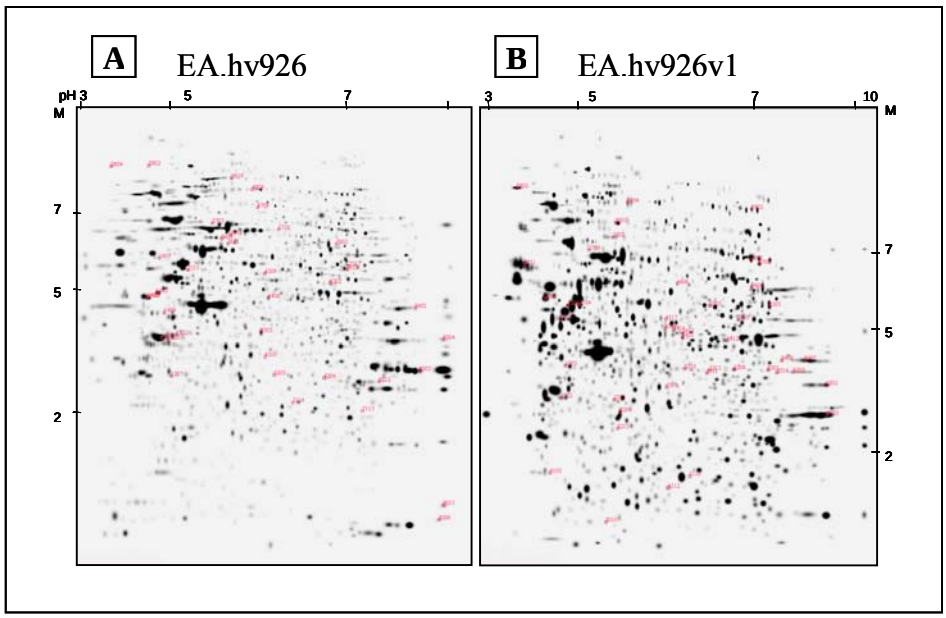

Figure 142. 2-DE gels of proteins extracted from human endothelial cell lines; EA.hy926 (A) and EA.hy926v1 (B). The 1st dimension IEF using pH gradient 3-10 NL, 2nd dimension 8% SDS-PAGE. Statistically significantly (t-test $p<0.05$) differing spots in the cell lines are numbered using PDQuest SSP numbers.

(A) EA.hy926 cell line - 38 statistically significantly differing spots. Four spots: vimentin (1402 and 1405), isocitrate dehydrogenase 3 (NAD+) alpha (4305), and heterogeneous nuclear ribonucleoprotein H1 (4406), were identified using mass spectrometry.

(B) EA.hy926v1 cell line; 45 statistically significantly differing spots.

Few of the protein spots, which expression was statistically significantly altered by the irradiation, were identified using MALDI-MS (Figure 143). In order to increase probability of a single protein present in the single spot, the protein spots that were selected for MALDI-MS analysis had to fulfil the following requirements: (i) spots were well separated from other spots in both 2-DE dimensions, (ii) spots were sufficiently large (Figure 143A). The MALDI-MS analysis service was purchased from the Protein Chemistry Laboratory of the Institute of Biotechnology at the Helsinki University, Finland. The selected spots were reduced with DTT and alkylated with iodoacetamide before overnight digestion with a sequence-grade modified trypsin (Roche, France). The peptide mixture was concentrated and desalted using Millipore ZipTip™ µ-C18 pipette tips. The peptide mass fingerprints were measured with Bruker Biflex™ MALDI-ToF mass spectrometer in a positive ion reflector mode using α-cyano-4-hydroxycinnamic acid as a matrix. The database searches were performed using ProFound and Mascot searches. The protein spots that were identified with MALDI-MS were as follows (Figure 143):

- Protein spot 4305 - isocitrate dehydrogenase 3 (NAD+) alpha (Kim et al. 1995) is a subunit of the mitochondrial enzyme, which catalyses the conversion of isocitrate to 2-oxoglutarate in the citric acid cycle. The expression level of this protein was moderately down-regulated in the exposed samples having a ratio exposed vs. control 0.72 with the p-value of 0.03. The down-regulation of this protein might affect cellular energy production.
- Protein spot 4406 - heterogeneous ribonucleoprotein H1 (Honore et al. 1995) is a component of the heterogeneous nuclear ribonucleoprotein (HNRNP) complexes which provide a substrate for the processing events which pre-mRNAs go through before becoming functional mRNAs in the cytoplasm. The expression level of this protein is slightly down-regulated in the exposed samples with a ratio exposed vs. control 0.61 with the p-value 0.03. The potential down-regulation of this protein might affect protein translation process.

- Protein spots 1402 and 1405 - vimentin (Ferrari et al. 1986) is a protein component of class III-intermediate filaments. In EA.hy926 cells it was found to be expressed in at least two different iso-forms differing in molecular weight and isoelectric point. Both vimentin iso-forms were up-regulated; spot 1402 (experimental MW/pI ca. 47 kDa/4.4) by 2.5-fold with p-value of 0.006 and spot 1405 (experimental MW/pI ca. 48kDa/4.8) by 2.2-fold with p-value of 0.02.

A

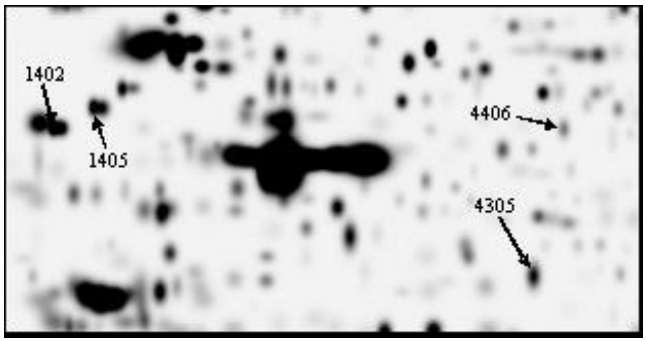

B

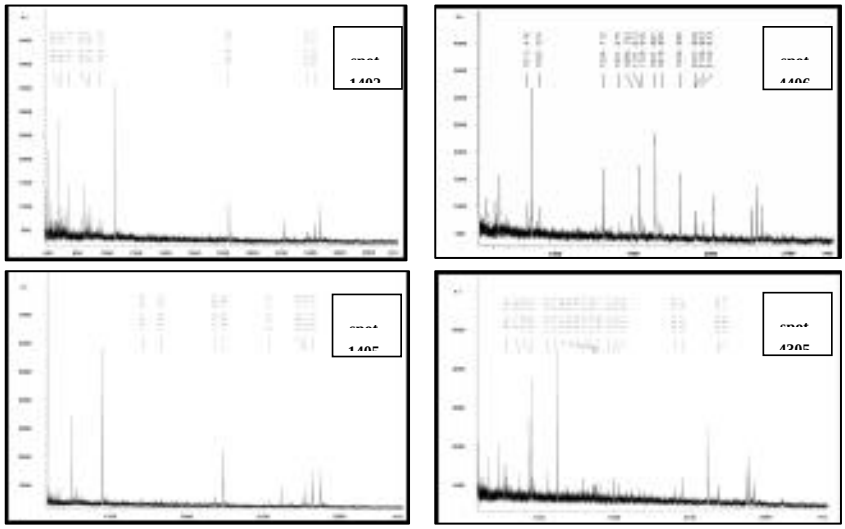

C

SSP	Protein name	Swiss-prot ID code	Sequence coverage	Swiss-prot annotations
4305	Isocitrate dehydrogenase 3 (NAD+) alpha	P50213	21%	component of enzyme complex catalysing conversion of isocitrate to 2-oxoglutarate
4406	Heterogeneous nuclear ribunocleoprote in H1	P31943	34%	component of HNRNP complex providing a substrate for pre-mRNA processing
1402	vimentin	P08670	19%	class III-intermediate filament
1405	vimentin	P08670	14%	class III-intermediate filament

Figure 143. (A) Fragment of the 2-DE gel of EA.hy926 cells with marked spots that were identified with MALDI-MS. (B) MALDI-MS spectra showing peptide finger prints of the four identified protein spots. (C) Table summarising the properties of the identified proteins**.**

Alterations in the vimentin expression suggest that some form of cytoskeletal response might be taking place in cells exposed to the mobile phone radiation. This notion agrees with our earlier observation of the effect of the mobile phone radiation on the stability of F-actin stress fibers (Leszczynski et al. 2002; Leszczynski et al. 2004). Changes in the vimentin expression observed in 2-DE were further confirmed by SDS-PAGE and western blotting and by cell staining using indirect immunofluorescence method. For SDS-PAGE/western blotting a standard protocol was used. Briefly, the cell lysates were separated using 7.5% SDS-PAGE, blotted to PVDF-membrane, blocked with 5% non-fat dry milk and exposed to the primary vimentin antibody (Zymed, USA) and the secondary antibody containing a HRP-conjugate (Dako, Denmark). The signal was detected using enhanced chemiluminescence (Pierce, UK). For immunocytochemistry cell were fixed in 3% paraformaldehyde, membranes were permeabilised in 0.5% Triton X-100 and as a primary antibody was used vimentin antibody (Zymed, USA) and the secondary antibody was TRICT-conjugated (Dako, Denmark). The images were captured using a Leitz fluorescence microscope and computerised image acquisition system (Metafer, Germany).

SDS-PAGE and western blot have confirmed that EA.hy926 cells express two iso-forms of vimentin. The higher molecular weight form (experimental MW ca. 57 kDa) was present both in control and in irradiated cells and its expression was not affected by the irradiation (Figure 144A). The lower molecular weight vimentin (experimental MW ca. 48 kDa) was not detectable in the non-irradiated cells but was expressed in the irradiated cells (Figure 144B). Indirect immunohistochemistry staining of vimentin has shown the change in the distribution pattern of the vimentin filaments after the exposure to the mobile phone radiation (Figure 143C, 143D). Together, the observed changes in the vimentin expression suggest that the mobile phone radiation might potentially alter cell physiology by affecting cellular cytoskeleton.

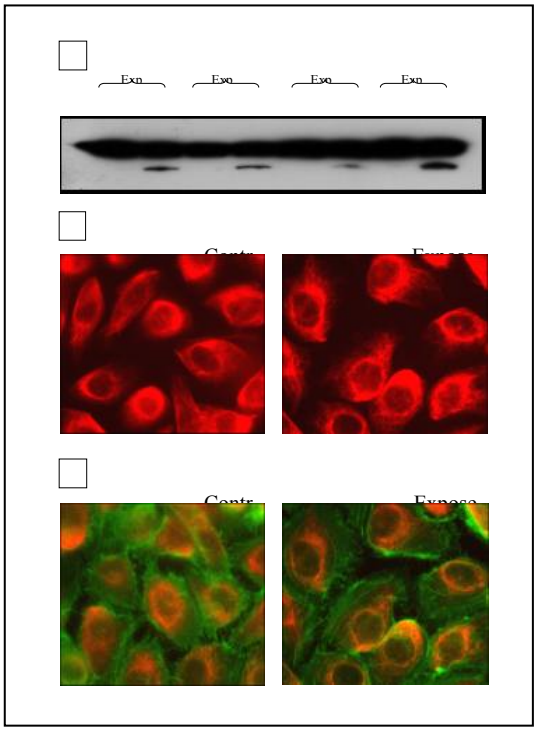

Figure 144. (A) Western blot-detected expression of vimentin in non-irradiated EA.hy926 cells (C-lanes) and in exposed cells (RF-lanes). MW ca. 57 kDa and ca. 48 kDa. Four separate experiments are shown. (B) Immunostaining of vimentin in non-exposed and in exposed EA.hy926; red colour – vimentin. Note diffuse-like staining for vimentin in non-exposed cells as compared with more filament-like expression in exposed cells.(C) Immunostaining of vimentin (red colour) and F-actin stress fibers (green colour) in non-exposed and in exposed EA.hy926. F-actin was detected with phalloidin-AlexaFluor. Note diffuse-like staining for both vimentin and F-actin in non-exposed cells as compared with more filament-like expression in exposed cells.

Transcriptomics approach

Using cDNA Expression arrays (Clontech, USA) we have determined that number of genes increased/declined expression in both cell lines following the exposure to mobile phone radiation (900 MHz GSM). Most strikingly, genes that were up regulated in one of the cell lines were down-regulated or not affected in the other cell line (Tables 29, 30, and 31). It suggests that the cell response might depend on the genotype.

Table 29. Genes which were up-regulated in EA.hy926 cell line following to the exposure to the 900 MHz GSM.

Gene name	**EA.hy926 (*fast proliferating*)**		**EA.hy926v1 (*slow proliferating*)**	
Increased expression in EA.hy926	**Ratio RF/sham**	**Difference RF-sham**	**Ratio RF/sham**	**Difference RF-sham**
proliferating cell nucleolar antigen P120; NOL1	**29,71**	**18734**	**0,38**	**-6343**
Homo sapiens mRNA for beta 2-microglobulin	**14,70**	**3895**	**0,50**	**-5312**
MCM7 DNA replication licensing factor; CDC47 homolog; p1.1-MCM3	**12,18**	**9029**	**0,98**	**-172**
zinc-finger protein (ZNFPT7) (fragment).	**8,43**	**15053**	**0,46**	**-2512**
chloride conductance regulatory protein ICLN; nucleotide-sensitive chloride channel 1A; chloride ion current inducer protein (CLCI); reticulocyte PICLN	**5,37**	**16944**	**0,79**	**-1686**
HHR23A; UV excision repair protein protein RAD23A	**4,42**	**20499**	**0,66**	**-7485**
ferritin heavy chain (FTH1); FTHL6	**4,30**	**6961**	**0,93**	**-2435**
CD166 antigen precursor (activated leukocyte-cell adhesion molecule) (ALCAM).	**4,09**	**3184**	**0,70**	**-2869**
nucleolar phosphoprotein B23; nucleophosmin (NPM); numatrin	**3,89**	**50540**	**0,97**	**-1699**
annexin IV (ANX4); lipocortin I; calpactin II; chromobindin 9; phospholipase A2 inhibitory protein	**3,68**	**7176**	**4,20**	**15254**
N4-(beta-N-acetylglucosaminyl)-L-asparaginase precursor (EC 3.5.1.26) (glycosylasparaginase) (aspartylglucosaminidase) (N4-(N-acetyl-beta-glucosaminyl)-L-asparagine amidase) (AGA).	**3,63**	**13266**	**0,55**	**-1060**
glial growth factor 2 precursor (GGFHPP2); neuregulin; heregulin-beta3 + neu differentiation factor + heregulin-alpha	**3,53**	**21908**	**0,70**	**-3070**
serine/threonine protein phosphatase PP1-alpha 1 catalytic subunit (PP-1A)	**3,31**	**7521**	**1,08**	**1402**
flavin reductase (EC 1.6.99.1) (FR) (NADPH-dependent diaphorase) (NADPH-flavin reductase) (FLR) (biliverdin reductase B) (EC 1.3.1.24) (BVR-B) (biliverdin-IX beta-reductase) (green heme binding protein) (GHBP)	**3,17**	**15395**	**0,77**	**-2827**
cytochrome c	**2,97**	**12337**	**0,82**	**-2047**
DNA-directed RNA polymerase II 19 kD polypeptide (EC 2.7.7.6) (RPB7).	**2,88**	**12043**	**0,88**	**-1360**

Table 30. Genes which were down-regulated in EA.hy926 cell line following to the exposure to 900 MHz GSM.

Gene name	EA.hy926 (*fast proliferating*)		EA.hy926v1 (*slow proliferating*)	
Decreased expression in EA.hy926	**Ratio RF/sham**	**Difference RF-sham**	**Ratio RF/sham**	**Difference RF-sham**
pyruvate kinase M2 isozyme (PKM2)	**0,33**	**-6273**	**0,90**	**-2490**
RAD51-interacting protein	**0,31**	**-3405**	**0,79**	**-510**
glutathione S-transferase mu1 (GSTM1; GST1); HB subunit 4; GTH4	**0,29**	**-3486**	**1,59**	**599**
glutathione S-transferase A1 (GTH1; GSTA1); HA subunit 1; GST-epsilon	**0,29**	**-4095**	**0,36**	**-2545**
early growth response protein 1 (hEGR1); transcription factor ETR103; KROX24; zinc finger protein 225; AT225	**0,28**	**-4223**	**0,54**	**-1932**
caspase-3 (CASP3); apopain precursor; cysteine protease CPP32; YAMA protein; SREBP cleavage activity 1; SCA-1	**0,27**	**-5844**	**1,04**	**79**
calpain 2 large (catalytic) subunit; M-type calcium-activated neutral proteinase (CANP)	**0,27**	**-3464**	**0,95**	**-1210**
ras-related C3 botulinum toxin substrate 1; p21-rac1; ras-like protein TC25	**0,26**	**-6905**	**1,10**	**730**
alpha-actinin 1 cytoskeletal isoform; F-actin cross linking protein	**0,25**	**-5276**	**0,82**	**-2597**
ras-related protein RAB-11B; YPT3	**0,24**	**-2870**	**0,79**	**-3643**
DNA ligase I; polydeoxyribonucleotide synthase (ATP) (DNL1) (LIG1)	**0,22**	**-2969**	**0,38**	**-2497**
ATP synthase lipid-binding protein P2 precursor (EC 3.6.1.34) (ATPase protein 9) (subunit C)	**0,19**	**-4520**	**0,80**	**-1486**
EDF-1 protein	**0,14**	**-6951**	**0,68**	**-2931**
coatomer delta subunit; delta-coat protein; delta-COP; archain (ARCN1)	**0,14**	**-4280**	**n/a**	**n/a**
nuclear transport factor 2 (NTF-2) (placental protein 15) (PP15).	**0,14**	**-2836**	**0,65**	**-2155**
fascin (actin bundling protein).	**0,14**	**-16072**	**0,54**	**-6852**
neurogranin (NRGN); RC3	**0,11**	**-18728**	**0,86**	**-2175**
MYLE	**0,11**	**-4959**	**0,81**	**-539**
sepiapterin reductase (EC 1.1.1.153) (SPR).	**0,10**	**-3467**	**0,63**	**-1123**
caspase-8 precursor (CASP8); ICE-like apoptotic protease 5 (ICE-LAP5); MORT1-associated CED-3 homolog (MACH); FADD-homologous ICE/CED-3-like protease (FADD-like ICE; FLICE); apoptotic cysteine protease MCH-5	**0,05**	**-3359**	**1,90**	**1080**

Table 31. Genes which were affected in EA.hy926v1 cell line following to the exposure to 900 MHz GSM.

Gene name	EA.hy926v1 *(slow proliferating)*		EA.hy926 *(fast proliferating)*	
Increased expression in EA.hy926v1	**Ratio RF/sham**	**Difference RF-sham**	**Ratio RF/sham**	**Difference RF-sham**
procollagen C-proteinase enhancer protein precursor.	**9,58**	**10373**	**1,09**	**5589**
HOMER-3.	**9,45**	**3027**	**0,98**	**-25**
T-lymphoma invasion and metastasis inducing TIAM1	**5,55**	**6554**	**0,01**	**-1335**
elafin precursor (elastase-specific inhibitor) (ESI) (skin-derived antileukoproteinase) (SKALP).	**5,33**	**10720**	**1,53**	**12919**
mitochondrial matrix protein P1 precursor; p60 lymphocyte protein; chaperonin homolog; HUCHA60; heat shock protein 60 (HSP-60); HSPD1	**4,43**	**8459**	**1,00**	**-89**
proteasome component C8; macropain subunit C8; multicatalytic endopeptidase complex subunit C8	**4,06**	**5029**	**1,10**	**5254**
special AT-rich sequence binding protein 1 (SATB1); MAR/SAR DNA-binding protein	**3,48**	**11151**	**0,99**	**-222**
HLA class I histocompatibility antigen C-4 alpha subunit (HLAC)	**3,12**	**2805**	**0,64**	**-1344**
ras-related protein RAP-1B; GTP-binding protein SMG p21B	**3,04**	**4820**	**63,80**	**2512**
phospholipase A2; tyrosine 3-monooxygenase/tryptophan 5-monooxygenase activation protein zeta polypeptide (YWHAZ); 14-3-3 protein zeta/delta; protein kinase C inhibitor protein 1 (KCIP1); factor activating exoenzyme S (FAS)	**2,93**	**4033**	**1,14**	**767**
Decreased expression in EA.hy926v1				
tuberin; tuberous sclerosis 2 protein (TSC2)	**0,33**	**-7082**	**0,42**	**-16846**
KIAA0115; dolichyl-diphosphooligosaccharide protein glycosyltransferase 48-kDa subunit precursor; oligosaccharyl transferase 48-kDa subunit; HA0643	**0,27**	**-3494**	**0,19**	**-1968**
sodium channel beta-1 subunit precursor (SCN1B)	**0,27**	**-2842**	**0,00**	**-1846**
embryonic growth/differentiation factor 1 (GDF1) + UOG-1	**0,21**	**-3542**	**0,00**	**-702**
SH3P18 SH3 domain-containing protein	**0,05**	**-3389**	**0,00**	**-949**

C. Comparison of the effect of CW and modulated RF-EMF on protein expression

Using cICAT method combined with liquid-phase chromatography and mass spectrometry we have compared protein expression changes in cells exposed either to continuous wave or to radiofrequency modulated ("talk" signal) RF-EMF (1800 MHz GSM). The cICAT reagent labelled samples were analysed using an automated mass spectrometric approach in which those proteins showing abundance differences between the two conditions being compared were selectively identified. In total, 58 unique proteins were identified and determined to show significant changes in abundance using this approach. These proteins were selected for identification by MS/MS analysis based upon the criteria that the measured abundance ratios ($C^{13}(0)/C^{13}(9)$) were either >1.7 or <0.60. The average abundance ratio for all detected cICAT reagent labelled peptide pairs (n=1476) was 1.26 +/-0.38, indicating that the vast majority of proteins within the two samples did not change in abundance. Peptides detected as singlets (i.e. having no corresponding $C^{13}(0)$ or $C^{13}(9)$ signal) were also selected for MS/MS analysis. The threshold abundance ratio values were selected based on the following criteria: 1) In relation to previously described errors of quantitative measurements using the ICAT reagent, these values represent conservative estimates of significant abundance changes; 2) These values are significant outliers relative to the average and median $C^{13}(0)/C^{13}(9)$ values for this dataset. The average $C^{13}(0)/C^{13}(9)$ value for all detected cICAT reagent labelled peptides (n = 1476) was 1.26 +/-0.38, and the median was 1.19. The threshold values for significant changes in abundance are therefore well outside the standard deviation for this dataset. Furthermore, the fact that the average and median values are close to one indicates the accuracy of the quantitative measurements used here, as it is expected that the majority of proteins will be constitutively represented, giving ratios close to one.

In conclusion it appears that the "talk" signal has caused increase in expression of a variety of proteins whereas CW did not (Table 32). It suggests that the modulation might have impact on cell response to RF-EMF.

Table 32. List of proteins induced by "talk" signal but not by the CW signal.

Protein name	Accession No.	$C^{13}(0)/C^{13}(9)$	Confidence score
serine-threonine protein kinase	NP_055212	1.9	0.996
GP:AF090929_1		1.8	0.912
RING finger protein 20	AAK58539	2.0	0.958
Homo sapiens cDNA FLJ20303	AK000310	2.4	0.957
hypothetical protein FLJ20420	NP_060282	2.0	0.984
fatty-acid synthase	PIR:G01880	2.2	0.993
hypothetical protein DKFZp434G171.1	T42678	1.9	0.855
hypothetical protein DKFZp564N1563.1 (2)	T46270	0.5	0.921
Serine/threonine protein phosphatase 2A	Q15173	1.8	0.950
Beta-adaptin 1	Q10567	2.0	0.813
Actin-like protein 2	O15142	2.0	0.993
Sarcoplasmic/endoplasmic reticulum calcium ATPase 2 (2)	P16615	1.9	0.944
CD59 glycoprotein precursor (6)	P13987	2.4	0.995
Chloride intracellular channel protein 1	O00299	2.7	0.997
Cellular nucleic acid binding protein (2)	P20694	2.2	0.980
Cofilin, non-muscle isoform	P23528	1.7	0.990
Coatomer alpha subunit	P53621	2.4	0.997
Coatomer beta subunit	P53618	2.0	0.993
Cleavage and polyadenylation specificity factor	Q9P2I0	1.9	0.994
Cyclophilin A (3)	P05092	2.2	0.975
Destrin (Actin-depolymerizing factor)	P18282	1.7	0.990
Aspartyl aminopeptidase	Q9ULA0	1.8	0.993
D-dopachrome tautomerase	P30046	1.7	0.952
Elongation factor 2	P13639	2.0	0.982
Alpha enolase	P06733	2.1	0.981
Fatty acid synthase (2)	P49327	2.1	0.975
Filamin A (2)	P21333	2.5	0.975
FL cytokine receptor precursor	P36888	1.9	0.970
Follistatin-related protein 1 precursor Q12841	Q12841	1.7	0.942
PROTEIN KINASE C SUBSTRATE	P14314	1.7	0.984
Transducin beta chain 1	P04901	1.9	0.993
Transducin beta chain 2	P11016	1.8	0.964
Guanine nucleotide-binding protein beta subunit-like protein (3)	P25388	2.9	0.998
Stress-induced-phosphoprotein 1	P31948	2.2	0.993
Pyruvate kinase, M1 isozyme	P14618	1.9	0.983
LAM2_HUMAN, partial CDS	AAC34573	0.6	0.994
Galectin-1 (3)	P09382	1.9	0.996
Myosin heavy chain, nonmuscle type A	P35579	0.6	0.996
Myoferlin (2)	Q9NZM1	2.9	0.940
NHP2-like protein 1 (3)	P55769	3.6	0.980
Nitric-oxide synthase, endothelial (2)	P29474	2.0	0.990
Purine nucleoside phosphorylase (2)	P00491	1.9	0.997
40S ribosomal protein S27a	P14798	3.0	0.974
Heterogeneous nuclear ribonucleoprotein D0	Q14103	3.0	0.984
Heterogeneous nuclear ribonucleoprotein K	Q07244	2.6	0.880
Heterogenous nuclear ribonucleoprotein U	Q00839	2.1	0.992
ribosomal protein S2 (2)	P15880	1.8	0.940
40S ribosomal protein S3a	P49241	2.1	0.991
Splicing factor, arginine/serine-rich 9	Q13242	2.0	0.986
Tubulin beta-2 chain	P05217	2.8	0.998
T-complex protein 1, theta subunit (2)	P50990	4.9	0.995
Transcription intermediary factor 1-beta	Q13263	2.3	0.995
Thioredoxin	P10599	2.1	0.935
Hypothetical UPF0123 protein BK223H9.2	Q9UH06	2.1	0.994
Splicing factor U2AF 35 kDa subunit (2)	Q01081	2.4	0.945
Ubiquitin-activating enzyme E1	P22314	1.8	0.963
Zinc finger protein 147	Q14258	3.7	0.995
Nuclear pore complex protein Nup133	Q8WUM0	2.3	0.914

3.2.4.7 Whole-genome analysis of various cell lines exposed to RF-EMF (Participant 12)

Altogether, 58 whole-genome analyses of 10 different cell lines (sham-exposed cells and control cells) were performed (Table 1). After primary data analysis, we only worked on genes which were reproducibly regulated in several experiments (see materials and methods) and which belonged to certain gene families (Table 33). We defined gene families which are potentially relevant for the cellular answer on EMF exposure: signal transduction, ion/electron transport, metabolism of energy/proteins, cell proliferation/apoptosis, immune answer/inflammation and extracellular matrix/cytoskeleton. Each gene family was sub-divided in subgroups again, e.g. GTP proteins in the signal transduction family (Tables 33, 11). In a first step, we did not go into single genes, but simply counted genes up- or down-regulated in the different gene families. The total number of regulated genes in a certain gene family is not very meaningful, because the sizes of the gene families are of course very different. Therefore, the total numbers of genes on the human array belonging to a gene family are shown in the first column of Tables 33 and 11. Although a single gene might appear in different categories (e.g. all small G proteins are GTP binding proteins), the tables give a good overview on what might happen in the cells after EMF exposure on the molecular level.

Although appearing regulated in all experiments, mitochondrial genes, ribosomal genes and cell cycle genes especially showed a high rate of regulation in the some RF-EMF experiments (U937 human monocytic cells and microglia cells, Participant 9; HL-60 human hematopoietic leukemia cells, Participant 2).

Moreover, the bio-statistical analysis of RF-EMF experiments (Participant 8, Dr. Remondini) allowed some interesting conclusions from the experiments with HL-60 cells (Participant 2), endothelial cells (Participant 6) and U937 cells (Participant 8, Table 34). Again, the regulation of mitochondrial and ribosomal genes was evident with this analysis. Most of the regulated genes in endothelial cells appear in the groups of ATP-associated genes (energy metabolism), transcription, and cytoskeleton. Remarkably, compared to ELF-EMF experiments, we find more up-regulated genes in RF-EMF experiments (Table 34, see also Table 12). However, the results do have to be interpreted in more detail, because down-regulation of a special gene does not mean that the respective process is down-regulated as well (for example, down-regulation of Bcl-2 might lead to up-regulation of apoptosis).

For T-lymphocytes (Participant 8) and microglia cells (Participant 9) the bio-statisitical analysis did not reveal significant data.

In detail, the following genes were extracted by bio-statistics so far:

Actin associated proteins (belong to cytoskeleton):
- Caldesmon (tropomysin binding, actin binding. Activation of ERK MAP kinases lead to phosphorylation of caldesmon. Regulatory protein of the contractile apparatus): down-regulated (endothelial cells, Participant 6).
- Gamma-actin: down-regulated ((endothelial cells, Participant 6, and U937 cells, Participant 8)
- “coactosin-like”: down-regulated (endothelial cells, Participant 6)
- “actin-binding”: down-regulated (endothelial cells, Participant 6)
- “procollagen-proline 2”: down-regulated (endothelial cells, Participant 6)
- “actin modulating activity”: up-regulated (endothelial cells, Participant 6)
- “actin-binding, calcium ion binding”: down-regulated (endothelial cells, Participant 6)
- CD2-associated protein, actin binding: down-regulated (endothelial cells, Participant 6)
- Tropomodulin 3: actin binding down-regulated (endothelial cells, Participant 6)

Calcium (Ca2+)-associated proteins:
- Ca: “hypothetical protein” (actin-binding): down-regulated (endothelial cells, Participant 6)
- “hypothetical protein”: down-regulated (endothelial cells, Participant 6)
- voltage-gated Ca channel: up-regulated (perhaps up-regulated, because Ca goes down? Endothelial cells, Participant 6)

Cytoskeleton (compare also actin and calcium-associated proteins):
- “hypothetical protein”: down-regulated (endothelial cells, Participant 6)
- “protein phosphatase 4, caldesmon): down-regulated (endothelial cells, Participant 6)
- “SH3 protein interacting with Nck”: down-regulated (endothelial cells, Participant 6)
- “in kinesin complex”: down-regulated (endothelial cells, Participant 6)

Table 33. Numbers of genes regulated within different gene families

Gene Family	total number of clones in Human Unigene RZPD-2	partner 8 U937 monocytes RF up-regulated genes	partner 8 microglia cells RF up-regulated genes	partner 8 U937 monocytes RF down-regulated genes	partner 8 microglia cells RF down-regulated genes	partner 6 endothelial cellsPr1 RF 900MHz up-regulated genes	partner 6 endothelial cells RF 1800 MHz Exp1 up-regulated genes	partner 6 endothelial cells RF 1800 MHz Exp2 up-regulated genes	partner 6 endothelial cellsPr1 RF 900MHz down-regulated genes	partner 6 endothelial cells RF 1800 MHz Exp2 down-regulated genes	partner 6 endothelial cells RF 1800 MHz Exp2 down-regulated genes	partner 2 HL-60 RF ON/OFF up-regulated genes	partner 2 HL-60 RF continuous waves Exp1 up-regulated genes	partner 2 HL-60 RF continuous waves Exp2 up-regulated genes	partner 2 HL-60 RF ON/OFF down-regulated genes	partner 2 HL-60 RF continuous waves Exp2 down-regulated genes	partner 2 HL-60 RF continuous waves Exp2 down-regulated genes	Gene "Superfamily"
Signal	2528	149	40	##	45	190	176	92	160	149	149	91	153	162	190	155	72	signal transduction
GTP	560	37	15	45	14	42	58	24	49	40	51	20	43	51	49	38	18	signal transduction
Small G	235	16	5	20	3	14	17	10	23	15	19	8	17	18	21	18	7	signal transduction
Jak	23	2	0	1	1	1	4	2	1	4	0	1	4	2	1	1	0	signal transduction
Rab	80	3	1	11	3	6	6	4	6	4	9	0	5	5	6	3	5	signal transduction
Ras	66	4	2	7	0	4	4	1	6	4	7	2	6	6	7	2	2	signal transduction
wnt	5	0	0	0	0	0	0	0	0	0	0	0	0	0	0	0	0	signal transduction
phosphatase	334	24	6	21	7	24	31	17	23	20	25	19	18	26	19	29	9	signal transduction
protein kinase	304	19	6	19	4	19	24	16	27	15	16	18	16	25	23	11	13	signal transduction
phospholipase	72	6	1	7	1	6	4	5	1	2	4	1	3	7	7	5	2	signal transduction
calcium	715	40	6	39	14	56	51	27	45	30	45	20	45	44	45	35	13	signal transduction
calmodulin	131	8	2	6	1	8	6	1	11	8	9	6	5	8	11	10	4	signal transduction
channel	348	12	1	18	7	12	12	8	16	12	11	12	28	11	16	13	6	ion/electron transport
voltage-gated	164	3	0	6	2	7	5	3	3	5	4	5	12	9	7	2	3	ion/electron transport
electron transport	423	25	11	29	6	35	44	20	37	17	34	25	19	36	26	18	15	ion/electron transport
ion transport	501	22	8	32	11	35	21	13	25	18	21	26	39	29	27	37	14	ion/electron transport
metaboli	1241	80	21	81	15	98	124	68	91	71	86	66	87	110	114	64	39	metabolism of energy/proteins
ATP	1234	81	27	92	24	75	116	49	111	77	83	86	102	104	111	82	47	metabolism of energy/proteins
mitochon	574	50	10	63	19	55	61	32	67	46	55	49	51	76	64	66	24	metabolism of energy/proteins
ribosom	254	39	14	39	19	32	35	15	30	25	32	33	31	23	26	37	13	metabolism of energy/proteins
translation	168	21	2	13	9	18	14	12	25	14	18	18	12	12	21	14	17	metabolism of energy/proteins
transcript	1991	116	39	##	41	172	142	78	144	120	129	122	143	138	138	130	75	metabolism of energy/proteins
cell cycle	478	34	11	39	14	42	46	28	46	37	39	44	49	42	46	22	23	cell proliferation/apoptosis/differentiation
apoptos	373	29	8	26	10	34	36	12	18	31	29	18	30	39	32	30	10	cell proliferation/apoptosis/differentiation
differentiat	177	17	2	20	1	14	11	8	5	6	13	6	7	9	12	7	4	cell proliferation/apoptosis/differentiation
immun	390	19	5	26	7	22	44	21	25	19	24	19	31	30	29	17	18	Immune answer/inflammation/stress answer
inflamma	184	8	1	6	3	15	15	8	13	13	9	10	11	6	12	14	2	immune answer/inflammation/stress answer
stress	118	5	6	7	2	8	16	5	8	5	13	5	8	12	10	11	4	immune answer/inflammation/stress answer
peroxidase	32	2	2	7	0	3	4	2	5	3	16	1	4	4	4	5	3	immune answer/inflammation/stress answer
heat shock	188	2	2	4	2	3	5	4	6	6	2	3	3	2	4	6	1	immune answer/inflammation/stress answer
DNA repair	154	10	3	17	4	11	15	6	13	16	15	7	13	12	17	7	8	immune answer/inflammation/stress answer
early	8	0	0	1	0	0	1	0	0	1	2	1	0	0	2	1	1	immune answer/inflammation/stress answer
adhesion	573	30	5	28	9	42	44	19	42	28	38	19	34	31	32	28	14	extracellular matrix/cytoskeleton/adhesion
extracellular matrix	226	14	4	7	5	12	12	7	7	8	8	5	11	10	11	10	8	extracellular matrix/cytoskeleton/adhesion
cytosk	529	33	9	36	21	39	41	19	33	37	43	24	30	46	48	32	21	extracellular matrix/cytoskeleton/adhesion
junction	129	0	3	11	5	3	10	2	9	3	10	5	5	7	4	8	2	extracellular matrix/cytoskeleton/adhesion
actin	494	35	7	35	19	42	39	24	38	41	40	28	30	34	44	40	21	extracellular matrix/cytoskeleton/adhesion

Table 34. Numbers regulated genes in different expression profiling experiments (bio-statistical analysis by Dr. Remondini/Participant 8)

GeneFamily	total number of clones in Human Unigene RZPD-2	partner 6 endothelial cells RF up-regulated genes	partner 6 endothelial cells RF down-regulated genes	partner 2 HL-60 cell RF up-regulated genes	partner 2 HL-60 cell RF down-regulated genes	partner 8 U937 cells RF up-regulated genes	partner 8 U937 cells RF down-regulated genes	Gene "Superfamily"
Signal	2528	4	9	1	0	1	1	signal transduction
GTP	560	1	2	1	0	0	0	signal transduction
Small G	235	0	1	0	0	0	0	signal transduction
Rab	80	0	1	0	0	0	0	signal transduction
Ras	66	0	0	0	0	0	0	signal transduction
phosphatase	334	0	1	0	0	1	0	signal transduction
protein kinase	304	0	2	0	0	0	0	signal transduction
calcium	715	1	2	0	0	0	0	signal transduction
calmodulin	131	0	1	0	0	0	0	signal transduction
channel	348	1	0	1	0	1	0	ion/electron transport
voltage-gated	164	1	0	0	0	0	0	ion/electron transport
ion transport	501	1	0	0	0	0	1	ion/electron transport
electron transport	423	1	1	0	0	1	0	ion/electron transport
metaboli	1241	3	0	0	0	2	0	metabolism of energy/proteins
ATP	1234	1	4	0	0	0	1	metabolism of energy/proteins
mitochon	574	2	1	0	0	0	0	metabolism of energy/proteins
ribosom	254	0	1	0	0	1	4	metabolism of energy/proteins
translation	168	0	0	0	0	0	0	metabolism of energy/proteins
transcript	1991	1	6	3	0	2	0	metabolism of energy/proteins
cell cycle	478	0	3	1	0	0	0	cell proliferation/apoptosis/differentiation
apoptos	373	1	0	0	0	0	0	cell proliferation/apoptosis/differentiation
differentiat	177	0	1	1	0	0	0	cell proliferation/apoptosis/differentiation
immun	390	0	0	0	0	0	0	immune answer/inflammation/stress answer
DNA repair	154	0	1	0	0	0	0	immune answer/inflammation/stress answer
inflamma	184	0	0	0	0	1	0	immune answer/inflammation/stress answer
adhesion	573	0	1	0	0	1	0	extracellular matrix/cytoskeleton/adhesion
extracellular matrix	226	1	0	0	0	1	0	extracellular matrix/cytoskeleton/adhesion
cytosk	529	0	5	0	0	1	1	extracellular matrix/cytoskeleton/adhesion
actin	494	0	4	0	0	1	1	extracellular matrix/cytoskeleton/adhesion
junction	129	0	1	0	0	1	0	extracellular matrix/cytoskeleton/adhesion

3.2.4.8 Summary (Participant 1)

Our data indicate an effect of RF-EMF on gene and protein expression in various cell systems. This conclusion is based on the following findings:

- RF-EMF exposure at a SAR value of 1.5 W/kg caused a transient up-regulation of p21 and c-myc genes and a long-term up-regulation of the stress response gene hsp70 in embryonic stem cells deficient of the p53 gene (3.2.4.1)
- RF-EMF exposure at a SAR value of 2 W/kg reduced the expression of the receptor FGFR1 of fibroblast growth factor (FGF) in human neuroblastoma cells (NB69) and in neural stem cells of rats (3.2.4.2).
- RF-EMF exposure at a SAR value of 1.3 W/kg up- or down-regulated the expression of various genes and proteins in HL-60 cells and in endothelial cells of human origin (3.2.4.3, 3.2.4.6, 3.2.4.7).
- RF-EMF exposure at a SAR value of 2.4 W/kg activated the p38MAPK/hsp27 stress response pathway in endothelial cells of human origin (3.2.4.6).
- RF-EMF exposure at a SAR value of 2.4 W/kg changed the global pattern of protein phosphorylation in endothelial cells of human origin with possible consequences for the signal transduction pathway (3.2.4.6).
- RF-EMF exposure at a SAR value at 2 W/kg did not significantly affect gene expression in human lymphocytes, although a few genes among several thousand tested with the micro-array system were found altered in two human immune cell lines (3.2.4.4, 3.2.4.5).
- RF-EMF exposure at a SAR value of 2 W/kg did not affect the expression and activity of the inducible nitric oxide synthase (iNOS) and the expression of hsp27 and hsp70 in nerve cells (3.2.4.5).
- The increased expression of hsp27 in endothelial cells (EA.hy926) after RF-EMF exposure as described in 3.2.4.6 could not be reproduced in another laboratory where slightly different methods were used (3.2.4.5).

4.0 DISCUSSION

4.1 Results obtained after ELF-EMF exposure

4.1.1 Genotoxic effects

4.1.1.1 Human fibroblasts, lymphocytes, monocytes, melanocytes and muscle cells and granulosa cells of rats (Participant 3)

Intermittent ELF-EMF exposure generated DNA strand breaks in various but not all cell lines.

Our results show, that intermittent exposure to a 50 Hz magnetic field causes a reproducible increase in DNA strand breaks in cultured human cells. These findings are in accordance with some recent studies with whole-body exposure of rodents to ELF-EMF which revealed DNA single- and double-strand breaks in the brain (Lai and Singh 1997c; Singh and Lai 1998; Svedenstal et al. 1999a/b). However, the majority of the studies investigating genotoxic effects of 50/60 Hz electromagnetic fields (McCann et al. 1993, 1998; Murphy et al. 1993; Moulder 1998) have reported a negative outcome on genotoxicity. Our results from tests with continuous exposure of fibroblasts to EMF corroborate these findings. Subjecting cells continuously to a constant field probably may induce adaptive mechanisms, protecting the genome from harmful influences. A regular change of environmental conditions might interfere with such mechanisms and lead to DNA damage. The extent of damage would depend on the duration of exposure and the time of recovery.

It is highly unlikely, that the observed genotoxic damage is caused non-specifically by spots of increased temperature within the cell layer as a secondary effect of the electromagnetic field. If so, the damage would increase with a prolongation of on-time during the intermittent exposure and would be largest at continuous exposure. The largest effects, however, are obtained at 5 min on/10 min off cycles, and continuous exposure had no effect at all. Therefore, we conclude, that the observed induction of DNA-single and double strand breaks is a direct consequence of an intermittent exposure to ELF-EMF.

Environmental exposure to continuous ELF-EMF is rather exceptional. Different electrical household devices (hair dryer, razor, vacuum cleaner) reaching peak values up to 1 mT are often used for a short period of time (5-10 min), producing a variety of exposure levels. To date, we could make out only one study dealing with genotoxic effects of ELF-EMF at intermittent exposure. This was done by Nordenson et al. (1994), who found a significant increase of chromosome aberrations in human amniotic cells (50 Hz, 30 µT, 20 s on-off). However, these results have not been corroborated by other studies as yet.

Genotoxic effects of ELF-EMF varied with exposure time.

We observed a time dependent increase of DNA breaks up to 15 to 19 hours of ELF-EMF exposure and then a decline to a steady state level of about 1.5 fold of the base line. This unexpected finding can be explained, if the exposure activates DNA repair processes and this activation takes a time of 10 to 12 hours. After this time the DNA damage is repaired then at an enhanced rate, which leads to a reduction of DNA breaks albeit not to a normalisation. This explanation is experimentally supported by the observation, that the single strand DNA breaks (alkaline conditions) are repaired after approximately 30 minutes, and double strand breaks 7 to 9 hours after finishing the exposure. Removal of damaged DNA-bases by induced repair enzymes (glycosylases) may lead to a temporary increase of abasic sites in the DNA (Friedberg et al. 1995). Abasic sites (alkali-labile sites) result in DNA single strand breaks after alkaline treatment (Tice et al. 2000). The alkali-labile sites generated after ELF-EMF exposure are therefore detected as peak at hour 12 to 17 at Comet assay conditions of pH > 13, but not of pH 12.1, the latter not being able to cleave the alkali sensitive sites.

It is well known, that the repair of single strand breaks is a fast and almost error free process, while the repair of more complex DNA damage (i.e. DNA double strand breaks) by homologous recombination, single strand annealing or non-homologous end joining require more time and are error prone in part (Van den Bosch et al. 2002). Therefore DNA double strand breaks may affect the integrity of the genome leading to cell death, uncontrolled cell growth or cancer (Van Gent et al. 2001).

Our results show, that intermittent exposure to a 50 Hz magnetic field causes a time dependent increase in micronuclei in cultured human fibroblasts. These findings are in accordance with Simko et al. (1998a/b), who could demonstrate an ELF-EMF-induced formation of micronuclei in human amnion and in human squamous cell carcinoma cells. In contrast, the greater part of studies performed as yet using different cell types did not point to direct clastogenic effects of ELF-EMFs (Livingston 1991; Scarfi et al. 1991, 1994; Paile et al. 1995), but they propose epigenetic or co-clastogenic mechanisms in combination with other genotoxic exposures (Lagroye et Poncy 1997; Cho and Chung 2003; Simko et al. 2001b). Micronucleus formation can either result from chromosomal non-disjunction due to damage of kinetochore proteins or from acentric fragments secondary to DNA double strand breaks. Since we did not use kinetochor antibodies to differentiate between these two possible mechanisms, the cause for the micronuclei induction remains an open question. At extended exposure times micronucleus frequencies reached a constant level, which is not in contrast to the results found in Comet assay since micronuclei cannot be repaired.

ELF-EMF produced DNA strand breaks in human fibroblasts in a dose dependent way.

We could demonstrate a dose dependent relationship between alkaline and neutral Comet assay tailfactors and applied magnetic flux density. The guidelines of the International Commission on Non-Ionizing Radiation Protection (ICNIRP 1998) are 500 µT during workday for occupational exposures and 100 µT for 24 h/day for the general population. The on-set of genotoxic effects in our tests was at a magnetic flux density as low as 35 µT at 15 hours and 70 µT at 24 hours of exposure, being well below these proposed guideline values. Moreover, these guidelines are dealing with continuous EMF exposure. No proposal how to handle intermittent exposures has been made by the ICNIRP as yet.

Generation of DNA strand breaks in human fibroblasts through ELF-EMF was related to the age of the donors.

Our findings of significant differences in basal DNA single and double strand break levels in fibroblasts of donors of different age are consistent with studies of several species and tissues (Mullaart et al. 1988; Holmes et al. 1992; Zahn et al. 1996; Diem et al. 2002). In addition, we here report differences in response to ELF-EMF exposure in relation to donor age, which point to a higher susceptibility of older donors to the genotoxic action of ELF-EMF. This could be interpreted by a later on-set of DNA repair. These findings are in agreement with age-related increases of DNA damage and mutations as a result of a reduced DNA repair capacity (Wolf et al. 2002; Bohr 2002; Cabelof et al. 2002; Ben Yehuda et al. 2000; Goukassian et al. 2000). Observations of an altered gene activity during ageing were reported for the rat brain, heart, and liver (Salehi et al. 1996; Goyns et al. 1998) and human fibroblasts (Linskens et al. 1995). This decline may be due to a reduction in chromatin associated RNA polymerase II activity (Rao and Loeb 1992), to mutation-induced changes in binding activity of transcription factors (Sheerin et al. 2001), or due to a decline in protein synthesis secondary to a decrease in the amount and activity of certain elongation factors (Shikama et al. 1994). Changes in the availability of proteins or enzymes may be critical if proteins of DNA repair machinery are affected.

Effects of ELF-EMF were cell type specific.

Our results point to cell type specific reaction and to differences in sensitivity of different tissues to ELF-EMF exposure. We could identify three responder (human fibroblasts, human melanocytes, transformed rat granulosa cells) and three non-responder cell types (human lymphocytes, monocytes and skeletal muscle cells). Up to date a plausible mechanism for these findings is mere speculation, but these data propose an epigenetic, indirect action of intermittent ELF-EMF. The observed cell specific response can not be explained by age-related effects, since the non-responding skeletal muscle cells are derived from the oldest donor.

In our experiments we exposed dividing and quiescent lymphocytes to ELF-EMF, and in both cases no induction of DNA strand breaks could be observed. Isolated monocytes did not respond either. The other cell types used were cells in the log-growing phase and some of them showed genotoxic effects, whereas dividing skeletal muscle cells did not react. Therefore, it is not likely that the observed effects could be due to differences in response between proliferating and non-proliferating cells. In addition, the observed effects can not be attributed to differences between adherent cells or suspension cultures, since there are non-responder cell types in both cases.

Based on the results with human fibroblasts, which suggest an induction of DNA repair upon intermittent ELF-EMF exposure, we speculate, that the effects reported here, may reflect differences in DNA repair

capacities between different tissues. This explanation, however, requires further assessment, e. g. evaluation of repair kinetics.

Generation of DNA strand breaks in human fibroblasts through ELF-EMF and their repair were modified by UVC or heat stress.

During ELF-EMF exposure UVC induced DNA-damage was repaired very slowly, although the maximum at 15h ELF-exposure could not be detected any more. The results were similar with the neutral Comet assay, but DNA damage (DNA double strand breaks) was repaired within a shorter time. These results suggest that ELF-EMF-exposure might impair and/or delay the onset of repair of DNA damage.

In regard to studies on repair kinetics, the exposure time dependent extent of DNA damage implicated an induction of DNA repair upon intermittent ELF-EMF exposure. We concluded that pre-exposure to intermittent ELF-EMF would have a protective effect and reduce genotoxic actions of additional exposures. In contrast to our assumption, pre-exposure to intermittent ELF-EMF for 20 hours resulted in an additive genotoxic effect of combined exposures and a reduced repair rate of UVC or heat stress induced DNA damage. A protective effect of ELF-EMF exposure could not be confirmed by these results. In contrast, they suggest an impairment or delay of DNA repair mechanisms due to ELF-EMF exposure.

Recently, Robison et al. (2002) have demonstrated that pre-exposure to ELF-EMF for 4 to 24 hours can decrease DNA repair rate and protect human HL-60 cells from heat induced apoptosis. Miyakoshi et al. (2000) showed that strong ELF-EMF for 2 hours can potentiate X-ray-induced DNA strand breaks in human malignant glioma cells, whereas others (Whitson et al. 1986; Frazier et al. 1990; Cantoni et al. 1996) found no evidence that ELF-EMF could inhibit repair of DNA damage induced by ionising radiation or UV light using different human cell types. However, in these experiments ELF-EMF exposure was not performed prior to UV or X-ray exposure, but afterwards. ELF-EMF preconditioning of cells may evoke different reactions. In addition, responses of the cells could differ with ELF-EMF exposure duration, applied exposure protocol (continuous vs. intermittent) or used cell type. Anyhow, these experiments may not overrule our theory of an induction of DNA repair upon ELF-EMF exposure, since repair processes are very complex and different mechanisms may engaged in the repair of UV or thermal stress induced DNA damage.

Generation of DNA strand breaks in human fibroblasts through ELF-EMF was dependent on the genetic background of cells.

We concluded that the cupola-shaped time dependent pattern of DNA breaks in the Comet assay mirrors the action of repair processes. This is supported by the more than two fold increased rate of DNA breaks in DNA repair deficient fibroblasts from a patient with Ataxia Telangiectasia after 24 hours of exposure. The increased DNA breaking rate seen in fibroblasts from this patient and in fibroblasts from older donors points to the significance of the genetic background regarding the response to ELF-EMF-exposure.

Generation of DNA strand breaks in human fibroblasts by ELF-EMF was dependent on the frequency of ELF-EMF.

Although intermittent ELF-EMF induced DNA strand breaks in the Comet assay at a broad frequency range between 3 and 550 Hz, there are noteworthy peak effects at 50 Hz and 16.66 Hz, these representing the commonly used frequencies of alternating current in Europe. However, this has been tested as yet at intermittent 5 min on /10 min off cycles only and may be different under changed intermittent conditions.

ELF-EMF generated chromosomal aberrations in human fibroblasts.

Structural chromosome aberrations result from breakage and abnormal rearrangement of chromosomes. They can be classified either to stable or unstable aberrations, depending upon their ability to persist in dividing cell populations. Unstable aberrations are ring chromosomes, dicentric chromosomes or acentric fragments, whereas stable aberrations, which result from repair processes, consist of balanced translocations or other symmetrical rearrangements. At exposure conditions producing maximum effects in micronucleus test and in Comet assay, we observed significant increases in gaps, breaks, ring chromosomes, dicentric chromosomes and acentric fragments, but not of translocations. These results are in accordance with studies performed by Nordenson et al. (1994) and Khalil and Quassem (1991), who applied intermittent or pulsed field ELF-EMF exposure. Several other studies performed at continuous ELF-EMF exposure could detect an increase in chromosomal damage (Jacobson-Kram et al. 1997; Galt et al. 1995; Scarfi et al. 1991; Paile et al. 1995).

The fate of a cell carrying a chromosomal aberration is crucial for the assessment of a possible cancer risk. Cells with unstable aberrations like rings, dicentrics or acentric fragments will be committed to apoptosis or cell death, whereas cells with repairable DNA damage like chromosomal gaps or breaks may survive. The repair process itself can lead to translocations, thereby creating a stable mutation. Surprisingly this could not be detected in 24-times 1,000 metaphases, when each chromosome had been separately painted.

Although no significant differences in cell numbers could be detected between ELF-EMF exposed and sham-exposed cells, a possible elimination of cells carrying non-stable chromosomal aberrations is not contradictory to these previous findings. Cell numbers were assessed directly after ELF-EMF exposure termination, whereas for evaluation of chromosomal aberrations, cells were maintained in culture. In addition, the total fraction of cells with non-stable aberrations in exposed cells was 0.8%. The method used for assessment of cell numbers (Coulter counter) is to imprecise to detect such o low number of cells.

Since experimental analyses have shown, that DNA double strand breaks are the principal lesions to produce chromosomal aberrations (Bryant 1998; Natarajan and Obe 1978; Obe et al. 1992), the induction of micronuclei and chromosomal aberrations is in good agreement with the previous demonstration of DNA strand breaks.

ELF-EMF did not influence the mitochondrial membrane potential.

Hitherto, response of $\Delta\Psi_m$ to ELF-EMF exposure has not been assessed and no data on EMF-induced modifications of the membrane potential of cells are available. Effects of electric fields on membrane ATPases (optimal ranges: 5 - 30 Vcm^{-1}, 10 Hz - 1 MHz) have been reported by several groups (Tsong 1992). Short pulses of electric field (100 µs decay time) of several $kVcm^{-1}$ have been used to trigger ATP synthesis in rat liver submitochondrial particles. The electric field-induced ATP synthesis was abolished by inhibitors of the F_0F_1-ATPase, oligomycin, *N,N´*dicyclohexylcarbodiimide, venturicidin and aurovertin, but occurs independently of components of the mitochondrial electron transport chain. In low field experiments (<75 Vcm^{-1}) Tsong showed a dependence of ATP yield on the field strength and frequency of the alternating current (AC) field. Effects of AC fields on the activity of Na^+,K^+-ATPase, the enzyme principally responsible for establishing ion gradients across the cell membrane, have also been reported by Blank (1992). Under normal conditions *in vitro*, the enzyme in weak electric fields has a decreased ability to split ATP (100 Hz, threshold for effects of 5 μVcm^{-1} estimated by extrapolation). When the enzyme activity was inhibited to less than half its optimal level by ouabain or low temperature, an increase in ATP splitting was observed. The greatest effects appear to be in the extremely low frequency range that includes 50 Hz.

Our data do not indicate an influence of intermittent ELF-EMF exposure of human fibroblasts on $\Delta\Psi_m$. Although these results cannot rule out rapid alterations of $\Delta\Psi_m$, we consider it to be unlikely that ELF-EMF-induced formation of DNA strand breaks is mediated via significant intracellular changes which affect $\Delta\Psi_m$.

4.1.1.2 Human fibroblasts and granulosa cells of rat (Participant 7)

The genotoxic effects induced by ELF-EMF are not reflected by physiological functions like volume regulation and free cytoplasmic Ca^{2+}-concentration.

The experiments have been performed on two different cellular levels, the genomic and the cellular level using cultured granulosa cells of rat (GFSHR-17) and human fibroblasts. On the genomic level the neutral and alkaline Comet assay has been applied to evaluate ELF-EMF (5min on/10 min off, 1 mT) induced effects on DNA single- and double-strand breaks. In parallel, the effects were compared with those obtained on the cellular level by analysis of volume regulation (Ngezahayo et al., 2003) and cytoplasmic free Ca^{2+} concentration (Pilger et al., submitted). Since Participant 3 observed no effect during permanent ELF-EMF exposure on the occurrence of DNA strand-breaks, but for intermittent exposure (Ivancsits et al. 2002a; Ivancsits et al. 2003b), we followed this exposure protocol.

The results of the alkaline Comet assay indicate that intermittent exposure to ELF-EMF induced a significant increase of single- and double-strand breaks in rat granulosa cells (Figure 26) with a maximum after exposure for 16h to 18h. The maximum is followed by a decline of DNA damage in the time range

of a few hours which can be attributed to the onset of DNA repair mechanisms (Ivancsits et al. 2002a). It should be noted that a similar time course of DNA damage was observed at an exposure frequency of 16 2/3 Hz for rat granulosa cells. The time course of DNA damage on rat granulosa cells is similar as reported for cultured human fibroblasts (Ivancsits et al. 2002a; Ivancsits et al. 2003b), CHO and HeLa cells, but appears to be more pronounced. Therefore, it seems to be reasonable to suggest that the sensitivity of cultured cell lines to ELF-EMF (intermittently applied) depends significantly on the cell type.

In addition the frequency dependence of DNA damage was studied. The quantity of DNA single-strand breaks appears to depend on the frequency of the applied ELF-EMF with a maximum at lower frequency within the applied sequence of frequencies (8 Hz, 16 2/3 Hz, 50 Hz, 1000 Hz) (Figure 27). Surprisingly, virtually no frequency dependence is found for the results of the neutral Comet assay (Figure 28).

The important question arises whether the ELF-EMF effects observed on the genomic level are reflected in a change of the macroscopic cellular behaviour, especially in basic regulatory physiological functions. As marker of physiological cell functions the regulatory volume decrease/increase of rat granulosa cells was considered. In response to a constantly applied hypotonic shock rat granulosa cells swell due to water influx like an osmometer and shrink thereafter to the original cell volume within the time scale of an hour. According to this physiological regulatory behaviour a hypertonic shock causes cell shrinkage. The results show no significant influence of ELF-EMF exposure at the additional stress condition caused by a non-isotonic bath medium (Figure 69). It could be argued that, since for technical reasons the regulation of cell volume was studied 10 min after the end of ELF-EMF exposure for 18h, the DNA repair mechanisms act significantly and thereby bias the results. But the time span for DNA repair after an exposure time of 18h occurs in the range of hours (Figures 16, 17), whereas the experiments focused to volume regulation were started 10 min after end of ELF-EMF exposure. Therefore it can be concluded that a significant increase of DNA single- and double-strand breaks by ELF-EMF exposure is virtually not reflected in a change of regulatory volume decrease/increase of granulosa cells. As second macroscopic cellular parameter the time course of free cytoplasmic Ca^{2+}-concentration ($[Ca^{2+}]_i$) was studied by fluorescence-spectroscopy after ELF-EMF exposure for 5h, 6h, 7h, 8h, and 18h. $[Ca^{2+}]_i$ was recorded in the absence (Figure 67, Table 9) and presence of a further stress factor, the exposure to H_2O_2 containing bath media (Figure 68, Table 10)). Also for this cellular parameter no significant influence of ELF-EMF exposure could be observed. In co-operation with Participant 3 a further cell-culture system, human fibroblasts, were used. In parallel to the results showing ELF-EMF induced DNA strand-breaks, the corresponding free Ca^{2+}-concentration was recorded. Also for this cell system the observed ELF-EMF induced DNA strand-breaks are not reflected in a change of the cellular level of free cytoplasmic Ca^{2+} (Figures 66, 67) or the mitochondrial potential (see also ref. Pilger et al., submitted). In contrast to our findings Tonini et al. (2001) reported a fast, within the time range of minutes, and significant increase of $[Ca^{2+}]_i$ in a cultured neuroblastoma cell line by ELF-EMF exposure at 50- to 60-Hz and 0.12 μT (0.24 μT). Surprisingly, the observations were made at continuous ELF-EMF exposure. The various findings could be related to the specific cell type, the different set-up used for ELF-EMF exposure or the method applied for analysis of $[Ca^{2+}]_i$.

4.1.1.3 Mouse embryonic stem cells (Participant 4)

ELF-EMF did not induce the formation of DNA strand breaks in embryonic stem cells.

The potential to induce primary DNA damage by ELF-EMF was analysed by the Comet assay, as a consequence of up-regulation of the DNA-damage inducible gene GADD45 after ELF-EMF exposure (4.1.3.1). In addition, it was shown by Participant 3 that the exposition of human fibroblasts to ELF-EMF results in the increase in DNA breaks suggesting a possible direct mutagenic effect (Ivancsits et al., 2002). A correlation has been described between up-regulation of GADD45, bcl-X_L, and increased DNA damage as determined on the basis of the alkaline Comet assay in human preneuronal cells (Santiard-Baron et al. 2001). However, we did not observe significant effects of 6h or 48h intermittent ELF-EMF exposure on single- and double-strand DNA break induction in the alkaline and neutral Comet assay. One reason for our negative results (as compared to the data presented by Participant 3 on human fibroblasts, e.g.) could be the different intermittency scheme of exposure, which was applied (5 min on/30 min off by Participant 4 vs. 5 min on/10 min off by Participant 3). Actually Ivancsits et al. did not observe effect by using an intermittency scheme of 5 min on/25 min off, but only for shorter off time durations. However, by RF-EMF exposure of ES cells using 5 min on/30 min off cycles, we found a low, but significant

increase in double-strand DNA breaks, suggesting that the EMF frequency has significance for the DNA damaging effects.

4.1.1.4 Summary (Participant 1)

As discussed by Participant 3 there has been sporadic literature concerning *in vitro* studies which demonstrate that ELF-EMF may possess a genotoxic potential (Lai and Singh 1997c; Singh and Lai 1998; Svedenstal et al. 1999a/b). However, the energy impact to the genome of livings cells exposed to ELF-EMF had been calculated to be too low to generate DNA damage. Since the mainstream literature contradicted the assumption of genotoxic effects (McCann et al. 1993; McCann et al. 1998; Murphy et al. 1993; Moulder 1998), these sporadic findings were considered more or less meaningless. Opposite to this widely accepted view, the data of the REFLEX study which were systematically investigated and confirmed in 4 laboratories, of which two were not members of the REFLEX consortium, support the view that ELF-EMF causes genotoxic effects in certain, but not all cell systems.

Based on the methodology used and the data obtained in the REFLEX study, the findings of genotoxicity caused by ELF-EMF are hard facts. DNA single and double strand breaks were observed in human fibroblasts exposed to ELF-EMF at a flux density as low as 35 µT, which is far below the presently valid safety limit. Increases in micronuclei and chromosomal aberrations were found at higher flux densities (3.1.1.1). These effects, although striking in fibroblast from normal donors and donors with a known repair deficiency, were not observed consistently in all cell types, e.g. in human lymphocytes. This suggests that the genetically determined defence mechanisms of cells play a decisive role as to whether or not the cells respond to ELF-EMF exposure. The question arises why the genotoxic potential of ELF-EMF was not confirmed many years ago when suitable biochemical methods became available the first time. One explanation may be that most of the experiments were carried out with lymphocytes which seem to be resistant to ELF-EMF, and that in experiments with different cell systems the exposure time and the exposure conditions may have been inadequate.

As already stated, for energetic reasons ELF-EMF can neither denature proteins nor damage cellular macromolecules directly. If the energy impact on the genome of living cells exposed to ELF-EMF is too low for damaging their DNA, the genotoxic alterations observed in the REFLEX project must be produced indirectly through intracellular processes. Participant 3 observed in its most recent experiments that the increase of DNA strand breaks in human fibroblasts after ELF-EMF exposure can partly be inhibited by oxygen radical scavengers. This finding speaks for the assumption that the observed DNA damage may be caused by free oxygen radicals which are released by ELF-EMF. This assumption is further supported by results obtained by Simko et al., who measured an increase of free oxygen radicals in macrophages derived from murine bone marrow after exposure to ELF-EMF at a flux density of 1 mT (Simko et al. 2001) and by Lupke et al. who observed an increase of free oxygen radicals in monocytes derived from umbilical cord blood and in a human monocytic leukaemia cell line also after exposure to ELF-EMF (50 Hz) at a flux density of 1 mT (Lupke et al. 2004). Into the same direction hint the results of Zymslony et al., who assessed the effects of ALF-EMF (50 Hz, 40 µT) on the oxidative deterioration of DNA in rat lymphocytes after *in vitro* irradiation by UVA (Zymslony et al. 2004). The free radical hypothesis is further supported by the studies of Lai and Singh (2004) who found that brain cells of rats after whole body-exposure to ELF-EMF (60 Hz) at very low flux densities (0.01-0.25 mT) for 2-48 hrs showed increases in DNA single and double strand breaks, and that these increases could be blocked by pre-treating the animals with the free radical scavengers melatonin, N-tert-butyl-α-phenylnitrone and Trolox (a vitamin E analogue). The work of Lai and Singh, which must still be reproduced by other independent research groups, deserves special attention, since the DNA damage reported by them was observed in the brain of whole-body exposed animals, not in isolated cells as in the REFLEX study.

Based on the data of the REFLEX project it must be assumed that ELF-EMF is able to damage the genome in certain, but not all cell systems after exposure *in vitro*. The work of Lai and Singh suggests that these effects might also be seen after exposure *in vivo*. The genotoxic effects of ELF-EMF may be best explained by an ELF-EMF induced increase of intracellular free radicals within the exposed cells and by the genetic background of the exposed cells. It is well known that a balanced free radical status is the prerequisite for maintaining health and that an unbalanced free radical status promotes the process of ageing and the development of chronic diseases such as cancer and neurodegenerative disorders. Whether the balance of free oxygen radicals can also be impaired through ELF-EMF *in vivo* as suggested by Lai and Singh (2004) needs to be further clarified.

4.1.2 Cell proliferation and differentiation

4.1.2.1 Human neuroblastoma cells (NB69 cell line) (Participant 5)

ELF-EMF enhanced proliferation and reduces spontaneous apoptosis of NB69 neuroblastoma cells.

The described results indicate that 42- or 63-hour exposure to 50 Hz magnetic fields at 10 or 100 μT can increase proliferation and reduce spontaneous apoptosis in human neuroblastoma cells. Initial evidence obtained through cell counting (Trypan blue exclusion) was subsequently confirmed through PCNA labelling, 5-bromo-2'-deoxyuridine (BrdU) labelling for identification of DNA-synthesizing cells, and flow cytometry. The modest, though statistically significant increase in the total number of cells in response to a 100-μT field estimated by the Trypan blue exclusion is consistent with the observed increase in the number of PCNA positive cells. This is also consistent with the increased numbers of cells in G2-M phase and of BrdU positive cells observed 24 hours before the increase in the number of cells was detected. The present data also indicate that a 50-Hz EMF at 100 μT can induce changes in the activation of the transcriptional factor CREB in a time-dependent manner.

A number of experimental studies investigating proliferative effects of EMF using in vitro or in vivo models (Kavet 1996), have provided limited evidence that ELF-EMF can represent a growth stimulus. Kwee and Raskmark (1995) have reported that a 24-h exposure to 50 Hz MF at 80 μT significantly increases the proliferation of transformed human epithelial amnion cells and K14 skin fibroblast cells. Wei et al. (2000) have reported that 60 Hz MF (30-120 μT, 3-72 h exposure) can induce proliferation in human astrocytoma cells and strongly strengthen the effect of two chemical agonists.

Some studies, however, have reported effects that are in apparent contrast to those described above. For instance, Conti et al. (1983) and Cleary (1993) have reported reduced ^{3}H-thymidine incorporation into lymphocyte DNA after exposure to 2.0 - 7.0 mT, 50-Hz magnetic fields. It has been proposed that several physical and biological variables, including different field parameters, exposure protocols, cell types and physiological conditions (degree of differentiation or activation) may account for the conflicting results reported in the literature (see for instance Schimmelpfeng and Dertinger 1997). In fact, the cellular response to the fields seems to be strongly dependent on biological parameters (Simko et al. 1998a/b; Wei et al. 2000). In addition, there is experimental evidence that specific combinations of AC/DC fields interact with biological systems (Blackman et al. 1994; Trillo et al. 1996) and the key to affecting proliferation of cells in a consistent manner might lie in the simultaneous control of the AC field amplitude and frequency, and the AD/DC field intensity ratio (Yost and Liburdy 1992; Blackman et al. 1985a,b; Trillo et al. 1996; Bauréus Koch et al. 2003).

Also, a recent study by Pirozzoli et al., (2003) has shown that the apoptosis induced by camptothecin in neuroblastoma cells (LAN-5) can be prevented by a 24-h exposure to 50 Hz, 1 mT MF. In addition, the cells respond to the stimulus with an increase in the proliferation index after seven days of continuous exposure to the field. In our cellular model (NB69) and under our experimental conditions, a 63-h exposure to 50 Hz, 100 μT MF significantly reduces the spontaneous rate of apoptosis while increasing proliferation in an extent that is similar to that reported by Pirozzoli et al.

The present data on PCNA, a protein that has been reported to be peak in proliferating cells at late G1 and S phases (Oue et al. 1995), indicate that the normal regulation of the PCNA positive cells is altered by the exposure to 50 Hz, 100 μT MF. In the MF-exposed samples the percent of PCNA-positive cells does not differ significantly from that at day 5 post plating, while in the control groups a significant reduction of PCNA positive cells was observed on day 6. These data are consistent with previous results reported by Cridland et al. (1999) on normal human fibroblasts showing a modest though significant increase in the length of the G1 phase when exposed to 50 Hz, 20 and 200 μT MF

The mechanism of interaction between ELF-EMF and NB69 neuroblastoma cells is not known yet.

Regarding the mechanism of interaction of magnetic fields that could underlay the herein described responses of NB69, the mobilization of cellular Ca^{2+} or some Ca^{2+}-regulatory process have been proposed as pre-eminent targets of the MF stimuli (Tonini et al. 2001). Also, in a recent work Zhou et al. (2002) have reported that ELF MF at 100 μT induced a time-dependent activation of CREB DNA binding in HL-60 cells. The effect was dependent on both the extracellular and intracellular Ca^{2+}, which suggests that ELF-EMF can activate CREB DNA binding through calcium-related signal transduction pathways. Similarly, in the present study, the activation of CREB was found to be influenced by the MF stimulus in

a time-dependent manner. Although additional research is needed to determine whether or not calcium is involved directly in the observed response of NB69 cells to 50-Hz MF, the present results are consistent with such a possibility. Further work is also necessary to determine the gene transcription pattern resulting from the increase of CREB activation after exposure to MF. Such an information would be crucial to identify the mechanism(s) by which MF interact with human neuronal cells in vitro. This hypothesis is not in contradiction with the recent results reported by Ivancsits et al. (2002b) and the studies by this group included in the REFLEX project. Their results showed that 50 Hz MF induced a dose dependent and time dependent DNA-single and double-strand breaks, with responses at a magnetic flux density as low as 35 μT.

4.1.2.2 Mouse embryonic stem cells (Participant 4)

ELF-EMF did not exert any influence on neuronal differentiation of embryonic stem cell.

We could not find evidence that under our experimental conditions, ELF-EMF exposure of ES cell derived neural progenitors affected the neural differentiation process, because we did not observe effects on transcript levels of genes involved in neuronal and glial differentiation (nestin, en-1, nurr1, tyrosine-hydroxylase and GFAP). Immunofluorescence analysis did not show any changes in the intracellular distribution and number of cells expressing neuronal markers (ßIII-tubulin, TH, GFAP).

4.1.2.3 Human lymphocytes and embryonic stem cells (Participant 8)

ELF-EMF did not affect proliferation, cell cycle and activation of lymphocytes.

Since the immune System has a key role in contrasting diseases, possible damages induced by exposure of immune cells, such as lymphocytes, could represent a great risk for human health. Thus, the objectives were to determine if different EMF exposures were able to modify human lymphocytes functionality and gene expression using appropriate in vitro tests. Moreover, since immune system efficiency is modified with ageing, a group of elderly donors was enrolled in order to study possible EMF effects age-related. On the whole, the results obtained show no differences between sham- and ELF-EMF exposed lymphocytes for most of the endpoints studied. Obviously, ELF-EMF is not able to modify proliferation, cell cycle and cell activation, which are fundamental phases of lymphocyte function. Negative results are extremely important for evaluations on human health risk.

ELF-EMF activated the expression of cardiac genes in embryonic stem cells thus enhancing their cardiac differentiation.

ELF - EMF were able to promote the differentiation of mice embryonic stem cells into a specific cardiac cell lineage, selectively promoting the expression of fundamental genes involved in the orchestration of cardiac differentiation. At the end of the differentiation process the expression of typical cardiac genes revealed that a specific direction of differentiation into a cardiac phenotype took place, which was also demonstrated by lack of expression of genes related to other cell lineages (e.g., skeletal muscle cells, neuronal cells, etc.).

4.1.2.4 Summary (Participant 1)

As discussed by Participant 5 (4.1.2.1) the findings reported in the literature about a possible influence of ELF-EMF on the proliferation and differentiation of various cell systems in vitro are controversial. Just recently, Lisi et al. (2004) demonstrated that exposure to ELF-EMF (50 Hz, 1 mT) triggered the differentiation of human pluripotent embryonic stem cells. In the REFLEX project, no data were obtained which suggest a major effect of ELF-EMF on cell proliferation and differentiation in human fibroblasts (4.1.1.1), embryonic stem cells (4.1.2.2), human lymphocytes (4.1.2.3) or neuroblastoma cells (3.1.4.2). On the other hand, some influence of ELF-EMF on proliferation and differentiation in certain cell systems cannot be excluded (4.1.2.1).

Participant 5 (3.1.2.1, 4.1.2.1) observed an inhibition of the spontaneous apoptosis in neuroblastoma cells which was followed by an increase of the proliferation rate, when the cells were exposed to ELF-EMF for 63h at a flux density of 50 or 100 μT. This observation is in line with the results of a recent study by Tokalov et al. (2003) and Tokalov and Gutzeit (2003) who reported that ELF-EMF alone does not have

any effect on the proliferation of HL-60 cells, while it protects heat shock treated HL-60 cells from becoming apoptotic. Quite obviously, ELF-EMF enabled heat shock treated HL-60 cells to escape the cell cycle arrest and to re-enter the normal cell cycle thus allowing the cell to continue the proliferation process. The authors explained this phenomenon by an ELF-EMF induced release of hsp-proteins which are thermo- or cytoprotective.

An answer of what may be the reason for the sporadically observed, but until now not unambiguously confirmed influence of ELF-EMF on cell proliferation and differentiation, may be provided by the REFLEX findings on gene and protein expression. As found by Participant 8 (3.1.4.3, 4.1.2.3), ELF-EMF accelerated the cardiac differentiation of embryonic stem cells through enhanced expression of cardiac genes. Further evidence for the validity of such an assumption comes from Participants 3 and 12 (3.1.4.5), who observed in human fibroblasts a remarkable influence of ELF-EMF on the expression of various genes, among them genes regulating Ca-metabolism, cell cycle, apoptosis, extracellular matrix, and cytoskeleton.

Of course, even if there is a relationship between ELF-EMF exposure and an acceleration of cell proliferation and differentiation in in vitro studies through the proposed mechanisms, it is at present not possible to draw any conclusion for the in vivo effects on man and animal.

4.1.3 Apoptosis

4.1.3.1 Mouse embryonic stem cells (Participant 4)

ELF-EMF altered the expression of bcl-2, bax and GADD45 gene in ES-cell derived neural progenitor cells.

In our experiments with ELF-EMF exposed wild-type mouse ES derived neural progenitors, we showed by Q-RT-PCR analysis significant changes in the transcript levels of the anti-apoptotic bcl-2 gene and the related pro-apoptotic bax gene. The biological significance of this finding and its relevance to the in vivo situation is not yet known. Apoptotic cell death is regulated by members of the bcl-2 family for differentiating mouse embryonic stem cells (Sarkar and Sharma 2002). Apoptosis plays an important role during embryonic development, including the development of the nervous system. Bcl-2 over expression was also reported to eliminate deprivation-induced cell death of brainstem auditory neurons (Mostafapour, 2002). Bcl-2 and bax mRNA transcripts in the hippocampus were significantly but transiently upregulated following the administration of the potent neurotoxin domoic acid (Ananth et al. 2001).

Another gene, whose expression was affected after ELF-EMF exposure, was the 'growth arrest DNA-damage' inducible GADD45 gene. The members of the GADD protein family are considered to play an important role in maintaining genomic stability and to regulate cell cycle activity (Chung et al. 2003).

Our results, which demonstrate changes of bcl-2, bax and GADD45 transcript levels indicate that ELF-electromagnetic signals could be perceived in ES cell-derived neural progenitors as environmental stress signals. These signals may trigger cellular responses for the maintenance of cellular homeostasis via alterations of genes that control cell cycle and apoptotic cell death.

In summary, we may conclude that exposure of ES-derived neural progenitor cells to magnetic fields simulating 50Hz power line ELF-EMF may influence transcript levels of genes encoding proteins of the bcl-2 family involved in apoptosis and the p53 responsive growth arrest and DNA damage inducible GADD45 gene. Since the fundamental processes of programmed cell death and cell cycle regulation are closely related to processes underlying cell transformation, the association of ELF-EMF with early stages of carcinogenesis cannot be excluded yet. Further investigations in vivo using genomics analyses and animal studies after EMF exposure have to be performed.

4.1.3.2 Neuroblastoma cells (NB69 cell line) (Participant 5)

ELF-EMF inhibited spontaneous apoptosis in neuroblastoma cells.

Environmental electromagnetic fields (EMF) such as those from electric power transmission and

distribution lines have been associated with increased risk of childhood leukaemia, cancer of the nervous system and lymphomas (Ahlbom et al. 2001; De Roos et al. 2001). In vitro studies of EMF effects have attempted to find an explanation to the epidemiological data and to determine the possible mechanism for cancer risk. Recent evidence has suggested that a common property shared by a number of known and suspected tumour promoters, is their ability to block the process of apoptosis (Jaattela et al., 1999). Therefore, one possible mechanistic explanation for the apparent effect of weak ELF magnetic fields would be their expression of tumour-promoting activities by interfering with the regulation of apoptosis. We have addressed this hypothesis by testing the effects of a 50 Hz 100 μT MF on apoptosis in the human neuroblastoma cell line.

Our data indicate that the field exposure can significantly inhibit spontaneous apoptosis of NB69 cells as revealed through TUNEL assay. This response was associated with significant increase in the number of cells as well as in BrdU incorporation into ADN. Besides, the immunoreactivity for Bcl-2 protein in exposed samples was also significantly increased at 60 min of exposure with respect to controls (data not shown). Regulation of apoptosis is delicately balanced by signalling pathways between apoptosis-promoting factors such as p53 and caspases, and antiapoptotic factors such as Bcl-2 and MDM2. Several lines of evidences have shown that the functional interaction between these factors play important roles in the control of cell growth and apoptosis.

Previous studies investigating changes in susceptibility to apoptosis after EMF exposure have reported both reduced (Simko et al. 1998b; Fanelli et al. 1999; Ding et al. 2001; Kumlin et al. 2002; Robison et al. 2002) and increased susceptibility (Ismael et al. 1998; Tofani et al. 2001; Mangiacasale et al. 2001; Liu et al. 2003). Other studies concerning DNA repair after EMF exposure have reported no effects (Cossarizza et al. 1989a; Frazier et al. 1990; Cantoni et al. 1996). In the majority of the studies reporting effects on apoptosis, cancer cells were exposed to MF (B>100 μT) after apoptosis induction by radiation or chemical treatments. The cellular susceptibility to such MF-driven apoptosis has been reported to be dependent on the cell type, the presence of genetic abnormalities, cell physiology and the MF exposure time. Cancer cells frequently have decreased cell death as a primary mode of increased cell proliferation. Attention has been focused on the expression of the p53 gene, which induces either a stable arrest of cell growth or apoptosis. The final outcome of the different mechanism of action of p53 is to maintain the genomic stability of the cell. Thus, the absent of this protein or their inactivation contributes to genomic instability, the accumulation of mutations and increased tumorigenesis. In the study by Czyz et al. (2004a, included in the present report) the exposure to 50 Hz EMF at 2.3 mT results in up-regulation of egr-1, c-jun and p-21 transcript levels in p53-deficient, but not in wildtype embryonic stem cells. These data indicate that loss of p53 may also affect the sensitivity of cells to external stress factors, such as EMF.

On the other hand, it has been reported (Tian et al. 2002b) that X-ray irradiation followed by 60 Hz EMF exposures can affect cell cycle distribution and transiently suppress apoptosis in xrs5 cells, which show a defect in rejoining of DNA double-strand breaks. The effect has been proposed to be exerted through EMF-induced decrease in the levels of caspase-3, p21, p53 and phospho-p53 and by increasing Bcl-2 expression. Our present results show that a 50 Hz 100 μT MF induces changes in the cell cycle together with a reduction of spontaneous apoptosis associated with increased Bcl-2 expression in NB69 cells. It is possible that a MF action on p53 and Bcl-2 is responsible for the effects on growth and apoptosis observed in our study. In addition we have investigated possible EMF-induced changes in the activation of the phosphorylated cyclic adenosine monophosphate response-element binding protein (p-CREB). CREB appears to be a primary transcriptional activator of the antiapoptotic gene Bcl-2 (Francois et al. 2000). Inhibition of CREB activity induces apoptosis in sympathetic neurones (Riccio et al. 1997) while CREB overexpression inhibits apoptosis induced by okadaic acid (Walton et al. 1999). Our data show that EMF exposure significantly increases the percent of p-CREB positive cells after 60-minute exposures. These results suggest that CREB may also be involved in the above-described effects of 50 Hz, 100 μT EMF on growth/apoptosis of NB69 cells.

4.1.3.3 Human fibroblasts (Participant 3)

ELF-EMF may not affect the apoptotic process in human fibroblasts after intermittent exposure for 24 hours at a flux density of 1 mT.

No differences in cell count between exposed and sham exposed human fibroblasts after any exposure duration could be detected. Therefore, an elimination of cells by apoptosis and cell death during ELF-EMF exposure can probably be ruled out (3.1.1.1).

4.1.3.4 Summary (Participant 1)

As discussed by Participant 5 (4.1.3.2), data reported in the scientific literature on possible effects of ELF-EMF on the apoptotic process are inconsistent. In many studies available to date, inhibition of apoptosis, enhancement of apoptosis and no effect at all have been reported. Most recently, Lai and Singh (2004) found a significant increase both in apoptosis and in necrosis in brain cells of rats after in vivo exposure to ELF-EMF which they explained by an increase in free radicals. Kim et al. (2004) demonstrated that apoptosis in testicular germ cells of mice can be induced by continuous exposure to ELF-EMF (60 Hz, 0.1 and 0.5 mT). The REFLEX findings did not show a significant effect of ELF-EMF on apoptosis in human fibroblasts (3.1.1.1, 4.1.3.3), embryonic stem cells (3.1.4.1, 4.1.3.1), human lymphocytes (3.1.2.3) and neuroblastoma cells (3.1.2.4).

On the other hand, some influence of ELF-EMF on the apoptotic process cannot be excluded at present. Participant 5 observed an inhibition of the spontaneous apoptosis in neuroblastoma cells which was followed by an increase of the proliferation rate, when the cells were exposed for 63 hours to ELF-EMF at a flux density of 50 or 100 µT (3.1.2.1, 4.1.2.1). A similar phenomenon was also reported by Tokalov and Gutzeit (2003) and Tokalov et al. (2003), who did not observe any direct effect of ELF-EMF on apoptosis in HL-60 cells either, while ELF-EMF protected heat shock treated HL-60 cells from becoming apoptotic, thus enabling cells arrested in the cell cycle to continue the proliferation process.

An answer of what may be the cause for the sporadically observed, but probably not systematically enough studied influence of ELF-EMF on apoptosis may be provided by the REFLEX findings on gene and protein expression. As found by Participant 4 (3.1.4.1, 4.1.3.1), ELF-EMF at a flux density of 2 mT up-regulated in neural progenitor cells the transcript levels of the bcl-2 and the GADD45 gene and down-regulated the transcript levels of the bax gene thus influencing cellular processes, which may result in an enhancement of the anti-apoptotic pathway. Further evidence for the validity of such a hypothesis comes from Participants 3 and 12 (3.1.4.5), who observed a remarkable influence of ELF-EMF on the expression of various genes, including those that regulate cell cycle and apoptosis.

From the physiological point of view, inhibition as well as promotion of apoptosis may be induced by ELF-EMF dependent on the type of cell exposed, its genetic background, its immediate metabolic stage and the pattern of exposure. The mechanisms may follow different routes. It may be possible, that two counteracting mechanisms balance out each other which would result in a zero outcome. Taken together, even if a relationship between ELF-EMF exposure and an inhibition or promotion of apoptosis in in vitro experiments were proven, it would in no way be possible to draw any conclusion for the in vivo situation in man and animal.

4.1.4 Gene and protein expression

4.1.4.1 Mouse embryonic stem cells (Participant 4)

Short-term high intensity exposure to ELF-EMF signals may cause a transient up-regulation of immediate early response and regulatory genes in p53-deficient ES cells.

It was found that a high flux density of 2.3 mT of 50 Hz ELF-EMF signals applied to p53-deficient ES cells at an intermittency scheme of 5 min on/30 min off induced a significant up-regulation of transcript levels of the immediate early growth response gene egr-1. This upregulation was paralleled by a transient upregulation of mRNA levels of the cyclin kinase inhibitor p21 and the AP-1 component c-jun in p53-deficient, but not in wt ES cells. This finding confirms our observation that loss of p53, affects the sensitivity of cells to external stress factors, such as GSM-signals. A correlation between loss of p53

function and external stress-induced expression of egr-1 has also been described by Zhang and Chen (2001), who reported experimental evidence for UV-induced egr-1 expression in p53-deficient mouse cells, whereas the effect was suppressed by functional p53. Our data indicate that a similar egr-1-dependent pathway may be triggered upon ELF-EMF exposure.

The role of c-jun and p21 in these processes has not been clarified so far. Egr-1 cooperates with c-jun in the regulation of DNA synthesis and cell survival in response to ionizing radiation (Hallahan et al. 1995). p21 is implicated in G1 arrest following ionizing radiation-induced DNA damage (Brugarolas et al. 1995). Therefore, one could speculate that the tumor suppressor p53 may be involved in the maintenance of cellular homeostasis of ES cells in response to external stress. However, there are also other data showing that despite abundant quantities of p53 in ES cells, the p53-mediated response is inactive, because of a predominantly cytoplasmic localisation and sequestration of p53 (Aladjem et al. 1998). In spite of this, undifferentiated ES cells are sensitive to DNA damage, because they activate a p53-independent apoptotic response. According to Sabapathy et al. (Sabapathy et al. 1997), the balance between positive and negative regulators of the cell cycle is critical for ES cell differentiation and, if disturbed by exogenous factors, this could lead to the activation of a tumorigenic pathway.

The nature of gene-expression responses to ELF-EMF was short-term only.

In our experiments, cellular responses to ELF-EMF signals were observed only immediately after the end of the 6h exposure and disappeared after an 18h recovery time. Similarly, a 48h exposure to ELF-EMF did not result in gene expression-related responses throughout the differentiation process. These results indicate a short-term nature of cell responses to ELF-EMF and the existence of pathways compensating potential stress-evoked effects of ELF-EMF.

There is some indication that threshold of field flux density exists for ELF-EMF biological effects.

We further investigated the influence of the signal strength and the quality of ELF-EMF exposure on cellular reactions in the ES cell system. Our data indicate the existence of threshold values of field flux density that are needed to evoke biological effects by ELF-EMF. Modifications of transcript levels in p53-deficient cells were observed only upon exposure to ELF-EMF signals applied at a high (2.3 mT) flux density, whereas weaker fields did not cause gene expression-related responses.

ELF-EMF effects in p53-deficient cells were dependent on intermittency cycles (on/off cycle duration).

The exposure protocols of ELF-EMF signals involving either intermittent (on/off cycles) or continuous exposure affected the responses of ES cells. Only an intermittency scheme of 5 min on/30 min off ELF-EMF signals exerted effects on transcript levels, whereas intermittency signals of 5 min on/10 min off exposure or continuous exposure showed no effects on transcript levels of ES cells. These findings demonstrate that a specific intermittency scheme of ELF-EMF exposure may be a critical factor to determine the interference of electromagnetic fields with biological systems (Murphy et al. 2002).

The mechanism of action induced by ELF-EMF exposure of living cells is not yet known.

Several hypothetical models have been proposed to explain the mechanisms of interference of ELF-EMF with biological systems, such as an induction of electric currents by acceleration of ions, resonant interactions involving driving vibrations or orbital transitions in biomolecules (Valberg et al. 1997), biochemical reactions involving free radicals (Brocklehurst and McLauchlan 1996; Eveson et al 2000) or direct interactions of EMF with moving electrons within DNA (Blank 1997). It was also suggested that external oscillating fields cause forced vibrations of free ions of the cellular surface and distort the gating of electro-sensitive channels on the plasma membrane. This would explain, why pulsed electromagnetic fields could have a higher biological activity than continuously applied fields (Panagopoulos et la. 2000, 2002). According to another model (Binhi and Goldman 2000), specific ‘windows’ of the electric-field frequency and amplitude might be predicted. These properties of ELF-EMF could explain the positive results of certain exposure schemes with a specific on/off cycle (in our case, 5 min on/30 min off) and the lack of biological effects at other experimental conditions.

4.1.4.2 Neuroblastoma cells (SY5Y cell line) (Participant 11)

The function of neuronal nicotinic receptors in the brain

Neuronal nicotinic receptors (nAchRs) are a family of ligand-gated cationic channels expressed both in the peripheral and central nervous system where they play a fundamental role in synaptic transmission. At the periphery nAchRs are expressed in post-ganglionic neurons of the autonomic nervous system (Wang et al. 2002 and references therein). In the CNS they seem to be located predominantly at the presynaptic and preterminal parts of the axons where they control the release of a number of different neurotransmitters, such as glutamate, GABA and dopamine (Wonnacott 1997).

nAchRs are composed of different subunits: so far nine ligand binding subunits, alpha 2 - alpha 10, and three structural subunits, beta2 - beta4, have been cloned from different species (Wang et al. 2002). Different combinations of alpha and beta subunits can form different receptor subtypes with their own pharmacological and biophysical characteristics. Neuronal nAchRs are involved in a number of functional processes including cognition, learning and memory (Jones et al. 1999). Alterations in the expression and/or activity of nAchRs have been implicated in different neurological disorders. For instance, mutations in the alpha4 or beta2 subunits produce in humans the autosomal dominant nocturnal frontal lobe epilepsy (Steinlein et al. 1995; De Fusco et al. 2000). Roles for the alpha7 subunit have been suggested in Alzheimer's disease (Dineley et al. 2001) and schizophrenia (Lindstrom 1997; Freedman 1999; Freedman et al. 2000). It has been recently shown that the expression of alpha7 is increased in a well-established mouse model of Alzheimer's disease, whereas the beta-Amyloid (1-42) peptide binds with high affinity to alpha7, suggesting a pathogenetic role for this receptor subtype (Grassi et al. 2003).

Insights into the functional role of nAchRs and their possible involvement in neurological disorders have been obtained by means of knock-out mice (Cordero-Erausquin et al. 2000). By this approach, it has been possible to show that the absence of the beta2 subunit as well as the hyperactivity of the alpha7 subunit are conditions sufficient to promote neurodegeneration. Epidemiological studies have shown that exposure to electromagnetic fields (EMF) might be responsible for neurodegenerative diseases such as Alzheimer's (Sobel et al. 1995, 1996). In light of the role of nAchRs in physiological and pathological conditions, we wondered whether EMF might affect the expression of these molecules. With this aim, we have characterized some neuronal cell lines for their ability to express nAchRs. We have identified some human neuroblastoma cell lines that are currently used to evaluate whether extremely low frequency EMF (ELF-EMF) can interfere with the expression of alpha3, alpha5 and alpha7 nAchR subunits. The expression of these subunits has been studied both at mRNA level by Northern blotting, and at protein level by radioligand assays, upon exposure to different protocol settings.

The function of the cathecolaminergic system in the brain

The cathecolaminergic system is very relevant for many brain functions. Moreover, in the periphery, cathecolamines, in particular norepinephrine, are released by the post-ganglionic neurons of the autonomic nervous system, representing the main neurotransmitters of the ortosympathetic division. In collaboration with Participant 1, we decided to investigate the expression of Dopamine beta-hydroxylase (DßH), the limiting enzyme for the synthesis of norepinephrine, in order to investigate whether ELF-EMF might modify its expression, therefore interfering with autonomic functions as it has been reported in some papers (Kim et al. 2002). With this aim, we carried out Northern blot analyses with RNA extracted from neuroblastoma cells exposed to ELF-EMF.

Finally, we have also been investigating the effects of ELF-EMF on the expression of two transcription factors, Phox2a and Phox2b. These homeodomain proteins are the main regulators of the expression of Dopamine beta-hydroxylase (Yang et al. 1998). In particular, they are responsible for the development of all three divisions of the autonomic nervous system (Lo et al. 1999; Stanke et al. 1999). Indeed Phox2b KO mice fail to develop the whole autonomic nervous system (Pattyn et al. 1999), whereas Phox2a mice show an apparently less severe phenotype, but die the day of birth (Morin et al. 1997). Furthermore, preliminary results from our laboratory have shown that they seem to play a role in the regulation and maintenance of the expression of nAchR alpha3 subunit gene (Flora, personal communication). In order to understand whether ELF-EMF can interfere with the expression of these transcription factors, therefore affecting the formation and function of the autonomic nervous system, we have been carrying out Northern blot experiments to evaluate possible variation in the expression of Phox2a and Phox2b mRNA.

ELF-EMF did not affect the expression of neuronal genes such as nAchRs, DβH, Phox2a and Phox2b, either at mRNA or protein level.

A human neuroblastoma cell line, SY5Y, was used in all the experiments, as it expresses the ganglionic-type nAchR subunits alpha3, alpha5 and alpha7 as well as DßH, Phox2a and Phox2b genes. Cells were

exposed by means of the ELF-EMF generator, setup by Participant 10, under different exposure protocol. The intensity of the electromagnetic field applied was always higher (2 mT and 1 mT) than that of a real life situation, in order to highlight possible, if any, macroscopic effect on gene expression due to ELF-EMF exposure. The duration time of the exposure varied from a relatively short period of time (16h) to a longer period (48h), in order to investigate a time-dependent effect upon exposure to EMF. Finally, the type of exposure, intermittent (5 min on/5 min off) rather than continuous was chosen in order to mimic different kinds of situations that may be encountered during the life-time of an individual. The cells were always collected immediately after the end of the exposure for gene expression analysis, except in one case (1 mT continuous exposure for 48h), when the cells were harvested 48 hours after the end of the exposure, in order to investigate possible indirect effects on the expression of nAchR subunits, DßH, Phox2a and Phox2b, due to the activation of second messenger cascades. We found that exposure of human neuroblastoma cells to continuous (magnetic field intensity of 2 mT and 1 mT) and intermittent (2 mT and 1 mT) low-frequency EMF either for a relatively short period (16h) as well as a longer period (48h) does not seem to influence the expression of neuronal genes for nAchRs, DßH, Phox2a and Phox2b, either at mRNA or protein level. In order to validate these negative results, every exposure condition was tested in at least three to nine independent experiments.

4.1.4.3 Embryonic stem cells of mice during cardiac differentiation (Participant 8)

ELF-EMF up-regulated the expression of cardiac specific genes thus promoting cardiogenesis.

The exposure of EC (P19) cells to ELF-EMF yielded conflicting results and poor reproducibility of the data. On the contrary, the development of a model of in vitro cardiogenesis based on "gene trapping" selection of cardiomyocytes from pluripotent (GTR1) cells provided a potentially homogenous and reproducible approach to assess whether ELF-EMF may afford developmental decisions (i.e. cardiogenesis) in ES cells. In this ES cell model, ELF-EMF afforded a consistent increase in the expression of genes tightly involved in coaxing ES cells to the cardiac lineage. As shown by in vitro run-off analyses, ELF-EMF affected the transcriptional machine of ES cells. These responses led to the expression of cardiac specific genes and ultimately ensued into a high-throughput of cardiogenesis, as shown by the increase in the number of spontaneously beating colonies in ELF_EMF-exposed cells. Failure of ELF-EMF to affect the transcription of a gene promoting skeletal muscle determination and the faint effect on neuronal specification seem to exclude a generalized activation of repressed genes and suggests that coupling of ELF-EMF with GATA-4, Nkx-2.5 and prodynorphin gene expression may represent a mechanism pertaining to ES cell cardiogenesis.

4.1.4.4 rCx46 in oocytes of *Xenopus laevis* (Participant 7)

The influence of ELF-EMF exposure on the expression of rCx46 in single and paired oocytes of *Xenupous laevis* was analysed. Especially the expression level as well as the corresponding regulatory properties of conducting hemi-channels and cell-to-cell channels (Bruzzone et al., 1996) were studied. ELF-EMF exposure neither significantly influenced the expression level of conducting hemi-channels composed of rCx46 (Figures 59 to 61), nor their gating properties by voltage, pH, Ca2+ (Figure 64). A similar result was found for cell-to-cell channels, which could be formed by pairing of oocytes expressing rCx46 (Figure 65). This finding is in contrast to the observation that in general ELF-EMF exposure causes a decrease of cell-to-cell coupling (Hu et al. 2001; Lohmann et al. 2003; Trosko and Ruch 1998; Vander Molen et al. 2000; Yamaguchi et al. 2002; Zeng et al. 2003), but different regulatory mechanisms were suggested. It was proposed that ELF-EMF increases Ca^{2+}-influx which in turn inhibits gap junctional coupling in synovial fibroblasts (Marino et al. 2003). But in osteoblast like cells such an increase of Ca^{2+} was not observed, despite the finding that ELF-EMF induced a decrease of gap junctional coupling (Yamaguchi et al. 2002). In contrast to further reports (Lohmann et al. 2003; Zeng et al. 2003) the authors showed that ELF-EMF does also not effect the distribution of the corresponding membrane protein connexin (Cx43) between the cytoplasmic and the membrane pool. Therefore, a change in the state of Cx-phosphorylation was considered as target of ELF-EMF exposure causing a decrease of cell-to-cell coupling (Yamaguchi et al. 2002, see also Lacy-Hulbert et al. 1998). By ELF-EMF exposure of oocytes expressing rCx46 cytoplasmic free Ca^{2+} and/or signal transduction pathways involved in protein phosphorylation also of rCx46 virtually remain unchanged. This conclusion can be drawn from the unchanged behaviour of the leak-current of the oocytes in the absence and presence of

ELF-EMF (Figure 58). The leak-current includes the sum of all electrogenic transport systems which are known to partially depend on cytoplasmic free Ca^{2+} and protein phosphorylation. At present the origin for the different response of cell systems expressing Cx43 (Hu et al. 2001; Lohmann et al. 2003; Trosko and Ruch 1998; Vander Molen et al. 2000; Yamaguchi et al. 2002; Zeng et al. 2003) and oocytes expressing rCx46 at ELF-EMF exposure remains unsolved.

4.1.4.5 Whole-genome analysis of various cell lines exposed to ELF-EMF (Participant 12)

If we look on the numbers in Table 12, it is obvious that members of some gene families are regulated predominantly. Moreover, repetitions of experiments with the same cell line and the same exposure conditions look more similar than repetitions with different cell lines or different exposure conditions. This might tell us that obviously something is happening on the gene-expression level after ELF-EMF exposure. Otherwise, if we only would see experimental variances (differences in experimental procedures, cell cycle stages, etc.), we would expect about the same numbers in each experiment, or higher similarities between same experiments as between different cell lines.

The results with the different cell lines obviously have not the same quality. For example, the results of profiling 1 and 2 of the fibroblasts (Participant 3) seem to be more similar than between the experiments between cells with differentiating potential. Also genes of different gene families react differently on certain influences. Whereas for example structural proteins like cell adhesion proteins are regulated slowly, certain proto-oncogenes like c-fos, c-fos or actin can be regulated within 10 to 30 min of growth factor addition (Quantin and Breathnach 1988). Moreover, the situation is different here from, for example, a disease situation with a certain defect in a single gene. We deal with environmental influences here, which are complex and variable. Even adaptation to the electromagnetic fields after some hours due to changes in gene expression cannot be excluded.

How the potential molecular changes after ELF-EMF exposure are regulated, remains speculative. However, if we look on the genes extracted by the bio-statistical analysis in more detail, some interesting points become obvious: A remarkable number of members of the actin cytoskeleton and associated proteins are down-regulated (also in RF-EMF experiments). Remarkably, in ELF-EMF treated cells (Participant 3) the actin-associated proteins obviously down-regulated seem to be regulated by Ca, and several Ca regulators were also down-regulated in our experiments. This would mean that the actin cytoskeleton as far as regulated by Ca is down-regulated. In addition to Ca^{2+}-associated proteins, proteins associated with other cations like Fe+, K+, and H+ are down-regulated. More experiments will be necessary for showing if these proteins might be involved in signalling or energy metabolism after ELF-EMF exposure.

4.1.4.6 Summary (Participant 1)

From the REFLEX data, the conclusion must be drawn that ELF-EMF may affect gene and protein expression in various cell systems. Based on the results of the genome analysis of human fibroblasts as carried out by Participant 12 (3.1.4.5), ELF-EMF appears to regulate the expression of a series of genes and proteins such as mitochondrial and ribosomal genes and Ca-, cell cycle-, apoptosis-, extracellular matrix-, and cytoskeleton-related genes. In particular, a number of G proteins and calcium associated proteins involved in signal transduction seem to be strongly regulated by ELF-EMF. Since the variances between the experiments were high, the significance of these findings is limited. Participant 4 observed a transient up-regulation of early response and regulatory genes only in embryonic stem cells deficient for p53 and not in wild type cells after ELF-EMF exposure. This suggests that the genetic background affects the responsiveness of the cells (3.1.4.1, 4.1.4.1). Participant 8 found that ELF-EMF up-regulates the expression of cardiac specific genes in cardiomyocytes derived from embryonic stem cells thus promoting cardiogenesis (3.1.4.3, 4.1.4.3). All these findings were obtained after ELF-EMF exposure at rather high flux densities. It remains, therefore, an open question whether or not these in vitro results are of any significance for the real life exposure of man and animal.

The REFLEX data on gene and protein expression due to ELF-EMF exposure are in line with the results of a series of studies already published in the literature. Goodman et al. (1994) and Lin et al. (2001) reported increased hsp70 transcript concentrations in HL-60 cells after exposure to weak ELF-EMF (60 Hz). Tokalov and Gutzeit (2004) observed an increase in several heat shock proteins in HL-60 cells after

exposure to ELF-EMF (50 Hz, 60 μT, 30 min), which was comparable to that after exposure to heat (41°C, 30 min) or X-ray (200 kV, 5 Gy). Most recently, Zeng et al. (2004a) and Xu et al. (2004) demonstrated that ELF-EMF (50 Hz, 0.4 mT, 24h) altered the signal transduction-related protein expression in human breast cancer cells (MCF-7). Mannerling et al. (2004) who studied the hsp70 expression in several human cell lines reported an increased expression after exposure to ELF-EMF (50 Hz, 0.1 or 0.2 mT, up to 24h). Of course, the expression of genes and proteins induced by ELF-EMF may again be dependent on the type of cell exposed, its genetic background and its immediate metabolic stage and, of course, the pattern of exposure. The available data indicate that the flux density (threshold) at which effects on gene and protein expression are at first found is in the range or not far above the presently valid safety levels of 100 μT for the general public or 400 μT for the workplace.

4.2 Results obtained after RF-EMF exposure

4.2.1 Genotoxic effects

4.2.1.1 Human promyelocytic cell line HL-60 (Participant 2)

Discussion on potential health effects of using mobile telephones has focused on possible cancer-enhancing effects. It seems quite clear that any cancer-related effects of radiofrequency electromagnetic waves cannot be based on direct genotoxic effects, since the energy level is not high enough to damage DNA. Most of RF-field studies concluded that RF-field exposure is not genotoxic or mutagenic. With respect to DNA strand breaks, there is no replicated evidence for DNA and/or repair damage due to RF-field exposure (Lai versus Malayapa, examples see literature cited). On the other hand, some studies have shown that radiofrequency-field/microwave (RF-fields/MW) radiation and extremely low frequency (ELF) fields cause increased DNA strand breakage and chromosome aberrations. This has been shown in cell lines (Phillips et al. 1998), human blood (Verschaeve et al. 1994), animals (Lai and Singh 1995, 1996a/b, 1997a/b/c, 2004) and living human beings (Fucic et al. 1992; Garaj-Vrhovac 1999). The basic strategy in our studies was to test whether RF-EMF are able to alter DNA integrity (MN induction and DNA strand breakage), cell proliferation, cell cycle kinetics and/or apoptosis using the promyelocytic leukaemia cell line HL-60 testing different SAR levels, exposure times and signal modulations. For the experiments a highly standardized exposure system setup was provided by Participant 10. This setup enabled the exposure of suspensions of cells with a highly standardized temperature constancy, an inhomogeneity of SAR of less than 30% and an efficiency of more than 20 W/kg per Watt input power. All experiments were performed blinded, i.e. not knowing, which of the waveguides was exposed to the RF-field and which was the sham control.

RF-EMF exposure for different SAR and different exposure times (1800 MHz, continuous wave) led to the induction of single and double DNA strand breaks.

DNA damage through RF-EMF was evaluated immediately after exposure using the alkaline single cell gel electrophoresis assay (Comet assay). RF-fields at 1800 MHz, continuous wave exposure for different exposure times caused the induction of single and double DNA strand breaks in HL-60 cells. No significant difference was seen between exposed and sham exposed cells at a SAR of 0.2 to 1.0 W/kg. An increase in the steepness of the dose response relation is observed between SAR 1.0 W/kg and 1.3 W/kg. A less expressed increase is observed between 1.6 W/kg and 3.0 W/kg (Figure 73).

Two other laboratories have recorded that RF-field/MW produced significant DNA stands breaks. Verschaeve et al. (1994), who used a GSM cell phone signal to expose human and rat peripheral blood lymphocytes, found significantly increased strand breaks at high, but non-thermal exposure levels. Phillips et al. (1998) exposed Molt-4 T-lymphoblastoid cells with cell phone radiation in the SAR range 0.0024 W/kg to 0.026 W/kg. A 2-hour exposure to these low levels of cell phone radiation significantly increased or decreased the DNA damage. Decreased DNA damage is evidence of increased repair that is, of course, evidence of damage (Meltz 1995). In some other studies the observations of significant increase in DNA single and double strand breaks in brain cells of rats whole body exposed to 2.45 GHz RF-field (Lai and Singh 1995, 1996a/b, 1997a/b) were not confirmed using rodent and human cells

exposed in vitro and in vivo to RF-fields (Malayapa et al. 1997, 1998; Maes et al., 1997; Vijayalaxmi et al., 2000; Li et al., 2001).

RF-EMF exposure for different SAR and different exposure times (1800 MHz, continuous wave) led to an increase in micronuclei.

Micronuclei are easily measured under day light microscopy. They consist of small amounts of DNA that arise in the cytoplasm when chromatid/chromosomal fragments or whole chromosomes are not incorporated into daughter nuclei during mitosis. We have used the conventional cytokinesis-block MN assay to assess induction of cytogenetic damage in HL-60 cells after exposure to RF fields. RF-EMF exposure on HL-60 cells at 1800 MHz, 24h, continuous wave, at the given experimental conditions, caused a significant increase of micronuclei induction in the same SAR-dependent manner as observed for the induction of DNA strand breaks. Whereas at a SAR of 1.0 W/kg no significant difference of micronuclei frequencies was noted compared to sham controls, a clear increase was observed at SAR of 1.3 W/kg and 1.6 W/kg, and, less expressed at a SAR of 2.0 W/kg and 3.0 W/kg (Figure 72).

Induction of both, micronuclei and Comet formation, by RF-EMF was dependent on the time of exposure. A short exposure period of 6 hours caused no increase in MN frequencies compared to longer exposure times of 24 and 72 hours, respectively. Exposure to a 1800 MHz magnetic field at SAR of 1.3 W/kg for 72 hours produces a similar micronucleus frequency in HL-60 cells as that caused by 0.5 Gy ionising radiation (exposure time: 5.2 s), i.e., an average of 22 MN per 1000 BNCs (Figures 75, 76). However, it is not likely that the two entities cause MN induction by similar mechanism and produce the same types of DNA damage. In contrast to these findings, Comet formation already started after short exposure periods of 2 and 6 hours, respectively, with a maximum after 24 hours, and a clear decline occurred towards a longer exposure period of 72 hours. Mechanistically, this finding may be explained by DNA repair phenomena in the case of the DNA strand breakage in contrast to MN induction.

On the other hand, data from several other studies have indicated in primary human lymphocytes an absence of significant differences in the incidence of CA, SCE and MN between RF-EMF-exposed and sham-exposed cells (Vijayalaxmi et al. 1997, 2001a/b; Bisht et al. 2002). The significant increase and a weak effect on sister chromatid exchanges in RF-field exposed human blood lymphocytes reported by Maes et al. (1996, 1997) was not confirmed in their own subsequent investigation (Maes et al. 2001). Some positive findings occurred under conditions in which RF exposure elevated the temperature (Manikowska-Czerska et al. 1985; Sarkar et al. 1994; Varma and Traboulay 1997).

RF-EMF-associated increase of DNA strand breaks and micronuclei (1800 MHz, 1.3 W/kg, 24h) in HL-60 cells was signal-independent.

Interestingly, DNA strand breaks and MN induction were similarly induced by different RF-EMF signal modulations including CW exposure, CW intermittent exposure (5 min on/10 min off), 217 Hz pulse modulation and GSM Talk each at 1800 MHz, SAR 1.3 W/kg for 24h (Figure 77, 78).

RF-EMF induced formation of reactive oxygen species as shown by flow cytometric detection of oxyDNA and rhodamine fluorescence.

ROS, including superoxide anion (O^{-}_{2}), hydrogen peroxide (H_2O_2), hydroxyl free radical ($OH\cdot$) and singlet oxygen ($^1O_2$), continuously generated from the mitochondrial respiratory chain, own a powerfully oxidative potential. ROS are capable of attacking lipids, nuclear acids and proteins, resulting in certain degrees of oxidative damage. The total ROS level in resting HL-60 cells, however, was directly measured in the present study, by flow cytometric detection of Rh123 and the oxidized nucleotide 8-oxoguanosine (Figures 86, 87). Detecting the ROS level by flow cytometry has been a novel approach with the characteristic of fastness, convenience and reproducibility and, to our knowledge, has not been frequently reported before. DHR123, one of common ROS captures, is membrane permeable. It is oxidized intracellularly by ROS to become fluorescent Rh123, which is pumped into mitochondria and remains there. After a period of accumulation it is then detectable by flow cytometry (e.g., Gao et al., 2002) The probe used in the Calbiochem OxyDNA Assay kit is specific for 8-oxoguanine, which, as part of the oxidized nucleotide 8-oxoguanosine, is formed during free radical damage to DNA and is thus a sensitive marker for differences of ROS levels (de Zwart et al. 1999; Kasai 1997; Cooke 1996) in HL-60 cells after exposure to RF-EMF compared to control and sham-exposed cells (Figure 86).

If an involvement of free radicals in the mechanism of RF-EMF induced DNA strand breaks in HL-60 cells could be shown, this would have an important implication on effects to cell integrity due to RF-EMF

exposure. The “free radical hypothesis” stating that EMF increase free radical activity has been proposed by various researchers (Grundler et al. 1992; Reiter 1997; Lai and Singh 2004). Involvement of free radicals in human diseases, such as cancer and atherosclerosis, have been suggested (Beckmann and Ames 1997). Free radicals also play an important role in aging processes (Reiter 1995).

Co-administration of ascorbic acid, a free radical scavenger, inhibited the effects of RF-EMF on HL-60 cells and may, thus, decrease DNA damage without affecting cellular growth.

Two plausible biological mechanisms involving free radicals have to be discussed for the RF-EMF effect. The first involves increased free radical formation and activity and genetic damage as a response to RF-field exposure. The second involves increased free radical activity and genetic damage because of an induced reduction of free radical scavenger, e.g. reduced SOD activity or melatonin (Reiter 1994). Indications were found in our investigations for increased free radicals activities and a correlation with genetic damage (Figures 86 to 89). Cells possess efficient antioxidant defence systems, mainly composed of the enzymes such as superoxide dismutase, glutathione peroxidase, and catalase, which can scavenge the ROS excessive to cellular metabolism, and make ROS level relatively stable under physiological conditions. Under the conditions used in our experiments, endogenous antioxidant enzyme activities of HL-60 cells (SOD and GPx activity) did not show pronounced alterations following RF-field exposure as compared to sham-exposure. Therefore, the first proposed mechanism mentioned above seems to be dominant.

In summary, the findings of an increase of micronuclei induction as well as Comet formation in HL-60 cells after exposure to RF-EMF at the conditions stated above indicate, that RF-EMF might generate genotoxic effects. The results obtained clearly show that RF-EMF under distinct exposure conditions cause DNA damage in human HL-60 cells. Since on the basis of these data RF-EMF have to be regarded as potentially genotoxic, it is pivotal to clarify first the molecular mechanisms involved in these potentially clastogenic effects in forthcoming experiments and secondly the biological consequences of DNA damage induced by RF-EMF, in particular the relevance for inducing mutations and changes in cellular signalling cascades. Responsive to the European Commission´s suggestions, additional independent verification experiments of the results obtained so far have to be conducted in the same cell line and other cell types, which are normal or similar in the metabolic process. Studies on indirect genotoxicity (e.g., reactive oxygen species, oxy-DNA, DNA repair) of RF-EMF on HL-60 cells, have to be extended. Studies on potential changes in gene expression profiles with respect to DNA repair have to be continued in co-operation with other groups.

4.2.1.2 Human fibroblasts and granulosa cells of rats (Participant 3)

RF-EMF generated DNA strand breaks in granulosa cells of rats and DNA strand breaks and chromosomal aberrations in human fibroblasts.

We could demonstrate an induction of DNA single and double strand breaks upon RF-EMF exposure in human diploid fibroblasts and in rat granulosa cells in culture. This induction depended on exposure duration as well as on the applied signal and could be determined in cells of different tissues. Based on the findings which we obtained with ELF-EMF, we also used for the intermittent RF exposure an “on” duration time of 5 minutes and an “off” duration time of 10 minutes. In contrast to ELF-EMF, RF-EMF induced DNA strand breaks also under continuous exposure conditions. However, the effects were more pronounced under intermittent exposure conditions at 5 min on /10 min off cycles.

The identification of the processes which lead to this DNA breakage will help to determine the extent of biological effects induced by RF-EMF exposure. Importantly, cellular effects observed in this study started already at an SAR of 0.3 W/kg which is far below 2 W/kg, the highest level allowed by the European safety limits. This suggests that the currently allowed radiation emission levels for the mobile phones, are clearly not sufficient to protect from biological effects. We have demonstrated, that the effect of ELF-EMF depends on the cell type and the on and off duration times used in research. The negative effects of RF-EMF reported in the literature (McNamee et al. 2002a, b; Tice and Hook 2002; d'Ambrosio and Scarfi 2002a), however, are based on lymphocytes and continuous exposure.

As with Elf-EMF, RF-EMF exposure of human fibroblasts induced also an increase in micronuclei and an even higher incidence of chromosome gaps, chromosome breaks, dicentrics and acentric fragments, which was 10-fold after ELF-EMF exposure as compared to control cells and 100-fold after RF-EMF

exposure. The RF-EMF results regarding chromosomal aberrations are of preliminary nature, but they are in line with the results obtained after ELF-EMF exposure. The evaluation of the micronulei carried out in our laboratory was reproduced blindly with coded slides in two independent laboratories that do not belong to the REFLEX consortium (Universities of Ulm and Kaiserslautern, Germany).

RF exposure revealed a significant decrease in the mitochondrial membrane potential in one experiment, which could not be reproduced. The RF induced formation of DNA strand breaks could not be related to changes in the membrane potential.

4.2.1.3 Mouse embryonic stem (ES) cells (Participant 4)

RF-EMF exposure of ES-derived neural progenitor cells induced a low transient increase of double DNA strand breaks measured by the neutral Comet assay.

Since we observed an up-regulation of GADD45, which is a DNA-damage inducible gene, it was logical to test the induction of primary DNA damages. It has been shown previously that EMF exposition of human HL-60 cells resulted in an increase of DNA breaks, suggesting a direct mutagenic effect (Ivancsits 2002). In addition, a correlation was found between up-regulation of GADD45, of the bcl-2 family member bcl-$X_{L,}$ and an increased amount of early DNA damage measured by the alkaline Comet assay in human preneuronal cells exposed to the amyloid protein (Santiard-Baron 2001). Therefore, we used the alkaline and neutral Comet assay to detect single, and double-strand DNA breaks, resp., in neural progenitors derived from murine pluripotent ES cells after RF-EMF exposure. Under our experimental conditions, 6 hours exposure to GSM signals induced a low transient increase of double-strand DNA breaks, whereas ELF-EMF did not induce a significant DNA damage. Our finding suggests that genotoxic effects of RF-EMF, at least *in vitro*, could not be excluded.

4.2.1.4 Summary (Participant 1)

As discussed by Participant 2 (4.2.1.1) there is sporadic literature about in vitro studies demonstrating that RF-EMF may possess a genotoxic potential (The Royal Society of Canada 1999; Stewart Report 2000). Since the energy impact on the genome of livings cells exposed to RF-EMF was calculated to be too low to cause DNA damage and since the mainstream literature contradicted the assumption of genotoxic effects (Moulder et al. 1999; Meltz 2003), these sporadic findings were considered more or less meaningless. Opposite to this widely accepted view, the data of the REFLEX study which were elaborated in a hitherto unknown systematic approach and confirmed in four laboratories, of which two were not members of the REFLEX consortium, support the view that RF-EMF causes genotoxic effects in certain, if not all cellular systems.

Based on the methodology used and the data obtained in the REFLEX study, the findings on genotoxicity caused by RF-EMF are hard facts. RF-EMF exposure at a SAR value below 2 W/kg induced an increase in DNA single and double strand breaks as well as in micronuclei in HL-60 cells. The DNA damage was dependent on the time of exposure, the field strength of RF-EMF and the type of RF-EMF signals. There is some indication that the effects may be caused via an increase in free oxygen radicals generated by RF-EMF (3.2.1.1, 4.2.1.1). RF-EMF exposure between SAR values from 0.3 to 2.0 W/kg made also DNA single and double strand breaks in human fibroblasts and in granulosa cells of rats dependent on the exposure time and the type of signals. This increase of DNA-strand breaks in human fibroblasts was accompanied by an increase in micronuclei and in chromosomal aberrations thus demonstrating that the DNA repair was not error-free (3.2.1.2, 4.2.1.2. In addition, RF-EMF exposure at a SAR value of 1.5 W/kg caused a slight, but significant increase in DNA double strand breaks in embryonic stem cells of mice (3.2.1.3, 4.2.1.3).

As already stated, for energetic reasons, RF-EMF can neither denature proteins nor damage cellular macromolecules directly. If the energy impact on the genome of living cells exposed to RF-EMF is too low for a DNA damage, the genotoxic alterations observed in the REFLEX project must be produced indirectly through intracellular processes in the course of RF-EMF exposure. In their experiments Participant 2 observed an increase of free radicals in HL-60 cells after RF-EMF exposure. With the oxygen radical scavenger ascorbic acid was it possible to inhibit the generation of DNA strand breaks and of micronuclei during RF-EMF exposure (3.2.1.1, 4.2.1.1). This findings support the assumption that the observed DNA damage may be caused by free oxygen radicals which are released by RF-EMF during

exposure. This possibility is further strengthened by the observation of Lai and Singh (1997a,b), who demonstrated that the increase in single and double DNA strand breaks in brain cells of RF-EMF exposed rats can be blocked with radicals scavengers. A final conclusion whether or not this finding is indisputable is still pending, since an increase in DNA strand breaks at the same model could not be confirmed by another research group (Malyapa et al. 1997, 1998).

Taken together, RF-EMF is able to damage the genome at least in certain cell systems after exposure in vitro. As with ELF-EMF, the genotoxic effects of RF-EMF may be best explained indirectly by an RF-EMF induced intracellular increase in free radicals. It is well known that a balanced free radical status is the prerequisite for maintaining health and that an unbalanced free radical status promotes the process of ageing and the development of chronic diseases such as cancer and neurodegenerative disorders. Whether the balance of free oxygen radicals can also be impaired through RF-EMF in vivo as suggested by the work of Lai and Singh (1997a,b) needs further clarification.

4.2.2 Cell proliferation and differentiation

4.2.2.1 NB69 neuroblastoma cells and neural stem cells (NSC) (Participant 5)

RF-EFM did not affect cell growth of NB69 and neural stem cells.

A short-tem (24h) exposure to the GSM-Basic signal does not modify the cell growth of NB69 cells and NSC. However, as described in 4.2.4.2, this signal induced in both cell a reduction in the proportion of cells expressing FGFR1. Signalling through fibroblast growth factor receptors (FGFRs) is essential for many cellular processes, including proliferation and differentiation (Kovalenko et al., 2003) and nervous system development (Oh et al. 2003). Our results indicate that in the selected exposure conditions, the GSM-basic signal does not induce changes in cell proliferation. Also, the short-term response induced by this GSM-signal on FGFR1 does not seem to be related to changes in cell growth.

4.2.2.2 Human lymphocytes and thymocytes (Participant 8)

RF-EMF may not affect proliferation, cell cycle, apoptosis and activation of human lymphocytes and thymocytes.

The immune system plays a decisive role in health and disease. Therefore, it was important to find out whether or not RF-EMF affect the immune system. Lymphocytes were exposed to RF-EMF at 1800 MHz with three different signals, such as GSM basic, Talk modulated and DTX only (SAR 1.4 - 2 W/kg).The in vitro tests were chosen in order to study the following endpoints: 1) cell proliferation; 2) cell cycle; 3) expression of membrane receptors on T lymphocytes, 4) spontaneous and induced apoptosis; 5) mitochondrial membrane potential (MMP) modifications in induced and spontaneous apoptosis ; 6) cytokine production; 7) Hsp70 levels in induced and spontaneous apoptosis; 8) thymocyte development and apoptosis; 9) T lymphocyte gene expression.

On the whole, the results obtained suggest that no differences exist for the most endpoints studied in RF-EMF exposure. Only some slight differences were observed in PBMCs; in particular, CD8+CD28+ appeared increased in exposed cultures, but the difference (3%) of the order of the calculated standard error did not indicate a relevant effect from a biological point of view. Actually, in a previous work we found that 900 MHz (SAR 76 mW/kg) RF seem to slightly decrease lymphocyte proliferation when these cells are low-stimulated (Capri et al., accepted 2004); thus our results suggest that RF effects on lymphocyte proliferation are frequency-dependent. However, the literature on this field is still scanty. Some groups showed different effect on cytolitic T lymphocyte proliferation (Cleary et al. 1996) and some groups did not found significant effects on mitotic indices between RF-exposed and sham-exposed lymphocytes (Vijayalaxmi et al. 1997).

A more interesting result appears the decrease of CD95 molecules on membrane surface of stimulated CD4 helper T cells, from elderly donors, which was found when cells were exposed to Talk modulated RF in comparison with sham exposed cells. Due to the importance of this receptor in the regulation and homeostasis of immune response, these results deserve further evaluations to confirm this decrease (around 9%) on CD^{4+} helper T lymphocytes from elderly and not from young donors.

An important observation was the observed decrease (around 13%) of IL-1 b production; this effects was found only in low-stimulated PBMCs exposed to DTX RF and suggest that a possible cell target of RF-EMF are monocytes rather than lymphocytes. Also this effect deserves further investigation in order to confirm possible interactions of RF-EMF exposure with human monocytes. Data in the literature are really scanty. A recent study, performed in vivo, demonstrated a transient increase of interferon-g (IFN-g) in mice exposed to GSM-modulated 900 MHz in mice exposed 2 hours/day for 1, 2 and 4 weeks in a TEM cell (Gatta et al. 2003)

Negative results are extremely important for evaluations on human health risk. RF-EMF exposure is obviously not able to interfere with cell cycle, spontaneous or chemically- induced apoptosis, mitochondrial membrane polarisation and cell activation. Negative results were also obtained on thymocyte development. This last result is extremely important, since it was observed in conditions very near to what happens in vivo. Moreover, results from gene expression of quiescent T lymphocyte confirm the absence of significant changes due to RF-EMF exposure.

4.2.2.3 Human promyelocytic cell line HL-60 (Participant 2)

RF-EMF generated genotoxic effects in HL-60 cells within a narrow energy window without affecting cell proliferation, cell progression and apoptosis.

Using the MTT assay, the annexin V assay, the TUNEL assay, cell counting, determination of cellular doubling time and thymidine kinase activity, it could be shown that the RF-field at 1800 MHz, SAR 1.3 W/kg and 24h exposure did not effect cell viability and cell growth, and did not induce apoptosis in HL-60 cells. These findings are in substantial agreement with previous literature reports on effects of RF-EMF in HL-60 cells and other human cells (e.g., Hambrook et al. 2002, Higashikubo et al. 2001). In contrast to the present results, induced cell proliferation and apoptosis have been reported in various other cell types after exposure to EMF (Blumenthal et al. 1997, Philips et al. 1997, Ismael et al. 1998, Kwee and Raskmark 1998, Simko et al. 1998, Velizarov et al. 1999).

4.2.2.4 Mouse embryonic stem (ES) cells (Participant 4)

RF-EMF exerted no influence on ES-derived cardiogenesis and did not affect DMSO-induced cardiac differentiation, proliferation and expression of regulatory genes in P19 EC cells.

Several in vitro studies report negative effects of high frequency EMF on cell cycle, gene expression and differentiation (Fritze et al. 1997; Cain et al. 1997; Goswami et al. 1999; Ivaschuk et al. 1997), DNA and chromatin structure (ICNIRP 1996; Repacholi 1998) and rat embryo development (Klug et al. 1997). In contrast, several reports described positive effects by high-frequency EMF exposure on the length of cell cycle phases, proliferation and gene expression levels in mammalian cells (Cleary et al. 1996; Czerska et al. 1992; Goswami et al. 1999; Lai and Singh 1996a; Sarkar et al. 1994). These studies, however, were performed with different experimental models, carrier frequencies (835 MHz to 2.45 GHz versus 1.71 GHz used in our study) and modulation schemes, and therefore, are not comparable. Moreover, positive RF-EMF effects were often observed at relatively high average SAR values (Cleary et al. 1996; Czerska et al. 1992; Fritze et al. 1997), which suggests that they could arise from RF-EMF-evoked thermal effects. In our studies, GSM signals were applied under conditions of the ICNIRP safety limit using an experimental set-up that enabled precise temperature control (Schönborn et al. 2000), and any temperature increase as a consequence of EMF exposure (Laurence et al. 2000) can be excluded.

For the evaluation of embryotoxic effects of chemical compounds in vitro, the mouse embryonic stem cell test (EST, (Spielmann et al. 1997) using cardiac differentiation of ES cells as endpoint has been established. Therefore, for a further specification of the effects of GSM-217 signals, we analysed EMF exposure during the process of cardiac differentiation. GSM-217 EMF exerted no influence on ES-derived cardiogenesis and did not affect DMSO-induced cardiac differentiation, proliferation and expression of regulatory genes in P19 EC cells. These data present evidence that wild-type ES cells are not sensitive during cardiac differentiation to EMF. However, this finding is in contrast to EMF-induced effects in ES-derived neural progenitors.

The differentiation process in cells is affected by RF-EMF exposure, when applied at the neural progenitor stage.

The intact nervous system might be very sensitive to induced electric fields and currents, due to the high level of spontaneous activity and the greater number of interacting neurons. It has been suggested that induced current densities above 10 mA/m^2 may have effects on some central nervous system functions (Saunders and Jefferys 2002). Because of the special public concern for neurotoxicity due to EMF exposure, we used an experimental protocol successful at selectively differentiating ES cells into the neural lineage (Rolletschek et al. 2001). It provides a tool to investigate in vitro neuropathogenic effects of environmental factors during early development. We exposed the cells to EMF during the differentiation stage when the first neural nestin-positive progenitors appear. This developmental stage is presumably very sensitive to environmental factors. In our experiments, we observed RF-EMF effects on neural differentiation. Among the investigated transcripts (the mRNA levels of the neuronal genes TH, Nurr1 and en-1, and the astrocyte-specific gene GFAP) we observed a statistically significant down-regulation of nurr at 4d+11d and TH at the terminal stage 4d+23d. This might indicate a delayed neural differentiation and would correlate with the up-regulation of the growth arrest gene GADD45 at terminal stage. The significant up-regulation of GADD45 at the terminal stage 4d+23d was also confirmed by quantitative RT-PCR with TaqMan probe. Bcl-2, whose transcript levels were found increased in our study, has also been shown to be involved in neuronal differentiation and axonal regeneration (Daadi et al. 2001). Human teratocarcinoma-derived neurons expressed bcl-2 in 85% of the implanted neurons after transplantation into the rat striatum. In addition, the in vitro induction into the neuronal lineage resulted in an up-regulation of bcl-2 expression. The authors suggested that neuronal differentiation could be mediated at least partially by bcl-2 (Daadi et al. 2001).

Since we observed an up-regulation of GADD45, which is a DNA-damage inducible gene, it was logical to measure the eventual induction of primary DNA damages (4.2.1.3)

4.2.2.5 Summary (Participant 1)

As discussed by Participant 4 (4.2.2.4), the results on possible effects of RF-EMF on cell proliferation and differentiation in vitro which are reported in the literature (The Royal Society of Canada 1999; Stewart Report 2000) are controversial. The REFLEX data do not reveal a significant effect of RF-EMF on proliferation and differentiation of various cell systems such as neuroblastoma cells (NB69) and neuronal stem cells (3.2.2.1, 4.2.2.1), embryonic cancer cells (P19) (3.2.4.1, 4.2.2.4), human lymphocytes and human thymocytes (3.2.2.2, 4.2.2.2) and HL-60 cells (3.2.2.3, 4.2.2.3). In neural progenitor cells only some effect on the differentiation process was observed at a SAR level of 1.5 W/kg (3.2.4.1, 4.2.2.4). Quite obviously, whether or not living cells respond to RF-EMF exposure in vitro may depend on the type of the cell, its genetic background, its metabolic state and, of course, on the exposure conditions.

An answer of what may be the reason for the sporadically observed, but until now not confirmed influence of RF-EMF on cell proliferation and differentiation may be provided by the REFLEX findings on gene and protein expression. As shown by Participant 5, RF-EMF reduced the expression of the receptor FGFR1 of fibroblast growth factor (FGF) in the human neuroblastoma NB69 cell line and in neural stem cells from rat embryonic nucleus striatum (3.2.4.2, 4.2.4.2). Participant 3 (3.2.4.3, 4.2.4.3), Participant 6 (3.2.4.6, 4.2.4.6), and Participant 12 (3.2.4.7, 4.2.4.7) observed, that RF-EMF enhanced the expression of various genes among them ribosomal and mitochondrial genes, ATP related genes and genes encoding calcium-associated proteins and cell cycle proteins.

Of course, the relationship between RF-EMF exposure and the acceleration or inhibition of cell proliferation and differentiation in vitro caused by alteration of gene and protein expression is not proven yet. Should that be shown one day, it is to be found out, whether such cellular events occur also in vivo in RF-EMF exposed man and animal. The most recent data of Weisbrot et al. (2003), who observed an increase in the numbers of off-springs, an elevation of the hsp70 levels, an increase in serum response element (SRE) DNA-binding and an induction of the phosphorylation of the nuclear transcription factor, ELK-1, in Drosophila melanogaster after RF-EMF discontinuous exposure (900/1900 MHz, 1.4 W/kg) during the 10 day developing period, speak in favour of such an assumption.

4.2.3 Apoptosis

4.2.3.1 Brain cells of different origin and human monocytes (Participant 9)

There is no indication that apoptosis is affected in nerve and immune cells after exposure to GSM-like RF-EMF.

Beside the importance of the apoptotic process in cellular homeostasis, only a few papers are available in the literature on the effects of ELF-EMF on apoptosis and almost no data were published on the interaction of RF fields with the apoptotic process. Thus, one of our objectives within the REFLEX programme was to investigate the potential role of environmental electromagnetic fields, specifically GSM-900 radiofrequency radiation (RFR) on the apoptotic process in critical cell types.

Briefly, apoptosis or programmed cell death plays a central role both in development and homeostasis of multicellular organisms (Skulachev 2002). A dual physio-pathological role of cellular apoptosis has been described (Rossi and Gaidano 2003). On the one hand, apoptosis is a major mechanism of protection against genotoxic agents since potential cancer cells are removed by apoptosis. On the other hand, dysregulation in the apoptotic pathways is involved in different pathologies since excessive apoptosis can contribute to diseases such as AIDS or neurodegenerative diseases (Olney 2003) whereas default in apoptosis is involved in cancer or autoimmune diseases (Burns and el-Deiry 2003). Moreover, inducing apoptosis in apoptosis-resistant tumour cells may lead to therapeutic applications (Tolomeo and Simoni 2002) while preventing apoptosis in apoptosis-sensitive cancer cells may be deleterious.

Because the phone is close to the head when in use, brain cells represent a major potential target for RFR emitted by the phones. Furthermore, one of the most critical cell types in the central nervous system is primary neurons. For our studies, we chose rat granule cells. Granule cells of the cerebellum constitute the largest homogeneous neuronal population of mammalian brain. Cerebellar granule cells are a model of election for the study of cellular and molecular correlates of mechanisms of survival/apoptosis and neurodegeneration/neuroprotection (Contestabile 2002). We failed to detect any influence of GSM-900 exposure on apoptosis in this highly critical cell type. All other nerve cell types tested, i.e. SH-SY5Y neuroblastoma cells, human U87 astrocytoma cells and rat C6 glioma cells - a priori less critical than granule cells - were not shown to be sensitive to GSM-900 exposure for up to 24 hours. Hence, no demonstration of an immediate or delayed effect of RFR on apoptosis in nerve cells has been made in rat primary cells and human cell lines. We conclude from our results that nerve cells do not represent a major target, in terms of apoptosis, for RFR emitted by mobile phones.

Because of the role of the immune system for cell homeostasis, cells from the immune system were to be tested. No evidence for an immediate, cumulative or delayed effect of RFR on apoptosis was shown in a human monocytic cell line. Gene expression experiments gave some confirmation that RF-EMF (GSM-900) had no influence on apoptosis in U937 cells as no significant effect was demonstrated on genes involved in apoptosis. We conclude from our results that U937 cells are not sensitive to GSM-900 exposure for up to 48 hours. Taken together, in our experiments, no substantial effect of exposure to RF-EMF (GSM-900) on spontaneous apoptosis of nerve and immune cells was found. No delayed effect could be evidenced either. When tested, interaction between GSM-900 exposure and pro-apoptotic chemicals could not be evidenced.

The results from the REFLEX programme strongly suggest that the apoptotic process may not be a major biological target for GSM mobile telephony-related signals. The REFLEX programme is contributing to most of our current knowledge on the effects of RF fields on cellular apoptosis. Two papers have been very recently published on that topics. Hook et al. (2004) found no evidence of programmed cell death in Molt 4 human lymphoblastoid cells after exposure to 4 different American signals for up to 24 hours at SAR ranging from 0.0024 and 3.2 W/kg. Markkanen et al. (2004) in Finland reported that 900-MHz CW or GSM-modulated RF fields at a SAR of 0.6 W/kg did not induce apoptosis in a control yeast strain and in its temperature-sensitive mutant of cdc48 (apoptosis strain). When yeast strains were pre-exposed to UV, GSM-900 only was able to enhance the UV-induced apoptosis in the mutant yeast strain only. In the REFLEX programme, no significant effect on spontaneous apoptosis was detected in cells from the immune system (human peripheral blood mononuclear cells, human U937 cells) and in EA.hy926 human endothelial cells exposed to RFR-fields (GSM-900 and GSM-1800). No delayed effect (time kinetics) after RFR exposure was demonstrated.

In the present body of work, the status (transformed or non-transformed) of cells used did not influence the effect of RF-fields. The signalling pathways involving bcl-2 was not affected in either $p53^{+/+}$ or $p53^{-/-}$ embryonic stem cells tested after exposure to RFR-fields. The activity of caspase3 was not altered in EA.hy926 cells. In all systems tested, intermittence in the signal did not elicit apoptosis. Data also suggest that for the exposure conditions tested, field effects were not substantially affected by the cell genetics (embryonic stem cells), or the age of the donor (human peripheral blood mononuclear cells).

Hence, no effects of GSM signals (GSM-900 and GSM-1800) have been detected on spontaneous apoptosis of mature and embryonic stem cells in the various groups involved in REFLEX, even in conditions reported to modify other biological endpoints (for instance, an increase of hsp27 expression was detected in EA.hy926 human endothelial cells, 4.2.4.6). However, the expression of the bcl-2 anti-apoptotic gene was shown to increase in murine differentiating embryonic stem cells after exposure to GSM-1800, which correlated with changes in the process of neural differentiation (down-regulation of certain neuronal genes, 4.2.2.4). This needs to be further investigated in order to understand the potential relevance for human health.

We then focused our research on the investigation of some interaction between RF-EMF and known pro-apoptotic drugs. Extension of studies on the expression of apoptosis-related genes was also performed. The data show that cells from the immune and the nervous systems did not exhibit any sensitivity in a concomitant or successive treatment with apoptogenic chemicals and GSM signals, by contrast to cells from the endothelium. However, even in that cell type, GSM-900 was shown to interact with only one chemical (polyHema) over the two chemicals tested. The effect observed was a partial prevention of chemically-induced apoptosis. In this cell line, a weak decrease in pro-apoptogenic genes after exposure to GSM-900 was correlated with the former effect observed. These data on endothelial cells have still to be independently replicated.

Moreover, apoptosis-related genes were shown only weakly affected after exposure to RFR when compared to other gene families such as the ribosomal-related genes (Participant 12). Compared to data of the Juutilainen group, experiments performed within the REFLEX consortium used mammalian cells instead of yeast cells. This, as well as the nature of apoptogenic agent (chemical versus physical), may account for the discrepancy observed in the interaction experiments.

These data suggest that, except for murine differentiating stem cells, low-level RFR are not able to interfere with the spontaneous integrative apoptotic process. If confirmed, interaction with pro-apoptotic chemicals is suggested to be highly dependent of the cell type and the chemical agent used.

4.2.3.2 Human lymphocytes (Participant 8)

RF-EMF may not affect apoptosis in human lymphocytes.

1800 MHz RF (GSM basic, Talk and DTX modulated; SAR 1.3 - 2 W/kg) is not able to modify spontaneous and chemical-induced apoptosis, when human PBMC were exposed 10 min on and 20 min off for 44 hours. This result was also confirmed using cells from old donors (GSM basic, SAR 2 W/kg), since their cells could result differently susceptible to undergo apoptosis (Salvioli et al. 2003). Data were further confirmed by the analysis of mitochondrial membrane potential, which was not affected by RF in all the conditions tested. Negative results were also obtained analysing thymocyte apoptosis during their differentiation. On the basis of these data we can conclude that these types of exposures do not affect apoptotic process, even if this is not established for longer or chronic exposures. (4.2.2.2)

4.2.3.3 Human promyelocytic cell line HL-60 (Participant 2)

Using the annexin V assay and the TUNEL assay, it could be shown that RF-EMF at 1800 MHz, SAR 1.3 W/kg and 24h exposure did not affect cell viability and cell growth, and did not induce apoptosis. (4.2.2.3**)**

4.2.3.4 Mouse embryonic stem (ES) cells (Participant 4)

RF-EMF affected the bcl-2 –mediated anti-apoptotic pathway in differentiating embryonic stem cells.

An up-regulation of bcl-2, bax and GADD45 transcript levels was observed after exposure of ES-derived neural progenitors at specific stages of differentiation to high frequency and extremely low frequency electromagnetic field. We studied the gene expression levels of regulatory genes like hsp70, p21 and apoptosis–related genes of the bcl-2 family (the anti-apoptotic bcl-2 and the pro-apoptotic bax gene). These regulatory genes were pre-selected after our previous experiments with undifferentiated p53-deficient ES cells, where we found significantly increased transcript levels of p21 and hsp70 (Czyz 2004a) after RF-exposure and of p21 after ELF-EMF exposure (50 Hz Powerline) (Czyz 2004b). Therefore, we analysed the effects of EMF on apoptosis-related genes in wild-type (wt) embryonic stem cells at the stage of neural differentiation. Our data demonstrated up-regulation of the transcript levels of bcl-2 in neuronally differentiated ES cells at terminal stages for RF-EMF. However, the biological significance of this finding and its relevance to the situation in vivo has to be clarified.

Apoptotic cell death is executed by caspases and can be regulated by members of the bcl-2 family as reported for differentiating murine embryonic stem cells (Sarkar and Sharma 2002). Apoptosis plays an important role during embryonic development, including the development of the nervous system. Studies applying the model of central axotomy in mouse have shown a degeneration of up to 70% of nigral neurons post transection due to the activation of c-jun, but bcl-2 over-expression leads to a reduced phosphorylation state of c-jun in transected neurons and protection against cell death (Winter et al. 2002). Bcl-2 over-expression was also reported to eliminate deprivation-induced cell death of brainstem auditory neurons (Mostafapour et al. 2002). In other studies, in situ hybridisation revealed a rapid and transient increase in bcl-2 mRNA in neurons following de-afferentation (Wilkinson er al. 2002).

In the RF-EMF experiments, we extended our study by including the analysis of mRNA levels of the growth arrest DNA-damage inducible (GADD45) gene and found a significant up-regulation at the terminal stage of differentiation (at 4+23d). The members of the GADD protein family are considered to play important roles in maintaining genomic stability and in regulating the cell cycle (Chung et al. 2003). The phenotype of GADD45-deficient mice is similar to the phenotype of p53-deficient mice, including genomic instability and sensitivity to radiation induced carcinogenesis (Hollander et al. 1999). GADD45 was found to promote G2/M arrest thus inhibiting entry of cells into S-phase and allowing genomic DNA repair in keratinocytes (Maeda et al. 2002). These findings suggest that GADD45 is a component of the p53 pathway that maintains genomic stability, albeit damage-induced transcription of the GADD45 gene is supposed to be mediated by both p53-dependent (Kastan et al. 1992) and p53–independent mechanisms (Jin et al.2001). Our results, which demonstrate an up-regulation of bcl-2 and GADD45 mRNA levels indicate, that electromagnetic signals are, probably, perceived in embryonic stem cell-derived neural progenitors as environmental stress signals at defined stages of differentiation. Such signals may trigger cellular responses for maintenance of the cellular homeostasis via mobilization of the mechanisms of DNA repair and protection against apoptotic cell death.

4.2.3.5 Human the endothelial cell lines EA.hy926 and EA.hy926v1 (Participant 6)

RF-EMF may affect the hsp27 mediated anti-apoptotic pathway in human endothelial cells.

Stress proteins are known to regulate cell apoptosis (Pandey et al. 2000; Mehlen et al. 1996; Creagh et al. 2000). RF-EMF-induced deregulation of apoptotic process might be a risk factor for tumour development because it could lead to the survival of cells that “should” die. This notion was suggested in the hypothesis presented recently by French et al. (2001). We suggest that the apoptotic pathway regulated by hsp27/p38MAPK might be the target of RF-EMF radiation (6.2.4.6).

4.2.3.6 Summary (Participant 1)

As discussed by Participant 9 (4.2.2.4), knowledge on a possible influence of RF-EMF on the apoptotic process in living cells *in vitro* is rather poor. In the two most recent studies no such effect of RF-EMF was observed (Hook et al. 2004; Markkanen et al. 2004). The REFLEX data did not reveal a significant influence of RF-EMF on apoptosis of various cell types such as brain cells and human monocytes (see 3.2.3.1 and 4.2.31), human lymphocytes (3.2.3.2, 4.2.3.2) and HL-60 cells (3.2.1.1, 4.2.3.3). On the other

hand, an indirect effect on apoptosis via the bcl-2 or hsp27 mediated anti-apoptotic pathway which was detected in differentiating embryonic stem cells (3.2.4.1, 4.2.3.4) and in endothelial cells, respectively (3.2.4.6, 4.2.3.5), cannot be excluded at this time.

Of course, based on the data on gene and protein expression obtained in the REFLEX project, an effect of RF-EMF on the apoptotic pathway, either through inhibition or promotion, seems to be possible. Whether or not cell cultures respond to RF-EMF may depend on the type of cell exposed, their genetic background, their metabolic state and, of course, on the pattern of exposure. But taken together, even if a relationship between RF-EMF exposure and an inhibition or promotion of apoptosis in *in vitro* experiments were proven, it would in no way be possible to draw any conclusion for the *in vivo* situation in man and animal.

4.2.4 Gene and protein expression

4.2.4.1 Mouse embryonic stem (ES) cells (Participant 4)

The genetic constitution of early differentiating embryonic stem cells may play a role on their responsiveness to differently modulated RF-EMF.

In ES cells deficient for the tumour promoter p53, a permanent up-regulation of mRNA levels of the stress response gene hsp70 paralleled by a slight and temporary increase of p21, c-jun and c-myc expression was found in response to GSM-217- but not GSM-Talk-modulated signals characterized by the presence of low frequency components. On the other hand, wt ES and EC cells exposed to GSM-217 signals revealed no effects on gene expression, cardiac differentiation and proliferation. This would indicate, that the genetic background of stem cells may potentially influence the response of early differentiating cells to GSM signals dependent on the modulation schemes, whereas wt cells analysed in this study remained insensitive to GSM-modulated EMF.

p53-/- mice are highly susceptible to the development of spontaneous tumours, in particular, of malignant lymphomas at early age (Attardi and Jacks 1999; Sigal and Rotter 2000). p53 is required for G1 arrest in response to DNA damage and is involved in apoptosis (Attardi and Jacks 1999) via modulating versatile regulatory genes. In our studies using mouse $p53^{-/-}$ ES cells, hsp70 mRNA levels were continuously elevated after 48h EMF exposition. Heat shock proteins act as chaperons whose expression is activated or up-regulated in response to external stress (Beere and Green 2001). Hsp70 has also been defined to regulate homoeostasis in response to external stress during early embryo development (Luft and Dix 1999), while up-regulated hsp70 levels were observed in tumour cells and are correlated with metastases and poor prognosis (Zylicz et al. 2001). A potential involvement of heat shock proteins in cell responses to EMF was reported recently: up-regulated hsp27 protein levels and a transient increase of hsp27 phosphorylation were found in human endothelial cells (Leszczynski et al. 2002).

However, if EMF act as inducers of cellular transformation processes, effects on expression levels of other early response genes should be expected. Indeed, we observed an up-regulation of c-myc, c-jun and p21 mRNA levels in $p53^{-/-}$ cells upon GSM-217 exposure. The same genes were previously shown to be affected by environmental factors, such as UV or X-irradiation in various systems (Amati et al. 1993; Angel et al. 1988; Jean et al. 2001). Because in our model, the shifts in gene expression were low and transient, it is conceivable that EMF signals, while affecting gene expression pattern in $p53^{-/-}$ cells, do not induce permanent cellular transformations in wt cells.

The response of early differentiating cells to RF-EMF is dependent mainly on the carrier frequency of the modulation schemes.

Contrary to GSM-217 signals, which elicited cellular responses in $p53^{-/-}$ ES cells, GSM-Talk modulation exerted no effects on gene expression in our model. This indicates that low frequency components generated by GSM-Talk (2 and 8 Hz) do not promote the action of EMF signals in our cell system. In contrast, time-averaged SAR values (1.5 W/kg for GSM-217 vs. 0.4 W/kg for GSM-Talk) may comprise a factor determining the biological activity of EMF. Furthermore, it cannot be excluded that the modulation scheme (time distribution of high SAR pulses) may also play a role in evoking biological

responses, because slot-averaged SAR values remained similar between the analysed modulation schemes.

The exposure duration may also influence the biological responses to RF-EMF.

In our in vitro studies, up-regulated transcript levels of regulatory genes in $p53^{-/-}$ ES cells were observed after 48 hours exposure to GSM-217 signals, whereas a short-term 6h exposure exerted no effects.

The parameters of genetic constitution, carrier frequency and exposure duration in determining the response of biological systems to RF-EMF have been proposed by in vivo studies using Eμ-Pim1-transgenic mice predisposed to develop spontaneous lymphomas. Repacholi et al. observed an increase in tumour formation after long-term, 18 months exposure of Eμ-Pim1-transgenic mice to 900 MHz EMF (Repacholi et al. 1997), which positive data suggest that mobile phone radiation-induced events may be hazardous to cells deficient in cell repair when occurring frequently over long periods.

It has been shown previously that the exposition of human HL-60 cells resulted in an increase in DNA breaks, suggesting a possible direct mutagenic effect (Ivancsits et al. 2002). In addition, there is a report about a correlation between up-regulation of GADD45, of the member of the Bcl-2 family bcl-$X_{L,}$ and an increased amount of early DNA damage as measured by the alkaline Comet assay in human preneuronal cells exposed to the amyloid protein (Santiard-Baron et al. 2001). Therefore, we used the alkaline and neutral COMET assay to detect single, and double-strand DNA breaks respectively, in the neuronal progenitors derived from murine pluripotent ES cells after ELF or RF-EMF exposure. Under our experimental conditions, however, we could not find a clear evidence of increased single-strand DNA break induction in the alkaline Comet assay. A low but significant increase in double-strand DNA breakage was observed only after a short (6h) RF-EMF exposure in the neutral Comet assay.

In summary, we found that RF-EMF simulating GSM signals caused a transient up-regulation of p21 and c-myc genes and a long-term up-regulation of the stress response gene hsp70 in ES cells deficient for p53 in response to GSM-217- but not GSM-Talk-modulated signals characterized by the presence of low frequency components. Here again we found that the genetic constitution (loss of p53 function) could alter the responsiveness of ES cells and render them sensitive to high frequency EMF, while wild-type cells were irresponsive. However, we did not observe any distinct direct genotoxic effects as measured by the Comet assay.

In ES cell-derived neuronal progenitors we found indication of growth arrest and effects on apoptosis (a significant up-regulation of the growth arrest and DNA damage inducible gene GADD45, the proapoptotic bax and the antiapoptotic gene bcl-2 mRNA levels), which correlated with changes in the process of neural differentiation (down-regulation of the neuronal genes Nurr1 at stage 4d+11d and TH at 4d +23d).

4.2.4.2 NB69 neuroblastoma cells and neural stem cells (NSC) (Participant 5)

RF-EMF reduced the expression of the receptor FGFR1 of fibroblast growth factor (FGF) in the human neuroblastoma NB69 cell line and in neural stem cells from rat embryonic nucleus striatum.

In NB69 cells, this response is similar to that induced by exogenous treatment with 20 ng/ml of bFGF, and by the combined treatment with bFGF plus EMF. In this biological system, an induction of morphological changes (increases in cell size and cell extensions) is also observed after 24 hours of treatment with bFGF. Such morphological changes are accompanied with a reduction in the proportion of cells expressing FGFR1-3 receptors. However, in cultures exposed to the GSM-Basic for 24 hours the effect on FGFR1 was not associated to changes in the cells′ morphology. Evidence exists that treatment of olfactory neuroblastoma cells with bFGF deregulates FGFR1 prior to differentiation (Nibu et al. 2000). It is possible that in our NB69 cells the response induced the GSM-Basic signal on FGFR1 can also be associated to a promotion of differentiation in long-term cultures. Additional work using differentiation markers for neuronal NB69 cells has to be done to verify the above hypothesis.

On the other hand, in neural stem cells, the 24h-exposure also induced a reduced expression of receptor FGFR1, and further significant changes in the cell morphology were observed six days later, in the absence of the GSM-exposure. The oligodendrocytes showed an advanced developmental stage with respect to controls. Similarly, the astrocytes showed longer cell-processes. The morphology of the neuronal progeny of NSC was not significantly changed by the exposure to the GSM-Basic signal.

Evidence exists that treatment of a human astrocytoma cell line, U-87 MG, with 835 MHz electromagnetic radiation induces alterations in F-actin distribution and cell morphology (French et al. 1997). Their astrocytes showed a similar response to that observed in our precursors lineage exposed to the GSM-signal: an increased cell spreading. Taken together, the present data suggest that the reduction of cells expressing FGFR1 induced by signal could be linked to a promotion of the differentiation of non-neuronal populations.

The changes in FGFR1 induced by RF-EMF are dependent mainly on the carrier frequency.

Both, basic and CW signal induced similar changes on FGFR1. This suggests that the cellular response is not dependent on the tested low-frequency modulation, but on the carrier frequency. The signals used in advanced telecommunication systems such as global system for mobile communications (GSM) and universal mobile communications system (UMTS) include extremely low frequency (ELF) amplitude modulation or pulse modulation components. There is a lack of scientific data on the possible health implications of such modulations. A recent study (Huber et al. 2002) has reported that a 30-minute exposure to 900 MHz, 1 W/kg GSM signal can influence the electrical activity of the brain, both before and after sleep onset, in young male test subjects. Both sleep and waking EEG changes were observed only with pulse modulated-EMF. Also, it has been reported a statistically significant micronucleus effect in peripheral blood cultures following 15-minute exposure to phase modulated field (Gaussian minimum shift keying, GMSK), 1.748 GHz, at SAR $\leq$ 5 W/kg (d'Ambrosio et al. 2002b). However, the micronucleus frequency result was not affected by CW exposure. No changes were found either in cell proliferation kinetics after exposure to both CW and phase modulated fields. In our present work we investigated whether fibroblast growth factor receptors (FGFR) could be influenced by the modulation of the GSM-signals. NB69 cells were exposed to GSM- Talk, GSM-Basic and CW signals, 2 W/kg SAR or to DTX-signal, 1W/kg SAR. The exposure to GSM 1800-Basic signal at a 2 W/kg SAR was found to induce a significant decrease in the number of cells expressing the FGFR-1 (15% reduction vs. controls) without affecting significantly the number of cells expressing receptors R2 and R3. The effect on R1 was equivalent to that induced by basic fibroblast growth factor (bFGF) at a 20 ng/ml concentration. The exposure to RF-CW signal (SAR 2 W/kg) induced effects on the expression of FGFR-1 equivalent to those induced by the GSM-Basic signal, whereas the exposure to GSM-Talk signal at the same SAR (2 W/kg) or to DTX-signal (1 W/kg SAR) did not modify significantly the normal expression of the FGF protein receptors R1. Our results indicate that the ELF modulation components resulting from the GSM signals shape (2, 8 and 217 Hz) and higher harmonics are not critical for the EMF-induced changes in FGFR-1 expression. Provided that the Talk mode is a temporal change between GSM Basic (66%) and DTX only (34%) our data together with those from Partner 4 indicate that the exposure duration could also be a critical factor for the herein described response. Future studies may also examine dose-response relationships by varying the exposure time and the specific absorption rate.

4.2.4.3 Human promyelocytic cell line HL-60 (Participant 2)

RF-EMF modulates the gene and protein expression in HL-60 cells.

Applying high resolution two-dimensional polyacrylamide gel electrophoresis to the HL-60 cell system, more than 4000 protein spots can be differentiated on the silver stained protein map. These spots were detected and the master gel image was calibrated. Clear differences in protein expression have been found for RF-field exposed HL-60 cells as compared to control and sham-exposed cells. The quantitative comparison has been completed. Further strategies in the future will include structural and biochemical identification of proteins significantly altered following RF-field exposure, beside mass spectrometry (MALDI-TOF) and mass spectrometric sequencing (ESI-MS/MS) and immunoblotting/functional protein assays, also by comparative studies with reference databases. Clarification of changes in protein expression after exposure to RF-fields will help to understand molecular pathomechanisms.

4.2.4.4 Human lymphocytes (Participant 8)

RF-EMF did not affect gene expression in human lymphocytes.

1800 MHz RF (DTX modulated, SAR 1,4 W/kg) is not able to modify gene expression profile when quiescent T lymphocyte are exposed 10 min on/20 min off for 44 hours. This result, obtained in collaboration with Participant 12 by means of micro-array technique, was expected because lymphocytes

were not stimulated and represents a first step toward a further evaluation in low-stimulated and RF-exposed T lymphocytes; future analyses should clarify the presence of potential gene targets for RF exposure in primary human cells.

4.2.4.5 Brain cells of different origin, human immune cells and human endothelial cell lines (Participant 9)

There is no indication that expression and activity of the inducible Nitric Oxide Synthase (iNOS or NOS_2) is affected in nerve cells after exposure to RF-EMF.

Under pathological conditions, nitric oxide, NO, can act as a neurotoxic agent (Leist and Nicotera 1998; Brown and Bal-Price 2003). A variety of stresses are known to induce neuronal cell death via NOS_2 (or inductible NOS, iNOS) activation and NO production in stimulated astrocytic cells. Hence, activated astrocytes may be involved in the pathogenesis of neurodegenerative diseases. Our goal was to determine whether exposure to a GSM-900 signal could activate C6 glioma cells by increasing the activity of the iNOS enzyme. A potential synergistic effect of such radiofrequency radiation (RFR) on cytokine-induced NO production was also investigated.

A few data are available in the literature on the effect of RF-EMF on nitric oxide, NO, production. Over three identified papers, only one used RF-EMF compatible with mobile telephony. Miura et al. (1993) reported that 10 MHz RFR (10 kHz bursts) caused an increase in NO production in rat cerebellum extracts. Using ultra-wideband pulses, Seaman et al. (2002) recently showed no influence of RFR in the Ultra Wide Band (UWB) range in RAW 264.7 macrophages except when nitrate was added to the culture medium. Paredi et al. (2001) showed a tendency for higher nasal NO levels in humans exposed to GSM-900 for 30 minutes that was due to skin heating experienced by the phone's users. As it has been clearly shown that heating from mobile phone microwaves is negligible, this effect was probably due to the battery's heating. Based on our data, GSM-900 did not appear to be able to alter chemically- induced activation in mammalian astrocytes and thus appeared unlikely to influence tumour cells characteristics and neuronal cells' viability via NO pathways.

There is no indication that expression of heat shock proteins is affected in nerve cells after exposure to RF-EMF.

The first objective was to determine whether exposure to GSM-900 microwaves could influence the expression of hsp70 proteins in neuronal and glial cell lines as reported in an endothelial cell line by Participant 6.

In response to environmental disturbances, cells respond by expressing heat shock proteins. Our study focuses on the 70-kDa family, which is the major form of stress proteins found in the brain (Pavlik et al. 2003) and on hsp27 that is expressed in endothelial cells (Loktionova et al. 1996).

Our data showed that exposure to GSM-900 microwaves were not able to induce hsp70 expression in rat and human nerve cells. These data are not in agreement with results of recent research showing that the expression of heat shock protein (hsp) may be induced in response to radiofrequency radiation exposure at non-thermal levels in different models (de Pomerai et al. 2000, in worms; Kwee et al. 2001, in human amnion cells; Leszczynski et al., 2002 in human EA-hy926 endothelial cells; Weisbrot et al. 2003, in Drosophilae). Thus, a common feature on the effect of GSM-900 at low SAR (about 2 W/kg) on the expression of hsp cannot be drawn. Different cell types could behave differently to exposure to a GSM-900 signal or different members of the hsp family could show a different sensitivity to exposure to GSM signals. Moreover, we can note that, so far, none of the "positive" effects have been independently replicated.

We failed to independently confirm that expression of heat shock proteins is affected in EA-hy926 cells after exposure to GSM-like RF-EMF.

The second objective was to confirm the data of Participant 6 on hsp27 in the EA-hy926 cells. Hsp27 is indeed the major form of stress proteins that is expressed in endothelial cells (Loktionova et al. 1996). Our results obtained by fluorescent image analysis in the two cell lines tested differed from those obtained in one of them by Participant 6 after western blotting experiments. A third method using Elisa test will allow us to quantify precisely if RFR are able to induce changes in hsp27 expression since the sensitivity reported is 1-10 ng for Western Blot and less than 1 ng for ELISA.

Here, with our semi-quantitative method and statistical analysis we were unable to confirm previous data on hsp27 expression in endothelial cell lines. Exposure set-up used in both groups also differed (water bath versus air cooling, homogeneity of SAR distribution at the cells level, …etc), which probably imply different dosimetric features. Whether this could account for the discrepancies observed could be determined (Participant 10). Meanwhile, we cannot conclude yet that RFR induce stress response. Hence, no implication for health hazard can be drawn at the moment based on Hsp expression in mammalian cells after low level RFR exposure.

The possible effect of low-level RFR on the expression of hsp is quite controversial. While some laboratories reported effects in mammalian cells (Leszczynski et al. 2002; Kwee et al. 2001) or simple organisms (de Pomerai et al. 2000; Weisbrot et al. 2003) as stated above, we (present work), as other groups (Cleary et al. 1997; Tian et al. 2002a; Miyakoshi et al. 2003) could not observe any effect in mammalian cells at SAR up to 10 W/kg. To date, no clear and satisfactory explanation can be given. However, we do think that the investigation of hsp expression after RFR exposure in *in vivo* mammalian models will help and enlighten the debate. Some but still sparse data are available, showing that heat shock proteins could not be induced in rat brain below 7 W/kg (Fritze et al., 1997).

There is some indication that gene expression is affected in immune cells after exposure to RF-EMF.

These data were obtained in collaboration with Participant 12 (4.2.4.7). First, these results gave a confirmation that GSM-900 had no influence on apoptosis in U937 cells as no significant effect was demonstrated on genes involved in apoptosis. Then, only a few genes among several thousand tested genes were shown altered after RFR exposure (increase or decrease) in two human immune cell lines. The largest modification in RNA expression corresponded to genes related to signal transduction and energy metabolism. Finally, amine oxidase activity-related genes experienced the largest changes after exposure to mobile phone-like RFR. This later gene is coding for an enzyme which is involved in cell growth and proliferation but also in immune regulation. This gene-profiling analysis showed that RFR can influence some biological processes and gave us trails for further investigations such as looking at energy metabolism in cells exposed to RFR using spectroscopic NMR. Comparing gene profiling obtained in different cell types may provide a "signature" for environmental RF-EMF exposure. It is however still unclear if and how those changes in gene expression can be related to human health.

Reported gene profiling after ethanol stress in yeast (Alexandre et al. 2001) showed that about 6% of the yeast genome were experiencing changes (about 3% upregulated and 3% downregulated). This represents 20 fold more genes than what was found affected after exposure to RF-EMF (0.3%). Genes identified were mainly involved in energetic metabolism, protein destination, ionic homeostasis and stress response with more than 10 hsp members. Stronger criteria were used in Alexandre et al. (2001) for significance of changes in gene expression compared to ours. When compared with the effect of a strong stress agent such as ethanol (in yeast), RF-EMF affected only a few genes in the human immune cell lines we tested. Whereas genes involved in energy metabolism seem to be a common feature for both types of exposure, none of the genes identified in human immune cells after RFR exposure belonged to the stress response family. Based of these comparisons, RF-EMF may be identified as a weak environmental stress, if any.

4.2.4.6 Human endothelial cell lines EA.hy926 and EA.hy926v1 (Participant 6)

RF-EMF induce cellular stress response.

Observed in this study changes in protein phosphorylation and activation of p38MAPK/hsp27 stress response pathway agree with the earlier studies suggesting that mobile phone RF-EMF radiation induces cellular stress response at non-thermal power level. In vitro, Cleary et al. (1997) claimed that RF-EMF exposure has no effect on stress proteins. However, because identification of stress proteins was based solely on their molecular weight in liquid chromatography, the exact identity of proteins claimed to be stress proteins remains unclear. Fritze et al. (1997b), using rat model, have shown increase in expression of stress protein hsp70 in brains of animals exposed for 4 hours to RF-EMF (890-915 MHz) at SAR of 1.5 W/kg. Daniells et al. (1998) and de Pomerai et al. (2000) have shown that overnight in vivo irradiation of nematode worms with RF-EMF (750 MHz) at SAR of 0.001 W/kg cause increase in expression of heat shock protein. Kwee et al. (2001) have shown induction of stress protein hsp70, but not hsp27, in cultures of transformed human epithelial amnion cells exposed for 20 min to RF-EMF (960 MHz) at SAR of 0.0021W/kg.

Because of the known broad spectrum of physiological processes that are regulated by stress proteins (Tibbles and Woodgett, 1999), and by hsp27 in particular, it is here hypothesized that mobile phone radiation-induced activation of hsp27/p38MAPK-dependent cellular stress response might: (i) lead to the development of brain cancer due to inhibition of cell apoptosis and (ii) cause increased permeability of blood-brain barrier due to stabilization of endothelial cell stress fibers (Figure 138).

Stress proteins are known to regulate cell apoptosis (Pandey et al. 2000; Mehlen et al. 1996; Creagh et al. 2000). RF-EMF-induced deregulation of apoptotic process might be a risk factor for tumour development because it could lead to the survival of cells that "should" die. This notion was suggested in the hypothesis presented recently by French et al. (2001). We suggest that the apoptotic pathway regulated by hsp27/p38MAPK might be the target of RF-EMF radiation. Hsp27, stress protein shown in this study to be affected by mobile phone radiation exposure, is a member of a family of small heat shock proteins that is ubiquitously expressed in most of cells and tissues under normal conditions in form of large-molecular complexes. In response to stress occurs rapid phosphorylation of hsp27 on serine residues (in human cells Ser-78 and Ser-82) what leads to dissociation of the large-molecular complexes into smaller units (Kato et al. 1994). Various stress factors have been indicated as inducers of changes in expression (accumulation) and/or phosphorylation (activity) of hsp27 (Ito et al. 1995; Deli et al. 1995; Garrido et al. 1997; Huot et al. 1997; Tibbles and Woodgett 1999). Activated (phosphorylated) hsp27 has been shown to inhibit apoptosis by forming complex with the apoptosome (complex of Apaf-1 protein, pro-caspase-9 and cytochrome *c*), or some of its components, and preventing proteolytic activation of pro-caspase-9 into active form of caspase-9 (Pandey et al. 2000; Concannon et al. 2001). This, in turn, prevents activation of pro-caspase-3 which, in order to become active, has to be proteolytically cleaved by caspase-9. Thus, induction of the increased expression and phosphorylation of hsp27 by the RF-EMF exposure might lead to inhibition of the apoptotic pathway that involves apoptosome and caspase-3. This event, when occurring in RF-EMF exposed brain cells that underwent either spontaneous or external factor-induced transformation/damage, could support survival of the transformed/damaged cells what, in favourable circumstances, could help clonal expansion of the transformed/damaged cells - a prerequisite for the tumour development. Furthermore, hsp27 in particular was shown to be responsible for the induction of resistance of tumour cells to death induced by anti-cancer drugs (Huot et al. 1996; Garrido et al. 1997). Thus, it appears possible that RF-EMF induced changes in hsp27 phosphorylation/expression might affect not only tumour development but also its drug-resistance.

Induction of the increase of the permeability of blood-brain barrier by RF-EMF exposure, which has been suggested by some animal and in vitro studies, is one of the controversial health issues that came up in relation to the use of mobile phones. It has been already established that, at thermal levels of exposure, microwave radiation causes increase in the permeability of blood-brain barrier (for review see Jokela et al. 1999; The Royal Society of Canada Report 1999, Stewart Report 2000, Zmirou Report 2001). However, the effect of non-thermal RF-EMF exposure on blood-brain barrier is still unclear. Some studies have suggested that mobile phone radiation, at non-thermal exposure levels, increases permeability of blood-brain barrier *in vivo* (Salford et al. 1994) and *in vitro* (Schirmacher et al. 2000), whereas others suggested lack of such effect (Fritze et al. 1997a; Tsurita et al. 2000). However, the no-effect claimed by Fritze et al. (1997a) is not so straight forward as suggested by the authors because they reported induction of stress response and increased permeability of the blood-brain barrier immediately after the end of irradiation. This effect was short lasting and, because of it, was considered by the authors as insignificant. Also, it remains unclear what would be the blood-brain barrier response to the repeated exposures to mobile phone radiation because the effect of repeated exposures was not examined. The increased blood-brain barrier permeability due to increase of endothelial pinocytosis was suggested by Neubauer et al. (1990) who have demonstrated increase in pinocytosis of cerebral cortex capillaries that were exposed to 2.45 GHz microwave radiation. Finally, the recently reported study by Töre et al. (2001) has shown that 2 hour exposure of rats to RF-EMF (900 MHz) at SAR of 2W/kg (averaged over the brain) causes increase in the permeability of blood-brain barrier. However, the molecular mechanism and the cellular signalling pathways that are involved in the induction of blood-brain barrier permeability are still unknown. We propose that the induction of hsp27 phosphorylation and increased expression by RF-EMF exposure, shown in this study to occur in vitro in human endothelial cells, might be the molecular signalling event that triggers the cascade of events leading to the increase in blood-brain barrier permeability. Phosphorylated hsp27 has been shown to stabilize endothelial cell stress fibers due to the increased actin polymerisation (for review see Landry and Huot 1995). The stabilisation of stress fibres was shown to cause several alterations to endothelial cell physiology: (i) cell shrinkage and opening of spaces between cells (Landry and Huot 1995; Piotrowicz and Levin 1997), (ii) increase in the

permeability of endothelial monolayer (Deli et al. 1995), (iii) increase in pinocytosis (Lavoie et al. 1993), (iv) formation of apoptosis-unrelated blebs on the surface of endothelial cells which may obstruct blood flow through capillary vessels (Becker and Ambrosio, 1987), (v) stronger responsiveness of endothelial cells to estrogen and, when stimulated by this hormone, secretion of larger than normally amounts of basic fibroblast growth factor (bFGF) (Piotrowicz et al. 1997) which could, in endocrine manner, stimulate de-differentiation and proliferation of endothelial cells leading to, the associated with proliferative state - cell shrinkage and unveiling of basal membrane. Occurrence of these events in brain capillary endothelial cells could lead to de-regulation of the mechanisms controlling permeability of blood-brain barrier. Furthermore, in addition to blood-brain barrier effects, the stabilization of stress fibres in endothelial cells may affect apoptotic process - it has been shown that the apoptosis-related cell surface blebbing is prevented by the stabilised stress fibres (Huot et al. 1998).

The proposed hypothetical molecular mechanism for the possible role of mobile phone radiation in development of brain cancer and in increasing permeability of the blood-brain barrier, although a hypothesis, it is reasonably supported by the evidence concerning both effects of microwaves on stress response and effects of hsp27 (increased expression and activity) on cell physiology. Proving or disproving of this hypothesis using in vitro and in vivo models will provide evidence to either support or to discredit the existence of some of the potential health risks that were suggested to be associated with the use of mobile phones.

The recently published hypothesis of French et al. (2001) of the possible effect of chronic/frequent exposure to mobile phone radiation that would induce abnormally high levels of stress proteins in cells still requires experimental confirmation that, indeed, repeating exposures to RF-EMF radiation could cause such an increase. On the other hand, proposed by us hypothetical mechanism of the mobile radiation effect on the brain relies on the single-exposure-induced transient increases in hsp27 phosphorylation and expression. We suggest that the transient effects, induced by repeated exposures, might, by chance of timing coincidence, led to survival of damaged/transformed cells and temporarily increase permeability of the blood-brain barrier. These events, when occurring repeatedly (on daily basis) over the long period of time (years) could become a health hazard because of the possibility of accumulating of brain tissue damage. Furthermore, our hypothesis suggests that other, than RF-EMF, cell-damaging factors might play a co-participating role in the tumour development caused by mobile phone radiation.

Finally, in addition to the p38MAPK/hsp27 stress pathway-induced effects, the extent of the global change of the pattern of protein phosphorylation observed in our study suggests that it is likely that multiple signal transduction pathways might be affected by the RF-EMF exposure. Identification of these pathways will help to determine the extent of biological effects induced by RF-EMF exposure. Importantly, cellular effects observed in this study were induced by RF-EMF irradiation at non-thermal levels, with SAR values set at the highest level that is allowed by the European safety limits. This suggests that the presently allowed radiation emission levels for the mobile phones, although low, might be sufficient to induce biological effects. However, determination of whether these effects might cause any significant health effects requires further studies.

5-step feasibility study of applying proteomics/transcriptomics to mobile phone research.

It has been suggested that high-throughput screening techniques (HTST) of transcriptomics and proteomics could be used to rapidly identify broad variety of potential molecular targets of RF-EMF and generate variety of biological end-points for further analyses (Leszczynski et al. 2004). Combination of data generated by transcriptomics and proteomics in search for biological effects is called the “discovery science”. This term has been coined-in by Aebersold et al. (2000) to define the new approach that will help in revealing biological mechanisms, some of which might be unpredictable using the presently available knowledge. This approach seems to be particularly suited for elucidation RF-EMF health hazard issue because it might reveal effects that are not possible to predict based on the present knowledge about the biological effects of RF-EMF. However, before committing large funds that are needed for HTST studies it is necessary to determine whether indeed this approach will be successful in unravelling physiologically significant biological events induced by RF-EMF. Due to their high sensitivity HTST are able to pick-up very small changes in protein or gene expression which changes might be of insufficient magnitude to alter cell physiology. Thus, although using HTST it might be possible to find biological effects induced by RF-EMF these effects might be of limited or no significance at all, from the physiological stand point. Therefore, to determine the usefulness of HTST

approach to the issue of bio-effects induced by RF-EMF, we have performed a 5-step feasibility study and have shown that HTST might indeed help to identify experimental targets for physiological studies of RF-EMF-induced biological responses. The obtained by us results clearly demonstrate that by using HTST it is possible to identify RF-EMF-induced molecular events that might alter cell physiology. Even though the increase in expression/phosphorylation of the examined hsp27 protein was very modest (ca. 2-3 folds increase) it was possible to determine impact of this event on cell physiology. Whether any impact on organ (e.g., brain) or whole body will be exerted by this change remains to be determined by in vivo studies. Although the use of discovery science-approach employing HTST will not provide direct evidence of health hazard or its absence, it will be essential in unravelling of possibly all biological effects exerted by RF-EMF exposure. Further elucidation of the physiological significance of these biological effects for the health and well-being, in short- and long-term exposure conditions, will allow determination whether any health hazard might be associated with the use of mobile phones at the presently allowed radiation safety levels.

Use of HTST to determine genotype-dependent and modulation-dependent cellular responses.

Our study has shown that proteomics transcriptomics and might be an efficient tool when searching for the proteins and genes responding to a weak stimulus, like the mobile phone radiation. In this pilot study we have found several tens of protein and gene targets of the mobile phone radiation. Functions of the few of the MALDI-MS-identified protein spots suggest possibility of the effects of the mobile phone radiation on such physiological functions as (i) cellular energy production, (ii) protein translation, and (iii) cytoskeleton-dependent processes (e.g. cell size, shape and cell-cell interactions). Potential effects on these processes were supported by the evidence gained with cDNA arrays. Further studies will be needed to determine whether there is any impact of these changes on cell physiology.

The other major finding of the study is the observation that the exposure of cells to the continuous-wave microwaves ("CW-signal" 1800 MHz GSM) does not induce changes in protein expression whereas radiofrequency modulated microwaves ("Talk-signal" 1800 MHz GSM) induces broad changes in protein expression. Analysis of changes in expression of some 1500 proteins using cICAT method combined with liquid chromatography and MS/MS identification of proteins has revealed several tens of affected proteins. Importantly, using other methods such as 2-DE and cDNA arrays the same cytoskeleton-related genes/proteins were detected as being affected by RF-EMF exposure up. It means that with two different proteomics approaches we have observed similar protein changes what strengthens the validity of our observations.

4.2.4.7 Effects of RF-EMF on gene expression in human cells analysed with the cDNA array (Participant 12)

The elevated turnover of ribosomal proteins and proteins involved in energy metabolism allows the hypothesis that the cellular turnover is increased after RF-EMF exposure. To prove this hypothesis for RF-EMF treated HL-60 cells (Participant 2), a very interesting additional comparison was performed: In the 1800 MHz continuous wave experiments (2 expression profiles, 4 hybridisations) we used two controls instead of one: One control in each experiment was a sham-exposed control as usual. Cells from another incubator, neither exposed nor sham-exposed, served as a second control. After both experiments we performed comparisons between both controls as well as between sham-exposed and RF-exposed cells (each comparison with 8 data points per gene, from 2 expression profiling experiments, 4 hybridisations). After going through all investigated gene families listed in Tables 30 and 31, with some gene families we found remarkable differences between the control comparison and the sham-RF comparison (Figure 144). As expected, again ribosomal and mitochondrial genes are much more upregulated in the sham-RF comparison than in the "blinded" comparison (Sham-Ctrl). But there are also other gene families showing the same tendency, as for example ATP related genes, genes encoding calcium-associated proteins and cell cycle proteins.

The increasing ribosomal turnover might lead to cell growth and, in the end, to mitosis and cell proliferation, respectively. This hypothesis has not been confirmed so far by the BrdU-incorporation assay, because no significant increase of DNA synthesis, and therefore, an increase in cell proliferation, could not detected (Participant 2). The same is true for the analysis of protein mass and the MTT assay for the detection of mitochondrial activity (Participant 2).

However, the changes in ribosomal protein synthesis are not so strong that we would expect a very strong increase in cell cycle progression. Ribosomal transcription rates have been found to vary by up to a factor of four (Derenzini et al. 2001; Leary and Huang 2001). It is known from stimulation by growth factors, that an increase of ribosomal activity not necessarily leads to significant changes in cell cycle (Stefanovsky et al. 2001; Bodem et al, 2000). We should investigate the cell cycle distribution after RF-EMF exposure in more detail. Also the analysis of the 45S precursor rRNA by real-time RT PCR or the analysis of the RNA polymerase I and associated proteins would help us to figure out if ribosomal transcription is elevated, which is a pre-requisite for an increase of ribosomal proteins (Stefanovsky et al. 2001; Jacob and Gosh 1999). Compared to the ELF-EMF results (Participant 3) the results with RF-EMF seem to be more uniform. The comparison of HL-60 profiling 2 and 3 for example (Participant 2), shows a much lower number of reproducibly regulated genes than after the analysis of only one experiment (compare Figure 139). If the reason for this is the differentiating potential of the cells (U937 cells of Participant 9, HL-60 cells of Participant 2, T-lymphocytes of participant 8), or the exposure conditions (homogenous ELF-EMF field with or without on/off cycles versus RF-EMF GSM talk signal), or both, remains to be elucidated. More cell lines, each exposed to different fields (ELF, RF), would have to be investigated to draw more reliable conclusions.

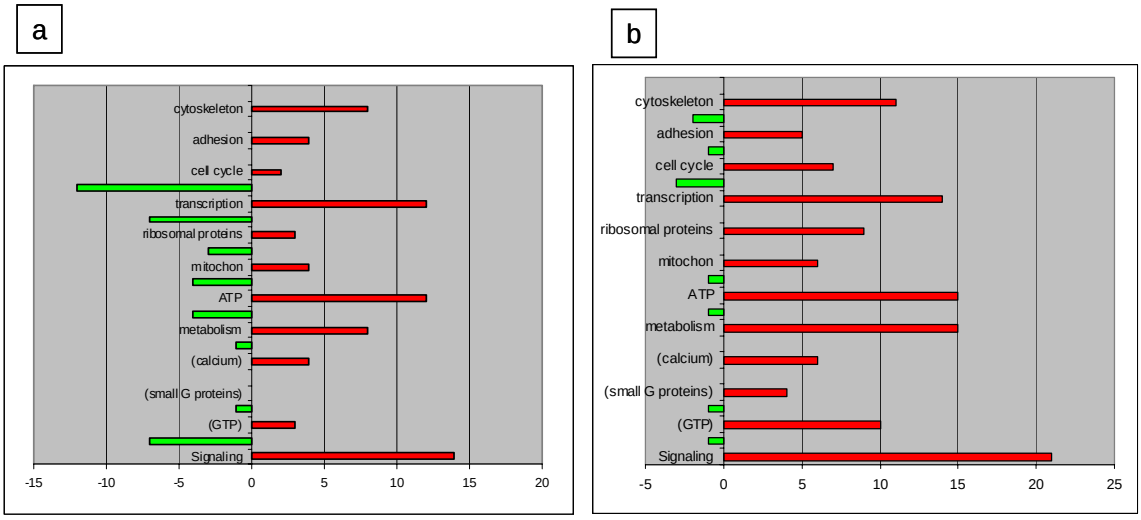

Figure 144. Numbers of regulated genes after RF-EMF exposure sorted according to different gene families. a, comparison between batches of control HL-60 cells (not exposed vs. sham exposed). Red: Genes appearing up-regulated in sham-exposed. Green: Genes appearing down-regulated in sham-exposed. b, comparison between sham-exposed (ctrl) and RF-EMF exposed HL-60 cells. Red: Genes showing up-regulation in RF-EMF. Green: Genes showing down-regulation in RF-EMF.

4.2.4.8 Summary (Participant 1)

Scientific work on gene and protein expression due to RF-EMF exposure using in vitro cell cultures and animal models is still in its early stages and as far as already published difficult to interpret (Independent Expert Group on Mobile Phones 2000). From the REFLEX data the conclusion can be drawn that RF-EMF may affect the gene and protein expression in various cell systems. RF-EMF exposure at a SAR value of 1.5 W/kg caused a transient up-regulation of the p21 and c-myc genes and a long-term up-regulation of the hsp70 gene in p53 deficient embryonic stem cells (3.2.4.1, 4.2.4.1). RF-EMF exposure at a SAR value of 2 W/kg reduced the expression of the receptor FGFR1 of fibroblast growth factor (FGF) in human neuroblastoma cells (NB69) and in neural stem cells of rats obviously without affecting protein transcription (3.2.4.2, 4.2.4.2). RF-EMF exposure up- or down-regulated the expression of various genes and proteins in HL-60 cells (1800 MHz, 1.3 W/kg) and in endothelial cells of human origin (900 MHz, 2.0 W/kg) (3.2.4.3, 3.2.4.6, 3.2.4.7, 4.2.4.3, 4.2.4.6, 4.2.4.7). RF-EMF exposure at a SAR value of 2.0 W/kg activated the p38MAPK/hsp27 stress response pathway and changed the global

pattern of protein phosphorylation in endothelial cells with possible consequences for the signal transduction pathway (3.2.4.6, 4.2.4.6).

Not unexpected, the available literature is controversial (Stewart Report 2000). While Lee et al. (2004) observed an alteration of gene expression in HL-60 cells after exposure to RF-EMF of 2450 MHz and Zeng et al. (2004a) an alteration of protein expression in human breast cancer cells (MCF-57) after exposure to RF-EMF of 1800 MHz, no such effects were found by Miyakoshi et al. (2004), who studied the influence of RF-EMF (1950 MHz) on the expression of hsp27 and hsp70 in human glioma cells (MO54). Opposite to the finding of Participant 6 (3.2.4.6, 4.2.4.6), no significant increase in hsp27 expression in endothelial cells was observed by Participant 9 who used a slightly different method (3.2.4.5, 4.2.4.5). Since the hsp27 expression was significantly increased in one laboratory, while this increase was near to significance in the other laboratory, this discrepancy seems to be neglectable. Furthermore, RF-EMF exposure (1800 MHz) at a SAR value of 1,4 W/kg did not affect gene expression in human lymphocytes (3.2.4.4, 4.2.4.4) and after RF-EMF exposure (900 MHz) at a SAR value of 2 W/kg only a few genes among several thousand tested with the micro-array system were found altered in two human immune cell lines (3.2.4.5, 4.2.4.5). Finally, RF-EMF exposure did not affect the expression and activity of the inducible nitric oxide synthase (iNOS) in nerve cells (3.2.4.5, 4.2.4.5).

The outcome of experiments following the genomics and proteomic approach may essentially depend on the cell system investigated and the RF-EMF signal used. Of course, the question remains as to whether or not these alterations in gene and protein expression are within the normal physiological range and if that is the case, they are without any biological relevance.

5.0 CONCLUSIONS

5.1 Conclusions based on the findings obtained in ELF-EMF research

5.1.1 Human fibroblasts, human lymphocytes, human monocytes, human melanocytes, human muscle cells and granulosa cells of rats (Participant 3)

These are the conclusions that Participant 3 draws from their findings:

1. The data strongly indicate a clastogenic potential of intermittent electromagnetic fields, which may lead to considerable chromosomal damage in dividing cells. However, the induced DNA damage did not persist in form of stable translocations.
2. The induced DNA damage was not based on thermal effects and arouses consideration about environmental safety limits for ELF-EMF exposure.
3. The effects were clearly more pronounced in cells from older donors, which could point to an age-related decrease of DNA repair efficiency of ELF-EMF induced DNA strand breaks.
4. In addition, three responder and three non-responder cell types could be identified, which could in part explain different results in reaction to ELF-EMF reported in the literature so far.
5. Fibroblasts from a donor with the genetically DNA repair defect Ataxia Telangiectasia had a more than two fold increase rate of ELF-EMF induced DNA breaks.
6. Between 3 and 550 Hz the largest DNA breaking effects were seen at 16.66 and 50 Hz, the most commonly used frequencies of alternating current in Europe.
7. Taken together, the results suggest that the observed effects of EMF exposure are caused by indirect mechanisms and are not inflicted due to changes in mitochondrial membrane potential.

5.1.2 Human neuroblastoma cell line NB69 and human hepatocarcinoma cell line HepG2 (Participant 5)

Our present results confirm preliminary observations that a 42- or 63-hour exposure to 50 Hz, sine wave MF at 10 or 100 μT (3 hours on/3 h off exposure cycle) can induce changes in the cell growth of NB69 human neuroblastoma cells. The data indicate that such an effect is exerted through an increase in cell proliferation, as revealed by BrdU-incorporation and flow cytometry.

1. In contrast, a 50-Hz MF at 2000 μT magnetic flux density, 5 min on/30 min off exposure cycle, did not affect significantly cell growth on the NB69 line. Thus, our cells were not responsive to these exposure parameters, which have been reported to be effective on differentiating neural embryonic stem cells (Participant 4). Additional experiments exposing NB69 cells to a 100 μT field in a 5 min on/30 min off cycle showed no significant responses. This indicates that the exposure cycle is crucial to eliciting a detectable cellular response.
2. In the NB69 line, the results on PCNA labelling show that at day 6 post-plating the percent of PCNA-positive cells in samples exposed to a 50-Hz, 100-μT field is significantly increased when compared to controls. Actually, the percent of PCNA positive cells significantly decreases in controls between the days 5 and 6 post-plating, whereas such a decrease did not occur in exposed cells. The results suggest that the MF could impair the normal cell cycle regulation through alterations in the late G1 and S-phases.
3. We have also investigated the response of a different human cancer line, the HepG2 human hepatocarcinoma cell line (data not shown), with a growth pattern different from that of the NB69 line. Fifty-Hertz magnetic fields at 10 or 100 μT elicited similar responses in both cell lines, consisting of significant increase in the number of cells at days 5 postplating. In HepG2, the melatonin, at a 10 nM concentration, inhibited the growth-promoting effect induced by the field (Cid et al., 11th International Congress of IRPA, 2004). In the HepG2 line, the growth effect became even stronger when the exposure was maintained until day 7 post-plating, whereas in the NB69 line, an equivalent extension of the exposure period results in a loss of the effect. The differential responses in both cell lines could be due to the fact that, in control conditions, NB69 cultures become saturated at day 7 post-plating and, consequently, their capability to respond to any stimulus is strongly impaired.

4. A 50-Hz, sine wave MF at 100-μT (3h on/3h off exposure cycle) induces a significant reduction in the spontaneous apoptosis of the human neuroblastoma cell line NB69. This response was associated to an increase in the total number of cells. The data suggest that both responses are a consequence of an effect of the field on cell cycle regulation.
5. In NB69 cells, a 50-Hz, sine wave MF at 100-μT (3h on/3h off exposure cycle) alters the activation of the phosphorylated cyclic adenosine monophosphate response-element binding protein (p-CREB) in a time-dependent manner. The results suggest that the activation of p-CREB is involved in the above described effects of this field on cell growth/apoptosis.

5.1.3 Human lymphocytes (Participant 8)

On the whole, data obtained indicate no response of human PBMCs to ELF-EMF exposure. Thus the conclusions are that ELF-EMF do not affect proliferation and cell activation, two fundamental phases of lymphocyte function. Since previous works indicated that pulsed ELF-EMF may interfere with human lymphocyte functionality (Cossarizza et al. 1989a/b, 1991, 1993), future experiments could be addressed to investigate the role of pulsed signal in biological systems in comparison with the negative results obtained with A.C. 50Hz ELF-EMF.

5.1.4 Mouse embryonic stem cells (Participant 4)

1. ELF-EMF signals at a high flux density are capable to transiently increase transcript levels of the regulatory genes egr-1, p21 and c-jun in ES cells deficient for the tumour suppressor p53.
2. The intermittency scheme of the ELF-EMF signals may play a critical role for changes in transcript levels of some regulatory genes.
3. The genetic constitution of pluripotent embryonic stem cells determined by loss of p53 function can influence ELF-EMF-related cellular responses, whereas wild-type cells are insensitive. It remains to be elucidated, whether ELF-EMF-induced changes of expression levels of regulatory genes may be compensated or normalized, or would result in sustained biological effects in vivo.
4. ELF-EMF exposure of ES-derived neural progenitor cells may influence transcript levels of genes of the bcl-2 family and the p53-responsive growth arrest and DNA damage inducible gene GADD45. This finding is an indication that ELF-EMF may affect, at least transiently, fundamental cellular processes including programmed cell death and cell cycle regulation.
5. Alkaline and neutral Comet assay failed to demonstrate a clear effect on the induction of single- and double-strand DNA breaks after ELF-EMF exposure of ES cell derived neural progenitors.

5.1.5 Experiments with embryonic stem cells of mice during cardiac differentiation (Participant 8)

In the ES cell model (GTR 1), ELF-EMF afforded a consistent increase in the expression of genes tightly involved in coaxing ES cells to the cardiac lineage. As shown by in vitro run-off analyses, ELF-EMF affected the transcriptional machine of ES cells. These responses led to the expression of cardiac specific genes and ultimately ensued into a high-throughput of cardiogenesis, as shown by the increase in the number of spontaneously beating colonies in ELF-EMF-exposed cells. Failure of EMF to affect the transcription of a gene promoting skeletal muscle determination and the faint effect on neuronal specification seem to exclude a generalized activation of repressed genes and suggests that coupling of MF with GATA-4, Nkx-2.5 and prodynorphin gene expression may represent a mechanism pertaining to ES cell cardiogenesis. This work represents, in our opinion, a first step toward an extensive investigation concerning the influence of EMF on the expression of a sequence of genes specifically involved in cell differentiation, and in particular the differentiation into a cardiac phenotype, using genomic and post-genomic techniques.

5.1.6 Experiments with the human neuroblastoma cell line SY5Y (Participant 11)

The results clearly demonstrate that, under the discussed exposure conditions, the expression of major components of the cholinergic and catecholaminergic systems is unresponsive to environmental exposure to ELF-EMF.

5.1.7 *Xenopus laevis* oocytes, human fibroblasts and granulosa cells of rats (GFSHR-17 cell line) (Participant 7)

1. For the applied three exposure protocols (50-Hz powerline, 1.0 mT or 2.3 mT continuously applied for 16 h; 50-Hz powerline, 1.0 mT and 2.3 mT intermittently (on/off: 5 min/10 min) applied for 16h the data indicate that the expression level as well as the voltage dependent gating of rCx46-connexons is not significantly affected. Since we could previously show that protein kinase C dependent phosphorylation processes affect the voltage-dependent gating of rCx46-connexons (Ngezahayo et al. 1998), a significant interaction of ELF-EMF on proteinphosphorylation can be neglected. The formation of cell-to-cell channels composed of two rCx46-hemi-channels, respectively, between a pair of mechanically contacting oocytes indicates an effect of ELF-EMF exposure. Exposure virtually suppresses the formation of cell-to-cell channels, but the effect is not significant on the level of three experiments analysed so far. The known $[Ca^{2+}]_o$-dependent gating property of hemi-channels appears not to be influenced by ELF-EMF exposure.
2. Continuous ELF-EMF exposure at high flux intensity 2.3 mT for 30 min did not significantly influence gap junctional coupling (cell-to-cell channels) of cultured pairs of rat granulosa cells as explored by the double whole cell patch-clamp technique.
3. The presented data indicate that intermittent exposure (5 min on / 10 min off) to ELF-EMF (50 Hz, 1 mT) neither generates a long lasting effect on the time course of $[Ca^{2+}]_i$ in cultured fibroblasts nor granulosa cells. This finding appears to be independent of an exposure for 5 to 18h. The corresponding observation of Ivancsits et al. (2003b), of a time dependent increase/decrease of DNA strand breaks with a maximum at about 15h, therefore seems not to be reflected in a corresponding long lasting change of $[Ca^{2+}]_i$. It is interesting to note that such a long lasting effect is also not found for the mitochondrial potential of fibroblasts. ELF-EMF exposure followed by exposure to further stressors, like 200 µM H_2O_2 or 30 mM KCl, also caused no significant change of $[Ca^{2+}]_i$.
4. Exposure experiments show no significant influence on volume regulatory mechanisms of granulosa cells. Further studies of intracellular signal transduction pathways should allow to understand the unsolved question whether significant effects of ELF-EMF on the genomic level are reflected on the cellular level. At present significant changes of cellular properties could not be derived from the analysed cellular parameters.
5. ELF-EMF exposure of cultured granulosa cells shows a significant time dependent increase of double DNA strand breaks with a maximum at about 18 h as observed by the neutral comet assay. This time dependence was also observed at 8 Hz, 16.66 Hz, 30 Hz, 50 Hz and 300 Hz. Therefore, it appears likely that for the chosen ELF-EMF exposure protocol the observed increase of double DNA strand breaks is not frequency dependent. But, the results of the alkaline comet assay indicate a frequency dependent effect of ELF-EMF exposure on the sum of double and single DNA strand breaks. The data obtained for the granulosa cells, after ELF-EMF exposure at 50 Hz, by the alkaline comet assay are comparable with those obtained by participant 3.

5.1.8 Effects of ELF-EMF on gene expression in human cells analysed with the cDNA array (Participant 12)

The gene expression analyses presented here make it very likely that EMFs – RF-EMF and ELF-EMF – can change gene expression in human cells. Although the in vitro studies do not allow any conclusions concerning health risk, the results are an important pre-requisite for further experiments to elucidate the detailed molecular changes in a cell, caused by EMFs.

The most obvious changes have been detected in the expression of genes involved in ribosomal biogenesis and energy metabolism. If the effects are momentary or lead to more dramatic changes like increase of cell proliferation has to be further investigated by molecular assays. The same is true for first ideas how the signalling after EMF exposure could work, referring to the bio-statistic analysis: The Ca-pathway (PIP3, PKC, ERK MAP and other pathways might be involved, but this is not obvious after our analysis) might be involved in regulation after EMF exposure. The actin cytoskeleton (e.g. stress fibers) and ECM possibly is down-regulated, which might lead to dedifferentiation of cells, again important for growth and proliferation of cells. The actin cytoskeleton behaves different in different cell types (adhesive, non-adhesive cells, cell migration etc.), and therefore also has to be investigated with the help of more specific assays.

5.1.9 Summary (Participant 1)

The ELF-EMF data obtained in the course of the REFLEX project allow the following conclusion:

1. ELF-EMF had genotoxic effects on primary cell cultures of human fibroblasts and on other cell lines. These observations were made in two laboratories within the REFLEX consortium (Participants 3 and 7) and confirmed by two other laboratories from outside the REFLEX project. ELF-EMF generated DNA strand breaks at a significant level at a flux density as low as 35 μT. A strong positive correlation was observed between both the intensity and duration of exposure to ELF-EMF and the increase in single and double strand DNA breaks and micronuclei frequencies. Surprisingly this genotoxic effect was only found when cells were exposed to intermittent ELF-EMF, but not to continuous exposure. Responsiveness of fibroblast to ELF-EMF increased with the age of the donor and in the presence of specific genetic repair defects. The effect also differed among the other types of cells examined. In particular, lymphocytes from adult donors were not responsive. Chromosomal aberrations were also observed after ELF-EMF exposure of human fibroblasts.
2. ELF-EMF at a flux density of 10 and 100 μT increased the proliferation rate of neuroblastoma cells (Participant 5) and at a flux density of 0.8 mT it enhanced the differentiation of mouse stem cells into cardiomyocytes (Participant 8). In contrast to these results, no clear-cut and unequivocal effects of ELF-EMF on DNA synthesis, cell cycle, cell differentiation, cell proliferation and apoptosis were found in the many other cell systems under investigation.
3. Elf-EMF inhibited the spontaneous apoptosis in neuroblastoma cells which was followed by an increase of the proliferation rate, when the cells were exposed for 63 hours to ELF-EMF at a flux density of 50 or 100 μT (Participant 5). In contrst to these results, no clear-cut and unequivoval effects of ELF-EMF on the apoptotic process were found in the many other cell systems under investigation.
4. ELF-EMF at a flux density of about 2 mT up-regulated the expression of early genes, such as p21, c-jun and egr-1, in p53- deficient mouse embryonic stem cells, but not in healthy wild-type cells (Participant 4) and, in addition, may affect the expression of genes and proteins in a variety of other cell systems. The results of the whole genome cDNA micro-array and proteomic analyses indicate that EMF may activate several groups of genes that play a role in cell division, cell proliferation and cell differentiation (Participant 12).

Taken together, the results of the REFLEX project were exclusively obtained in in vitro studies and are, therefore, not suitable for the conclusion that ELF-EMF exposure below the presently valid safety limits causes a risk to the health of people. They move, however, such an assumption nearer into the range of the possible. Furthermore, there exists no justification anymore to claim, that we are not aware of any pathophysiological mechanisms which could be the basis for the development of functional disturbances and any kind of chronic diseases in animal and man.

5.2 Conclusions based on the findings obtained in RF-EMF research

5.2.1 Human promyelocytic cell line HL-60 (Participant 2)

1. Different SAR levels have been examined with respect to the effect on comet formation and micronuclei induction in HL 60-cells. Comparing RF-EMF exposure (1800 MHz, continuous wave, 24h) at SAR levels ranging from 0.2 W/kg to 3.0 W/kg indicate that both effects appear to be energy dependent. Whereas at SAR of 0.2 W/kg and 1.0 W/kg both, comet formation and micronucleus frequency, were not significantly different from that observed in sham-exposed control cells, comet formation as well as micronucleus frequency were significantly increased at SAR of 1.3 W/kg, 1.6 W/kg and 2.0 W/kg. The maximal effect was observed at a SAR of 1.3 W/kg. At higher SAR levels from 2.0 to 3.0 W/kg micronucleus frequencies and comet formation were less expressed as compared to the effect noted at a SAR of 1.3 W/kg.
2. In order to extend the statistical basis of evaluation average numbers of micronuclei (micronuclei per 1000 BNC) in different experimental groups were calculated comparing cells exposed either at (i) all SAR tested (0.2 W/kg, 1.0 W/kg, 1.3 W/kg, 1.6 W/kg, 2.0 W/kg, 3.0 W/kg, (ii) higher SAR (1.0 W/kg, 1.3 W/kg, 1.6 W/kg, 2.0 W/kg, 3.0 W/kg) or (iii) lower SAR of 0.2 W/kg or 1.0 W/kg. In both groups (i) and (ii) the number of micronuclei was increased at a significant level ($p<0.001$) as

compared to sham-exposed controls, while in group (iii) micronuclei numbers per 1000 BNC were not significantly different from that observed in sham-exposed controls.

3. Likewise, in order to extend the statistical basis of evaluation average values of Olive Tail Moments as a measure of comet formation were calculated in different experimental groups comparing cells exposed either at (i) all SAR tested (0.2 W/kg, 1.0 W/kg, 1.3 W/kg, 1.6 W/kg, 2.0 W/kg, 3.0 W/kg, (ii) higher SAR (1.0 W/kg, 1.3 W/kg, 1.6 W/kg, 2.0 W/kg, 3.0 W/kg) or (iii) lower SAR of 0.2 W/kg or 1.0 W/kg. In both groups (i) and (ii) the comet formation was increased at a significant level (group (i) $p<0.01$; group (ii) $p<0.001$) as compared to sham-exposed controls, while in group (iii) comet formation was not significantly different from that observed in sham-exposed controls.
4. Experiments on the influence of the duration of exposure showed that short exposure period (6h) caused no (MN) or less (Comet) pronounced effects on micronuclei induction and comet formation as compared to longer exposure periods of 24h. While micronucleus frequencies were further increased after exposure for 72h, comet formation after 72h of exposure was less expressed as compared to 24h exposure.
5. Experiments on the influence of RF-signals showed that at a SAR level of 1.3 W/kg all RF-signals tested, i.e. continuous wave (C.W.), C.W. 5 min on/10 min off, GSM-217 Hz, and GSM-Talk exhibited similar effects on micronuclei induction and on comet formation.
6. By applying sequential approaches for the detection of reactive oxygen species (ROS) in HL-60 cells, an increase in the intracellular generation of free radicals accompanying RF-EMF exposure could be clearly demonstrated by flow cytometric detection of the oxidized nucleotide 8-oxoguanosine (oxy-DNA assay) and the fluorescent Rhodamine 123 (DHR 123 assay), respectively.
7. RF-EMF exposure (1800 MHz, 1.3 W/kg, 24h) had no effect on the cellular doubling time and the activity of the enzyme thymidine kinase of HL 60 cells, indicating that RF-EMF exposure does not influence cellular growth rates.
8. RF-EMF exposure (1800 MHz, 1.3 W/kg, 24h) did not induce apoptosis in HL-60 cells.
9. Within the investigated SAR energy ranges RF-EMF under the in-vitro conditions used are genotoxic in HL-60 cells without affecting cell-cycle distribution cell proliferation or cell progression.
10. The partial-body SAR for any 10-gram tissue like for example the head as exposed region to mobile phone electromagnetic fields should not exceed 2 W/kg according to the Radio-Radiation Protection Guidelines. Notably, our findings on genotoxic effects of RF-fields in HL-60 cells have been shown for SAR levels below these acceptable partial-body SAR levels.
11. These results on genotoxicity in the HL-60 cell line cannot be transferred automatically to other cells, especially to primary cells, and definitely not to whole organism.
12. Clear differences in protein expression have been shown for RF-exposed HL-60 cells as compared to control and sham-exposed cells. This indicates that, as also demonstrated by genetic profiling, RF-EMF exposure has an influence on as well the transcriptional as the translational level in these cells. Clarification of changes in protein expression with respect to functional analysis will help to understand molecular pathomechanisms.

5.2.2 Human fibroblasts and granulosa cells of rats (Participant 3)

Our results imply a genotoxic action of RF-EMFs below proposed radiation safety levels.

1. RF-EMFs were able to induce DNA single and double strand breaks in human fibroblasts and SV40 transformed rat granulosa cells. In contrast to ELF-EMF, genotoxic effects were also observed at continuous exposure.
2. In addition, the decline of DNA strand break levels at elongate exposure (16-24 h), which was found in ELF-EMF exposed cells, could not be demonstrated after RF-EMF exposure. These results could point to differences in mechanisms between the genotoxic action of RF and ELF-EMF
3. Differences in genotoxic effects between different cell types after EMF exposure could be found in RF as well as in ELF-EMF exposed cells.
4. RF-EMF exposure of human fibroblasts was able to induce higher incidences of chromosome aberrations than which was found in ELF-EMF exposed cells.
5. No effects of RF-EMF exposure on mitochondrial membrane potential could be observed. These findings are in accordance with the results obtained with ELF-EMF.

5.2.3 Human lymphocytes and thymocytes (Participant 8)

On the whole, the data obtained indicate a very low response of human PBMCs and no response of thymocytes to RF-EMF exposure. Concerning PBMCs, some results suggest a possible effect on the number of CD95 surface molecules in stimulated T lymphocytes from aged donors. Moreover, other results seem to indicate a greater susceptibility to RF of monocytes with respect to lymphocytes, as demonstrated by a decrease of IL-1 b cytokine, specifically produced by monocytes, in RF-exposed cultures. Future work could be addressed to analyse further effects on these type of human cells.

5.2.4 Human neuroblastoma cell line NB69 and neural stem cells (Participant 5)

1. When administered alone, the exposure to the GSM-Basic signal at a 2W/kg SAR induced a decrease in the number of cells expressing the fibroblast growth factor receptor-1 (FGFR-1), both in NB69 cells and NSC, without affecting significantly the number of cells expressing receptors R2 and R3. The magnitude of the effect on R1 was equivalent to that induced by 20 µg/ml bFGF. Since the GSM-Basic treatment did not affect significantly the total cell number or the cell viability, the above data indicate that RF-induced effect in FGFR-1 is not due to a reduction in the number of cells, but to a loss of the cellular expression of receptor-1.
2. The results also indicate that the exposure to GSM 1800-CW signals at a 2 W/kg SAR induced effects on the expression of FGFR-1 equivalent to those described above for the GSM 1800-Basic signal. No significant effects on the expression of FGFR-1 were observed after exposure to GSM 1800-Talk and DTX signals at 2 W/kg SAR and 1 W/kg SAR, respectively. The data obtained with the different GSM-signals suggest that the cellular response is not dependent on the tested low-frequency modulation.
3. The exposure to the GSM-basic signal induces specific, morphological changes in oligodendrocytes and astrocytes derived from neural stem cells, at day 9 post-plating. These results are indicative that GSM-basic radiation at SAR = 2 W/kg can promote differentiation in NSC. The effect would be exerted through short-term changes in the expression of FGF receptor-1. In contrast, the GSM-Basic signal does not influence cytodifferentiation in NB69 cells or in the neuronal progeny of NSC, as revealed with anti-beta-tubulin antibody.

5.2.5 Brain cells of different origin and human monocytes (Participant 9)

1. Our results strongly suggest that the spontaneous apoptotic process is not a biological target for GSM mobile telephony-related signals. This was shown in different primary cells and cell lines from both nerve and immune systems.
2. Based on the expression and activity of inducible nitric oxide synthase (NOS2) in an astrocytic cell line, GSM-like signals did not “activate” the inflammatory process in nerve cells.
3. No evidence was found of effects of GSM-like signals on heat shock proteins in different mammalian nerve cells. Replication of the previously reported increase in hsp27 expression in a human endothelial cell line after exposure failed.
4. Based on the whole data set, our conclusion is that exposure to low-level GSM-900 signal is unlikely to lead to neurodegeneration or to favour tumour development via pathways involving apoptosis, nitric oxide or heat shock proteins.

5.2.6 Mouse embryonic stem cells (Participant 4)

1. Our present data suggest that currently applied GSM radiation levels under certain circumstances might induce biological effects, at least in cells generated from embryonic stem cells in vitro.
2. The genetic constitution of pluripotent embryonic stem cells determined by loss of p53 function influences RF-EMF-related cellular responses at the level of gene expression, whereas wild-type cells are insensitive. It remains to be elucidated, whether RF-EMF-induced changes of mRNA levels of regulatory genes may be compensated or normalized, or would result in sustained biological effects in vivo.
3. RF-EMF exposure of ES-derived neural precursor cells influences the bcl-2 mediated anti-apoptotic pathway, affects the growth arrest and DNA damage inducible gene GADD45 and the neuronal differentiation by inhibition of Nurr1.

4. Short exposure to RF-EMF could induce double-strand DNA breaks in ES-derived neural progenitor cells (as measured by the neutral Comet assay).

5.2.7 Human the endothelial cell lines EA.hy926 and EA.hy926v1 (Participant 6)

1. RF-EMF appears to be recognized by the cells as an external stress factor because it in response to exposure phosphorylation status of several hundreds proteins was altered either up or down; identification of these proteins will be done in due time.
2. RF-EMF appears to be a weak inducer of cellular stress response because it increases expression and phosphorylation of heat shock protein-27 (hsp27) - a known marker of cellular stress response.
3. RF-EMF induced phosphorylation of Hsp27 appears to be regulated by the activation of up-stream stress kinase p38MAPK.
4. RF-EMF-induced hsp27 activation appears to affect down-stream physiological processes in cell - stabilization of F-actin stress fibers what, in turn, alters cell size and shape (causes rounding-up of cells).
5. Using cDNA Expression Arrays and protein separation by 2-dimensional electrophoresis followed by mass spectrometric identification of individual proteins we have determined that the cellular skeleton appears to be a target of RF-EMF exposure as changes in gene/protein expression of some dozen cytoskeletal proteins were induced by RF-EMF exposure.
6. RF-EMF-induced phosphorylation of hsp27 is followed by translocation of hsp27 to cell nucleus where it appears to interfere with the gene expression processes.
7. RF-EMF causes changes in the expression of several tens of genes and proteins as determined by high-throughput screening technologies - cDNA Expression Arrays and protein separation by 2-dimensional electrophoresis followed by mass spectrometric identification of individual proteins.
8. RF-EMF-induced changes in gene and protein expression appear to be dependent on the cell genotype/phenotype what suggests that some cell types might be more and some less responsive to RF-EMF exposure.
9. RF-EMF induced changes in protein expression appear to be modulation dependent since RF-EMF exposure caused changes whereas CW-EMF did not.
10. the ability of RF-EMF to induce cellular stress response indicates that cells recognize this radiation in spite of it low energy but the induction of stress response per se can not be considered as any indicator of potential health risk.
11. We have practically demonstrated that the use of high-throughput screening methods of transcriptomics and proteomics is useful tool in determining the potential targets of RF-EMF exposure in cells.

5.2.8 Effects of RF-EMF on gene expression in human cells analysed with the cDNA array (Participant 12)

The gene expression analyses presented here make it very likely that EMFs – RF-EMF and ELF-EMF – can change gene expression in human cells. Although the in vitro studies do not allow any conclusions concerning health risk, the results are an important pre-requisite for further experiments to elucidate the detailed molecular changes in a cell, caused by EMFs.

The most obvious changes have been detected in the expression of genes involved in ribosomal biogenesis and energy metabolism. If the effects are momentary or lead to more dramatic changes like increase of cell proliferation has to be further investigated by molecular assays. The same is true for first ideas how the signalling after EMF exposure could work, referring to the bio-statistic analysis: The Ca-pathway (PIP3, PKC, ERK MAP and other pathways might be involved, but this is not obvious after our analysis) might be involved in regulation after EMF exposure. The actin cytoskeleton (e.g. stress fibers) and ECM possibly is down-regulated, which might lead to dedifferentiation of cells, again important for growth and proliferation of cells. The actin cytoskeleton behaves different in different cell types (adhesive, non-adhesive cells, cell migration etc.), and therefore also has to be investigated with the help of more specific assays.

5.2.9 Summary (Participant 1)

The RF-EMF data obtained in the course of the REFLEX project allow the following conclusion:

1. RF-EMF produced genotoxic effects in fibroblasts, HL-60 cells, granulosa cells of rats and neural progenitor cells derived from mouse embryonic stem cells (Paticipants 2, 3 and 4). Cells responded to RF-EMF exposure between SAR levels of 0.3 and 2 W/kg with a significant increase in single and double strand DNA breaks and in micronuclei frequency (Participants 2 and 3). Chromosomal aberrations in fibroblasts were also observed after RF-EMF exposure (Participant 3). In HL-60 cells an increase in the intracellular generation of free radicals accompanying RF-EMF exposure could clearly be demonstrated (Participant 2).
2. No clear-cut and unequivocal effects of RF-EMF on DNA synthesis, cell cycle, cell proliferation, cell differentiation and immune cell functionality were found in the cell systems under investigation. (Participants 2, 3, 4, 5, 6, 8). There is some indication that RF-EMF may affect the growth arrest and DNA damage inducible gene GADD45 and the neuronal differentiation by inhibition of Nurr1 in neural progenitor cells (Participant 4).
3. No clear-cut and unequivocal effects of RF-EMF on apoptosis were fond in the cell systems under investigation was observed (Participants 2, 3, 4, 5, 6, 8 and 9). There is some indication that RF-EMF may have some influence on the bcl-2 mediated anti-apoptotic pathway in neural progenotor cells (Participant 4) and on the the p38MAPK/hsp27 stress response pathway in endothelial cells of human origin (Participant 6) which may in turn exert an inhibitory effect on apoptosis.
4. RF-EMF at a SAR of 1.5 W/kg down-regulated the expression of neuronal genes in neuronal precursor cells and up-regulated the expression of early genes in p53-deficient embryonic stem cells, but not in wild-type cells (Participant 4). Proteomic analyses on human endothelial cell lines showed that exposure to RF-EMF changed the expression and phosphorylation of numerous, largely unidentified proteins. Among these proteins is the heat shock protein hsp27, a marker for cellular stress responses (Participant 6). The results of the whole genome cDNA micro-array and proteomic analyses indicated that EMF may activate several groups of genes that play a role in cell division, cell proliferation and cell differentiation (Participants 2, 6 and 12).

Taken together, the results of the REFLEX project were exclusively obtained in in vitro studies and are, therefore, not suitable for the conclusion that RF-EMF exposure below the presently valid safety limits causes a risk to the health of people. They move, however, such an assumption nearer into the range of the possible. Furthermore, there exists no justification anymore to claim, that we are not aware of any pathophysiological mechanisms which could be the basis for the development of functional disturbances and any kind of chronic diseases in animal and man.

6.0 EXPLOITATION AND DISSEMINATION OF RESULTS

6.1 Coordination (Participant 1)

a. Scientific publications, meetings, interviews, and round tables

Adlkofer F et al.: Brochure presenting the REFLEX project, June 2001 (*for distribution*)

Adlkofer F et al.: Oral presentation of results. Bundesamt für Strahlenschutz, Salzgitter/Germany, June 21-22, 2001, p. 18-19

Adlkofer F et al.: Oral presentation of the project. EBEA, Helsinki/Finland, Sep 6-8, 2001. Proceedings, p. 54-56, 269-270

Adlkofer F et al.: Oral presentation of results. EU/Japan/Korea/US workshop on EMF, mobile telephony and health. Brussels/Belgium, Oct 29-30, 2001, Proceedings, p. *(not numbered)*

Adlkofer F et al.: Oral presentation of results. Institut für Zoologie, Technical University of Dresden/ Germany, April 2, 2002

Adlkofer F et al.: Oral presentation of results. COST281/EBEA Forum, Rome/Italy, May 2-5, 2002

Adlkofer F et al.: Oral presentation of the project.. 24th BEMS Meeting, Quebec City/Canada, June 23-27, 2002, Proceedings, p. 91-92, 95, 98-100

Adlkofer F et al.: Oral presentation of the project and of results. PIERS, Cambridge/Mass/USA., July 1-5, 2002. Proceedings, p. 498

Adlkofer F et al.: Oral presentation of results. Cursos de Verano Universidad de Malaga, Ronda/Spain, July 22-26, 2002

Adlkofer F et al.: Oral presentation of the project. Biological Effects of EMF, Rhodes/Greece, Oct 7-11, 2002. Proceedings, p. 514-522

Adlkofer F, Rüdiger HW, Wobus AM: DNA-Doppelstrangbrüche bei intermittierender Exposition. Diskussionsbeitrag. Deutsches Ärzteblatt, Nov 15, 2002, p. 3114-3115

Adlkofer F et al.: Oral presentation of results. Elektromagnetische Felder in der Umwelt, Umwelt-ministerium Nordrhein-Westfalen, Dortmund/Germany, Nov 28, 2002

Adlkofer F et al.: Oral presentation of results. The EMF Biological Research Trust, London/UK, Jan 16, 2003

Adlkofer F et al.: Oral presentation of results. WHO EMF Project, Research Coordination Meeting, Geneva/Switzerland, June 12-13, 2003

Adlkofer F et al.: Oral presentation of the project. 25th BEMS Meeting, Maui/Hawaii, June 22-27, 2003. Proceedings, p. 127, 135 - 136

Adlkofer F: Interview. Television feature on “Elektrosmog”, ARD Germany, Aug 7, 2003

Adlkofer F et al.: Oral presentation of results. 3rd Int. EMF Seminar, Guilin/China, Oct 13-17, 2003. Proceedings, p. 23 - 24

Adlkofer F et al.: Oral presentation of results. O_2 Telecommunication Company, München/Germany, Oct 22, 2003

Adlkofer F et al.: Oral presentation of results. Die Umwelt-Akademie e.V., München/Germany, Dec 5, 2003

Adlkofer F: Interview. Bayer. landwirtschaftliches Wochenblatt, Heft 5, Jan 2004, p. 48

Adlkofer F: Interview. life + sciences, Heft 1, Feb - April 2004, p. 30-31

Adlkofer F et al.: Oral presentation of results. Bündnis 90/Die Grünen, Bavarian State Parliament, München/Germany, April 2, 2004

Adlkofer F: Round Table Discussion. Bayer. Akademie der Wissenschaften, München/Germany,

April 29, 2004

Adlkofer F et al.: Oral presentation of results. EMF-NET, Brussels/Belgium, April 30, 2004

Adlkofer F et al.: Oral presentation of results. BUND, 3. Rheinland-Pfälzisch-Hessisches Mobilfunk-symposium, Mainz, June 12, 2004. Tagungsband, p. 33 - 49

b. Posters

Adlkofer F et al.: Poster presentation. EBEA, Helsinki/Finland, Sep 6-8, 2001

Adlkofer F et al.: Poster presentation. An Environment for Better Health Conference, Arhus/Denmark, May 8-11, 2003

6.2 Experiments with the human promyelocytic cell line HL-60 (Participant 2)

Research performed is basic research with relevance for life science and techniques, respectively. The results obtained by participant 2 have been subsequently actualised and reported in the usual scientific manner. These reports included confidential Annual Reports as progress reports to the European Commission (1st, 2nd, 3rd Annual Report) and public presentations at the following scientific meetings: BEMS 2002 (Radiofrequency EMF and DNA strand breaks), BEMS 2002 (RF-EMF genotoxic effects), PIERS 2002 (1800 MHz radiofrequency exposition of human HL-60 cells induces DNA strand breaks as measured by the alkaline comet assay), BEMS 2003 (Genotoxic effects of RF-EMF on cultured cells in vitro), Deutscher Ärztekongress 2002 (Workshop in German), Deutscher Ärztekongress 2003 (Workshop in German). Peer-reviewed publications have been prepared and will be submitted after the end of the project.

a. Scientific papers

in preparation:

Schlatterer K., Gminski R., Tauber R., Fitzner R. (2004) Radiofrequency (1800 MHz) electromagnetic fields cause DNA strand breaks and micronuclei formation in HL-60 human promyelocytic cells.

b. Scientific meetings

Fitzner R, Gminski R, Schlatterer K (2004) 1800 MHz radiofrequency electromagnetic fields cause energy-dependent genotoxic effects in human promyelocytic HL-60 cells. Session 14: Non thermal biological effects of EM Fields used for mobile communication. Progress In Electromagnetic Research Symposium (PIERS 2004), Pisa, March 28-31, 2004 (oral presentation)

Fitzner R (2004) In-vitro-Untersuchungen an HL-60-Zellen – Einfluss niederfrequenter Magnetfelder (50 Hz; 162/3 Hz). Umweltmedizin – Elektromagnetfelder, Zellen, Gesundheit, 53. Deutscher Ärztekongress, 3.-5. Mai, Berlin 2004 (oral presentation)

Schlatterer-Krauter, K (2004) Einfluss hochfrequenter Elektromagnetfelder des Mobilfunks – Erbgut-veränderungen direkt oder indirekt verursacht. Umweltmedizin – Elektromagnetfelder, Zellen, Gesundheit, 53. Deutscher Ärztekongress, 3.-5. Mai, Berlin 2004 (oral presentation)

c. Posters

Fitzner R, Gminski R, Schlatterer K (2004) Radiofrequency electromagnetic fields (1800 MHz) induce elevated production of reactive oxygen species in human promyelocytic HL-60 cells. Poster presentation. Bioelectromagnetics Society 26th Annual Meeting, 20-24th June, Washington, 2004

6.3 Experiments with human fibroblasts, human lymphocytes, human monocytes, human melanocytes, human muscle cells and granulosa cells of rats (Participant 3)

a. Scientific papers

published:

Ivancsits S, Diem E, Rüdiger HW, Jahn O (2002) Induction of DNA strand breaks by intermittent exposure to extremely-low-frequency electromagnetic fields in human diploid fibroblasts. Mutation Res 519: 1-13

Ivancsits S, Diem E, Jahn O, Rüdiger HW (2003) Intermittent extremely low frequency electromagnetic fields cause DNA damage in a dose dependent way. Int Arch Occup Env Health 76: 431-436

Ivancsits S, Diem E, Jahn O , Rüdiger HW (2003) Age-related effects on induction of DNA strand breaks by intermittent exposure to electromagnetic fields. Mech Age Dev 124: 847-850

submitted:

Diem E, Jahn O, Rüdiger HW. Non-thermal DNA breakage by mobile phone radiation in human fibroblasts and transformed GFSH-R17 (rat granulosa) cells in vitro. Mutation Research

Ivancsits S, Diem E, Jahn O, Rüdiger HW. Chromosomal damage in human diploid fibroblasts by intermittent exposure to extremely low frequency electromagnetic fields. Mutation Research

Ivancsits S, Diem E, Jahn O, Rüdiger HW. Cell type specific genotoxic effects of intermittent extremely low frequency electromagnetic fields. Mutation Research

Ivancsits S, Diem E, Jahn O, Rüdiger HW. Intermittent exposure to extremely low frequency electromagnetic fields increases the genotoxic sensitivity to UV-light or mild thermal stress in cultured human fibroblasts. J Toxicol Envir Health

Pilger A, Ivancsits S, Diem E, Steffens M, Kolb HA, Rüdiger HW. No long-lasting effects of intermittent 50 Hz electromagnetic field on cytoplasmic free calcium and mitochondrial membrane potential in human diploid fibroblasts. Radiat Envir Biophysics

b. Scientific meetings

Wiener Forum Arbeitsmedizin, April 2000 Vienna,"Elektrosmog – Neue Untersuchungen zur gentoxischen Wirkung elektromagnetischer Felder" Oswald Jahn Oral presentation

26th International Conference of Occupational Health (ICOH), 27th August-1st September2000, Singapore, In vitro evaluation of genotoxic potential of low EMF of 50 Hz" Oswald Jahn, Eva Valic, Elisabeth Diem, Hugo W. Rüdiger Oral presentation

Tagung der Österreichischen Gesellschaft für Arbeitsmedizin (ÖGAM), 27-28th September 2002, Vienna. Sabine Ivancsits, Elisabeth Diem, Hugo W. Rüdiger and Oswald Jahn „Biologische Wirkung elektromagnetischer Felder" Oral presentation

Bioelectromagnetics Society 24th Annual Meeting, 23rd-26th June, Quebec, 2002

H.W. Rüdiger, S. Ivancsits, E. Diem, A. Pilger, F. Bersani, O. Jahn. „Genotoxic effects of extremely-low-frequency electromagnetic fields on human cells in vitro" Oral presentation

Gesellschaft für Umwelt und Mutationsforschung 20. Jahrestagung, 17-20th March 2003, Mainz. Sabine Ivancsits, Elisabeth Diem, Oswald Jahn and Hugo W. Rüdiger „Dosisabhängige Induktion von DNA-Strangbrüchen nach niederfrequenter elektromagnetischer Bestrahlung" Oral presentation

Bioelectromagnetics Society 25th Annual Meeting, 22-27th June, Maui, 2003

H.W. Rüdiger, S. Ivancsits, E. Diem, O. Jahn. „Genotoxic effects of extremely-low-frequency electromagnetic fields on human cells in vitro" Oral presentation

Tagung der Österreichischen Gesellschaft für Arbeitsmedizin (ÖGAM), 19-20th September 2003, St. Pölten.. Sabine Ivancsits, Elisabeth Diem, Oswald Jahn and Hugo W. Rüdiger „Induktion von chromosomalen Aberrationen durch niederfrequente elektromagnetische Felder" Oral presentation.

6th Congress of European Bioelectromagnetics Association (EBEA), November 13–15th 2003, Budapest. S. Ivancsits, E. Diem, O. Jahn, H.W. Rüdiger "In vitro genotoxic effects of extremely-low-frequency electromagnetic fields" Oral presentation

c. Poster

Tagung der Österreichischen Gesellschaft für Arbeitsmedizin (ÖGAM), 28-29th September 2001, Salzburg, Sabine Ivancsits, Elisabeth Diem, Hugo W. Rüdiger and Oswald Jahn „Gentoxische Wirkung

von elektromagnetischen Feldern“ Poster presentation

Conference on RF interactions with Humans: Mechanisms, Exposure and MedicalApplications, 27-28th February 2003, London. E. Diem, S. Ivancsits, H.W. Rüdiger “Non-thermal DNA breakage by mobile phone radiation in human fibroblasts and transformed GFSH-R17 (rat granulosa) cells” Poster presentation

Gesellschaft für Umwelt und Mutationsforschung 20. Jahrestagung,17-20th March 2003, Mainz. E. Diem, S. Ivancsits, H.W. Rüdiger “Non-thermal DNA breakage by mobile phone radiation in human fibroblasts and transformed GFSH-R17 (rat granulosa) cells” Poster presentation

4. Gemeinsame Jahrestagung der Österreichischen und Deutschen Gesellschaft für Arbeitsmedizin, April 22-24th 2004, Innsbruck. S. Ivancsits, E. Diem, O. Jahn, H.W. Rüdiger “Induktion von chromosomalen Schäden durch niederfrequente elektromagnetische Felder“ Poster presentation

4. Gemeinsame Jahrestagung der Österreichischen und Deutschen Gesellschaft für Arbeitsmedizin, April 22-24th 2004, Innsbruck. A. Pilger, S. Ivancsits, E. Diem, M. Steffens, H.A. Kolb, H.W. Rüdiger „Intermittierende Belastung mit 50 Hz ELF-EMF bewirkt keine Veränderungen des mitochondriellen Menbranpotentiales und freien Kalziums in humanen Fibroblasten“ Poster Presentation

6.4 Embryonic stem cells (Participant 4)

a. Scientific papers

published:

Jaroslaw Czyz, Kaomei Guan, Qinghua Zeng, Teodora Nikolova, Armin Meister, Frank Schönborn, Jürgen Schuderer, Niels Kuster, and Anna M. Wobus. High frequency electromagnetic fields affect gene expression levels in tumor suppressor p53-deficient embryonic stem cells. Bioelectromagnetics (2004) 25: 296-307.

Jaroslaw Czyz, Teodora Nikolova, Jürgen Schuderer, Niels Kuster, and Anna M. Wobus. Non-thermal effects of power-line magnetic fields (50 Hz) on gene expression levels of embryonic stem cells – the role of tumour suppressor p53. Mutation Research (2004) 557(1): 63-74.

submitted:

Teodora Nikolova, Jaroslaw Czyz, Alexandra Rolletschek, Przemyslaw Blyszczuk, Jürgen Schuderer, Niels Kuster, and Anna M. Wobus. Electromagnetic fields affect the transcript levels of apoptosis-related genes in embryonic stem cell-derived neural progenitor cells. Submitted to Environ Health Persp.

Part of our results were presented by Participant 8 of the REFLEX Project at the International BEMS 2003 Conference in June, 2003 in Maui, Hawaii.

6.5 Experiments with the human neuroblastoma cell line NB69 and neural stem cells (Participant 5)

For our REFLEX studies a specific software for the analysis of immunocytochemical images was developed in collaboration with Escuela Universitaria de Ingeniería Técnica Industrial (Erasmus-Socrates arrangement between Madrid-Belgium).

Part of the results has been presented in different meetings: BEMS, EBEA, and 2nd International Workshop on Biological Effects of EMF.

a. Scientific papers:

published:

Carlos Platero, Kristof Verbiest, Alejandro Úbeda, M-Angeles Trillo, Jaime Gosalvez, and Javier Bartolomé. Platform opened for the processing and management of biomedical images. XXI Jornadas of

Automática 1-7. ISBN: 84-699-3163-6 (2000)

Carlos Platero, M-Angeles Trillo and Alejandro Úbeda. Processing of biomedical images for the study of the potential influence of GSM electromagnetic radiation on neural stem cells. XXIII Jornadas of Automática 1-7. ISBN: 84-699-8916-2 (2002)

in preparation:

M-Angeles Trillo, M-Antonia Cid, M-Antonia Martinez, Vicente-J. Garcia, Alejandro Úbeda and Jocelyne Leal. Influence of 50 Hz magnetic fields on the proliferation and apoptosis of human neuroblastoma cells *in vitro"*.

M.A.Trillo, G. Alegría, M.A. Martínez, D. Reimers, E. Bazán, A. Úbeda, Jürgen Schuderer and J. Leal. Influence of RF fields (GSM signals, 1800 MHz) on the expression of FGFR1 by NB69 human neuroblastoma cell line and neural stem cells from rat embryonic nucleus striatum".

M.A. Trillo, M.A. Martínez, M.A. Cid A. Úbeda and J. Leal. 50 Hz sinus wave magnetic field at 100 μT activates phosphorilated cyclic adenosine monophosphate response-element binding protein (P-CREB) in NB69 human neuroblastoma cell line.

6.6 Human the endothelial cell lines EA.hy926 and EA.hy926v1 (Participant 6)

a. Scientific papers

published:

Leszczynski D, Joenväärä S, Reivinen R, Kuokka R. Non-thermal activation of hsp27/p38MAPK stress pathway by mobile phone radiation in human endothelial cells: Molecular mechanism for cancer- and blood-brain barrier-related effects. Differentiation 70, 2002, 120-129

Leszczynski D, Nylund R, Joenväärä S, Reivinen J. Applicability of Discovery Science-Approach to Determine Biological Effects of Mobile Phone Radiation. Proteomics 4, 2004, 426-431

Nylund R, Leszczynski D. Proteomics analysis of human endothelial cell line EA.hy926 after exposure to GSM 900 radiation. Proteomics, 4, 2004, 1359-1365

submitted:

Leszczynski D. Mobile phone radiation and blood-brain barrier: The available scientific evidence is insufficient to support or dismiss claims of an effect.

in preparation:

Nylund R, Griffin T, Maercker Ch, Schuderer J, Kuster N, Aebersold R, Leszczynski D. Effect of low-energy microwaves on protein expression in human endothelial cell line might be frequency modulation-dependent

Nylund R, Toivo T, Sihvonen AP, Jokela K, Schuderer J, Kuster N, Landry J, Leszczynski D. Mobile phone radiation-induced activation of cellular stress response induces cytophysiological effects.

Nylund R, Reivinen J, Leszczynski D. Cellular response to mobile phone radiation is proteome- and genotype-dependent

Leszczynski D. Induction of Cellular Stress Response by Mobile Phone Radiation: Possible mechanism behind the effects – a molecular biologists perspective. invited review for IEEE Transactions

Nylund R, Toivo T, Sihvonen AP, Schuderer J, Jokela K, Kuster N, Leszczynski D. Mobile phone radiation-induced Hsp27 stress response in human endothelial cell line EA.hy926 is a non-thermal effect.

b. Scientific meetings and reports for the media

invited lectures:

Harvard University, Boston, MA, USA, 15.11.2000, Proteomics: a novel approach to determine health effects of mobile phone radiation.

Centre for Immunology at St. Vincent's Hospital, Sydney, Australia, 11.02.2002, Possible Effects of Mobile Phones on Brain - Should We Be Afraid?

Telstra Laboratories, Melbourne, Australia, 12.02.2002, Mobile Phones and Health Risk: Why Do We Know So Little?

Department of Physics, Sydney University, Sydney, Australia, 15.02.2002, Mobile Phones, Cancer and Blood-Brain Barrier: A Possible Molecular Mechanism.

Zheijang University, School of Public Health, Hangzhou, China, 10.10.2003; Biological effects of mobile phone radiation.

Brooks AFB, San Antonio, TX, USA, 3.12.2003; Application of transcriptomics and proteomics in search for the potential health effects of EMF.

invited presentations at the conferences:

24th Annual Meeting of Bioelectromagnetics Society, Quebec City, Canada, 23-27.06.2002, Effect of mobile phone radiation on gene and protein expression.

27th General Assembly of the International Union of Radio Science (URSI), Maastricht, The Netherlands, 17-24.08.2002, Effect of GSM mobile phone radiation on blood-brain barrier: Use of proteomics approach to define the hypothetical molecular mechanism.

COST 281 Seminar "Subtle Temperature Effects of RF-EMF", 12-13.11.2002, London, UK, Indirect evidence of non-thermal biological effects induced by mobile phone radiation in vitro.

FGF & COST 281 Workshop on "Genetic and Cytogenetic Aspects of RF-Field Interaction", 24-27.11.2002, Löwenstein, Germany, Mobile phone radiation-induced gene expression might be cell genotype-dependent.

Proteomica Symposium, University of Madrid, 4-8.02.2003, Cordoba, Spain, Use of discovery science-approach to elucidate bio-effects of electromagnetic fields.

25th Annual Meeting of Bioelectromagnetics Society, Maui, HI, USA, 23-27.06.2003, Use of discovery science-approach to elucidate bio-effects of electromagnetic fields. (Plenary talk)

25th Annual Meeting of Bioelectromagnetics Society, Maui, HI, USA, 23-27.06.2003, Cellular response to mobile phone radiation appears to be cell genotype-dependent.

WHO & ICNIRP & China Health Ministry, 3rd International EMF Seminar in China: Electromagnetic Fields and Biological Effects, 14-17.10.2003, Guilin, China, Discovery science and mobile phone safety: a need for the new research approach. (Keynote talk)

FGF & COST281 Workshop "The Blood-Brain Barrier (BBB) - Can it be influenced by RF-field interactions?", 3-6.11.2003, Reisensburg, Germany, Mobile Phone Radiation and Blood-Brain Barrier: The available scientific evidence is insufficient to dismiss or to support claims of a health risk in humans.

6th Meeting of the European BioElectromagnetics Association, Budapest, Hungary, 12-16.11.2003, New research approach in EMF research - proteomics and transcriptomics (Plenary talk)

IEEE ICES (SCC-28) meeting, San Antonio TX, USA, 4-7.12.2003; Use of high-throughput screening techniques to determine biological effects of mobile phone radiation.

26th Annual Meeting of the Bioelectromagnetics Society, Washington, DC, USA, 20-25.06.2004; Biological effects of EMF: do they exist and what might be their biophysical mechanism - a molecular biologists perspective.

6.7 rCx46 in oocytes of *Xenopus laevis* and human fibroblasts and granulosa cells of rats (Participant 7)

a. Scientific papers

submitted:

Pilger A., Ivancsits S., Diem E., Steffens M., Kolb H-A., Rüdiger H. W. No long-lasting effects of intermittent 50 Hz electromagnetic field on cytoplasmic free calcium and mitochondrial membrane potential in human diploid fibroblasts Radiation and Environmental Biophysics.

in preparation:

Steffens M., Enders O., Behnsen J., Kolb H.-A. Effects of intermittent 50 Hz electromagnetic field on gap junctional coupling of paired *Xenopus laevis* oocytes expressing rCx46.

Steffens M., H.-A. Kolb; Effects of intermittent 50 Hz on conducting connexons of rCx46 expressed in oocytes of *Xenopus laevis*.

Steffens M., Kolb H.-A. Frequency dependent induction of DNA strand breaks by intermittent exposure to extremely low frequency electromagnetic field in various cultered cell lines.

b. Scientific meetings and reports

Steffens M., Kolb, H.-A. Gene expression of rCx46 in *Xenopus* oocytes is not affected by 50 Hz electro-magnetic radiation. Pflügers Arch. 443 (Plenary Lectures, Oral Sessions, Poster Sessions, Symposia) : S280 (2002)

Wobus A.M., Trillo M.A., Ubeda A., Kolb H.-A. Effects of ELF-and RF-EMF on cell proliferation and cell differentiation. 25th Annual Meeting of the BEMS, Maui, USA (June 2003). Proceedings: p. 133

Kolb, H.-A. Die Angst vor dem Strom. Neue Presse. Hannover (September 05, 2003)

Kolb, H.-A. Biologische Wirkungen ELF- und RF- elektromagnetischer Felder (EMF) (Nicht-ionische Wirkungen). 1.Nationaler Kongress Elektrosmog-Betroffener, Biel, Switzerland (22.11.2003)

Kolb, H.-A. Interview with Südwestfunk: Wirkung von EMF auf biologische Systeme. Hannover (July 07, 2004)

c. Poster

M. Steffens, H.-A. Kolb; Gene expression of rCx46 in *Xenopus* oocytes is not affected by 50 Hz electro-magnetic radiation. The Physiological Society Scandinavian Physiological Society, Deutsche Physiologische Gesellschaft (81st Annual Meeting), Tübingen, Germany (15–19 March 2002)

6.8 Experiments with human lymphocytes and thymocytes and with mice embryonic stem cells during cardiac differentiation (Participant 8)

a. Scientific papers

published:

Capri M, Scarcella E, Bianchi E, Fumelli C, Mesircas P, Agostini C, Remondini D, Schuderer J, Kuster N, Franceschi C, Bersani F (2004) 1800 MHz radiofrequency (mobile phones, different Global System for Mobile communication modulations) does not affect apoptosis and heat shock protein 70 level in peripheral blood mononuclear cells from younf and old donors. Int J Radiat Biol, Vol 80, No 6: p. 389 - 397

Ventura C, Maioli M, Asara Y, Santoni D, Mesirca P, Remondini D, Bersani F (2004) Turning on stem cell cardiogenesis with extremely low frequency magnetic fields. The FASEB J, published online Oct 26, 2004.

in preparation:

Magnetic fields and cell fate specification in embryonic stem cells. In preparation for Science

b. Scientific meetings

Effects of ELF-EMF on gene expression of various cell lines. 25th Annual BEMS Meeting 2003, Abstract book, p. 131

6.9 Experiments with brain cells of different origin and human monocytes (Participant 9)

a. Scientific papers

in preparation:

Poulletier de Gannes F. et al., Effects of GSM-900 radiofrequency radiation on apoptosis in brain cells. (Ready to be submitted to Radiation Research)

Lagroye I. et al., GSM-900 signal does not affect iNOS expression in rat C6 glioma cells (in preparation for Radiation Research)

Lagroye I. et al., Apoptosis in U937 after exposure to 217 Hz-modulated GSM-900 radiofrequency radiation. (in preparation for Bioelectromagnetics)

Poulletier de Gannes F. et al., Expression of heat shock proteins in brain cells after exposure to GSM-900 radiofrequency radiation (in preparation for International Journal of Radiation Biology)

b. Scientific meetings

Lagroye I., E. Haro, P.-E. Dulou, B. Billaudel, B. Veyret. Effect of GSM-900 exposure on NOS-II expression in rat C6 glioma cells. 24st Annual Meeting of the BEMS, Quebec, Canada (June 2002)

Lagroye I., E. Haro, P.-E. Dulou, B. Billaudel, B. Veyret. Effect of GSM-900 exposure on NOS-II expression in rat C6 glioma cells. 24st Annual Meeting of the BEMS, Quebec, Canada (June 2002).

Leszczynski, D., Billaudel, B., Czyz, J., Dulou, P-E., Guan, K., Haro, E., Joenväärä, S., Kuokka, R., Lagroye, I. , Meister, A., Reivinen, J., Veyret, B., Wobus, A.M., Zeng. Q. Effects of mobile phone radiation on gene and protein expression in vitro. 24st Annual Meeting of the BEMS, Quebec, Canada (June 2002).

Lagroye I, Bersani F., Billaudel B., Capri M., Czyz J., Dulou P-E., Guan K. Haro E., Joenväärä S., Kuokka R., Kuster N.,., Leszczynski D., Meister A., Reivinen J., Schuderer J., B. Veyret, A.M. Wobus, Q. Zeng. Do ELF or RF fields affect the apoptotic process? Data from the REFLEX programme. 24st Annual Meeting of the BEMS, Québec, Canada (June 2002).

Lagroye I., Poulletier de Gannes F., Haro E., Billaudel B., Dulou P.E., Veyret B. Effect of GSM-900 radiofrequency on apoptosis of immune and nervous cells. 27ème assemblée générale de l'URSI, Maastricht, Pays-Bas, (August 2002).

Lagroye I., Bersani F., Agostini C., Bianchi E.,Billaudel B., Capri M., Dulou P.E., Fumelli C., Haro E., Mesirca P., Poulletier de Gannes F., Scarcella E., Veyret B., Do GSM signals induce apoptosis in mammalian immune and nervous cells? 2nd International Workshop on Biological effects of EMF's, Rhodes, Crète, (October 2002).

Lagroye I., Bersani F., Agostini C., Bianchi E., Billaudel B., Capri M., Dulou P.E., Fumelli C., Haro E., Mesirca P., Poulletier de Gannes F., Scarcella E., Veyret B. Do GSM-900 signals induce apoptosis in mammalian immune and nervous cells? 2nd International Workshop on Biological Effects of Electromagnetic Fields, Rhodes, October 7-11, 2002, page 404-408.

Adlkofer F., R. Tauber, H.W. Rüdiger, A.M. Wobus, A. Trillo, D. Leszczynski, H.-A. Kolb, F. Bersani, I. Lagroye, N. Kuster, F. Clementi, C. Maercker, Risk Evaluation of Potential Environmental Hazards from Low Energy Electromagnetic Field Exposure Using Sensitive in vitro Methods (REFLEX), 2nd International Workshop on Biological effects of EMF's, Rhodes, Crète, (October 2002).

Poulletier de Gannes F., I. Lagroye, E. Haro, P.E. Dulou, B.Billaudel, B. Veyret. Heat shock proteins as sensors of nonthermal effects? Subtil effects of temperature, Cost 281 meeting, London, UK, (november 2002).

Lagroye I., Bersani F., Billaudel B., Capri M., Czyz J., Dulou P-E., Guan K., Haro E., Joenväärä S., Kuokka R., Kuster N., Leszczynski D., Meister A., Poulletier de Gannes F., Reivinen J., Schuderer J., Veyret B., Wobus A.M., Zeng Q. Effects of ELF- and RF-EMF on the apoptotic process. Abstract for the BEMS 25th annual meeting - Maui, Hawaii, June 22-27, 2003, page 134.

Poulletier de Gannes F., I. Lagroye, E. Haro, M. Taxile, P.E. Dulou, B. Billaudel, B. Veyret, Effects of GSM-900 on apoptosis in brain cells. 6th International Congress of the European BioElectromagnetics Association, 2003, Budapest, Hongrie (November 2003).

Lagroye I., Haro E., Billaudel B., Veyret B. The effect of GSM-900 radiofrequency radiation on camptothecin-induced apoptosis in human U937 lymphoblastoma cells. 6th International Congress of the European BioElectromagnetics Association, 2003, Budapest, Hongrie (November 2003).

Poulletier de Gannes, F., Sanchez, S., Lagroye, I., Haro, E., Dulou, P.-E., Billaudel, B., Veyret. B. In vitro and in vivo studies of the effects of GSM-900 microwave exposure on heat shock proteins in the brain and skin. 25th Annual Meeting of the BEMS, Maui, USA (June 2003).

Lagroye I, Bersani F, Billaudel B, Capri M, Czyz J, Dulou P-E., Guan K., Haro E., Joenväärä S., Kuokka R., Kuster N., Leszczynski D., Meister A., Poulletier de Gannes F. Reivinen J., Schuderer J., B. Veyret, A.M. Wobus, Q. Zeng. Effects Of ELF And RF Fields On Apoptosis In Different Cell Lines. . 25th Annual Meeting of the BEMS, Maui, USA (June 2003).

F. Poulletier de Gannes, S. Sanchez, I. Lagroye, E. Haro, B. Billaudel, B. Veyret. Effects of GSM-900 microwave exposure on heat shock proteins: *in vitro* and *in vivo* studies on different models in PIOM laboratory. COST 281bis workshop on "Influence of RF Fields on the Expression of Stress Proteins". April 28-29 2004, STUK Helsinki, Finland.

F. Poulletier de Gannes, I. Lagroye, S. Sanchez, B. Billaudel, B. Veyret. Effect of GSM-900 exposure on hsp27 expression in EA-hy926 endothelial cells: a replication study. 26th Annual Meeting of the BEMS, Washington DC, USA (June 2004).

6.10 Provision of exposure setups and technical quality control (Participant 10)

Exploitation

The success of the exposure setups developed under the umbrella of REFLEX have resulted in additional demands for similar setups being used in further European research programs, e.g. PERFORM B.

Dissemination

a. Scientific papers

published:

J. Schuderer, T. Schmid, G. Urban, N. Kuster, “Novel High Resolution Temperature Probe for RF Dosimetry”, Physics in Medicine and Biology, vol 49, pp. N83-N92, 2004.

J. Schuderer, T. Samaras, W. Oesch, D. Spät, N. Kuster, “High Peak SAR Exposure Unit with Tight Exposure and Environmental Control for In Vitro Experiments at 1800 MHz”, IEEE Transactions on Microwave Theory and Techniques, vol 52, No 8, 2004: 2057-2066

J. Schuderer, D. Spät, T. Samaras, W. Oesch, N. Kuster, “In Vitro Exposure Systems for RF Exposures at 900 MHz”, IEEE Transactions on Microwave Theory and Techniques, vol 52, No8, 2004: 2067-2075

J. Schuderer, W. Oesch, N. Felber, N. Kuster, “In Vitro Exposure Apparatus for ELF Magnetic Fields”, Bioelectromagnetics, in press, 2004.

J. Schuderer, "EMF Risk Assessment: *In Vitro* Research and Sleep Studies", Dissertation, ETH, 2003

J. Schuderer, N. Kuster, “The Effect of the Meniscus at the Solid/Liquid Interface on the SAR Distribution in Petri Dishes and Flasks”, Bioelectromagnetics, vol. 24, pp.103-108, 2003.

submitted:

J. Schuderer, U. Lott, N. Kuster, “UMTS In Vitro Exposure System and Test Signal for Health Risk Research”, Bioelectromagnetics, submitted 2004

in preparation:

W. Oesch, J. Schuderer, N. Kuster, R. Mertens, R. Adey, "Selection of Specific EMF Exposure Conditions for Bioexperiments in the Context of Health Risk Assessments", in preparation, 2004.

b. Scientific meetings

J. Schuderer, T. Samaras, W. Oesch, N. Nikoloski, D. Spät, N. Kuster, "Electromagnetic Field Exposure of Cells at 900 and 1800 MHz: Requirements, Dosimetry and Performance Comparison of Different Setups", FGF & COST281 Workshop on the Influcence of RF Fields on the Expression of Stress Proteins, April, Helsinki, Finland, pp. 21-22, 2004.

J. Schuderer, W. Oesch, U. Lott, N. Kuster, "In Vitro Exposure Setup for Risk Assessment Studies with UMTS Signal Schemes at 1950 Mhz", 25th Annual Meeting of the Bioelectromagnetics Society, June, Maui, USA, p. 68, 2003.

J. Schuderer, W. Oesch, R. Mertens, U. Frauenknecht, N. Kuster, "Exposure Systems, Dosimetry and Quality Control", 25th Annual Meeting of the Bioelectromagnetics Society, June, Maui, USA, pp. 127-128, 2003.

T. Samaras, J. Schuderer, N. Kuster, "Temperature Distributions Inside Cell Cultures Exposed to Electromagnetic Fields In Vitro", Cost 281 Management Committee Meeting, London, GB, Nov. 12-13, 2002.

J. Schuderer, T. Schmid, G. Urban, N. Kuster, "Novel High Resolution Temperature Probe for Micro-dosimetry", 27th General Assembly of the International Union of Radio Science, Maastricht, Netherlands, August, paper No. 2110 (2.p), 2002.

J. Schuderer, W. Oesch, N. Kuster, "In Vitro Exposure Setup for ELF Magnetic Fields Enabling Flexible Signal Schemes and Double Blind Protocols", 24th Annual Meeting of the Bioelectromagnetics Society, June, Quebec, Canada, pp. 105-106, 2002.

J. Schuderer, W. Oesch, R. Mertens, U. Frauenknecht, N. Kuster, "Exposure Systems and Dosimetric Quality Control in the REFLEX Project", 24th Annual Meeting of the Bioelectromagnetics Society, June, Quebec, Canada, pp. 93-94, 2002.

R. Mertens, W. Kainz, N. Kuster, "Simulating Environmental GSM Features for Use in Bioexperiments", 24th Annual Meeting of the Bioelectromagnetics Society, June, Quebec, Canada, p. 105, 2002.
J. Schuderer, R. Mertens, W. Oesch, U. Frauenknecht, N. Kuster, "Flexible and Efficient In Vitro Exposure Setup for Risk Assessment Studies at 1800 MHz Enabling any Modulation Scheme from Sub-Hz up to 15MHz and Double Blind Protocols", 23rd Annual Meeting of the Bioelectromagnetics Society, St. Paul, Minnesota, USA, p. 26, 2001.

N. Kuster, W-R. Adey, "Criteria for Selecting Specific EMF Exposure Conditions for Bioexperiments in the Context of Health Risk Assessments", 23rd Annual Meeting of the Bioelectromagnetics Society, St. Paul, Minnesota, USA, p. 24, 2001.

J. Schuderer, N. Kuster, "The Effect of the Meniscus at the Solid-Liquid Interface on the SAR Distribution in Petri Dishes and Flasks", Millenium Workshop on Biological Effects of Electromagnetic Fields, Heraklion, Greece, pp. 203-207, 2000.

c. Posters

W. Oesch, H-U. Gerber, N. Kuster, "Requirements for Controlling & Monitoring Software of Expoure Systems in (Double-)Blinded Bio Experiments", 24th Annual Meeting of the Bioelectromagnetics Society, June, Quebec, Canada, pp. 152-153, 2002.

d. Reports in the general media

J. Schuderer, "EMF Risk Assessment: In Vitro Research and Sleep Studies", Diss. ETH 15347, 2003.

N. Kuster, "Latest Progress in Experimental Dosimetry for Human Exposure Evaluations and for Characterization and Optimization of Exposure", in "Communication Mobile – Effects Biologique", ed. Claude Legris, CADAS, Académie des Sciences, Paris, France, pp. 63-69, 2001.

6.11 Experiments with the human neuroblastoma cell line SY5Y (Participant 11)

a. Scientific papers

The results described in this final report will be *submitted* for two publications in international scientific journals.

Benfante R., Antonini R.A., Gotti C., Moretti M., Kuster N., Schuderer J., Clementi F, and Fornasari D. – "Extremely low-frequency electromagnetic field (ELF-EMF) does not affect the expression of α3, α5 and α7 nicotinic receptor subunit genes in SY5Y neuroblastoma cell line". Manuscript in preparation

Antonini R.A:, Benfante R., Flora A., Kuster N., Schuderer J., Adlkofer F, Clementi F., and Fornasari D. – "The expression of DβH (dopamine-β-hydroxylase) and noradrenergic phenotype specifying genes Phox2A and Phox2B is unresponsive to exposure to extremely-low-frequency electromagnetic field (ELF-EMF)". Manuscript in preparation

6.12 Effects of EMF on gene expression in human cells analysed with the cDNA array (Participant 12)

a. Scientific publications

submitted:

Schlatterer K, Gminski R, Hermann S, Tauber R, Fitzner R, Maercker C. Gene expression profiling identifies differences in ribosome biogenesis of human promyelocytic leukemia HL-60 cells following exposure to 1800 MHz radiofrequency electromagnetic fields.

in preparation:

Remondini D, Leszczynski D, Nylund R, Ivancsits S, Rudiger HW, Bersani B, Maercker C. The bio-statistical analysis of micro-array data give indications for the induction of calcium-related signaling pathways after exposure of primary fibroblasts and endothelial cells to electromagnetic fields.

Kuokka R, Griffin T, Maercker C, Schuderer J, Reivinen J, Kuster N, Aebersold R, Leszczynski D. Effect of low-energy microwaves on protein expression in human endothelial cell line: Microwave modulation might be the cause of biological response.

b. Oral presentations at scientific meetings and round tables

Maercker C, Czyz J, Ivancsits S, Ruediger HW, Jahn O, Diem E, Pilger A, Rolletschek A, Schuderer J, Kuster N, Guan K, Trillo A, Bazán E, Reimers D, Fornasari D, Clementi F, Schlatterer K, Tauber R, Fitzner R, Adlkofer F, Wobus AM (2002) Gene expression profiling studies on global cDNA arrays show sensitivity of human and mouse cell lines to extremely-low frequency (ELF-EMF) and radiofrequency (RF-EMF) exposure. 24th annual BEMS Meeting, Quebec, Canada.

Maercker C, Wobus AM, Huber W, Poustka A, Ivancsits S, Rüdiger HW, Jahn O, Diem E, Schuderer J, Kuster N, Fornasari D, Clementi F, Schlatterer K, Tauber R, Fitzner R, Reivinen J, Adlkofer F, Leszczynski D (2002) An EU-wide initiative to characterize the biological effects of EMF on human and mouse cell lines by gene expression profiling. 2nd Int. Workshop on Biolocical Effects of Electromagnetic Fields, Rhodes, Greece. Proceedings, pp. 588-594.

Maercker C (2003) In-vitro investigation of molecular effects of electromagnetic fields by high-throughput techniques. Deutscher Ärztekongress, Berlin, Germany.

Maercker C, Schlatterer K, Gminski R, Schuderer J, Kuster N, Adlkofer F, Fitzner R, Tauber R (2003) RF-EMF exposure increases protein synthesis in human promyelocytic cells. 25th annual BEMS Meeting, Hawaii, USA.

Maercker C (2003) Effects of electromagnetic fields on the human genes – expererimental results and assessment of the potential of molecular biology in environmental research. Workshop of the ministry for environment in Nordrhein-Westfalen, Universität Witten-Herdecke, Germany.

Maercker C, Schlatterer K, Gminski R, Schuderer J, Kuster N, Adlkofer F, Fitzner R, Tauber R (2003) In vitro studies on promyelocytic cells with the help of gene expression profiling on cDNA microarrays show an increase of protein synthesis after RF-EMF exposure. EBEA2003 meeting, Budapest, Hungary.

Maercker C (2004) Genomics and proteomics approaches in EMF research. Erice School in Bioelectromagnetics, Erice, Italy.

Maercker C (2004) Invited participant in a round table discussion about research needs in European EMF research. Erice School in Bioelectromagnetics, Erice, Italy.

Maercker C (2004) Do electromagnetic fields induce stress responses? A whole-genome approach helps to identify cellular pathways modulated by RF-EMF and ELF-EMF" COST Workshop "Influence of RF Fields on the Expression of Stress Proteins" Helsinki, Finland.

Maercker C, Schlatterer K, Gminski R, Remondini D, Leszczynski D, Rüdiger H, Bersani F, Fitzner R, Tauber R (2004) The whole-genome gene expression analysis as a powerful method to detect molecular effects of electromagnetic fields. Deutscher Ärztekongress, Berlin, Germany.

Maercker C, Remondini D, Nylund R, Lezczynski D, Schlatterer K, Fitzner R, Tauber R, Ivancsits S, Rudiger H, Bersani F (2004) Analysis of gene expression in EMF research. 26th Annual Meeting of the Bioelectromagnetic Society (BEMS), Washington, USA.

Maercker C (2004) Molecular investigation of the effects of electromagnetic fields. T-Mobile GmbH, Darmstadt, Germany.

c. Posters

Maercker C, Czyz J, Wobus AM, Huber W, Poustka A, Ivancsits S, Ruediger HW, Reivinen J, Leszczynski D, Schlatterer K, Tauber R, Fitzner R, Fornasari D, Clementi F, Schuderer J, Kuster N, Adlkofer F (2002) An EU-wide initiative to characterize the biological effects of electromagnetic fields on different human and mouse cell lines by gene expression profiling. Annual Meeting of the "Nationales Genomforschungsnetz" (NGFN) in Berlin, Germany.

Maercker C, Kuokka R, Reivinen J, Ivancsits S, Ruediger HW, Schuderer J, Kuster N, Fornasari D, Clementi F, Schlatterer K, Tauber R, Fitzner R, Adlkofer F, Leszczynski D (2003) Whole-genome gene expression profiling: a big challenge to find out the molecular answer to EMF exposure. 25th annual BEMS Meeting, Hawaii, USA.

Lupke M, Maercker C, Simkó M (2004) Alteration in gene expression after 50 Hz ELF-MF exposure in human umbellical cord blood-derived monocytes. 3nd Int. Workshop on Biolocical Effects of Electromagnetic Fields, Kos, Greece.

7.0 POLICY RELATED BENEFITS

7.1 Studies on the human promyelocytic cell line HL-60 (Participant 2)

Research performed is basic research with relevance for life science and techniques, respectively. Our results obtained with human promyelocytic HL-60 cells have made a substantial addition to the data base relating to genotoxic and phenotypic effects of RF-EMF in vitro. Its value lies in providing new data that will enable mechanisms of RF-EMF effects to be studied more effectively (e.g. ROS effects) than in the past. Proteomics studies should be extended to identify possible, potential biological and molecular markers. Furthermore, our data provide new information that will be used for risk evaluation by WHO, IARC and ICNIRP.

7.2 Studies on human fibroblasts, human lymphocytes, human monocytes, human melanocytes, human muscle cells and granulosa cells of rats (Participant3)

Based on our findings we propose the suitability of the comet assay, micronucleus test and evaluation of chromosomal aberrations for monitoring and surveillance of EMF exposed subjects. Due to possible cell specific differences in response to EMF the biological material chosen for biomonitoring could be crucial. Our findings arouse concern about environmental threshold limit values and protective measures regarding EMF exposure in particular with respect to older individuals or people suffering from repair syndroms. The observed activation of DNA repair could display beneficial health effects and could be applied for medical treatment.

7.3 Studies on mouse embryonic stem cells (Participant 4)

Our research results confirmed subtle biological effects emanating from both extremely low frequency fields (simulating the magnetic components of 50 Hz power line fields) and high-frequency (RF) electromagnetic fields (EMF) simulating GSM-modulated schemes. The effects were dependent on the genetic constitution of the cells, and especially the transcription of apoptotic/anti-apoptotic related genes was shown to be affected. Neural progenitor cells appeared to perceive EMF at certain stages of differentiation as external stress signals, which may activate at least, a bcl-2 mediated anti-apoptotic pathway.

1. Important for the quality of life and for human health could be the improvement of products emitting EMF. In this context, 'no effect-levels' were observed with regard to flux density, which can be used to determine threshold values more precisely.
2. The analysis of transcript levels affected by EMF should be extended by genomics and proteomics studies in animals, but also in human populations, to identify further potential molecular markers which may serve as "EMF-responsive bio-indicator".
3. Cell biological studies should be continued to elucidate the molecular processes that may be affected by EMF, especially in the context of carcinogenesis.

7.4 Studies on the human neuroblastoma cell line NB69 and neural stem cells (Participant 5)

The described results indicate that a human neuroblastoma cell line can be sensitive to the in vitro exposure to power frequency, sine wave EM fields at magnetic flux densities that are equal to or lower than the exposure threshold (100 μT) recommended by ICNIRP and UE for the general public. The effects, which include changes in the cells' proliferation, apoptosis or the cellular response to growth factors, among others, were found to be dependent on the ELF-EMF density, the exposure time, the cell passage or the cell cycle. The same human cancer cell line, as well as neural stem cells from rat's embryonic nucleus striatum, was found to be sensitive to the in vitro exposure to GSM-1800 signals at a SAR of 2 w/kg, the exposure threshold recommended by ICNIRP and UE for the general public. The effects included changes in the expression of fibroblast growth factor receptor-1, accompanied or not with changes in the cellular morphology linked to a potential promotion of non-neuronal precursors of NSC' progeny. No differential responses were detected when the cells were exposed to GSM signals with

different ELF modulation patterns, suggesting that the observed effects reflect a cellular sensitivity to the RF carrier wave, rather than to the ELF modulation.

1. These data identify cellular mechanisms of response to specific parameters of exposure to ELF and RF electromagnetic fields that are ubiquitous in today's human environment. Such information can significantly contribute to the establishment of adequate strategies for the protection against non-ionising radiation in public, residential or occupational environments.
2. The study of the cellular mechanisms of response to ELF and RF EMF should be extended to properly identify the biophysical phenomena underlying the potential health effects of the exposure to environmental, non-ionising radiation. In this context, two types of studies are of crucial interest. A) Studies aimed to identify potential markers or bio-indicators of EM sensitivity; B) Studies on human cancer cells and the in vitro response to chemicals that could prevent the EMF effects.

7.5 Studies on the human endothelial cell lines EA.hy926 and EA.hy926v1 (Participant 6)

We have found that 900 and 1800 MHz GSM radiation at SAR of 2.0-2.4W/kg causes activation of stress response in human endothelial cell line. The stress response was followed by a physiological response on a single cell level. Cellular stress fibers were stabilized what was followed by the changes in cellular size and shape (cells contraction). Also we have observed effect on other cytoskeletal proteins, in particular on vimentin and formed of it - vimentin filaments. In respect of cell apoptosis we have observed decline in the expression of nearly all proteins involved in Fas/TNFα-dependent apoptosis pathway. This suggests that the mobile phone radiation might have some potential to prevent apoptosis of cells - a possibility that is currently being explored in further research. All-in-all, results of our research suggest that cells recognize mobile phone radiation as an external stress and this in spite of the very low energy of the exposure. Part of the results of our research has been already published in three articles (one in Differentiation 2002; two in Proteomics 2004). These results, although directly can not be used for prediction of any health hazard, they are available for the scientific evaluation of the potential risks associated with the use of mobile phones and for recommendations of further research needs. The remaining experimental data obtained by us within REFLEX is in process of submission for publication (3 manuscripts) and will be available for the scientific community in 2005.

7.6 Studies on rCx46 in oocytes of Xenopus laevis and human fibroblasts and granulosa cells of rats Participant 7)

On the level of DNA we found significant evidence for DNA damage by ELF-EMF for cultured human fibroblasts and granulosa cells of rats. The findings were strongly related to the exposure protocol. At intermittent ELF-EMF exposure maximal effects were observed after 16-18 h of exposure independently on the applied frequency in the range of 8 Hz to 300 Hz.

The effects appeared not to be reflected on the cellular level of free cytoplasmic calcium. Also cellular studies on the expression level of connexin 46 in oocytes of *Xenopus laevis* showed no significant effect on ELF-EMF exposure. Therefore, it is tempting to suggest that significant effects by ELF-EMF exposure on the genomic level appear not to be reflected on the cellular level. But is has to be taken into account that the methods which are applied to study DNA damage are quite different and most probably more sensitive than those for studying cellular parameters.

7.7 Studies on embryonic stem cells during cardiac differentiation and human lymphocytes and thymocytes (Participant 8)

Studies on embryonic stem cells open a totally new perspective: on one side, the possibility to study in a reproducible way the effects of ELF-EMF on cell differentiation and in particular on cardiogenesis; on the other side, the possibility to direct in some way the differentiation processes of stem cells into specific cell phenotypes.

The more or less negative results studies on human lymphocytes and thymocytes are of paramount importance for risk evaluation since they show that the immune system cells are nearly insensitive to ELF and RF EMF exposure.

7.8 Studies on brain cells of different origin and human monocytes (Participant 9)

We have found no evidence of biological effects of GSM-like signals on mammalian immune and nerve cells. The endpoints were apoptosis and the expression of stress- or inflammation induced proteins. Protocols included exposures at SAR levels corresponding to the public limit for local exposure (2 W/kg) and prolonged exposure duration (24 to 48 hours) that represent a "worst-case" exposure condition. These in vitro results will add to the database, on which the next scientific evaluation of RF-EMF health effects will be based. Although the present findings do not suggest a need for a revision of the local exposure limits to RF-EMF (1999/519/CE), more investigations on animal models of neurodegenerative diseases are needed.

7.9 Provision of exposure set-ups and technical quality control (Participant 10)

Our research is basically aimed at guaranteeing appropriate exposure setups and thorough quality control of the engineering aspects of the various experiments. High technical quality control is of special interest, since the variability of experiments within REFLEX is rather broad. Solid risk assessment will contribute to the future development of new communications technologies.

7.10 Studies on the human neuroblastoma cell line SY5Y (Participant 11)

Our results fit in a scientific debate around the contribution of ELF-EMF on brain neurodegenerative diseases, with particular emphasis on Alzheimer's disease (AD). Epidemiological studies showed that workers with likely electromagnetic field exposure may have an elevated risk of AD. On the other hand, experimental studies employing animal models failed to confirm these observations. In our studies we demonstrate that, at molecular level, the cholinergic system, which is one of the most affected neurotransmission system in AD, did not undergo any modification in the expression of relevant nAChR subtypes.

7.11 cDNA array analysis (Participant 12)

The micro-array technique is a state-of-the-art tool to investigate changes in gene expression and therefore molecular defects in human cells. Whereas in the field of medicine this kind of technique is on the way to get a diagnostic standard for certain diseases (e.g. cancer), it is not common so far for the detection of environmental effects. With our study we have shown that the whole-genome analysis is a suitable method to detect potential molecular effects of EMF. Since the different labs participating in the REFLEX project have worked with the same exposure setups (Participant 10) and we have done all hybridisations and data analyses in the same way, we have created a platform which can work with comparable material (RNA) of different cell lines and different experimentators. A quality control of the RNA (test for degradation, concentration) allowed us to make experiments with very different cell lines under comparable conditions and therefore to produce reliable results. This is a big difference to other assays (e.g. microscopical analysis), which strongly depend on people and software. In the near future, whole-genome approaches might support or even replace other measurements of the effects of electromagnetic fields or related environmental influences. Since the technique is very sensitive and specificly applicable for human cells, it also should be applied for in vivo studies in upcoming projects.

7.12 Summary (Participant 1)

The policy related benefits of the REFLEXproject consist in the fact that new knowledge has been generated independent of whether one likes it or not. Biological effects of extremely low-frequency (ELF) and radio-frequency (RF) electromagnetic fields (EMFs) the exposure to which is constantly increasing especially in Europe with its high density of population and industry and with the omnipresence of EMFs in infrastructures and consumer products have become a topic of public concern. This is due to the fear of people that based on the many conflicting research data a risk to their health cannot be excluded with some certainty. Therefore, the overall objective of REFLEX was to find out whether or not the fundamental biological processes at the cellular and molecular level support such an assumption. For this purpose, possible effects of EMFs on cellular events controlling key functions, including those involved

in carcinogenesis and in the pathogenesis of neurodegenerative disorders, were studied through focussed research. Failure to observe the occurrence of such key critical events in living cells after EMF exposure would have suggested that further research efforts in this field could be suspended and financial resources be reallocated to the investigation of more important issues. But as clearly demonstrated, the results of the REFLEX project show the way into the opposite direction.

The REFLEX project has made a substantial contribution to the data base on biological effects of both ELF-EMF and RF-EMF on in vitro cellular systems. The study was designed to investigate whether or not EMF exposure below the energy density reflected by the present safety levels generates in vitro critical cellular events. Gene mutations, deregulated cell proliferation and suppressed or exaggerated programmed cell death (apoptosis) that are caused by or result in an altered gene and protein expression profile are such critical events, the convergence of which is required for the development of chronic diseases. Genotoxic effects and a modified expression of numerous genes and proteins after EMF exposure could be demonstrated with great certainty, while effects on cell proliferation, cell differentiation and apoptosis were much less conclusive. Since all these observations were made in in vitro studies, the results obtained neither preclude nor confirm a health risk due to EMF exposure, but they speak in favour of such a possibility. Because of their fundamental character the findings will be presented to WHO, IARC and ICNIRP. It will be up to these organisations to make use of them for risk evaluation, in combination with findings from animal and epidemiological studies.

A major European added value of REFLEX consists also in the fact that the need for further research and especially how it should look alike have clearly been demonstrated. Furthermore, the outcome of the project should stimulate the research and development departments of the electrical, electronic, and telecommunication industry to make use of the methods developed in order to better adjust the state of technology to the conditions of life, and prompt the European governments to ensure multidisciplinary EMF research in order to take care, that the solution of the presently existing problem of uncertainty about a possible health risk for the people in Europe and beyond due to EMF exposure will not be postponed in the far future.

8.0 References

Aebersold R, Hood LE, Watts JD (2000) Equipping scientists for the new biology. Nature Biotechnology 18: 359

Ahlbom IC, Cardis E, Green A, Linet M, Savitz D, Swerdlow A (2001) Review of the epidemiologic literature on EMF and health. Environ Health Perspect 109: 911-933

Aladjem MI, Spike BT, Rodewald LW, Hope TJ, Klemm M, Jaenisch R, Wahl GM (1998) ES cells do not activate p53-dependent stress responses and undergo p53- independent apoptosis in response to DNA damage. Curr Biol 8:145-155

Alexandre H, Ansanay-Galeote V, Dequin S, Blondin B (2001) Global gene expression during short-term stress in Saccharomyces cerevisiae. FEBS letters 498: 98-103

Amati B, Littlewood TD, Evan GI, Land H (1993) The c-Myc protein induces cell cycle progression and apoptosis through dimerization with Max. EMBO J 12: 5083-5087

Ananth C, Thameem DS, Gopalakrishnakone P, Kaur C (2001) Domoic acid-induced neuronal damage in the rat hippocampus: changes in apoptosis related genes (bcl-2, bax, caspase-3) and microglial response. J Neurosci Res 66: 177-190

Anderson D, Yu TW, Phillips BJ, Schmerzer P (1994) The effect of various antioxidants and other modifying agents on oxygen-radical-generated DNA damage in human lymphocytes in the Comet assay. Mutat Res 307: 261-271

Anderson G, Jenkinson EJ (2000) Review article: thymus organ cultures and T-cell receptor repertoire development. Immunology 100(4): 405-10

Angel P, Allegretto EA, Okino ST, Hattori K, Boyle WJ, Hunter T, Karin M (1988) Oncogene jun encodes a sequence-specific trans-activator similar to AP-1. Nature 332: 166-171

Attardi LD, Jacks T (1999) The role of p53 in tumour suppression: lessons from mouse models. Cell Mol Life Sci 55: 48-63

Bachelet M, Mariethoz E, Banzet N, Souil E, Pinot F, Polla CZ, Durand P, Bouchaert I, Polla BS (1998) Flow cytometry is a rapid and reliable method for evaluating heat shock protein 70 expression in human monocytes.Cell Stress Chaperones 3(3):168-76 / Erratum in: Cell Stress Chaperones 3(4): 273

Bauréus Koch LLM, Sommarin M, Persson BRR, Salford LG, Eberhardt LL (2003) Interaction between weak low frequency magnetic fields and cell membranes. Bioelectromagnetics 24: 395-402

Becker LC, Ambrosio G (1987) Myocardial consequences of reperfusion. Progr Cardiovasc Dis 30: 23-44

Beckman KB, Ames BN (1997) Oxidative decay of DNA. J Biol Chem. 272: 19633-19636

Beere HM, Green DR (2001) Stress management - heat shock protein-70 and the regulation of apoptosis. Trends Cell Biol 11: 6-10

Ben Yehuda A, Globerson A, Krichevsky S, Bar On H, Kidron M, Friedlander Y, Friedman G, Ben Yehuda D (2000) Ageing and the mismatch repair system. Mech Age Dev 20: 173-179

Biben C, Harvey RP (1997) Homeodomain factor Nkx-2.5 controls left/right asymmetric expression of bHLH gene eHand during murine heart development. Genes Dev. 11: 1357-1369

Binhi VN, Goldman RJ (2000) Ion-protein dissociation predicts 'windows' in electric field-induced wound-cell proliferation. Biochim Biophys Acta 1474: 147-156

Bisht KS, Moros EG, Straube WL, Baty JD, Roti Roti JL (2002) The effect of 835.62 MHz FDMA or 847.74 MHz CDMA modulated radiofrequency radiation on the induction of micronuclei in C3H 10T(1/2) cells. Radiat Res 157(5): 506-15

Blackman CF, Benane SG, House DE, Joines WT (1985a) Effects of ELF (1-120 Hz) and modulated (50 Hz) RF fields on the efflux of calcium ions from brain tissue in vitro. Bioelectromagnetics 6(1): 1-11

Blackman CF, Benane SG, Rabinowitz JR, House DE, Joines WT (1985b) A role for the magnetic field in the radiation-induced efflux of calcium ions from brain tissue in vitro. Bioelectromagnetics 6: 327-337

Blackman CF, Benane SG, House DE, Pollock MM (1993) Action of 50 Hz magnetic fields on neurite outgrowth in pheochromocytoma cells. Bioelectromagnetics 14: 273-286

Blackman CF, Blanchard JP, Benane SG, House DE (1994) Empirical test of an ion parametric resonance model for magnetic field interactions with PC-12 cells. Bioelectromagnetics 15: 239-260

Blackmann CF, Benane SG, House DE (1995)Frequency-dependent interference by magnetic fields of nerve growth factor-induced neurite outgrowth with PC-12 cells. Bioelectromagnetics 16: 387-395

Blank M (1992) Na,K-ATPase function in alternating electric fields. FASEB J 6: 2434-2438

Blank M, Goodman R (1997) Do electromagnetic fields interact directly with DNA? Bioelectromagnetics 18: 111-115

Blumentahl NC, Ricci J, Breger L, Zychlinsky A, Solomon H, Chen GG, Kuznetsov D, Dorfman R (1997) Effects of low-intensity AC and/or DC electromagnetic fields on cell attachment and induction of apoptosis. Bioelectromagnetics 18 (3): 264-272

Bodem J, Dobreva G, Hoffmann-Rohrer U, Iben S, Zentgraf H, Delius H, Vingron M, Grummt I (2000) TIF-IA, the factor mediating growth-dependent control of ribosomal RNA synthesis, is the mammalian homolog of yeast Rrn3p. EMBO Rep 1: 171-175

Boer JM, Huber WK, Sultmann H, Wilmer F, von Heydebreck A, Haas S, Korn B, Gunawan B, Vente A, Fuzesi L, Vingron M, and Poustka A (2001) Identification and classification of differentially expressed genes in renal cell carcinoma by expression profiling on a global human 31,500-element cDNA array. Genome Res. 11: 1861-1870

Bohr VA (2002) Repair of oxidative DNA damage in nuclear and mitochondrial DNA, and some changes with aging in mammalian cells (1,2). Free Radic Biol Med 32: 804-812

Borbely AA, Huber R, Graf T, Fuchs B, Gallmann E, Achermann P (1999) pulsed high-frequency electromagnetic field affects human sleep and sleep electroencophalogramm. Neuroci Lett 275: 207

Böyum A (1968) Separation of lymphocytes from blood and bone marrow. Scand. J. Clin. Lab. Invest. 21 (suppl.97): 1-7

Brocklehurst B, McLauchlan JA (1996) Free radical mechanism for the effects of environmental electromagnetic fields on biological systems. Int J Radiat Biol 69: 3-24

Brown GC, Bal-Price A (2003) Inflammatory neurodegeneration mediated by nitric oxide, glutamate, and mitochondria. Mol Neurobiol. 27: 325-355.

Brugarolas J, Chandrasekaran C, Gordon JI, Beach D, Jacks T, Hannon GJ (1995) Radiation-induced cell cycle arrest compromised by p21 deficiency. Nature 377: 552-557

Bruzzone R, White TW, Paul DL (1996) Connections with connexins: the molecular basis of direct intercellular signaling. Eur J Biochem FEBS, Vol. 238: 1-27

Bryant P (1998) The signal model: a possible explanation or the conversion of DNA double-strand breaks into chromatid breaks. Int J Radiat Biol 73: 243-251

Burns TF, el-Deiry WS (2003) Cell death signaling in maligancy. Cancer Treat. Research 115: 319-343

Cabelof DC, Raffoul JJ, Yanamadala S, Ganir C, Guo Z, Heydari AR (2002) Attenuation of DNA polymerase beta-dependent base excision repair and increased DMS-induced mutagenicity in aged mice. Mutat Res 500: 135-45

Cain CD, Thomas DL, Adey WR (1997) Focus formation of C3H/10T1/2 cells and exposure to a 836.55 MHz modulated radiofrequency field. Bioelectromagnetics 18: 237-243

California EMF Program: Neutra RR, Delpizzo V, Lee GE (2002) An evaluation of the possible risks from electric and magnetic fields (EMFs) from powerlines, internal wiring, electrical occupations, and appliances. California Department of Health Services, Oakland, CA, USA

Cantoni O, Sestili P, Fiorani M, Dachà M (1996) The effect of 50 Hz sinusoidal electric and/or magnetic fields on the rate of repair of DNA single strand breaks in cultured mammalian cells exposed to three different carcinogens: methylmethane sulphonate, chromate and 254 nm U. V. radiation. Biochem Molec Biol Internat 38: 527-533

Capri M, Scarcella E, Fumelli C, Bianche E, Salvioli S, Mesirca P, Agostini C, Antolini A, Schiavoni A, Castellani G, Bersani F, Franceschi C (2004) In vitro exposure of human lymphocytes to 900 MHz CW and GSM modulated radiofrequency: studies on proliferation, apoptosis and mitochondrial membrane potential. Accepted by Radiat Res with minor modifications

Chang ZF (1990) Post-transcriptional regulation of thymidine kinase gene expression during monocytic differentiation of HL60 promyelocytes. Biochem Biophys Res Commun 169: 780-787

Chini B, Clementi F, Hukovic N, and Sher E (1992) Neuronal-type a-bungarotoxin receptors and the a5-nicotinic receptor subunit gene are expressed in neuronal and non-neuronal human cell lines. Proc. Natl. Acad. Sci. U.S.A. 89: 1572-1576

Cho YH, Chung HW (2003) The effect of extremely low frequency electromagnetic fields (ELF-EMF) on the frequency of micronuclei and sister chromatid exchange in human lymphocytes induced by benz(a)pyrene. Toxicol Lett 143: 37-44

Chomczynski P, Sacchi N (1987) Single-step method of RNA isolation by acid guanidinium thiocyanate- phenol-chloroform extraction. Anal Biochem 162: 156-159

Chung H, Yi YW, Jung NC, Kim D, Suh JM, Kim H, Park KC, Song JH, Kim DW, Hwang ES, Yoon SH, Bae YS, Kim JM, Bae I, Shong M (2003) CR6 interacting factor 1 (CRIF1) interacts with Gadd45 family proteins and modulates the cell cycle. J Biol Chem 278: 28079-28088

Cleary SF (1993) A review of in vitro studies: Low-frequency electromagnetic fields. Am. Ind. Hyg. Assoc. J. 54: 178-185

Cleary SF, Du Z, Cao G, Liu LM, McCrady C (1996) Effect of isothermal radiofrequency radiation on cytolytic T lymphocytes. FASEB J 10: 913-919

Cleary SF, Cao G, Liu LM, Egle PM, Shelton KR (1997) Stress proteins are not induced in mammalian cells exposed to radiofrequency or microwave radiation. Bioelectromagnetics 18: 499-505

Concannon CG, Orrenius S, Samali A (2001) Hsp27 inhibits cytochrome c-mediated caspase activation by sequestering both pro-caspase-3 and cytochrome c. Gene Expression 9: 195-201

Contestabile A (2002) Cerebellar granule cells as a model to study mechanisms of neuronal apoptosis or survival in vivo and in vitro. Cerebellum 1: 41-55.

Conti P, Gigante GE, Cifone MG, Alesse E, Ianni G, Reale M, Angeletti PU (1983) Reduced mitogenic stimulation of human lymphocytes by extremely low frequency electromagnetic fields. FEBS Lett. 162: 156-160

Cooke C (1996) UV-mediated DNA damage and its assessment. Toxicol Ecotoxicol News 3: 101-109

Cordero-Erausquin M, Marrubio LM, Klink R, Changeaux JP (2000) Nicotinic receptor function: new perspectives from knockout mice. Trends Pharmacol. Sci. 21: 211- 217

Cossarizza A, Monti D, Bersani F, Cantini M, Cadossi R, Sacchi A, Franceschi C (1989a) Extremely low frequency pulsed electromagnetic fields increase cell proliferation in lymphocytes from young and aged subjects. Biochem Biophys Res Commun 160(2): 692-698

Cossarizza A, Monti D, Bersani F, Paganelli R, Montagnani G, Cadossi R, Cantini M, Franceschi C (1989b) Extremely low frequency pulsed electromagnetic fields increase interleukin-2 (IL-2) utilization and IL-2 receptor expression in mitogen-stimulated human lymphocytes from old subjects.FEBS Lett 248(1-2): 141-144

Cossarizza A, Monti D, Bersani F, Scarfi MR, Zanotti M, Cadossi R, Franceschi C (1992) Exposure to low-frequency pulsed electromagnetic fields increases mitogen-induced lymphocyte proliferation in Down's syndrome. Aging, Milan/Italy 3(3): 241-246

Cossarizza A, Angioni S, Petraglia F, Genazzani AR, Monti D, Capri M, Bersani F, Cadossi R, Franceschi C (1993a) Exposure to low frequency pulsed electromagnetic fields increases interleukin-1 and interleukin-6 production by human peripheral blood mononuclear cells. Exp Cell Res. 204(2): 385-387

Cossarizza A, Baccarani-Contri M, Kalashnikova G, Franceschi C (1993b) A new method for the cytofluorimetric analysis of mitochondrial membrane potential using the J-aggregate forming lipophilic cation 5,5',6,6'-tetrachloro-1,1'3,3'-tetraethylbenzimidazolcarbo-cyanine iodide (JC-1). Biochem Biophys Res Comm 197: 40-45

Cotter TG (1992) Induction of apoptosis in cells of the immune system by cytotoxic stimuli. Semin Immunol 4: 399-405.

Creagh EM, Sheehan D, Cotter TG. (2000). Heat shock proteins--modulators of apoptosis in tumour cells. Leukemia 14: 1161-1173

Cridland NA, Haylock RGE, Saunders RD (1999) 50 Hz magnetic field exposure alters onset of S-Phase in normal human fibroblasts. Bioelectromagnetics 20: 446-452

Czerska EM, Elson EC, Davis CC, Swicord ML, Czerski P (1992) Effects of continuous and pulsed 2450-MHz radiation on spontaneous lymphoblastoid transformation of human lymphocytes in vitro. Bioelectromagnetics 13: 247-259

Czyz J, Guan K, Zeng Q, Nikolova T, Meister A, Schönborn F, Schuderer J, Kuster N, Wobus AM (2004a) High frequency electromagnetic fields affect gene expression levels in tumor suppressor-deficient embryonic stem cells. Accepted in Bioelectromagnetics

Czyz J, Nikolova T, Schuderer J, Kuster N, Wobus AM (2004b) Non-thermal effects of power-line magnetic fields (50 Hz) on gene expression levels of pluripotent embryonic stem cells – the role of tumour suppressor p53. Mutat Res 557: 63-74

D´Ambrosio G, Scarfi MR (2002a) Cytogenetic damage in human lymphocytes following GSM modulated microwave exposure. Bioelectromagnetics 23: 7-13

D'Ambrosio G, Massa R, Scarfi MR, Zeni O (2002b) Cytogenetic damage in human lymphocytes following GMSK phase modulated microwave exposure. Bioelectromagnetics 23(1): 7-13

Daadi MM, Saporta S, Willing AE, Zigova T, McGrogan MP, Sanberg PR (2001) In vitro induction and in vivo expression of bcl-2 in the hNT neurons. Brain Res Bull 56: 147-152

Daniells C, Duce I, Thomas D, Sewell P, Tattersall J, de Pomerai D. (1998). Transgenic nematodes as biomonitors of microwave-induced stress. Mutat. Res. 399, 55-64

De Fusco M, Becchetti A, Patrignani A, Annesi G, Gambardella A, Quattrone A, Ballabio A, Wanke E, Casari G (2000) The nicotinic receptor beta2 subunit is mutant in nocturnal frontal lobe epilepsy. Nat Genet 26: 275-276

De Pomerai D, Daniells C, David H, Allan J, Duce I, Mutwakil M, Thomas D, Sewell P, Tattersall J, Jones D, Candido P (2000) Non-thermal heat-shock response to microwaves. Nature 405: 417-418

De Roos AJ, Teschke K, Savitz DA, Poole C, Grufferman S, Pollock BH, Olshan AF (2001) Parental occupational exposures to electromagnetic fields and radiation and the incidence of neuroblastoma in offspring. Epidemiology. 12(5): 508-517

De Zwart LL, Meerman JH, Commandeur JN, Vermeulen NP (1999) Biomarkers of free radical damage applications in experimental animals and in humans. Free Radic Biol Med 26(1-2): 202-26

Deli MA, Descamps L, Dehouck MP, Cecchelli R, Joo F, et al. (1995) Exposure of tumor necrosis factor-alpha to luminal membrane of bovine brain capillary endothelial cells cocultured with astrocytes induces a delayed increase of permeability and cytoplasmic stress fiber formation of actin. J Neurosci Res 41: 717-726

Derenzini M, Trere D, Pession A, Govoni M, Sirri V, Chieco P (2000) Nucleolar size indicates the rapidity of cell proliferation in cancer tissues. J Pathol 191: 181-186

Diem E, Ivancsits S, Rüdiger HW (2002) Basal levels of DNA strand breaks in human leukocytes determined by comet assay. J Toxicol Enviro Health A 65: 641-648

Dineley KT, Westerman M, Bui D, Bell K, Ashe KH, Sweatt JD (2001) Beta-amyloid activates the mitogen-activated protein kinase cascade via hippocampal alpha7 nicotinic acetylcholine receptors: In vitro and in vivo mechanisms related to Alzheimer's disease. J Neurosci 21: 4125-4133

Ding GR, Nakahara T, Tian FR, Guo Y, Miyakoshi J (2001) Transient suppression of X-ray-induced apoptosis by exposure to power frequency magnetic fields in MCF-7 cells. Biochem Biophys Res Commun 7; 286(5): 953-957

Doetschman TC, Eistetter H, Katz M, Schmidt W, Kemler R (1985) The in vitro development of blastocyst-derived embryonic stem cell lines: formation of visceral yolk sac, blood islands and myocardium. J Embryol Exp Morphol 87: 27-45

Edgell CJS, McDonald CC, Graham JB (1983) Permanent cell line expressing human factor VIII-related antigen established by hybridization. Natl. Acad. Sci. USA 80: 3734-3737

Edwards MK, McBurney MW (1983) The concentration of retinoic acid determines the differentiated cell types formed by a teratocarcinoma cell line. Dev Biol 98: 187-191

Eveson RW, Timmel CR, Brocklehurst B, Hore PJ, McLauchlan KA (2000) The effects of weak magnetic fields on radical recombination reactions in micelles. Int J Radiat Biol 76: 1509-1522

Fairbairn DW, Olive PL, O´Neill KL (1995) The comet assay: a comprehensive review. Mutat Res 339: 37-59

Falasca L, Marcellini P, Ara C, Rufo A, Devirgiliis LC (1999) Growth inhibition and induction of specific hepatic phenotype expression by retinoic acid in HEPG2 cells. Anticancer Res. 19(4B): 3283-3292

Fanelli C, Coppola S, Barone R, Colussi C, Gualandi G, Volpe P, Ghibelli L (1999) Magnetic fields increase cell survival by inhibiting apoptosis via modulation of Ca+ influx. The FASEB Journal 13: 95-102

Fenech M, Morley AA (1985) Measurement of Micronuclei in Lymphocytes. Mutat Res 147: 29 -36

Fenech M, Morley AA (1986) Cytokinesis-block micronucleus method in human lymphocytes: Effect of in vivo aging and low dose X-irradiation . Mutat Res 161: 193-198

Fenech M (1993) The cytokinesis-block micronucleus technique: A detailed description of the method and its application to genotoxicity studies in human population. Mutat Res 285: 35-44

Fenech M, Neville S, Rinaldi J (1994) Sex is an important variable affecting spontaneous micronucleus frequency in cytokinesis-blocked lymphocytes. Mutat Res 313: 203-207

Fenech M, Rinaldi J (1995) A comparison of lymphocyte micronuclei in plasma micronutrients in vegetarians and non-vegetarians. Carcinogenesis 16: 223-230

Fenech M (2000) The in vitro micronucleus technique. Mutat Res 455: 81-95

Ferrari S, Battini R, Kaczmarek L, Rittling S, Calabretta B, de Riel JK, Philiponis V, Wei JF, Baserga R (1986) Coding sequence and growth regulation of the human vimentin gene. Mol Cell Biol 11: 3614-3620

Flora A, Schulz R, Benfante R, Battaglioli E, Terzano S, Clementi F, Fornasari D (2000) Neuronal and extraneuronal expression and regulation of the human alpha5 nicotinic receptor subunit gene. J Neurochem 75: 18-27

Flora A, Lucchetti H, Benfante R, Goridis C, Clementi F, Fornasari D (2001) Sp proteins and Phox2B regulate the expression of the human Phox2a Gene. J Neurosci 21: 7037-7045

Fornasari D, Battaglioli E, Flora A, Terzano S, Clementi F (1997) Structural and functional characterization of the human alpha3 nicotinic subunit gene promoter. Mol Pharmacol 51: 250-261

François F, Godinho MJ, Grimes M (2000) CREB is cleaved by caspases during neural cell apoptosis. FEBS Letters 486: 281-284

Frazier ME, Reese JA, Morris JE, Jostes RF, Miller DL (1990) Exposure of mammalian cells to 60 Hz magnetic or electric fields: Analysis of DNA repair of induced single-strand breaks. Bioelectromagnetics 11: 229-234

Freedman R, Adler LE, Leonard S (1999) Alternative phenotypes for the complex genetics of schizophrenia. Biol. Psychiatry 45: 551-558

Freedman R, Adams CE, Leonard S (2000) The alpha 7-nicotinic acetylcholine receptor and the pathology of hippocampal interneurons in schizophrenia. J Chem Neuroanat 20: 299-306

French P, Donnellan M, McKenzie D (1997) Electromagnetic radiation at 835 MHz changes the morphology and inhibits proliferation of a human astrocytoma cell line. Bioelectrochemistry and Bioenergetics 43: 13-18

French PW, Penny R, Laurence JA, McKenzie DR. (2001). Mobile phones, heat shock proteins and cancer. Differentiation 67: 93-97

Friedberg EC, Walker GC, Siede W (1995) DNA repair and mutagenesis. ASM Press, Washington, DC: 135-178

Fritze K, Sommer C, Schmitz B, Mies G, Hossman KA, Kiessling M, Wiessner C. (1997a) Effect of global system for mobile communication (GSM) microwave exposure on blood-brain barrier permeability in rat. Acta Neuropathol. 94, 465-470

Fritze K, Wiessner C, Kuster N, Sommer C, Gass P, Hermann DM, Kiessling M, Hossmann KA. (1997b). Effect of global system for mobile communication microwave exposure on the genomic response of the rat brain. Neuroscience 81: 627-639

Fucic A, Garaj-Vrhovac V, Skara M, Dimitrovic B (1992) X-rays, microwaves and vinyl chloride monomer: their clastogenic and aneugenic activity, using the micronucleus assay on human lymphocytes. Mutat Res 282: 265-271

Galt S, Wahlström J, Hamnerius Y, Holmqvist D, Johannesson T (1995) Study of effects of 50 Hz magnetic fields on chromosome aberrations and the growth-related enzyme ODC in human amniotic cells. Bioelectrochem Bioenerg 36: 1-8

Gao F, Yi J, Shi GY, Li H, Shi XG, Tang XM (2002) The sensitivity of digestive tract tumor cells to As_2O_3 is associated with the inherent cellular level of reactive oxygen species. World J Gastroenterol 8(1): 36-39

Garaj-Vrhovac V (1999) Micronucleous assay and lymphocyte mitotic activity in risk assessment of occupational exposure to microwave radiation. Chemosphere 39: 2301-2312

Garrido C, Ottavi P, Fromentin A, Hammann A, Arrigo AP, Chauffert B, Mehlen P. (1997). HSP27 as a mediator of confluence-dependent resistance to cell death induced by anticancer drugs. Cancer Res. 57: 2661-2667

Garriott ML, Phelps JB, Hoffman WP (2002) A protocol for the in vitro micronucleus test. I. Contributions to the development of a protocol suitable for regulatory submission from an examination of 16 chemicals with different mechanisms of action and different levels of activity. Mutat Res 517: 123-134

Gatta L, Pinto R, Ubaldi V, Pace L, Galloni P, Lovisolo GA, Marino C, Pioli C (2003) Effects of in vivo exposure to GSM-modulated 900 MHz radiation on mouse peripheral lymphocytes. Radiat Res 160(5): 600-605

Goodman R, Henderson A (1988) Exposure of salivary gland cells to low-frequency electromagnetic fields alters polypeptide synthesis. Proc Natl Acad Sci USA 85: 3982

Goodman R, Blank M, Lin H, Khorkova O, Soo L, Weisbrot D, Henderson A (1994) Increased level of hsp70 transcripts induced when cells are exposed to low-frequency electromagnetic fields. Biochem and Bioenergetics 33: 115-120

Goodman R, Blank M (1998) Magnetic field stress induces expression of hsp70. Cell Stress Chaperones 3: 79

Goswami PC, Albee LD, Parsian AJ, Baty JD, Moros EG, Pickard WF, Roti Roti JL, Hunt CR (1999) Proto-oncogene mRNA levels and activities of multiple transcription factors in C3H 10T 1/2 murine embryonic fibroblasts exposed to 835.62 and 847.74 MHz cellular phone communication frequency radiation. Radiat Res 151: 300-309

Goukassian D, Gad F, Yaar M, Eller MS, Nehal US, Gilchrest BA (2000) Mechanisms and implications of the age-associated decrease in DNA repair capacity. FASEB J 14: 1325-1334

Goyns MH, Charlton MA, Dunford JE, Lavery WL, Merry BJ, Salehi M, Simoes DCM (1998) Differential display analysis of gene expression indicates that age-related changes are restricted to a small cohort of genes. Mech Age Dev 101: 73-90

Grassi F, Palma E, Tonini R, Amici M, Ballivet M, Eusebi F (2003) Amyloid beta (1-42) peptide alters the gating of human and mouse alpha-bungarotoxin-sensitive nicotinic receptors. J Physiol 547: 147-157

Green AM, Steinmetz N.D (2002) Monitoring apoptosis in real time. Cancer J 8(2): 82-92

Grepin C, Robitaille L, Antakly T, Nemer M (1995) Inhibition of transcription factor GATA-4 expression blocks in vitro cardiac muscle differentiation. Mol Cell Biol 15: 4095-4102

Groot Kormelink PJ, Luyten WHML (1997) Cloning and sequence of full-length cDNAs encoding the human neuronal nicotinic acetylcholine receptor (nAchR) subunits b3 and b4 and expression of seven nAchR subunits in the human neuroblastoma cell line SH-SY5Y and/or IMR-32. FEBS Letter 400: 309-314

Grundler W, Kaiser F, Keilmann F, Walleczek J (1992) Mechanisms of electromagnetic interaction with cellular systems. Naturwissenschaften 79: 551-559

Grynkiewicz G, Poenie M, Tsien RY, (1985): A new generation of Ca^{2+} indicators with greatly improved fluorescence properties. J Biol Chem 260: 3440-3450

Hallahan DE, Dunphy E, Virudachalam S, Sukhatme VP, Kufe DW, Weichselbaum RR (1995) C-jun and Egr-1 participate in DNA synthesis and cell survival in response to ionizing radiation exposure. J Biol Chem 270: 30303-30309

Hambrook JL, Simpson R, Lindsay CD, Holden SJ, Inns RH (2002) Investigation into cellular effects of exposure to UWB radiation. Workshop on Biological Effects of EMFs, Rhodes/Greece, Proceedings

Hardell L, Mild KH, Carlberg M (2003) Further aspects of cellular and cordless telephones and brain tumours. Int J. Oncol 22: 399-407

Hewett SJ, Corbett JA, McDaniel ML, Choi DW (1993) Interferon-g and interleukin-1ß induce nitric oxide formation from primary mouse astrocytes. Neurosci Letts 164: 229-232

Higashikubo R, Ragouzis M, Moros EG, Straube WL, Roti Roti JL (2001) Radiofrequency electromagnetic fields do not alter the cell cycle progression of C3H10T and U87MG cells. Radiat Res 156: 786-795

Holden JA (2001) DNA topoisomearses as anticancer drug targets: from the laboratory to the clinic. Curr Med Chem Anti-Canc Agents1: 1-25

Hollander MC, Sheikh MS, Bulavin DV, Lundgren K, Augeri-Henmueller L, Shehee R, Molinaro TA, Kim KE, Tolosa E, Ashwell JD, Rosenberg MP, Zhan Q, Fernandez-Salguero PM, Morgan WF, Deng CX, Fornace AJ (1999) Genomic instability in Gadd45a-deficient mice. Nat Genet 23: 176-184

Holmes GE, Bernstein C, Bernstein H (1992) Oxidative and other DNA damages as the basis of aging: a review. Mutat Res 275: 305-315

Honore B, Rasmussen HH, Vorum H, Dejgaard K, Liu X, Gromov P, Madsen P, Gesser B, Tommerup N, Celis JE. (1995) Heterogeneous nuclear ribonucleoproteins H, H', and F are members of a ubiquitously expressed subfamily of related but distinct proteins encoded by genes mapping to different chromosomes. J Biol Chem 270: 28780-28789

Hook GJ, Zhang P, Lagroye I, Li L, Higashikubo R, Moros EG, Straube WL, Pickard WF, Baty JD, Roti Roti JL (2004) Measurement of DNA damage and apoptosis in molt-4 cells after in vitro exposure to radiofrequency radiation. Radiat Res 161(2): 193-200

Hu GL, Chiang H, Zeng QL, Fu YD (2001) ELFMagnetic Field Inhibits Gap Junctional Intercellular Communication and Induces Hyperphosphorylation of Connexin43 in NIH3T3 Cells. Bioelectromagnetics 22: 568-573

Huber R, Borbely AA, Graf T, Fuchs B, Gallmann E, Achermann P (2000) Pulsed high-frequency EMF affects human sleep and sleep EEG. Neurosc Letts 275: 207-210

Huber R, Graf T, Cote KA, Wittmann L, Gallmann E, Matter D, Schuderer J, Kuster N, Borbely AA, Achermann P (2000) Exposure to pulsed high-frequency electromagnetic field during waking affects human sleep EEG. Neuroreport, Oct 20; 11 (15): 3321-3325

Huber R, Treyer V, Borbely AA, Schuderer J, Gottselig JM, Landolt HP, Werth E, Berthold T, Kuster N, Buck A, Achermann P (2002) Electromagnetic fields, such as those from mobile phones, alter regional cerebral blood flow and sleep and waking EEG. J Sleep Res 11(4): 289-295

Huot J, Houle F, Spitz DR, Landry J (1996). HSP27 phosphorylation-mediated resistance against actin fragmentation and cell death induced by oxidative stress. Cancer Res. 56: 273-279

Huot J, Houle F, Marceau F, Landry J (1997) Oxidative stress-induced actin reorganization mediated by the p38 mitogen-activated protein kinase/heat shock protein 27 pathway in vascular endothelial cells. Circulation Res. 80: 383-392

Huot J, Houle F, Rousseau S, Deschenes RG, Shah GM, Landry J (1998) SAPK2/p38-dependent F-actin reorganization regulates early membrane blebbing during stress-induced apoptosis. J. Cell Biol. 143: 1361-1373

IARC Monographs (2000): Non-ionizing radiation, Part 1. Static and extremely low-frequency (ELF) electric and magnetic fields. IARC Monogr Eval Carcinog Risks Hum, 80: 1-395

ICNIRP, International Commission on Non-Ionizing Radiation Protection (1996): Health issues related to the used of hand-held radiotelephones and base transmitters. Health Phys 70: 587-593

ICNIRP, International Commission on Non-Ionizing Radiation Protection (1998): Guidelines for limiting exposure to time-varying, magnetic, and electromagnetic fields (up to 300 GHz). Health Phys 74: 494-522

IEC, International Electrotechnical Commission (1995): Limitations of Emission of Harmonic Currents for Equipment Connected to Medium and High Power Supply Systems. Technical Report, IEC 1000 Electromagnetic Compatibility, Part 3: Limits, Section 6

Ismael SJ, Callera F, Garcia AB, Baffa O, Falcao RP (1998) Increased dexamethasone-induced apoptosis of thymocytes from mice exposed to long-term extremely low frequency magnetic fields. Bioelectromagnetics 19: 131-135

Ito H, Hasegawa K, Inahuma Y, Kozawa O, Asano T, Kato K. (1995) Modulation of the stress-induced synthesis of stress proteins by phorbol ester and okadaic acid. J. Biochem. 118, 629-634

Ivancsits S, Diem E, Pilger A, Rüdiger HW, Jahn O (2002a) Induction of DNA strand breaks by exposure to extremely-low frequency electromagnetic fields in human diploid fibroblasts. Mutat Res 519: 1-13

Ivancsits S, Pilger A, Diem E, Schaffer A, Rudiger HW (2002b) Vanadate induces DNA strand breaks in cultured human fibroblasts at doses relevant to occupational exposure. Mutat Res 519: 25-35

Ivancsits S, Diem E, Jahn O, Rüdiger HW (2003a) Age-related effects on induction of DNA strand breaks by intermittent exposure to electromagnetic fields. Mech Ageing Dev 124: 847-850

Ivancsits S, Diem E, Jahn O, Rüdiger HW (2003b) Intermittent extremely low frequency electromagnetic fields cause DNA damage in a dose-dependent way. Int Arch Occup Environ Health 76: 431–436

Ivaschuk OI, Jones RA, Ishida-Jones T, Haggren W, Adey WR, Phillips JL (1997) Exposure of nerve growth factor-treated PC12 rat pheochromocytoma cells to a modulated radiofrequency field at 836.55 MHz: effects on c-jun and c-fos expression. Bioelectromagnetics 18: 223-229

Jaattela M (1999) Escaping cell death: Survival proteins in cancer. Exp Cell Res 248: 30-43

Jacks T, Remington L, Williams BO, Schmitt EM, Halachmi S, Bronson RT, Weinberg RA (1994) Tumor spectrum analysis in p53-mutant mice. Curr Biol 4: 1-7

Jacob ST, Gosh AK (1999) Control of RNA polymerase I-directed transcription: recent trends. J Cell Bioch Suppl 32: 41-50

Jacobson-Kram D, Tepper J, Kuo P, San RHC, Curry PT, Wagner VO, Putman DL (1997) Evaluation of the genotoxicity of pulsed electric and electromagnetic field used for bone growth stimulation. Mutat Res 388: 45-57

Jean S, Bideau C, Bellon L, Halimi G, De Meo M, Orsiere T, Dumenil G, Berge-Lefranc JL, Botta A (2001) The expression of genes induced in melanocytes by exposure to 365-nm UVA: study by cDNA arrays and real-time quantitative RT-PCR. Biochim Biophys Acta 1522: 89-96

Jin M, Blank M, Goodman R (2000) ERK1/2 phosphorylation, induced by electromagnetic fields, diminishes during neoplastic transformation. J Cell Biochem 78: 371

Jin S, Fan F, Fan W, Zhao H, Tong T, Blanck P, Alomo I, Rajasekaran B, Zhan Q (2001) Transcription factors Oct-1 and NF-YA regulate the p53-independent induction of the GADD45 following DNA damage. Oncogene 20: 2683-2690

Johnson LF, Rao LG, Muench AJ (1982) Regulation of thymidine kinase enzyme level in serum-stimulated mouse 3T6 fibroblasts. Exp Cell Res 138(1): 79-85

Jokela K, Leszczynski D, Paile W, Salomaa S, Puranen L, Hyysalo P. (1999). Radiation safety of handheld mobile phones and base stations. STUK-A161 Report, OY Edita Ab Helsinki, Finland

Jones S, Sudweeks S, Yakel JL (1999) Nicotinic receptors in the brain: correlating physiology with function. Trends Neurosci 22: 555-561

Kasai H (1997) Analysis of a form of oxidative DNA damage, 8-hydroxy-2'-deoxyguanosine, as a marker of cellular oxidative stress during carcinogenesis. Mutat Res 387: 147-163

Kashima T, Vinters HV,Campagnoni AT (1995) Unexpected expression of intermediate filament protein genes in human oligodendrioma cell lines. J Neurophathol Exp Neurol 54: 23-31

Kastan MB, Zhan Q, el Deiry WS, Carrier F, Jacks T, Walsh WV, Plunkett BS, Vogelstein B, Fornace AJ (1992) A mammalian cell cycle checkpoint pathway utilizing p53 and GADD45 is defective in ataxia-telangiectasia. Cell 71: 587-597

Kato K, Hasegawa K, Goto S, Inaguma Y. (1994). Dissociation as a result of phosphorylation of an aggregated form of the small stress protein, hsp27. J. Biol. Chem. 269: 11274-11278

Kavet R (1996) EMF and current cancer concepts. Bioelectromagnetics 17: 339-357

Kawasaki H, Mukai K, Yajima S, Tanaka R, Takayama J, Takasaki Y, Ohira M (1995) Prognostic value of proliferating cell nuclear antigen (PCNA) immunostaining in neuroblastoma. Med Pediatr Oncol 24(5): 300-304

Keren-Tal I, Dantes A, Sprengel R., Amsterdam A (1993) Establishment of steroidegenic granulosa cell lines expressing follicle stimulating hormone receptors. Mol. Cell Endocrinol 95: R1–R10

Khalil AM, Qassem W (1991) Cytogenetic effects of pulsing electromagnetic field on human lymphocytes in vitro: chromosome aberrations, sister-chromatid exchanges and cell kinetics. Mutat Res 247: 141-146

Kim CH, Zabetian CP, Cubells JF, Cho S, Biaggioni I, Cohen BM, Robertson D, Kim KS (2002) Mutations in the dopamine beta-hydroxylase gen are associated with human norepinephrine deficiency. Am J Med Genet 108: 140-147

Kim YO, Oh IU, Park HS, Jeng J, Song BJ, Huh TL. (1995) Characterization of a cDNA clone for human NAD(+)-specific isocitrate dehydrogenase alpha-subunit and structural comparison with its isoenzymes from different species. Biochem J. 308, 63-68

Kim YW, Lee JS, Ahn SS, Jung KC, Lee SK, Lee JY, Gimm YM (2004) Study on testicular germ cell apoptosis of mice to 60 Hz magnetic field exposure. 26th Annual BEMS Meeting, Proceedings: 283

Kit S (1976) Thymidine kinase, DNA synthesis and cancer. Mol Cell Biochem 11: 161-182

Klaude M, Eriksson S, Nygren J, Ahnstrom G (1996) The comet assay: mechanisms and technical considerations. Mutat Res 363: 89-96

Klose J and Kobalz U (1995) Two-dimensional electrophoresis of proteins: an updated protocol and implications for a functional analysis of the genome. Electrophoresis 16: 1034-1059

Klug S, Hetscher M, Giles S, Kohlsmann S, Kramer K (1997) The lack of effects of nonthermal RF electromagnetic fields on the development of rat embryos grown in culture. Life Sci 61: 1789-1802

Koivisto M, Revonsuo A, Krause CM, Haarala C, Sillanmäki L, Laine M, Hämäläinen H (2000) Effects of 902 MHz electromagnetic field emitted by cellular phones on response times in humans. NeuroReport 11: 413

Kovalenko D, Yang X, Nadeu RJ, Harkins LK, Friesel R (2003) Sef inhibits fibroblast growth factor signaling by inhibiting FGFR1 tyrc phosphorilation and subsequent ERK activation. J Biol Chem 278(16): 14087.91

Krause CM, Sillanmäki L, Koivisto M, Häggqvist A, Saarela C, Revonsuo A, Laine M, Hämäläinen H (2000) Effects of electromagnetc field emitted by cellular phones on the EEG during a memory task. NeuroReport 11: 761

Kumlin T, Heikkinen P, Kosma VM, Alhonen L, Janne J, Juutilainen J (2002) p53-independent apoptosis in UV-irradiated mouse skin: possible inhibition by 50 Hz magnetic fields. Radiat Environ Biophys 41(2): 155-158

Kwee S, Raskmark, P (1995) Changes in cell proliferation due to environmental non-ionizing radiation: 1. ELF electromagnetic fields. Bioelectrochem Bioenerg 36: 109-114

Kwee S, Raskmark P, Velizarov S (2001) Changes in cellular proteins due to environmental non-ionizing radiation. I. Heat-shock proteins. Electro Magnetobiol 20: 141-152

Lacy-Hulbert A, Metcalfe JC, Hesketh R (1998) Biological responses to electromagnetic fields. FASEB J 12: 395-420.

Lagroye I, Poncy JL (1997) The effect of 50 Hz electromagnetic fields on the formation of micronuclei in rodent cells exposed to gamma irradiation. Int J Radiat Biol 72: 249-254

Lai H, Singh NP (1995) Acute low-intensity microwave exposure increases DNA single-strand breaks in rat brain cells. Bioelectromagnetics 16: 207-210

Lai H, Singh NP (1996a) Single- and double-strand DNA breaks in rat brain cells after acute exposure to radiofrequency electromagnetic radiation. Int J Rad Biol 69(4): 513-521

Lai H, Singh NP (1996b) Reply to "Comment on 'Acute low-intensity microwave exposure increases DNA single-strand breaks in rat brain cells' ". Bioelectromagnetics 17: 166

Lai H, Singh NP (1997a) Melatonin and N-tert-butyl-a-phenylnitrone Block 60 Hz magnetic field-induced DNA single- and double-strands breaks in rat brain cells. J Pin Res 22: 152-162

Lai H, Singh NP (1997b) Melatonin and a spin-Trap compound block radiofrequency electromagnetic radiation-induced DNA strands breaks in rat brain cells. Bioelectromagnetics 18: 446-454

Lai H, Singh NP (1997c) Acute exposure to a 60 Hz magnetic field increases DNA strand breaks in rat brain cells. Bioelectromagnetics 18(2): 156-165

Lai H, Singh NP (2004) Magnetic- field-induced DNA strand breaks in brain cells of the rat. Environ Health Perspect 112(6): 687-694

Landry J, Huot J (1995) Modulation of actin dynamics during stress and physiological stimulation by a signaling pathway involving p38 MAP kinase and heat-shock protein 27. Biochem Cell Biol 73: 703-707

Lasne C, Gu ZW, Venegas W, Chouroulinkov I (1984) The in vitro micronucleus assay for detection of cytogenetic effects induced by mutagen-carcinogens: comparison with the in vitro sister-chromatid exchange assay. Mutat Res 130: 273-282

Laurence JA, French PW, Lindner RA, Mckenzie DR (2000) Biological effects of electromagnetic fields-mechanisms for the effects of pulsed microwave radiation on protein conformation. J Theor Biol 206: 291-298

Laval L, Leveque P, Jecko B (2000) A new in vitro Exposure Device for the Mobile Frequency of 900 MHz. Bioelectromagnetics 21: 255-263

Lavoie JN, Hickey E, Weber LA, Landry J (1993) Modulation of actin microfilament dynamics and fluid phase pinocytosis by phosphorylation of heat shock protein 27. J Biol Chem 268: 24210-24214

Leary DJ, Huang S (2001) Regulation of ribosome biogenesis within the nucleolus. FEBS Lett 509: 145-150

Lee S, Tseng CC, Chen J, Sun M, Gerber HL, Zhou CQ, Johnson DS, Dunbar K, Wang SM (2004) The 2.45 GHz radio frequency fields alter human gene expression. 25th Annual BEMS Meeting, Proceedings: 184

Leist M, Nicotera P (1998) Apoptosis, excitotoxicity, and neuropathology. Exp Cell Res 239: 183-201

Leszczynski D (2001) Mobile phones, precautionary principle, and future research. Lancet 358: 1733

Leszczynski D, Joenvaara S, Reivinen J, Kuokka R (2002) Non-thermal activation of the hsp27/p38mapk stress pathway by mobile phone radiation in human endothelial cells: Molecular mechanism for cancer- and blood-brain barrier-related effects. Differentiation 70: 120-129

Leszczynski D, Nylund R, Joenväärä S, Reivinen J (2004) Applicability of discovery science approach to determine biological effects of mobile phone radiation. Proteomics 4, 426-431; Nylund R, Leszczynski D (2004) Proteomics analysis of human endothelial cell line EA.hy926 after exposure to GSM 900 radiation. Proteomics 4, 1359-1365

Leszczynski, D (2004) Mobile Phones and Blood-Brain Barrier: The available scientific evidence is insufficient to dismiss or to support claims of a health risk in humans. Environ. Health Perspect. submitted

Li L, Bisht KS, LaGroye I, Zhang P, Straube WL, Moros EG, Roti Roti JL (2001) Measurement of DNA damage in mammalian cells exposed in vitro to radiofrequency fields at SARs of 3-5 W/kg. Radiat Res 56(3): 328-332

Liburdy RP, Callahan DE, Harland J, Dunham E, Sloma TR, Yaswen P (1993) Experimental evidence for 60 Hz magnetic fields operationg through the signal transduction cascade. Effects on Calcium influx and c-MYC mRNA induction. FEBS Lett 334(3): 301-308

Lin H, Blank M, Rossol-Haseroth K, Goodman R (2001) Regulating genes with electromagnetic response elements. J Cell Bioch 81: 143-148

Lindstrom J (1997) Nicotinic Acetylcholine Receptors in health and disease. Mol Neurobiol 15: 193-222

Linskens MHK, Feng J, Andrews WH, Enloe BE, Saati SM, Tonkin LA, Funk WD, Villepontoau B (1995) Cataloging altered gene expression in young and senescent cells using enhanced differential display. Nucl Acid Res 23: 3244-3251

Lints TJ, Parsons LM, Hartley L, Lyons I, Harvey RP (1993) Nkx-2.5: a novel murine homeobox gene expressed in early heart progenitor cells and their myogenic descendants. Development 119: 419-431

Lisi A, Ledda M, Patti AM, Vulcano A, Rieti S, Rosola E, Grimaldi S (2004) Low-frequency electromagnetic field as a tool to trigger pluripotent human stem cells diffrenetiation. 26th Annual BEMS Meeting, Proceedings: 223

Liu Y, Hong R, Yu YM, Weng EQ (2003) Effects of extremely low frequency electromagnetic fields on apoptosis and cell cycle of mouse brain and liver cells. Zhonghua Lao Dong Wei Sheng Zhi Ye Bing Za Zhi. 21(5): 339-341

Livingston GK, Witt KL, Gandhi OP, Chatterjee I, Roti Roti J (1991) Reproductive integrity of mammalian cells exposed to power frequency electromagnetic fields. Environ Mol Mutagen 17: 49-58

Lo L, Morin X, Brunet JF, Anderson DJ (1999) Specification of neurotransmitter identità by Phox2 proteins in neural crest stem cells. Neuron 22: 693-705

Lohmann CH, Schwartz Z, Liu Y, Li Z, Simon BJ, Sylvia VL, Dean DD, Bonewald LF, Donahue HJ, Boyan BD, (2003) Pulsed electromagnetic fields affect phenotype and connexin 43 protein expression in MLO-Y4 osteocyte-like cells and ROS 17/2.8 osteoblast-like cells. J Orthop Res 21(2): 326-34

Loktionova SA, Ilyinskaya OP, Gabai VL, Kabakov AE (1996) Distinct effects of heat shock and ATP depletion on distribution and isoform patterns of human Hsp27 in endothelial cells. FEBS Letts 392: 100-104

Lopez-Ongil S, Hernandez-Perera O, Navarro-Antolin J, Perez de Lema G, Rodriguez-Puyol M, Lamas S, Rodriguez-Puyol D (1998) Role of reactive oxygen species in the signalling cascade of cyclosporine A-mediated up-regulation of eNOS in vascular endothelial cells. Br J Pharmacol 124: 447-454

Luft JC, Dix DJ (1999) Hsp70 expression and function during embryogenesis. Cell Stress Chaperones 4: 162-170

Lupke M, Rollwitz J, Simko M (2004) Cell Activating Capacity of 50 Hz Magnetic Fields to Release Reactive Oxygen Intermediates in Human Umbilical Cord Blodd-derived Monocytes and in Mono Mac 6 Cells. Free Radical Res, Vol 38 (9): 983-993

Maeda T, Hanna AN, Sim AB, Chua PP, Chong MT, Tron VA (2002) GADD45 regulates G2/M arrest, DNA repair, and cell death in keratinocytes following ultraviolet exposure. J Invest Dermatol 119: 22-26

Maes A, Collier M, Slaets D, Verschaeve L (1996) 954 MHz microwaves enhance the mutagenic properties of mitomycin C. Environ Mol Mutagen 28(1): 26-30

Maes A, Collier M, Van Gorp U, Vandoninck S, Verschaeve L (1997) Cytogenetic effects of 935.2-MHz (GSM) microwaves alone and in combination with mitomycin C. Mutat Res 18, 393(1-2): 151-156

Maes A, Collier M, Verschaeve L (2001) Cytogenetic effects of 900 MHz (GSM) microwaves on human lymphocytes. Bioelectromagnetics 22(2): 91-96

Malyapa RS, Ahern EW, Straube WL, Moros EG, Pickard WF, Roti Roti JL (1997a) Measurement of DNA damage following exposure to 2450 MHz electromagnetic radiation. Radiat Res 148(6): 608-617

Malyapa RS, Ahern EW, Bi C, Straube WL, LaRegina M, Pickard WF, Roti Roti JL (1998) DNA damage in rat brain cells after in vivo exposure to 2450 MHz electromagnetic radiation and various methods of euthanasia. Radiat Res 149(6): 637-645

Mangiacasale R, Tritarelli A, Sciamanna I, Cannone M, Lavia P, Barberis MC, Lorenzini R, Cundari E (2001) Normal and cancer-prone human cells respond differently to extremely low frequency magnetic fields. FEBS Letts 487: 397-403

Manikowska-Czerska E, Czerski P, Leach, W (1985) Effects of 2.45 GHz microwaves on meiotic chromosomes of male CBA/CAY mice. J Heredity 76: 71-73

Mannerling AC, Hannemann S, Simko M, Hansson Mild K, Mattson MO (2004) Hsp70 regulation in human cells after exposure to 50 Hz magnetic fields. 26th Annual BEMS Meeting, Proceedings: 240

Marino AA, Kolomytkin OV, Frilot C (2003) Extracellular currents alter gap junction intercellular communication in synovial fibroblasts. Bioelectromagnetics, 24(3): 199-205

Markkanen A, Penttinen P, Naarala J, Pelkonen J, Sihvonen AP, Juutilainen J (2004) Apoptosis induced by ultraviolet radiation is enhanced by amplitude modulated radiofrequency radiation in mutant yeast cells. Bioelectromagnetics 25(2): 127-133

McCann J, Dietrich F, Rafferty C, Martin AO (1993) A critical review of the genotoxic potential of electric and magnetic fields. Mutat Res 297: 61-95

McCann J, Dietrich F, Rafferty C (1998) The genotoxic potential of electric and magnetic fields: an update. Mutat Res 411: 45-86

McFarlane EH, Dawe GS, Marks M, Campbell IC (2000) Changes in neurite outgrowth but not in cell division induced by low EMF exposure: influence of field strength and culture conditions on responses in rat PC12 pheochromocytoma cells. Bioelectrochem 52(1): 23-28

McNamee JP, Bellier P V, McLean J R, Marro L, Gajda G B, Thansandote A (2002a) DNA damage and apoptosis in the immature mouse cerebellum after acute exposure to a 1 mT, 60 Hz magnetic field. Mutat Res 513(1-2): 121-133

McNamee JP, Bellier PV, Gajda GB, Miller SM, Lemay EP, Lavalleé BF, Marro L, Thansandote A (2002b) DNA damage and micronucleus induction in human leukocytes after acute in vitro exposure to a 1.9 GHz continuous-wave radiofrequency field. Radiat Res 158: 523-533

Mehlen P, Schultze-Osthoff K, Arrigo AP. (1996). Small stress proteins as novel regulators of apoptosis. Heat shock protein 27 blocks Fas/APO-1- and staurosporine-induced cell death. J. Biol. Chem. 271: 16510-16514

Melchiorri D, Reiter RJ, Sewerynek E, Chen LD, Nistico G (1995) Melatonin reduces □ignall-induced lipid peroxidation in homogenates of different brain regions. FASEB J 9: 1205–1210

Meltz ML (1995) Biological effects versus health effects: an investigation of the genotoxicity of microwave radiation. In: Radiofrequency Radiation Standards, NATO ASI Series (B.J. Klauebberg ed). New York, Plenum Press: 235-241

Meltz ML (2003) Radiofrequency Exposure and Mammalian Cell Toxicity, Genotoxicity, and Transformation. Bioelectromagnetics Suppl 6: S196-S213

Mena MA, Casarejos MJ, Bonin A, Ramos JA,García de Yébenes J (1995) Effects of dibutyryl cyclic AMP and retinoic acid on the differentiation of dopamine neurons: Prevention of cell death by dibutyryl cyclic AMP. J Neurochem 65: 2612-2620

Miles AM, Wink DA, Cook JC, Grisham MB (1996) Determination of nitric oxide using fluorescence spectroscopy. Methods Enzymol 268: 105-120

Miura M, Takayama K, Okada J (1993) Increase in nitric oxide and cyclic GMP of rat cerebellum by radio frequency burst-type electromagnetic field radiation. J Physiol 461: 513-524

Miyakoshi J, Yoshida M, Shibuya K, Hiraoka M (2000) Exposure to strong magnetic fields at power frequency potentiates X-ray induced DNA strand breaks. J Radiat Res 41: 293-302

Miyakoshi J, Ding GR, Hirose H, Koyama S (2003) Effects of exposure to 1950 MHz radio-frequency fields on expression of Hsp27 and Hsp70 in human glioma MO54 cells; EBEA Congress, Budapest/Hungary, Nov 13-15 2003; Proceedings: 190

Miyakoshi J, Takashima Y, Ding GR, Hirose H, Koyama S (2004) Effects of exposure ro 1950 MHz radi-frequency field on expression of hsp27 and hsp70 in human glioma MO54 cells. 26 Annual BEMS Meeting, Proceedings: 220-221

Monti D, Salvioli S, Capri M, Malorni W, Straface E, Cossarizza A, Botti B,Piacentini M, Baggio G, Barbi C, Valensin S, Bonafe M, Franceschi C (2000) Decreased susceptibility to oxidative stress-induced apoptosis of peripheral blood mononuclear cells from healthy elderly and centenarians. Mech Ageing Dev 121(1-3): 239-250

Morin X, Cremer H, Hirsch MR, Kapur RP, Goridis C, Brunet JF (1997) Defects in sensory and autonomic ganglia and absence of locus coeruleus in mice deficient for the homeobox gene Phox2a. Neuron 18: 411-423

Moros EG, Pickard WF (1999) On the assumption of negligible heat diffusion during the thermal measurement of a nonuniform specific absorption rate. Radiat Res, Sep, 152 (3): 312-320

Morris EJ, Dreixler JC, Cheng KY, Wilson PM, Gin RM, Geller HM (1999) Optimization of single-cell gel electrophoresis (SCGE) for quantitative analysis of neuronal DNA damage. Biotechniques 26: 282-289

Mostafapour SP, Del Puerto NM, Rubel EW (2002) bcl-2 Overexpression eliminates deprivation-induced cell death of brainstem auditory neurons. J Neurosci 22: 4670-4674

Moulder JC (1998) Power-frequency fields and cancer. Crit Rev Biomed Eng 26: 1-116

Moulder JE, Erdreich LS, Malyapa RS, Merritt J, Pickard WF, Vijayalaxmi (1999) Cell Phones and Cancer: What Is The Evidence for a Connection? Radiat Res 151: 513-531

Mullaart E, Boerrigter METI, Brouwer A, Berends F, Vijg J (1988) Age-dependent accumulation of alkali-labile sites in DNA of post-mitotic but not in that of mitotic rat liver cells. Mech Age Dev 45: 41-91

Murphy JC, Kaden DA, Warren J, Sivak A (1993) Power frequency electric and magnetic fields: a review of genetic toxicology. Mutat Res 296: 221-240

Murphy LO, Smith S, Chen RH, Fingar DC, Blenis J (2002) Molecular interpretation of ERK signal duration by immediate early gene products. Nat Cell Biol 4: 556-564

Nagy A, Rossant J, Nagy R, Abramow-Newerly W, Roder JC (1993) Derivation of completely cell culture-derived mice from early-passage embryonic stem cells. Proc Natl Acad Sci USA 90: 8424-8428

Natarajan AT, Obe G (1978) Molecular mechanisms involved in the production of chromosomal aberrations. Part I. Utilization of neurospora endonuclease for the study of aberration production in G2 stage of the cell cycle. Mutat Res 52: 137-149

Natarajan AT, Darroudi F (1991) Use of human hepatoma cells for in vitro metabolic activation of chemical mutagens/carcinogens. Mutagenesis 6: 399-403

Neubauer C, Phelan AM, Kues H, Lange DG. (1990). Microwave irradiation of rats at 2.45 GHz activates pinocytotic-like uptake of tracer by capillary endothelial cells of cerebral cortex. Bioelectromagnetics 11: 261-268

Ngezahayo A, Zeilinger C, Todt I, Marten I, Kolb HA (1998): Inactivation of expressed and conducting rCx46 hemichannels by phosphorylation. The J Membrane Biol, Vol. 436: 627-629

Ngezahayo A, Altmann B, Kolb HA (2003) Regulation gap junctional coupling, ion fluxes and cell volume by cGMP in GFSHR-17 granulosa cells. J Membr Biol 194: 165-176

Nibu K, Li G, Kaga K, Rothstein JL (2000) Basic-FGF induces differentiation and death of olfactory neuroblastoma cells. Biochem Biophys Res Commun 279(1): 172-180

Nomura Y (1998) A transient brain ischemia- and bacterial endotoxin-induced glial iNOS expression and NO-induced neuronal apoptosis. Toxicol Letts 102-103: 65-69

Nordenson I, Mild KH, Andersson G, Sandström M (1994) Chromosomal aberrations in human amniotic cells after intermittent exposure to 50 Hz magnetic fields. Bioelectromagnetics 15: 293-301

NRPB (2001) ELF electromagnetic fields and the risk of cancer. Documents of the National Radiological Protection Board (NRPB), Vol 12, No. 1

Nüsse M, Kramer J (1984) Flow cytometric analysis of MN found in cells after irradiation. Cytometry 5: 20-25

Nüsse M, Marx K (1997) Flow cytometric analysis of micronuclei in cell cultures and human lymphocyte: advantages and disadvantages. Mutat Res 392: 109-115

Obe G, Johannes C, Schulte-Frohlinde D (1992) DNA double strand breaks induced by sparsely ionizing radiation and endonucleases as critical lesions for cell death, chromosomal aberrations, mutations and oncogenic transformation. Mutagenesis 7: 3-12

Oh LY, Denninger A, Colvin JS, Vyas A, Tole S, Ornitz DM (2003) Fibroblast growth factor receptor 3 signaling regulates the onset of oligodendrocyte terminal differentiation. J Neurosci 23(3): 883-894

Öllinger K, Brunmark A (1994) Effect of different oxygen pressures and N,N-diphenyl-p-phenylenediamine on adriamycin toxicity to cultured neonatal rat heart myocytes. Biochem Pharmacol 48: 1707-1715

Olney JW (2003) Excitotoxicity, apoptosis and neuropsychiatric disorders. Curr Opin Pharmacol 3: 101-109

Östling O, Johanson KJ (1984) Microelectrophoretic study of radiation-induced DNA damages in individual mammalian cells. Biochem Biophys Res Com 123: 291-298

Oue T, Fukuzawa M, Kamata S, Okada A (1995) Immunohystochemical analysis of proliferating cell nuclear antigen expression in human neuroblastoma. J pediatric surgery 30(4): 528-532

Paile W, Jokela K, Koivistoinen A, Salomaa S (1995) Effects of 50 Hz sinusoidal magnetic fields and spark discharges on human lymphocytes in vitro. Bioelectrochem Bioenerg 36: 15-22

Panagopoulos DJ, Messini N, Karabarbounis A, Philippetis AL, Margaritis LH (2000) A mechanism for action of oscillating electric fields on cells. Biochem Biophys Res Commun 272: 634-640

Panagopoulos DJ, Karabarbounis A, Margaritis LH (2002) Mechanism for action of electromagnetic fields on cells. Biochem Biophys Res Commun 298: 95-102

Pandey P, Farber R, Nakazawa A, Kumar S, Bharti A, Nalin C, Weichselbau R, Kufe D, Kharabanda S. (2000). Hsp27 functions as a negative regulator of cytochrome c-dependent activation of procaspase-3. Oncogene 19: 1975-1981

Paredi P, Kharitonov SA, Hanazawa T, Barnes PJ (2001) Local vasodilator response to mobile phones. Laryngoscope 111: 159-162

Pattyn A, Morin X, Cremer H, Goridis C, Brunet JF (1999) The homeobox gene Phox2b is essential for the development of autonomic neural crest derivatives. Nature 399: 366-370

Pavlik A, Aneja IS, Lexa J, Al-Zoabi BA (2003) Identification of cerebral neurosn and glial cell types inducing heay shock protein Hsp70 following heat stress in the rat. Brain research: 179-189

Pelka-Fleischer R, Ruppelt W, Wilmanns W, Sauer H, Schalhorn A (1987) Relations between cell cycle stage and the activity of DNA-synthesizing enzymes in cultured human lymphoblasts: investigations on cell fractions enriched according to cell cycle stages by way of centrifugal elutriation Leukemia 1: 182-187

Phillips JL, Ivaschuk O, Ishida-Jones T, Jones RA, Campbell-Beachler M, Haggnen W (1998) DNA damage in Molt-4 T-lymphoblastoid cells exposed to cellular telephone radiofrequency fields in vitro. Bioelectrochem Bioenerg 45: 103-110

Pilger A, Ivancsits S, Diem E, Steffens M, Stranzl T, Kolb HA, Rüdiger HW (2002) No long lasting effects of intermittent 50 Hz electromagnetic field on cytoplasmic free calcium and mitochondrial membrane potential in human diploid fibroblasts. Submitted

Piotrowicz RS, Levin EG (1997a) Basolateral membrane-associated 27-kDa heat shock protein and microfilament polymerization. J Biol Chem 272: 25920-25927

Piotrowicz RS, Martin JL, Dillman WH, Levin EG (1997b) The 27-kDa shock protein facilitates basic fibroblast growth factor release from endothelial cells. J Biol Chem 272: 7042-7047

Piper AA, Tattersall MHN, Fox RM (1980) The activities of thymidine metabolizing enzymes during the cell cycle of a human lymphocyte cell line LAZ-007 synchronised by centrifugal elutriation. Biochim Biophys Acta 633: 400-409

Pirozzoli MC, Marino C, Lovisolo GA, Laconi C, Mosiello L, Negroni A (2003) Effects of 50 Hz electromagnetic field exposures on apoptosis and differentiation in a neuroblastoma cell line. Bioelectromagnetics 24(7): 510-516

Preece AW, Iwi G, Davies-Smith A, Wesnes K, Butler S, Lim E, Varey A (1999) Effects of a 915 MHz simulated mobile phone signal on cognitive function in man. Int J Radiat Biol 75: 447

Quantin B and Breathnach R (1988) Epidermal growth factor stimulates transcription of the c-jun proto-oncogene in rat fibroblasts. Nature 334: 538-539

Rao KS, Loeb LA (1992) DNA damage and repair in brain: relationship to ageing. Mutat Res 275: 317-329

Rao S, Henderson AS (1996) Regulation of c-fos is affected by electromagnetic fields. J Cell Biochem 63: 358

Reimers D, López-Toledano A, Mason I, Cuevas P, Redondo C, Herranz AS, Lobo MVT, Bazán E (2001) Developmental expression of fibroblast growth factor (FGF) receptors in neural stem cell progeny. Modulation of neuronal and glial lineages by basic FGF treatment. Neurological Res 23: 612-620

Reiter RJ (1994) Pineal function during aging: attenuation of the melatonin rhythm and its neurobiological consequences. Acta Neurobiol Exp Warsz 54 Suppl: 31-39

Reiter RJ (1995) Oxygen radical detoxification processes during aging: the functional importance of melatonin. Aging, Milan/Italy 7(5): 340-351

Reiter RJ (1997) Melatonin aspects of exposure to low frequency electric and magnetic fields. In: Advances in electromagnetic fields in living systems, Vol. 2 (Lin JC ed). Plenum Press, New York: 1-27

Repacholi MH, Basten A, Gebski V, Noonan D, Finnie J, Harris AW (1997) Lymphomas in E µu-Pim1 transgenic mice exposed to pulsed 900 MHZ electromagnetic fields. Radiat Res 147: 631-640

Repacholi MH (1998) Low-level exposure to radiofrequency electromagnetic fields: health effects and research needs. Bioelectromagnetics 19: 1-19

Riccio A, Pierchala BA, Ciarallo CL, Ginty DD (1997) An NGF-TrkA-mediated retrograde signal to transcription factor CREB in sympathetic neurons. Science 22, 277(5329): 1097-1100

Robison JG, Pendelton AR, Monson KO, Murray BK, O´Neill KL (2002) Decreased DNA repair rates and protection from heat induced apoptosis mediated by electromagnetic field exposure. Bioelectromagnetics 23: 106-112

Rogalla T, Ehrnsperger M, Preville X, Kotlyarov A, Lutsch G, Ducasse C, Paul C, Wieske M, Arrigo AP, Buchner J, Gaestel M. (1999). Regulation of Hsp27 oligomerization, chaperone function, and protective activity against oxidative stress/tumor necrosis factor alpha by phosphorylation. J. Biol. Chem. 274: 18947-18956

Rolletschek A, Chang H, Guan K, Czyz J, Meyer M, Wobus AM (2001) Differentiation of embryonic stem cell-derived dopaminergic neurons is enhanced by survival-promoting factors. Mech Dev 105: 93-104

Roschke J, Mann K (1997) No short-term effects of digital mobile radio telephone on the awake human electroencephalogram. Bioelectromagnetics 18: 172

Rossi D, Gaidano G (2003) Messengers of cell death: apoptotic signalling in health and disease. Haematologica 88: 212-218

Sabapathy K, Klemm M, Jaenisch R, Wagner EF (1997) Regulation of ES cell differentiation by functional and conformational modulation of p53. EMBO J 16: 6217-6229

Salehi M, Hodgkins M, Merry B, Goyns MH (1996) Age-related changes in gene expression identified in the rat brain by differential display. Experientia 52: 888-891

Salford LG, Brun A, Sturesson K, Eberhard JL, Persson BR. (1994). Permeability of the blood-brain barrier induced by 915 MHz electromagnetic radiation, continuous wave and modulated at 8, 16, 50, and 200 Hz. Microsc. Res. Tech. 15: 535-542

Salvioli S, Ardizzoni A, Franceschi C, Cossarizza A (1997) JC-1, but not DiOC6(3) or rhodamine 123, is a reliable fluorescent probe to assess ΔΨ changes in intact cells: implications for studies on mitochondrial functionality during apoptosis. FEBS Lett 411: 77-82

Salvioli S, Capri M, Scarcella E, Mangherini S, Faranca I, Volterra V, De Ronchi D, Marini M, Bonafe M, Franceschi C, Monti D (2003) Age-dependent changes in the susceptibility to apoptosis of peripheral blood CD4+ and CD8+ T lymphocytes with virgin or memory phenotype. Mech Ageing Dev 124(4): 409-418

Sambrook J, Fritsch EF, Maniatis T (1989) Molecular Cloning. A Laboratory Manual. Cold Spring Harbor Laboratory Press, Cold Spring Harbor, New York

Santiard-Baron D, Lacoste A, Ellouk-Achard S, Soulie C, Nicole A, Sarasin A, Ceballos-Picot I (2001) The amyloid peptide induces early genotoxic damage in human preneuron NT2. Mutat Res 479: 113-120

Sarkar S, Ali A, Behari J (1994) Effect of low power microwave on the mouse genome: a direct DNA analysis. Mutat Res 320: 141-147

Sarkar SA, Sharma RP (2002) Expression of selected apoptosis related genes, MIF, IGIF and TNF alpha, during retinoic acid-induced neural differentiation in murine embryonic stem cells. Cell Struct Funct 27: 99-107

Saunders RD, Jefferys JG (2002) Weak electric field interactions in the central nervous system. Health Phys 83: 366-375

Scarfi MR, Bersani F, Cossarizza A, Monti A, Castellani D, Cadossi R, Franceschetti G, Franceschi C (1991) Spontaneous and mitomycin-C induced micronuclei in human lymphocytes exposed to extremely low-frequency pulsed magnetic fields. Biochem Biophys Res Commun 176: 194-200

Scarfi MR, Lioi MB, Zeni O, Franceschetti G, Franceschi C, Bersani F (1994) Lack of chromosomal aberration and micronucleus induction in human lymphocytes exposed to pulsed magnetic fields. Mutat Res 306: 129-133

Schimmelpfeng J, Dertinger H (1997) Action of a 50 Hz magnetic field on proliferation of cells in culture. Bioelectromagnetics 18: 177-183

Schirmacher A, Winters S, Fisher S, Goeke J, Galla HJ, Kullnick U, Ringelstein EB, Stogbauer F. (2000). Electromagnetic fields (1.8 GHz) increase the permeability to sucrose of the blood-brain barrier in vitro. Bioelectromagnetics 21: 338-345

Schönborn F, Pokovic K, Wobus A, Kuster N (2000) Design, Optimization, Realization, and Analysis of an In Vitro System for the Exposure of Embryonic Stem Cells at 1.71GHz. Bioelectromagnetics 21: 372-384

Schreiber E, Matthias P, Müller MM, Schaffner W (1989) Rapid detection of octamer binding proteins with 'mini-extracts" prepared from a small number of cells. Nucleic Acids Res 17: 6419

Schuderer J, Mertens R, Oesch W, Frauenknecht U, Kuster N (2001) Flexible and efficient in vitro exposure setup for risk assessment studies at 1800 MHz enabling any modulation scheme from sub-Hz up to MHz and double blind protocols. 23th BEMS Meeting, St. Paul, MI, USA. Proceedings: 26

Seaman RL, Parker JE, Kiel JL, Mathur SP, Grubbs TR, Prol HK (2002) Ultra-wideband pulses increase nitric oxide production by RAW 264.7 macrophages incubated in nitrate. Bioelectromagnetics 23: 83-87

Sehlmeyer U, Meister A, Beisker W, Wobus AM (1996) Low mutagenic effects of mitomycin C in undifferentiated embryonic P19 cells are correlated with efficient cell cycle control. Mutat Res 354: 103-112

Sewerynek E, Melchiorri D, Chen LD and Reiter R J (1995) Melatonin reduces both basal and bacterial lipopolysaccharide-induced lipid peroxidation in vitro. Free Radical Biol and Med 19: 903–909

Sheerin A, Thompson KSJ, Goyns MH (2001) Altered composition and DNA binding activity of the AP-1 transcription factor during the ageing of human fibroblasts. Mech Age Dev 122: 1813-1824

Shikama N, Ackermann R, Brack C (1994) Protein synthesis elongation factor EF-1α expression and longevity in Drosophila melanogaster. Proc Natl Acad Sci USA 91: 4199-4203

Sigal A, Rotter V (2000) Oncogenic mutations of the p53 tumor suppressor: the demons of the guardian of the genome. Cancer Res 60: 6788-6793

Simko M, Kriehuber R, Lange S (1998a) Micronucleus formation in human amnion cells after exposure to 50 Hz MF applied horizontally and vertically. Mutat Res 418: 101-111

Simko M, Kriehuber R, Weiss DG, Luben RA (1998b) Effects of 50 Hz EMF exposure on micronucleus formation and apoptosis in transformed and nontransformed human cell lines. Bioelectromagnetics 19(2): 85-91

Simko M, Droste S, Kriehuber R, Weiss DG (2001a) Stimulation of phagocytosis and free radical production in murine macrophages by 50 Hz electromagnetic fields. Eur J Biol 80: 562-566

Simko M, Richard D, Kriehuber R, Weiss DG (2001b) Micronucleus induction in Syrian hamster embryo cells following exposure to 50 Hz magnetic fields, benzo(a)pyrene and TPA in vitro. Mutat Res 495: 43-50

Simmons DM, Arriza IL, Swanson LW (1989) A complete protocol for in situ hybridization of messenger RNAs in brain and other tissues with radilabeled single stranded RNA probes. Histotechnol 12: 169-181

Singh NP, McCoy MT, Tice RR, Schneider EL (1988) A simple technique for quantitation of low levels of DNA damage in individual cells. Exp Cell Res 175: 184-191

Singh NP, Tice RR, Stephens RE, Schneider EL (1991) A microgel electrophoresis technique for direct quantitation of DNA damage and repair in individual fibroblasts cultured on microscope slides. Mutat Res 252: 289-296

Singh NP, Lai H (1998) 60 Hz magnetic field exposure induces DNA crosslinks in rat brain cells. Mutat Res 400: 313-320

Skulachev VP (2002) Programmed death phenomena: from organelle to organism. Ann NY Acad Sci 959: 214-237

Smiley ST, Reers M, Mottola-Hartshorn C, Lin M, Chen A, Smith TW, Steele GD Jr, Chen LB (1991) Intracellular heterogeneity in mitochondrial membrane potentials revealed by a J-aggregate-forming lipophilic cation JC-1. PNAS USA 88: 3671-3675

Sobel E, Davanipour Z, Sulkava R, Erkinjuntti T, Wikstrom J, Henderson HW, Buckwalter G, Bowman JD, Lee PJ (1995) Occupations with exposure to electromagnetic fields: a possibile risk factor for Alzheimer's disease" Am J Epidemiol 142: 515

Sobel E, Dunn M, Davanipour Z, Qian Z, Chui HC (1996) Elevated risk of Alzheimer's disease among workers with likely electromagnetic field exposure. Neurology 47: 1477

Speit G, Dennog C, Eichhorn U, Rothfuss A, Kaina B (2000) Induction of heme oxygenase-1 and adaptive protection against the induction of DNA damage after hyperbaric oxygen treatment. Carcinogenesis 21: 1795-1799

Spielmann H, Pohl I, Doring B, Liebsch M, Moldenhauer F (1997) The embryonic stem cell test, an in vitro embryotoxicity test using two permanent mouse cell lines: 3T3 fibroblasts and embryonic stem cells, In Vitr. Toxicol. In Vitr Toxicol 10: 119-127

Stanke M, Junghans D, Geissen M, Goridis C, Ernsberger U, Rohrer H (1999) The Phox2 homeodomain proteins are sufficient to promote the development of symapathetic neurons. Development 126: 4087-4094

Stefanovsky VY, Pelletier G, Hannan R, Gagnon-Kugler T, Rothblum LI, Moss T (2001) An immediate response of ribosomal transcription to growth factor stimulation in mammals is mediated by ERK phosphorylation of UBF. Mol Cell 8: 1063-1073

Steinlein OK, Mulley JC, Propping P, Wallace RH, Phillips HA, Sutherland GR, Scheffer IE, Berkovic SF (1995) A missense mutation in the neuronal nicotinic acetylcholine receptor alpha 4 subunit is associated with autosomal dominant nocturnal frontal lobe epilepsy. Nat Genet 11: 201-203

Stewart Report (2000) Mobile Phones and Health. Report of the Independent Expert Group on Mobile Phones. National Radiation Protection Board (NRPB), London, UK; http://www.iegmp.org.uk

Svedenstal BM, Johanson KJ, Mild KH (1999a) DNA damage induced in brain cells of CBA mice exposed to magnetic fields. In Vivo 13: 551-552

Svedenstal BM, Johanson KJ, Mattsson MO, Paulsson LE (1999b) DNA damage, cell kinetics and ODC activities studied in CBA mice exposed to electromagnetic fields generated by transmission lines. In Vivo 13: 507-513

The Royal Society of Canada (1999) A Review of the Potentail Health Risks of Radiofrequency Fields from Wireless Telecommuinication Devices. An Expert Panel Report, ISBN 920064-68-X (www.rsc.ca)

Tian F, Nakahara T, Wake K, Taki M, Miyakoshi J (2002a) Exposure to 2.45 GHz electromagnetic fields induces hsp70 at a high SAR of more than 20 W/kg but not at 5W/kg in human glioma MO54 cells. Int J Radiation Biol 78(5): 433-440

Tian F, Nakahara T, Yoshida M, Honda N, Hirose H, Miyakoshi J (2002b) Exposure to power frequency magnetic fields suppresses X-ray-induced apoptosis transiently in Ku80-deficient xrs5 cells. Biochem Biophys Res Commun 29; 292(2): 355-361

Tibbles LA, Woodgett JR (1999) The stress-activated protein kinase pathways. Cell. Mol. Life Sci. 55, 1230-1254

Tice RR, Andrews PW, Singh NP (1990) The single cell gel assay: a sensitive technique for evaluating intercellular differences in DNA damage and repair. Basic Life Sci 53: 291-301

Tice RR, Agurell E, Anderson D, Burlinson B, Hartmann A, Kobayashi H, Miyamae Y, Rojas E, Ryu JC, Sasaki YF (2000) Single cell gel/comet assay: guidelines for in vitro and in vivo genetic toxicology testing. Environ Mol Mutagen 35: 206-221

Tice RR, Hook GJ (2002) Genotoxicity of radio frequency signals. Investigation of DNA damage and micronuclei induction in cultured human blood cells. Bioelectromagnetics 23: 113-126

Tofani S, Barone D, Cintorino M, De-Santi MM, Ferrara A, Orlassino R, Ossola P, Peroglio F, Rolfo K, Ronchetto F (2001) Static and ELF magnetic fields induce tumor growth inhibition and apoptosis. Bioelectromagnetics 22(6): 419-428

Toivo T, Sihvonen A-P, Puranen L, Keskinen K (2001) Water Cooled Waveguide Chambers for Exposure of Cells In Vitro at 900 MHz. EBEA Congress, Helsinki, Finland. Proceedings: 62-63

Tokalov SV, Gutzeit HO (2003) The heat shock-induced cell cycle arrest is attenuated by weak electromagnetic fields. Cell Prolif 36(2): 101-111

Tokalov SV, Pieck S, Gutzeit HO (2003) Comparison of the reactions to stress produced by X-rays or electromagnetic fields (50Hz) and heat: induction of heat shock genes and cell cycle effects in human cells. J Appl Biomed 1: 85-92

Tokalov SV, Gutzeit HO (2004) Weak electromagnetic fields (50 Hz) elicit a stress response in human cells. Environ Res, Vol 94 (2): 145-151

Tolomeo M, Simoni D (2002) Drug resistance and apoptosis in cancer treatment: development of new apoptosis-inducing agents active in drug resistant malignancies. Curr Med Chem Anti-Canc Agents 2: 387-401

Tonini R, Baroni MD, Masala E, Micheletti M, Ferroni A, Mazzanti M (2001) Calcium protects differentiating neuroblastoma cells during 50 Hz electromagnetic radiation. Biophysical J 81: 2580-2589

Töre F, Dulou PE, Haro E, Veyret B, Aubineau P. (2001). Two-hour exposure to 2-W/kg, 900-MHZ GSM microwaves induces plasma protein extravasation in rat brain and dura matter. Proceedings of the 5th International congress of the EBEA, pp43-45

Trillo MA, Úbeda A, Blanchard JP, House DE, Blackman CF (1996) Magnetic fields at resonant conditions for the hydrogen ion affect neurite outgrowth in PC-12 cells: A test of the ion parametric resonance model. Bioelectromagnetics 17: 10-20

Trosko JE, Ruch RJ (1998): Cell-Cell Communication in Carcinogenesis. Frontiers in Bioscience, Vol. 3, d208-236

Tsong TY (1992) Molecular recognition and processing of periodic signals in cells: study of activation of membrane ATPases by alternating electric fields. Biochim Biophys Acta 1113: 53-70

Tsurita G, Nagawa H, Ueno S, Watanabe S, Taki M. (2000) Biological and morphological effects on the brain after exposure of rats to a 1439MHz TDMA field. Bioelectromagnetics 21, 364-371

Valberg PA, Kavet R, Rafferty CN (1997) Can low-level 50/60 Hz electric and magnetic fields cause biological effects? Radiat Res 148: 2-21

Van den Bosch M, Lohman PHM, Pastink A (2002) DNA double strand break repair by homologous recombination. Rev Biol Chem 383: 873-892

Van Engeland M, Nieland LJW, Ramaekers FCS, Schutte B, Reutelingsperger CPP (1998) Annexin V-affinity assay: a review on an apoptosis detection system based on phosphatidylserine exposure. Cytometry 31: 1-9

Van Gent DC, Hoeijmakers JH, Kanaar R (2001) Chromosomal stability and the DNA double-strand break connection. Nature Rev Genet 2: 196-206

Vander Molen MA, Donahue HJ, Rubin CT, McLeod KJ (2000): Osteoblastic networks with deficient coupling: differential effects of magnetic and electric field exposure. Bone 27(2): 227-231

Varma MM, Traboulay EA (1997) Comparison of native and microwave irradiated DNA. Experientia 33(12): 1649-1650

Velizarov S, Raskmark P, Kwee S (1999) The effects of radiofrequency fields on cell proliferation are non-thermal. Bioelectrochemistry and Bioenergetics 48: 177-180

Ventura C, Pintus G, Fiori MG, Bennardini F, Pinna G, Gaspa L (1997) Opioid peptide gene expression in the primary hereditary cardiomyopathy of the Syrian hamster. Part I: Regulation of prodynorphin gene expression by nuclear protein kinase. C J Biol Chem 272: 6685-6692

Ventura C, Maioli M (2000) Opioid peptide gene expression primes cardiogenesis in embryonal pluripotent stem cells. Circ Res 87: 189-194

Ventura C, Zinellu E, Maninchedda E, Fadda M, Maioli M (2003a) Protein kinase C signaling transduces endorphin-primed cardiogenesis in GTR1 embryonic stem cells. Circ Res 92: 617-622

Ventura C, Zinellu E, Maninchedda E, Maioli M (2003b) Dynorphin B is an agonist of nuclear opioid receptors coupling nuclear protein kinase c activation to the transcription of cardiogenic genes in GTR1 embryonic stem cells. Circ Res 392: 623-629

Verschaeve L, Slaets D, Van Gorp U, Maes A, Vanderkom J (1994) In vitro and in vivo genetic effects of microwaves from mobile phone frequencies in human and rat peripheral blood lymphocytes. In: Proceedings of Cost 244 Meetings on Mobile Communication and Extremely Low Frequency field: Instrumentation and Measurements in Bioelectromagnetics Research (Simunic D ed.): 74-83

Veskovic M, Mattson MO, Hansson Mild K (2002) Dose and Exposure in Mobile Phone Research. Arbetslivrapport 04, ISSN 1401-2928, http://www.arbetslivinstitutet.se/publikationer

Vijayalaxmi, Mohan N, Meltz ML, Wittler MA (1997) Proliferation and cytogenetic studies in human blood lymphocytes exposed in vitro to 2450 MHz radiofrequency radiation. Int J Radiat Biol 72(6): 751-757

Vijayalaxmi, Leal BZ, Szilagyi M, Prihoda TJ, Meltz ML (2000) Primary DNA damage in human blood lymphocytes exposed in vitro to 2450 MHz radiofrequency radiation. Radiat Res 153(4): 479-486

Vijayalaxmi, Pickard WF, Bisht KS, Prihoda TJ, Meltz ML, LaRegina MC, Roti Roti JL, Straube WL, Moros EG (2001a) Micronuclei in the peripheral blood and bone marrow cells of rats exposed to 2450 MHz radiofrequency radiation. Int J Radiat Biol 77(11): 1109-1115

Vijayalaxmi, Leal BZ, Meltz ML, Pickard WF, Bisht KS, Roti Roti JL, Straube WL, Moros EG (2001b) Cytogenetic studies in human blood lymphocytes exposed in vitro to radiofrequency radiation at a cellular telephone frequency (835.62 MHz, FDMA). Radiat Res 155(1 Pt 1): 113-121

Vilim V, Wilhelm J (1989) What do we measure by luminol-dependent chemiluminescence of phagocytes. Free Radical Biol Med 6: 623-629

Wagner P, Roschke J, Mann K, Hiller W, Frank C (1998) Human sleep under the influence of pulsed radiofrequency electromagnetic fields: a polysomnographic study using standardized conditions. Bioelectromagnetics 19: 199

Wagner M, Hermanns I, Bittinger F, Kirkpartick CJ (1999) Induction of stress proteins in human endothelial cells by heavy metal ions and heat shock. Am. J. Physiol. 277: L1026-L1033

Walton M, Woodgate AM, Muravlev A, Xu R, During MJ, Dragunow M (1999) CREB phosphorylation promotes nerve cell survival. J Neurochem 73(5): 1836-1842

Wang JF, Komarov P, Sies H, de Groot H. (1991) Contribution of nitric oxide synthase to luminal-dependent chemiluminescence generated by phorbol-ester-activated Kupffer cells. Biochem J 279: 311-314

Wang N, Orr-Urtreger A, Korczyn AD (2002) The role of neuronal nicotinic acetylcholine receptor subunits in autonomic ganglia: lessons from knock-out mice. Progress in Neurobiol 68: 341-360

Wassermann TH, Twentyman P (1988) Use of a colorimetric microtiter (MTT) assay in determining the radiosensitivity of cells from murine solid tumors. Int J Radiat Oncol Biol Phys 15 (3): 699-702

Wei M, Guizzetti M, Yost M, Costa LG (2000) Exposure to 60-Hz magnetic fields and proliferation of human astrocytoma cells in vitro. Toxicology and Applied Pharmacology 162 (3): 166-176

Weisbrot D, Lin H, Ye L, Blank M, Goodman R (2003) Effects of mobile phone radiation on reproduction and development in Drosophila melanogaster. J Cell Biochem 89: 48-55

Wessels JM, Nüsse M (1995) Flow cytometric detection of MN by combined staining of DNA and membranes. Cytometry 19: 201

Whitson GL, Carrier WL, Francis AA, Shih CC, Georghiou S, Regan JD (1986) Effects of extremely low frequency (ELF) electric fields on cell growth and DNA repair in human skin fibroblasts. Cell Tissue Kinet 19: 39-47

WHO (1985) Guide to short-term tests for detecting mutagenic, carcinogenic chemicals. World Health Organization, Geneva, Switzerland. Env Health Crit 51: 57-67

Wilkinson BL, Sadler KA, Hyson RL (2002) Rapid deafferentation-induced upregulation of bcl-2 mRNA in the chick cochlear nucleus. Brain Res Mol Brain Res 99: 67-74

Winter C, Weiss C, Martin-Villalba A, Zimmermann M, Schenkel J (2002) JunB and Bcl-2 overexpression results in protection against cell death of nigral neurons following axotomy. Brain Res Mol Brain Res 104: 194-202

Wobus AM, Kleppisch T, Maltsev V, Hescheler J (1994) Cardiomyocyte-like cells differentiated in vitro from embryonic carcinoma cells P19 are characterized by functional expression of adrenoceptors and Ca^{2+} channels. In Vitro Cell Dev Biol Anim 30A: 425-434

Wobus AM, Guan K, Yang HT, Boheler KR (2002) Embryonic stem cells as a model to study cardiac, skeletal muscle, and vascular smooth muscle cell differentiation. Methods Mol Biol 185: 127-156

Wolf FI, Torsello A, Covacci V, Fasanella S, Montanari M, Boninsegna A, Cittadini A (2002) Oxidative DNA damage as a marker of aging in WI-38 human fibroblasts. Exp Gerontol 37: 647-56

Wonnacott S (1997) Presynaptic nicotinic Ach receptors. Trends Neurosci 20: 92-98

Xu ZP, Chen GD, Zemg QL, Lu DQ, Chiang H (2004) Changes in gene expression profile of MCF-7 cell after exposure to ELF MFs. 26th Annual BEMS Meeting, Proceedings: 99

Yamaguchi DT, Huang J, Ma D, Wang PK (2002): Inhibition of gap junction intercellular communication by extremely low-frequency electromagnetic fields in osteoblast-like models is dependent on cell differentiation. J Cell Physiol, 190(2): 180-188

Yang C, Kim HS, Seo H, Kim CH, Brunet JF, Kim KS (1998) Paired-like homeodomain proteins, Phox2a and Phox2b, are responsible for noradrenergic cell-specific transcription of the dopamine beta-hydroxylase gene. J Neurochem 71: 1813-1826

Yost MG, Liburdy RP (1992) Time-varying and static magnetic fields act in combination to alter calcium signal transduction in the lymphocyte. FEBS Lett 296: 117-122

Zahn RK, Jaud S, Schröder HC, Zahn-Daimler G (1996) DNA status in brain and heart as prominent co-determinant for life span? Assessing the different degrees of DNA damage, damage susceptibility, and repair capability in different organs of young and old mice. Mech Age Dev 89: 79-94

Zamzami N, Marchetti P, Castedo M, Decaudin D, Macho A, Hirsch T, Susin SA, Petit PX, Mignotte B, Kroemer G (1995) Sequential reduction of mitochondrial transmembrane potential and generation of reactive oxygen species in early programmed cell death. J Exp Med 182(2): 367-377

Zeng QL, Chiang H, Hu GL, Mao GG, Fu YT, Lu DQ (2003): ELF magnetic fields induce internalization of gap junction protein connexin 43 in Chinese hamster lung cells. Bioelectromagnetics 24(2): 134-138

Zeng QL, Li H, Lu DQ, Chiang H, Xu ZP (2004a) The protein expression profiling of MCF-7 cells induced by ELF MF exposure. 26th Annual BEMS Meeting, Proceedings: 61-62

Zeng QL, Weng Y, Li H, Lu DQ, Chianh H, Xu ZP (2004b) Preliminary proteomic evidence of 1.8 GHz mobile phone signal-induced cellular reaction in vitro. 26th Annual BEMS Meeting, Proceedings: 174-175

Zhang W, Chen S (2001) EGR-1, a UV-inducible gene in $p53^{(-/-)}$ mouse cells. Exp Cell Res 266: 21-30

Zhou J, Yao G, Zhang J, Chang Z (2002) CREB DNA binding activation by a 50-Hz magnetic field in HL60 cells is dependent on extra- and intracellular Ca^{2+} but not PKA, PKC, ERK, or p38 MAPK. Biochem Biophys Res Commun 296: 1013-1018

Zmirou Report to the French Health General Directorate (2001) (http://www.sante.gouv.fr/htm/dossiers/telephon_mobil/index.htm)

Zylicz M, King FW, Wawrzynow A (2001) Hsp70 interactions with the p53 tumour suppressor protein. EMBO J 20: 4634-4638

Zmyslony M, Palus J, Dziubaltowska E, Politanski P, Mamrot P, Rajkowska E, Kamedula M (2004) Effects of In Vitro Exposure to Power Frequency Magnetic Fields on UV-Induced DNA Damage of Rat Lymphocytes. Bioelectromagnetics 25: 560-562

ANNEX I - Results submitted after deadline

A) ELF-EMF

1) Re-evaluation of micronucleus frequencies on slides prepared by Participant 3 in two additional laboratories which are not members of the REFLEX consortium

Micronucleus frequencies in fibroblasts which were exposed to ELF-EMF (50 Hz, 1 mT, 15h, 5 min on/10 min off) or sham-exposed in the laboratory of Participant 3 (Vienna, see 2.2 and 3.1.1.1) were re-evaluated under blinded conditions.

a) Prof. Guenter Speit, Medizinische Fakultaet/Humangenetik, University of Ulm, Albert-Einstein-Allee 7, 89081 Ulm, Germany

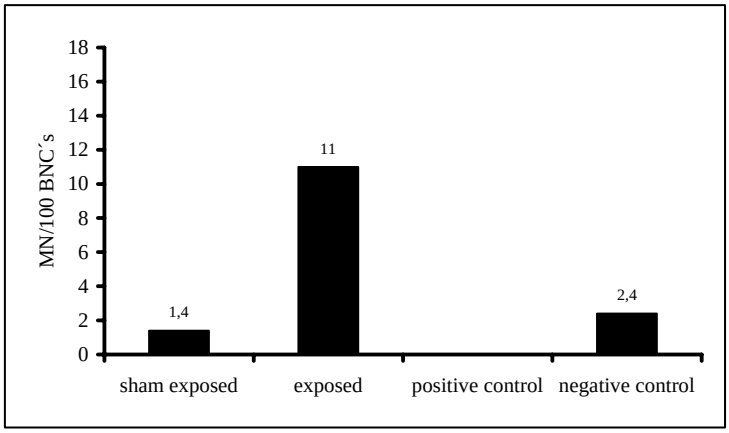

Figure 1: Micronucleus frequencies in ELF-EMF exposed cultured human fibroblasts (50 Hz, 1 mT, 15h, 5 min on/10 min off) and in control cells. Bleomycin treated cells (10µg/ml) were used as a positive control.

b) Prof. Heinrich Zankl, Fachbereich Biologie der Technischen Universitaet Kaiserslautern, Paul-Ehrlich-Strasse 7, 67663 Kaiserslautern, Germany

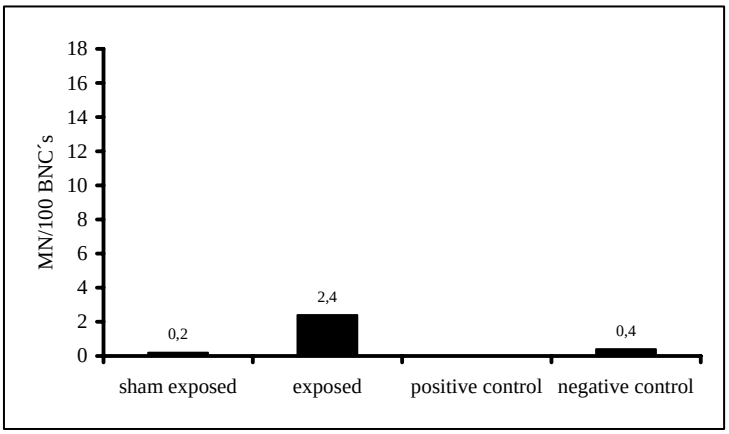

Figure 2: Micronucleus frequencies in ELF-EMF exposed cultured human fibroblasts (50 Hz, 1 mT, 15h, 5 min on/10 min off) and in control cells. Bleomycin treated fibroblasts (10 µg/ml) were used as a positive control.

ELF-EMF exposed cells showed an increase in micronucleus frequencies, which was about 6 to 10-fold as compared to sham exposed cells and negative controls. Although basal levels of micronuclei correlated well with the results obtained in the laboratory of Participant 3, exposed cells showed definitely higher values. The variability in micronuleus frequencies between the laboratories maybe due to the fact that different staining techniques were applied: Vienna and Ulm used a more sensitive fluorescent dye (DAPI), whereas the laboratory in Kaiserslautern stained the slides with GIEMSA. In addition, the laboratories in Ulm and Kaiserslautern scored 500 binucleated cells only instead of 2,000 processed in Vienna.

In conclusion, in three independent laboratories micronucleus frequencies showed a consistent increase in cultured human fibroblasts after ELF-EMF exposure. Differences in micronucleus frequencies between the laboratories can be attributed to different staining techniques and the different a numbers of scored cells.

2) Evaluation of genotoxic effects on human fibroblasts following intermittent exposure to 50 Hz powerline magnetic fields by Participant 8 (Bologna/Naples)

Some experiments related to the evaluation of the induction of genotoxic effects following intermittent (5 min field on/10 min field off) exposures to 50 Hz ELF magnetic fields, 1 mT field intensity, were carried out on human diploid fibroblasts (ES-1). In particular, to evaluate the induction of DNA single strand breaks the alkaline comet assay was applied following 15, 18 and 24 hours exposures, while the induction of micronuclei (MN) was measured following 24 h exposure.

Moreover, positive controls were also provided by treating cells with hydrogen peroxide (Alkaline Comet Assay) or Mitomycin-C (MMC; micronucleus assay) at several concentrations.

The results obtained do not indicate induction of genotoxic effects, neither in terms of comets induction nor in terms of MN frequency increase. On the contrary, positive controls showed an increase in DNA damage, as expected.

Experimental conditions and cytogenetic analysis

Human diploid fibroblasts (ES-1) were cultured in DMEM containing 10% FBS, 20 mM Hepes buffer, 2mM L-glutamine, 100 IU/ml penicillin and 100 µg/ml streptomycin at 37°C in a humidified atmosphere of 5% CO_2. Cells were supplied with fresh culture medium every 48 h and splitted once a week. Cells were received at passage 6 and a master bank was established with cells at passage 8. For experiments, cells from passages 10-16 were used.

Preliminary experiments were devoted to find the dose of chemicals to be used to provide positive controls for both the assays employed. Dose-response curves were set up by treating ES-1 cells with H_2O_2 ranging from 25-100 µM final concentration for 30 minutes (alkaline comet assay) and with MMC ranging form 0,005 – 0,05 µg/ml final concentration for the whole culture period (MN assay). For both chemicals a dose-dependent increase in DNA damage was detected, even for the lowest doses tested. However, the best compromise between induced damage and cell survival was found at 50 µM H_2O_2 and 0,025 µg/ml MMC and these concentrations were used for the experiments.

A second set of preliminary experiments was devoted to define the cell cycle duration of ES-1 cells to block cytokinesis for micronucleus test: it resulted of 28 h (data not shown).

The exposures were carried out at 50 Hz (1 mT field intensity) and the signal used was powerline. Several exposure durations were tested, as reported below.

Alkaline Comet Assay

Ten independent experiments (5 by exposing cells for 24 h, 2 by exposing cells for 18 h, 3 by exposing cells for 15 h) were carried out by setting up 8 cultures each: 4 to be exposed and 4 to be sham exposed.

Moreover, positive controls were provided by treating cultures for 30 min with hydrogen peroxide (H_2O_2, 50 µM). 24 hours before the experiments, 50000 cells/3 ml complete medium were seeded into 35 mm Petri dishes (Corning, cat. 430165). Following the intermittent exposure cultures were processed for the comet assay as described in details in (1). Slides were stained, just before the analysis, with ethidium

bromide (12 μg/ml) and images of 1000 randomly selected cells (250 from each of four replicated cultures) were analyzed by a computerized image analysis system (Delta Sistemi, Rome, Italy) fitted with a Leica DM BL fluorescence microscope at 250 X magnification. This system acquires images, computes the integrated intensity profile for each cell, estimates the comet cell components, head and tail, and evaluates a range of derived parameters. DNA damage was evaluated by calculating the tail factor, as reported in (1). Moreover, tail moment, comet moment and percentage of tail DNA were also measured.

Cytokinesis-block Micronucleus Assay

4 independent experiments were carried out by exposing cells for 24 h. For each experiment 4 cultures were set up: 2 to be exposed and 2 to be sham exposed. Positive controls were provided by adding MMC (0,025 μg/ml) 24 h after the seeding.

50000 cells/5 ml complete medium were seeded in slide flasks (NUNCLON, cod. 170920, 9 cm^2 growth area) and recovered for 24 h. To block cytokinesis, 4 hours before the end of the first cycle (48 h after seeding), Cytochalasin-B (3 μg/ml final concentration) was added and at the end of the second replication cycle (80 h after seeding), cells were incubated for 30 min at 37°C with hypotonic solution (KCl 0,075 M) and fixed for 10 min (methanol 80% in distilled water). Air dried slides were stained for 8 min (10% Giemsa in phosphate buffer pH 6.8). The intermittent MF exposure was carried out during the first 24 hours following the recovery.

MN were scored in binucleated cytokinesis-blocked (CB) cells with well preserved cytoplasm by using a light microscope, and for each experiment their frequency was evaluated in 2000 cells (1000 cells for each duplicate slide). The results were expressed as micronucleated binucleated (MNBN) cells per thousand binucleated cells.

The morphological criteria for MN scoring in binucleated cells were similar to those reported by Fenech for human lymphocytes (2). By classifying 500 cells according to the number of nuclei, the binucleate cell index (BCI) and the cytokinesis-block proliferation index (CBPI) were evaluated for each culture, as reported in (3) and (4), respectively.

Statistical analysis

Differences between treated and untreated samples (sham exposed vs. exposed; sham exposed vs. positive controls) were tested by using the two tailed paired Student's t test. P values lower than 0.05 were considered as statistically significant.

RESULTS

Comet assay

Following 24 h intermittent exposure (5 min on/10 min off) to 50 Hz powerline MF, human diploid fibroblasts did not show statistically significant differences in all the parameters investigated when sham-exposed samples were compared to exposed ones. The results obtained are reported in table 1 as mean ± standard error of 5 independent experiments. Same results have been obtained when cultures exposed for 18 h (2 experiments) and 15 h (3 experiments) were compared to their own sham exposed cultures, as shown in table 2 and 3, respectively.

On the contrary, when sham exposed cultures were compared to H_2O_2 -treated samples, a significant increase in all the parameters investigated was detected following treatments of 30 minutes ($p<0.05$). The results obtained are reported in figure 1 as mean ± standard error of all the parameters investigated.

Micronucleus assay

Following 24 h exposure no genotoxic effects were detected by comparing sham-exposed with exposed samples. The proliferation index (CBPI) also resulted not affected by the exposure. The results are reported in table 4 (4 independent experiments), where data related to MMC treatments are also shown. By comparing sham-exposed with MMC treated cultures a statistically significant increase in MN frequency was detected, together with a decrease of cell proliferation and of percentage of binucleated cells ($p<0.05$ in all cases).

DISCUSSION

The data here reported do not support the hypothesis that intermittent exposures to 50 Hz MF (powerline signal) induce genotoxic effects in human diploid fibroblasts.

Concerning the alkaline comet assay, our finding is also supported by the results obtained by treating cells with hydrogen peroxide as positive control, where an increase in all the comet parameters investigated has been detected. Moreover, the cells investigated showed an high sensitivity to 30 min treatment already at 25 µM final concentration (data not shown), while most of the data reported in literature on several cell types indicate that 30 min treatments at concentrations between 50 and 100 µM are needed to induce a statistically significant effect.

Concerning the data on the induction of micronuclei (MN), also in this case we have not found genotoxic effects induced by the field. On the contrary, MMC treatments at doses of 0,025 µg/ml resulted cytotoxic (CBPI: 1,18 vs. 1,45 in treated and untreated cultures, respectively) while a dose of 0,033 µg/ml is necessary to induce MN increase in human peripheral blood lymphocytes without affecting cell proliferation.

The data here reported refer only to the exposures performed with the powerline signal: experiments devoted to test the sinusoidal signal are in progress.

REFERENCES

[1] Ivancsits S, Diem E, Pilger A, Rüdiger W, Jahn O. (2002) Mutation Res., 519, 1-13.

[2] Fenech, M. (1993) Mutation Res. 285: 35-44

[3] Tice RR, Hook GG, Donner M, McRee DI, Guy AW. (2002) Bioelectromagnetics 23, 113-126

[4] Surralles J, Xamena N, Creus A, Catalan J, Norppa H, Marcos R. (1995) Mutation Res. 341: 169-184

Table 1 – mean values ± standard error of the parameters investigated following alkaline comet assay in ES-1 human fibroblasts exposed for 24 h to 50 Hz powerline magnetic field. Results of 5 independent experiments (1000 cells/treatment investigated)

Parameters	Sham-exposed	MF-exposed
Tail Factor (%)	5.65 ± 0.98	6.36 ± 0.93
Comet Moment	1.86 ± 0.43	2.01 ± 0.49
% DNA	3.8 ± 0.97	4.12 ± 1.12
Tail Moment	1.10 ± 0.32	1.29 ± 0.36

Table 2 – mean values ± standard error of the parameters investigated following alkaline comet assay in ES-1 human fibroblasts exposed for 18 h to to 50 Hz powerline magnetic field. Results of 2 independent experiments (1000 cells/treatment investigated)

Parameters	Sham-exposed	MF-exposed
Tail Factor (%)	6.24 ± 0.25	6.11 ± 0.26
Comet Moment	2.32 ± 0.04	2.25 ± 0.04
% DNA	4.37 ± 0.22	4.20 ± 0.22
Tail Moment	1.56 ± 0.05	1.54 ± 0.11

Table 3 – mean values ± standard error of the parameters investigated following alkaline comet assay in ES-1 human fibroblasts exposed for 15 h to to 50 Hz powerline magnetic field. Results of 3 independent experiments (1000 cells/treatment investigated)

Parameters	Sham-exposed	MF-exposed
Tail Factor (%)	5.23 ± 0.26	5.20 ± 0.63
Comet Moment	1.76 ± 0.08	1.68 ± 0.18
% DNA	3.07 ± 0.29	3.08 ± 0.68
Tail Moment	0.89 ± 0.03	0.88 ± 0.15

Table 4 – MN frequency, proliferation index (CBPI) and binucleate cell index (BCI) in cultures sham-exposed, exposed for 24 h and positive controls. Data are reported as mean ± SD of 4 independent experiments. * Sham-exposed vs. MMC treated cultures: $p<0.05$.

Parameters	Sham-exposed	MF-exposed	MMC (0.025 µg/ml)
MN/1000 CB cells	0.45±0.06	0.43±0.07	2.35±0.35*
CBPI	1.45±0.02	1.43±0.02	1.15±0.01*
% BCI	45.2±2.45	43.3±2.01	15.0±1.41*

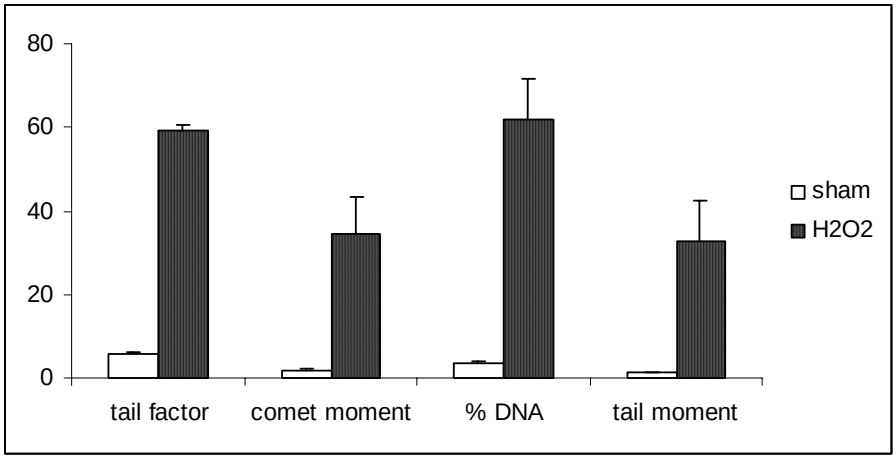

Figure 1 – mean values ± standard error of the parameters investigated following alkaline comet assay in ES-1 human fibroblasts treated for 30 min with 50µM hydrogen peroxide compared to sham-exposed samples.

B) RF-EMF

1) Re-evaluation of micronucleus frequencies on slides prepared by Participant 3 in two additional laboratories which are not members of the REFLEX consortium

Micronucleus frequencies in fibroblasts which were exposed to RF-EMF (GSM basic 1950 MHz, 15h, 2 W/kg) or sham-exposed in the laboratory of Participant 3 (Vienna, see 2.2 and 3.2.1.2) were re-evaluated under blinded conditions.

a) Prof. Guenter Speit, Medizinische Fakultaet/Humangenetik, University of Ulm, Albert-Einstein-Allee7, 89081 Ulm, Germany

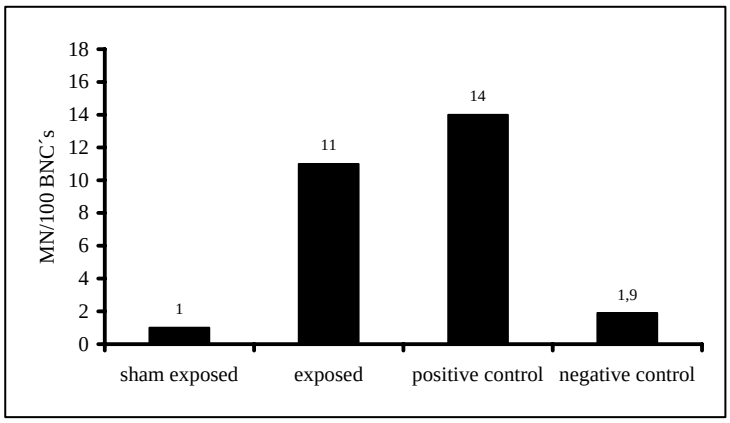

Figure 1: Micronucleus frequencies of RF-EMF exposed (GSM basic 1950 MHz, 15h, 2 W/kg) cultured human fibroblasts and control cells. Bleomycin-treated cells were used as a positive control.

b) Prof. Heinrich Zankl, Fachbereich Biologie der Technischen Universitaet Kaiserslautern, Paul-Ehrlich-Strasse 7, 67663 Kaiserslautern, Germany

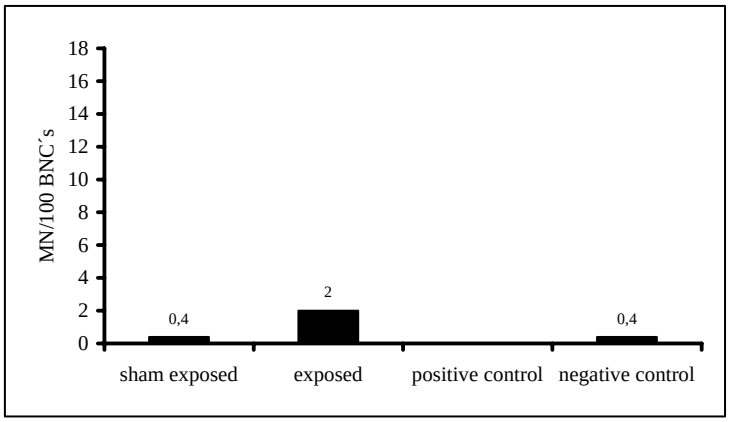

Figure 2: Micronucleus frequencies of RF-EMF exposed (GSM basic 1950 MHz, 15h, 2 W/kg) cultured human fibroblasts and control cells. Bleomycin-treated cells were as a positive control.

RF-EMF exposed cells showed an increase in micronucleus frequencies, which was about 5-fold compared to sham exposed cells and negative controls. Although, basal levels of micronuclei correlated well with the results obtained in the laboratory of Participant 3, exposed cells showed definitely lower levels. These variability could be attributed to different staining techniques. Laboratories in Vienna and Ulm used a more sensitive fluorescent dye (DAPI), whereas the laboratory in Kaiserslautern stained the slides with GIEMSA. Positive controls could not be evaluated, due to a too low number of assessable cells.

In conclusion, in three independent laboratories micronucleus frequencies showed a consistent increase in cultured human fibroblasts after RF-EMF exposure. Differences in micronucleus frequencies between the laboratories can be attributed to different staining techniques and a various number of scored cells.

IT'IS FOUNDATION
Foundation for Research on Information Technologies in Society

Prof. Dr. Niels Kuster
Director Foundation IT'IS
Professor of Swiss Federal Institute of Technology – ETHZ
Phone +41 1 245 9690 · kuster@itis.ethz.ch

ANNEX II

Technical support (Participant 10)

OBJECTIVES

To be able to compare the results of investigations carried out in the different laboratories and to ensure the conclusiveness of the data obtained in the studies, it is of the utmost importance that the conditions of exposure to EMFs be strictly controlled. Therefore, the objective are:

- Evaluation of existing setups
- Development of an optimised ELF setup
- Development of an optimised RF setup (900 MHz)
- Development of an optimised RF setup (1800 MHz)
- Comprehensive dosimetry ELF setup
- Comprehensive dosimetry RF setups
- Technical quality control during the entire period of exposure

Detailed information about the applied exposure systems and their dosimetry are given in

- [Schuderer et al., 2004a] for the ELF setup
- [Schuderer et al., 2004b] for the RF setup (GSM)
- [Schuderer et al., 2003] for the RF setup (UMTS)
- [Schönborn et al., 2000] for the waveguide setup of Participant 4
- [Laval et al., 2000] and [Schuderer et al., 2004c] for the Wire-patch cell of Participant 9
- [Toivo et al., 2001] and [Schuderer et al., 2004c] for the resonator setup of Participant 6
- [Kuster et al., 2002] for the choice of the exposure signals

REQUIREMENTS

The requirements for the exposure systems are formulated in Kuster and Schönborn (2001). In particular, the following parameters need to be fulfilled:

ELF setup:

- large loading volume with uniform exposure
- high dynamic (µT - mT) and frequency ranges (subHz - kHz)
- enabling complex signals and intermittent exposure
- good isolation between exposure and sham
- identical atmospheric parameters for exposed and sham cells (preferably placed in the same incubator)
- blinded exposure protocols by a computer-controlled random decision maker
- continuous monitoring of all environmental and technical parameters in order to detect any malfunctions
- evaluation of possible artefacts such as parasitic E-fields, temperature loads, vibrations, etc.

RF setup:

- peak SAR exposure: >100 W/kg
- maximum time averaged SAR exposure for thermal load < 0.1°C: > 2 W/kg
- deviations from uniformity of exposure: < 30%
- variability of exposure: < 10%
- loading volume with uniform exposure: min. 50 cm^2
- flexible signal unit with high dynamic range enabling complex modulation such as:
  - continuous wave (CW)
  - pulse or sinusoidal modulation at any frequency and repetition rate
  - GSM DTX (discontinuous transmission mode)
  - GSM non-DTX
  - GSM talk (temporal changes between non-DTX and DTX)
  - UMTS signal schemes
- flexible intermittent exposure protocols: seconds to hours
- good isolation between exposure and sham: > 30 dB
- identical atmospheric parameters for exposure and sham: μT < 0.1°C
- blinded exposure protocols
- continuous monitoring of exposure and environmental parameters
- detailed numerical modelling including meniscus
- evaluation of SAR distribution and experimental verification by dosimetric measurements
- uncertainty and variability analysis for SAR
- evaluation of the temperature load
- reliability, user-friendliness and self-detection of malfunctions
- minimal setup cost

MATERIAL AND METHODS

Overview

High-end exposure setups for ELF, RF-GSM and RF-UMTS were developed and fully characterized with respect to exposure parameters, design and possible artifacts.

Since the budget did not allow to equip every laboratory with these setups, existing setups were evaluated with respect to their suitability.

Evaluation of Existing Setups

In order to assess the performance of the already existing setups, the exposure systems in the laboratories of Participants 2 - 9 were evaluated with respect to dosimetric performance and characterization. Possible modifications to improve the performance were also evaluated.

In addition to the newly developed exposure systems, it was decided to use five existing setups (Participants 4, 5, 6, 8, 9) and to modify and improve the two RF setups of Particioants 4 and 9. Similar methods for dosimetry and characterization as described for the newly developed RF setups were used.

ELF setups:

- *Helmholtz coils (Participant 5)*: A pair of Helmholtz coils is placed inside a μ-metal shield; exposure and sham are kept in different incubators; and sinusoidal B-fields (50 Hz) up to 0.1 mT can be applied.
- *4-coil system (Participant 8)*: Two unshielded 4-coil systems are arranged in the same incubator; B-fields up to 1 mT (50 Hz) can be applied.

Both setups provide acceptably uniform B-fields, and no further modification and optimisation was applied.

RF setups:

- *Waveguide setup (Participant 4)*: The waveguide setup of Participant 4 is operated at 1710 MHz and allows the exposure of eight 60 mm diameter Petri dishes. The original system [Schönborn et al., 2000] was enhanced with
  - a new signal unit, allowing complex GSM modulation
  - field sensors to monitor the exposure
  - temperature sensors to monitor the incubator environment
  - an optimised air flow system to reduce temperature differences between both chambers
- *Wire-patch cell (Participant 9)*: The Wire-patch cell is an open radiating setup operated at 900 MHz. The setup is based on a 150 mm x 150 mm parallel plate configuration (distance 29 mm), short-circuited at the edges by four plots [Laval et al., 2000]. Eight 35 mm Petri dishes (placed inside a 60 mm dish with distilled water) are arranged symmetrically around the central coaxial feed. Since the WP cell is an open setup, exposure and sham groups need to be placed in two different incubators. For the purpose of REFLEX, the original system was enhanced by
  - distance keepers for the Petri dishes,
  - optimised Petri dish loading (to reduce the thermal load, distilled water instead of cell medium is used for the 60 mm dish),
  - E-field sensors for monitoring and regulation
  - A computer-controlled signal unit, allowing complex GSM modulation
- *Resonator setup (Participant 6)*: The resonator setup consists of a short-circuited waveguide chamber at 900 MHz [Toivo et al., 2001]. Four 60 mm diameter Petri dishes are exposed in a standing wave E-field maximum in E-polarization. The dishes are placed on a glass plate which is water-cooled from below. In this way a temperature stability of ± 0.3°C over the range from 0 – 10 W/kg average SAR is achieved. No modification of the resonator setup was performed.

Development of ELF Exposure Setup

An ELF setup was developed and four copies were installed in the laboratories of Participants 3, 4, 7 and 11. The following methods have been applied to achieve an optimised design for the ELF exposure system:

- Two coil chambers are placed inside the same incubator to guarantee identical environmental parameters for exposure and sham groups. A fan system serves for enhanced atmospheric exchange between coil chambers and incubator.
- µ-metal shielding is applied for the coils in order to provide sufficient sham isolation.
- E-field shielding of the exposure area is applied to remove parasitic E-fields, generated by the voltage drop over the inductive coils.
- Elastically damped dish holders are used to minimize the coupling of the mechanical vibrations to the Petri dishes.
- Numerical field calculation was used to optimise the 4-coil system within the µ-metal shielded exposure chamber. Optimisation parameters were size of the coils, number of windings and distance between the windings. B-field uniformity was used as an optimisation target.
- Exposure control is realized by monitoring and feedback regulation of the coil currents.
- Complex ELF signals can be applied by using an arbitrary function generator together with a custom-made current source to generate any signal with a point length of 16000 points, a point resolution of 12 bit and frequencies up to 1.5 kHz.
- A power-line signal was defined as the maximum accepted distortion for low- to medium-voltage power systems by the IEC (spectral components up to 1250 Hz are present).
- Environmental monitoring is applied with temperature sensors inside the chambers and by controlling the fan system (current measurement).
- Computer control allows blind protocols and easy handling of the system.

Development of RF Exposure Setup (GSM)

An RF setup (GSM) was developed and four copies were installed in the laboratories of Participants 2, 5, 6 and 8. The following methods have been applied to achieve an optimised design for the RF exposure system:

- The study from Schönborn et al. (2001) showed that the most suited setup with respect to highly uniform cell monolayer exposures should be based on waveguides.
- A waveguide setup was numerically analysed by using the FDTD method. The length of the waveguides was optimised, so that the system is operated at a fundamental resonator mode at 1800 MHz. In this way, superior power efficiency can be achieved.
- The required uniformity and maximum SAR is achieved for a fan-cooled cell monolayer exposure in E-polarization, which provides minimum temperature load.
- Exposure control is realized by field sensors.
- Environmental control is realized by placing the waveguides inside an incubator and using fans for atmospheric exchange. A common air inlet of the fan system was realized in order to reduce temperature differences between both waveguides.
- Environmental monitoring is applied with air temperature sensors and fan monitoring.
- Low variability is realized with a field sensor feedback regulation and by using dish holders together with distance keepers to provide defined positions of the Petri dishes with respect to the incident fields.
- Flexible signal schemes and blinded protocols are realized with a computer-controlled signal unit. AM modulation of the RF generator is applied via an arbitrary function generator and additionally via software commands. Temporal changes between different modulation modes like GSM DTX and non-DTX is realized with a GSM frame unit, blanking the output of the RF amplifier.

Development of RF Exposure Setup (UMTS)

An RF setup (UMTS) was developed and installed in the laboratory of Participant 3. Similar methods as for the RF setup (GSM) have been applied to achieve an optimised design for the UMTS exposure system:

- Similar to the GSM setup, two waveguides are used, equipped with field and temperature sensors and an optimized fan cooling system.
- Due to the different carrier frequency at 1950 MHz, new positions for the Petri dishes inside the waveguide are necessary. Because of the 5 MHz bandwidth of the UMTS signal, a broadband coax-to-waveguide adapter was required.
- The signal unit was updated by a UMTS signal generator. The fast power control of the signal is realized by AM modulation of the RF generator with a fading function stored on the arbitrary function generator.
- A UMTS test signal was defined, which represents worst-case exposure with respect to ELF spectral content. The signal is based on closed loop power controlled fades and additionally covers compressed mode and an open loop power controlled sequence for the physical random access channel.

Dosimetry ELF Exposure Setup

The following methods for dosimetry of the ELF setup were applied:

- *Numerical B-field characterization*: Mathematica V4.1 was used for analytical calculation of the B-field distribution as resulting from the 4-coil configuration.
- *Experimental B-field characterization*: A 3-axis Gaussmeter (FH49, Magnet-Physik, Germany) was used to measure the B-field distribution inside the exposure chamber.
- *Uncertainty and variability*: Uncertainty of the dosimetric assessment and exposure variability were analyzed for the applied numerical and experimental methods.
- *Induced E-field characterization*: The distribution of the induced E-fields within the cell medium was assessed by calculation.
- *Artefact characterization*:
  - *Parasitic E-fields*: A Wandel and Goltermann EFA-3 sensor system was used to determine the electric fields inside the exposure chamber as produced by the setup.
  - *Temperature*: Temperature was measured inside the cell medium with a SPEAG T1V3 probe as well

as for several positions inside the exposure chamber with Thermometrics Pt100 temperature sensors.

- *Vibrations*: To assess the acceleration resulting from coil vibrations, a Wilcoxon Research accelerometer Model 728T equipped with an amplifier unit P704T was applied.

Dosimetry RF Exposure Setup (GSM, UMTS, Wire-Patch Cell)

The following methods for dosimetry of the RF setups were used:

- *Numerical field simulation*: The FDTD simulation platform SEMCAD was applied for a full 3D electromagnetic field analysis.
- *Numerical modelling*: High resolution numerical models including menisci at the solid/liquid interfaces have been used to achieve realistic modelling. SAR extrapolation to the monolayer was applied to compensate discretization error in the strong SAR gradients.
- *Experimental verification*: Simulation was experimentally verified using the DASY3 near-field scanner equipped with 3-axis free space E- and H-field probes (SPEAG EF3DV2, H3DV6) and a dosimetric E-field probe with a diameter of only 1 mm [Pokovic et al., 2000].
- *Uncertainty and variability*: The uncertainty of the SAR assessment was evaluated with respect to the applied numerical and experimental methods. Possible variability of SAR values was additionally evaluated.
- *Thermal load*: The thermal load for the exposed group was assessed by measurement and simulation: A SPEAG T1V3 temperature probe was used for a single-point measurement of the temperature response of the medium (probe was fixed in the temperature maximum). Additionally, a coupled electro-thermal FDTD simulation was used for the 3D assessment of the temperature distribution as a function of exposure duration.

Quality Control and Maintenance

Quality control is ensured by the analysis of the exposure data as recorded from the monitoring unit and stored within an encoded file. All experimental settings and software commands are saved together with the sensor data for field exposure and environment. The monitoring sampling rate is 0.1 Hz. Decoding of the data files can only be provided by a dedicated software and is done by the quality assurance group after biological evaluation. A detailed report of all exposure parameters is then provided.

Furthermore the controlling and monitoring software is able to self-detect malfunctions and responds with warnings or abortions if required (tracing and handling of 60 errors).

For the RF setups, the ambient ELF-fields in the different laboratories were determined for several positions within the incubator and laboratory using a Wandel & Golterman EFA-3 sensor system.

RESULTS

Dosimetry ELF Exposure Setup

The performance of the ELF setup can be summarized by:

- Dynamic range for B-field amplitude (50 Hz): 0.02 – 3.6 mT_{rms}
- Dynamic range for B-field frequency: mHz –1500 Hz
- Nonuniformity of B-field: < 1%
- Uncertainty for B-field assessment: 4.3%
- Variability of exposure: 1.6%
- Loading volume: 3500 cm^3
- Parasitic E-fields (50 Hz): < 1 V/m
- Vibrations:
  - < 0.1 m/s^2 for elastically damped holder
  - < 1 m/s^2 for non-damped holder

- Signal schemes:
  - Sinusoidal 3 –1000 Hz
  - 50 Hz power-line signal (components up to 1250 Hz)
  - Arbitrary intermittency
- Exposure control and monitoring: provided by current measurements (sampling rate 0.1 Hz)
- Environmental control: provided by incubator and fan system (air temperature difference between exposure and sham: < 0.1°C)
- Environmental monitoring: provided by temperature probes and fan current sensing (sampling rate 0.1 Hz)

Dosimetry RF Exposure Setup (GSM)

The performance of the RF setup (GSM) can be summarized by:
- Dynamic range for peak SAR: 0.01 W/kg to > 100 W/kg
- Nonuniformity of SAR: < 30%
- Thermal load: < 0.03 °C / (W/kg)
- Uncertainty of SAR assessment: 20%
- Variability of exposure: 5.1%
- Loading surface for cell monolayers: 60 cm^2
- Signal schemes:
  - Continuous wave
  - 217 Hz pulse modulation
  - GSM non-DTX
  - GSM DTX
  - GSM Talk
  - Arbitrary intermittency
- Exposure control and monitoring: provided by field sensor (sampling rate 0.1 Hz)
- Environmental control: provided by incubator and fan system (air temperature difference between exposure and sham: < 0.1°C)
- Environmental monitoring: provided by temperature probes and fan current sensing (sampling rate 0.1 Hz)

Dosimetry RF Exposure Setup (UMTS)

The performance of the RF setup (UMTS) can be summarized by:
- Dynamic range for peak SAR: 0.01 W/kg to > 200 W/kg
- Nonuniformity of SAR: < 26%
- Thermal load: < 0.03 °C / (W/kg)
- Uncertainty of SAR assessment: 18%
- Variability of exposure: 1.9%
- Loading surface for cell monolayers: 60 cm^2
- Signal schemes:
  - Continuous wave
  - UMTS test signal (maximized ELF spectral content)
  - 217 Hz pulse modulation
  - GSM DTX
  - GSM non-DTX
  - GSM Talk
  - Arbitrary intermittency
- Exposure control and monitoring: provided by field sensor (sampling rate 0.1 Hz)

- Environmental control: provided by incubator and fan system (air temperature difference between exposure and sham: < 0.1°C)
- Environmental monitoring: provided by temperature probes and fan current sensing (sampling rate 0.1 Hz)

Quality Control and Maintenance

Quality Control:

- In the course of the REFLEX project, approximately 1800 *in vitro* experiments have been performed. Each of these experiments is documented with a dosimetric evaluation report covering the time courses and statistics for the field values, air temperatures and fan currents as well as all experimental settings.
- Average ambient ELF B-fields in the incubators of laboratories 2, 3, 4, and 8 are:
  - Participant 2: $B = 0.3 \pm 0.2\ \mu T_{rms}$
  - Participant 4: $B = 3.2 \pm 2.0\ \mu T_{rms}$
  - Participant 5: $B = 3.5 \pm 2.2\ \mu T_{rms}$
  - Participant 8: $B = 2.8 \pm 1.9\ \mu T_{rms}$

Maintenance:

Maintenance and assistance was provided in the course of the project for:

- installation of the setups
- handling of the setups
- exchange of several Pt100 temperature probes
- exchange of some RF dish holders
- exchange of one malfunctioning ELF current source
- exchange of one malfunctioning RF generator
- provision of software updates
- evaluation of data files

DISCUSSION

All tasks except development of an optimised RF setup at 900 MHz have been fully solved. More setups than initially planned needed to be developed, since the quality of the setups available in the laboratories were not sufficient to meet the requirements of the project. In order to stay within the budget, the consortium decided to develop a new RF setup only for 1800 MHz and use already available setups for 900 MHz (setups of Participants 6 and 9). Furthermore, the setup of Participant 9 was updated to allow complex GSM modulation. In addition to the required deliverables, a novel UMTS exposure system was developed.

CONCLUSIONS

High-end exposure systems for conducting *in vitro* laboratory studies in several European research institutes were realized and characterized. These systems have already become standard exposure setups for bioexperiments around the world.

An ELF exposure system that allows flexible signal and intermittent exposure schemes has been developed and characterized. It is easy to handle due to automated software control. Coil currents, chamber temperatures and fan speed are continuously monitored and allow the experimental history to be traced with 10 s resolution. B-field and E-field distributions were characterized. The B-field shielding of the 4-coil configuration considerably enhances the uniformity of the field distribution, and a highly efficient E-field shielding inhibits strong parasitic electric fields generated by the coils. Temperature differences between exposed and sham-exposed cells are kept below 0.1°C. The vibration load on the

exposed Petri dishes is sensitive to mechanical resonance; however, a mechanically isolated and elastically damped dish holder limits this to less than $0.1 m/s^2$, which is no more than twice the background vibration of the sham setup.

The waveguide-based, computer-controlled RF (GSM) setup enables the exposure of cell monolayers with excellent efficiency > 20 W/kg /W. The flexible signal unit allows the generation and control of complex modulated signals, e.g. temporal changes between different GSM operation modes (DTX/non-DTX). Exposure field strength and environmental parameters (air temperature, fan system) are continuously monitored. Due to the field regulation, exposure variability is kept below 10%. A coupled electro-thermal FDTD analysis was performed and resulted in a nonuniformity of SAR of < 30%. The temperature load was assessed by measurement and simulation, and a maximum temperature increase of less than 0.03°C was found. No localized temperature hot "spots" are generated within the cell medium. All simulations were verified by dosimetric measurements.

An exposure setup allowing the blinded exposure of cell monolayers to UMTS signal schemes was developed and dosimetrically analysed. Cells can be exposed to up to 17 W/kg/W with less than 26% nonuniformity of SAR. The temperature load for the exposed cells is less than 0.03°C /(W/kg). The UMTS specifications have been analysed in order to identify ELF spectral components in the signal. These mainly result from inner loop power control; however, pulsed signal structures due to compressed mode and PRACH/PCPCH procedures also contribute to the ELF components. A test signal is proposed which is compliant to the 3GPP FDD modulation specifications and is optimised for maximized ELF spectral power (1 Hz harmonics).

Quality control for the entire duration of the project is ensured due to automatically generated data files. Exposure field strength, temperature, fan currents and all settings and computer commands are stored in the data files with a sampling rate of 0.1 Hz. Evaluation reports are available for every experiment performed in the REFLEX consortium.

LITERATURE CITED

N. Kuster, F. Schönborn, "Recommended Minimal Requirements and Development Guidelines for Exposure Setups of Bio-experiments Addressing the Health Risk Concern of Wireless Communications", Bioelectromagnetics 21:508-514, 2000.

N. Kuster, W-R. Adey, "Criteria for Selecting Specific EMF Exposure Conditions for Bioexperiments in the Context of Health Risk Assessments", 23rd Annual Meeting of the Bioelectromagnetics Society, St. Paul, Minnesota, USA, p. 24, 2001.

L. Laval, P. Leveque, B. Jecko,"A new in vitro Exposure Device for the Mobile Frequency of 900 MHz", Bioelectromagnetics 21:255-263, 2000.

K. Pokovic, T. Schmid, N. Kuster "Millimeter-Resolution E-Field Probe for Isotropic Measurement in Lossy Media Between 100 MHz and 20 GHz", IEEE Transactions on Instrumentation and Measurement 49:873-878, 2000.

F. Schönborn, K. Pokovic, A. Wobus A, N. Kuster, "Design, Optimization, Realization, and Analysis of an In Vitro System for the Exposure of Embryonic Stem Cells at 1.71GHz", Bioelectromagnetics 21:372-384, 2000.

J. Schuderer, W. Oesch, N. Felber, N. Kuster, "In Vitro Exposure Setup for ELF Magnetic Fields", Bioelectromagnetics, in press, 2004a.

J. Schuderer, T. Samaras, W. Oesch, D. Spät, N. Kuster, "High Peak SAR Exposure Unit with Tight Exposure and Environmental Control for In Vitro Experiments at 1800 Mhz", IEEE Transactions on Microwave Theory and Techniques, vol 52, No. 8, pp. 2057-2066, 2004b.

J. Schuderer, D. Spät, T. Samaras, W. Oesch, N. Kuster, "In Vitro Exposure Systems for RF Exposures at 900 Mhz", IEEE Transactions on Microwave Theory and Techniques, vol 52, No. 8, pp. 2067-2075, 2004c.

J. Schuderer, W. Oesch, U. Lott, N. Kuster, "In Vitro Exposure Setup for Risk Assessment Studies with UMTS Signal Schemes at 1950 Mhz", 25th Annual Meeting of the Bioelectromagnetics Society, June, Maui, USA, p. 68, 2003.

T. Toivo, A-P. Sihvonen, L. Puranen, K. Keskinen, "Water Cooled Waveguide Chambers for Exposure of Cells In Vitro at 900 MHz", Proc. EBEA 2001, Helsinki, Finland. pp 62-63, 2001.